NASA CR-120943
AT-6133-R

F

ADVANCED TWO-STAGE COMPRESSOR PROGRAM DESIGN OF INLET STAGE

by

Dr. C. A. Bryce
C. J. Paine
Dr. A. R. S. McCutcheon
Dr. R. K. Tu
G. L. Perrone

AIRESEARCH MANUFACTURING COMPANY OF ARIZONA

Prepared for

NATIONAL AERONAUTICS AND SPACE ADMINISTRATION

NASA Lewis Research Center
Contract NAS 3-15324

P-13432

NOTICE

Requests for copies of this report should be referred to:

National Aeronautics and Space Administration
Scientific and Technical Information Facility
P. O. Box 33
College Park, Maryland 20740

1. Report No.	2. Government Accession No.	3. Recipient's Catalog No.
NASA CR-120943		

4. Title and Subtitle	5. Report Date
ADVANCED TWO-STAGE COMPRESSOR PROGRAM DESIGN OF INLET STAGE	August 1973
	6. Performing Organization Code
7. Author(s) Dr. C.A. Bryce, C.J. Paine, Dr. A.R.S. McCutcheon, Dr. R.K. Tu, G.L. Perrone	8. Performing Organization Report No. AT-6133-R
9. Performing Organization Name and Address AiResearch Manufacturing Company of Arizona Phoenix, Arizona 85010	10. Work Unit No.
	11. Contract or Grant No.
12. Sponsoring Agency Name and Address National Aeronautics and Space Administration Washington, D.C. 20546	13. Type of Report and Period Covered Contractor Report
	14. Sponsoring Agency Code

15. Supplementary Notes

Program Monitor, Robert Y. Wong, NASA-Lewis Research Center, Cleveland, Ohio

16. Abstract

This final report covers the aerodynamic design of an inlet stage for a two-stage, 10/1 pressure ratio, 2 lb/sec flow rate compressor. Initially a performance comparison was conducted for an axial, mixed flow and centrifugal second stage. A modified mixed flow configuration with tandem rotors and tandem stators was selected for the inlet stage. The term "conical flow compressor" was coined to describe a particular type of mixed flow compressor configuration which utilizes axial flow type blading and an increase in radius to increase the work input potential. Design details of the conical flow compressor are described.

17. Key Words (Suggested by Author(s))	18. Distribution Statement
Compressor/Impeller Inlet Stage Two-Stage Compressor Program	Unclassified-unlimited

19. Security Classif. (of this report)	20. Security Classif. (of this page)	21. No. of Pages	22. Price*
Unclassified	Unclassified	300	3.00

*For sale by the National Technical Information Service, Springfield, Virginia 22151

Page Intentionally Left Blank

FOREWORD

This is the final report covering work performed under Contract No. NAS 3-15324 during the period May 1, 1971 through April 30, 1972.

This contract was under the technical direction of Mr. R. Wong, Lewis Research Center, of the National Aeronautic and Space Administration.

Mr. K. W. Benn was program manager, Mr. G. R. Metty, the project engineer, and Mr. G. L. Perrone, principal investigator. Recognition is given to Mr. J. R. Erwin for frequent consultations and to Mr. P. Dodge for his assistance in developing one of the computer programs required to analyze this design.

Page Intentionally Left Blank

TABLE OF CONTENTS

ADVANCED TWO-STAGE COMPRESSOR PROGRAM DESIGN OF INLET STAGE

SUMMARY

The objective of this program was to design an inlet stage for an advanced two-stage compressor for an overall pressure ratio of 10/1 and 2.0 pounds per second mass flow. As a part of this program, an optimization study was conducted for various inlet stages in combination with a centrifugal compressor second stage. Axial, mixed flow, and centrifugal compressors were examined as inlet stages with analyses made for the optimum pressure ratio split between stages and the optimum speed for each combination. A form of mixed flow compressor, with a tandem bladed rotor and a tandem bladed stator, was selected for detailed design on the basis of performance potential.

The flow path in the selected mixed flow compressor incorporates axial flow type blading and a substantial change in radius along streamlines across each blade row to increase the work input without exceeding the loading criteria established for axial flow blading. The change in radius renders conventional methods for finding flow deviation largely inaccurate. An improved method for computing flow deviation was developed which essentially coupled the axisymmetric, radial equilibrium flow solution to a finite difference, blade-to-blade solution thereby yielding a quasi three-dimensional model of the flow through each blade row (secondary flows excluded). A complete description of the design philosophy used to establish blade sections for each blade row is presented. Predicted performance for the conical compressor looks favorable and, if experimentally verified, this design concept could have a wide range of applications.

Page Intentionally Left Blank

INTRODUCTION

In order to achieve low specific fuel consumption (SFC) and high specific thrust, high compressor pressure ratios and high turbine inlet temperature are required, while at the same time maintaining high component efficiencies. These objectives become progressively more difficult to achieve as gas turbine engines are reduced in size or power output. In the small power range (500 horsepower or less), the relative size of the components make manufacturing tolerances and minimum clearances critical factors in attaining high efficiencies.

In small engines it is desirable to employ a relatively simple compressor with a minimum number of stages consistent with performance goals and weight considerations. In this class of engine, the Lewis Research Center is particularly interested in a two-stage compressor with an overall pressure ratio of 10/1 and 2.0 pounds per second mass flow rate. Thus a compressor program was initiated to study a two-stage compressor consisting of a second-stage centrifugal compressor which is preceded by an inlet stage operating at the same shaft speed. The inlet stage may be an axial, centrifugal, or a mixed flow design. The first objective of this program was to optimize these combinations of stages for various pressure ratio splits and rotative speeds. Consideration was also given to turbine speed limitations in an actual engine application. From this study, a two-stage compressor was selected on the basis of performance potential, stage compatibility, size, weight, volume, and resistance to foreign object damage. A second objective was to incorporate the first stage of the selected configuration into a research package for delivery to the Lewis Research Center for experimental evaluation. This research package was to be complete with drive turbine and research instrumentation. Funding limitations resulting mainly from the need to develop analytical methods for handling a novel impeller prevented the completion of all of these objectives.

This report will describe the work that was completed under contract with the Lewis Research Center. Included in this report are a description of the optimization study of the three candidate configurations, trade-offs made in making the final selections, the detailed aerodynamic design of the first stage of the selected compressor configuration, the detailed aerodynamic design of the crossover duct between the two stages, and the detailed aerodynamic design of the drive turbine for the research package. The drive turbine was designed to have the capability of driving the combined two-stage configuration to a speed of 110-percent of design speed. Also included in this report are:

(a) Blade shapes, coordinate, and stacking information for (1) the first stage of the selected compressor (Appendix A) and (2) the research package drive turbine (Appendix C)

(b) A complete non-isentropic radial equilibrium flow solution for all blade rows (Appendix D)

(c) Mechanical design analysis of first-stage compressor blade and disk (Appendix E)

COMPRESSOR SELECTION

The selection of the two-stage compressor configuration for 10/1 pressure ratio and 2 lb/sec flow rate is based on an optimization study of each candidate configuration for efficiency as a function of speed and pressure ratio split. The configurations examined analytically were (1) an axial stage followed by a centrifugal stage, (2) a mixed flow stage followed by a centrifugal stage, and (3) a centrifugal stage, and (3) a centrifugal stage followed by a second centrifugal stage. The results of this study were then used with the criteria listed below to select the compressor configuration for this application.

(a) Overall compressor efficiency

(b) Aerodynamic compatibility of the two stages

(c) Potential for boundary layer control

(d) Stage size and weight considerations

(e) Impeller erosion considerations

Centrifugal-Centrifugal Compressor Configuration

The prediction of performance of a centrifugal compressor is based on a correlation of polytropic efficiency against specific speed. The use of a specific speed correlation originates from pump practice where peak adiabatic efficiency has been experimentally found to be uniquely related to this parameter. Published derivations of specific speed correlations rely on dimensional analysis and certain intuitive arguments. A theoretical basis for the application of specific speed as a correlating parameter for compressor performance can be derived from the corresponding momentum equations in nondimensional form. The subject derivation indicates that dynamic similarity for solutions to the equations of motion depends on specific speed and certain dimensionless geometric parameters for the rotor. In the AiResearch derivation, the specific speed is based on a mean volume flow through the compressor. This formulation uses the square root of the product of the compressor inlet and outlet volumetric flow rates instead of the usual specific speed definition based on the inlet volumetric flow. AiResearch experience has shown that the mean effective definition of specific speed best describes conditions for dynamic similarity in a centrifugal compressor.

Polytropic efficiency is used to correlate centrifugal compressor performance since it represents the true aerodynamic efficiency exclusive of pressure ratio of preheat effects. An empirical correlation of experimental results from a variety of centrifugal compressor tests with inlet tip relative Mach numbers up to 1.3 has shown that polytropic efficiency is essentially independent of compressor pressure ratio. Therefore, obtainable performance for centrifugal compressors can be represented by a single line on a plot of polytropic efficiency against specific speed as shown on figure 1. This correlation is restricted to compressors with throughflows (W_{corr}) of 7 pounds per second or greater, nominal clearances of 0.010 inch or less, and a Reynolds number (Re) of 3×10^6 or higher. Scaling these results to lower flow rates is a separate problem and will be discussed later in this report. This polytropic efficiency correlation is used in the design point computer program to compute state and overall efficiency for a given overall pressure ratio, rotative speed, and first-stage pressure ratio.

With several assumed values of first-stage pressure ratio at constant rotating speed and overall pressure ratio, the program will curve fit the resulting overall efficiencies and determine the optimum stage pressure ratios. Results from this program are presented on figure 2. This figure shows overall compressor efficiency for two centrifugal stages with an overall pressure ratio 10/1 as a function of first-stage pressure ratio and rotating speed. Peak stage efficiency is indicated for each speed in figure 2 corresponding to the optimum pressure ratio split between stages. A crossplot of the peak efficiency results against rotating speed is shown in figure 3. This plot is used to determine design conditions tabulated below for the optimum centrifugal-centrifugal configuration for this application.

Note that the first stage of a two-stage compressor does not require diffusion to as low a Mach number as the second stage and thus the diffusion losses are lower. Experience has indicated, however, that the turning and ducting losses associated with the interstage duct are sufficiently high to compensate for the reduced diffusion. Therefore in the above analysis, the efficiency correlations that are based primarily on single-stage performance with diffusers are also assumed to apply to stages with interstage ducts.

DESIGN CONDITIONS FOR THE OPTIMUM
CENTRIFUGAL-CENTRIFUGAL COMPRESSOR CONFIGURATION

	First Stage	Second Stage	Overall
Rotor speed, rpm	75,500	72,500	72,500
Pressure ratio	4.75/1	2.1/1	10/1
Specific speed, N_s	70	64	N/A
Adiabatic efficiency, η_{ad}	0.84	0.862	0.826

Previous AiResearch test experience with a two-stage centrifugal compressor at approximately 11/1 pressure ratio has demonstrated an adiabatic efficiency of 80.3 percent with a corrected

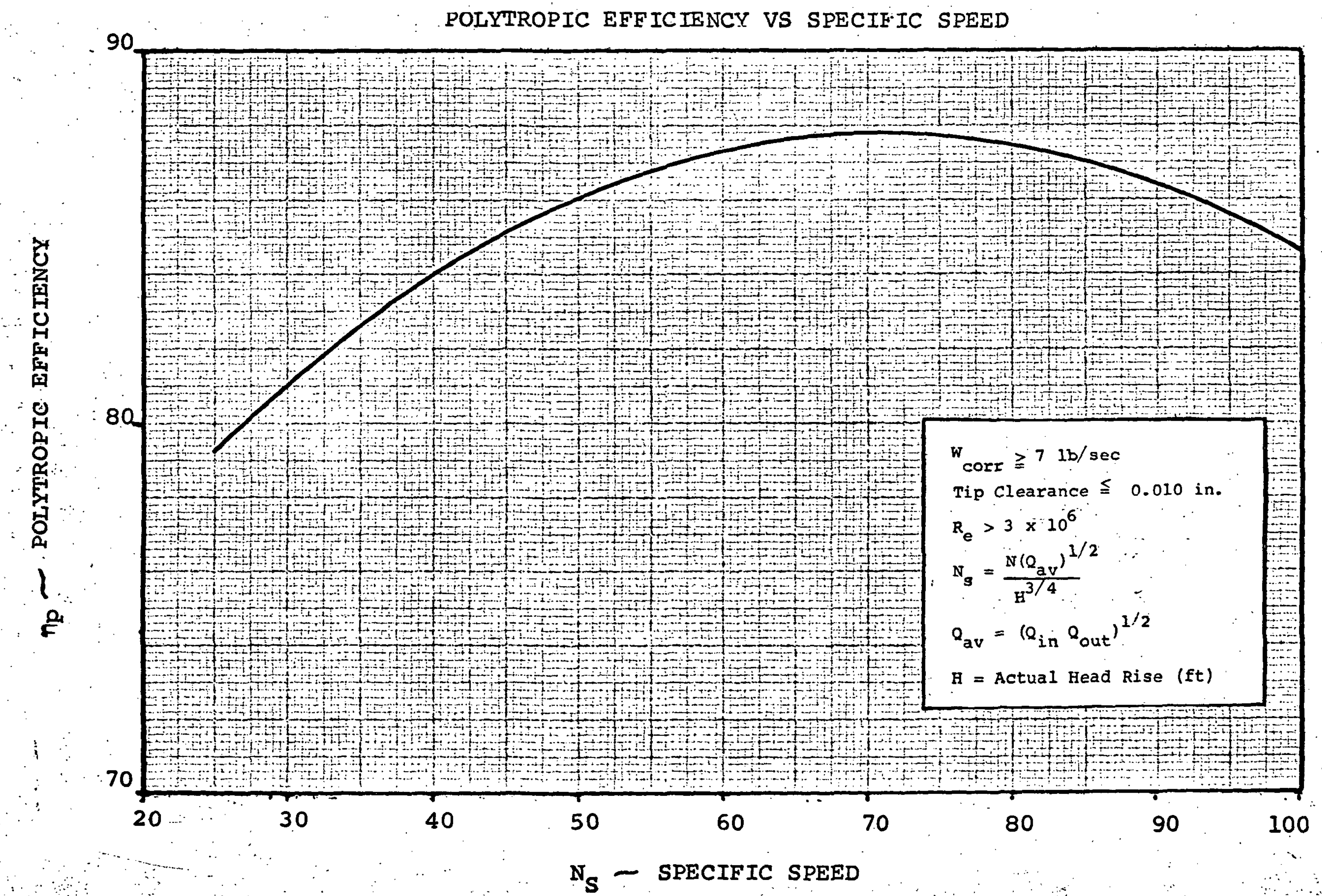

Figure 1. - Centrifugal Compressor Performance.

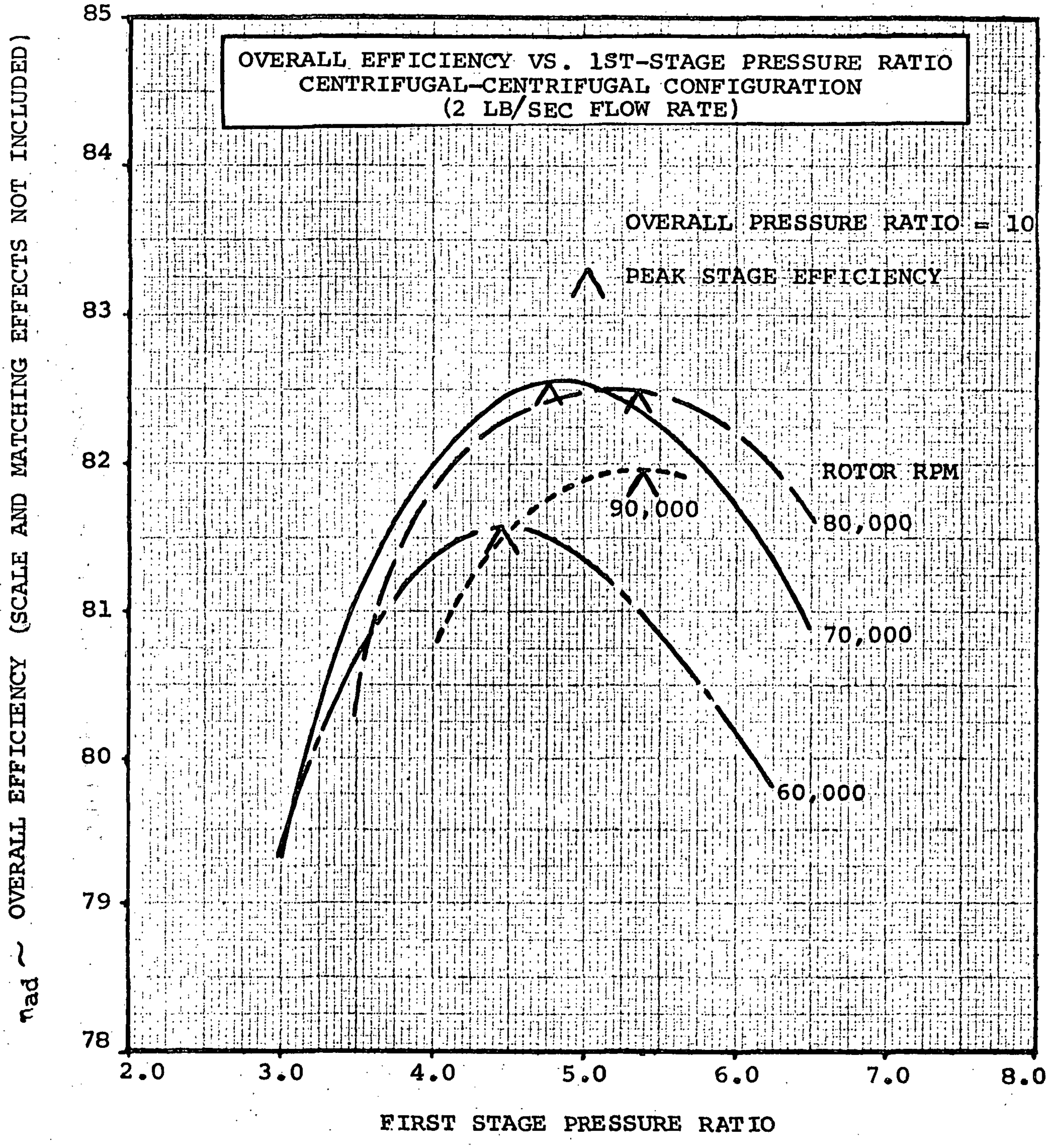
OVERALL EFFICIENCY VS. 1ST-STAGE PRESSURE RATIO
CENTRIFUGAL-CENTRIFUGAL CONFIGURATION
(2 LB/SEC FLOW RATE)
OVERALL PRESSURE RATIO = 10
PEAK STAGE EFFICIENCY
ROTOR RPM
90,000
80,000
70,000
60,000
η_{ad} ~ OVERALL EFFICIENCY (SCALE AND MATCHING EFFECTS NOT INCLUDED)
85
84
83
82
81
80
79
78
2.0
3.0
4.0
5.0
6.0
7.0
8.0
FIRST STAGE PRESSURE RATIO

Figure 2.

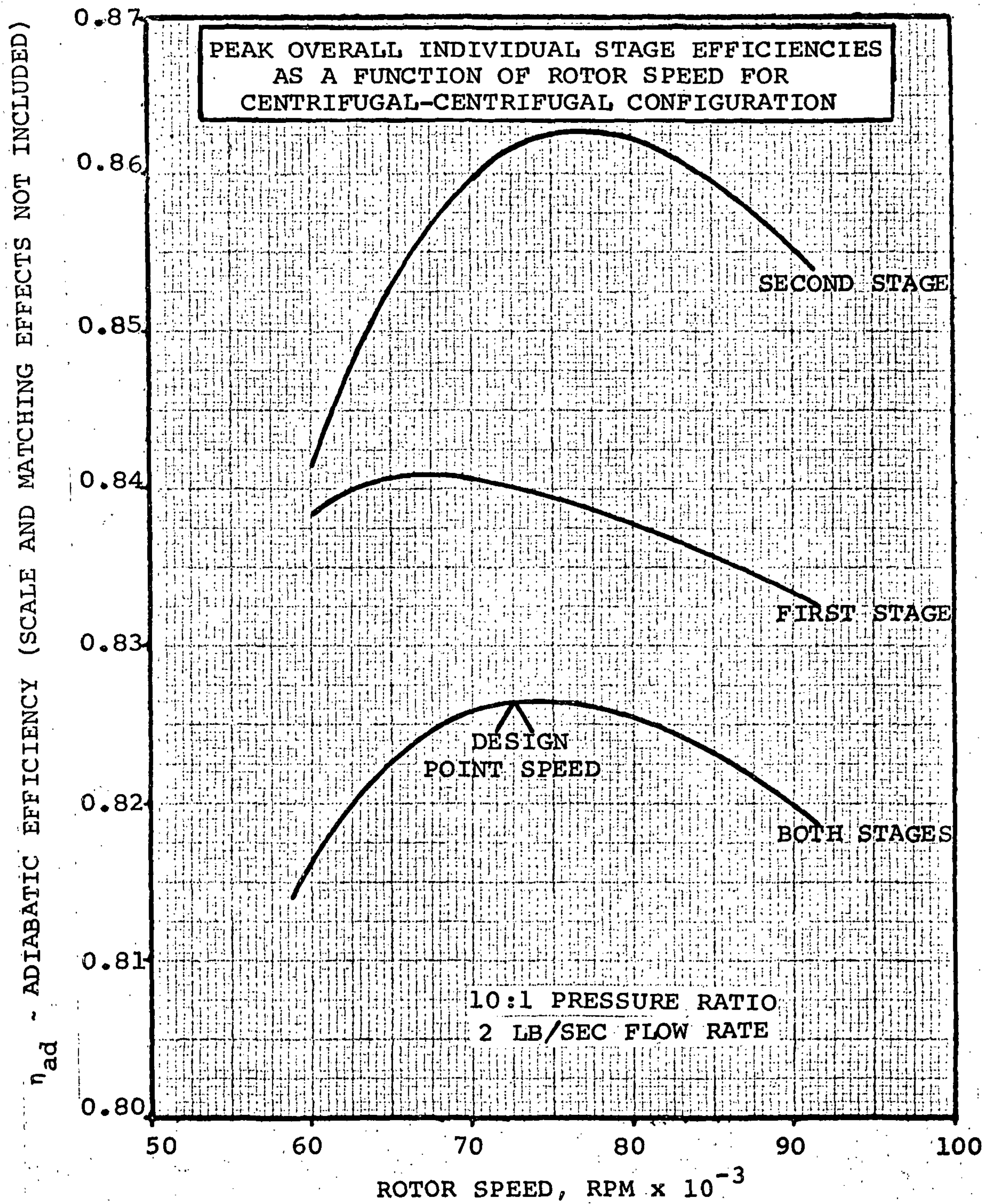
PEAK OVERALL INDIVIDUAL STAGE EFFICIENCIES
AS A FUNCTION OF ROTOR SPEED FOR
CENTRIFUGAL-CENTRIFUGAL CONFIGURATION
SECOND STAGE
FIRST STAGE
DESIGN
POINT SPEED
BOTH STAGES
10:1 PRESSURE RATIO
2 LB/SEC FLOW RATE
η_{ad} - ADIABATIC EFFICIENCY (SCALE AND MATCHING EFFECTS NOT INCLUDED)
0.87
0.86
0.85
0.84
0.83
0.82
0.81
0.80
50
60
70
80
90
100
ROTOR SPEED, RPM x 10^{-3}

Figure 3.

flow to the first stage of 8.0 pounds per second. Predicted performance for this configuration from the polytropic efficiency correlation is 81.6 percent. The difference, 1.3 points, is attributed to the fact that in order to obtain the operating range required for a practical two-stage compressor, it is often necessary to match the two stages so that their individual peak efficiencies do not coincide at the design operating point. Thus, even though each stage may achieve the peak efficiency level indicated by the specific speed correlation, the overall compressor peak efficiency may be significantly lower than the value obtained by assuming both stages to be operating at their peaks simultaneously.

It seems logical to assume that the 10/1 compressor would require a similar matching to insure good range and, therefore, the overall optimum efficiency should be lowered about 1.3 points to account for this effect.

In addition to a stage matching correction, a scale must be applied to the predicted performance to account for the lower airflow of the present design. Predicted efficiency from the polytropic performance correlations is based on experimental data for centrifugal compressors with corrected flows of 7.0 pounds per second or higher. At the 2.0 pounds per second airflow of the present design, clearance problems and secondary flow effects are more severe than for a corresponding condition in the empirical correlation. Experience has shown that a decrement of 2.3 points in the overall adiabatic efficiency is necessary to account for scaling down to the 2.0 pounds per second airflow. Thus, the combined correction for the two-stage centrifugal combination is 3.6 points (staging loss plus flow rate scaling). This results in a predicted overall adiabatic efficiency for the centrifugal-centrifugal configuration of 79 percent.

A sketch showing a meridional view of the flowpath for the centrifugal-centrifugal configuration is presented as figure 4. In this design the Mach number at the entrance to the transition section between stages is 0.3. This is a reasonable level for efficient turning in the transition duct. Flow leaves the second-stage diffuser at an average Mach number of 0.2. This value was a requirement of the contract.

Axial-Centrifugal Compressor Configuration

Axial compressor performance prediction requires much more parametric definition than for centrifugal compressor performance. A computer program has been developed by AiResearch which predicts stage efficiency of an axial compressor for specified conditions of inlet corrected flow, rotational speed, and stage pressure ratio. The program solves for conditions along the pitch line with continuity being satisfied on a one-dimensional basis. The rotor and

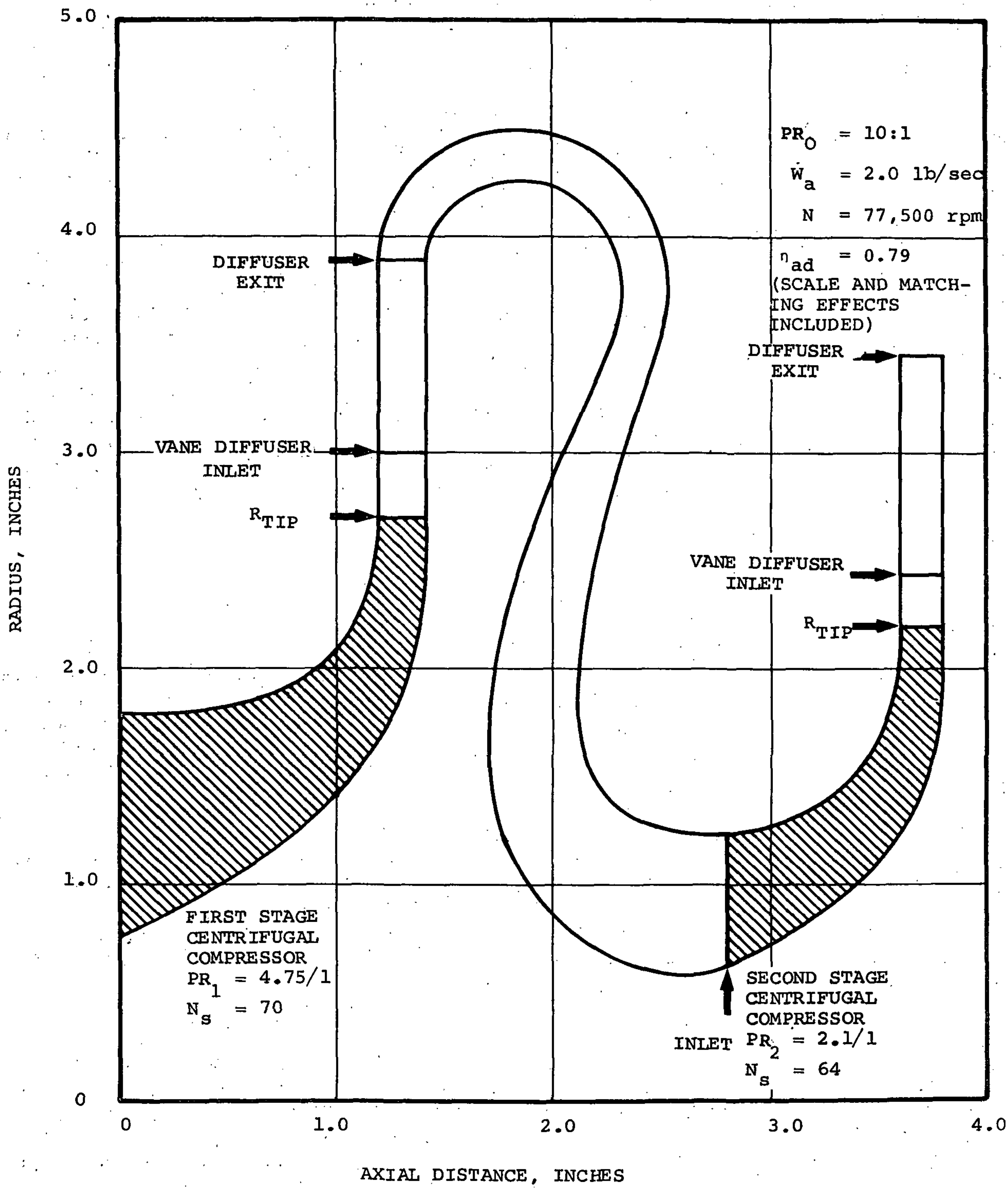

Figure 4. - Meridional View At Flow Path For Centrifugal-Centrifugal Configuration.

stator efficiencies are calculated from mean effective profile loss coefficients using pitch line flow conditions. Loss coefficients for both shock losses and profile losses are computed as briefly discussed in the following paragraph.

The shock loss in the blade tip regions is directly related to boundary layer separation along the blade which is governed by the static pressure rise across the shock. If the shock is strong enough to separate the boundary layer, the losses will be greater than that associated with a normal shock at the inlet relative Mach number. However, if the boundary layer does not separate, the shock losses can be lessened. A correlation of the limiting static pressure rise that the boundary layer can sustain before separating was derived from shock separation data for turbulent boundary layers on a flat plate as a function of Mach number (ref. 1).* An average pitch line Mach number corresponding to:

$$M_{avg} = \frac{1.0 + M_{tip}}{2}$$

was used to calculate a normal shock loss for the entire blade. This value of loss was then multiplied by a ratio of total pressure rise across the blade to the limiting value for boundary layer separation to obtain shock-related losses. The blade element profile losses were based on a correlation of AiResearch experimental data (airflow of 20 to 30 lb/sec) in the form of loss coefficent versus D-factor as done in Reference 2.

The rotational speed is determined from the inlet conditions, the desired work input, and hub turning across the rotor. This speed is continuously corrected as the work input is varied to achieve the required overall pressure ratio. After the program results converge, the vector diagram for the rotor and stator are calculated and a preliminary size established for the compressor stage.

The results from this computer program are plotted (figure 5) in nondimensional form for an assumed absolute inlet Mach number of 0.6 and an air angle of ten degrees at the rotor hub exit station. Several different hub exit air angles were investigated (β_{H2} = 0; 10°, and 20°) with the results showing the same general trend with hub radius ratio and pressure ratio. The selected air angle at the rotor hub exit (β_{H2} = 10°) was found to be a good representation of several existing axial compressor stages. Measured performance of these axial stages compare quite favorably with that calculated by the program. It should be noted that these axial stages are larger and have design corrected flows much higher than the present design. nitial design calculations were made without any scaling

*Refer to Appendix F for list of references.

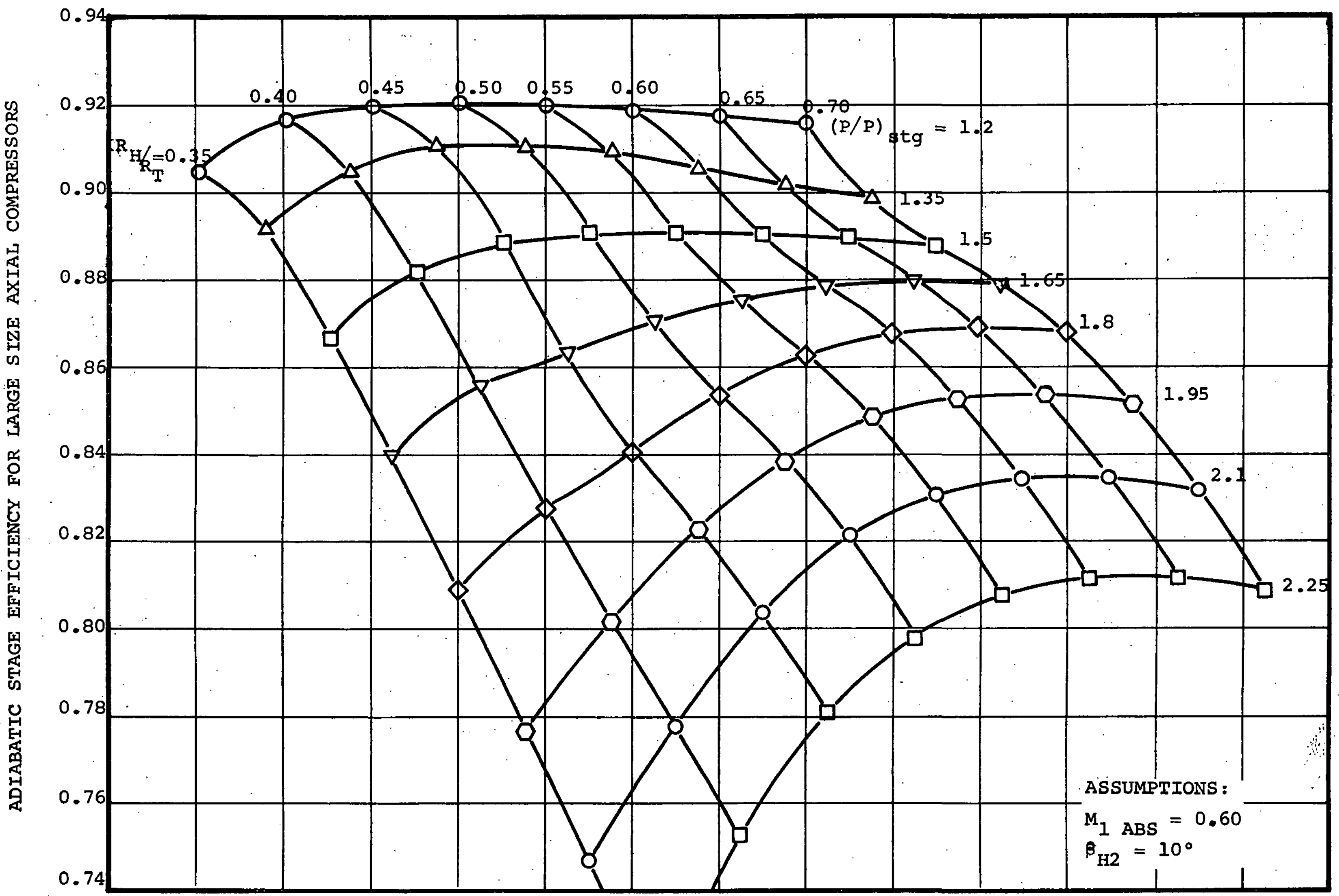

Figure 5. - Axial Compressor Stage Performance As A Function Of Hub/Tip Ratio.

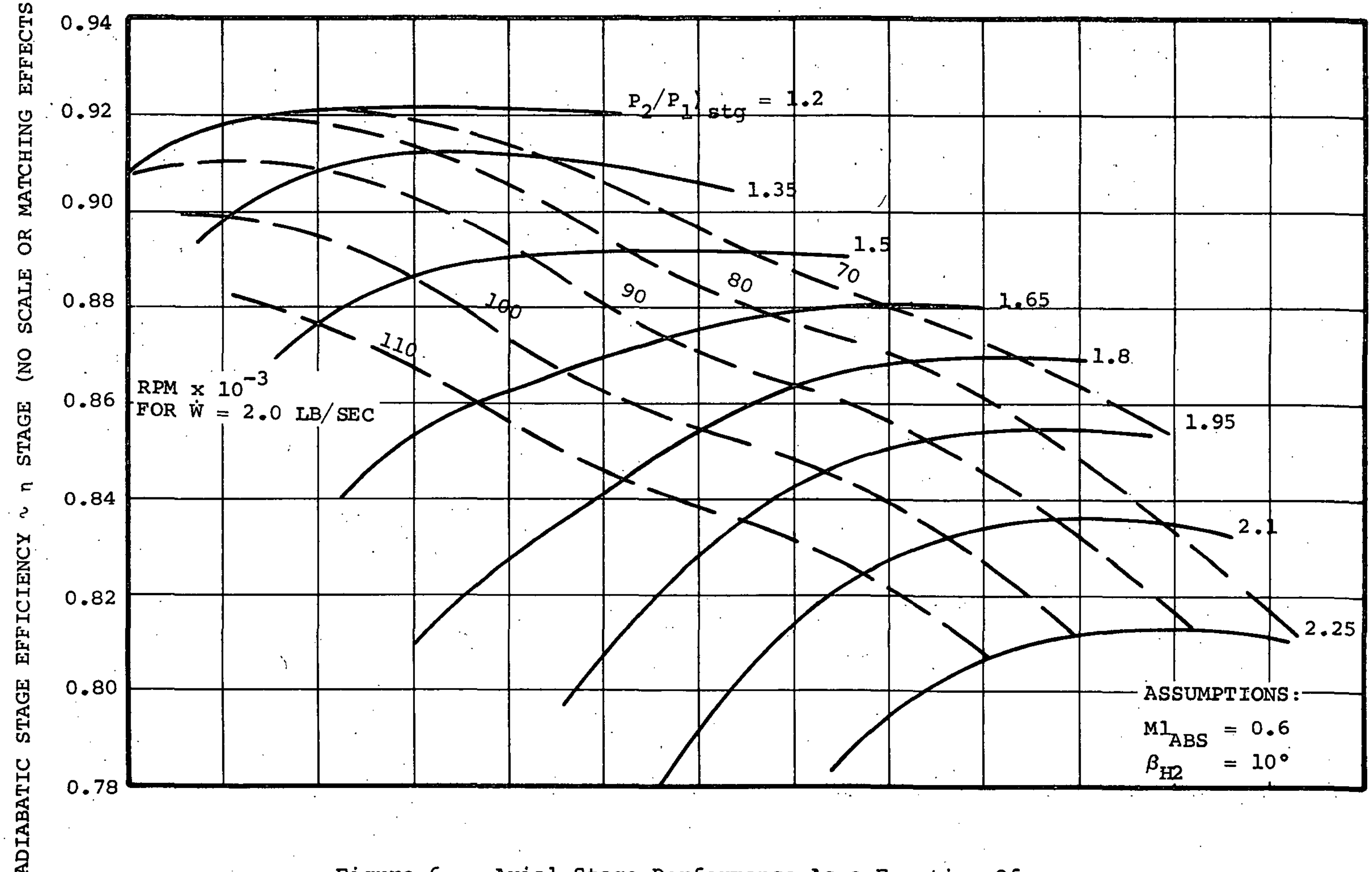

Figure 6. - Axial Stage Performance As a Function Of Rotor Speed For 2 lb/sec Flow.

effects on performance included. A discussion of overall scaling effects is undertaken in the latter portion of this section. The nondimensional results in figure 5 are converted to dimensional results in figure 5 are converted to dimensional results by specifying the stage weight flow and inlet conditions. Axial-stage performance at constant values of rotative speed for 2 lb/sec flow rate is presented in figure 6.

Overall compressor performance for an axial first-stage followed by a centrifugal compressor second stage is obtained from the design point matching program. In this program, the axial-stage performance is input as a function of first-stage pressure ratio at constant wheel speed. The centrifugal stage performance is obtained from the specific speed correlation described previously. The program computes overall performance for a 10/1 pressure ratio stage as a function of input first-stage pressure ratio values and curve fits the results to define the optimum pressure ratio split between stages. No matching penalty has been included.

A summary of the predicted overall performance for the axial-centrifugal compressor configuration is presented in figure 7. Overall compressor efficiency is shown as a function of pressure ratio across the axial stage for several values of rotor speed. Peak overall compressor efficiency for each speed is indicated by the arrows in this figure. Note that overall efficiency increases with rotor speed. The increase is directly attributable to the centrifugal stage operating at a more favorable specific speed condition at higher rotor speeds. The optimum wheel speed for peak overall compressor efficiency is above 100,000 rpm. Turbine stress considerations for this size engine have shown the wheel speed should be limited to approximately 90,000 rpm. Therefore, no attempt was made to define an optimum efficiency above 100,000 rpm in the axial-centrifugal combination. Design point wheel speed was set at 90,000 rpm for this configuration. Design conditions for this configuration are summarized in the following tabulation:

DESIGN CONDITIONS
AXIAL-CENTRIFUGAL COMPRESSOR

	First-Stage	Second-Stage	Overall
Compressor Type	Axial	Centrifugal	-
Rotor Speed, rpm	90,000	90,000	90,000
Tip Relative Mach Number	1.4	1.192	-
Pressure Ratio	1.73/1	5.78/1	10/1
Specific Speed	235	54.2	N/A
η_{ad} (no scale or matching effects included)	0.866	0.821	0.813

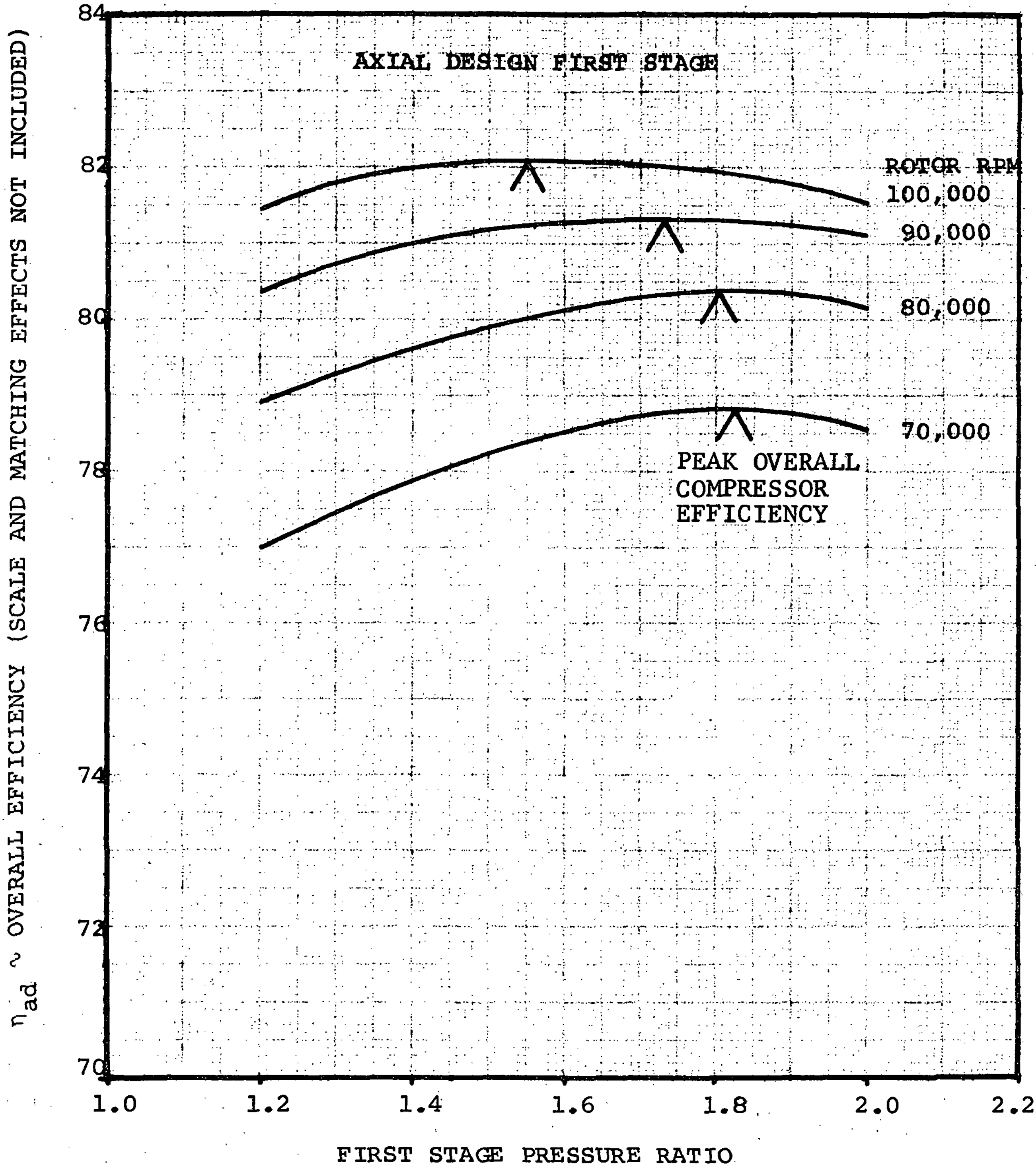

Figure 7. - Overall Efficiency vs 1st Stage Pressure Ratio Axial-Centrifugal Configuration, 2 lb/sec Flow Rate, 10/1 Overall Pressure Ratio.

Again, it should be noted that scaling and stage matching effects have not been included in the efficiencies stated above. Little data is available to estimate the effects of scaling axial flow compressors to low airflows. Therefore, in scaling the axial-centrifugal configuration, the incremental effect of size on overall efficiency was assumed to be the same as that estimated for the centrifugal-centrifugal configuration. Application of a total correction of 3.6 points to the axial-centrifugal configuration indicates that this configuration should have an overall adiabatic efficiency of 77.7 percent at design conditions (turbine speed limit). This assumes that the axial stage scales identically with a centrifugal stage. In the axial-centrifugal stage combination, the centrifugal stage does about five times as much work as the axial first-stages. Therefore a scaling effect error for the axial stage would have a minimum effect on the overall efficiency.

A meridional view of the flow path through the axial-centrifugal compressor combination is presented as figure 8. Mach number in the transition section between stages is approximately 0.43. Diffuser exit conditions for the second-stage centrifugal compressor correspond to an average Mach number of 0.2 as required.

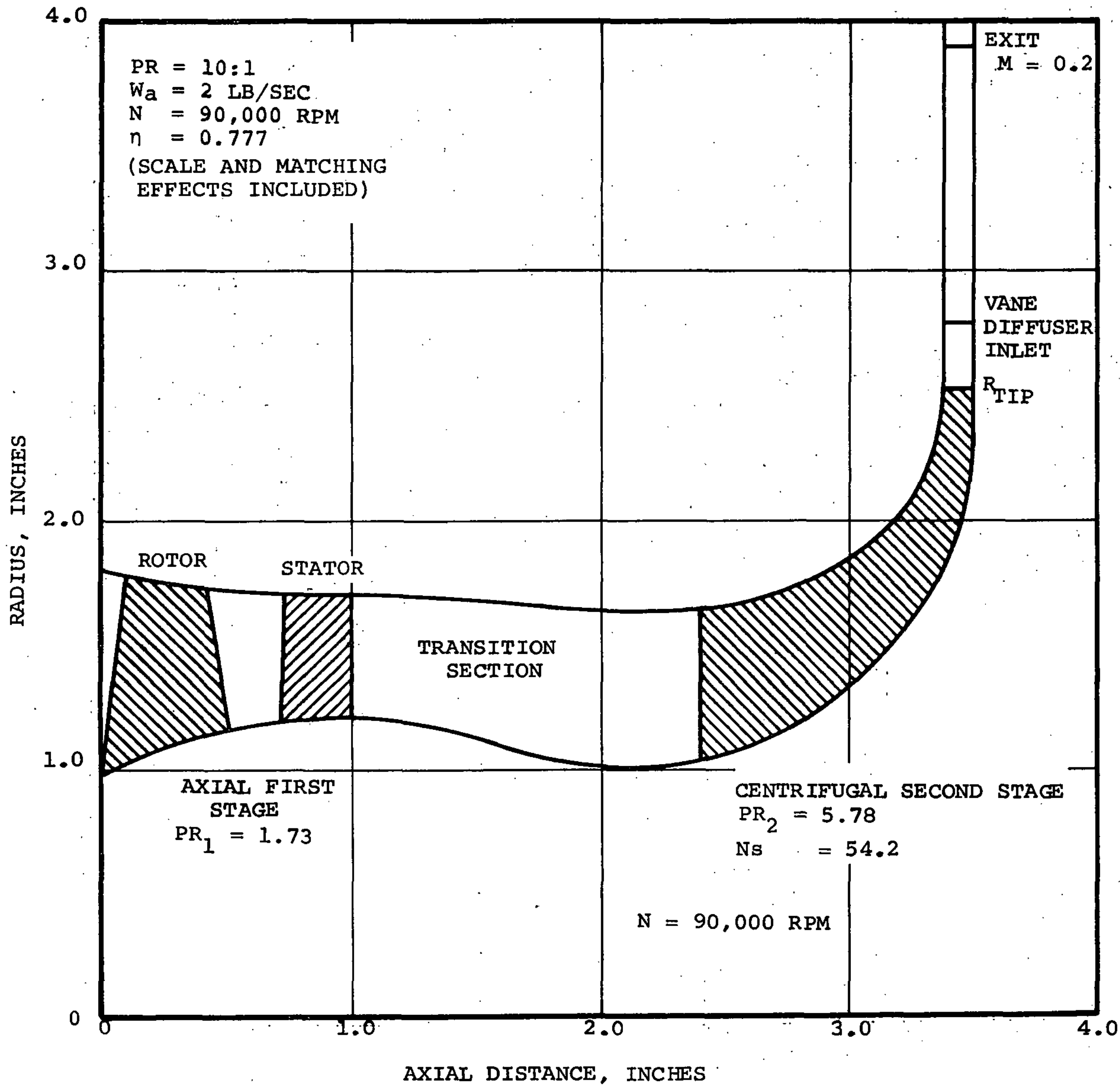

Figure 8. - Meridional View of Flow Path For Axial-Centrifugal Configuration.

MIXED-FLOW CENTRIFUGAL CONFIGURATION

The design technique employed for a conventional mixed-flow compressor is identical to that currently used for centrifugal compressor design. Based on this fact, the specific speed efficiency correlation for centrifugal compressors is also used to predict the efficiency level for the mixed-flow configuration. This, of course, yields the same result as the two-stage centrifugal configuration analysis, except that the mixed-flow configuration has a longer axial length.

In an attempt to improve the efficiency potential of a mixed-flow type of compressor, a new mixed-flow compressor concept was proposed. This concept which embodies a combination of axial design techniques with a mixed-flow type of flowpath was given the name conical-flow compressor to distinguish it from the conventional mixed-flow compressor.

Fundamentally, the conical-flow compressor combines axial flow compressor blade shapes with a large radius change (analogous to that occurring across a mixed-flow or centrifugal compressor rotor). Axial compressor design criteria are used to select blade loadings and loss estimates. Centrifugal compressor design criteria are used in selecting the design relative velocity ratios across the rotor. The capability for improved performance arises from the use of a large change in radius, which gives increased static pressure rise, with blade loadings designed to axial compressor loading criteria. If blade aspect ratios are kept similar to those acceptable to axial compressor design criteria, it is felt that secondary flow losses, which comprise a large portion of conventional mixed-flow losses, will be minimized. Frictional losses due to large blade surface areas will also be reduced. Additional advantages may be achieved by use of a tandem blading in the conical flow rotor and/or stator.

There is no data available for this type of compressor on which to base a performance prediction. Therefore, the approach used in making performance calculations on the conical-flow compressor was to assume that the pressure rise occurring due to radius change did not directly influence boundary layer growth. This approach has been used in the calculation of boundary layer growth in centrifugal impellers at AiResearch. Reasonable agreement has been achieved between losses based on loss correlations and boundary layer calculations up to the point of separation. Good agreement has also been obtained between the predicted point of boundary layer separation and experimental indication of boundary layer separation using lamp black traces on the surface of impellers. This assumption permits use of criteria established for axial flow blading to calculate blade losses for conical-flow compressor.

Various conical flow configurations were examined analytically. The performance prediction computations involved an iteration process where a meridional shape was assumed to specify a radius change across the blade row. From the desired pressure ratio and assumed loss coefficients, inlet and outlet velocity diagrams were calculated at several radial positions. These velocity diagrams were used to compute D-factors and shock losses (similar to procedure used for axial stages described earlier) which were converted into loss coefficients from a loss correlation for axial flow blading (Reference 2) for the computation of new velocity diagrams. Once there were no further changes in the loss coefficients between successive calculations, a satisfactory flow solution was assumed.

After a satisfactory flow solution was obtained, the hub, mean, and tip vector diagrams were examined at the blade inlet and exit stations. The variation in velocities from hub-to-tip, the air angle changes across the blade, and the relative velocity ratio across the rotor tip sections were critically examined for consistency with axial flow design practice. Where a single rotor was used, the relative velocity ratio for the tip section was limited to approximately 0.6. With two rotor blade rows, this limit was increased to the neighborhood of 0.65 for each row to provide additional stall margin and a small degree of conservatism to the design. Where undesired values were evident from the vector triangles, a change in meridional contours (i.e., flow width, wall shape, and/or wall curvature) was necessary and a new flow solution obtained.

A summary of the configurations examined by the method just described is shown on table I. These are listed in chronological order to illustrate the direction in which the study progressed. In the first two cases investigated, a single rotor and single stator were employed in a conical flow configuration with a 45-degree meanline slope at the stator exit. Based on previous computations made for the axial-centrifugal arrangement, a design pressure ratio of 2.5 at wheel speeds of 65,000 and 80,000 rpm was examined.

At the lower speed, the flow solution indicated that too much turning was needed to reach the design pressure ratio (the rotor hub exit flow was overturned to discharge the flow in the direction of rotor rotation). The operating characteristics in an engine would be undesirable with this velocity diagram because, as weight flow is reduced, the hub work decreases. Thus, engine acceleration characteristics might be undesirable. Furthermore, the compressor would be more sensitive to inlet distortion. A high rotor speed would avoid this situation by meeting the work requirements with less turning in the blades. At 80,000 rpm, the required flow turning was satisfactory but the diffusion factors across the blades were greater than the normal range for moderate loss coefficients. Thus, the profile losses for a single rotor would be too high to efficiently produce a pressure ratio of 2.5. Consequently, a conical flow rotor with two

TABLE I.

CONICAL FLOW FIRST STAGE

TWO STAGE, 10/1 PRESSURE RATIO PERFORMANCE SUMMARY

N	$(PR)_1$	$(\eta_{ad})_1^*$	$(\eta_{ad})_2^*$	$(\eta_{ad})_0^*$	DESCRIPTION
		SINGLE BLADES			
65,000	2.5	Too Much Turning Required			Single Rotor/ Single Stator
80,000	2.5	"D" Factors Off Curve			Single Rotor/ Single Stator
		TANDEM ROTORS			
65,000	2.5	0.9	0.802	0.8151	Tandem Rotor/ +Single Stator
70,000	2.0	0.9431	0.7975	0.8192	Tandem Rotor/ +Single Stator
70,000	2.5	0.9150	0.8123	0.8289	Tandem Rotor/ +Single Stator
70,000	3.0	0.8758	0.8248	0.8233	Tandem Rotor/ +Single Stator
		TANDEM ROTORS AND STATORS			
70,000	2.5	0.9308	0.8123	0.8370	Tandem Rotor/ Tandem Stator
70,000	2.96	0.8983	0.8241	0.8345	Tandem Rotor/ Tandem Stator
		REALIGNED ROTORS (TANDEM STAGES)			
70,000	2.5	0.9395	0.8123	0.8406	Tandem Rotors/ Tandem Stators
70,000	3.06	0.9067	0.8265	0.8413	Tandem Rotors/ Tandem Stators

*Efficiency level valid for compressors with corrected flows of 8 lb/sec or more.

blade rows in tandem was investigated in order to lower diffusion factors and, thus the rotor losses.

The initial tandem rotor configuration investigated was with a design pressure ratio of 2.5 and a design speed of 65,000 rpm. The flow solution for the tandem rotor configuration for these conditions indicated that the flow overturning problem of the single rotor was eliminated as a result of a larger radius change across the rotor with this tandem configuration. Computed stage efficiency for this tandem rotor-single stator configuration was 90.0 percent. (It should be noted that these efficiency values have not been depreciated for size effects. A discussion of size effects on performance will be presented later.) When this configuration was matched to a second-stage centrifugal compressor, the estimated overall efficiency for both stages was 81.5 percent at 10/1 pressure ratio. A meridional view of this tandem rotor-single stator configuration is presented in figure 9.

Another tandem rotor-single stator conical flow compressor was examined at a pressure ratio of 2.5 but with a wheel speed of 70,000 rpm. The effects of wheel speed on component and overall efficiencies are shown on table II.

A clear performance advantage for the higher wheel speed is evident since the rotor and stator efficiencies are higher due to reduced blade loadings. It is quite possible that further increases in rotational speed would show some performance improvement based on the analytical model used here, which define losses in terms of a normal shock loss at the inlet relative Mach number and a blade profile loss. Experience has shown that, above an inlet relative Mach number of approximately 1.3, the shock strength is often sufficient to cause boundary layer separation on the suction surface of the rotor. When this happens, the losses increase rapidly and the loss model used here is no longer applicable. The inlet relative Mach number for the rotor tip section at 70,000 rpm is 1.29. Therefore, design wheel speed for the remaining mixed-flow configurations analyzed here was specified at 70,000 rpm in an attempt to avoid shock-separation problems at design conditions.

The effect of first-stage pressure ratios of 2.0, 2.5, and 3.0 on component and overall efficiency at 70,000 rpm was investigated and is shown on table III. These results are for one tandem rotor-single stator conical flow configuration in combination with a second-stage centrifugal compressor. These results show first-stage efficiency decreases with increasing stage pressure ratio as might be expected. At the same time, the centrifugal stage performance increases with first-stage pressure ratio reflecting more favorable specific speed values. The combined effect on the overall efficiency at 10:1 pressure ratio produces an optimum first-stage pressure ratio for the tandem rotor-single stator conical flow configuration of approximately 2.5 to 2.6.

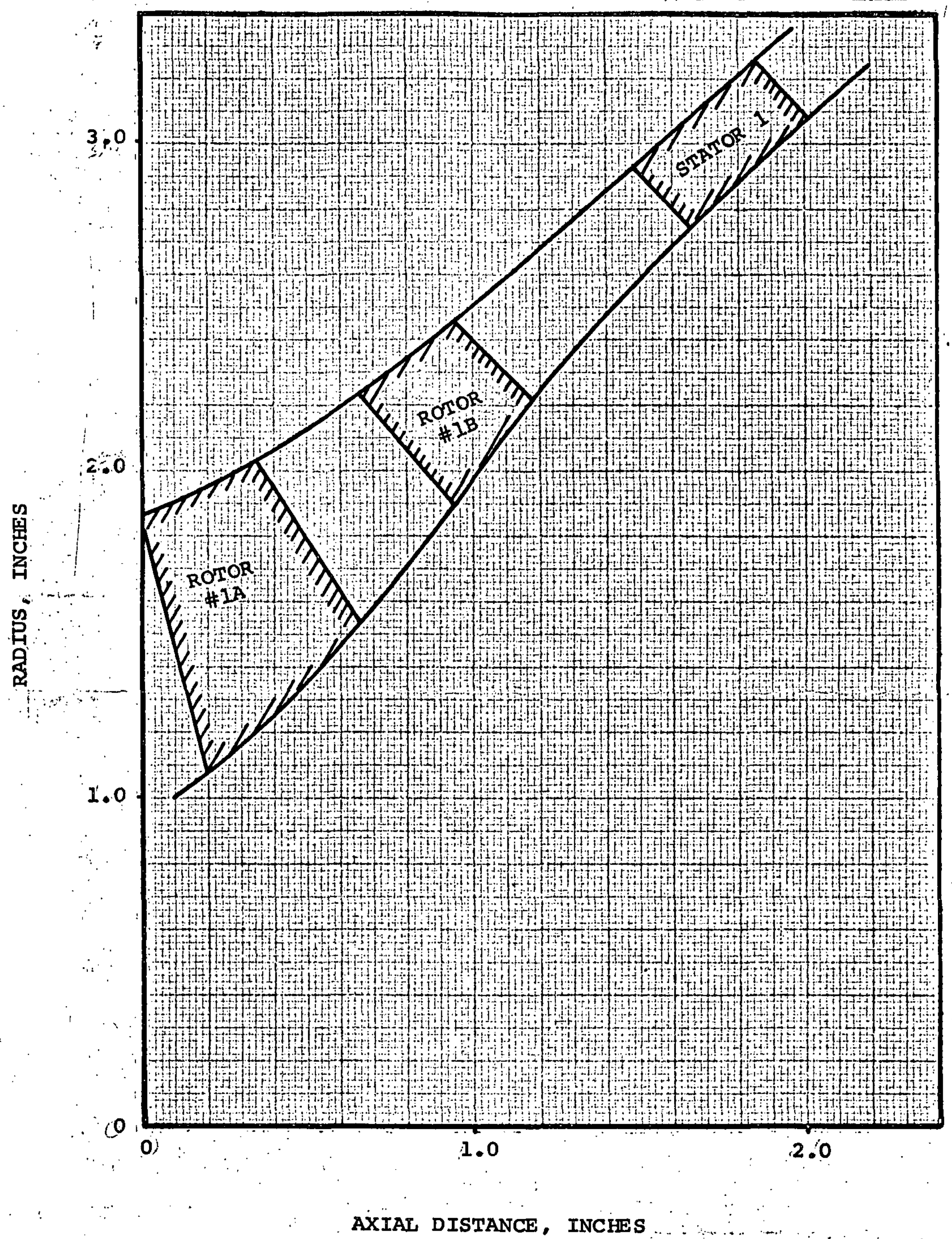

Figure 9. - Meridional View - Conical Flow Stage - Tandem Rotor and Single Stator.

TABLE II.

EFFECT OF WHEEL SPEED ON PERFORMANCE
OF CONICAL-CENTRIFUGAL COMPRESSOR

Wheel speed	65,000 rpm	70,000 rpm
Conical flow stage		
(a) Pressure ratio	2.5	2.5
(b) Rotor efficiency, η_{ad}*	0.959	0.963
(c) Stage efficiency, η_{ad}*	0.90	0.915
Centrifugal stage		
(a) Pressure ratio	4.0	4.0
(b) Specific speed	41.3	44.9
(c) Stage efficiency, η_{ad}*	0.802	0.822
Combined stages		
(a) Pressure ratio	10.0	10.0
(b) Overall efficiency, η_{ad}*	0.815	0.829

*Efficiency level valid for compressors with corrected flow of 8 lb/sec or larger.

TABLE III.

FIRST STAGE PRESSURE RATIO COMPARISON
TANDEM ROTOR, SINGLE STATOR

1.	Wheel speed, rpm	70,000	70,000	70,000
2.	Conical flow stage			
	(a) Pressure ratio	2.0	2.5	3.0
	(b) Rotor efficiency, η_{ad}*	0.969	0.963	0.946
	(c) Stage efficiency, η_{ad}*	0.943	0.916	0.876
3.	Centrifugal stage			
	(a) Pressure ratio	5.0	4.0	3.33
	(b) Specific speed, Ns	42.4	44.9	47.6
	(c) Stage efficiency, η_{ad}*	0.798	0.812	0.825
4.	Combined stages			
	(a) Pressure ratio	10.0	10.0	10.0
	(b) Overall efficiency *	0.819	0.829	0.823

*Efficiency level valid for compressors with equivalent flows of 8 lb/sec or more.

At this point in the investigation, it became evident that the blade loadings for the single-stator configurations were quite large and that there could be an overall performance improvement associated with tandem stators. A conical flow compressor configuration was then laid out which included a tandem rotor and a tandem stator. The effect of tandem stators on the first-stage component efficiencies is listed as follows:

COMPARISON OF TANDEM AND SINGLE STAGE STATOR

Number of stators	Single	Two
Wheel speed, rpm	70,000	70,000
Conical flow stage:		
(a) Pressure ratio	3.0:1	2.96:1
(b) Rotor efficiency, η_{ad}*	0.946	0.944
(c) Stage efficiency, η_{ad}*	0.876	0.898

*Efficiency levels valid for compressors with equivalent flows of 8 lb/sec or more.

The comparison indicates that the tandem stator configuration is 2.2 points better in stage efficiency than the single stator design at a stage pressure ratio of 3/1. This difference is equivalent to a gain of 1.2 points of overall efficiency for the combined two-stage performance as shown on table III. A similar comparison can be made for a 2.5:1 pressure ratio first stage by referring to the results on table III. This indicates the first-stage performance for tandem stators is 1.6 points higher than a single stator with the overall two-stage efficiency gain of approximately 0.8 point. The relative comparison of component efficiencies between the different first-stage pressure ratio cases appears reasonable considering the fact that stator loadings are much higher for the 3/1 pressure ratio stage. Therefore, there is more to be gained by the use of a tandem stator configuration for the higher first-stage pressure ratio design.

Preliminary stress calculations made for the initial rotor blade configuration, shown in figure 10 by dashed line, indicated that orientation of the blade approximately normal to the flow direction could cause blade stress problems because of the overhung blade configuration. As a result, a blade stacking arrangement where the blade edges are placed more nearly in a radial direction, as shown by the solid line in figure 10 was examined for efficiency and stress. This arrangement was found to be satisfactory from a stress standpoint and also produces a backward swept blade configuration

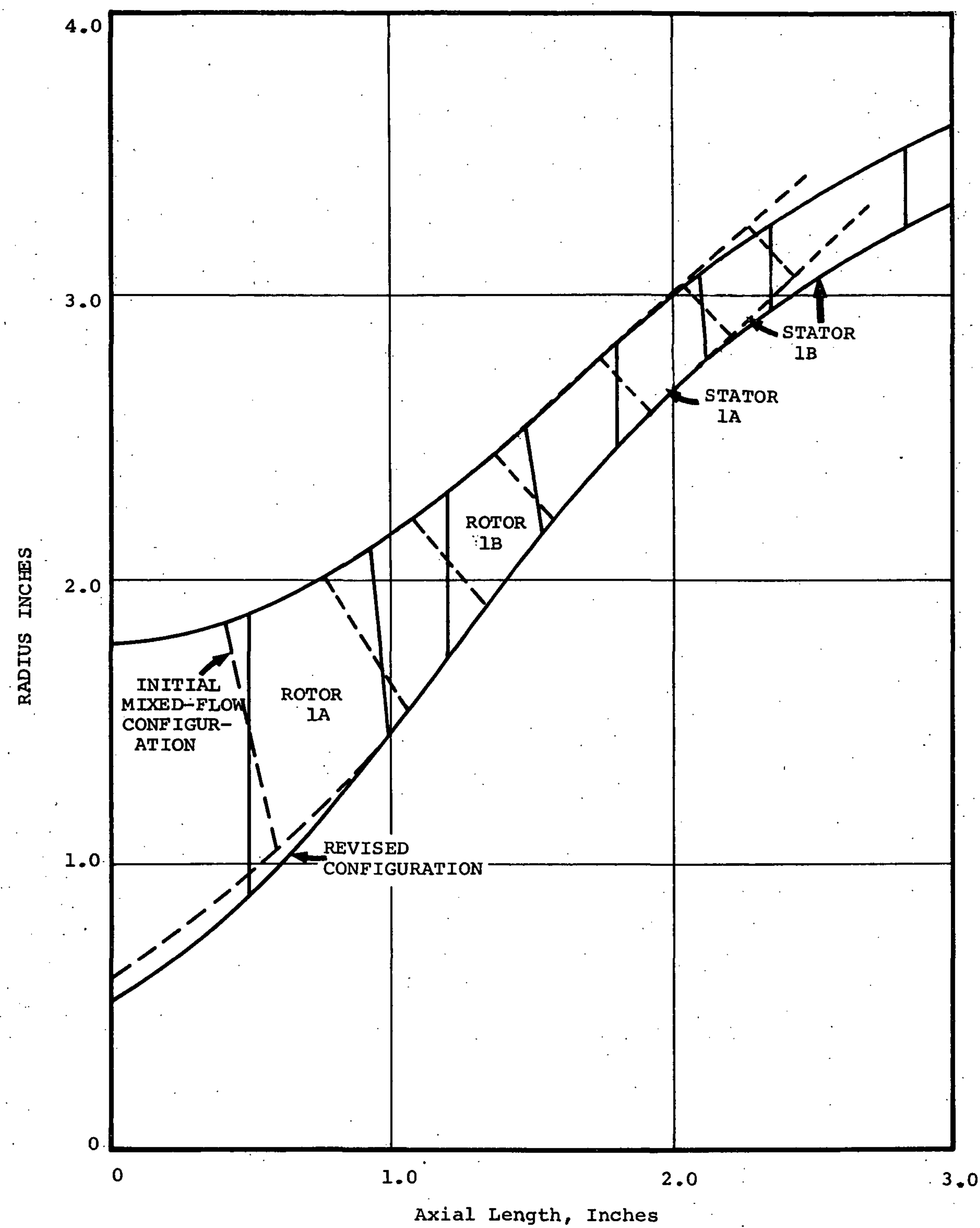

Figure 10. - Meridional View of Conical - Flow Stage.

with respect to the streamline flow path over the blades. Investigators of swept blades for axial compressors have indicated favorable effects of transonic compressors (References 3 to 7). The advantages of swept wings on high-speed aircraft are well understood at this time. The aerodynamic performance of a swept wing has been related to the component of relative velocity normal to the leading edge. Using this loss model, lower losses would be predicted for the backswept blade configuration. In the preliminary design calculations for the revised stacking arrangement, no attempt was made to include any benefit of leading edge sweep on the predicted performance results.

Performance for the different blade stackings is shown on table IV. This comparison indicates a slight performance advantage for the revised stacking arrangement despite the fact that blade sweep effects were not taken into consideration. Investigation of the detailed flow calculations indicated the revised stacking arrangement had a higher radius change between rotor inlet and exit stations than for the initial design. This, in effect, reduced the loadings for each rotor blade with a greater portion of the static pressure ratio generated by centrifugal forces.

The effects of first-stage pressure ratio on overall stage efficiency for tandem-rotor/single-stator configurations as previously discussed show that optimum first-stage pressure ratio was approximately 2.5:1. With the tandem-rotor/tandem-stator configurations the optimum first-stage pressure ratio shifts toward a value in the neighborhood of 3/1 (Table V). However, the difference in overall performance between the 2.5/1 and 3/1 cases is essentially insignificant in light of the approximate nature of the design calculations performed here. The true optimum condition appears to be within this range of design pressure ratios for the first stage. Therefore the 3/1 design was selected as the best configuration for a mixed-flow first stage based on the premise that the higher pressure ratio value would permit a better demonstration of the performance potential of the tandem-rotor/tandem-stator configuration.

A design overall efficiency of 84.1 percent was predicted for the selected conical flow compressor configuration. To be consistent with the performance estimates of the other candidate compressors, an efficiency decrement of 3.6 points was assumed for scaling and matching effects resulting in an adjusted efficiency of 0.805.

A meridional view of the two stage 10/1 pressure ratio conical-centrifugal compressor configuration is presented in figure 11. This shows the tandem-rotor/tandem-stator conical flow first-stage followed by a transition duct leading to the centrifugal compressor second stage. Average Mach number for the transition section is approximately 0.32 and the design Mach number for the second-stage diffuser exit is 0.2. Total stage length is approximately four

TABLE IV.

CONICAL-CENTRIFUGAL COMPRESSOR WITH INITIAL AND REVISED ROTOR BLADE STACKING (SEE Figure 10)

		Initial	Revised
1.	Blade stacking	Initial	Revised
2.	Wheel speed, rpm	70,000	70,000
3.	Conical flow stage		
	(a) Pressure ratio	2.96	3.06
	(b) Rotor efficiency, η_{ad}*	0.944	0.955
	(c) Overall efficiency, η_{ad}*	0.898	0.907
4.	Centrifugal stage		
	(a) Pressure ratio	3.38	3.27
	(b) Specific speed, N_s	47.5	48.1
	(c) Stage efficiency, η_{ad}*	0.824	0.827
5.	Overall compressor		
	(a) Pressure ratio	10.0	10.0
	(b) Overall efficiency, η_{ad}*	0.834	0.841

*Efficiency level valid for compressors with equivalent flows of 8 lb/sec or more.

TABLE V.

DESIGN PARAMETERS AND PERFORMANCE RESULTS

TANDEM CONICAL FLOW COMPRESSOR

	Tip	Mean	Hub
ROTOR 1A (20 BLADES, AR = 1.028)			
SOLIDITY	1.25	1.5	2.33
TOTAL PRESSURE RATIO	1.82	1.78	1.75
EFFICIENCY, η_{ad} *	0.874	0.971	0.987
DIFFUSION FACTOR	0.443	0.418	0.399
ROTOR 1B (40 BLADES, AR = 0.84)			
SOLIDITY	1.57	1.68	1.79
TOTAL PRESSURE RATIO	3.27	3.19	3.32
EFFICIENCY, η_{ad} *	0.883	0.977	0.988
DIFFUSION FACTOR	0.441	0.362	0.333
STATOR 1A (53 BLADES, AR = 0.584)			
SOLIDITY	1.73	1.75	1.76
TOTAL PRESSURE RATIO	3.1	3.1	3.1
EFFICIENCY, η_{ad} *	0.837	0.948	0.922
DIFFUSION FACTOR	0.535	0.502	0.525
STATOR 2A (53 BLADES, AR = 0.495)			
SOLIDITY	1.5	1.57	1.69
TOTAL PRESSURE RATIO	3.06	3.07	3.04
EFFICIENCY, η_{ad} *	0.827	0.939	0.905
DIFFUSION FACTOR	0.523	0.483	0.502

*Efficiency level valid for compressors with corrected flows of 8 lb/sec or more.

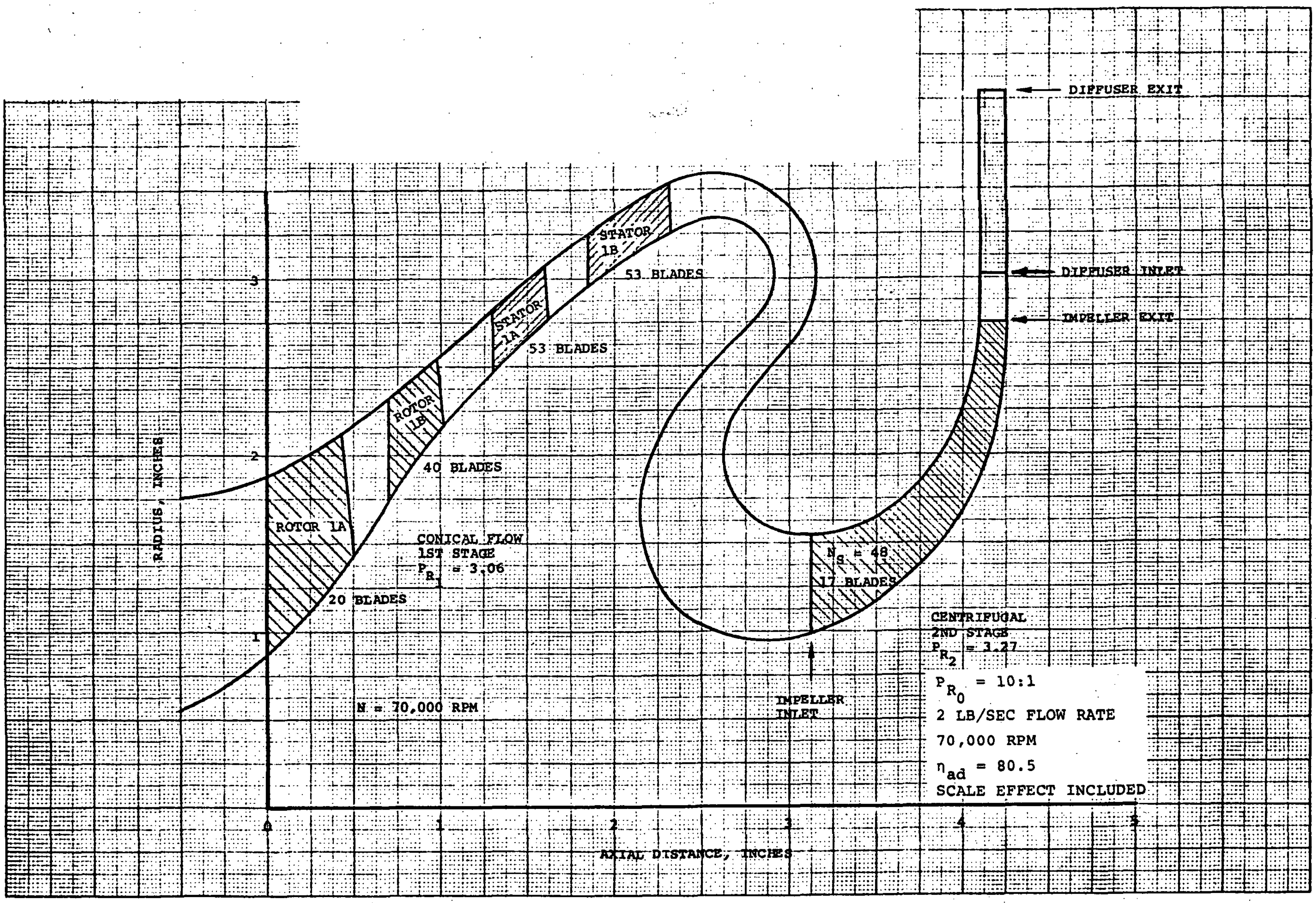

Figure 11. - Meridional View of Flow Path For The Mixed-Centrifugal Compressor Configuration.

inches with the maximum diameter of the mixed flow first stage being less than seven inches. Preliminary design vector triangles for the tandem-rotor/tandem-stator configuration are presented in figures 12 and 13. Additional design parameters and performance information along the tip, mean, and hub streamlines are presented on table V.

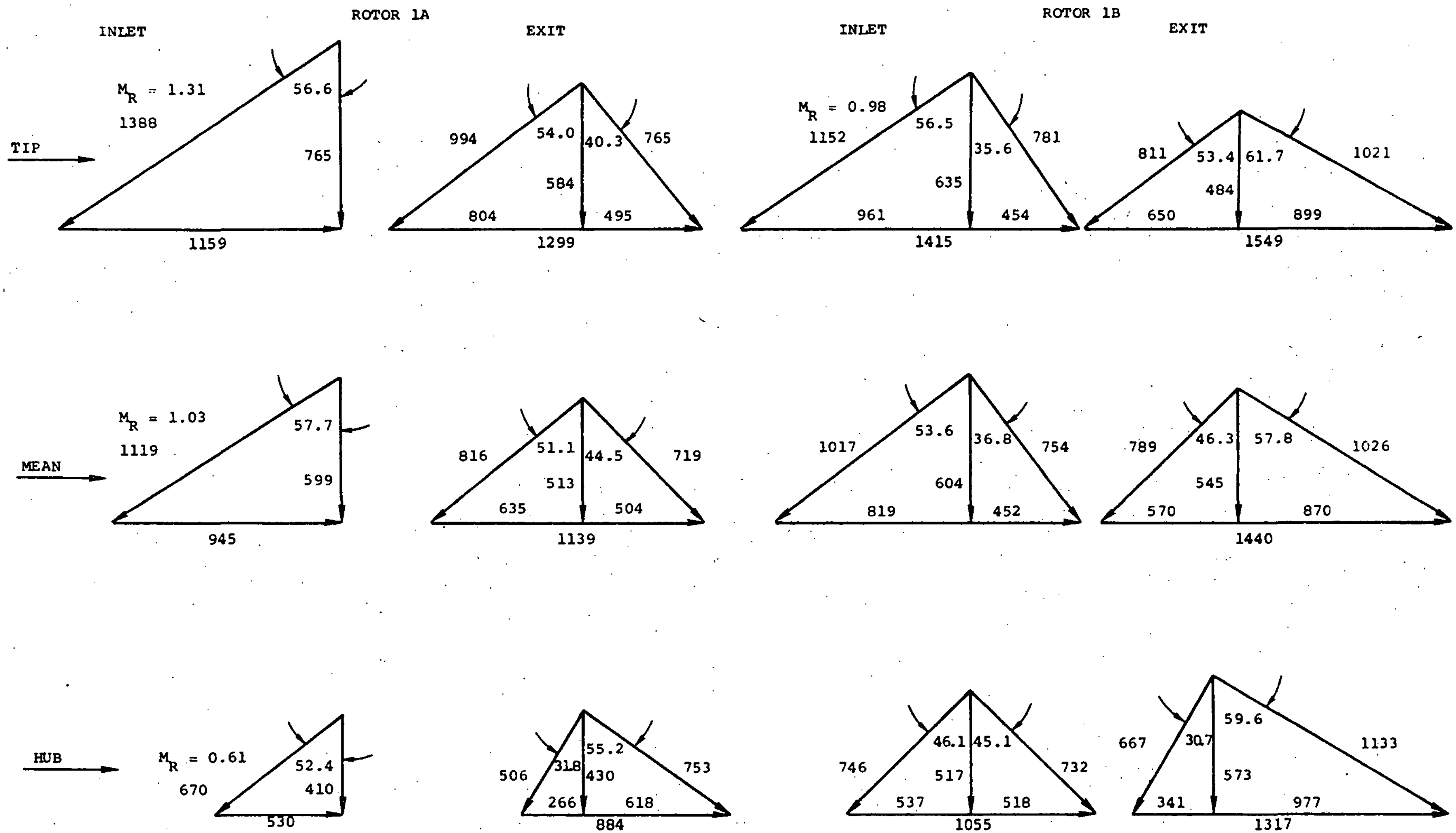

Figure 12. - Conical Flow Tandem Rotor Preliminary Design Vector Triangles.

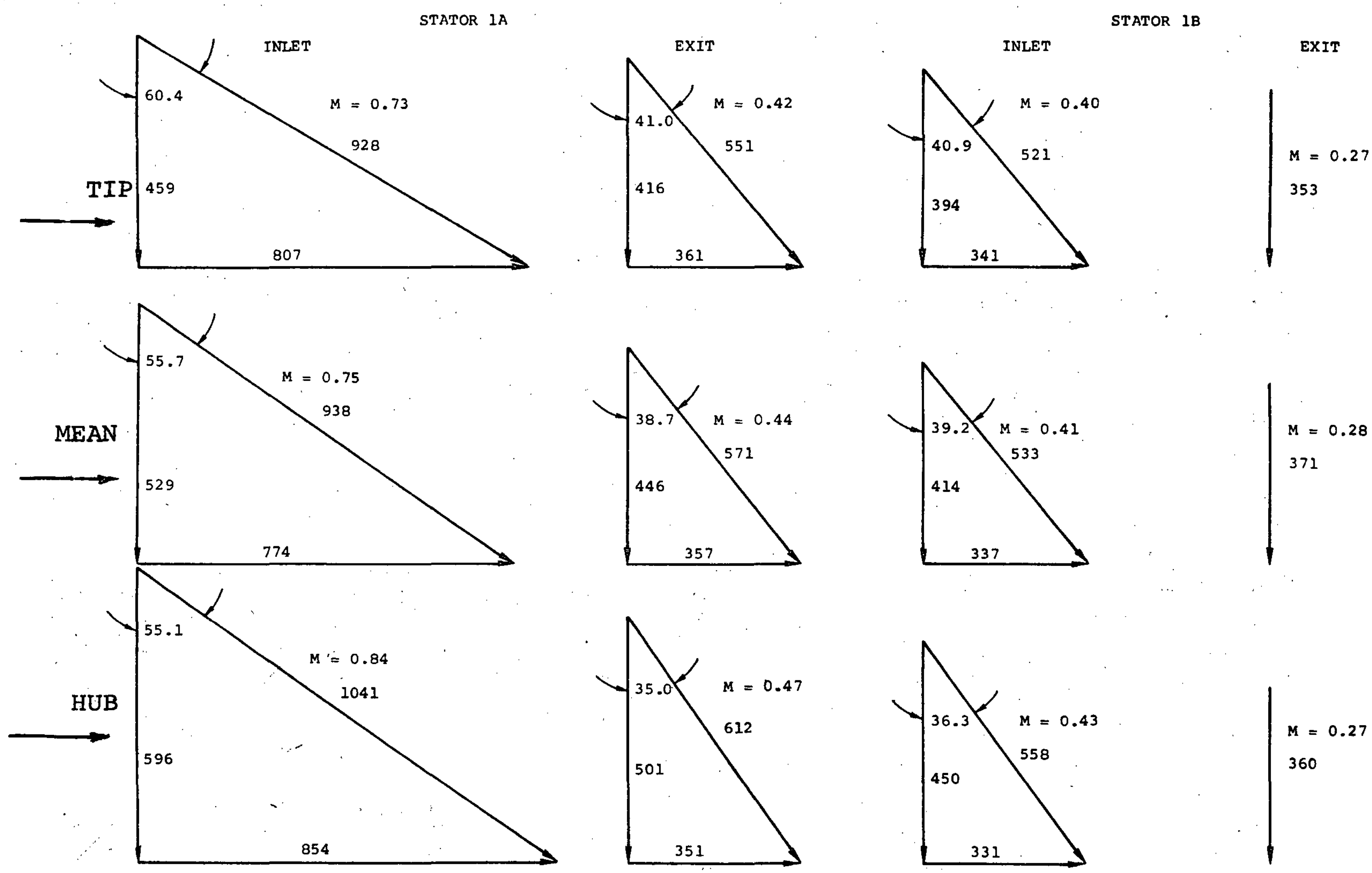

Figure 13. - Conical Flow, Tandem Stator Preliminary Design Vector Triangles.

COMPARISON OF CANDIDATE COMPRESSORS

In order to facilitate a comparison of the different candidate configurations, selected speeds, work splits, stage characteristics, and overall efficiency are tabulated on table VI.

The predicted overall efficiency of 0.790 for the centrifugal-centrifugal configuration is the most reliable because of recent AiResearch experience with a similar 11/1 pressure ratio compressor with eight pounds-per-second weight flow. The dominating factor in the overall efficiency is the rotating speed which was set at 72,500 rpm in order to place both stages as close to their optimum specific speed as possible.

The predicted overall efficiency of 0.777 for the axial-centrifugal configuration is less reliable than the centrifugal-centrifugal configuration due to a lack of scaling effect data on axial compressors. As discussed, this performance adjustment, of 3.6 efficiency points, used for the centrifugal-centrifugal configuration was also applied to this configuration. The predominating factor in the low overall efficiency of the axial-centrifugal compressor is the low specific speed of the second stage. It was indicated that operation at a higher rotative speed would improve the second-stage specific speed and, therefore, the overall compressor efficiency. Increasing the rotative speed was ruled out because the calculated turbine blade stress in an engine application would be excessive above 90,000 rpm.

The predicted efficiency for the conical-centrifugal configuration is the least reliable because of the complete lack of experimental data on the conical flow type compressor. However, the concept is believed to have an excellent chance for success because, based on axial flow design criteria, the design is conservative. The tip inlet relative Mach number was limited to 1.3 and the diffusion factor at the tip was limited to 0.44 for the rotors and 0.54 for the stator.

The overall efficiency for the conical-centrifugal configuration adjusted for scaling effects and matching is 1.5 points higher than the centrifugal-centrifugal configuration and 2.8 points higher than the axial-centrifugal configuration. The higher performance shown for the conical-centrifugal configuration is primarily a result of the high efficiency predicted for the conical flow first stage. This stage operates at a pressure ratio of 3.06/1 with a calculated adiabatic efficiency of 90.7 percent.

If this concept is successful, a less conservative first-stage design could give greatly improved second-stage specific speed and,

TABLE VI.

PREDICTED OVERALL PERFORMANCE COMPARISON

		Cent-Cent	Axial-Cent	Conical-Cent
1.	Wheel speed, rpm	72,500	90,000	70,000
2.	First stage	centrifugal	axial	conical
	(a) Pressure ratio	4.75/1	1.73/1	3.06/1
	(b) Specific speed	70	235	95
	(c) Adiabatic efficiency*	0.84	0.866	0.907
3.	Second stage	centrifugal	centrifugal	centrifugal
	(a) Pressure ratio	2.11/1	5.78/1	3.27/1
	(b) Specific speed	64	54	48
	(c) Adiabatic efficiency*	0.862	0.821	0.827
4.	Overall compressor			
	(a) Pressure ratio	10/1	10/1	10/1
	(b) Adiabatic efficiency*	0.826	0.813	0.841
	(c) Scaled performance, η_{ad}	0.790	0.777	0.805

*Efficiency level valid for compressors with corrected flows of 8 lb/sec or larger.

therefore, greater gains in overall compressor efficiency than predicted herein. It is believed that the relative level of efficiency computed for large compressors is valid for the scaled compressors. Thus, only the magnitude of the difference between the centrifugal-centrifugal compressor and the other two configurations is subject to question. The use of a constant correction factor maintains the relative levels of efficiency and gives an indication of the levels of efficiency expected. A check was made to see how much error would be required in the conical flow stage efficiency prediction to make the overall conical-centrifugal performance equivalent to the two-stage centrifugal combination. The required value was 3.2 efficiency points. This means that the conical-compressor loss factors would have to be more than 30 percent in error, which is unlikely.

Before making a final selection of candidate compressors, several additional considerations were explored. These are discussed in the following sections.

STAGE COMPATIBILITY

Aerodynamic compatability between the two stages is concerned with:

(a) Design of the interstage duct for an efficient transition between stages

(b) The off-design operation with regard to inlet guide vane requirements

(c) The influence of compressor configuration on engine mechanical problems

With a two-stage centrifugal compressor combination, the transition duct makes a 180-degree turn followed by a 90-degree turn. While this would seem to be a rather tortuous flow path, AiResearch experience with similar transition sections has demonstrated very good performance with proper design. Recommended design practice in this case is to accelerate the flow through each turn; this practice results in very little distortion at the inlet to the second stage. By setting the Mach number at the diffuser exit from the first stage reasonably lower than the impeller inlet Mach number of the second stage, the necessary acceleration can be designed into the turns. The final meridional shape is analytically evaluated using the radial equilibrium flow program to ensure a favorable velocity distribution downstream of the transition duct.

The transition section for the conical-centrifugal stage combination is quite similar to that shown for the centrifugal stages but may require somewhat less overall turning, since the flow has an axial component at the impeller exit. This should make the design and performance of the transition duct for the conical-centrifugal stages more favorable than the corresponding centrifugal stage combination design. Again, the flow accelerates through each bend in the transition duct, and the velocity distribution to the second-stage is evaluated analytically. The first-stage exit and second-stage inlet Mach numbers can be adjusted to accomplish the desired acceleration. Therefore, the design and performance of the transition section for the conical-centrifugal stage combination would seem to present few, if any, problems based on AiResearch experience with staged centrifugal compressors.

A cursory look at the transition section between an axial stage followed by a centrifugal stage would seem to indicate few reasons for concern to the designer. The interstage flow requires little turning and the duct lengths are quite short. For high pressure ratio, low hub/tip ratio designs, the absolute Mach number at the rotor hub discharge can be an the order of 1.0. This value must then be diffused to approximately M = 0.45 which requires a large amount of diffusion. This situation requires special design consideration to prevent deteriorated flow conditions at the centrifugal stage inlet.

Careful attention to design details can minimize or eliminate many pitfalls in the transition region design. As a first step, the axial stage should be designed to deliver as low a discharge Mach number as feasible while still maintaining high stage efficiency. Secondly, the inlet hub and tip diameters of the centrifugal stage are matched closely to the corresponding diameters on the axial stage are minimize any necessary turning of the flow. Then, potential flow and boundary layer analyses are made on the design meridional shape to assure that there are no flow separation problems and that the velocity distribution to the centrifugal stage inlet meets design requirements.

In summary, transition section design and performance for the conical-centrifugal stages and the combined centrifugal stages are normally quite satisfactory with sufficient attention to current design techniques. Transition section design for an axial-centrifugal stage combination requires careful attention be given to the rate of diffusion between stages. Here, again, a reasonable design with good performance characteristics is obtainable with astute design practice. In this light, the transition section design and performance do not seem to favor any one of the different two-stage configurations.

Stage compatability with respect to off-design operation of two centrifugal stages in series is normally not a problem. AiResearch experience has shown that two centrifugal stages in series will match quite satisfactorily over a wide range of operating conditions without requiring guide vanes. An example of two-stage centrifugal compressor operating characteristics and performance is presented as figure 14. This stage combination has good design and off-design operation as is readily apparent from the experimental data shown on this figure.

The off-design operation of an axial first stage followed by a centrifugal second stage results in certain matching problems that normally require inlet guide vanes for the axial stage. At design speed, where the stages are usually matched, the range of the combined stages is often greater than demonstrated by the axial stage alone. This seems to be due to the centrifugal stage actually stabilizing flow through the axial stage when the first stage is supposedly in surge. However, low speed and start-up operation of the combined stages results in a mismatch between the stages. The axial stage wants to pass more flow than the centrifugal stage will accept,

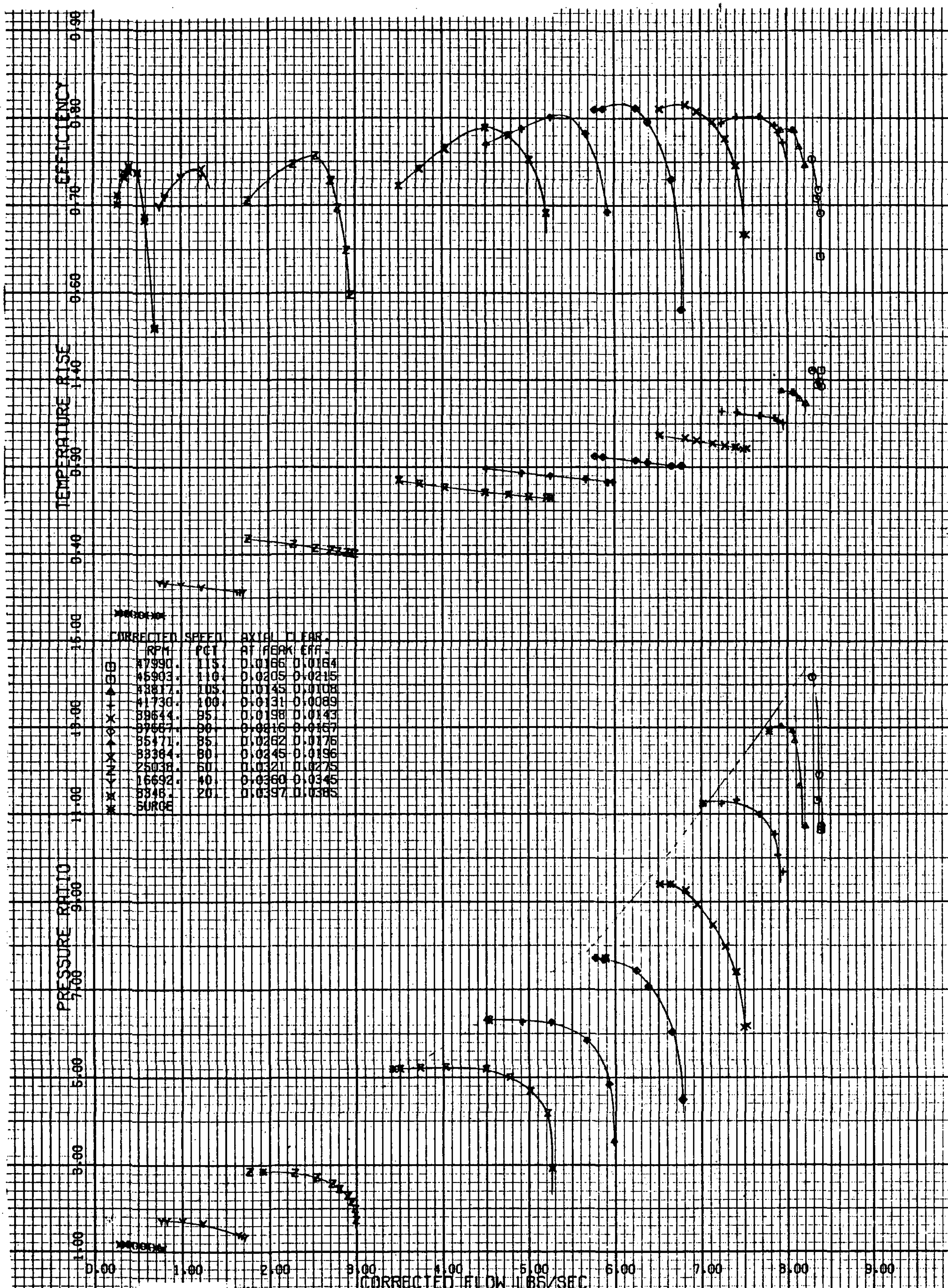

Figure 14. - Example Two-Stage Centrifugal Compressor Map.

tending to choke the back stage and stall the first stage. Therefore, inlet guide vanes are needed to limit the flow through the axial stage during low speed and/or start-up operation. This complicates somewhat the construction and operation of an axial-centrifugal stage combination and may result in this combination being unacceptable for certain applications.

In the conical-centrifugal stage combination, the off-design operating characteristics are expected to fall somewhere between the axial-centrifugal and centrifugal-centrifugal conditions. Low speed and start-up operation may be a problem since the tandem rotors and stators of the conical compressor are basically axial blade shapes. However, there is a significant radius change across each rotor section of the conical compressor which yields some static pressure rise during low speed operation. This would help the second stage to pass more flow and it is quite possible that the conical-centrifugal stage combination could start without variable inlet guide vanes. If this is the case, then off-design operation of the conical-centrifugal combination would be as good as two centrifugal stages in series and much better than an axial-centrifugal combination.

From a mechanical standpoint, a design goal of the program is to have a resonant-free operational speed range and a sufficient margin between the operating speed range and the criticals to ensure reasonable bearing life. The axial-centrifugal stage combination followed by a drive turbine can possibly be designed to meet this goal, despite its much wider operating speed range. Design speed for the axial-centrifugal combination is limited at 90,000 rpm so that it is desirable to set the first bending mode of the shaft critical above $\sim$120,000. For this compressor to work, it must be straddled between the two bearings and the bearing span minimized to increase the first bending mode critical to help meet the design goal.

Overhanging the inlet impeller of the centrifugal-centrifugal compressor results in an unacceptable condition and, thus, straddle mounting the compressor stages is required. The only problem with the straddle-mounted bearing arrangement in the vertical shaft orientation specified by NASA is that it is difficult to get oil to and from the outboard bearing. It is obvious that the conical-centrifugal compressor exhibits a similar mechanical characteristic to the centrifugal-centrifugal stage. However, straddle-mounting the compressor stages is an acceptable solution and the final design of the conical-centrifugal stage is calculated to operate below the critical resonant frequency for bending.

Boundary Layer Control

The application of boundary layer control techniques to axial compressors has received considerable attention during recent years. Research has been conducted in the areas of:

(a) Casing treatments over rotor tips

(b) Slotted and tandem blading

(c) Boundary layer suction along the blade surface

(d) Wall suction

The effect of boundary layer control techniques on overall compressor performance is of primary interest in this program. A portion of the above research was conducted for the purpose of extending the stall margin and reducing noise. However, in most cases, the effect on compressor performance has been measured and presented as part of the test results. Therefore, it appears that there is sufficient data available, both in-house and in the literature, to select a reasonably effective boundary layer control technique for an axial stage should this type compressor be selected for the final configuration.

While there is considerable information available concerning boundary layer control with axial compressors, there is almost nothing available concerning this subject in centrifugal compressors.

The conical flow compressor is sufficiently different from conventional compressor design to warrant a somewhat closer examination of the boundary layer techniques. Obviously, this examination will have to draw extensively on related experience in axial compressors with consideration given to the larger radius change associated with the conical design.

In a recently completed program for NASA (Contract No. NAS3-14306), two forms of boundary layer control are built into the centrifugal compressor configuration. First, the centrifugal impeller is made up of separate inducer and impeller sections in tandem. As such, the configuration can be adjusted to discharge the inducer flow from the inducer pressure surface to energize the suction surface boundary layer on the downstream impeller. The second boundary layer control mechanism incorporated in this design is wall suction on the impeller shroud at two meridional locations and suction on both walls in the diffuser between stages of a cascade diffuser. These can be employed singly or in any desired combination. Both concepts of boundary layer control look quite feasible for application to centrifugal compressor stages. However, experimental evaluation of the effectiveness of these techniques has not been established at this time.

In recent years, boundary layer removal from the junction of the convex stator surfaces and the convex inner wall of compressor and turbine casings has been found to be economically feasible (Reference 13 and unpublished American and British industrial data). Withdrawal of one percent or less of the flow through narrow slots has been found to improve performance.

The rotor and stator of the conical-flow first-stage compressor have been examined to determine the most logical location for boundary layer control slots. The junctions of the convex blade surfaces and the disks (or platforms) of rotors 1A and 1B are logical candidates for boundary layer removal, but these zones experience a relief due to the presence of the blade, the wall slope, and rotational effects. For a given level of diffusion, the rotor blade-disk junctions appear to be less critical than stator-casing intersections.

Spanwise boundary layer flow along the conical-flow rotor blades will be proportionately stronger than along axial blades due to the sweep of the blades adding to the normal outward forces on axial-blade boundary layers. If this outward flow is sufficient to interfere with proper performance of the outboard region of tandem rotor 1B, fences attached to rotor 1A blades near mid-span should be considered. Such fences would discharge the excess boundary layer near mid-passage. Energy addition to this wake-fluid would be rapid from the surrounding free-stream. The flow into the tip-section of rotor 1B should remain strong, since shock losses will be low due to the use of only moderate Mach numbers relative to the blades. Tip clearances can be held to low values through the use of soft, abradable inserts in the shroud, so tip clearance flows could be kept small.

The stator blades will not experience relief due to rotation, but will inhibit spanwise flow of low energy fluid if swept. To prevent separation and the generation of excessive quantities of low energy fluid, small narrow slots at the critical convex-blade/convex-wall chord length, located toward the rear, and sized to remove about 0.5 percent of the flow at design speed.

SIZE AND WEIGHT CONSIDERATIONS

In a volume and/or weight limited system, the axial-centrifugal stage combination would seem to offer a potential advantage over the other stage combinations under consideration. Obviously this is a result of the small stage diameter and relative stage length associated with the axial inlet stage.

An overall summary of the pertinent stage dimensions and a relative stage weight comparison is presented on Table VII. This tabulation includes the maximum diameter and length of each stage and both stages together for the three compressor combinations considered herein. Diameters for the centrifugal stages have been adjusted to account for the design as it would appear in an actual engine configuration. In an engine, the diffuser for the centrifugal stage would normally be divided between two stages. The initial diffuser would be oriented radially and diffuse to an intermediate Mach number ($M \sim 0.35$). Then the flow is turned to an axial orientation where further diffusion takes place. It was felt that a more valid size comparison could be made by comparing each configuration as it would appear in an actual engine installation. Also included on table VII is a relative weight comparison for the combined compressor stages above (not a complete engine), where the weights are normalized to the weight of the two centrifugal stages in series. These weights are estimated from existing hardware where applicable with considerable scaling involved. Because of the approximate nature of the weight estimates it was felt that this information could best be presented on a relative basis. Additional size and weight of inlet guide vanes, actuator and control, normally required for off-design operation and starting of an axial-centrifugal combination, have not been included in this comparison.

The size comparisons show the axial-centrifugal stage combination will fit in a smaller diameter and have a shorter stage length than the other combinations. As a result, the axial-centrifugal stage combination also weighs less than the other designs. On a relative weight basis, the axial-centrifugal stage combination weighs about 18 percent less than the two-stage centrifugal combination. These weights are representative of the impellers, stators, housings, bearings, shaft, and transition section for both compressor stages. The effect of the compressor configuration on the remaining engine component weights has been neglected.

The conical-centrifugal can be fit into a smaller diameter than the two-stage centrifugal combination because of the width of the transition section on the latter configuration. Stage length for the conical-centrifugal stages is greater than for the other two cases. However, the stage weight for the conical-centrifugal

TABLE VII.

ENGINE SIZE AND WEIGHT COMPARISON

1. First Stage	Axial	Centrifugal	Conical
Max Diameter, in.	3.7	9.0	6.94
Stage Length, in.	2.4	2.8	2.7
2. Second Stage	Centrifugal	Centrifugal	Centrifugal
Max Diameter, in.	7.0	6.4	7.2
Stage Length, in.	1.1	1.0	1.2
3. Both Stages	(1) Axial-Centrifugal	(2) Centrifugal-Centrifugal	(3) Conical-Centrifugal
Max Diameter, in.	7.0	9.0	7.2
Combined Length, in.	3.5	3.8	4.2
4. Relative Weights			
Two Stages	(4) 0.82	1.0	0.91

NOTE:

(1) Reference flowpath (see Figure 8)

(2) Reference flowpath (see Figure 4)

(3) Reference flowpath (see Figure 11)

(4) Does not include inlet guide vanes nor actuator/control

combination. Thus it appears that the conical-centrifugal combination would compare quite favorably with two centrifugal stages in series for a volume and/or weight limited system. But the axial-centrifugal stage combination still offers the most size and weight advantages of the combinations investigated.

IMPELLER EROSION CONSIDERATIONS

Foreign object damage (FOD) and performance degradation effects due to large amounts of sand, dust, and other foreign substances are significant factors that must be considered in the design of engines for aircraft installations. Various engine test programs and a USAF study (NASA Technical Report No. 54, Factors That Affect Operational Reliability of Turbojet Engines) conclude that centrifugal-type compressors afford inherently better protection from FOD and minimal performance degradation when compared with axial-type compressors.

A comparison of power decay due to erosion is tabulated below for several engines that utilize axial compressors as compared to AiResearch T76 and TPE331 engines that employ centrifugal compressors:

Engine	Operating Period	Power Decay Percent	Remarks	Source
T76 (Centrifugal)	1600 hr	1.35	Data from OV-10A operation Viet Nam (eight engines)	Third Quarterly Progress Report, AiResearch Document PE-8088-R2
TPE331 (Centrifugal)	1000 hr	5	Turbo-Porter STOL rough field operation	"Turboprop Operation in STOL Aircraft" SAE Paper 680228
T64 (Axial)	400 landings	14	CH53 Patuxent River tests	"Problems and Solutions for Sand Environment Operation" ASME Paper 68GT37
T63 (Axial)	10 hr	5	T-63-A-5A Qualification Test (0.0015 gm/cu ft)	"T63 Sand and Dust Tolerance....." SAE Paper 670334
	50 hr	10	LOH Test Data - Ft. Benning, Ga.	

This illustrates dramatically the severe effect erosion can have on axial compressor performance.

Blade configurations of the tandem rotors for the conical flow compressor are similar to an axial rotor configuration. However, the inlet flow intersects the leading edge of the conical flow blades at a relatively steep angle producing a swept effect across the blade rows. Sweeping the leading edge of an erosion specimen 45 degrees or more has been shown to dramatically reduce the rate of erosion. Apparantly the effect of sweep is to convert the direct impact of the hard particles to glancing blows. The acceleration of the glancing particles, and the normal force developed due to the collision is greatly reduced. For a given foreign particle concentration, the number of impacts per unit leading-edge-length is reduced. In the case of transonic Mach numbers, the shock wave preceding the swept leading edge produces a static pressure gradient which helps divert the particles, causing some to miss the airfoil and to increase the "glancing" angle. All of these factors tend to reduce the amount of erosion caused by hail, rain, sand, and dust.

Conventional transonic and supersonic compressors require very small radius, essentially sharp, leading edge to minimize the strength and the extent of the detached bow waves and the aerodynamic losses associated with strong shock waves. Sharp edges are subject to rapid erosion damage. The use of swept blades reduces the Mach number normal to the leading edge to subsonic values. Subsonic-type airfoils having larger leading edge radii can be employed without suffering excessive losses. One method of explaining this behavior is to consider that the weak three-dimensional shock which precedes the blade leading edge generates a pressure gradient which "forewarns" the air particles that a blade is approaching and causes them to divert automatically. Thus, larger leading edge radii and thicker leading edge regions to support the impact zone against local fracture are available. Therefore, it is quite possible that the conical flow compressor may show considerable resistance to erosion and low FOD.

CONFIGURATION SELECTION

The axial-centrifugal stage combination appears to offer the least potential advantages for this application. Examination of the two-stage performance results showed this combination is the least efficient of those considered. The low efficiency is directly attributable to the second-stage centrifugal compressor which operates at a low design specific speed. There could also be stage compatibility problems associated with the axial-centrifugal stage combination. First, diffusion is required between the stage, in the transition duct, and at off-design operation, a definite need for variable inlet guide vanes in front of the axial stage for start-up and low speed operation is indicated. Engine size and weight considerations would favor the axial-centrifugal combination in a volume and/or weight limited system. However, for the application considered, the axial-centrifugal compressor is least favorable based on performance potential, susceptability to foreign object damage, and potential stage compatibility problems.

The centrifugal-centrifugal stage combination clearly showed higher design performance than the axial-centrifugal stage combination but somewhat less performance potential than the conical-centrifugal stage combination. In the stage compatibility comparison, the centrifugal-centrifugal stage combination and conical-centrifugal stage combination were essentially identical. In a volume limited system where compressor diameter is a concern, the conical-centrifugal stage combination may also have a slight weight advantage over the centrifugal-centrifugal stage combination. From an erosion and foreign object damage standpoint, the conical compressor is probably better than a typical axial but inferior to a centrifugal.

With all criteria considered, the conical-centrifugal was selected to meet the objective of this contract primarily because of its improved performance potential. Therefore, the mixed flow or conical flow compressor was subjected to the detailed design analysis discussed in the subsequent sections of this report.

GENERAL DESIGN LOGIC

The logic used in the calculation of blade shapes for the conical compressor is diagramatically presented in Figure 15. The various calculation procedures encompassed by the logic are discussed in the following paragraphs. Details of the various program input requirements and selection of blade element airfoil sections will be given in ensuing sections.

The air inlet and exit vector triangles were calculated in the optimization study using the non-isentropic, radial equilibrium program. This calculation has been referred to as the across-the-blade solution, where calculations were made just outside of the leading and trailing edges of each blade (and vane) row. The detailed blade shape design uses the same program with calculations made inside of each blade row. This is referred to as the through-the-blade calculation. Each rotor blade was designed separately, i.e., the aerodynamic calculations were made with only one rotor blade in the flow field. This was done for expendiency. However, the stator vanes were analyzed aerodynamically in tandem. When all blade shapes were finalized, a through-the-blade solution was made with all blades in place. This was done to evaluate the aerodynamic interaction between blade rows.

A second aerodynamic calculation program, referred to as a blade-to-blade calculation (also Katsanis), was used for the twofold purpose of calculating inviscid flow deviation at the blade exit, where applicable, and the rate of change in angular momentum along each axisymmetric stream surface through a blade. Both results are used (except as noted) in the through-the-blade calculation. Details of this calculation procedure are contained in Appendix D.

Both the through-the-blade analysis and the blade-to-blade analysis require a definition of the blade geometry. This information is obtained from a blade stacking program. The function of this calculation procedure is to take the specified aerodynamic blade element along each stream surface of a given blade and generate stacked blade properties for both aerodynamic programs. Details of this calculation procedure are contained in Appendix B.

From the across-the-blade calculation, initial setting of each blade element leading edge is made, based on incidence angle criteria. The blade element deviation angle is estimated from Carter's rule. A specification of the aerodynamic blade element shape can then be made for input to the blade stacking program. A through-the-blade calculation is now made with initial assumptions of the loss, aerodynamic blockage, and energy distributions.

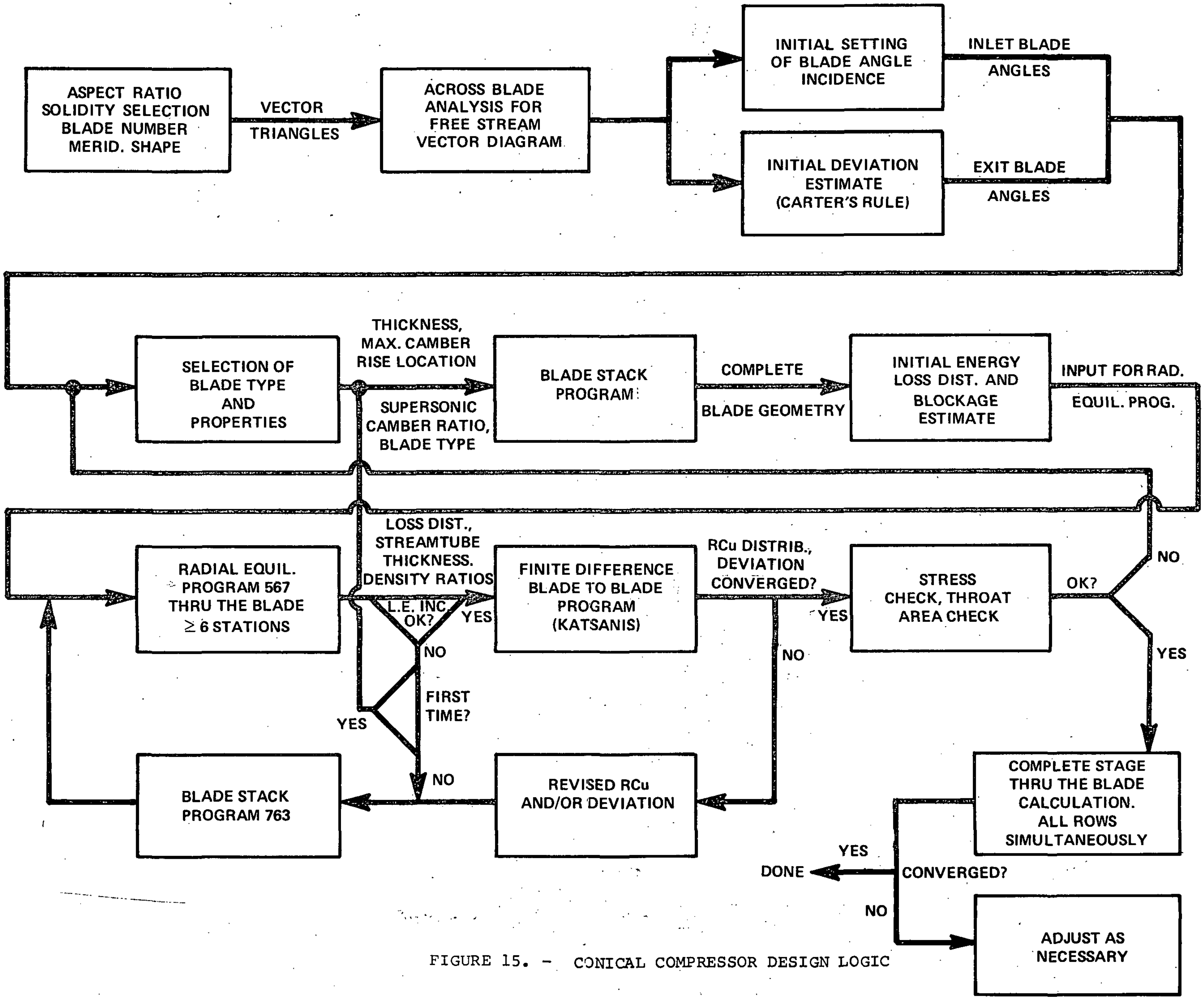

FIGURE 15. - CONICAL COMPRESSOR DESIGN LOGIC

The thermodynamic properties along each axisymmetric stream surface from the through-the-blade calculation are used to calculate a stream-surface height distribution from inlet to exit of the blade row. This distribution of stream-surface height, along with the definition of blade suction and pressure surfaces bounding the stream surface, are input to the blade-to-blade calculation. The inviscid deviation calculated by the blade-to-blade program added to an estimated viscous deviation (see Appendix A) is now compared to the across-the-blade vector triangle (for each streamline). The blade element camber is then changed by the amount of the difference. Also, the energy addition distribution is adjusted, where applicable, according to this calculation.

A revised blade shape is then calculated with the blade stacking program. The through-the-blade analysis is then rerun with the new blade shape and energy distribution. This iterative loop is continued until the through-the-blade vector triangles agree reasonable well with the across-the-blade solution. The blade is then checked for choke flow margin and a stress analysis performed.

The final individual rotor blade designs and the tandem stator design were then analyzed in a full through-the-blade calculation. In this way, blade interactions attributable to streamline slope and curvatures effects were established. Ideally, blade designs should then be adjusted if significant difference exist between the inlet and exit vector diagrams from the individual designs compared to the complete solution.

ROTOR AND STATOR GEOMETRY SELECTION

The performance of each rotor blade row and stator vane row is strongly dependent upon the selection of aspect ratio and solidity. The blade element aspect ratio, defined as

$$AR = \text{mean blade height/mean chord}$$

requires rotor blade and stator vane chords to be quite small if the aspect ratio is to be within the limit of current experience. For rotors and stators, a lower limit for aspect ratio is 1.25. A minimum chord length value acceptable to stress and manufacturing criteria is approximately 0.5 inch. For rotors, chord length may be adjusted upwards for stress reasons, depending upon the aspect ratio selected.

As the flow path height is contracted through each blade row to maintain acceptable meridional velocity ratios and D-factors, the aspect ratio is no longer under control of the designer. Hence, the aspect ratio of rotor 1B and stators 1A and 1B was considerably less than desired. For this reason, blade element losses used in the analysis tend to be optimistic and must be verified by an experimental test program.

Rotor 1A tip solidity was selected to be consistent with current AiResearch design experience for transonic rotor blading. Rotor 1B required twice the number of blades 1A to account for radius increase and a decreased chord length. Stator solidities were selected to give acceptable blade loadings while being maintained within current design experience.

Selection of the type of airfoil section to be used along each axisymmetric stream surface of a given blade was determined by the inlet relative Mach number. These section types were subject to modification if the resultant blade loading was not satisfactory. In rotors 1A and 1B, a combination of multiple circular arc (MCA) and double circular arc (DCA) sections were used. Double circular arcs were used throughout both stator vane designs. A general MCA section with pertinent parameters required for definition is shown in Figure 17. Upper and lower surfaces and meanline are made up of arcs which have tangency at the point of maximum thickness. The DCA section is a specific form of the MCA section in which the maximum camber rise and maximum thickness occur at 50 percent of the chord length and the camber is distributed uniformly along the entire meanline. Parameters required for specification of a section are total camber (Φ), maximum thickness, location of maximum thickness, amount of front (or supersonic) camber, and leading edge meanline direction.

DETAILED AERODYNAMIC DESIGN

The section will cover in detail the aerodynamic design of the inlet stage of the conical-centrifugal compressor, the interstage duct between the conical flow inlet stage and the centrifugal second stage, and the drive turbine for the proposed research package.

General

As seen in the discussion of the design logic, three computer programs were required to design each blade. To carry out a through-the-blade, non-isentropic radial equilibrium calculation, an initial estimate of the blade geometry was required for stacking the blade. For this design, six streamlines were used in each blade design analysis.

Experience at AiResearch and elsewhere (Reference 14) indicates that for supersonic relative Mach numbers, the leading edge suction surface should be made parallel with the inlet relative air angle (0° incidence). As the Mach number decreases below 1.0, the suction surface incidence (i) was decreased to -2.0 degrees. At the blade trailing edge, deviation (δ) was initially estimated using Carter's rule. The total amount of blade element camber along the streamline can then be calculated from

$$\Phi = (\beta_1' - \beta_2') - i + \delta$$

Ensuing iterations used the value calculated by the blade-to-blade plus a viscous correction, where applicable.

With the airfoil shape, position of each surface (r, Z) and stack axis specified, a blade shape can be calculated. For all blades in this design, the blade leading and trailing edges were held fixed in the meridional view with sections stacked on their respective center of mass in the circumferential direction only (Appendix B). This calculation provided input of blade geometry for the through-the-blade analysis and blade-to-blade analysis.

Additional information needed in the through-the-blade calculation are the rate of change in the angular momentum, distribution of the loss, and distribution of the aerodynamic blockage along each streamline. For blade rows operating with supersonic relative inlet Mach numbers, the angular momentum change was approximated for all iterations by a sinusoidal function of axial length given by:

$$\frac{r\,V_u - r_1\,V_{u1}}{r_2\,V_{u2} - r_1\,V_{u1}} = \sin^A\left[\frac{\pi}{2}\left(\frac{Z - Z_1}{Z_2 - Z_1}\right)\right]$$

The value of A was varied from 2.0 to 1.50 based on previous design experience. The initial estimate of angular momentum distribution for streamlines with subsonic inlet relative Mach numbers was linear. In subsequent iterations, the distribution resulting from the blade-to-blade solution was used. The loss and aerodynamic blockage were distributed linearly with axial distance for all blade rows. The loss values were held constant on the basis that the final through-the-blade calculation would give the same diffusion factors as the across-the-blade solution.

Rotor 1A Design

The final rotor 1A design parameters are as follows:

Corrected flow, lb/sec	2.0
Tip diffusion factor	0.443
Tip relative velocity ratio	0.7068
Inlet hub/tip ratio	0.45
Tip relative Mach number	1.26
Aspect ratio	1.028
Tip solidity	1.34
Number of blades	20

Figure 16 shows a meridional view of the final blade shape. Radial equilibrium calculation station lines are shown along with straight line approximations of the six streamlines on which each airfoil section was specified for stacking the blade. Details of the final airfoil sections specified along each of the conical stream surfaces are contained in table VIII. Figure 17 provides a schematic representation of symbols used to describe the airfoil section.

Selection of the airfoil sections used along each axisymmetric stream surface of rotor 1A was initially based on the inlet relative Mach number shown in figure 18. The multiple circular arc (MCA) type was used for all streamlines except the hub. Here an MCA meanline with an arbitrary thickness distribution was used to adjust the loading as discussed at the end of this design section (figure 19).

A comparison of the resulting and design minimum loss incidence angles are presented in figure 20. The two angles are not the same due to changes which occurred in the meridional velocity distribution at the rotor leading edge during the design iteration. The difference from design intent was deemed acceptable on the basis of the lower relative Mach number at which the maximum difference occurred, i.e., the low loss incidence range is somewhat wider for that Mach number level. Also shown are the incidence angles based on the complete through-the-blade solution.

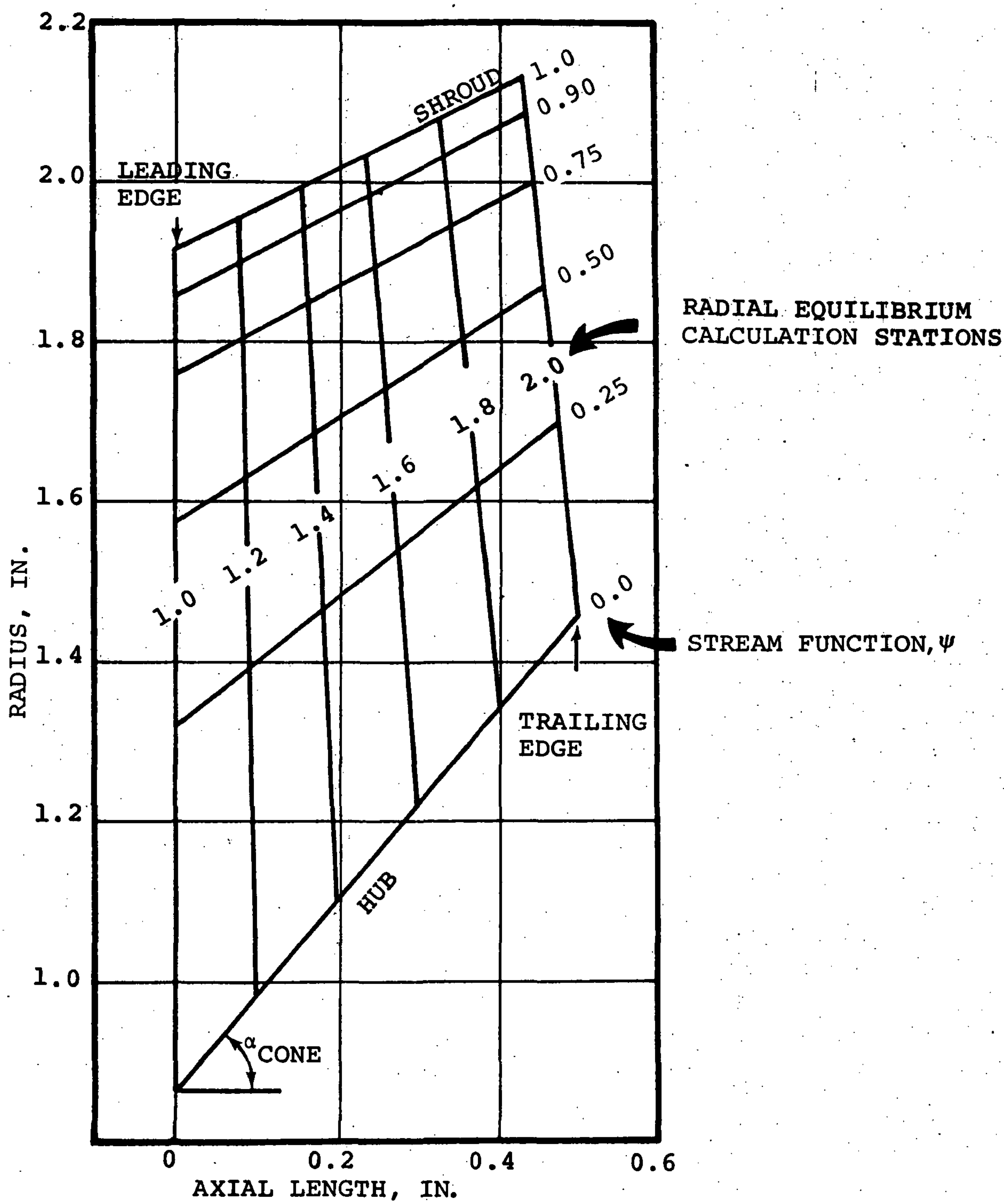

Figure 16.- Meridional Flow Path for Conical Flow Compressor, Rotor 1A.

TABLE VIII.

BLADE SETTING FOR ROTOR 1A

ψ	$M1_{REL}$	β_1(Air)	β_1(Blade)	i	$\beta_{1SS}-\beta_{1MC}$	t_{LE}
Shroud	1.256	59.95	57.72	2.22	2.65	0.007
0.9	1.214	59.80	56.93	2.87	3.07	0.0075
0.75	1.153	59.21	55.83	3.38	3.70	0.0081
0.5	1.035	58.13	54.57	3.56	4.72	0.0095
0.25	0.865	58.10	53.77	4.33	5.84	0.0116
Hub	0.585	54.82	49.79	5.03	8.08	0.0178

ψ	β_2(Air)	β_2(Blade)	δ	t_{TE}	t_{max}/C_T
Shroud	55.78	50.54	5.24	0.0081	0.0395
0.9	55.44	50.15	5.29	0.0082	0.0423
0.75	53.97	49.11	4.86	0.0086	0.0470
0.5	50.66	44.89	5.77	0.0098	0.0550
0.25	44.31	35.25	9.06	0.0110	0.0630
Hub	28.95	14.76	14.19	0.0140	0.0850

ψ	C_T	Φ_T	a/C_T	Φ_{SS}/Φ_T	δ
Shroud	0.852	7.18	0.73	0.15	1.342
0.9	0.854	6.78	0.68	0.24	1.383
0.75	0.847	6.72	0.61	0.37	1.438
0.5	0.839	9.68	0.53	0.48	1.562
0.25	0.860	18.52	0.50	0.50	1.841
Hub	0.825	35.03	0.45	0.55	2.265

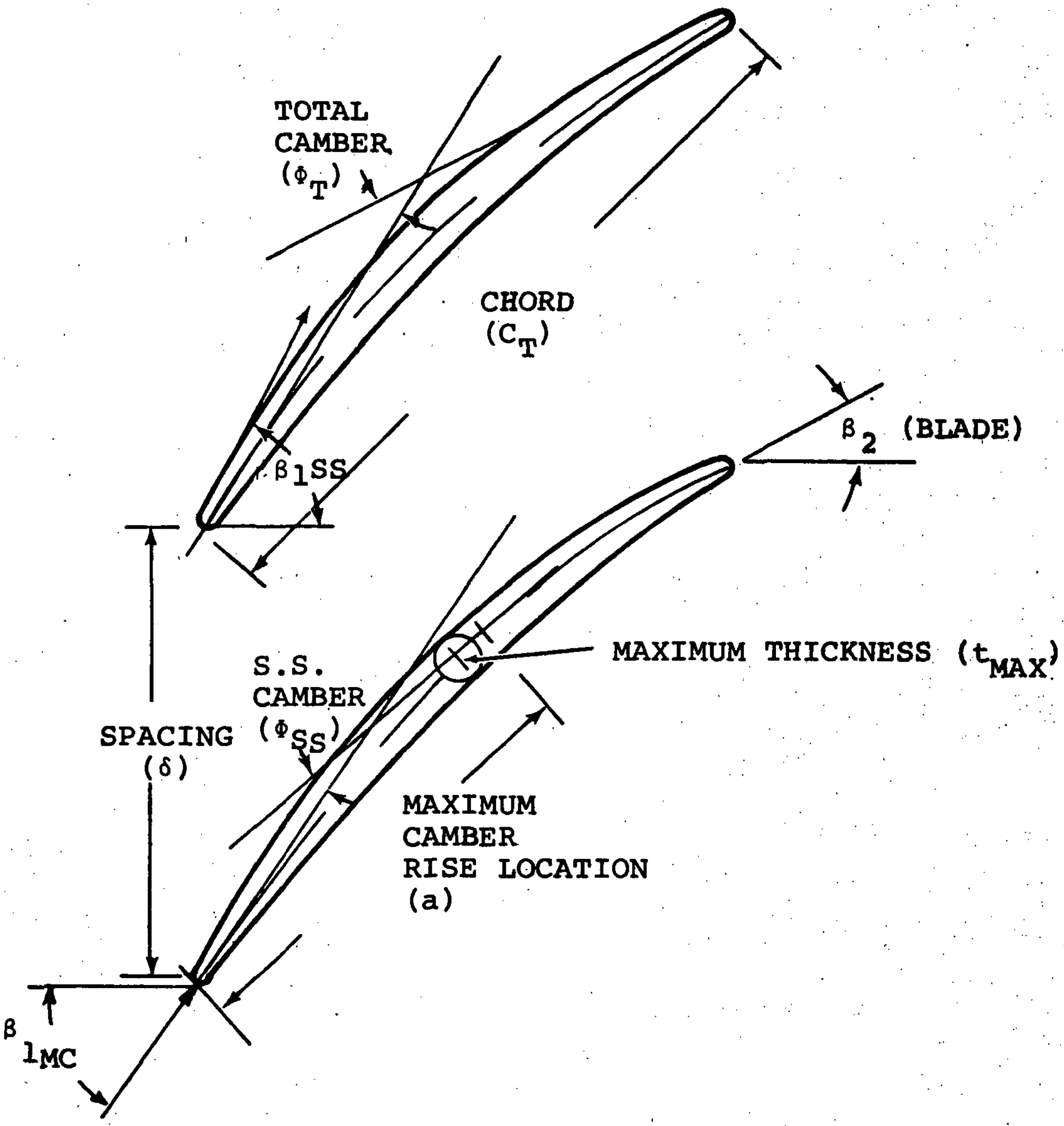

Figure 17. - Multiple-circular-arc airfoil description.

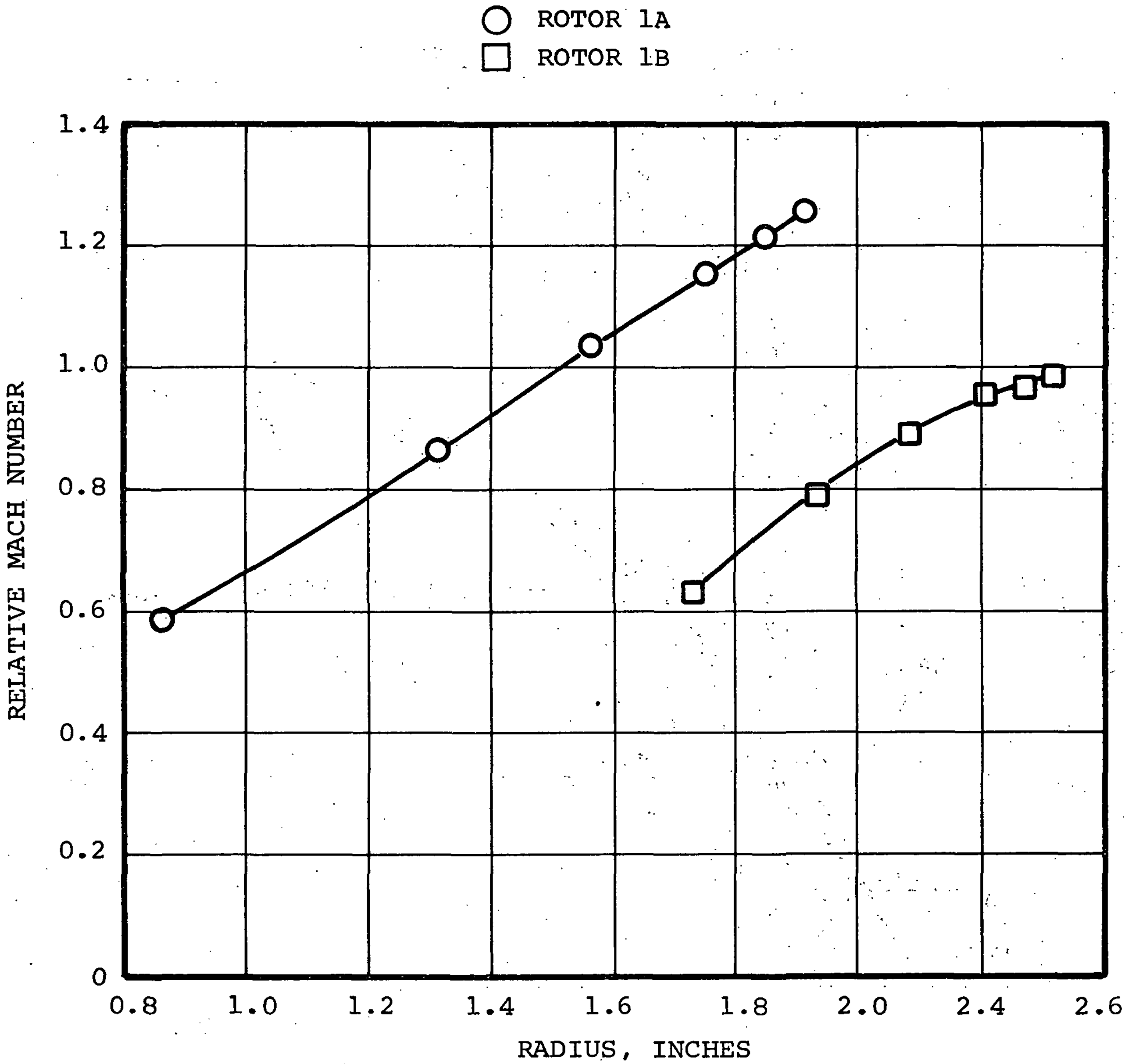

Figure 18. Inlet Relative Mach Number For Rotors 1A and 1B.

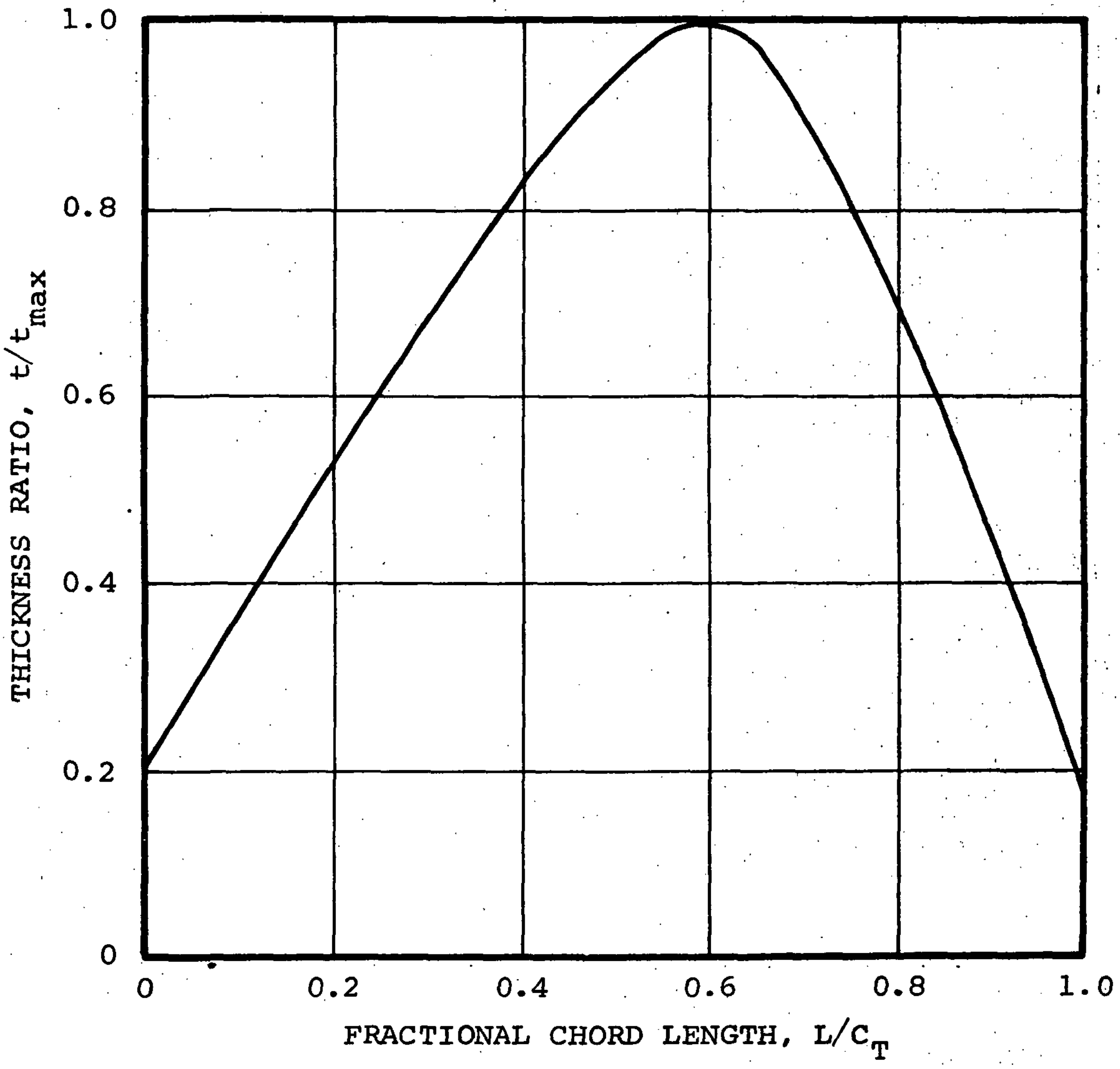

Figure 19. Final Thickness Distribution For Rotor 1A Hub Section.

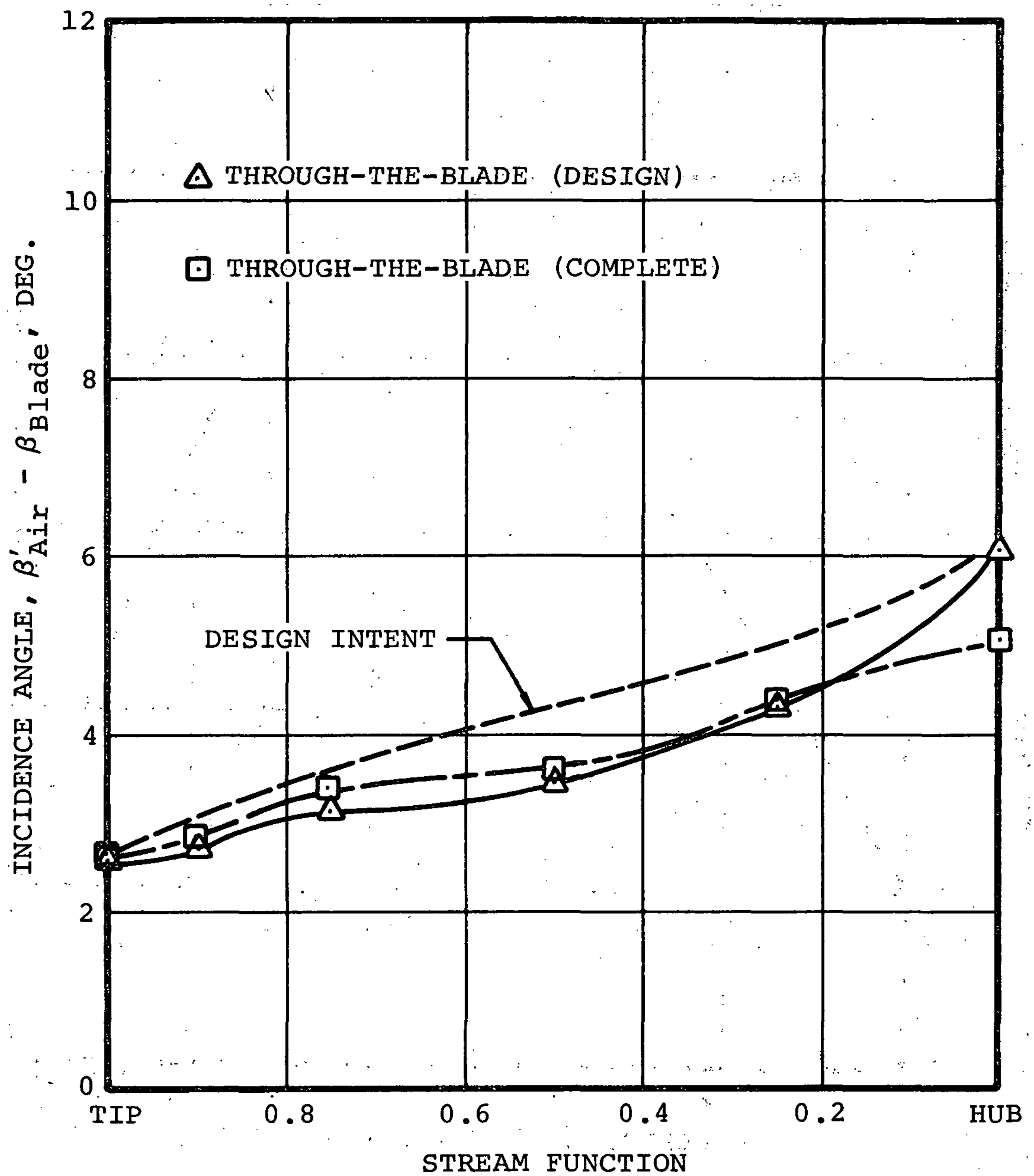

Figure 20.- Design Incidence Angles for Rotor 1A.

Final design deviation angle is shown in figure 21. These values were calculated to satisfy the angular momentum addition criteria from the across-the-blade analysis. As seen from the comparison of inlet and exit relative air angle distributions (figure 21), a difference exists between the across-the-blade analysis exit angle and those from the final through-the-blade design. The difference arises from introducing the blade into the flow field solution. Also included is the deviation calculated from the complete through-the-blade flow solution. The difference was insignificant implying virtually no blade interaction based on the analytical model.

The aerodynamic and blade blockage distributions used in the through-the-blade analysis along shroud, 50-percent flow and hub streamlines are shown in figures 22 and 23. Aerodynamic blockage along each streamline was distributed linearly with meridional distance, while the radial distribution (at each station calculation line) was held constant.

The distribution of angular momentum normalized to a reference velocity for the through-the-blade analysis is shown for all streamlines in figures 24 and 25. The hub and 25-percent streamline distributions were taken from the blade-to-blade Katsanis solution while the remaining streamlines used the sinusoidal distribution discussed previously on Page 54 because of their supersonic velocities.

A comparison of calculated diffusion factors at the rotor blade trailing edge for the preliminary across-the-blade solution and the design through-the-blade solution are shown in figure 26. Agreement is good except at the hub streamline. This difference was not accounted for due to the approximate nature of the estimated loss.

Only one blade loading is presented for Rotor 1A. This loading corresponds to the hub streamline and is shown on figure 27. The blade surface velocities were obtained from the blade-to-blade program. The resultant loading for the hub section streamline, while considered satisfactory for design purposes, has some undesirable features that could not be corrected in the time available for this design. One problem area associated with this loading is that the mean velocity initially accelerates and then diffuses quite rapidly toward the blade exit. It would be desirable to minimize the velocity peak. However, an adjustment of this condition may have an adverse influence on the total flow field, requiring considerable redesign to achieve the desired overall design intent.

The final step in the aerodynamic design of Rotor 1A involved a throat area check for each streamline to insure that the rotor will pass the design flow. This calculation is approximate in that mean flow properties and a constant height are employed to calculate flow

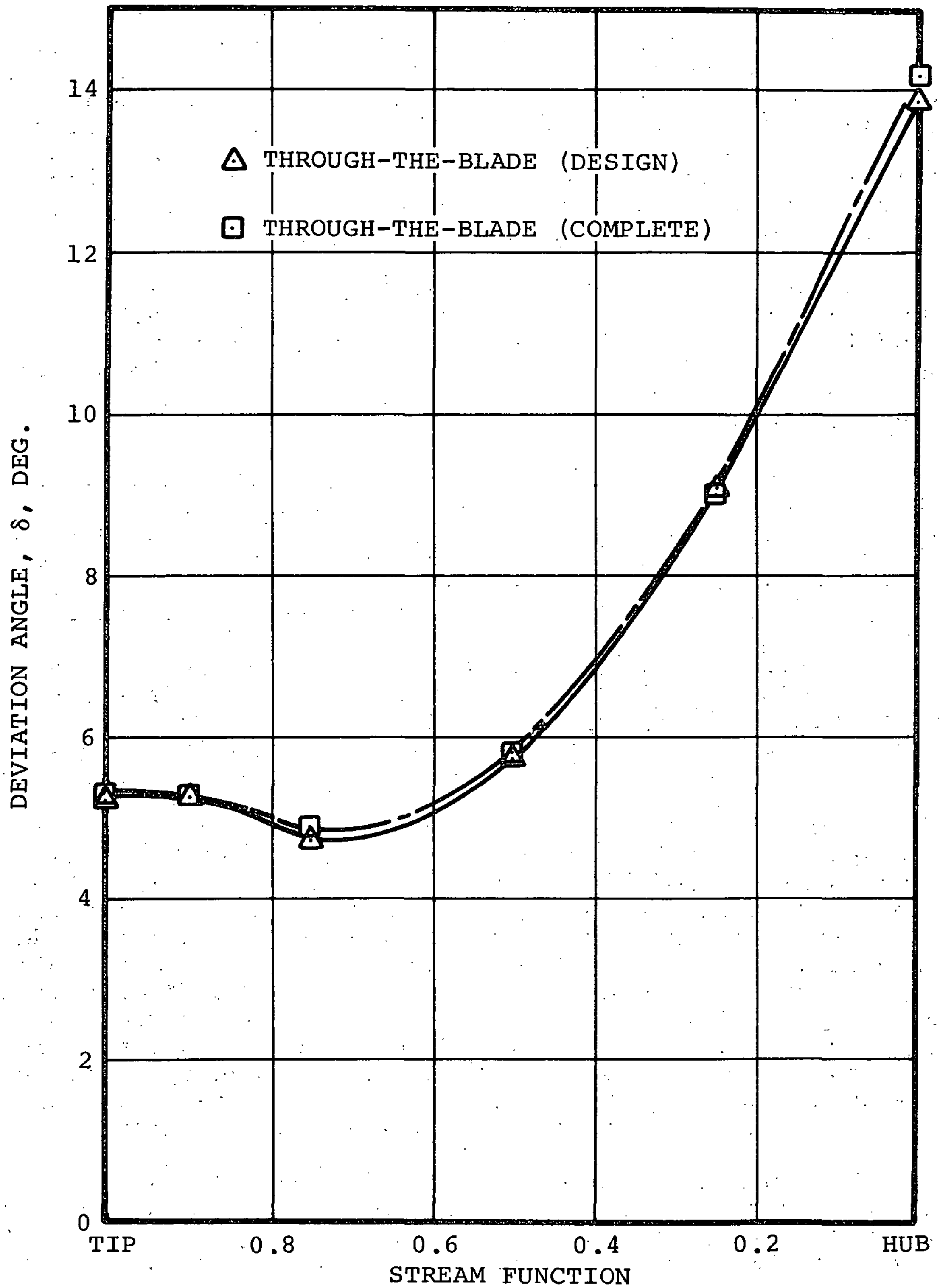

Figure 21.- Deviation Angle Agreement for Rotor 1A.

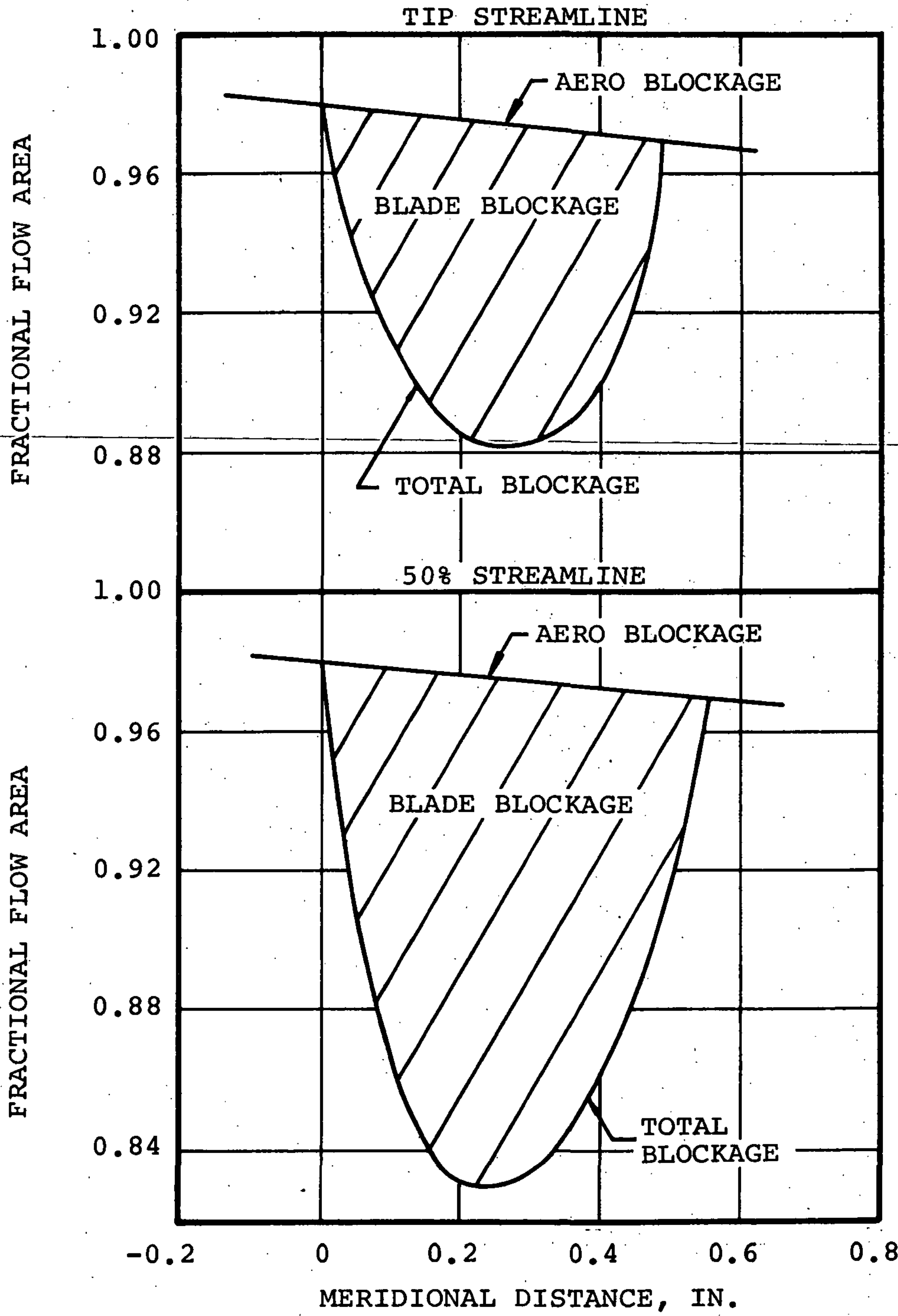

Figure 22.- Blockage Distribution for Rotor 1A
Tip and 50% Streamline.

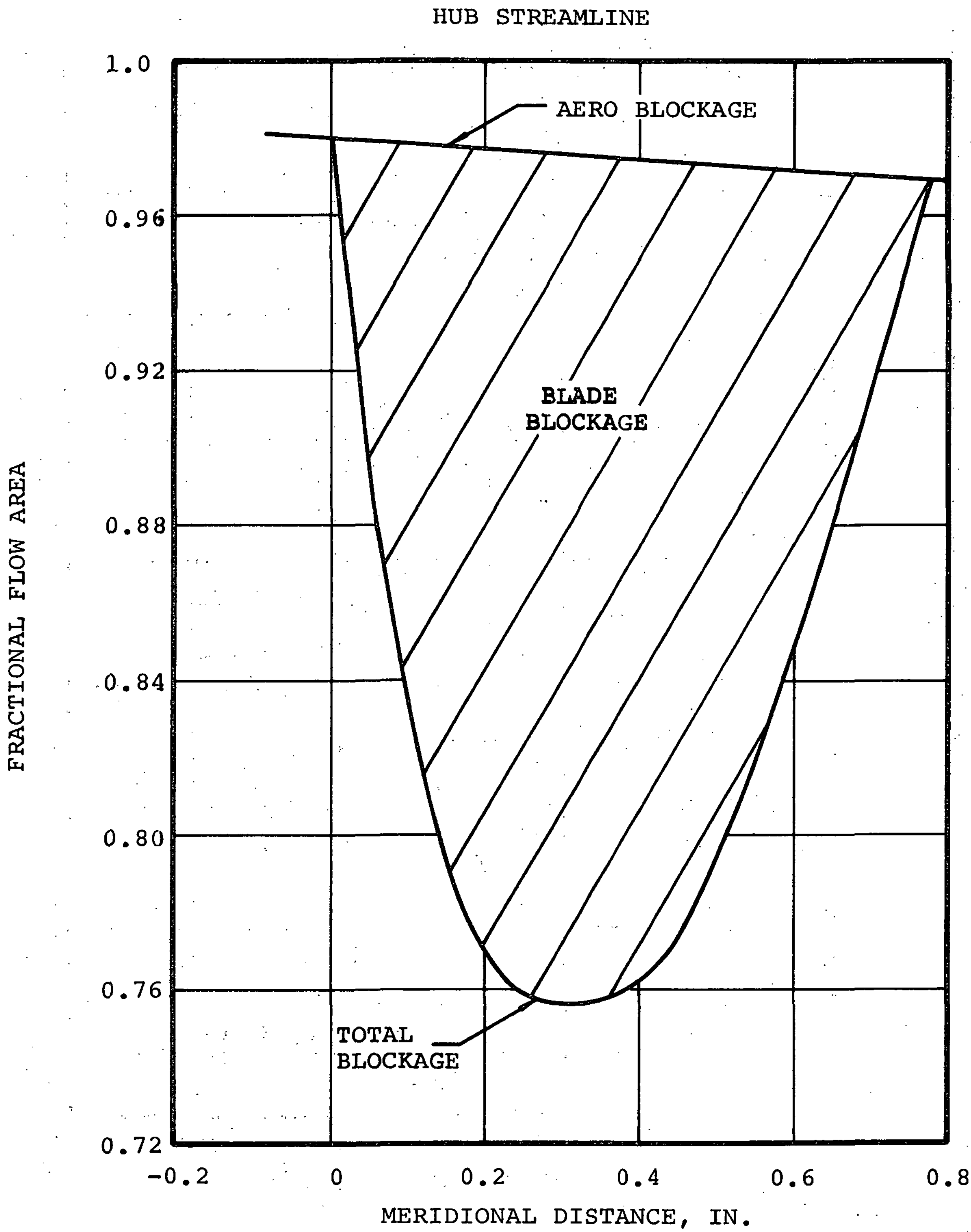

Figure 23.- Blockage Distribution for Rotor 1A Hub Streamline.

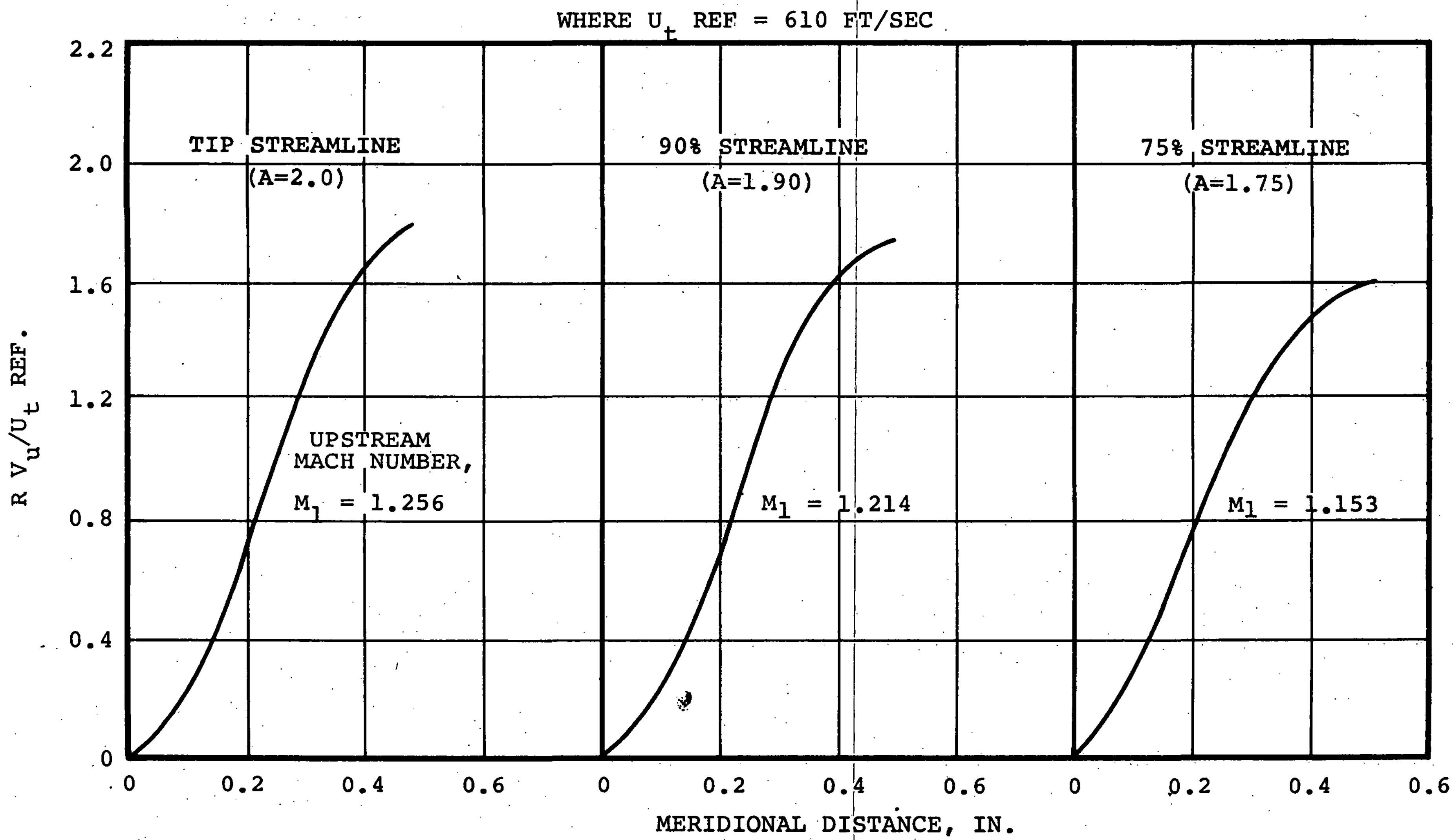

Figure 24.- Streamline Energy Distribution for Rotor 1A.

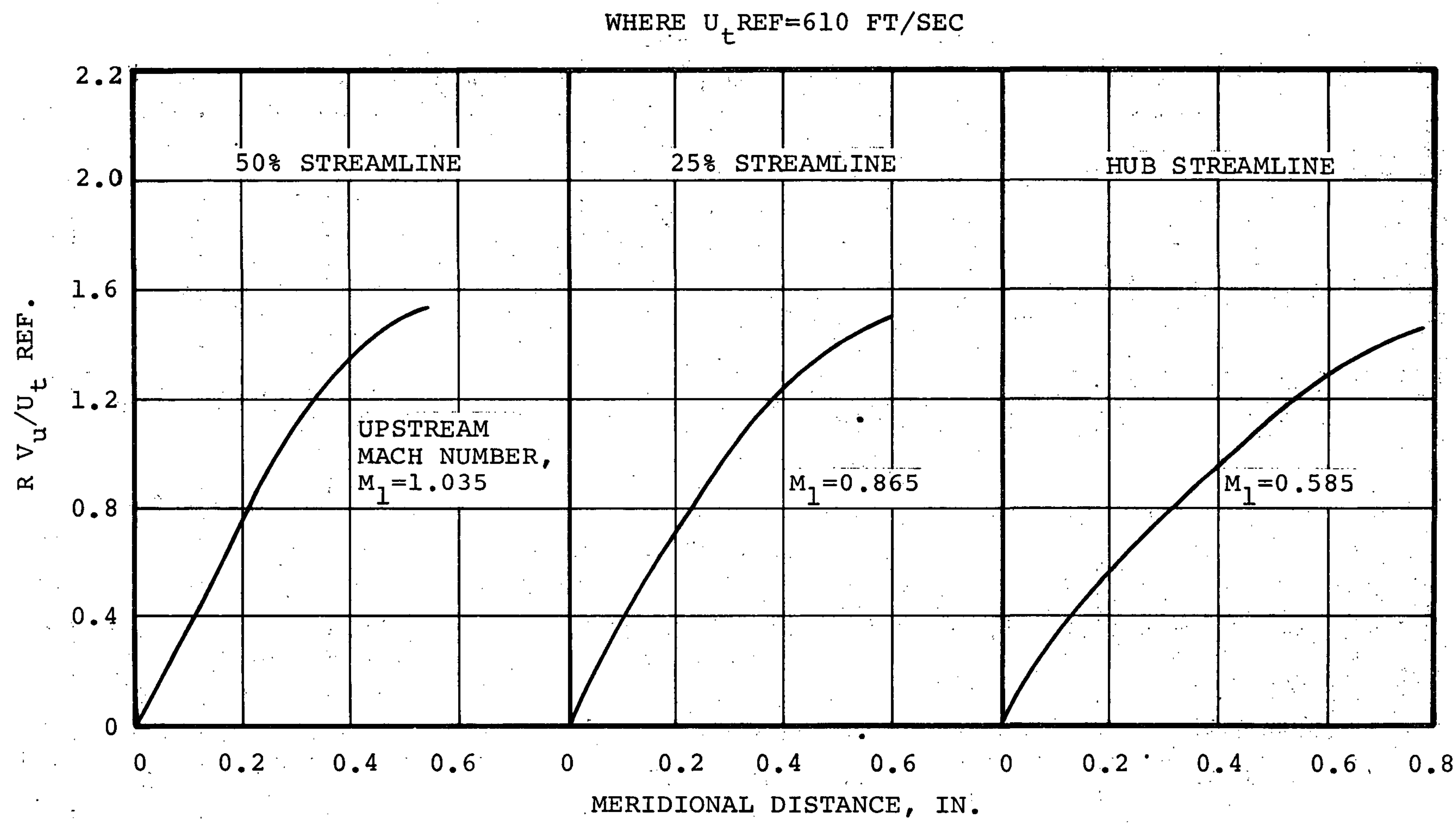

Figure 25.- Streamline Energy Distribution for Rotor 1A.

$$D = 1.0 - \frac{V_2'}{V_1'} + \frac{r_2 V_{u_2} - r_1 V_{u_1}}{2\bar{r}\,\sigma V_1'}$$

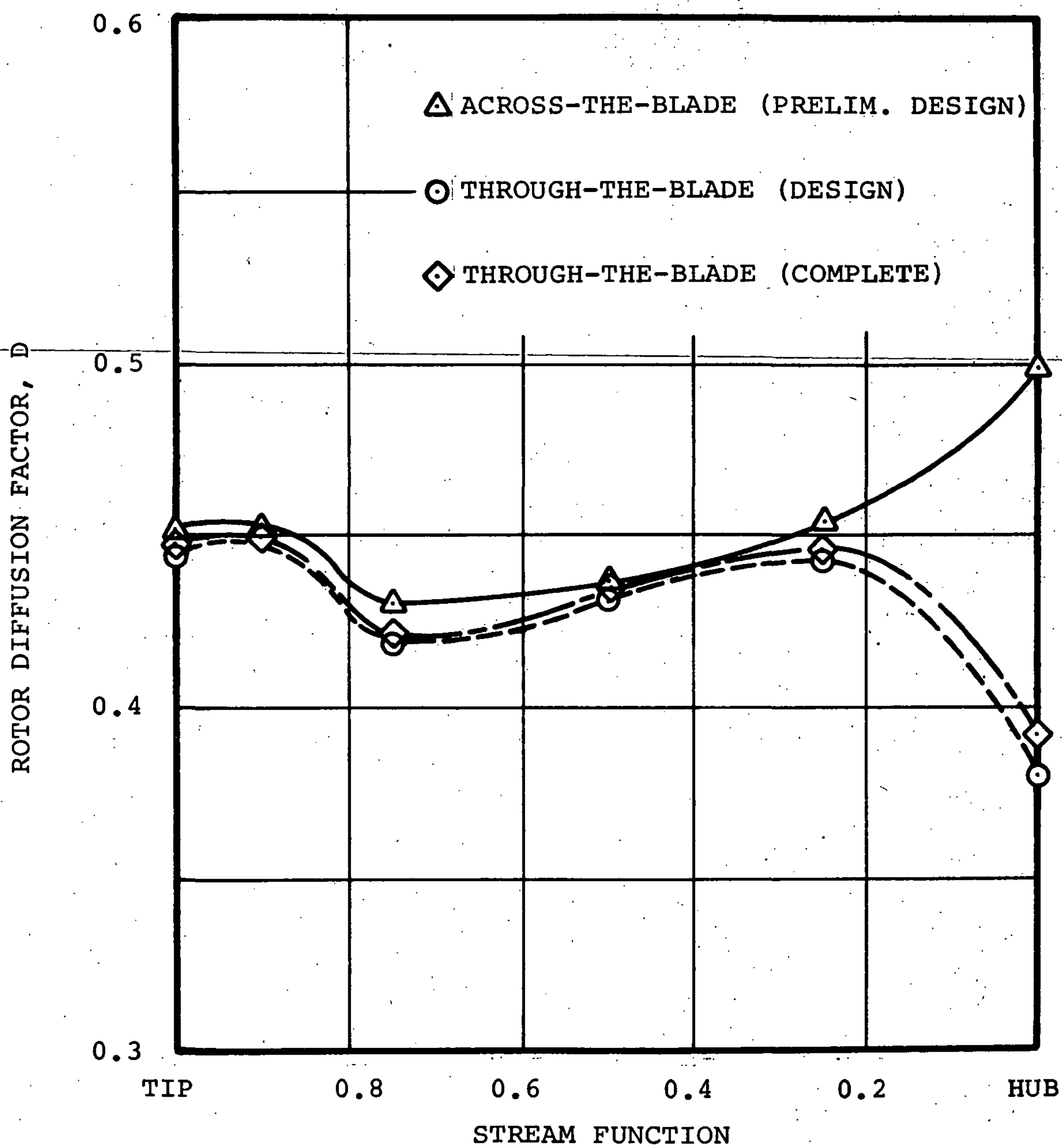

Figure 26.- Diffusion Factors for Rotor 1A.

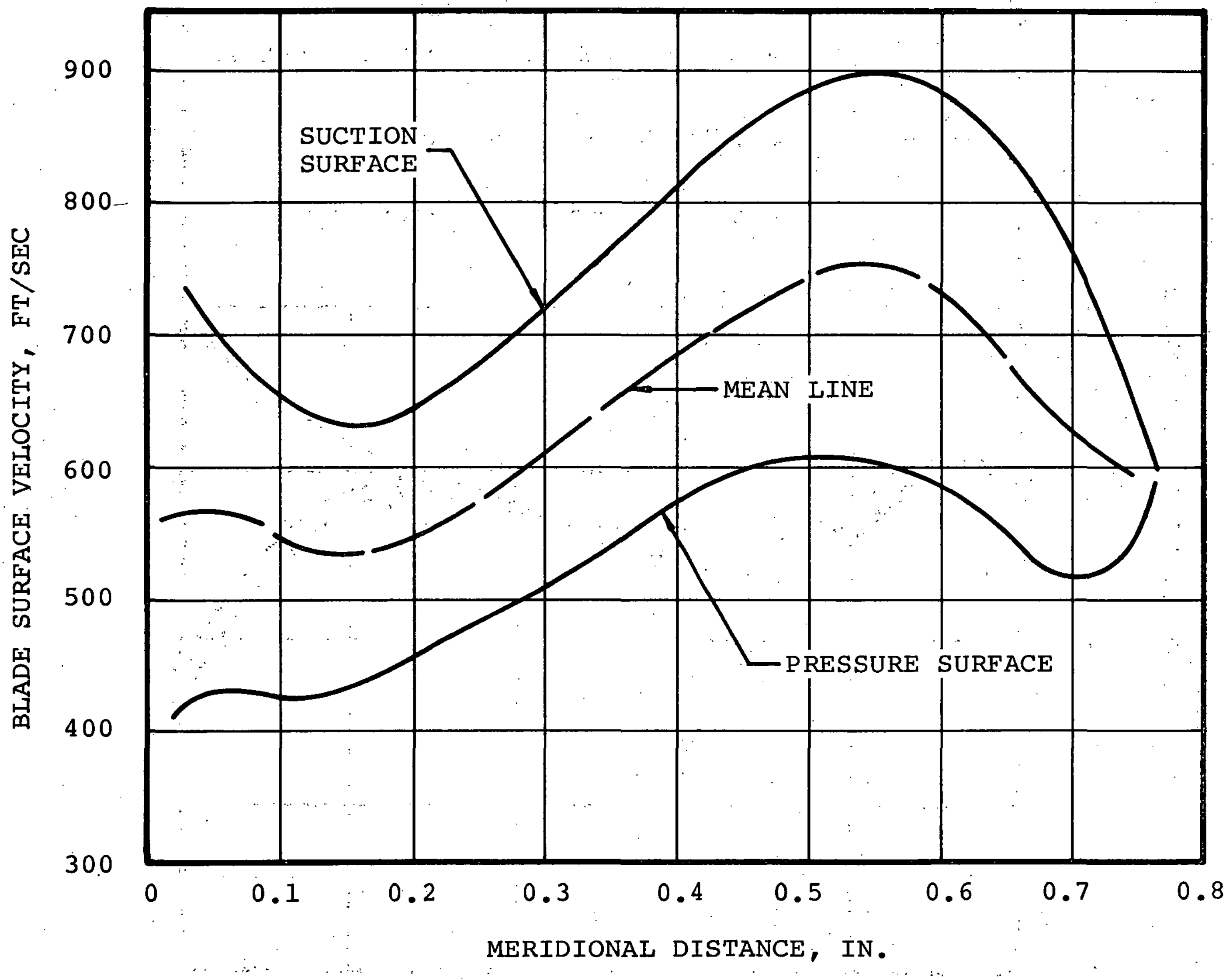

Figure 27.- Final Blade Loading for Rotor 1A Hub Streamline.

areas at a particular meridional streamline location. The passage width is obtained geometrically. Obviously, this does not account for secondary flows and/or warped stream surface thicknesses that are known to exist in the real case. In essence, the throat area check made here uses one-dimensional flow properties with area change to calculate the minimum passage area along a particular streamline.

Results of the throat area check for all the streamlines in Rotor 1A are presented on figure 28. These are shown as the flow area divided by the critical area for choked flow versus meridional distance along each streamline. Note that the first four streamlines indicate a choke margin of 2 percent or greater and that the throat location moves from the middle of the blade to near the leading edge going from the blade tip to the 50-percent streamline.

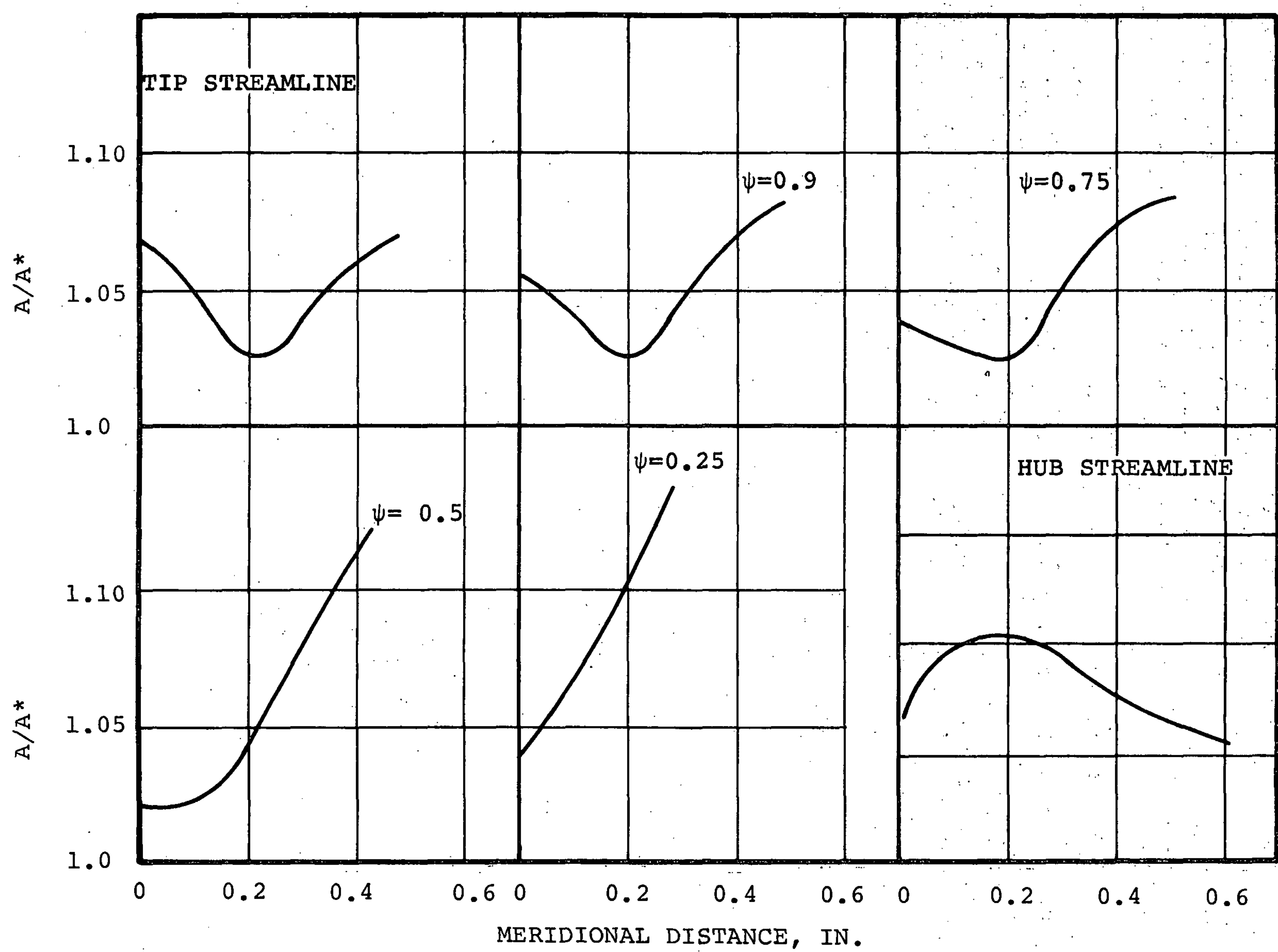

Figure 28.- Throat Area Check for Rotor 1A.

ROTOR 1B DESIGN

The final rotor 1B design parameters are as follows:

Corrected flow, lb/sec	1.225
Tip diffusion factor	0.493
Tip relative velocity ratio	0.655
Inlet hub/tip ratio	0.746
Tip relative Mach number	0.981
Aspect ratio	0.84
Tip solidity	1.57
Number of blades	40

The final meridional shape is shown in figure 29. Also included are the through-the-blade calculation stations and final streamline positions. Details of the final airfoil sections specified along each of these axisymmetric stream surfaces are contained in table IX.

The rotor 1B inlet relative Mach number distribution is shown in figure 18. For this range of Mach numbers, the double circular arc meanline was selected for initial through-the-blade analysis. This selection was subsequently changed to the more general multiple circular arc to adjust blade loadings and to shift flow streamlines. The flow streamline shift was required to match, as closely as possible, the across-the-blade inlet and exit vector diagrams.

A comparison of design intent incidence angle and the resulting through-the-blade values are shown in figure 30. The two values do not agree perfectly, again due to the change (from the across-the-blade calculation) through-the-blade solution. However, the differences were judged acceptable based on the calculated loadings from the blade-to-blade program and the wider loss versus incidence characteristic associated with the lower Mach number level.

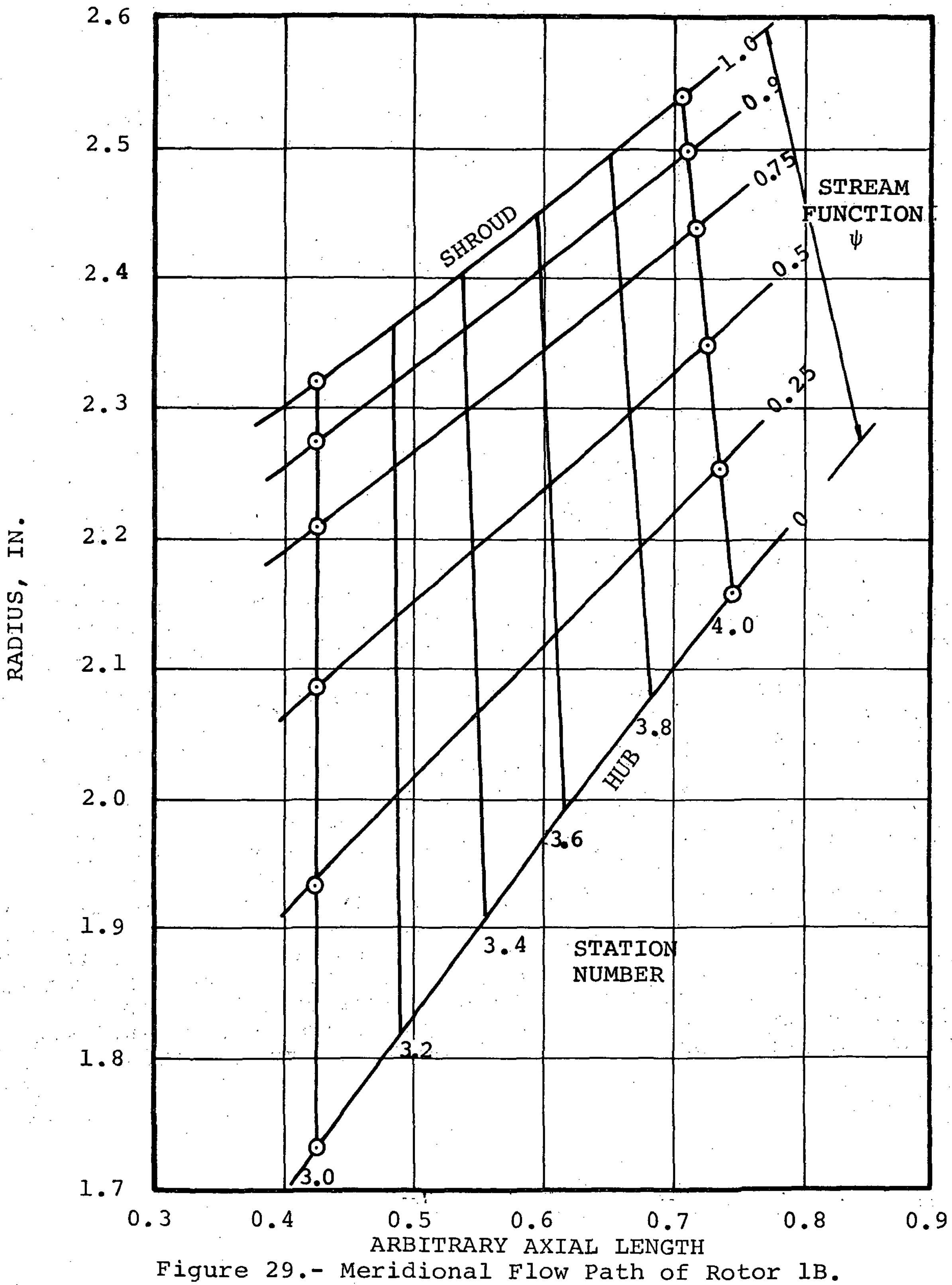

Figure 29.- Meridional Flow Path of Rotor 1B.

TABLE IX.

BLADE SETTING FOR ROTOR 1B

ψ	$M1_{REL}$	$\beta 1$(Air)	$\beta 1$(Blade)	i	$\beta 1_{SS}-\beta 1_{MC}$	t_{LE}
Shroud	0.981	55.02	53.04	1.98	3.08	0.0060
0.9	0.965	54.54	52.06	2.48	2.00	0.0064
0.75	0.955	54.38	51.00	3.38	2.60	0.0070
0.5	0.888	52.67	49.64	3.03	3.83	0.0080
0.25	0.784	50.89	47.00	3.89	5.34	0.0090
Hub	0.624	47.85	43.92	4.12	4.17	0.0116

ψ	$\beta 2$(Air)	$\beta 2$(Blade)	δ	t_{TE}	t_{max}/C_T
Shroud	57.23	49.89	7.34	0.0066	0.035
0.9	53.81	48.74	5.07	0.0075	0.0392
0.75	50.12	46.58	3.54	0.0086	0.0462
0.5	45.41	40.09	5.32	0.011	0.0586
0.25	37.74	30.65	7.09	0.0132	0.07
Hub	27.61	15.78	11.83	0.0144	0.0866

ψ	C_T	Φ_T	a/C_T	Φ_{SS}/Φ_T	δ
Shroud	0.572	3.15	0.583	0.25	1.487
0.9	0.568	3.32	0.570	0.345	1.49
0.75	0.566	4.42	0.554	0.427	1.532
0.5	0.560	9.55	0.483	0.625	1.59
0.25	0.5625	16.35	0.466	0.74	1.707
Hub	0.6027	28.14	0.465	0.81	1.973

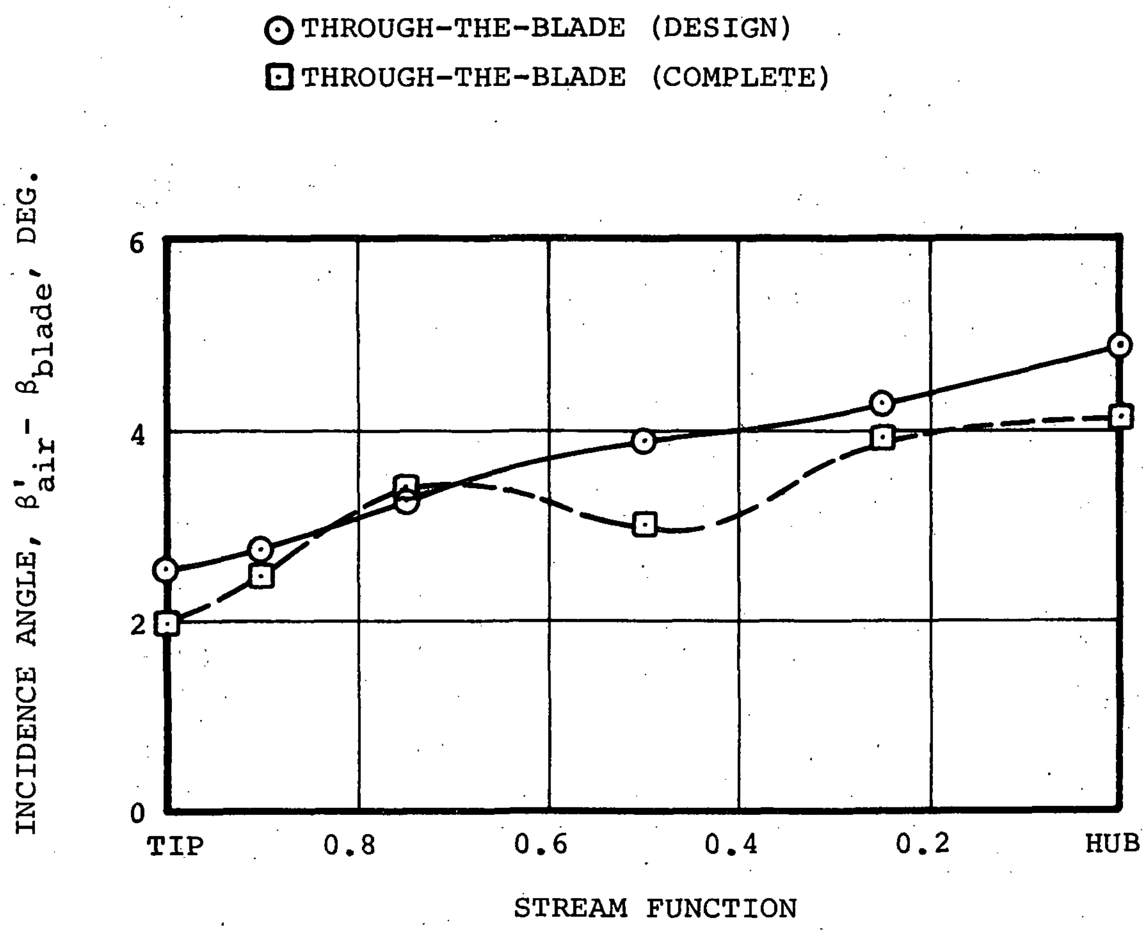

Figure 30.- Design Incidence for Rotor 1B.

The final design deviation angles are shown in figure 31. These values were calculated to give the correct angular momentum change across the second rotor blade. As seen from figure 32, the exit relative air angles from the across-the-blade solution do not agree with those from the final through-the-blade design. The trends are identical to those of the rotor 1A design. Also included are the complete through-the-blade values. Agreement is very good which assures the correct energy condition.

Final aerodynamic and blade blockage distributions are shown for the shroud, 50-percent flow, and hub streamlines in figures 33 and 34. The aerodynamic blockage was distributed linearly with streamline meridional distance and held constant across each calculation station line.

For rotor 1B, since all inlet relative velocities were subsonic, distribution of angular momentum from the blade-to-blade program was used for all streamlines. The final design distributions for the shroud, 50-percent flow, and hub streamlines are shown in figures 35, 36, and 37.

A comparison of across-the-blade diffusion factor distribution at rotor 1B exit to the final design solutions is shown in figure 38. Small differences exist across the entire blade. However, these differences were not felt to be significant enought to change the original loss values.

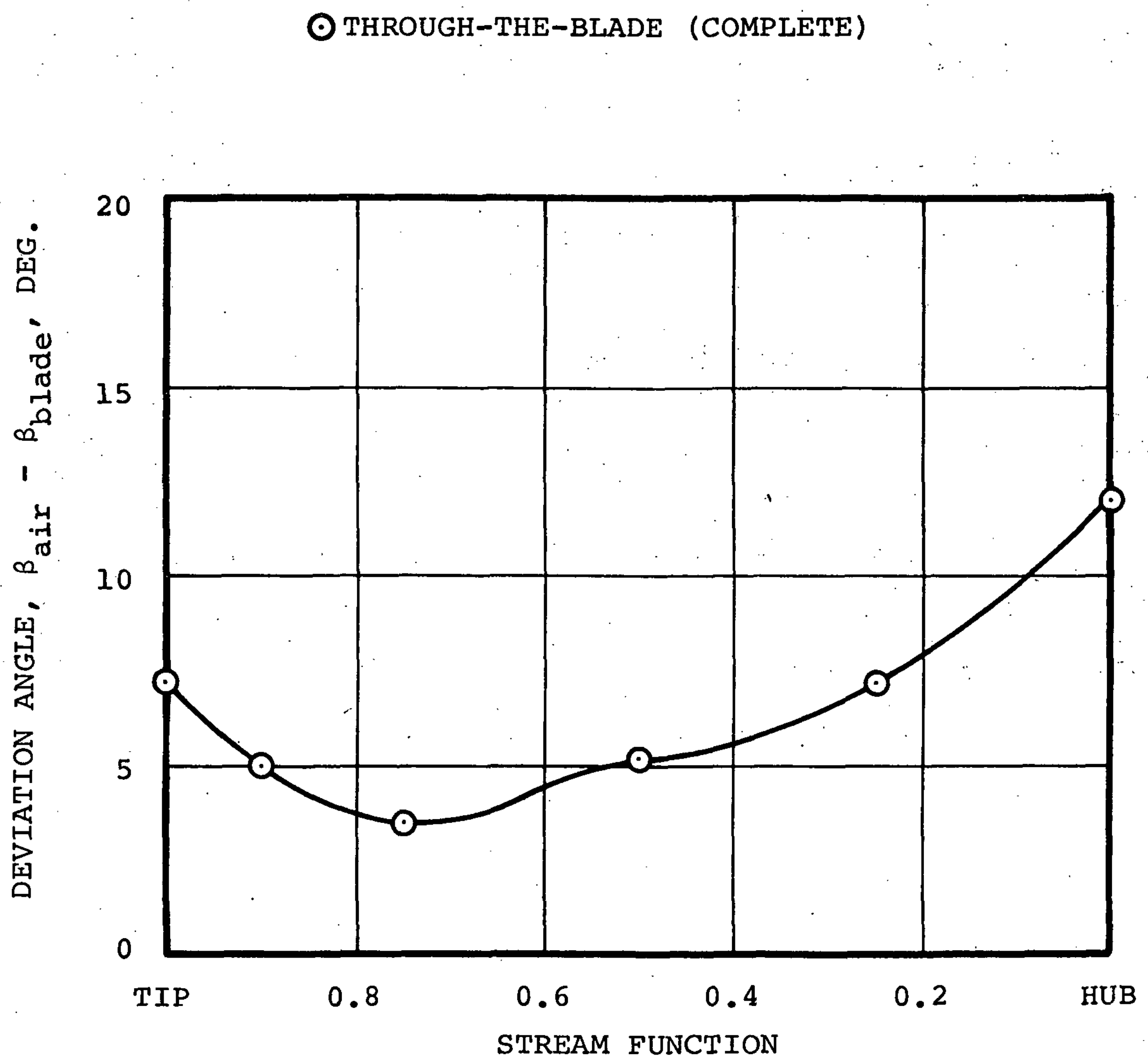

Figure 31.- Rotor 1B Final Design Deviation Angle.

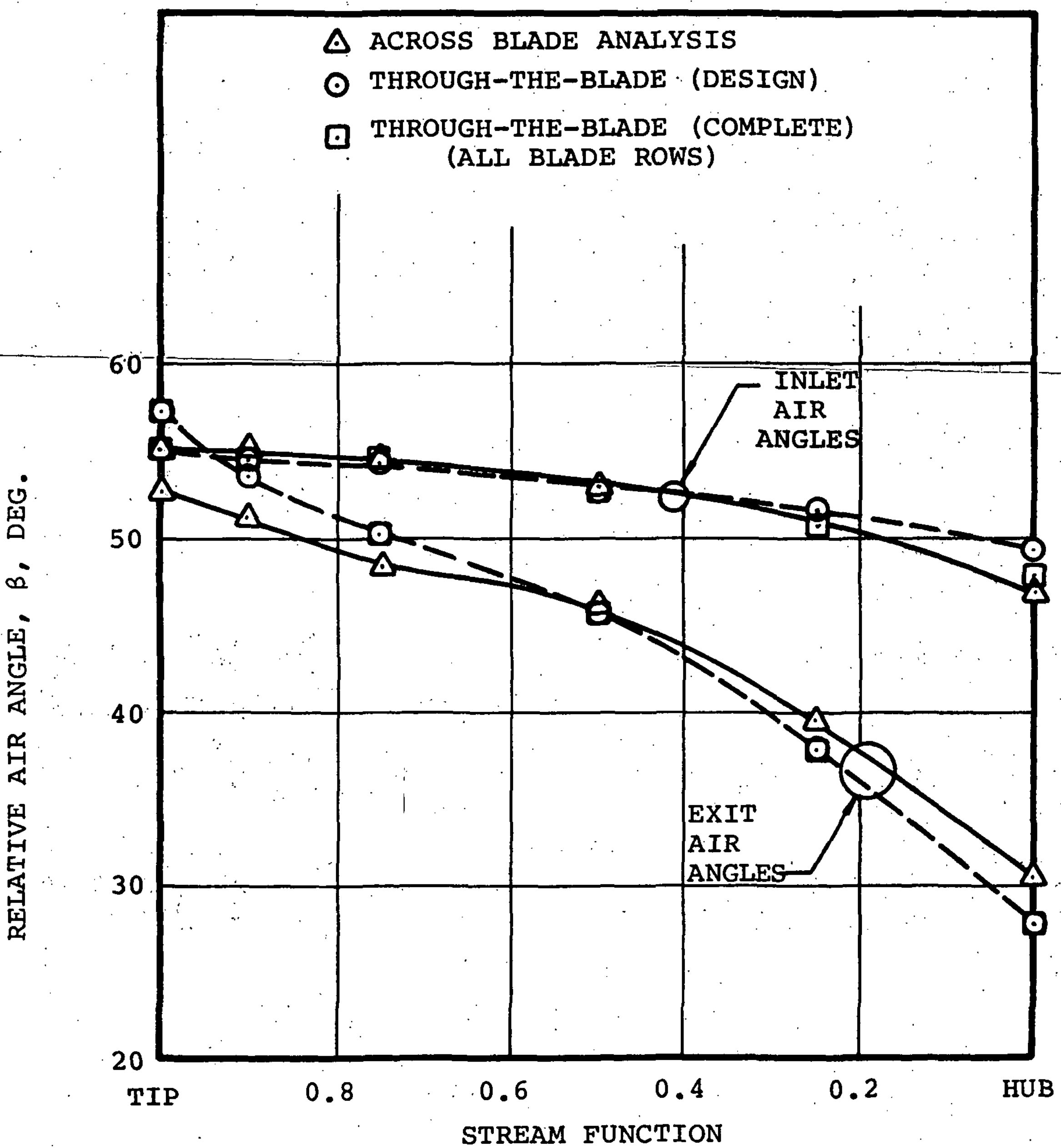

Figure 32.- Comparison of Rotor 1B Relative Air Angles.

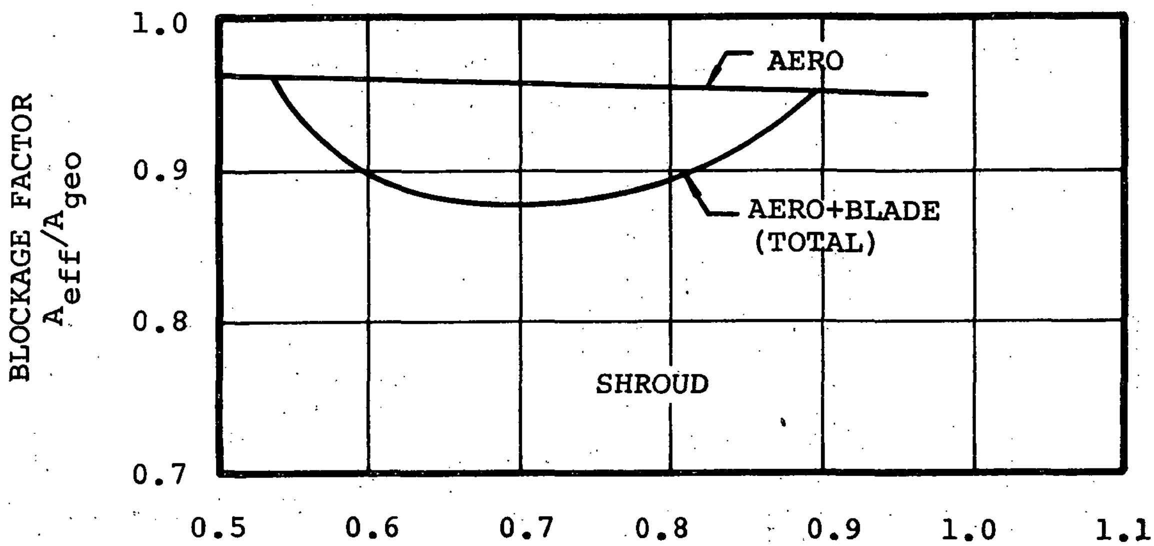

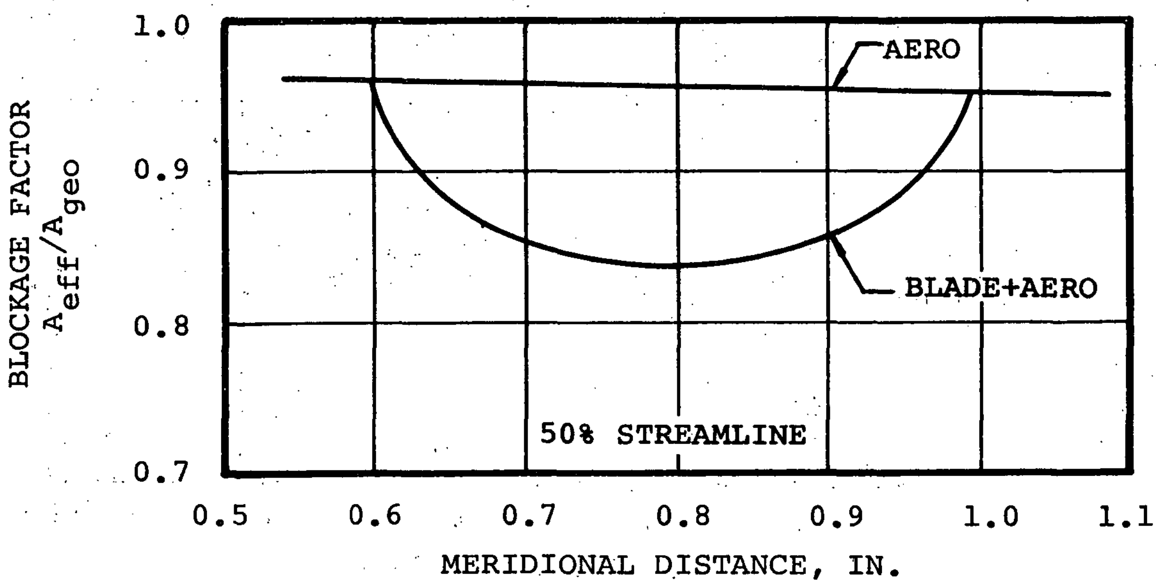

Figure 33.- Rotor 1B Blade Blockage Distribution.

HUB STREAMLINE

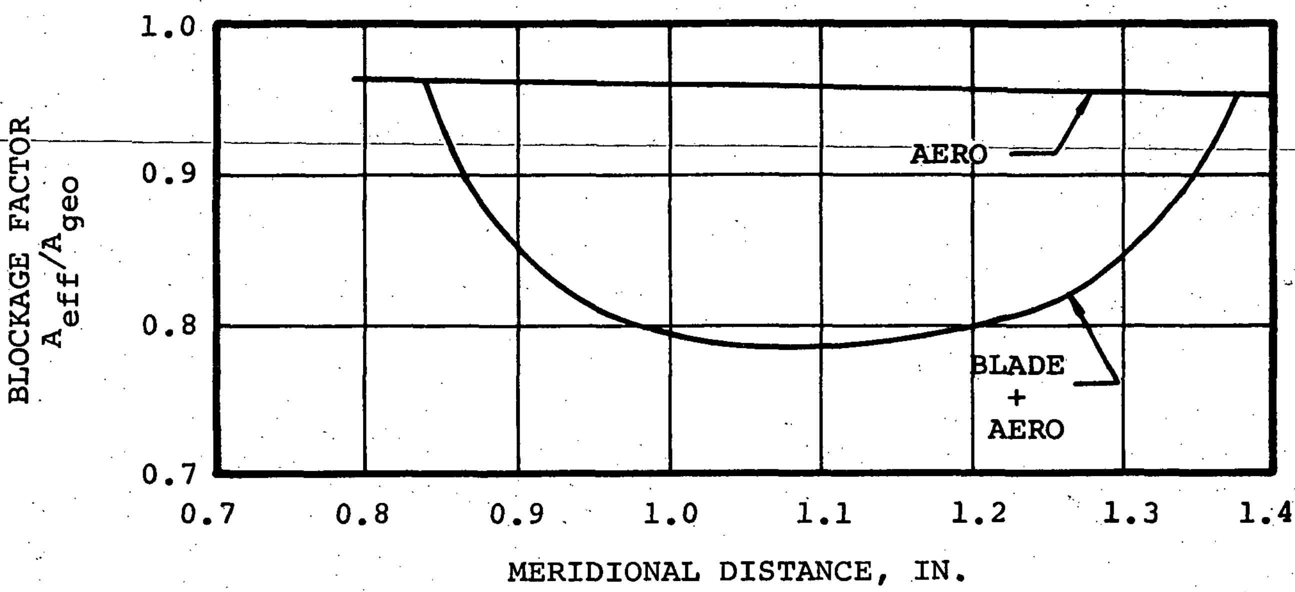

Figure 34.- Rotor 1B Blade Blockage Distribution.

WHERE U_t REF = 610 FT/SEC.

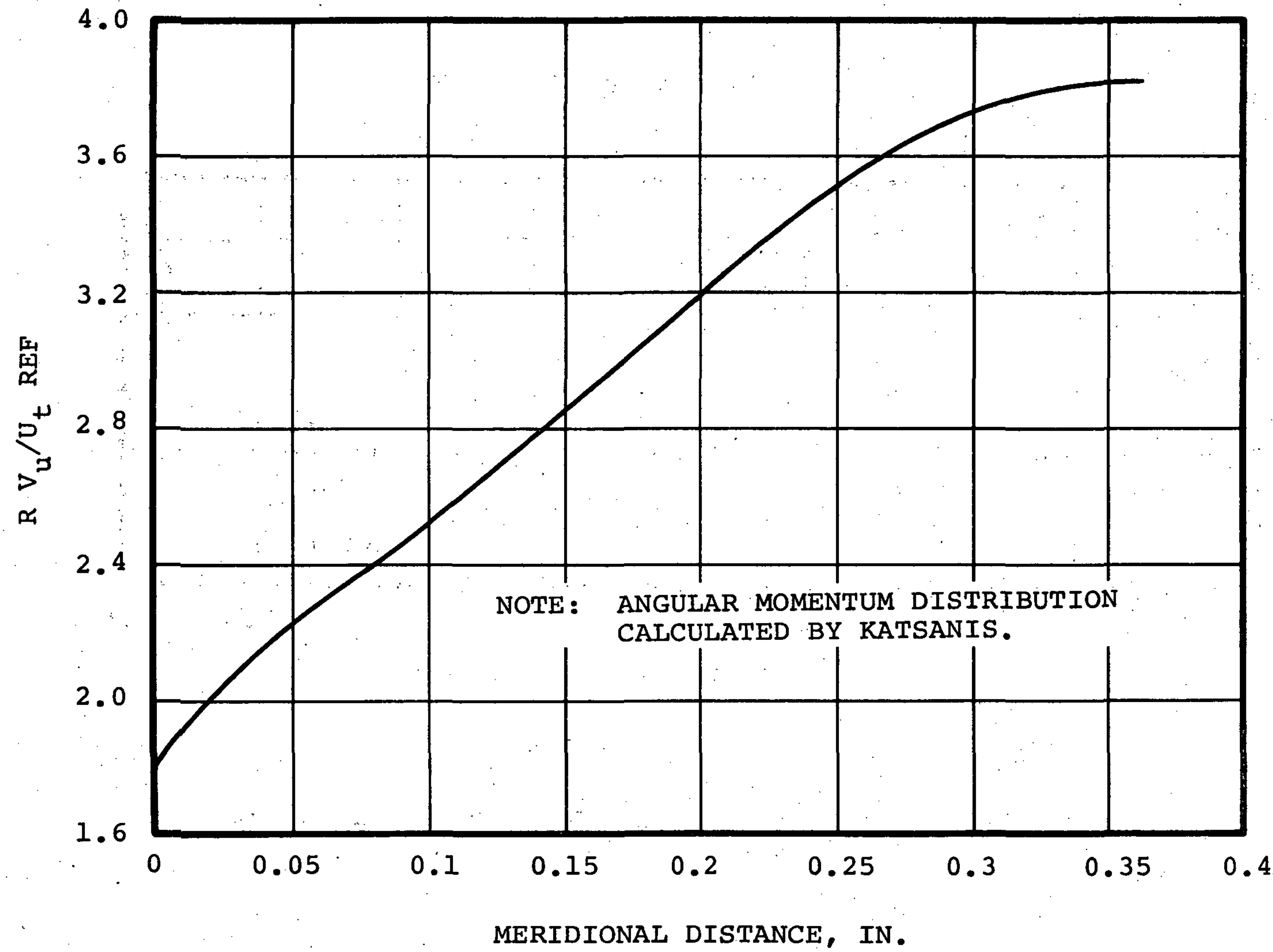

Figure 35.- Rotor 1B Tip Streamline Energy Distribution.

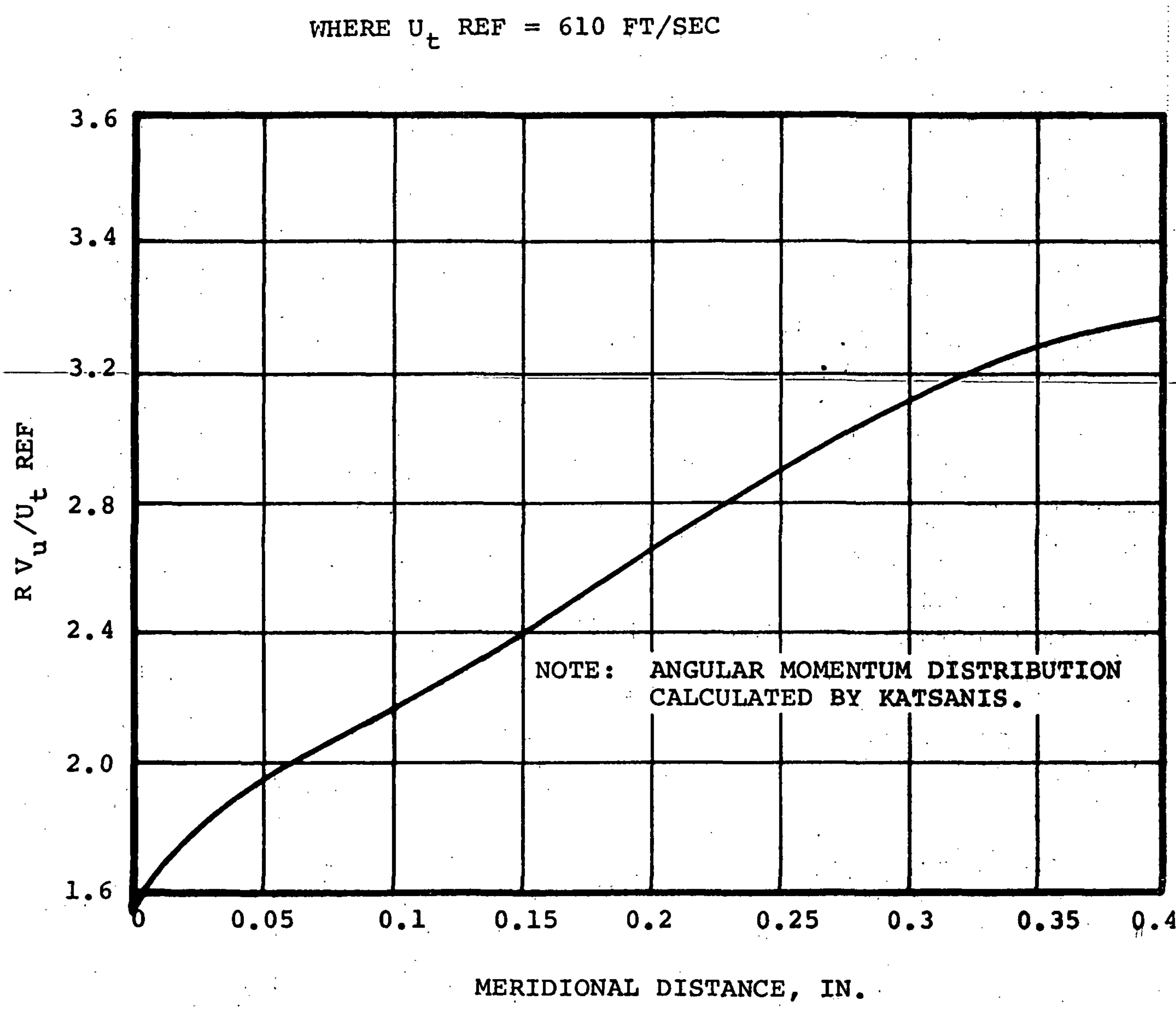

Figure 36.- Rotor 1B Fifty-Percent Streamline Energy Distribution.

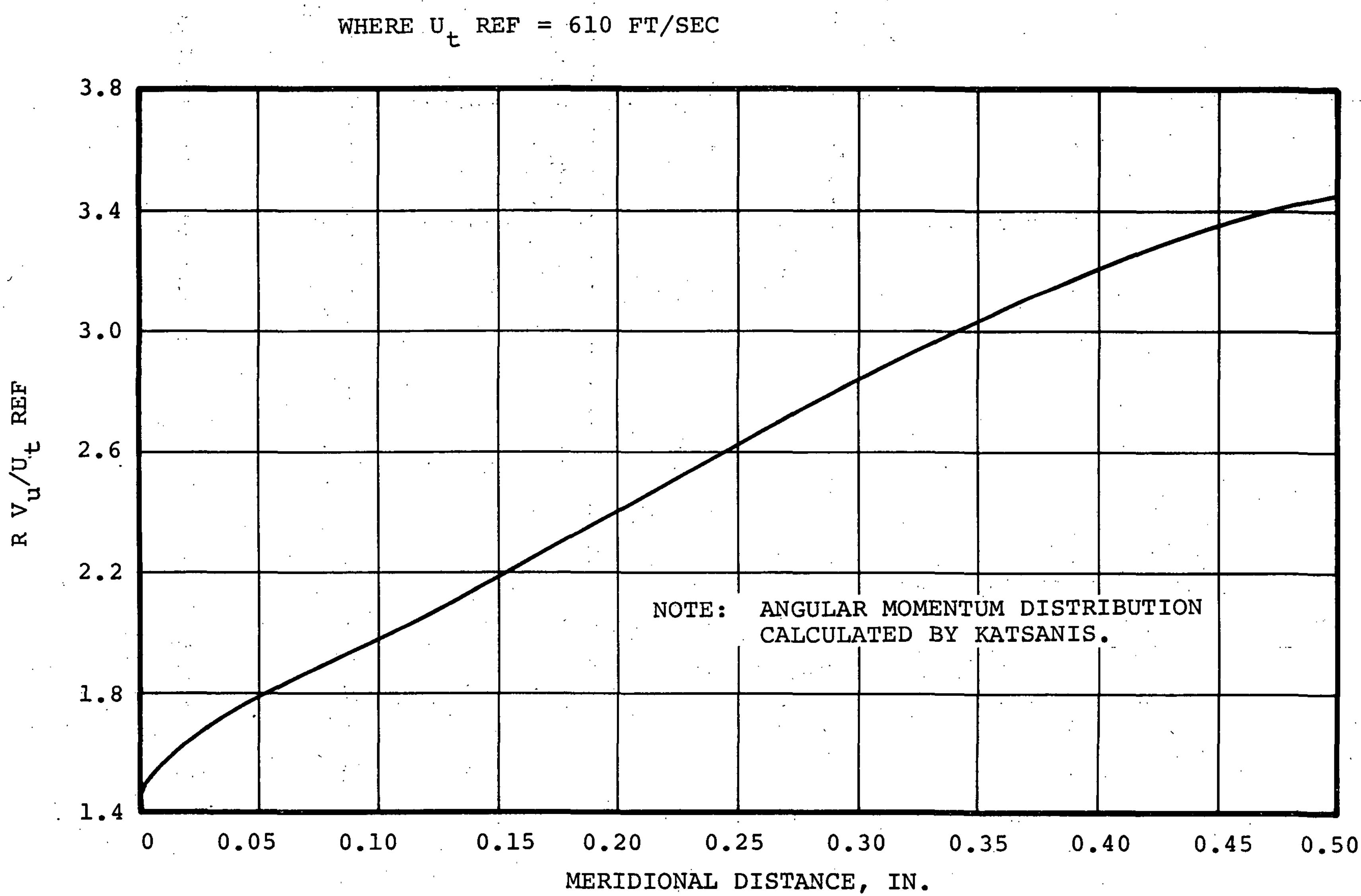

Figure 37.- Rotor 1B Hub Streamline Energy Distribution.

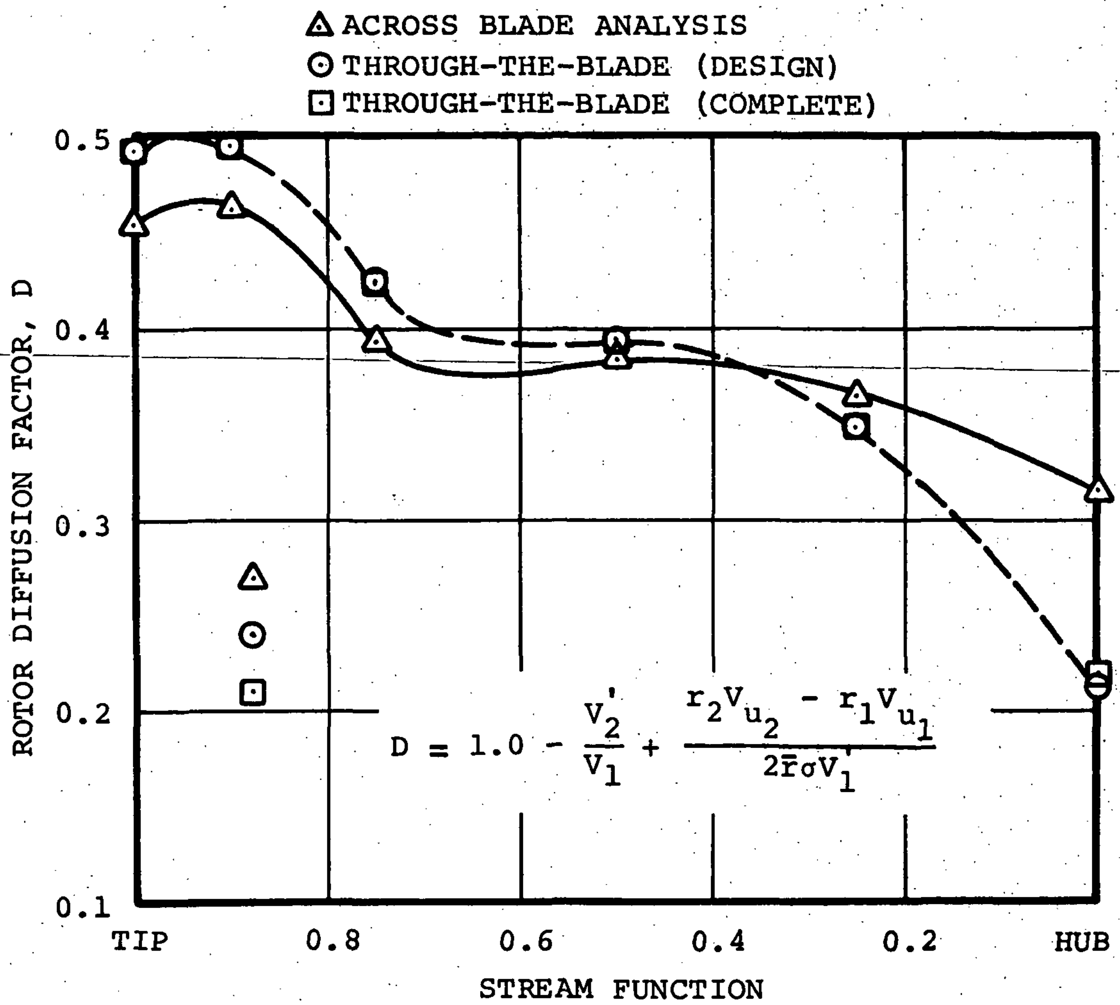

Figure 38. - Comparison of Rotor 1B Exit Diffusion Factor Distribution.

The final loadings from the blade-to-blade program for the shroud, 50-percent flow, and hub streamlines are shown in figures 39, 40, and 41. All distributions are uniform in their deceleration rate.

Throat area checks were made for each of the streamlines to preclude the possibility of rotor 1B choking at the design condition. The minimum area ratio occurred for streamlines 1 through 4 at 1.04 of the minimum value. Streamlines 5 and 6 were had considerably more margin.

A final comparison is the distribution of inlet and exit relative air angles (Figure 32) as calculated by the initial across-the-blade analysis and by the two through-the-blade analysis. This result is similar to that observed in the rotor 1A design.

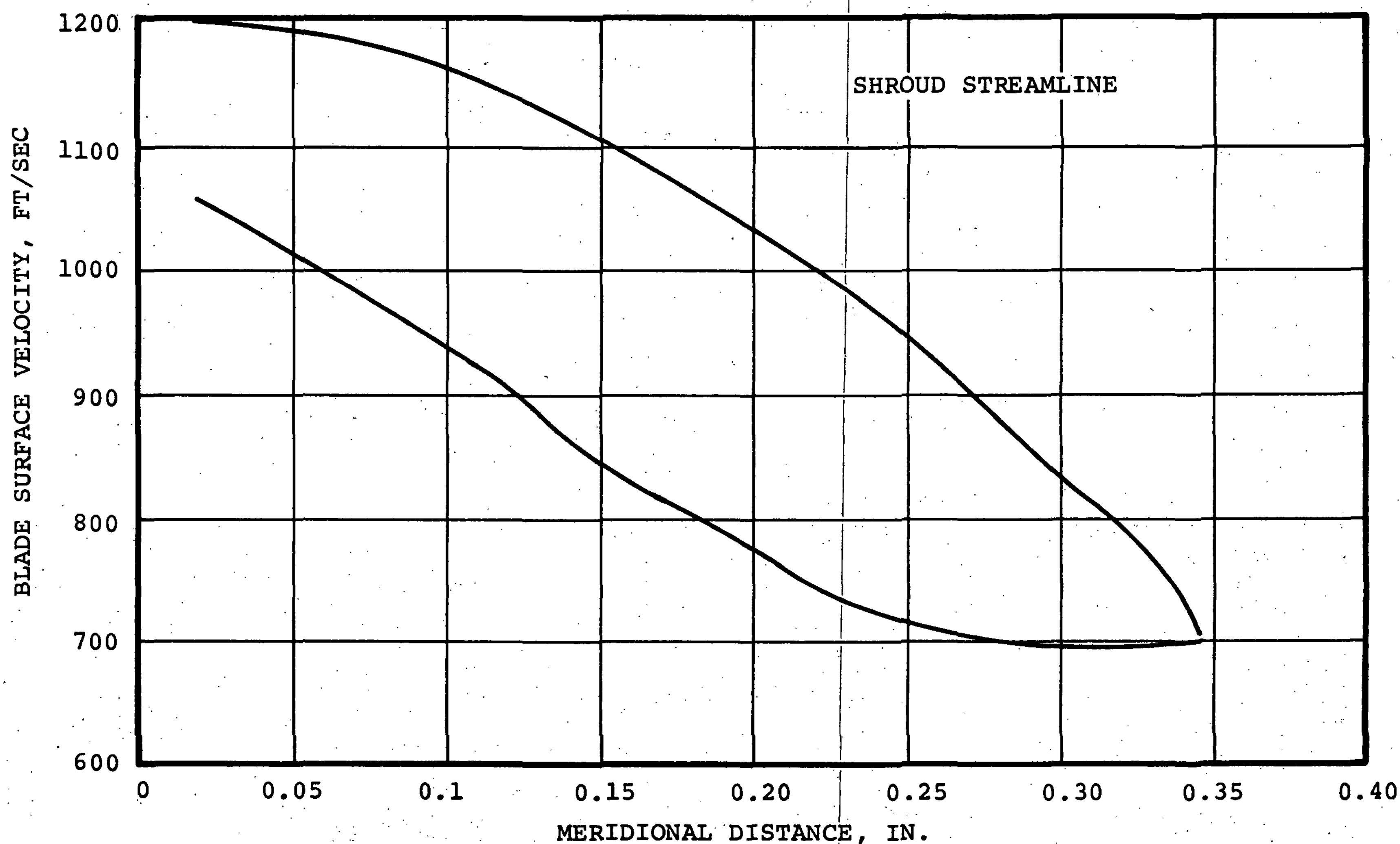

Figure 39. - Rotor 1B Final Blade Loading From The Blade-To-Blade Program Analysis.

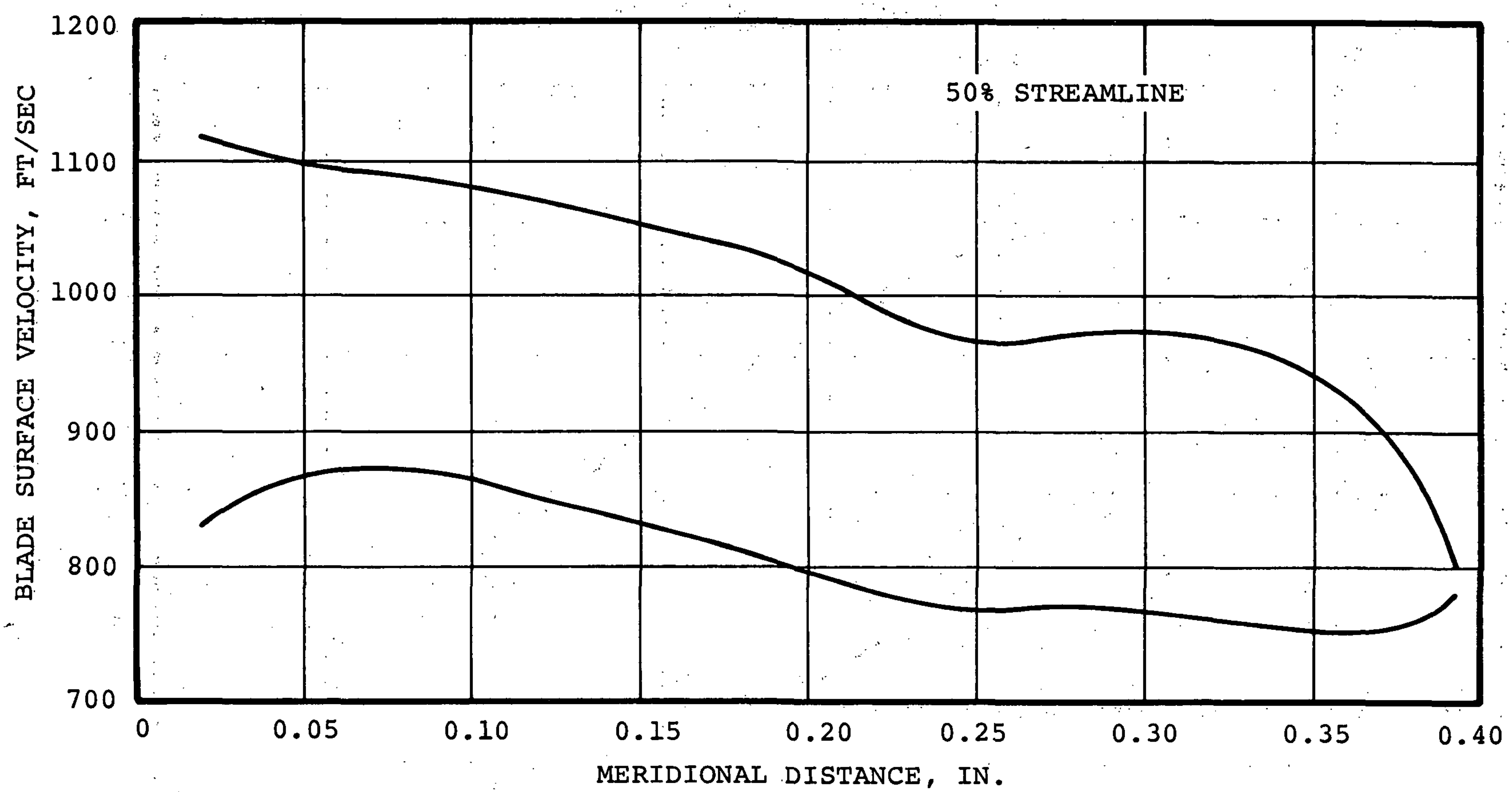

Figure 40. - Rotor 1B Final Blade Loading From The Blade-To-Blade Program Analysis.

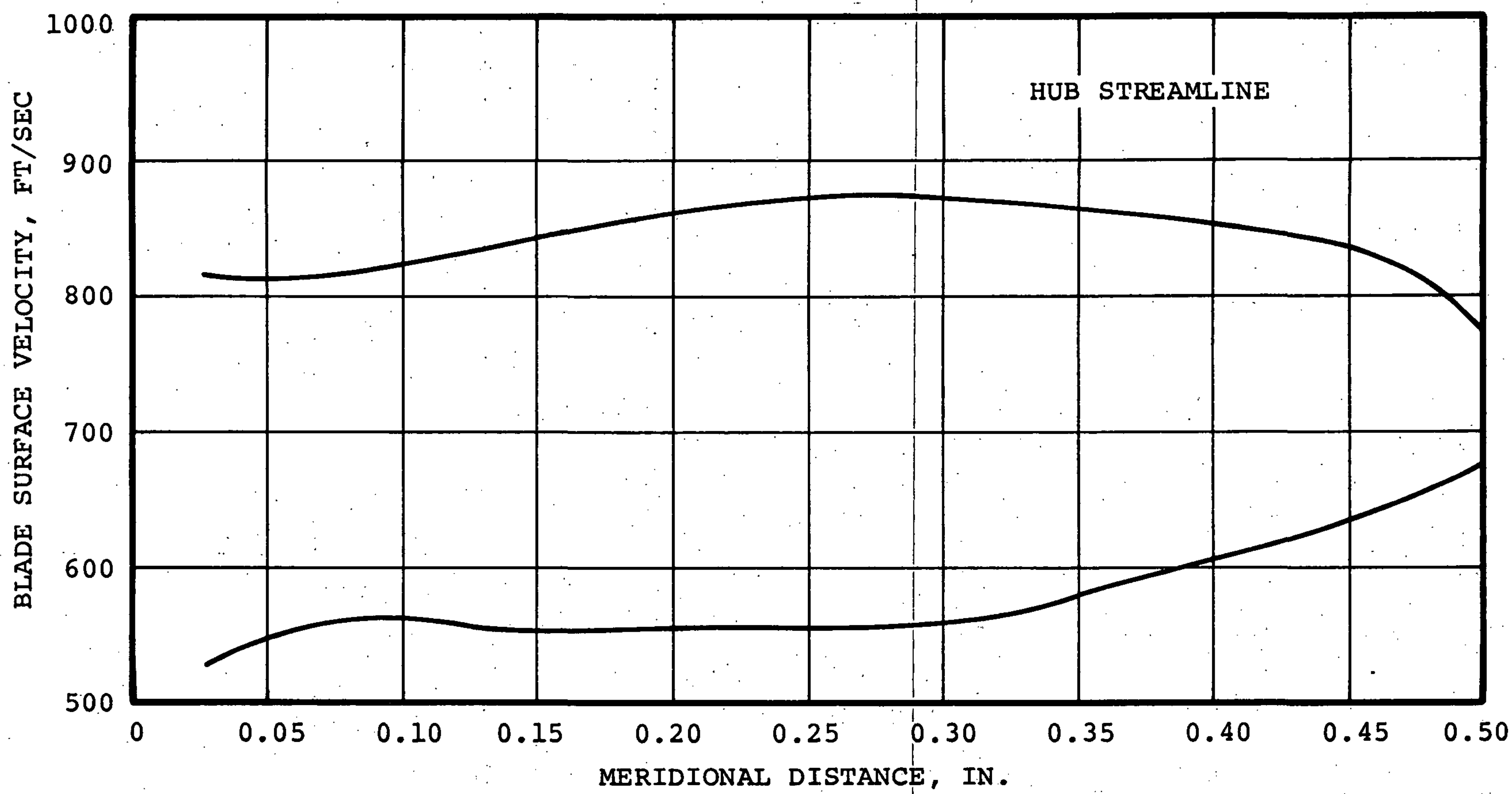

Figure 41. - Rotor 1B Final Blade Loading From The Blade-To-Blade Program Analysis.

TANDEM STATOR DESIGN

The final design parameters for stators 1A and 1B are as follows:

	Stator 1A	Stator 1B
Hub inlet Mach number	0.845	0.423
Hub solidity	1.891	1.63
Number of vanes	53	53
Aspect ratio	0.604	0.494

The meridional shape and calculation station locations are shown in figure 41a for the first row and figure 41b for the second row. Appendix B presents plots of the stacked blades and the section coordinators.

The distribution of inlet Mach number for both stators is shown in figure 42. For these levels of Mach number, double circular arc airfoils were used throughout both stator vane designs.

The design incidence angle for both stators, based on current stator technology (Reference 10), was -2.0 degrees to the suction surface. A comparison of the design intent to the final values is shown in figure 43 for both stators. Deviations from the design intent vary approximately ±2 degrees for stator 1A and from +0.8 degrees to -2.0 degrees for stator 1B. Time limitations prevented better matching with the design intent. However, the blade-to-blade analysis did not indicate excessive leading edge loadings.

The final stator deviation angles are as shown in figure 44. These values were required to achieve the correct amount of diffusion in each vane row. Air angles for the across-the-blade and through-the-blade analysis at the inlet and exit of each stator vane row are compared in figures 45 and 46. Good agreement (within 1 degree) was achieved at the inlet to each row whereas discrepancies up to 3.0 degrees occurred at the exit of each vane row.

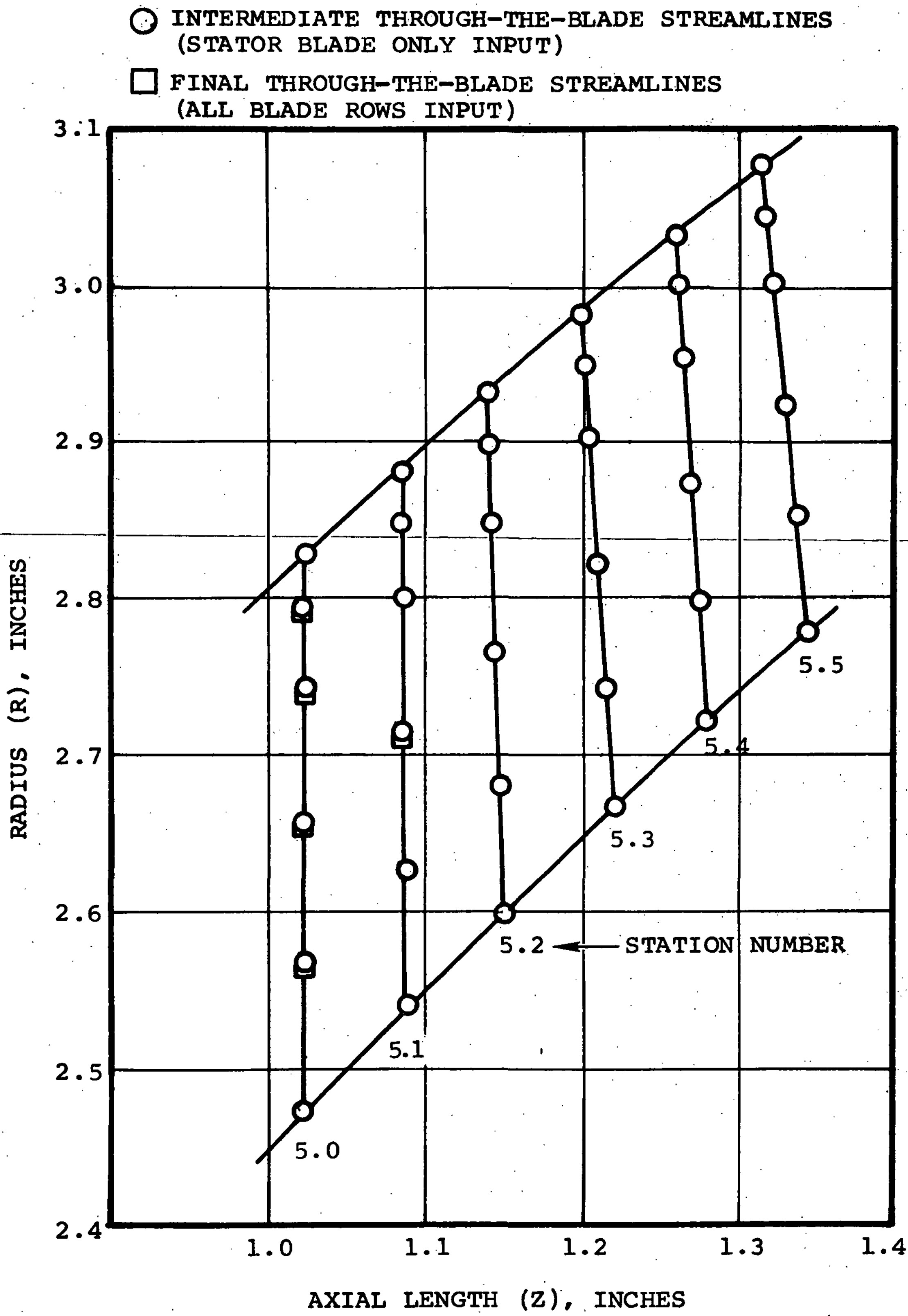

Figure 41a. - Meriodional Shape for Stator 1A.

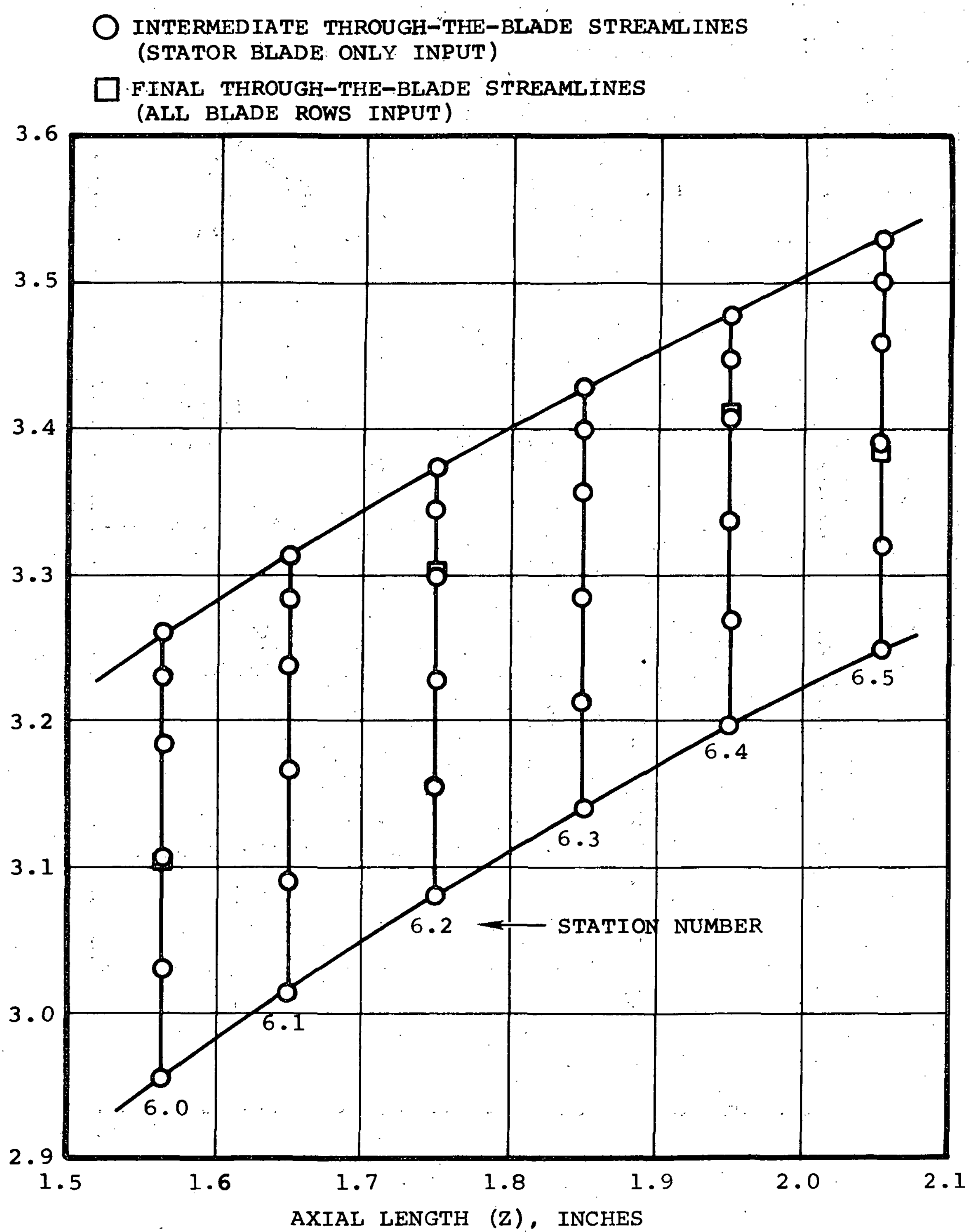

Figure 41b. - Meriodional Shape for Stator 1B.

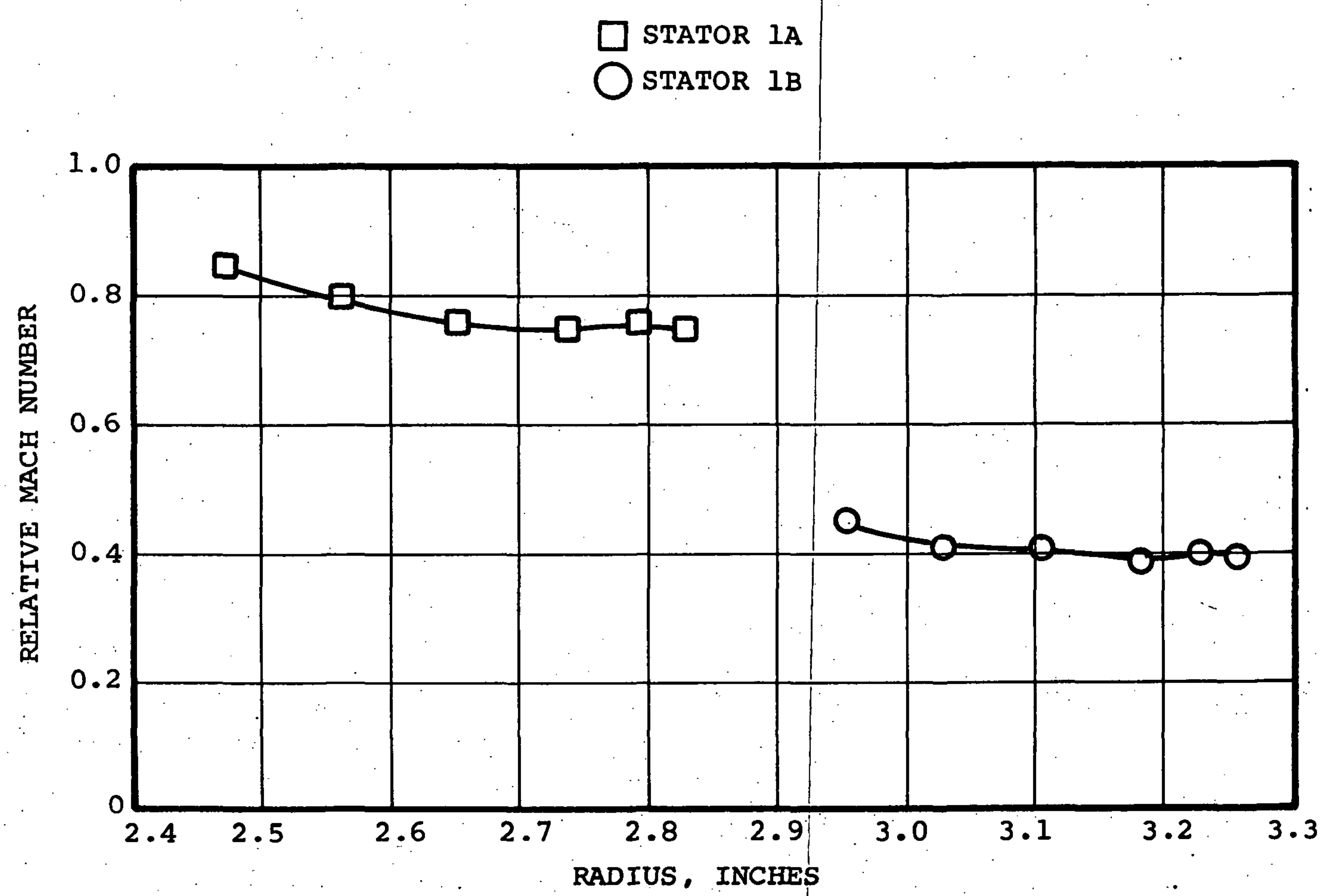

Figure 42. Inlet Mach Number For Stators 1A and 1B.

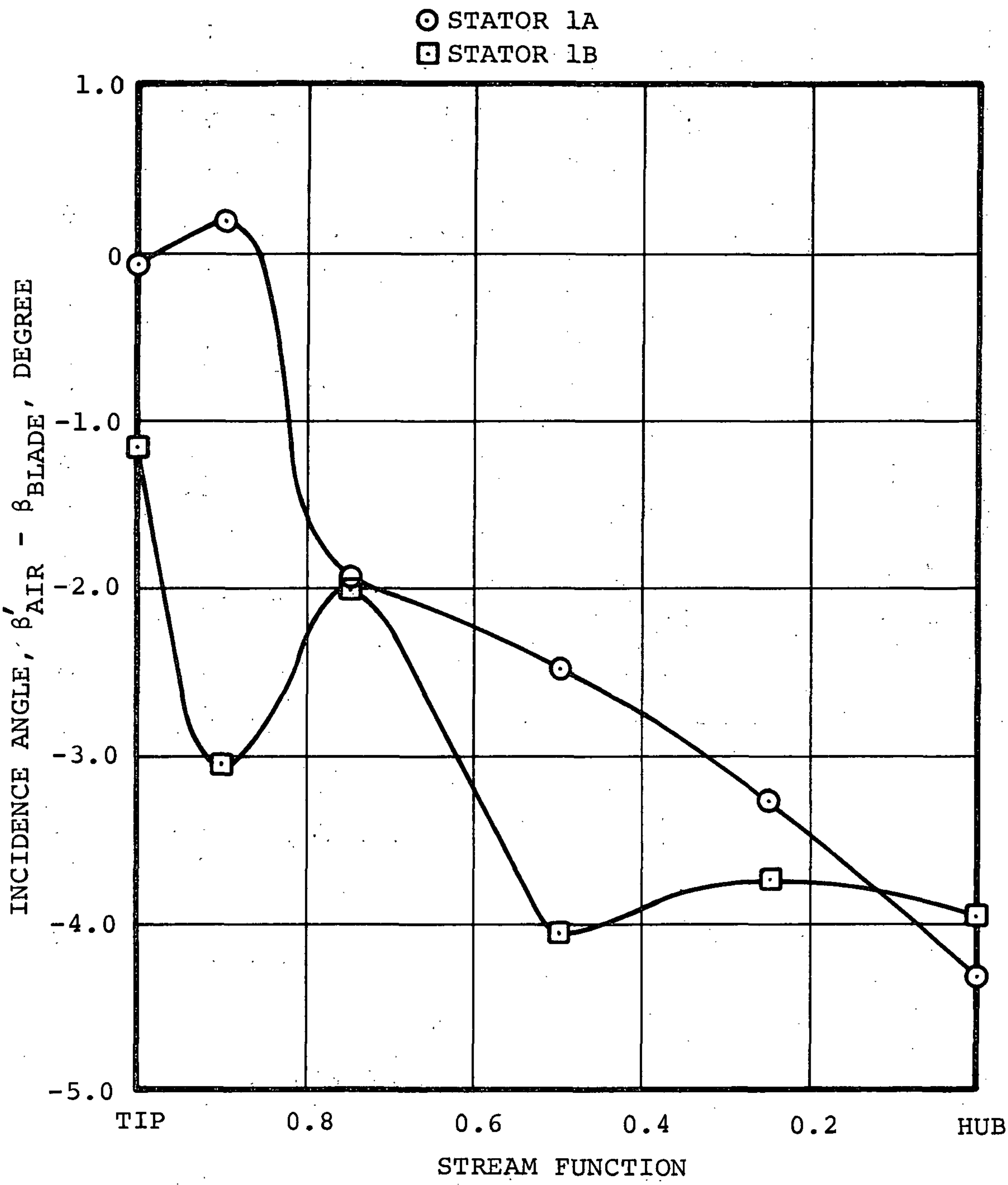

Figure 43. - Design Incidence Angles For Both Stators.

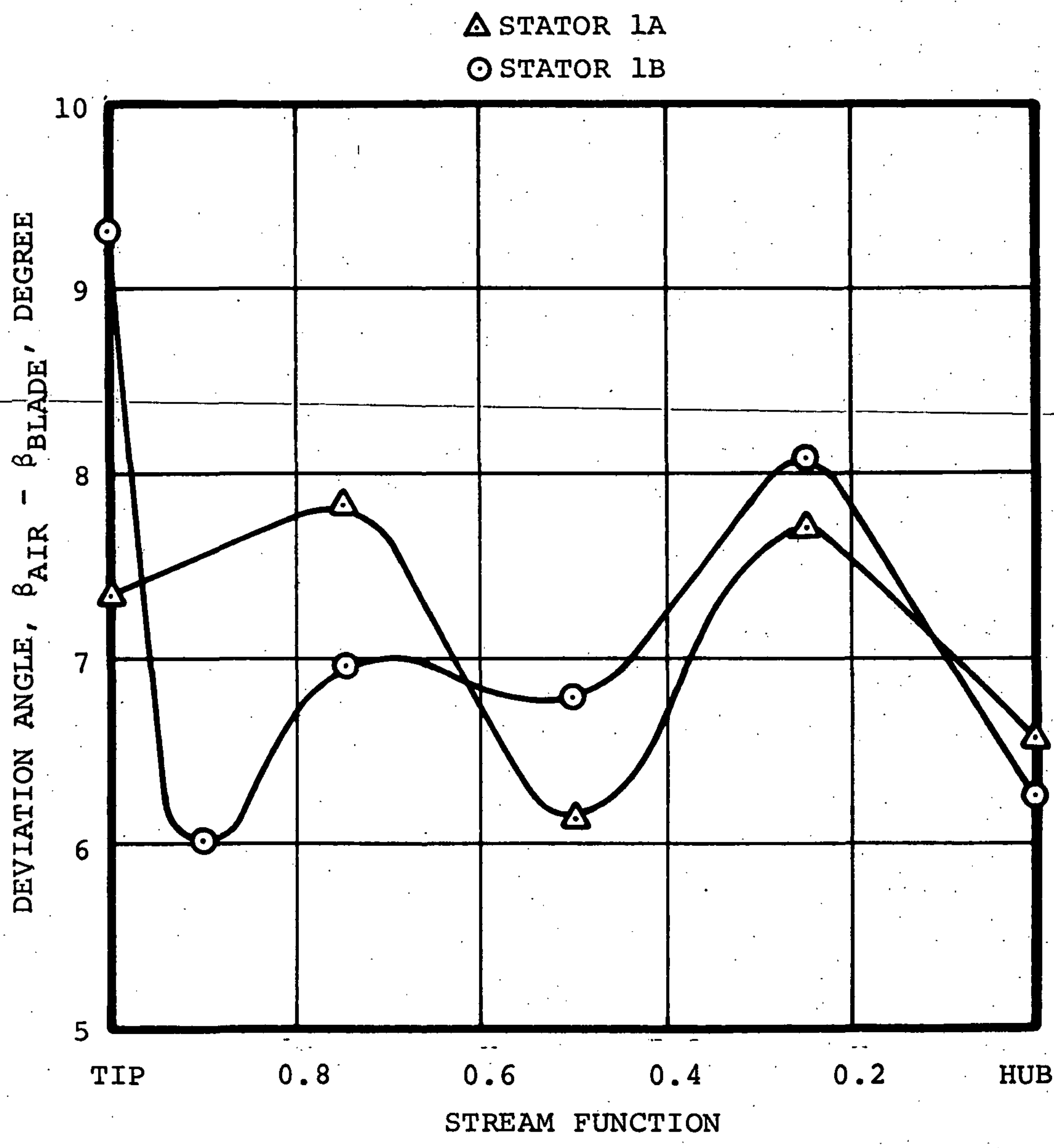

Figure 44. - Design Deviation Angles For Both Stators.

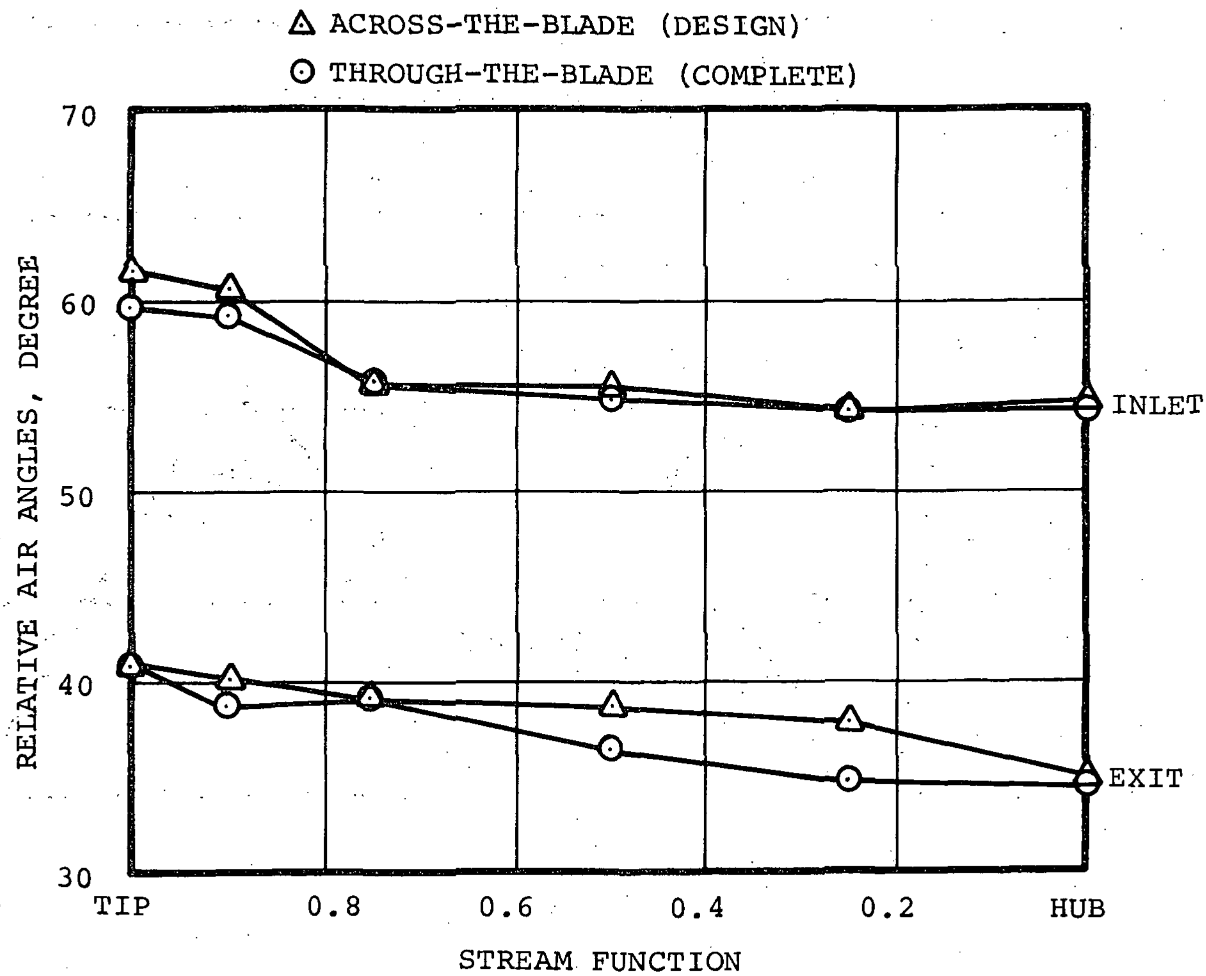

Figure 45. - Comparison of Stator 1A Relative Air Angles Between Initial and Final Design Solutions.

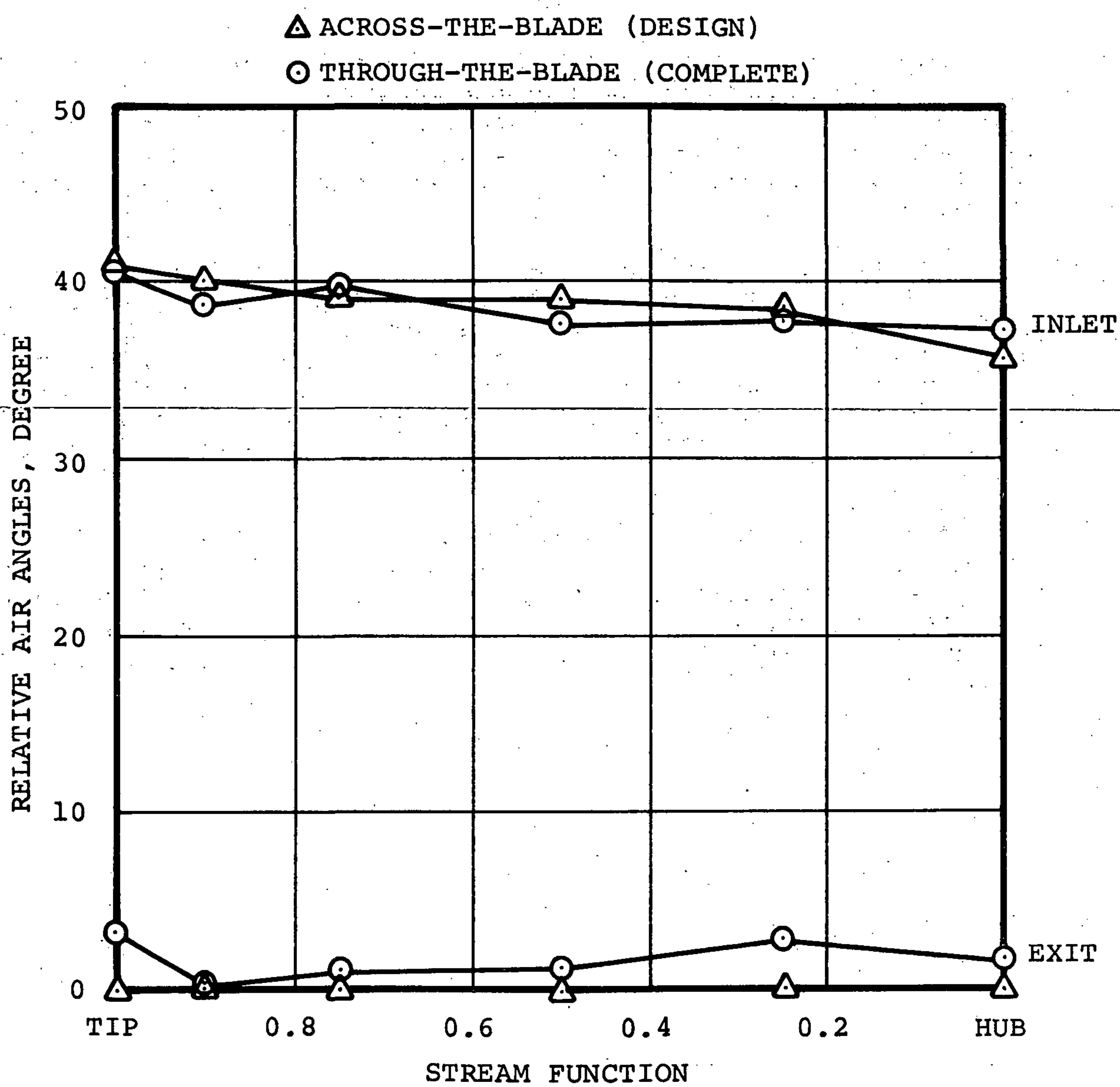

Figure 46. - Comparison of Stator 1B Relative Air Angles Between Initial and Final Design Solutions.

Distribution of the aerodynamic and blade blockage for the tip, 50-percent flow, and hub streamline for each stator vane are contained in figures 47 through 52. Aerodynamic blockage was again distributed as in the tandem rotor design.

The rate of angular momentum decreases through each of the stators as shown in figures 53 through 56. These values were obtained from the blade-to-blade calculation. Complete deswirl of the air was not achieved by the second stator. However, the amount of remaining angular momentum was not considered detrimental to the performance of a second stage.

Stator diffusion factors are compared in figures 57 and 58. Final 1A values for the design and complete through-the-blade analysis are somewhat lower than the across-the-blade analysis. For 1B, however, the design and complete through-the-blade analysis are not consistent due to streamline shifts caused by the rotor/stator blade interaction. Where the difference is largest, toward the hub in stator 1B, the diffusion factor is less which is advantageous from a loss consideration.

Final stator loadings along the tip, 50-percent flow, and hub streamlines for stators 1A and 1B are shown in Figures 59 through 64. The tip streamline loadings for both stators display the highest loading near the leading edge due to the more positive incidence angles. However, loadings are smooth and should provide acceptable performance.

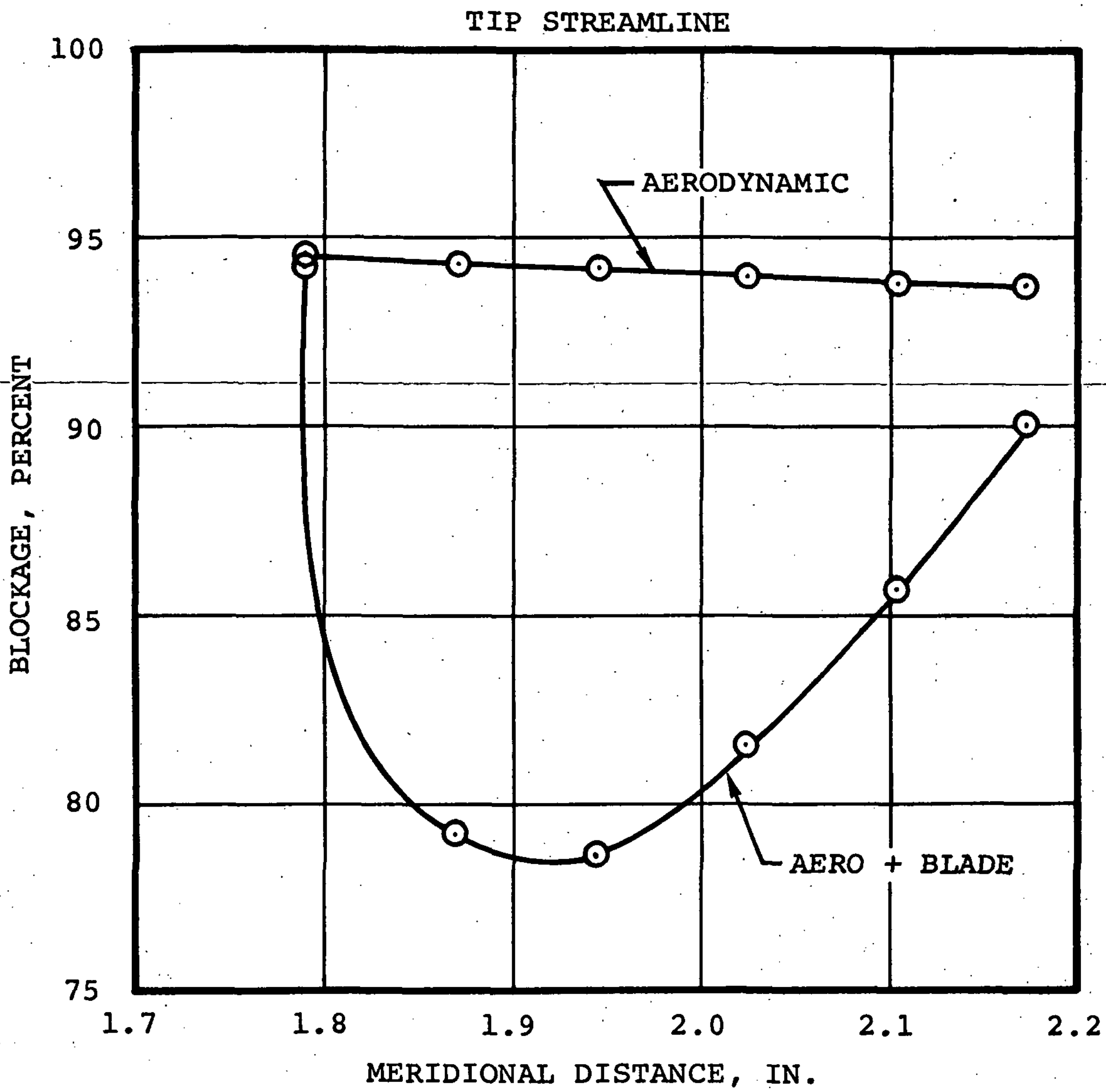

Figure 4. - Stator 1A Blockage Distribution.

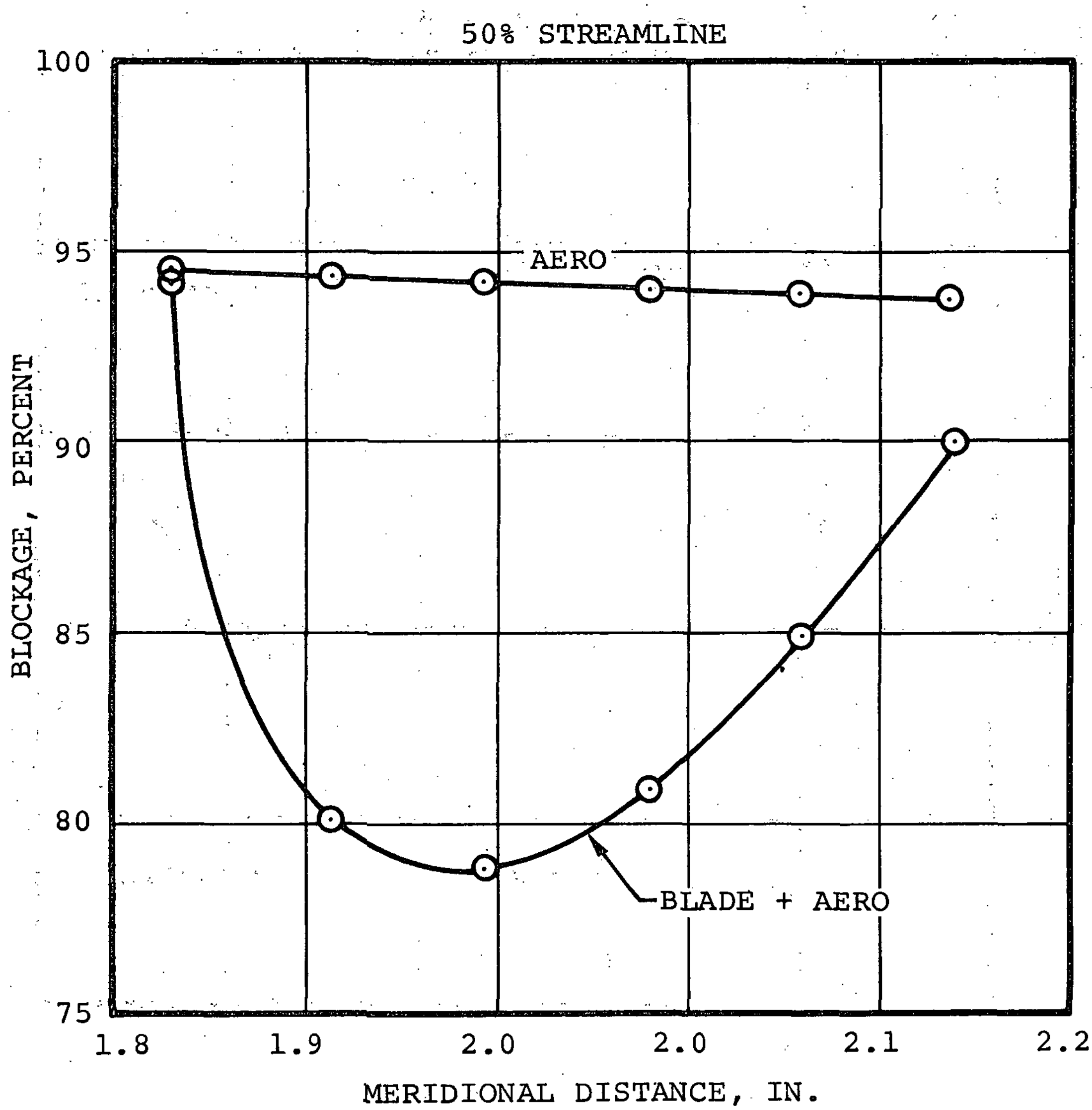

Figure 48. - Stator 1A Blockage Distribution.

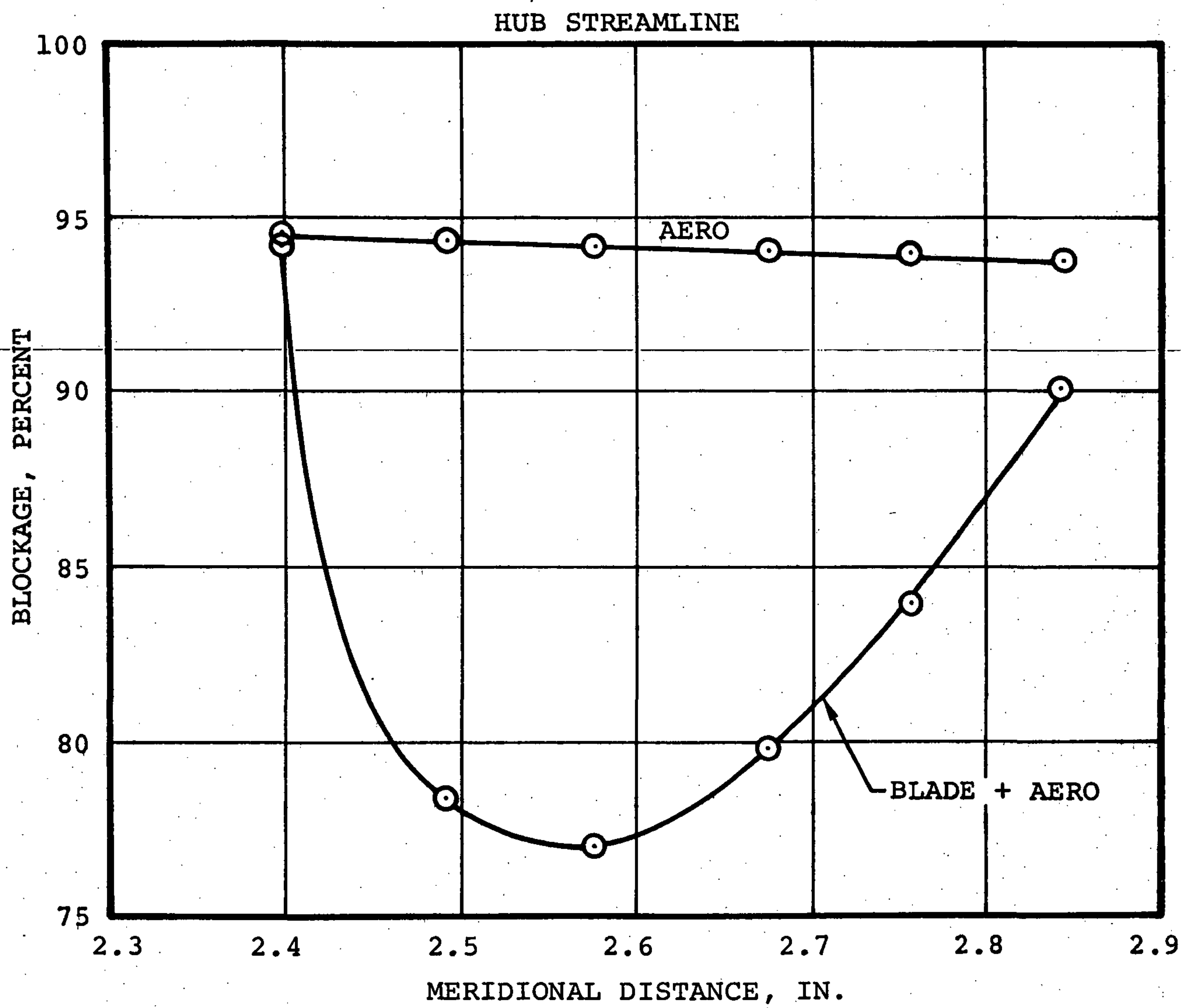

Figure 49. - Stator 1A Blockage Distribution.

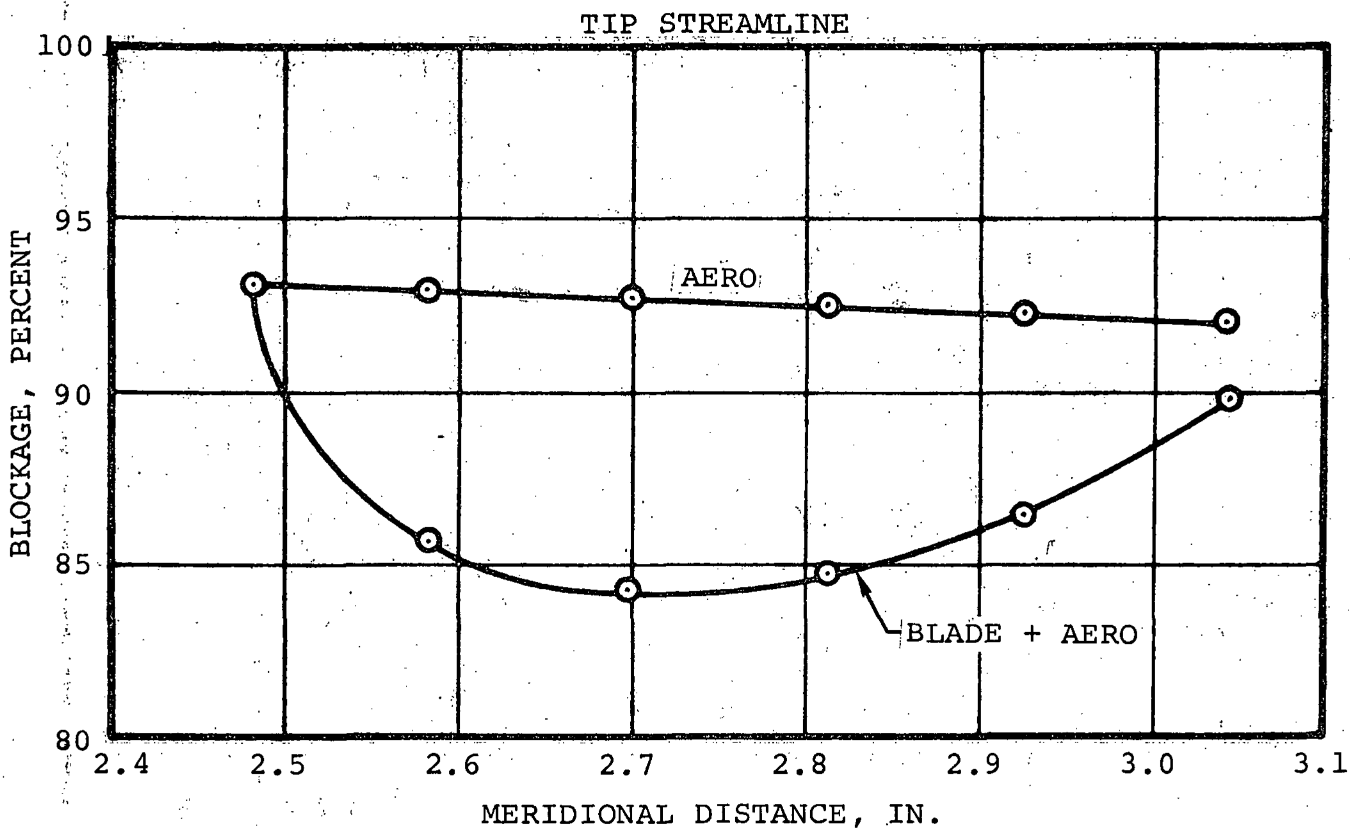

Figure 50. - Stator 1B Bockage Distribution.

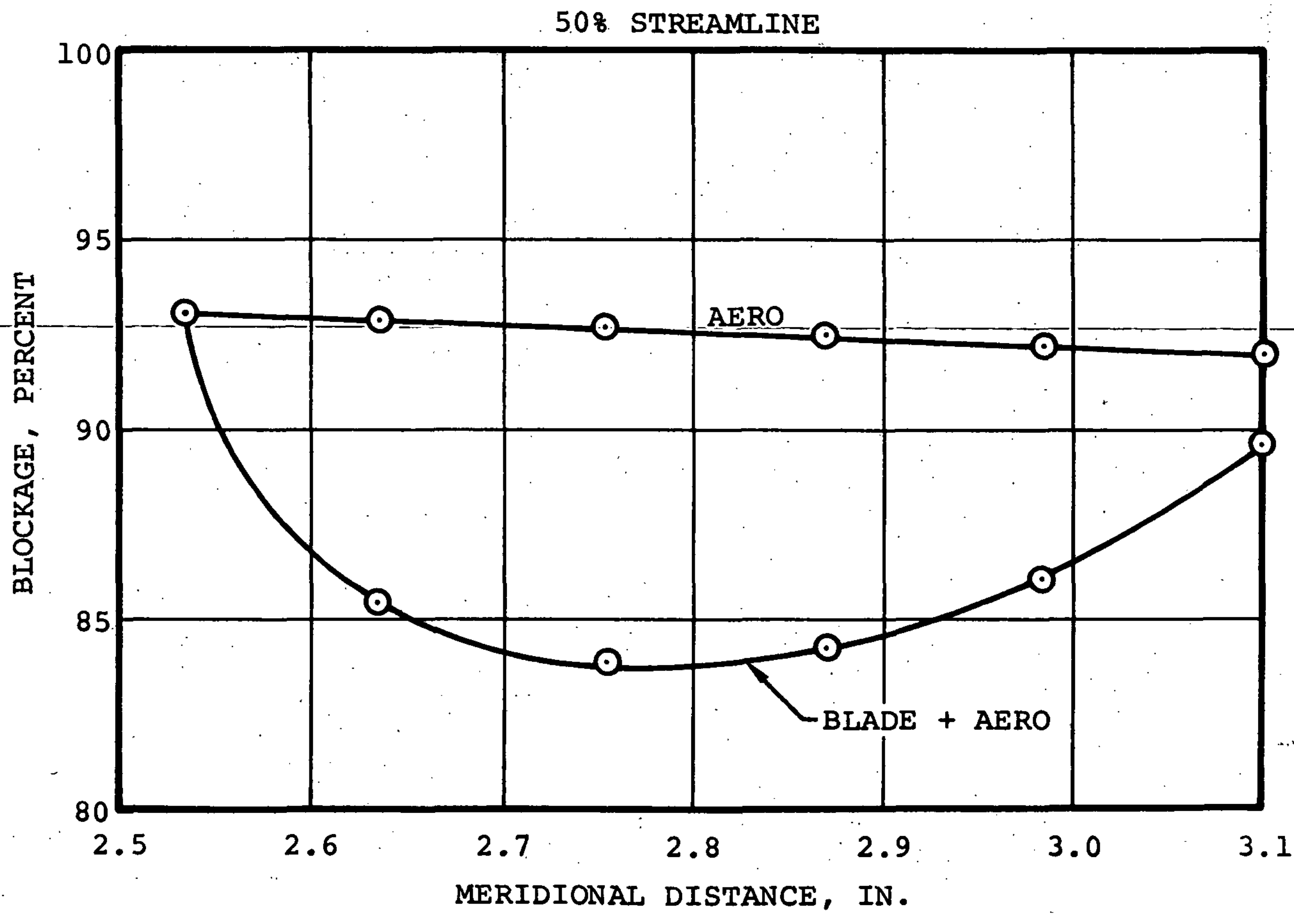

Figure 51. - Stator 1B Blockage Distribution.

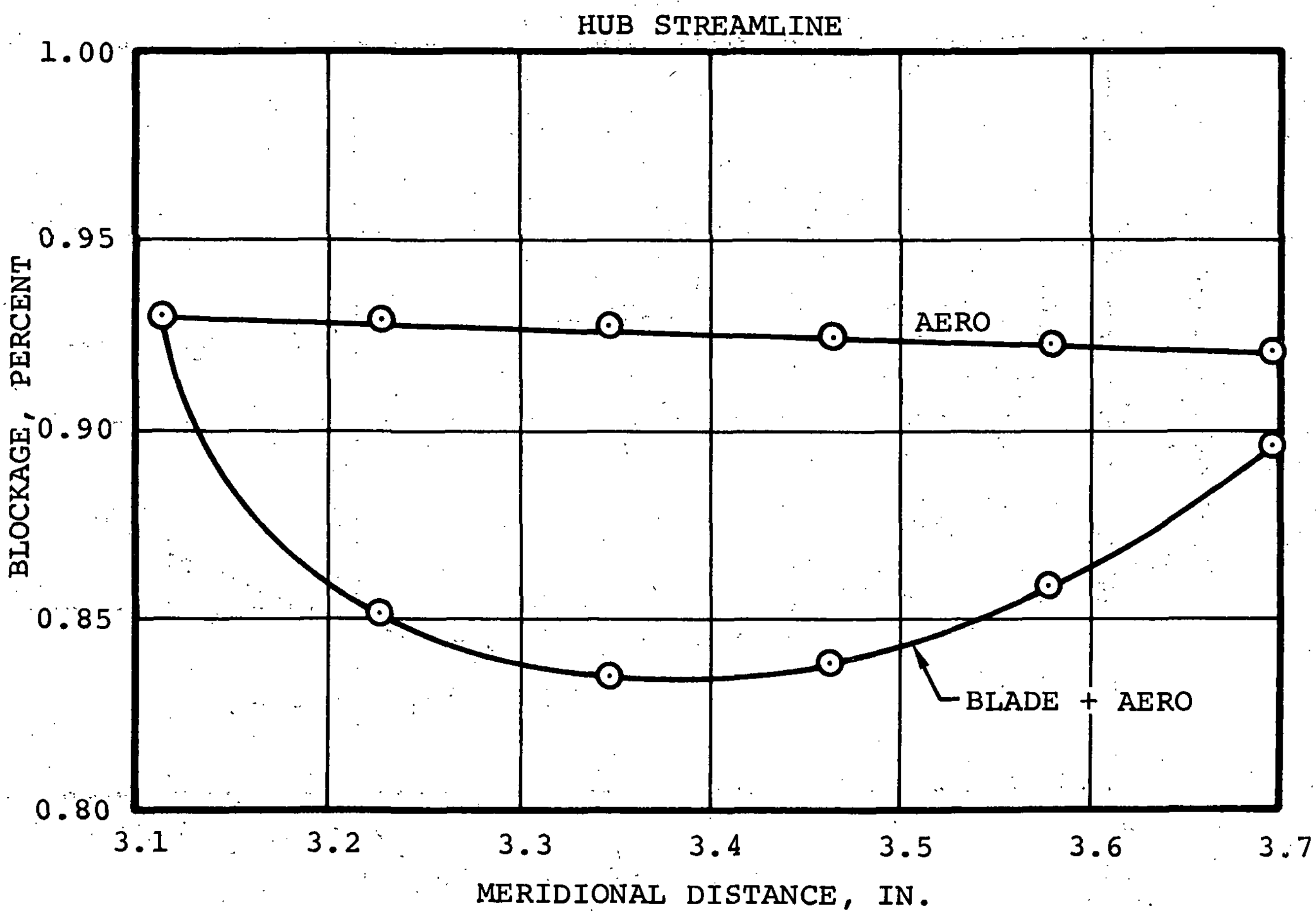

Figure 52. - Stator 1B Blockage Distribution.

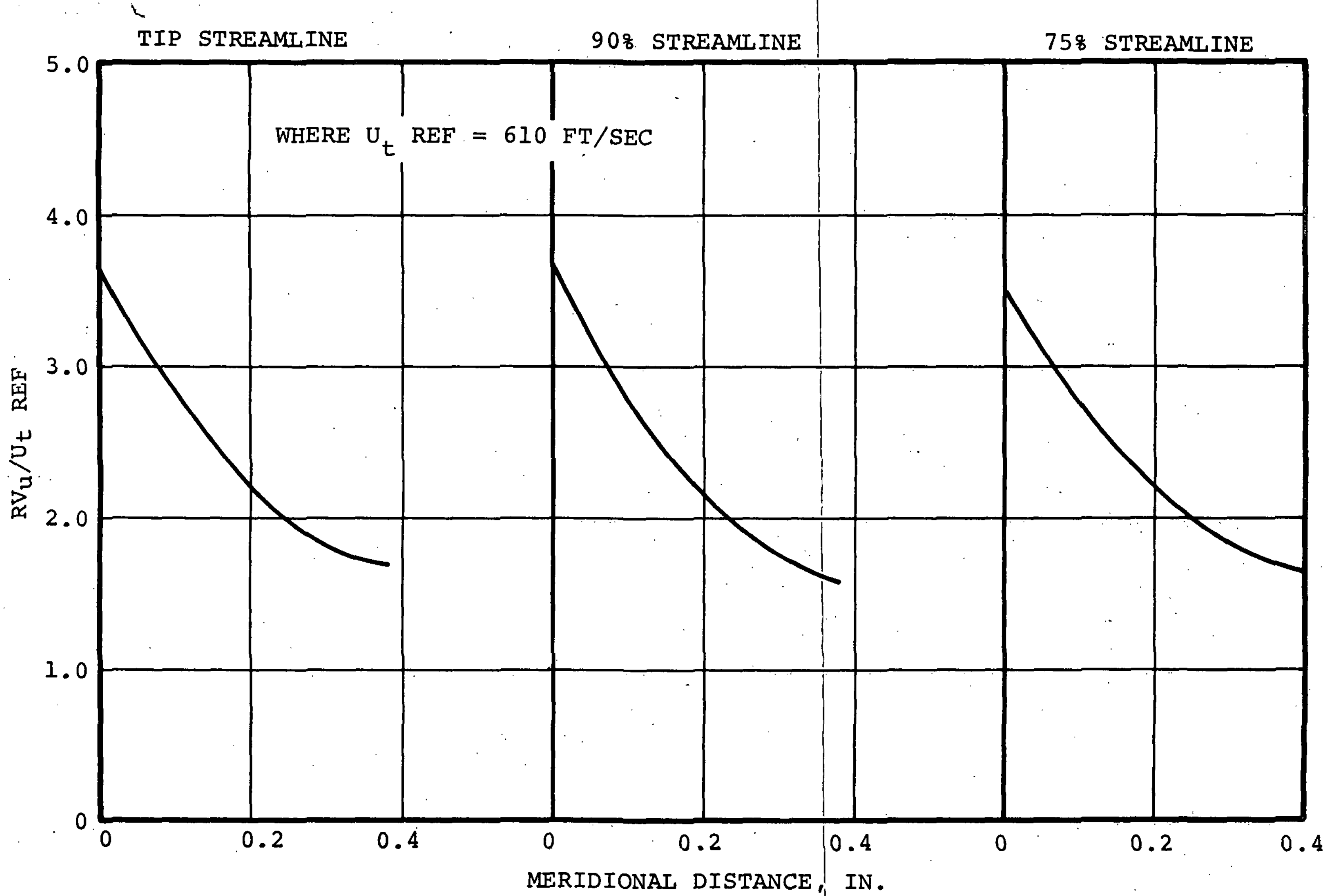

Figure 53. - Stator 1A Streamline Energy Distribution.

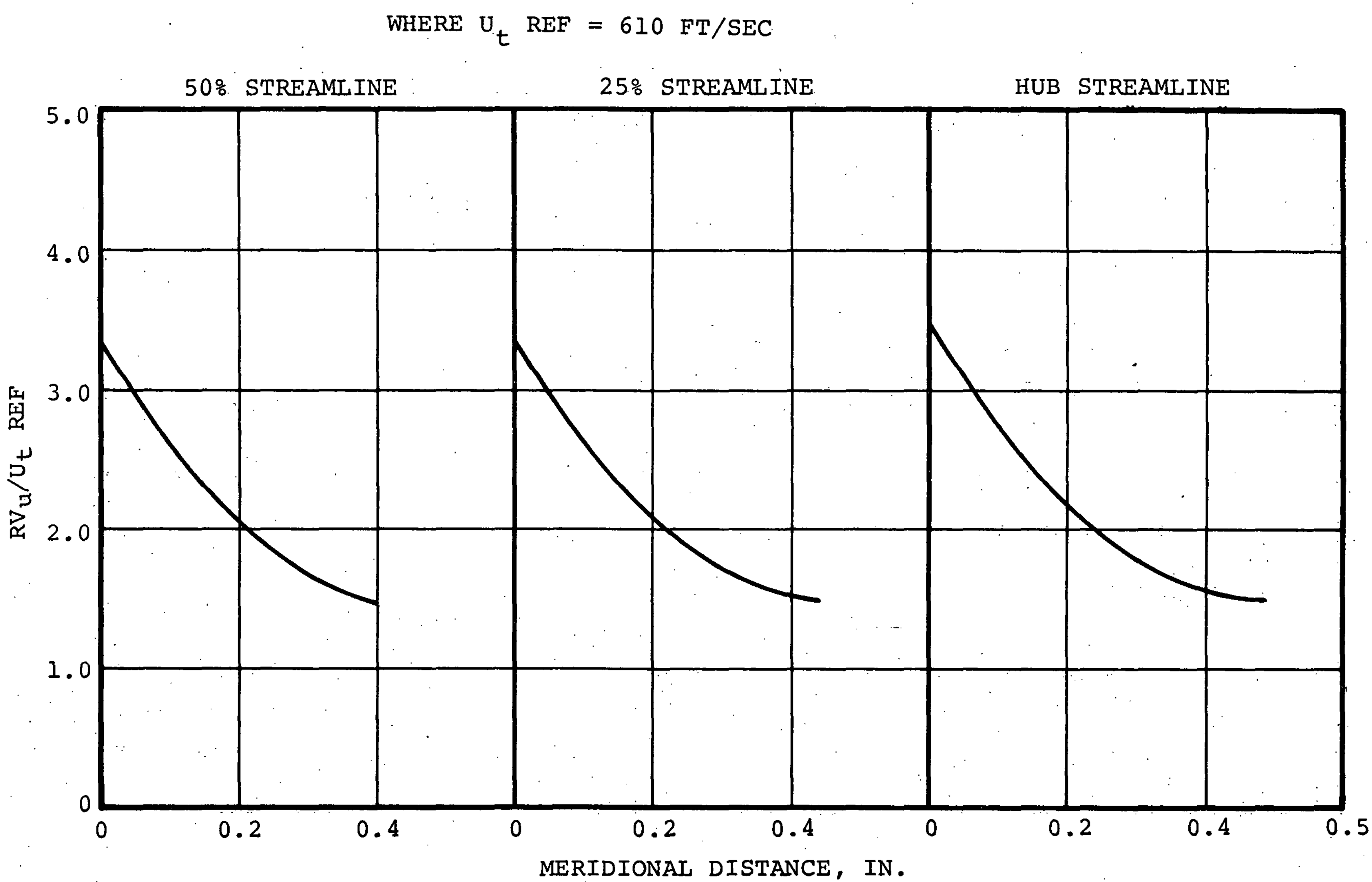

Figure 54. - Stator 1A Streamline Energy Distribution.

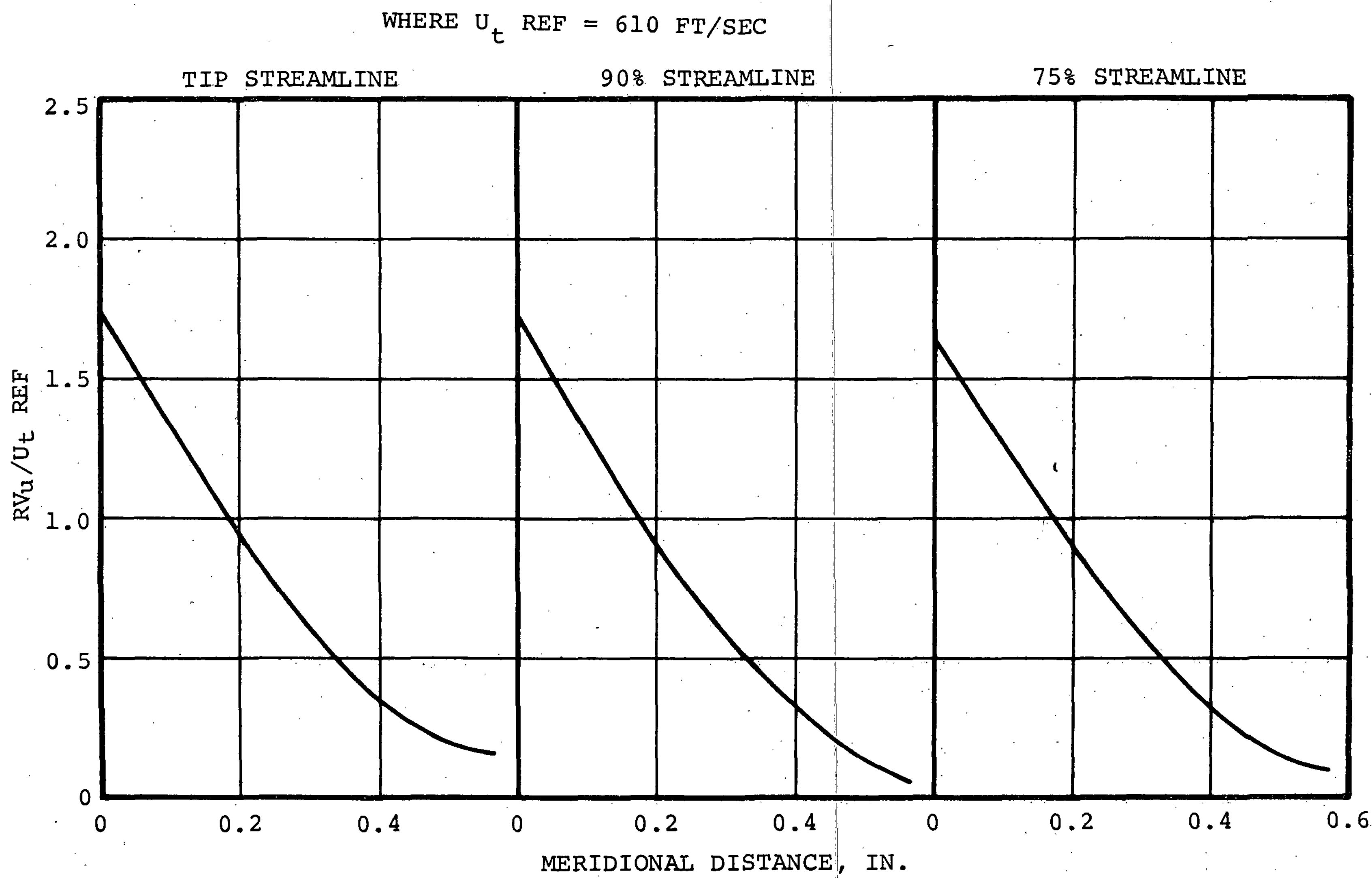

Figure 55. - Stator 1B Streamline Energy Distribution.

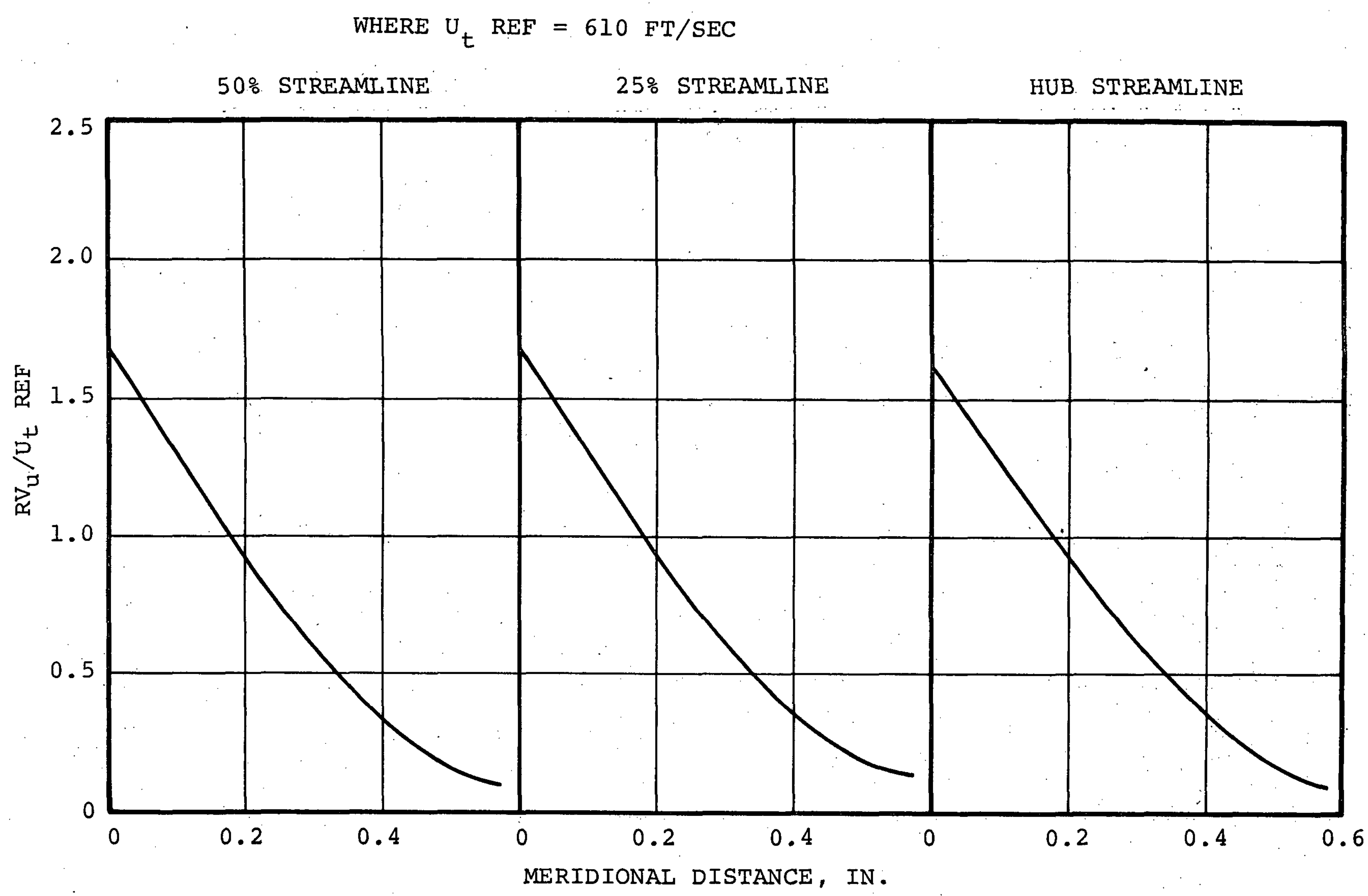

Figure 56. - Stator 1B Streamline Energy Distribution.

$$D = 1.0 - \frac{V_2}{V_1} + \frac{r_2 V_{u_2} - r_1 V_{u_1}}{2\bar{r}\sigma V_1}$$

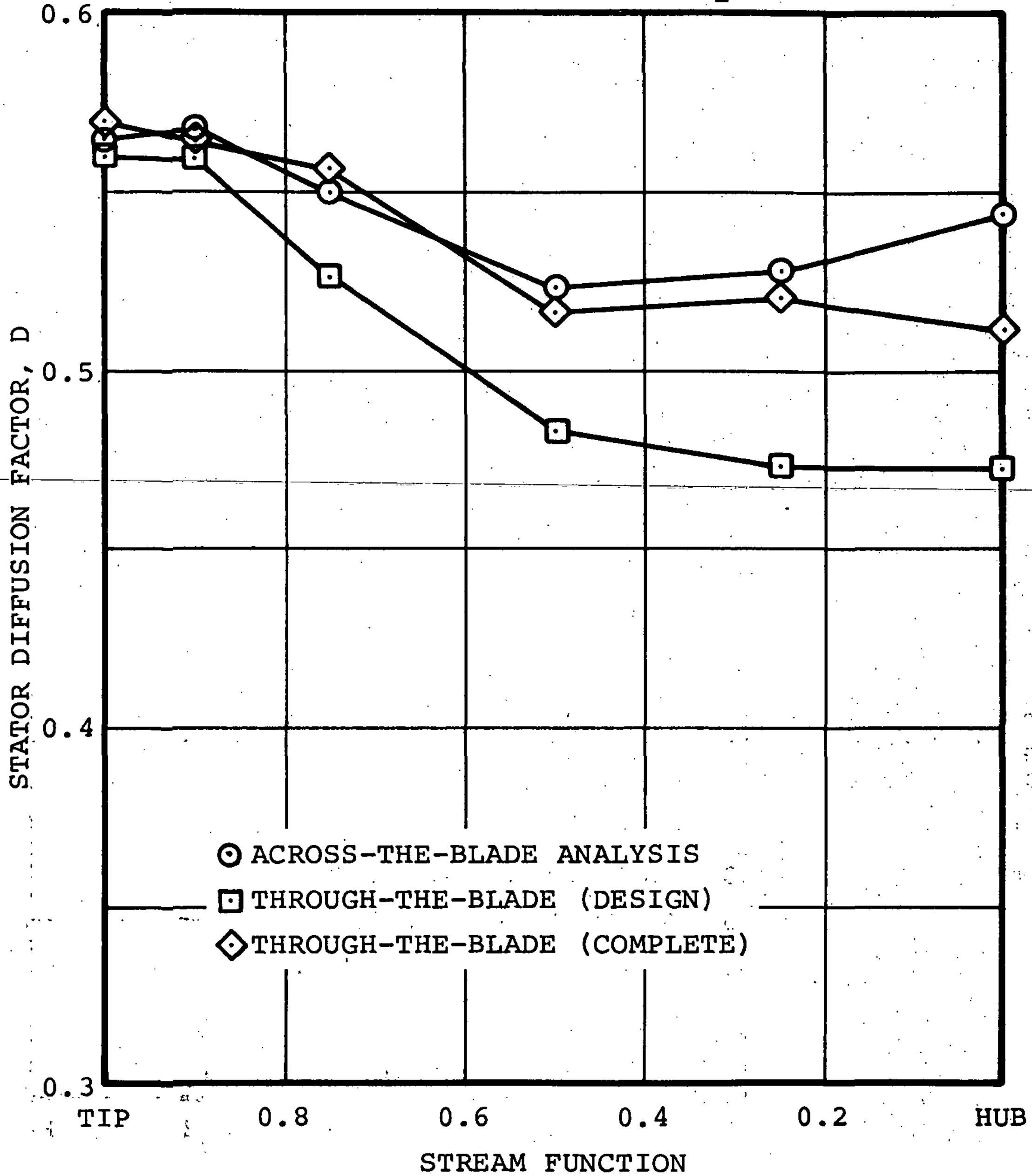

Figure 57. - Stator 1A Diffusion Factor Distribution.

$$D = 1.0 - \frac{V_2}{V_1} + \frac{r_2 V_{u_2} - r_1 V_{u_1}}{2\bar{r}\sigma V_1}$$

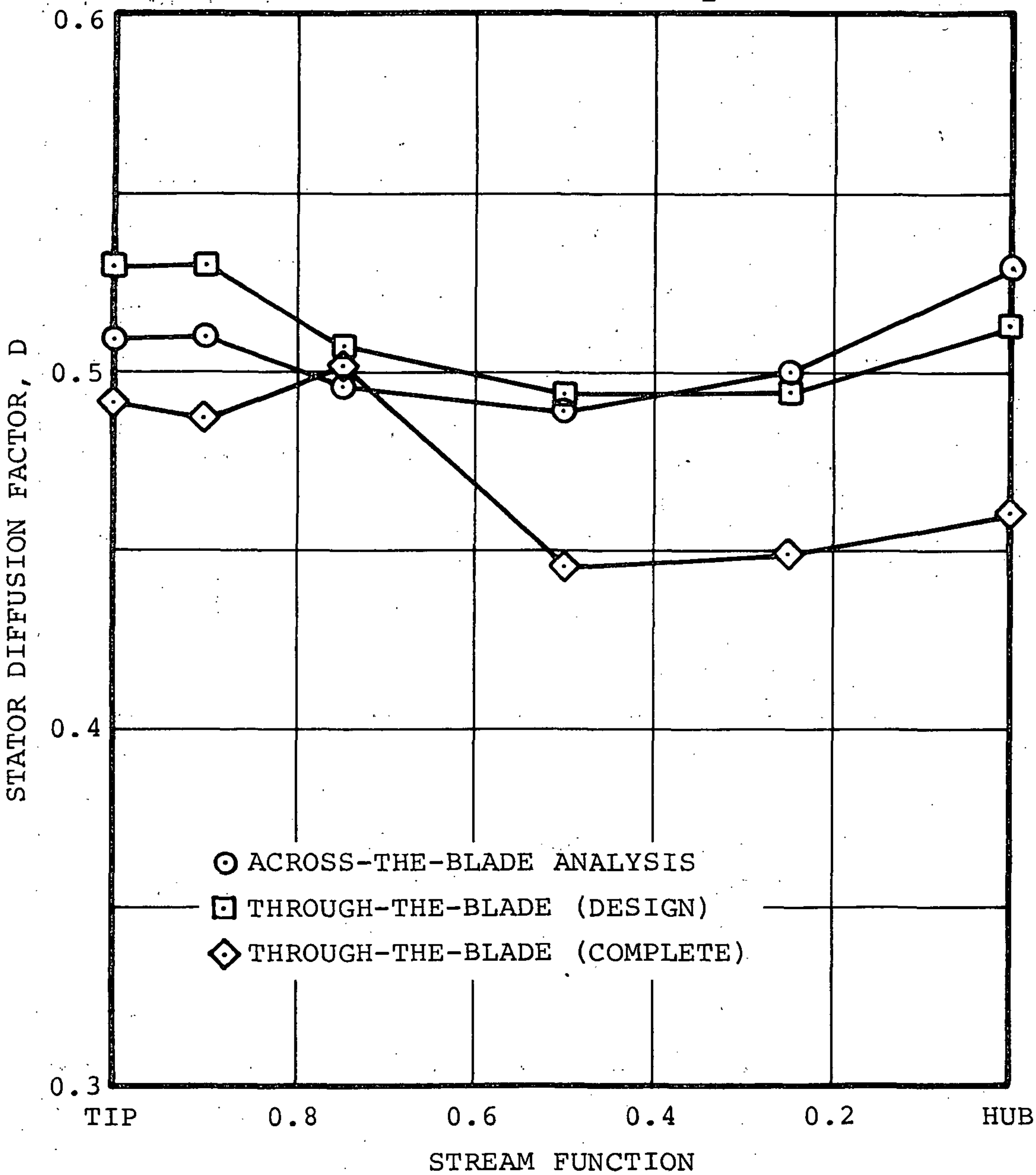

Figure 58. - Stator 1B Diffusion Factor Distribution.

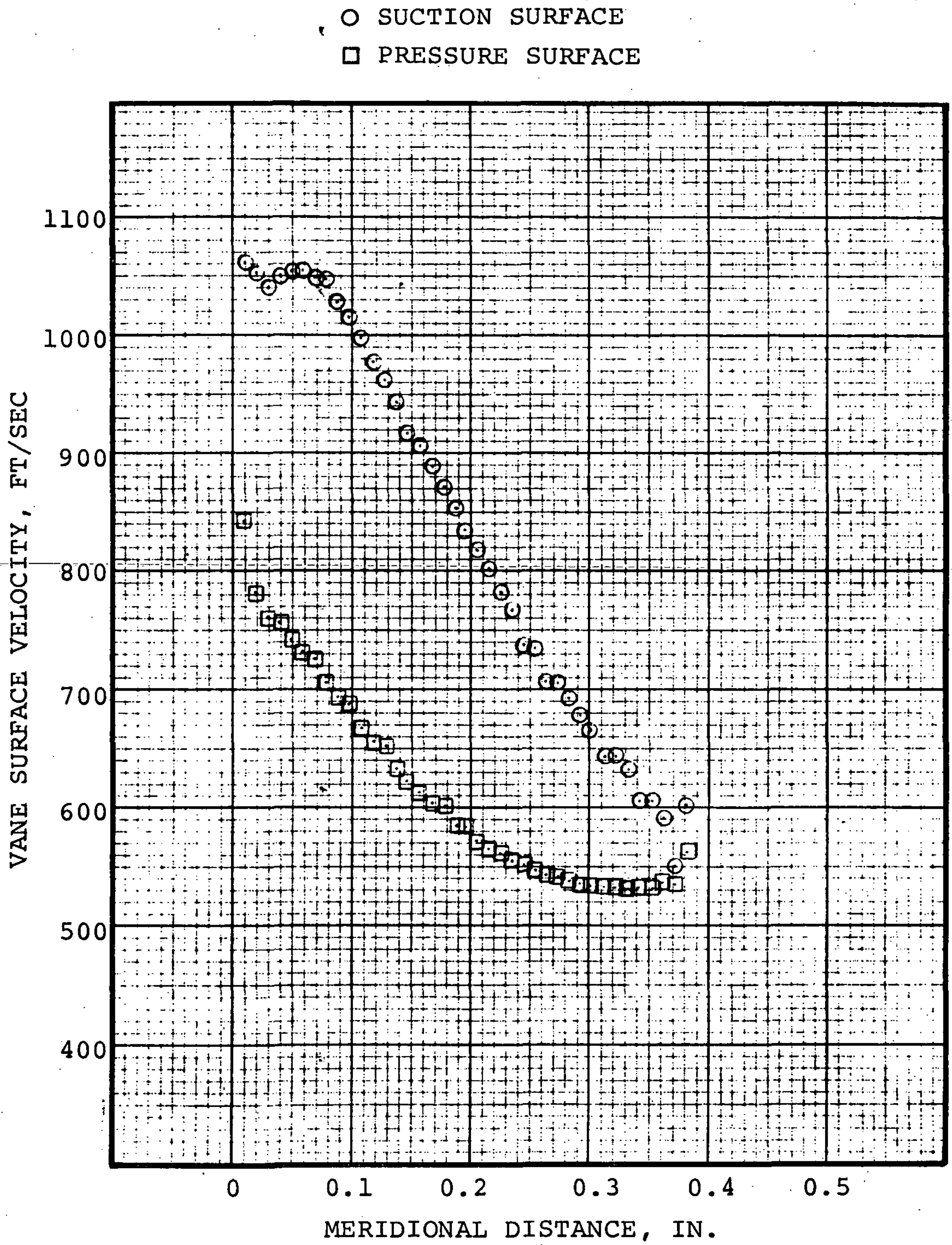

Figure 59. - Stator 1A Loading - Tip Streamline.

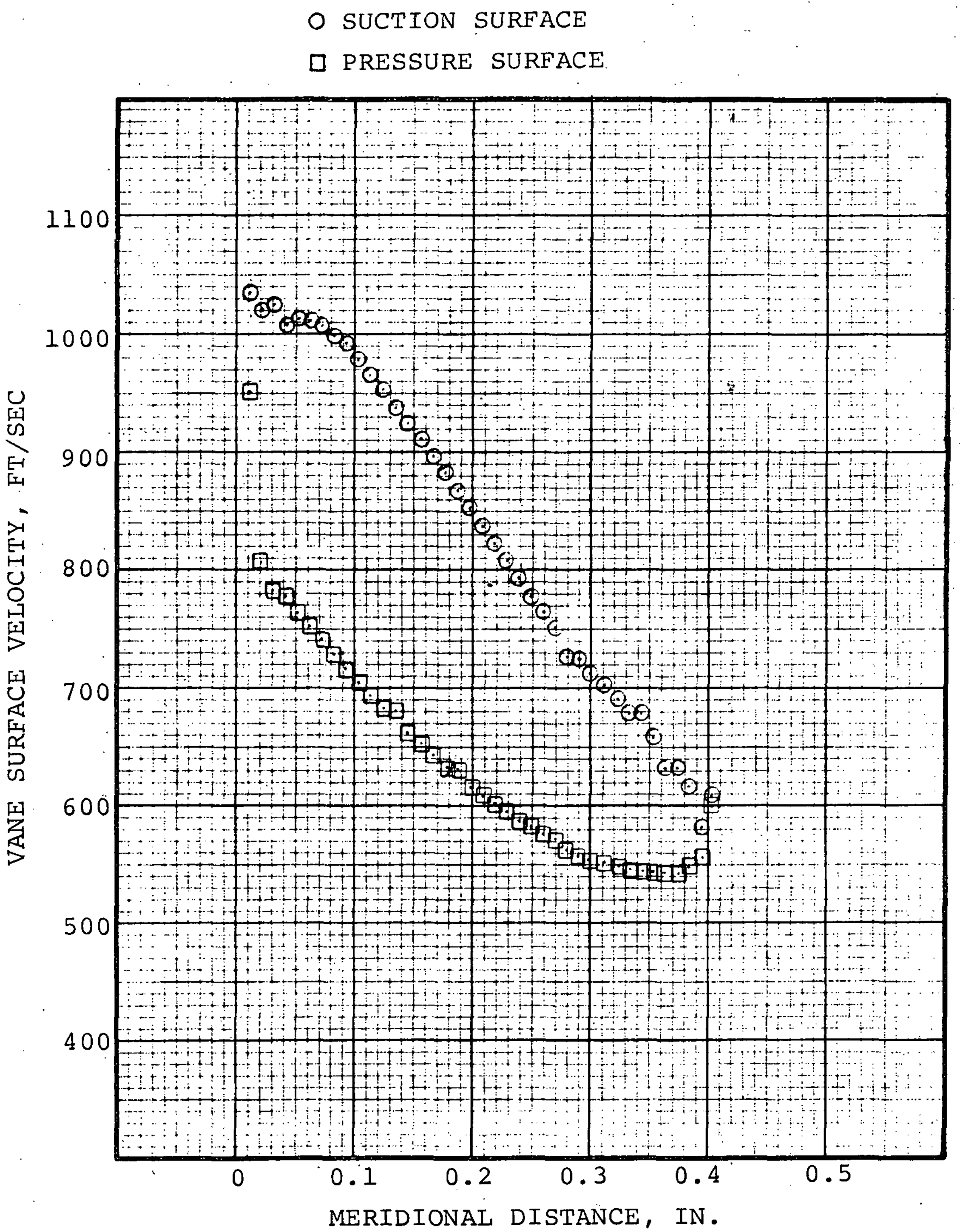

Figure 60. - Stator 1A Loading - Mean (50%) Streamline.

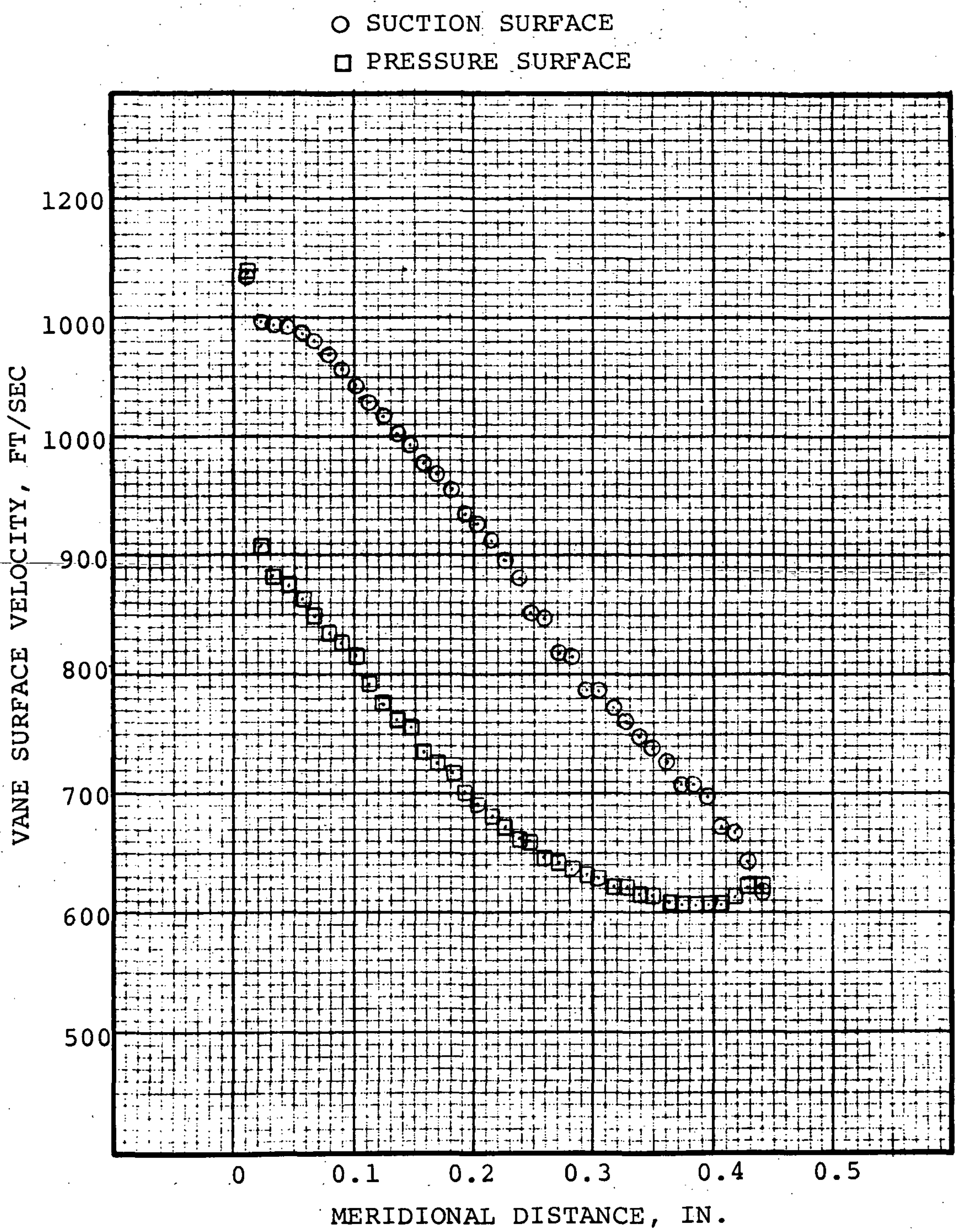

Figure 61. - Stator 1A Loading - Hub Streamline.

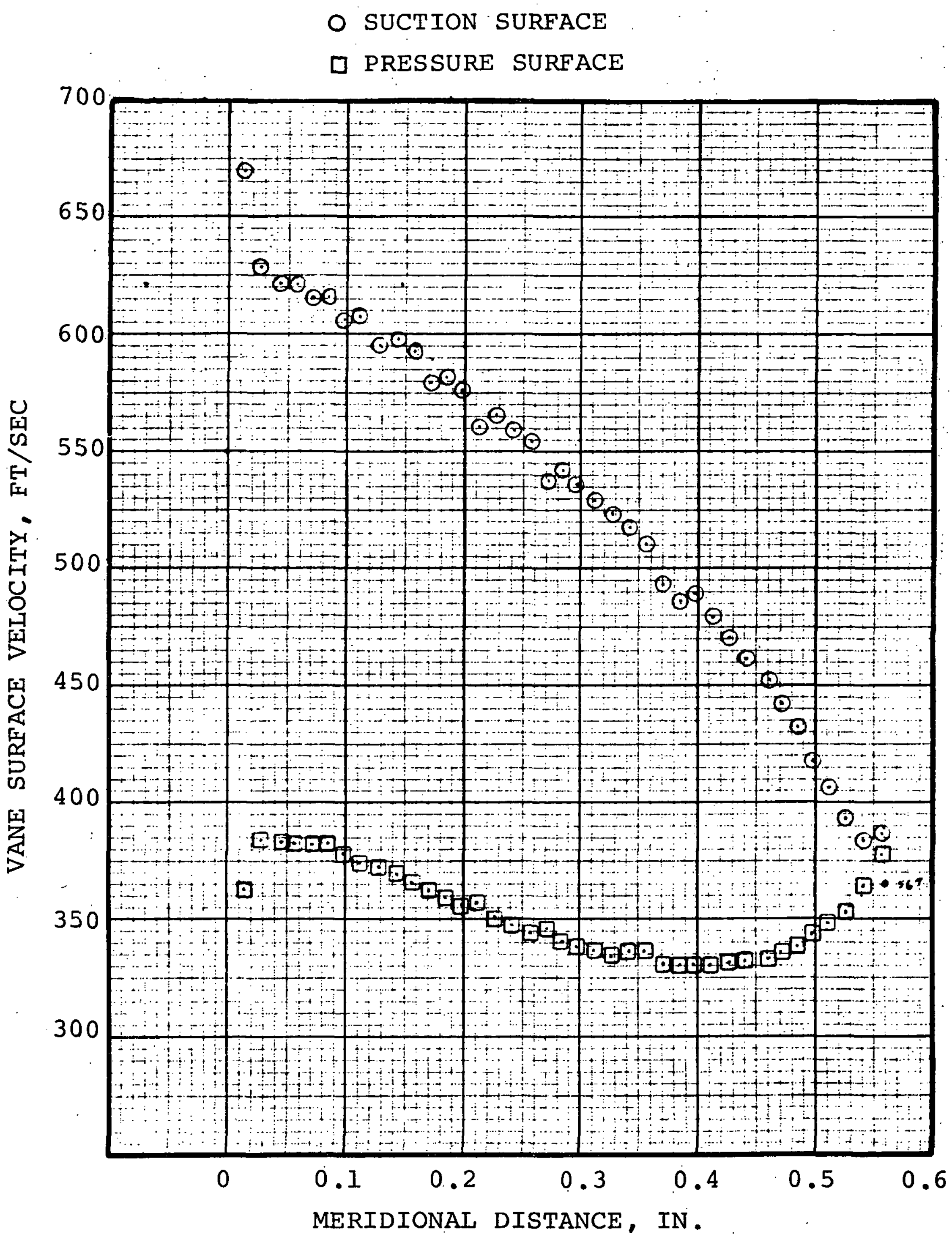

Figure 62. - Stator 1B Loading - Tip Streamline.

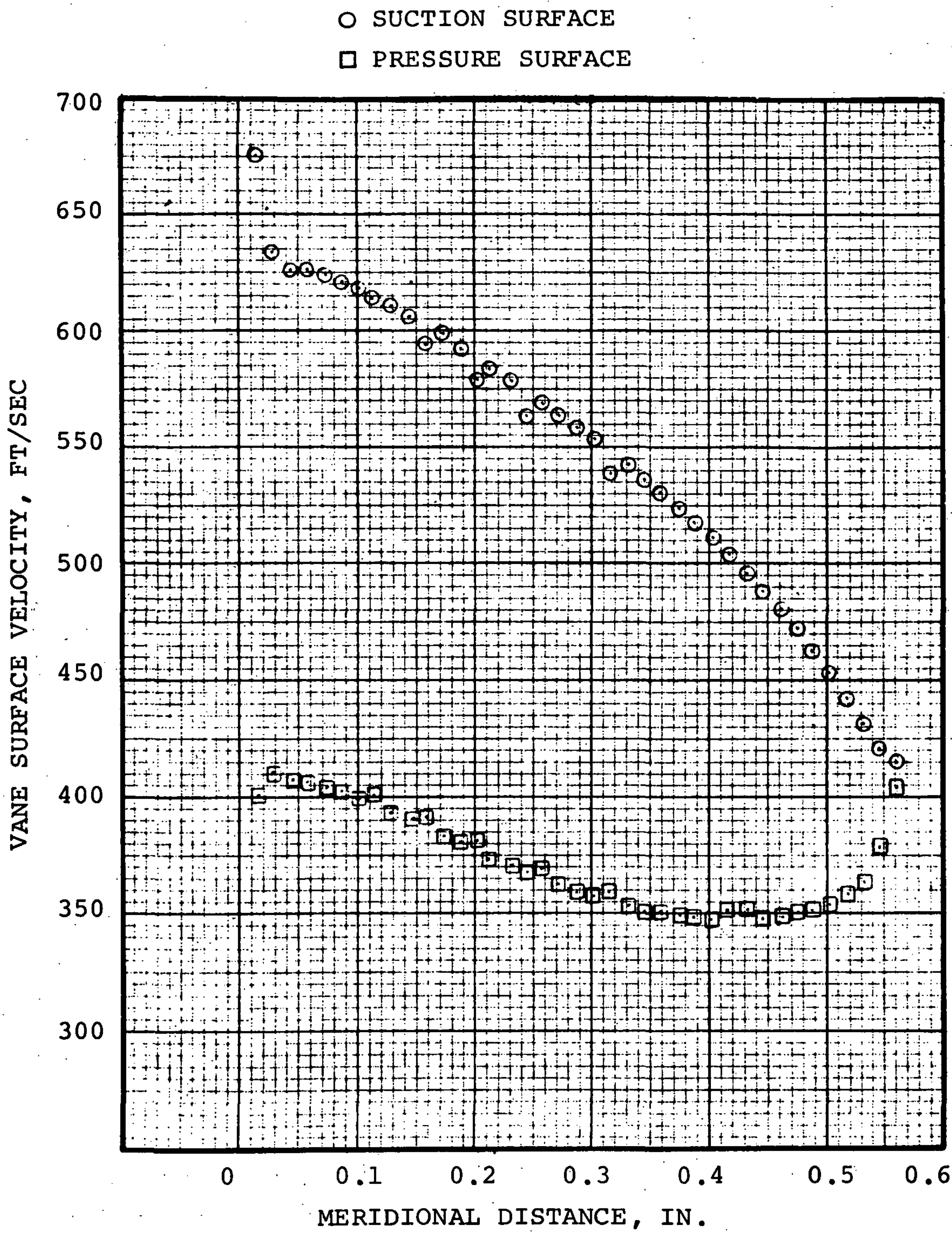

Figure 63. - Stator 1B Loading - Mean (50%) Streamline.

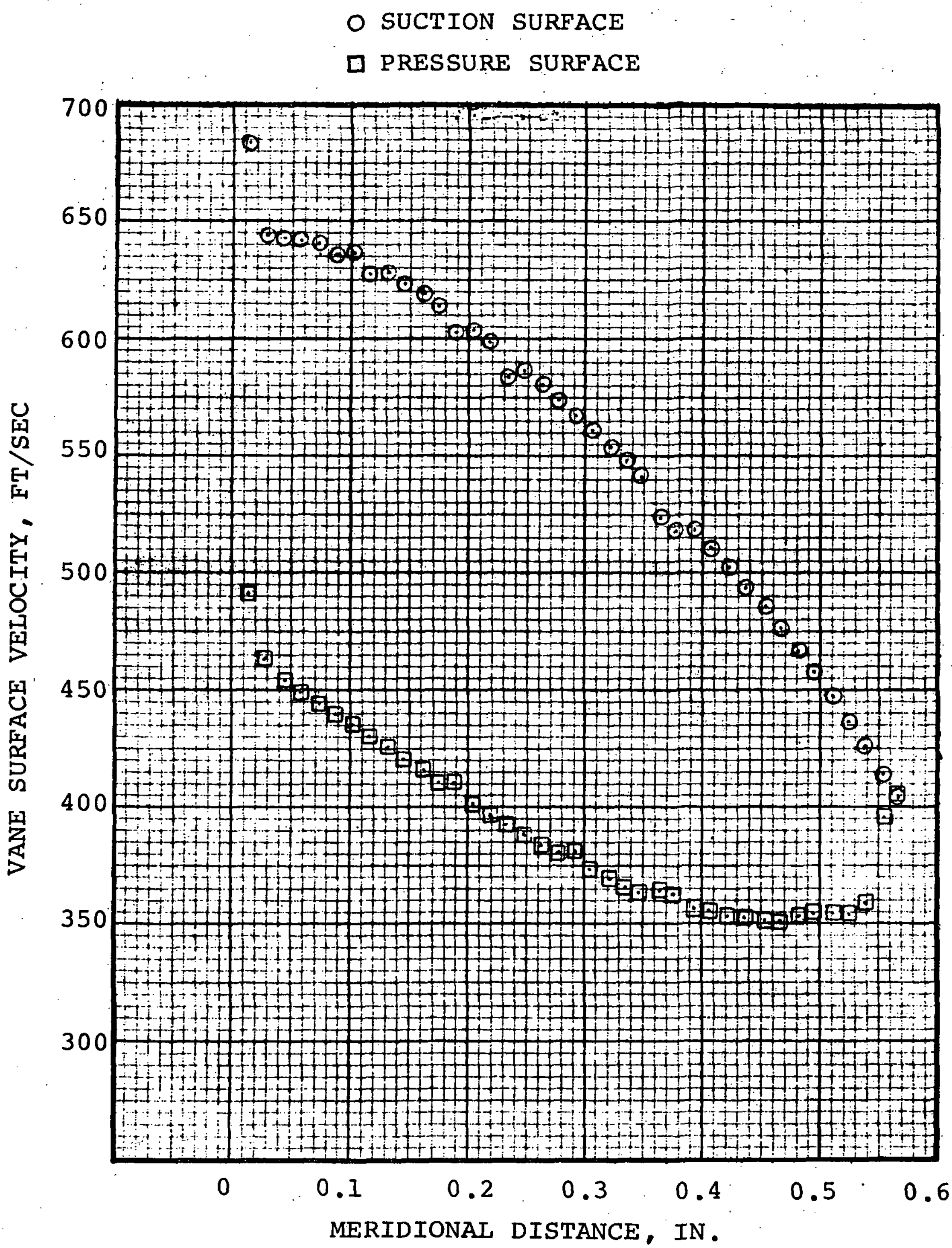

Figure 64. - Stator 1B Loading - Hub Streamline.

Boundary Layer Control

The purpose of any boundary layer control device is to prohibit flow separation from the confining walls. As a result of the inherent diffusion for the compression process, the boundary layers within a compressor are subject to adverse pressure gradients and, therefore, grow rapidly. Judicious design can minimize, but not eliminate, this growth. One of the objects for using tandem rotors and stators is to start each blade row with a new boundary layer. This permits the mixing and re-energization of low energy fluid at several points within the stage. Another attractive technique for removing boundary layers internal to the compressor stage is to bleed off fluid through the shroud or hub walls. Since these boundary layers grow continuously through the stage, a significant benefit should be possible. Location of bleed parts should be such that boundary layer removal is accomplished prior to probable separation regions. The new boundary layer created by the removal of low energy fluid is then better able to withstand adverse pressure gradient conditions, thereby inhibiting flow separation.

Analysis of the impeller boundary layers was accomplished as part of the finite difference blade-to-blade program. The subroutine for computing boundary layer properties is based on the method of Von Doenhoff and Tetervin (Ref. 11) as modified by Garner (Ref. 12). This program uses the free-stream velocities along flow surfaces, as predicted by the potential flow solution, to calculate boundary layer properties along streamlines. Flow separation is said to occur at the location where the shape factor (H) is equal to 2.2

In examining the blade row boundary layers, the hub and tip streamlines are of primary interest since flow separation on the blade surface in these locations may influence conditions circumferentially across the end walls. The blade surface boundary layers of interest have been plotted as curves (figures 65 through 71) with momentum thickness as a function of surface length. Results for Rotor 1A are shown on figure 65. Only the hub streamline was analyzed here. The potential flow field for the tip section is not adequately defined from the standpoint of the actual shock structure interval to the blade row to permit a valid solution of boundary layer conditions. The hub region of the first rotor does not indicate any regions of incipient separation. In general, the flow conditions exiting the first rotor should be sufficiently stable such that an external bleed system is not necessary prior to the second rotor.

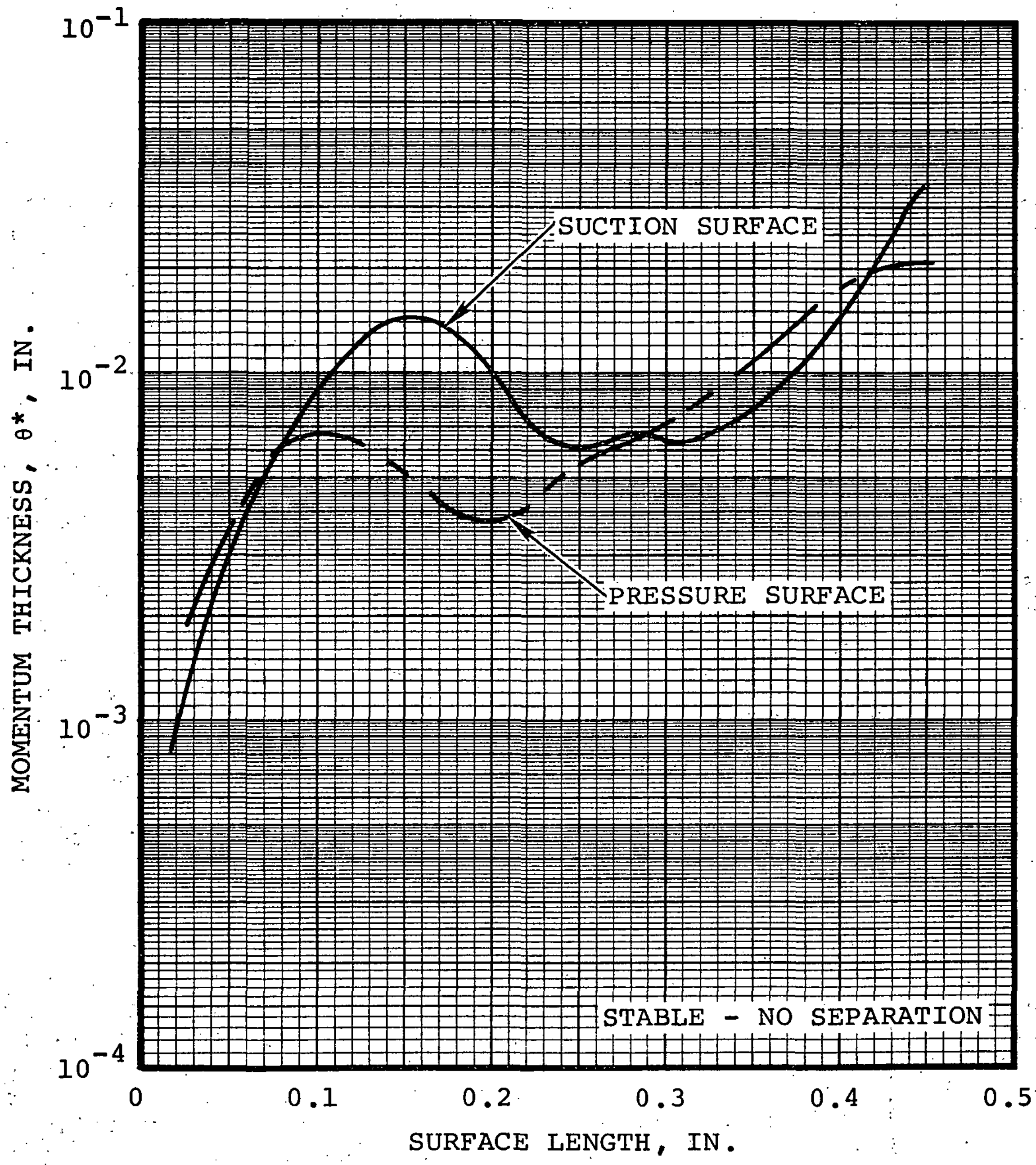

Figure 65. - Rotor 1A Blade Surface Boundary Layers - Hub Streamline.

Blade surface boundary layers for Rotor 1B are shown on figures 66 and 67 for the tip and hub streamlines, respectively. Note that a possible separation condition is predicted along the blade suction surface for the tip streamline. This potential separation zone occurs near the trailing edge of the blade in a region which should have little influence on the overall rotor performance. However, this might affect flow conditions entering the first stator row so that it may be desirable to install a series of bleed ports in the shroud wall between the second rotor row and first stator row. The consideration here being that a separated zone or a region of low energy fluid could possibly propagate a stall condition within the stators, thereby seriously penalizing the pressure recovery in this region. Thus, provision will be made for the installation of bleed ports on the shroud wall between the second rotor and first stator rows to permit experimental evaluation of this potential problem area.

Blade surface boundary layers on Stator 1A are shown on figures 68 and 69 for the tip and hub streamlines, respectively. Both streamlines indicate the possibility of separation on the suction surface of the blade. This is not an unusual circumstance and is experienced quite often with high turning stator rows in axial compressors. In fact, previous experience has shown good performance can be obtained with stator sections which are marginally stable with some portion of the blade exhibiting potential flow separation. A stator system was designed and tested where the calculations indicated an even greater separated condition than indicated here. Stage performance was not degraded for these stators, indicating either: (1) the separated area may have been localized to a small region on the blade followed by re-attached flow, or (2) the calculation may be in error such that separation is predicted prematurely. The instrumentation employed in these tests was insufficient to evaluate the existence or extent of flow separation in the stator system.

Since both the hub and tip sections for the first stator indicate a possibility of separated flow, it seems advisable to include bleed ports on both walls between the tandem stator rows. These should be set up to be operated either separately, or simultaneously with the rotor bleed. The recommended bleed port locations for the first-stage conical compressor are shown on figure 70.

Boundary layer conditions for the hub and tip streamlines on Stator 1B are presented on figures 71 and 72, respectively, computed for meanline loading. These results show a small region of possible flow separation along the suction surface for both cases. The effect of a small separated region in this part of the blade should be minimal and, therefore, does not require a bleed system for boundary layer stabilization.

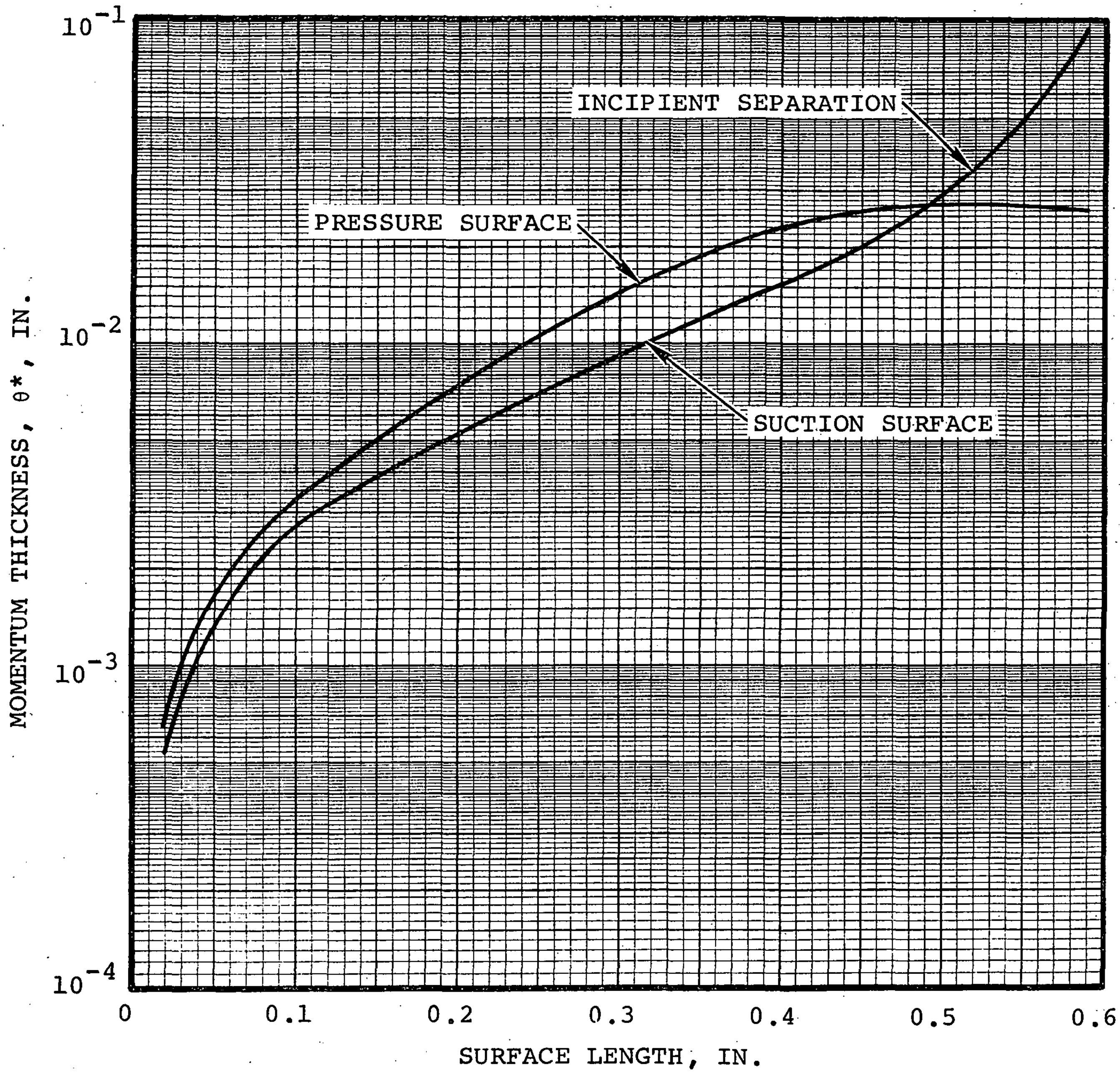

Figure 66. - Rotor 1B Blade Surface Boundary Layers - Tip Section Streamline.

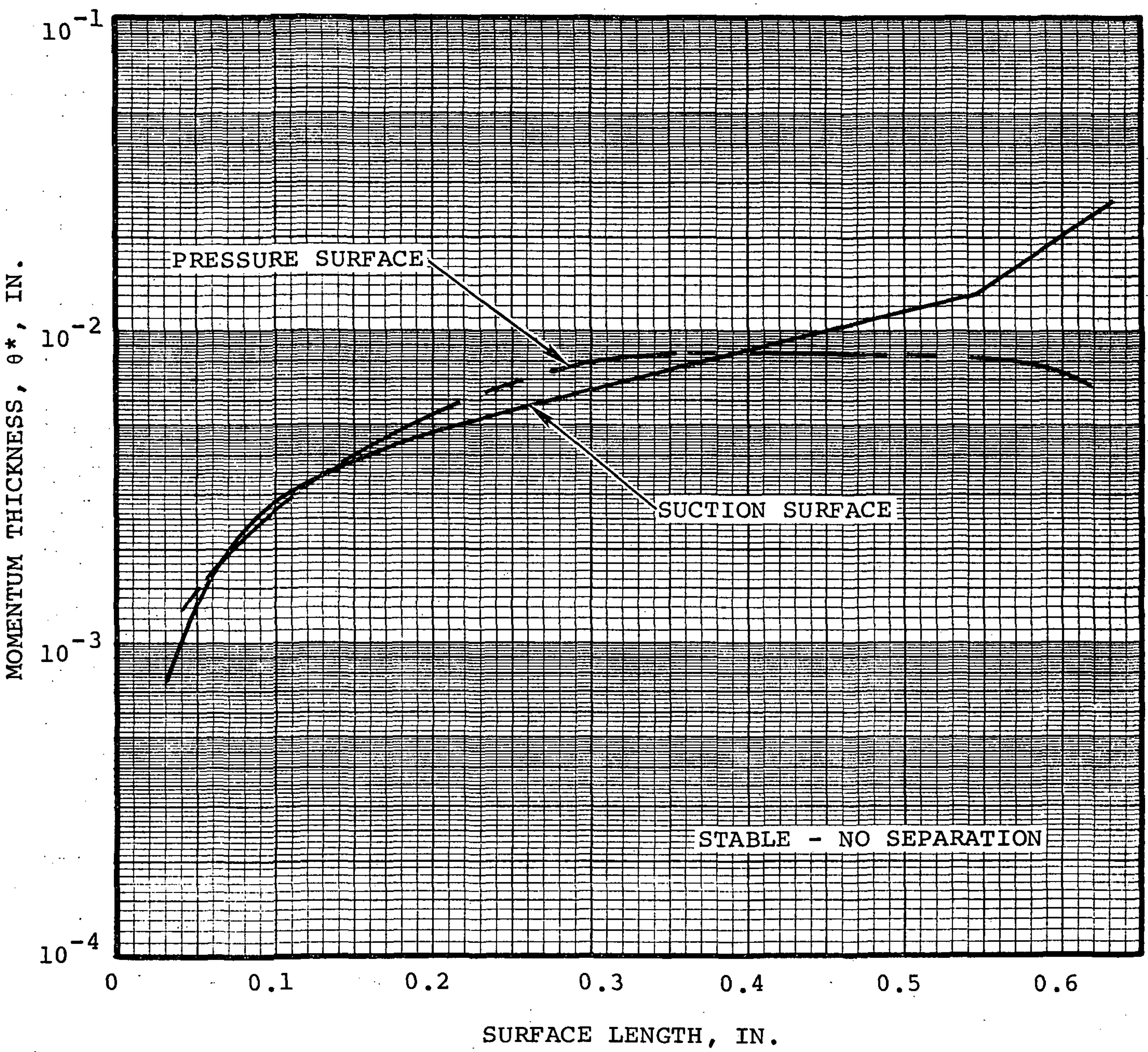

Figure 67. - Rotor 1B Blade Surface Boundary Layers - Hub Streamline.

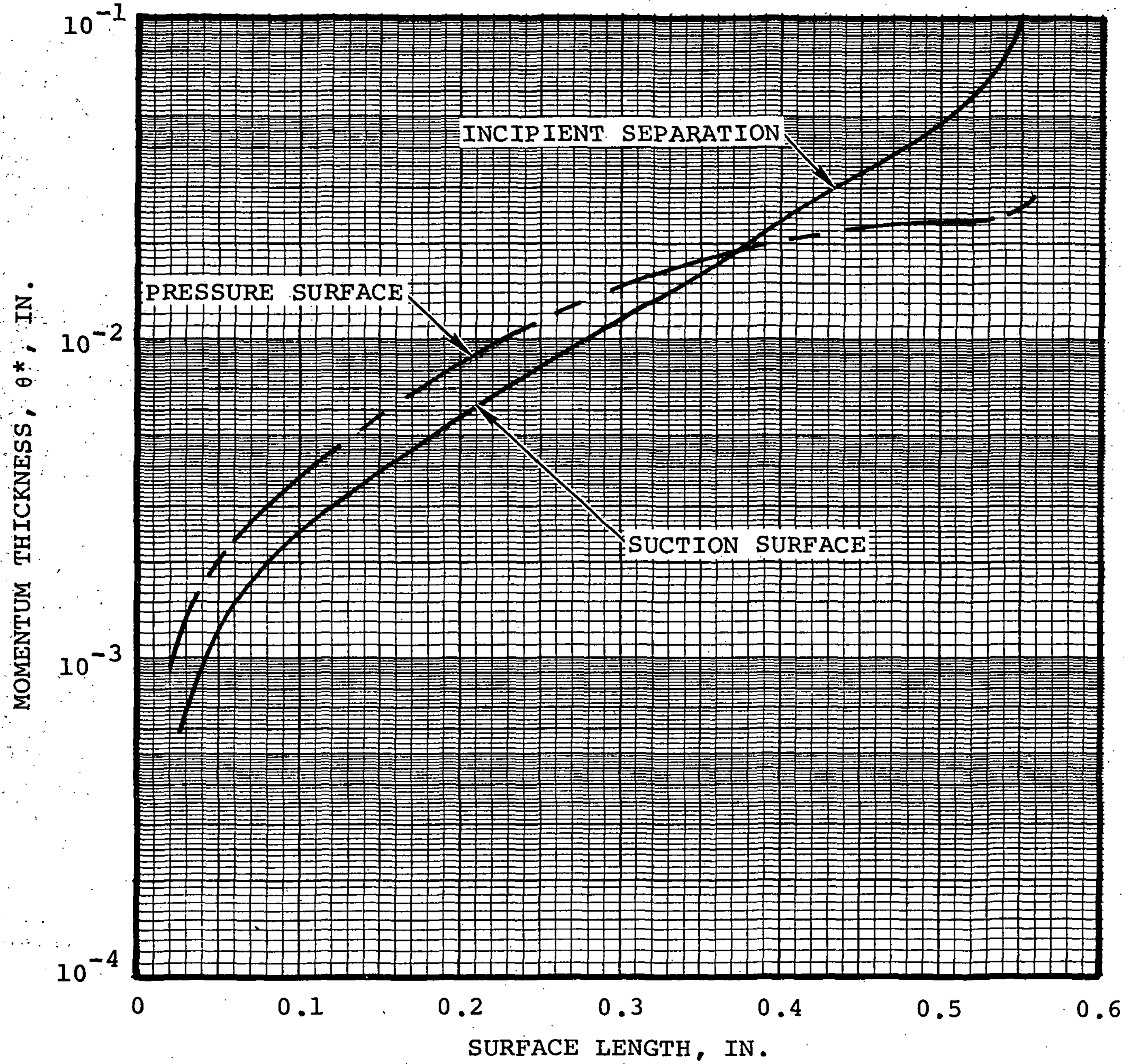

Figure 68. - Stator 1A Blade Surface Boundary Layers - Tip Streamline.

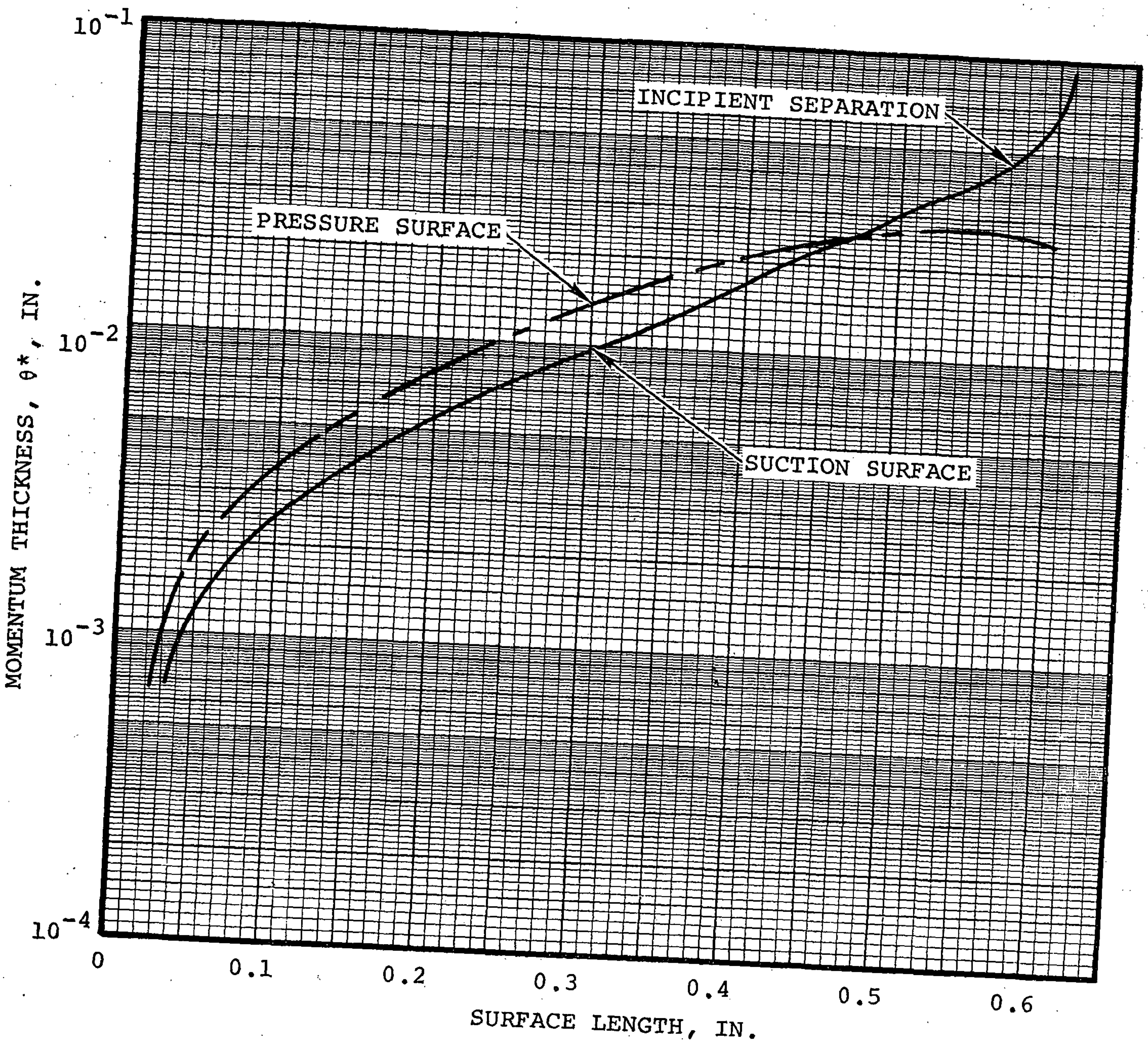

Figure 69. - Stator 1A Blade Surface Boundary Layers - Hub Streamline.

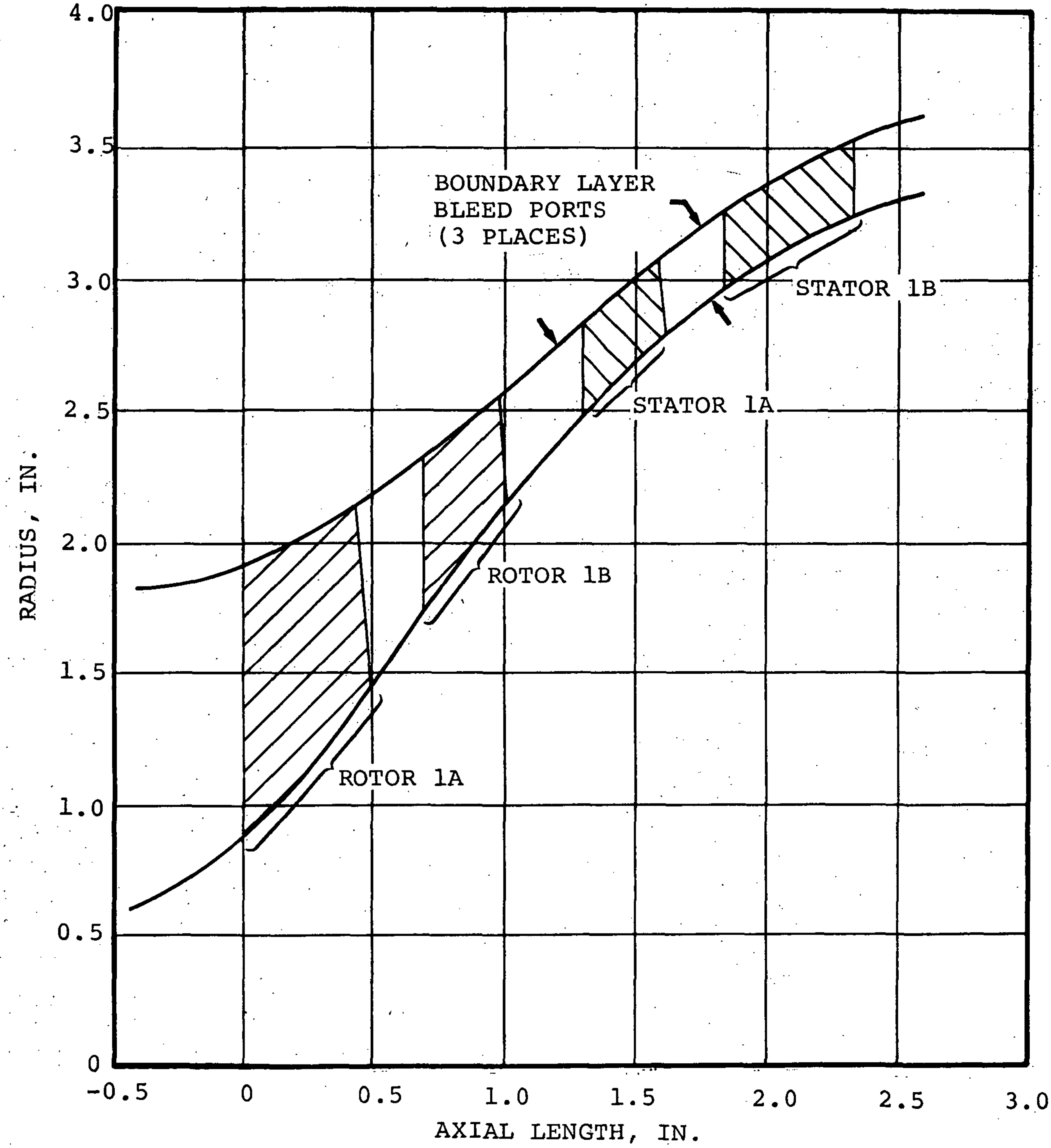

Figure 70. - Recommended Location of Boundary Layer Bleed Ports In Conical Compressor.

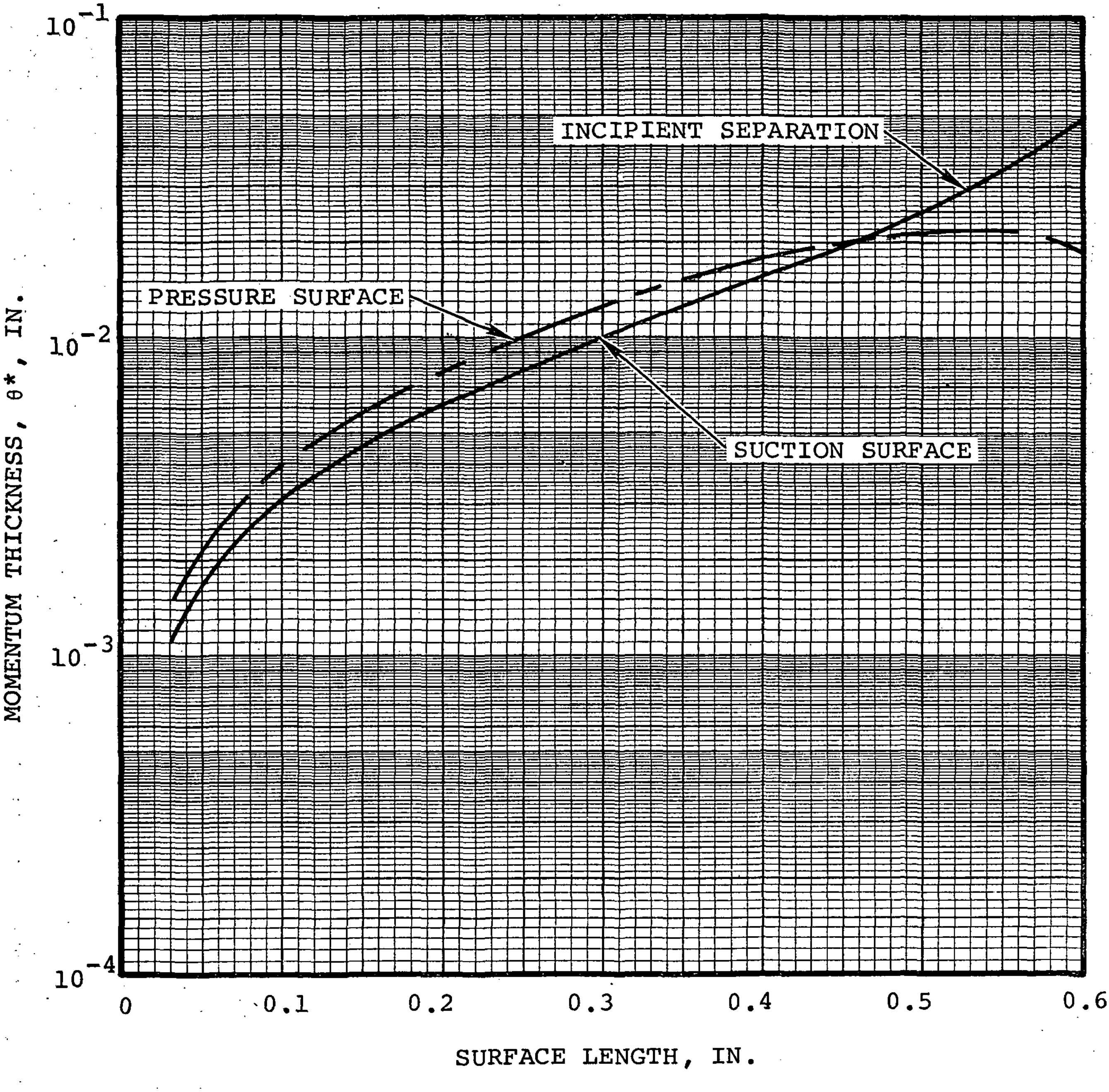

Figure 71. - Stator 1B Blade Surface Boundary Layers - Hub Streamline.

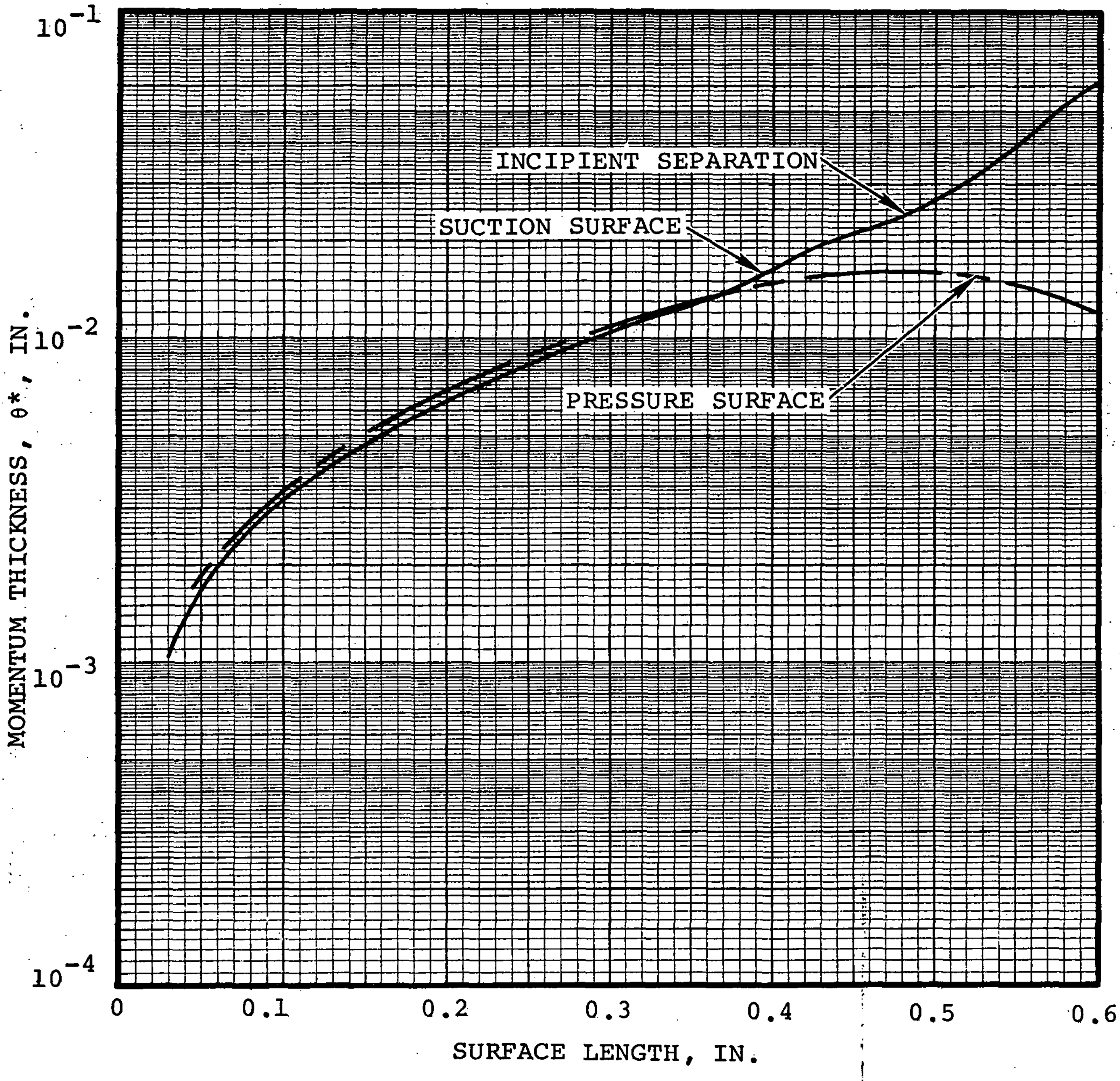

Figure 72. - Stator 1B Blade Surface Boundary Layers - Tip Streamline.

The design of the transition duct is such that the initial passage is converged slightly prior to any diffusion. This should tend to stabilize the flow prior to the turning section in the transition duct.

The boundary layer bleed ports will consist of a series of 40 holes, equally spaced circumferentially around the wall at each specified location. The diameters of the bleed ports should be 3/32nd of an inch, which will take a bleed flow ratio of two percent of the main flow. For the boundary layer bleed system to show a favorable performance trade-off, it will be necessary to operate the bleed systems at less than the design flow ratio (less than 2.0 percent). Optimum operating conditions will have to be determined experimentally since there are too many unknowns to permit this problem to be solved analytically.

Inlet Flowpath Design

Analysis of flow conditions in the inlet duct employed an axisymmetric flow program to solve for the potential velocity field. A boundary layer program was used to examine wall effects. Basically it is desirable to have the flow continuously accelerate throughout the entrance region to avoid excessive boundary layer buildup with the possibility of flow separation. The analytical programs were employed to examine various duct shapes on an essentially trial and error basis to arrive finally at an acceptable entrance configuration.

The selected inlet duct configuration is shown on figure 73. Also included on this figure are several streamlines in the flow field and the velocity distribution presented as lines of constant velocity. The upstream portion of their duct has several support struts which pass through the flow field. The blockage of the struts has been included in the potential flow calculations. This is evidenced by the hump in the velocity profile across the strut. The fact that the struts have been placed in a relatively low velocity region tends to minimize their effects on the downstream flow field. The resulting velocity distribution in the entrance duct looks quite satisfactory from the standpoint of potential core flow calculations. Examinations of the boundary layers along both walls also indicated a reasonable rate of boundary layer build-up with distance. A check of the resulting displacement thickness calculations as affecting blockage indicated the aerodynamic blockages assumed in the potential flow calculations were quite satisfactory. This final comparison then completed the analytical examination of the inlet duct configuration.

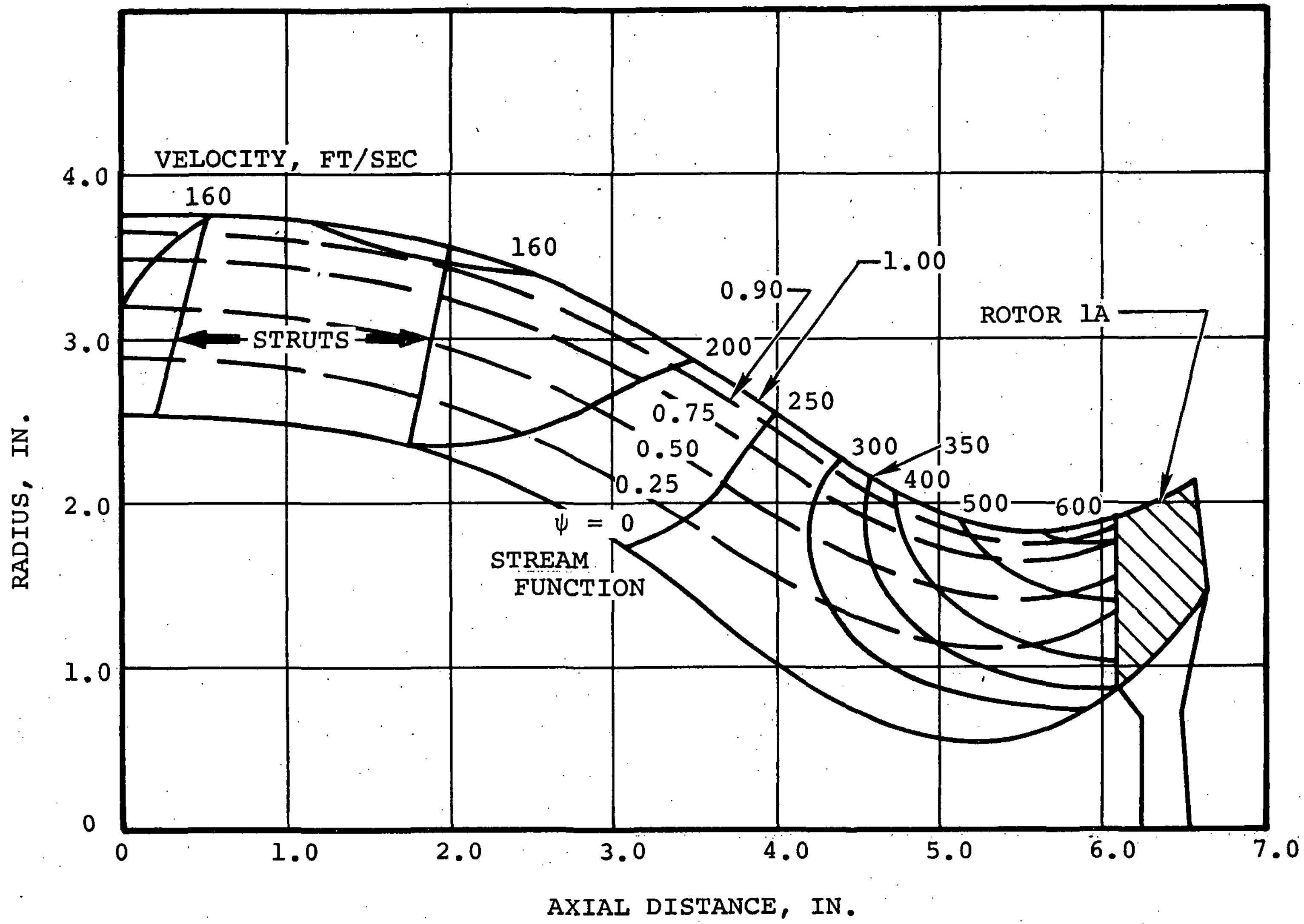

Figure 73. - Inlet Duct for Conical Flow Compressor - Velocity Distribution.

Transition Duct Design

A cross-section of the final flowpath from the second row stator exit down to the inducer leading edge of the second stage compressor is shown in figure 74. The resultant surface velocities (for the design point) are presented in figure 75.

This design involved a trade-off between the area ratio distribution along the meanline and local wall curvatures to achieve hub and shroud wall velocity distributions which minimized the possibility of boundary layer separation. The final design was made within geometric constraints of radius and axial distance fixed by the mechanical considerations, and the aerodynamic constraint of a second-stage inlet shroud to meanline velocity ratio consistent with current radial compressor design technology requirements. (The second-stage inducer geometry was obtained from a preliminary design discussed earlier in this report.)

A calculation of the boundary layer conditions was conducted for each of the final hub and shroud wall velocity distributions. In each case, depending upon the assumed initial conditions of the boundary layer, a region exists where the shape factor value, H, indicates probable separation. These regions are shown on the meridional flowpath view (figure 74). Due to the positive wall curvature in each of these regions, the centrifugal body force will act opposite to the adverse pressure gradient tending to hold the fluid to the wall and the separated zone is expected to be small with rapid reattachment.

Considerable effort was expended in obtaining this situation since some separation is inevitable because of the severity of the curvature required to satisfy the envelope restrictions. The design is considered conservative in that the boundary layer blockage was not included in the flow-field solution. The inclusion of this blockage would decrease the effective area and increase the velocity level, the increase being greatest where the diffusion is greatest. This type solution requires an iterative process between the boundary layer program and the radial equilibrium program. A time limitation prevented this more detailed analysis.

The final configuration is representative of crossover ducts currently in use on production engines at AiResearch.

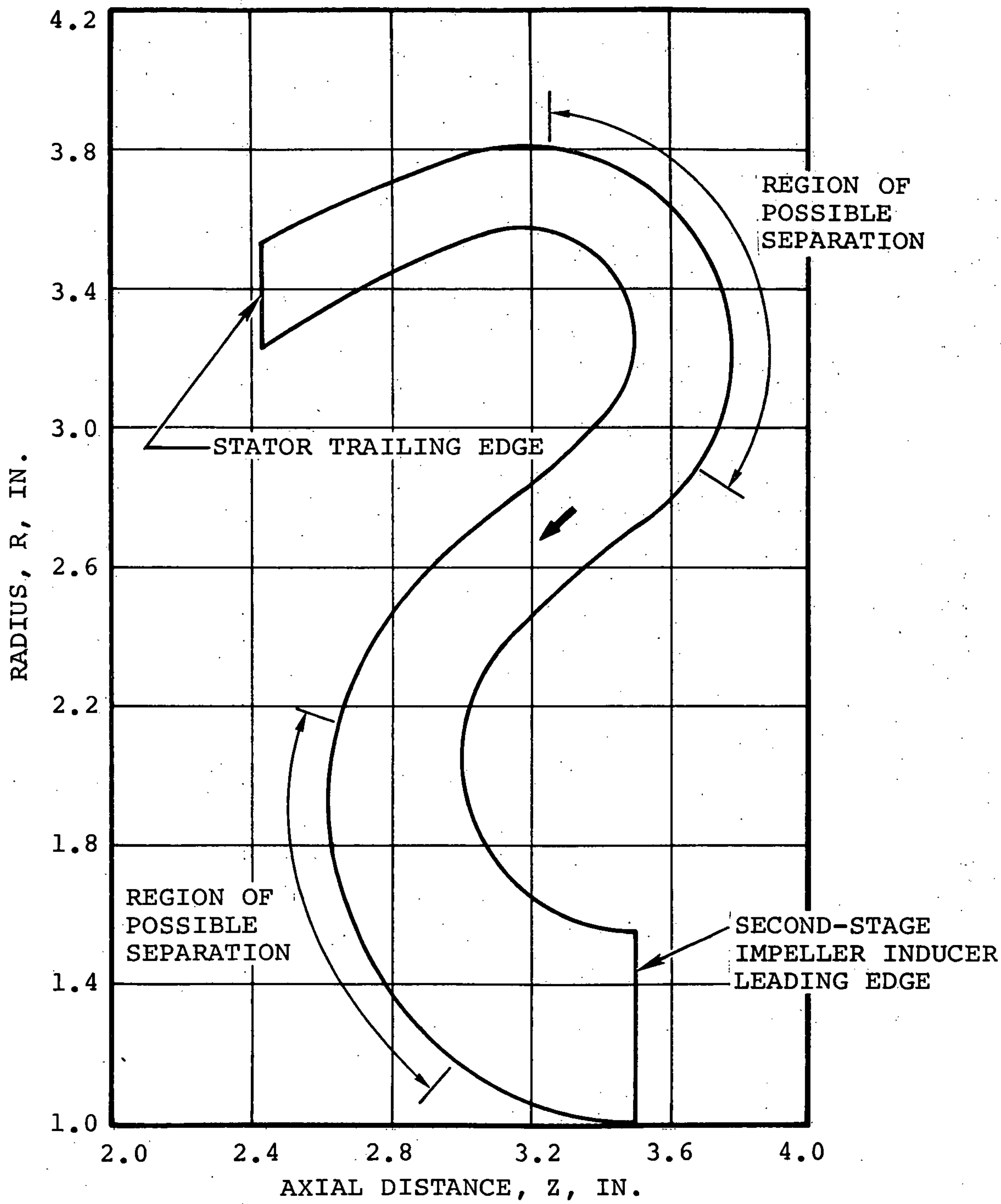

Figure 74. - Transition Duct Size and Shape.

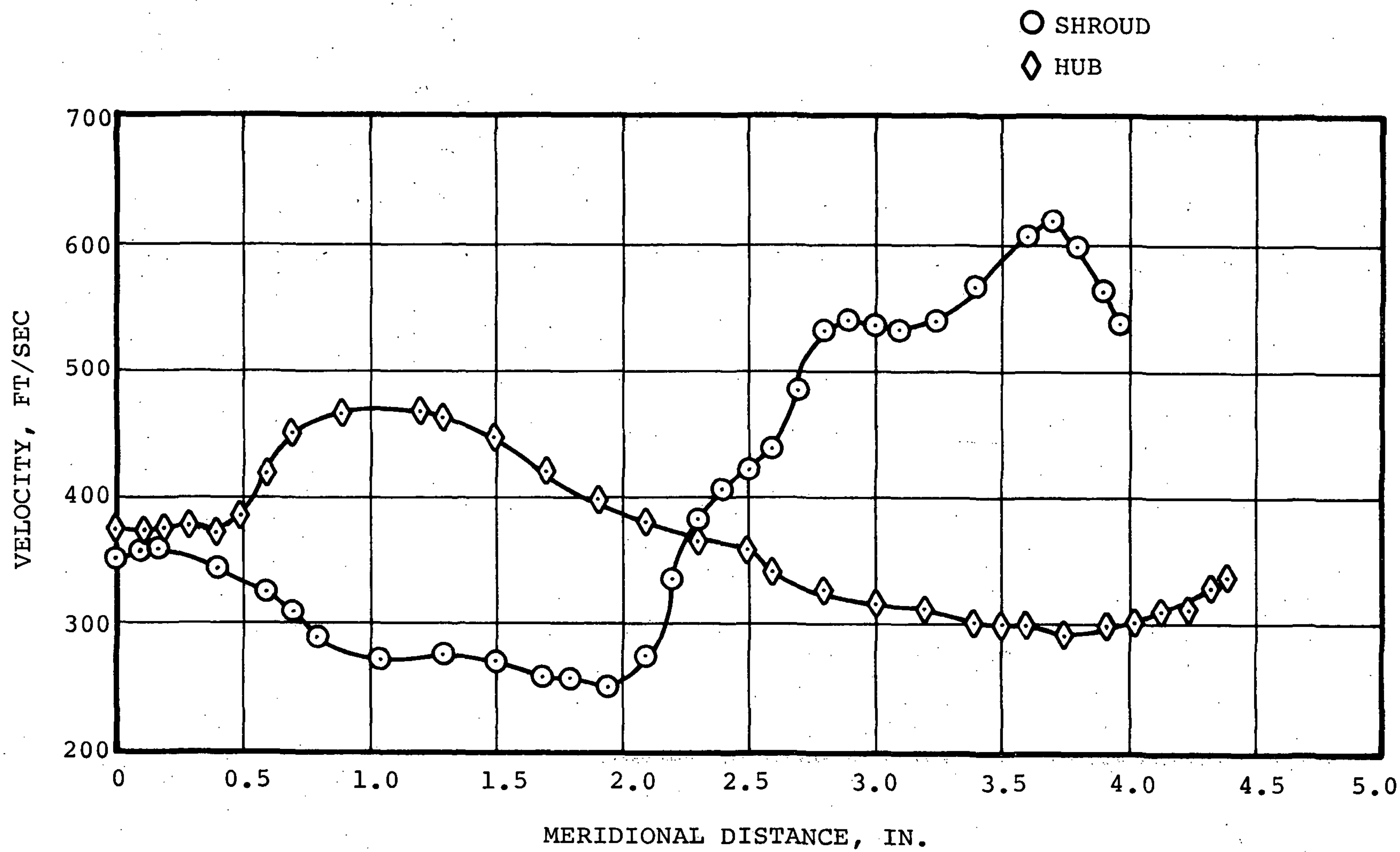

Figure 75. - Transition Duct Velocity Distribution.

Drive Turbine Aerodynamic Design

An existing radial inflow turbine design has been selected to drive the 10/1 compressor research rig. This selection is based on consideration of power capability, mechanical integrity, and contractually stipulated turbine inlet conditions. Of the two candidate drive turbines considered (radial and axial), the radial inflow design selected to drive the rig is superior in available power and mechanical integrity. It can also produce maximum power at lower turbine inlet temperature and integrates well with the research rig. An aerodynamic design summary follows. The blading geometry is defined in Appendix A.

Drive Turbine Aerodynamic Design Summary

The drive turbine for the NASA 10/1 compressor is required to produce sufficient power to test the two-stage compressor to 110 percent of design speed. The compressor design point used to size the turbine is as follows:

$$P_r = 10.0$$

$$W\sqrt{\theta}/\delta = 2.0 \text{ lb/sec}$$

$$\eta_{ad} = 0.805$$

$$N/\sqrt{\theta} = 70{,}000 \text{ rpm}$$

Achievement of this design goal requires an input horsepower of 411 and an overspeed power requirement of 547 horsepower based on the cubic power law. These horsepower requirements will be provided by the following available energy source:

Maximum flow: 7 lb/sec

Maximum T_{in} : 1000°R

Maximum P_{in} : 350 psia

Maximum P_{out}: 4 psia

From this energy source and the required overspeed of 77,000 rpm, an examination of existing turbines was made to determine which, if any, could produce the required 547 horsepower at 77,000 rpm and not exceed the available energy source. As a result of the examination, a radial inflow turbine design was selected for use in the research rig. The design point of the turbine is:

Speed, rpm:	81,800
$W\sqrt{\theta}/\delta$, lb/sec:	0.474
P_r, T-T:	4.167
η, T-T:	89.7
$\Delta H/\theta$, Btu/lb:	37.6

The performance of the selected turbine was tested in an actual size cold air rig. The test results are given in figures 76 through 82. Using the turbine performance test data, a computer model that would predict turbine performance at any desired operating point was created. Figure 78 shows the comparison between the measured performance and predicted performance based on the computer model. The agreement shown in figure 78 and like agreement at other test speeds indicates that the computer model could reliably predict performance at any operating condition. Using the computer model, a maximum power curve for the radial turbine was generated for a range of compressor speeds and inlet temperatures. Figure 82 presents a carpet plot of this information and clearly shows that the required objective of 547 horsepower and 110-percent compressor speed can be obtained without exceeding the facility limitations.

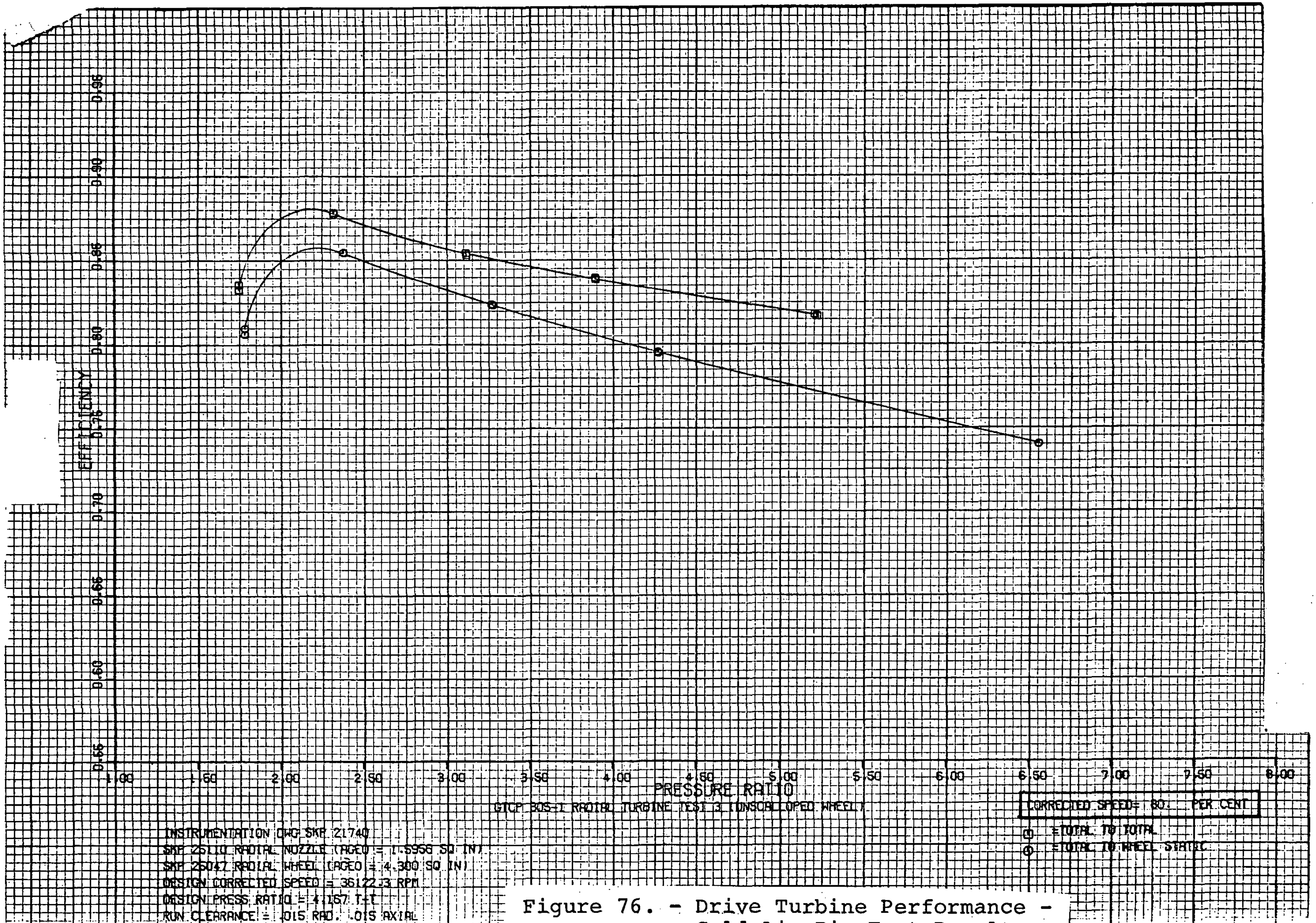

Figure 76. - Drive Turbine Performance - Cold-Air Rig Test Results.

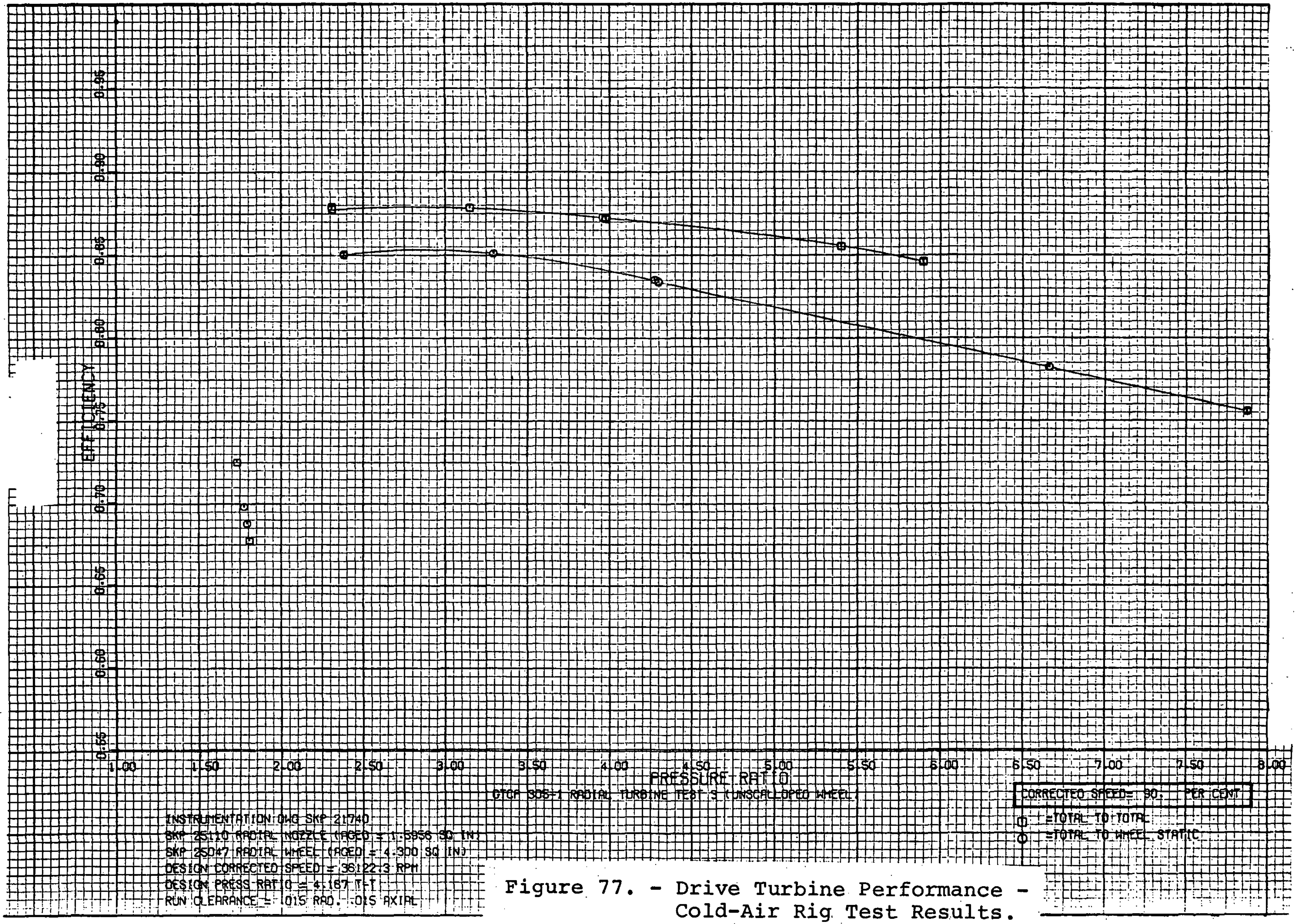

Figure 77. - Drive Turbine Performance - Cold-Air Rig Test Results.

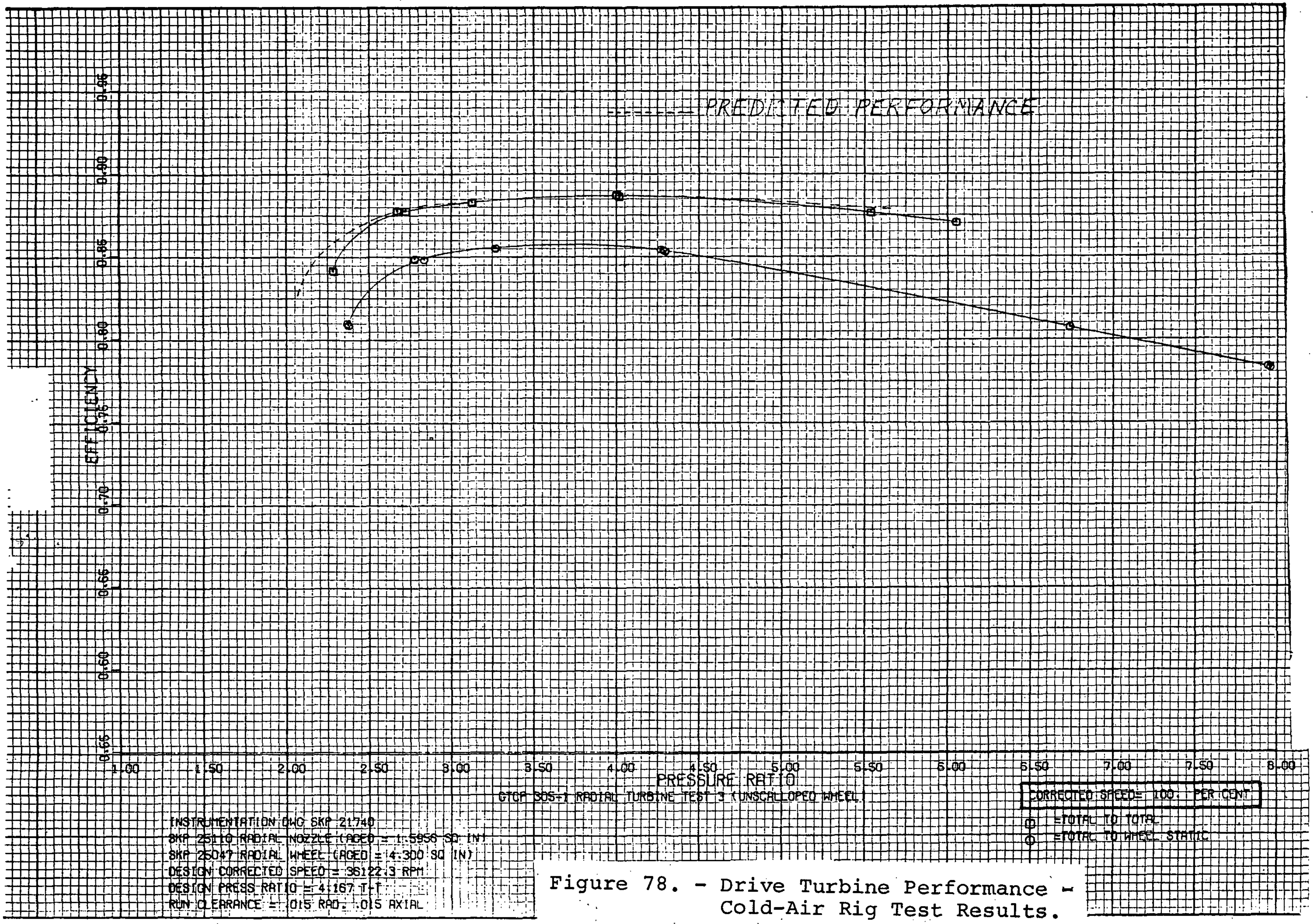

Figure 78. - Drive Turbine Performance - Cold-Air Rig Test Results.

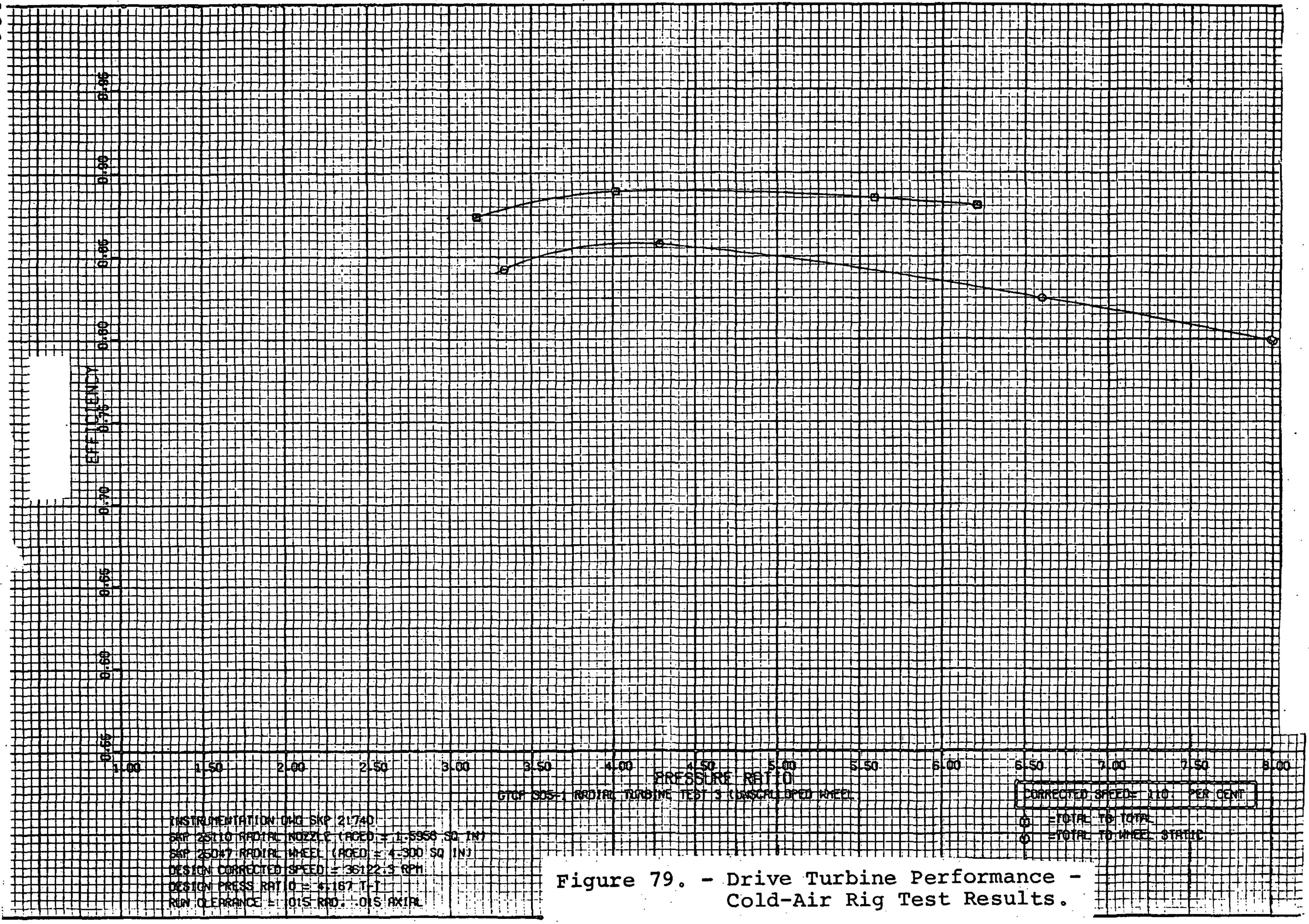

Figure 79. - Drive Turbine Performance - Cold-Air Rig Test Results.

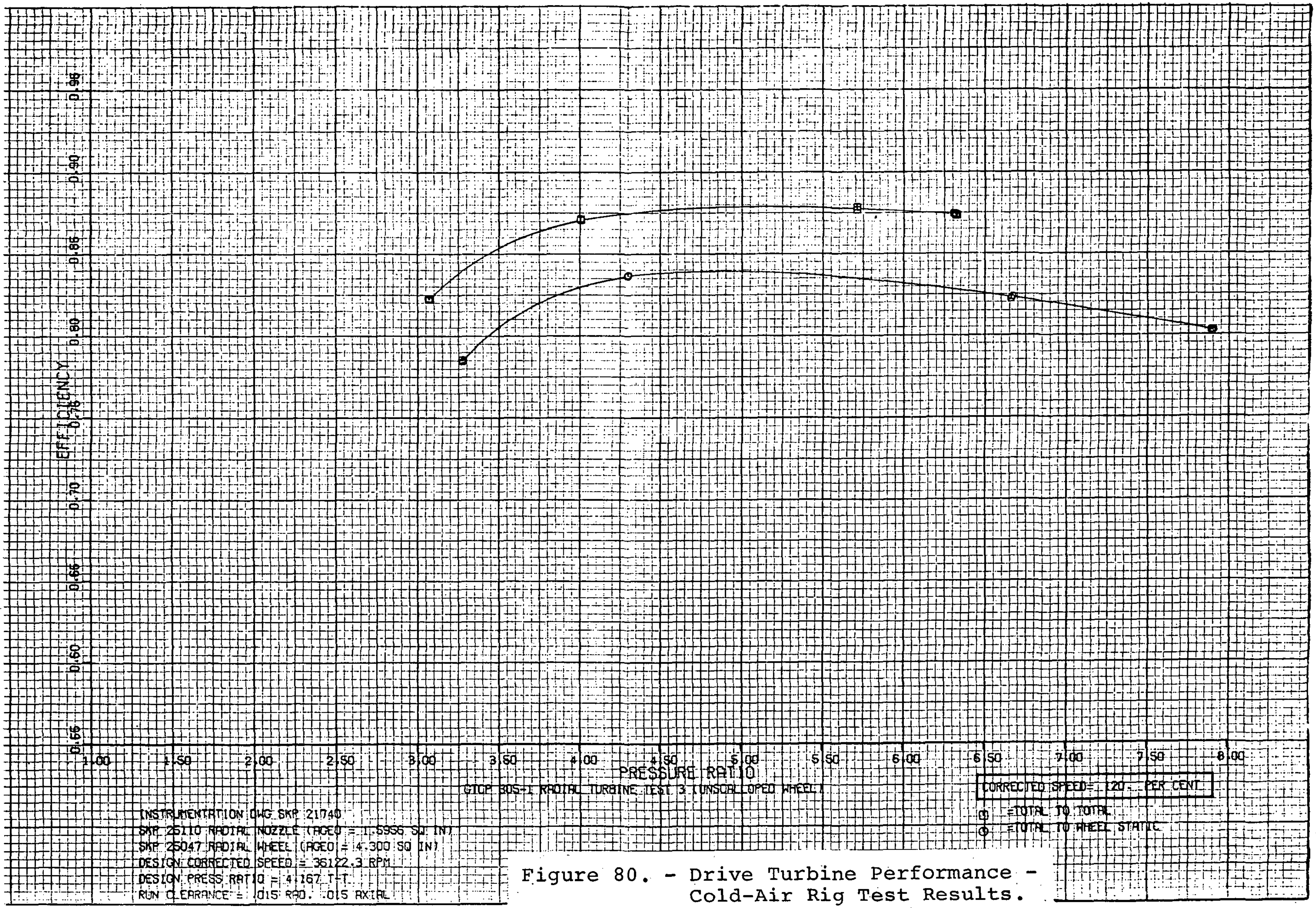

Figure 80. - Drive Turbine Performance - Cold-Air Rig Test Results.

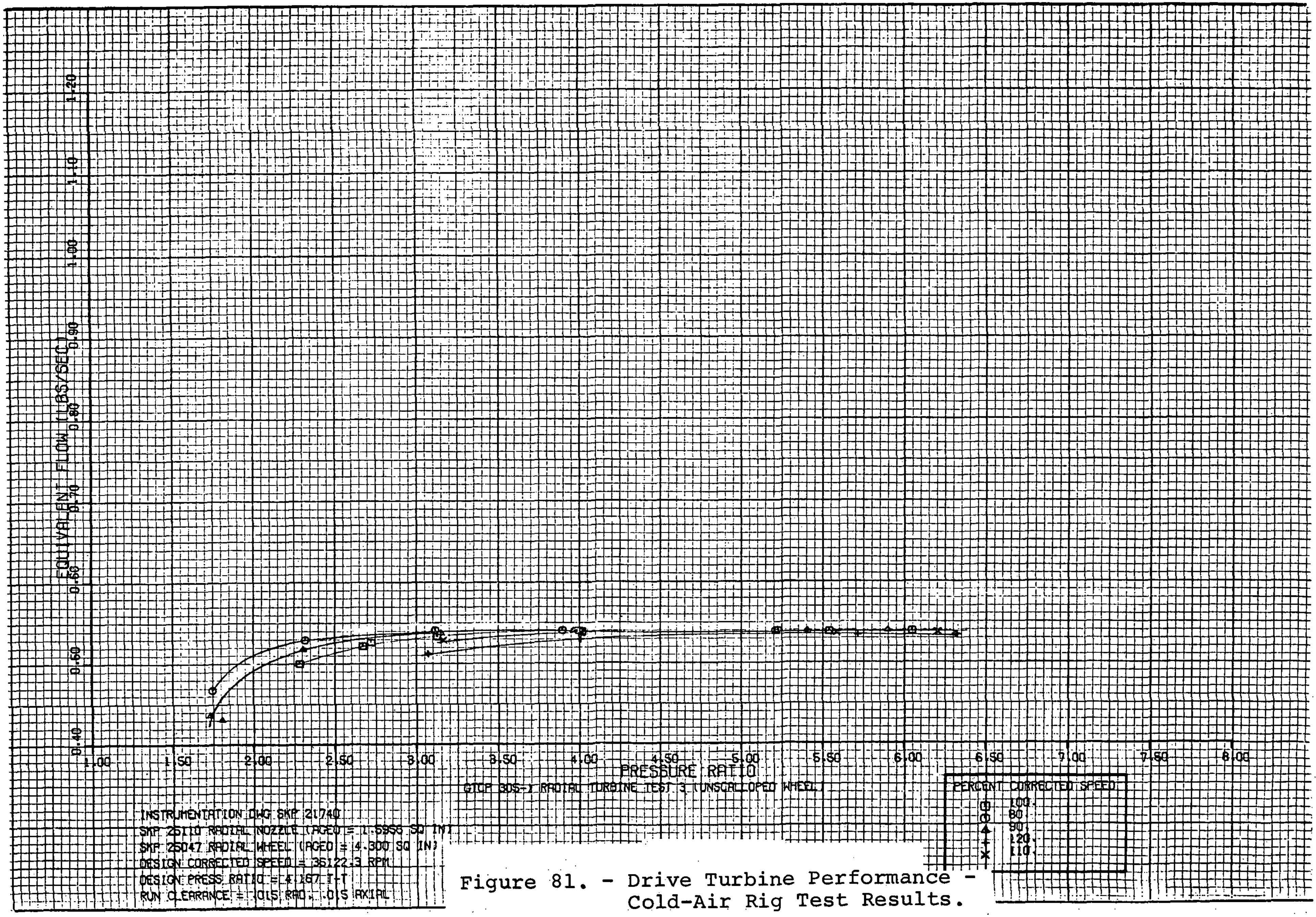

Figure 81. - Drive Turbine Performance - Cold-Air Rig Test Results.

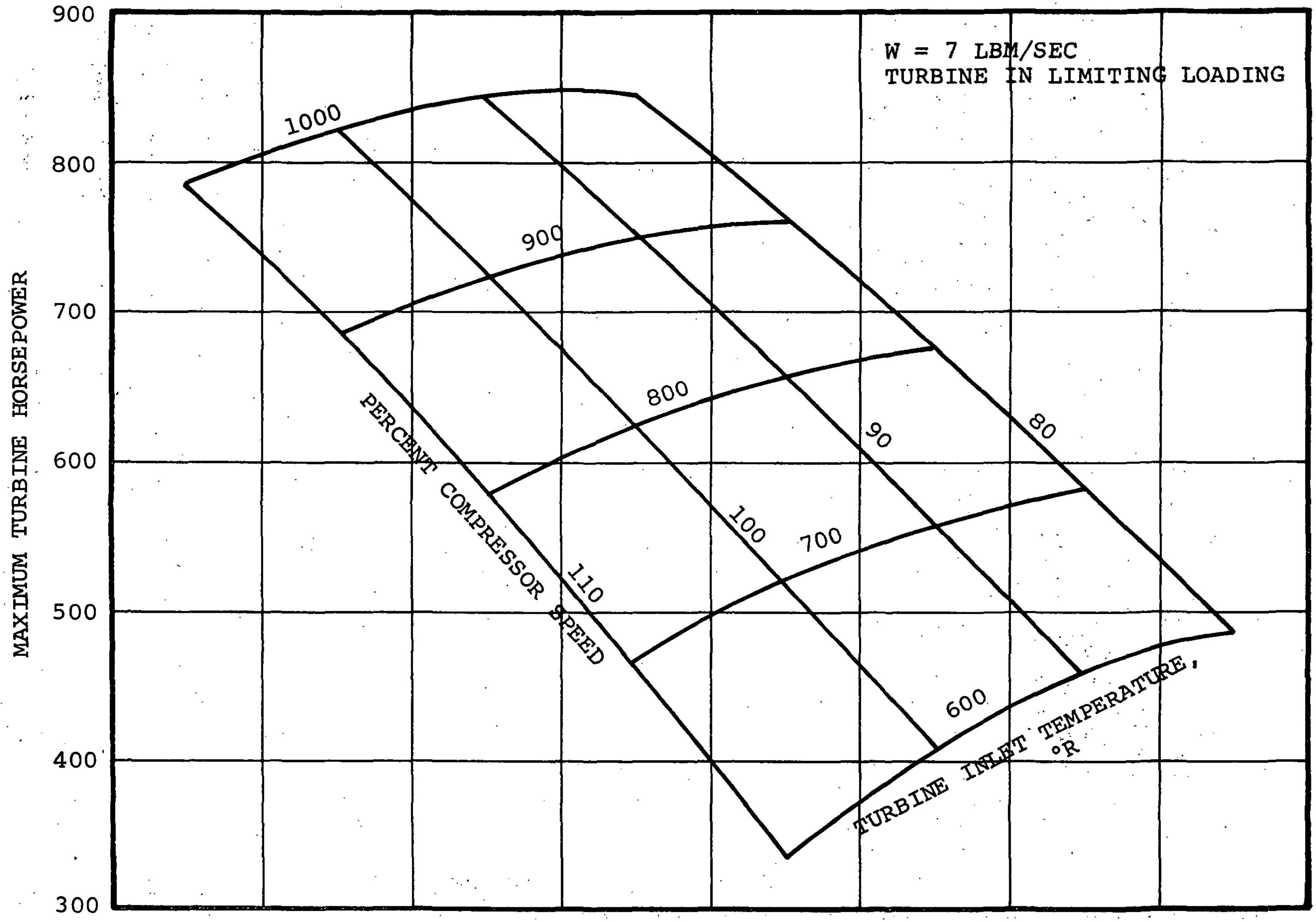

Figure 82. - Maximum Available Radial Turbine Horsepower.

Turbine Design Point

Despite the fact that the radial turbine will operate at higher than design pressure ratios, the initial selection of design point was critical to the proper prediction of the off-design performance. The following aerodynamic summary is based on the design point previously given in the preceding section of this report.

Figure 83 presents a vector diagram of design point, figures 84 through 87 are loading diagrams at the hub, mean, and shroud streamtube for the meridional shape shown in figure 88. The loading diagrams present the nondimensional velocity ratios for the pressure, average, and suction surfaces of the blade as a function of percent meridional distance. The symbols used in figures 83 and 84 through 91 are defined as follows:

- Z - axial distance
- R - radial distance
- m - meridonal distance
- t_n - thickness normal to blade
- t_t - thickness tangential to blade
- β_B - blade angle
- θ_B - blade tangential angle
- V - velocity
- a'_{cr} - $\sqrt{\frac{2\gamma}{\gamma+1} gRT'}$, velocity of sound based on stagnation temperature
- T' - stagnation temperature
- T'' - relative stagnation temperature

The objective of utilizing loading diagrams is to produce a geometry that will minimize blade surface diffusion while achieving the desired blade circulation. Since actual cold air test data indicates that measured efficiency is very close to design efficiency, the objective was achieved. The geometry required to produce these loadings and efficiency is illustrated in figures 89 through 91. In these figures, the streamtube axial distance (Z), radial distance (R), normal (t_n) and tangential (t_t) thickness, blade beta angle (β_B). and blade theta angle (θ_B) are presented as a function of percent meridional distance.

A complete geometrical description of the turbine wheel and nozzle is given in Appendix B.

NOZZLE EXIT   R = 3.1599 IN.   19 VANES

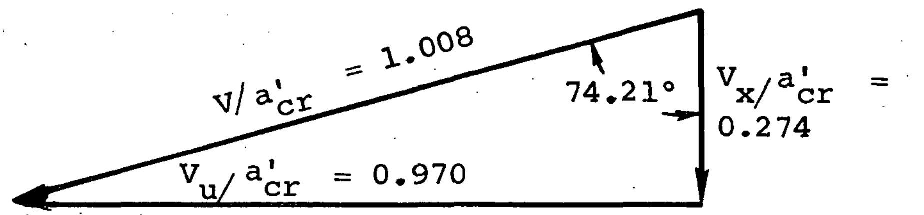

ROTOR TIP   R = 3.0679 IN.

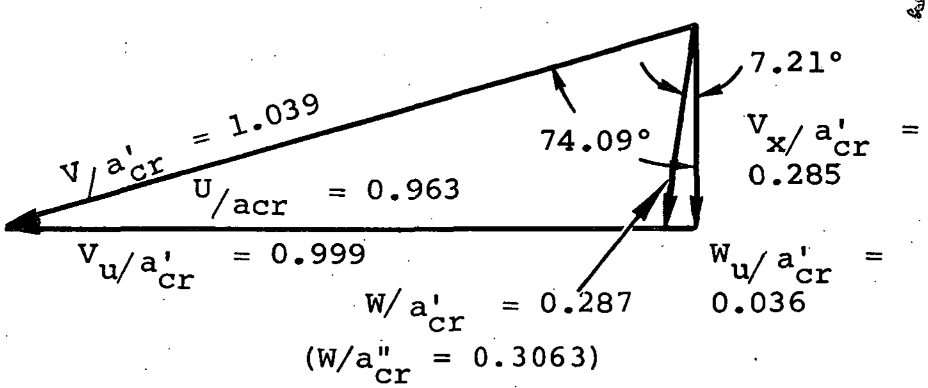

ROTOR EXIT HUB   R = 1.2500 IN.

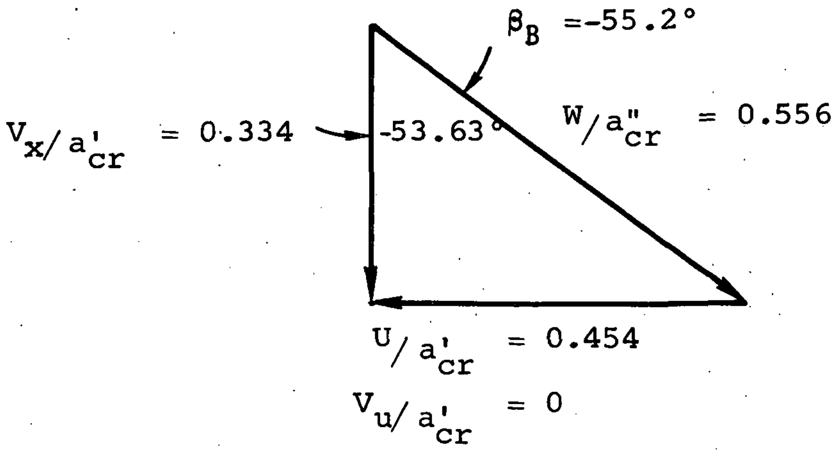

Figure 83. - Radial Turbine Vector Diagram (Sheet 1 of 2).

ROTOR EXIT MEAN LINE R = 1.75 IN.

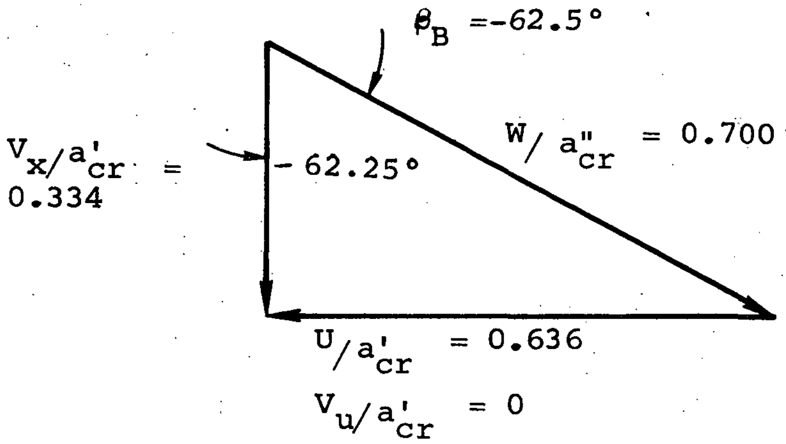

ROTOR EXIT TIP , R = 2.183 IN.

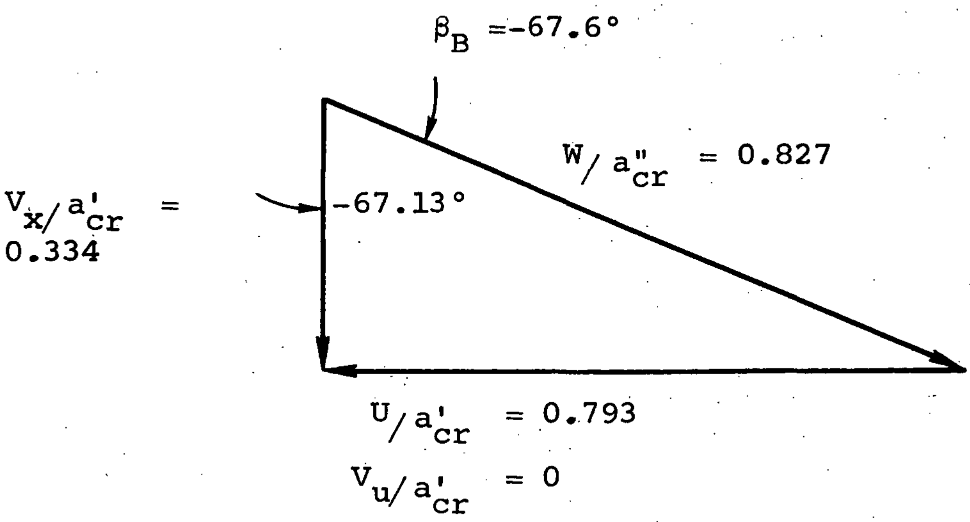

Figure 83. - Radial Turbine Vector Diagram (Sheet 2 of 2).

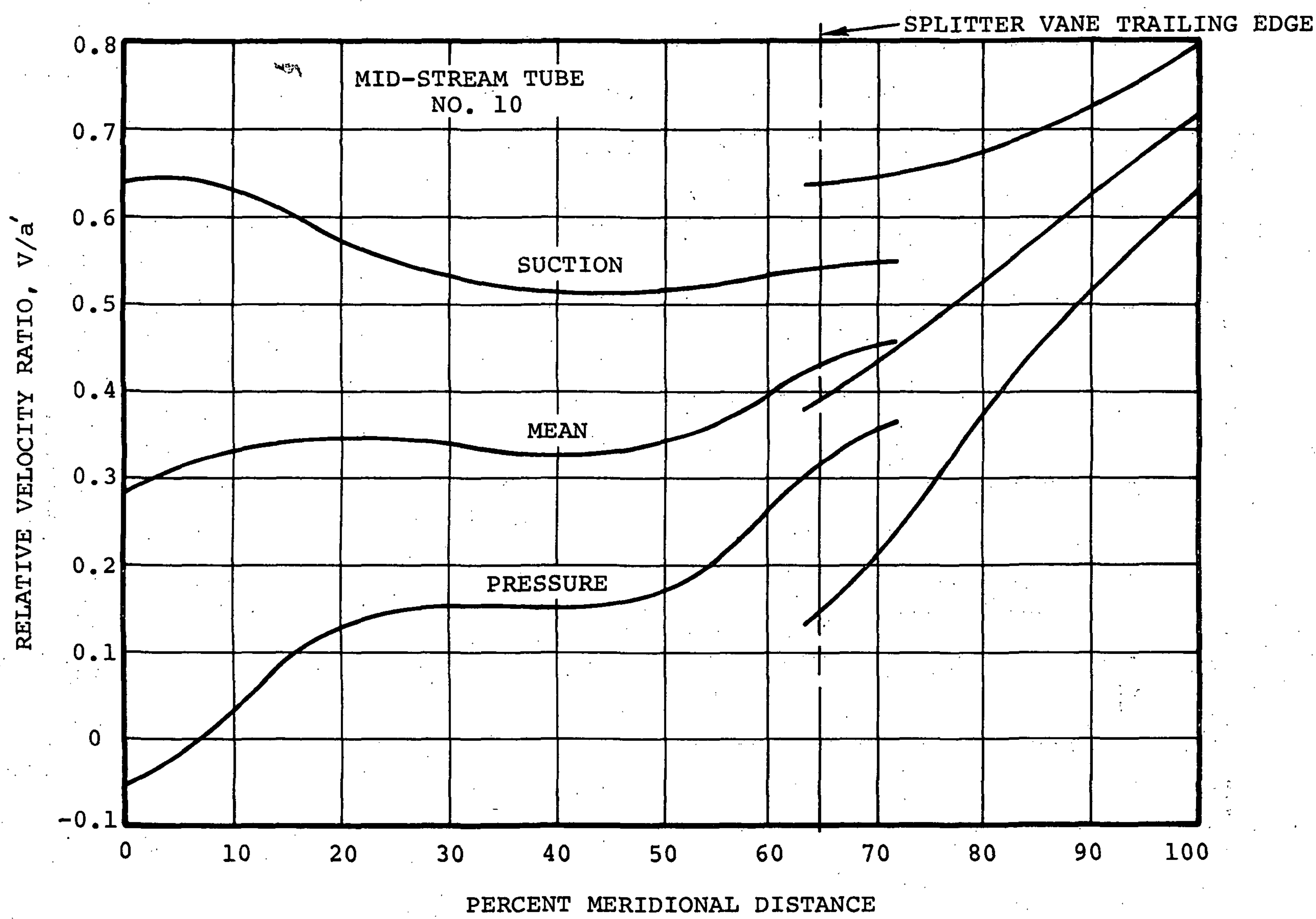

Figure 84. - Radial Turbine - Mean Streamtube Blade Loading.

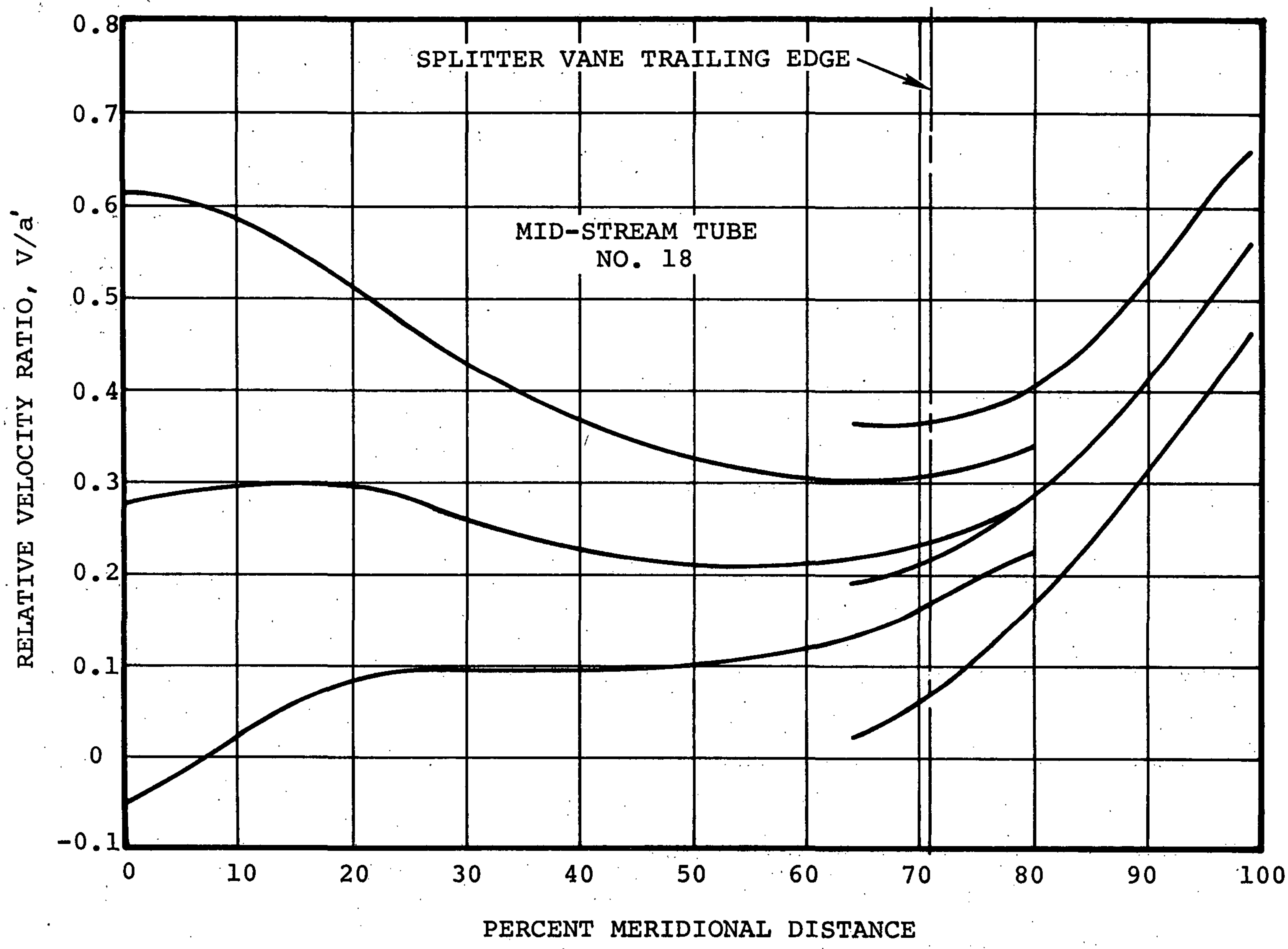

Figure 85. - Radial Turbine - Hub Streamtube Blade Loading.

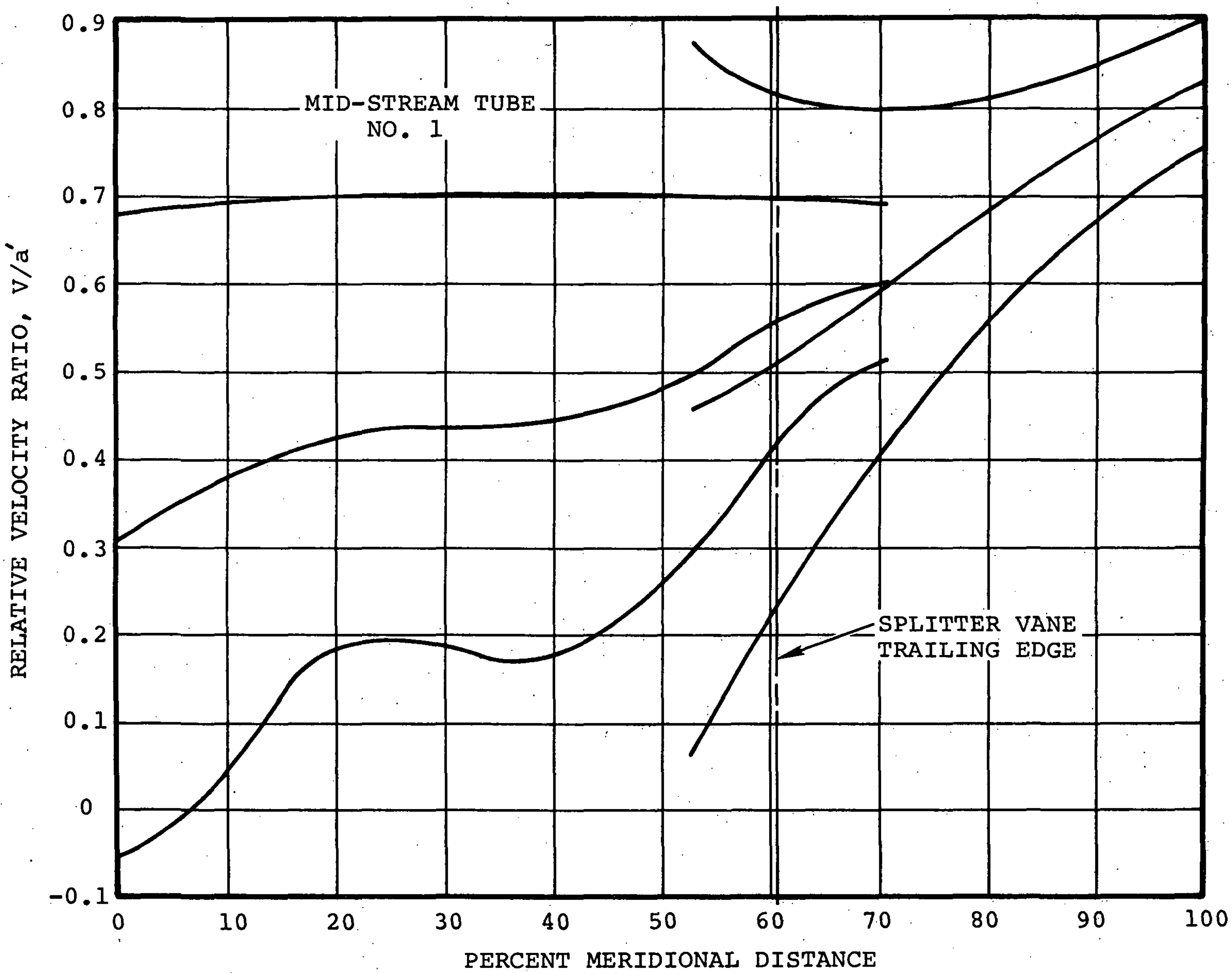

Figure 86. - Radial Turbine - Shroud Streamtube Blade Loading.

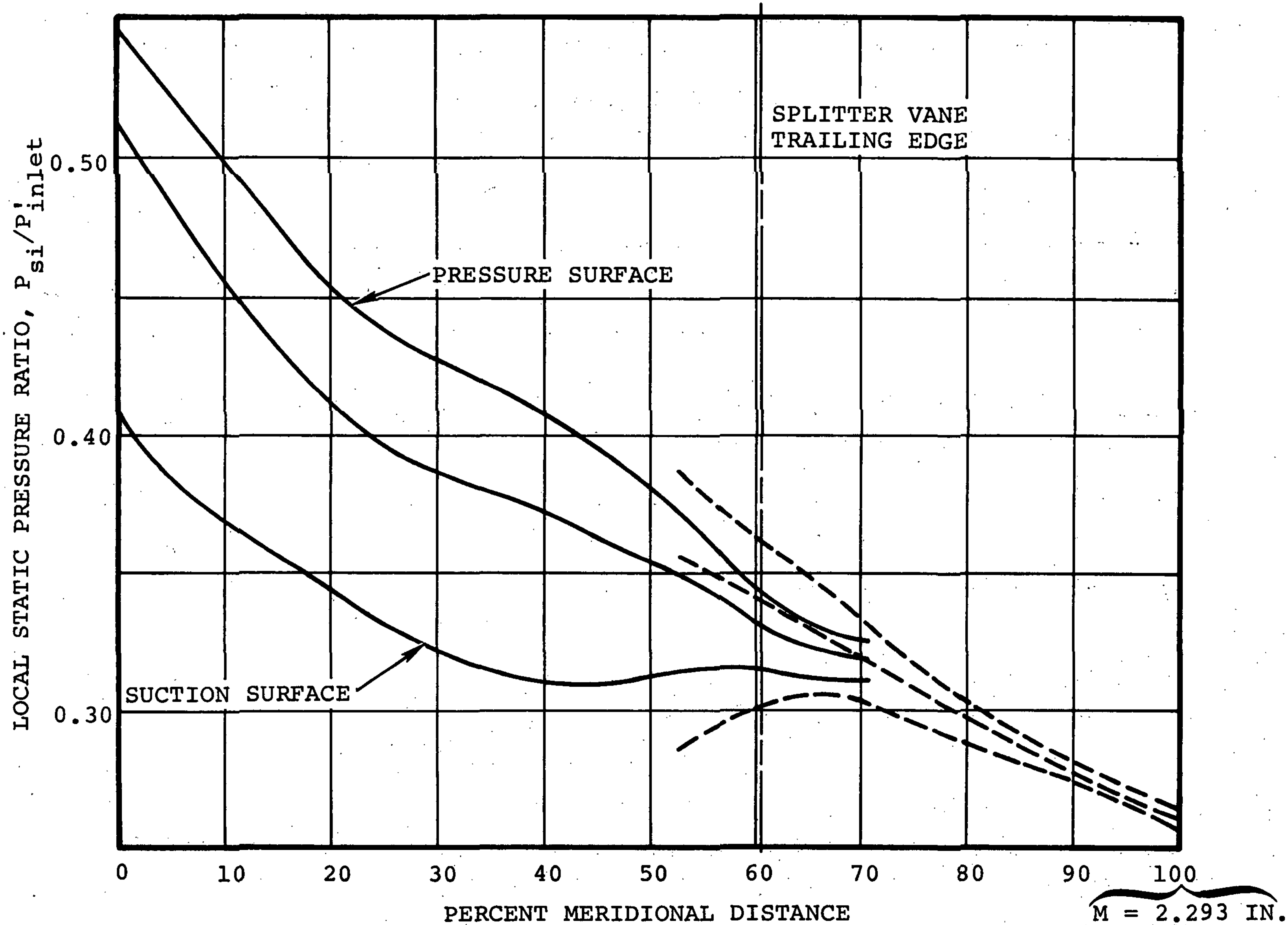

Figure 87. - Radial Turbine - Streamtube 1 - Shroud.

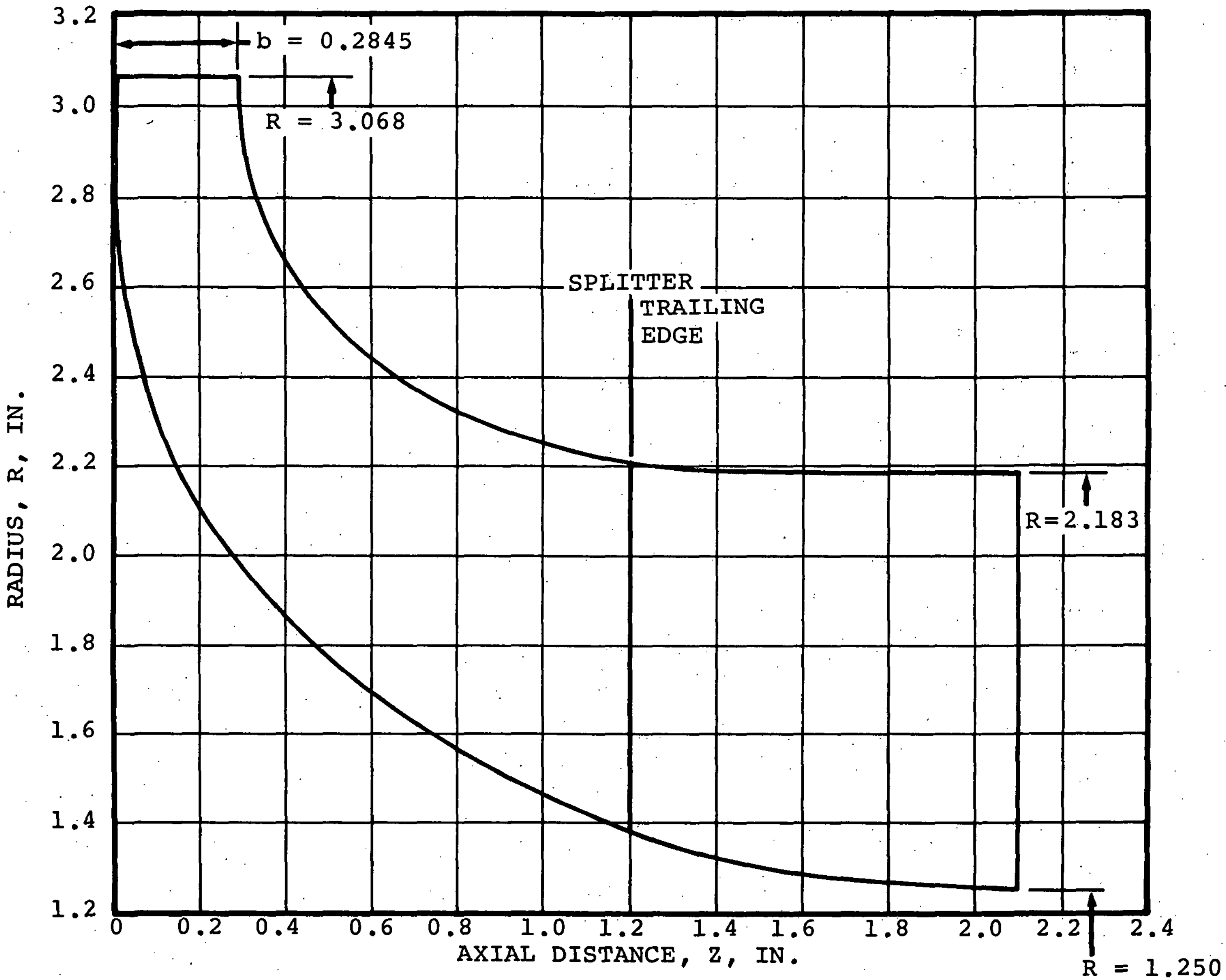

Figure 88. - Meridional Plane View of Radial Turbine.

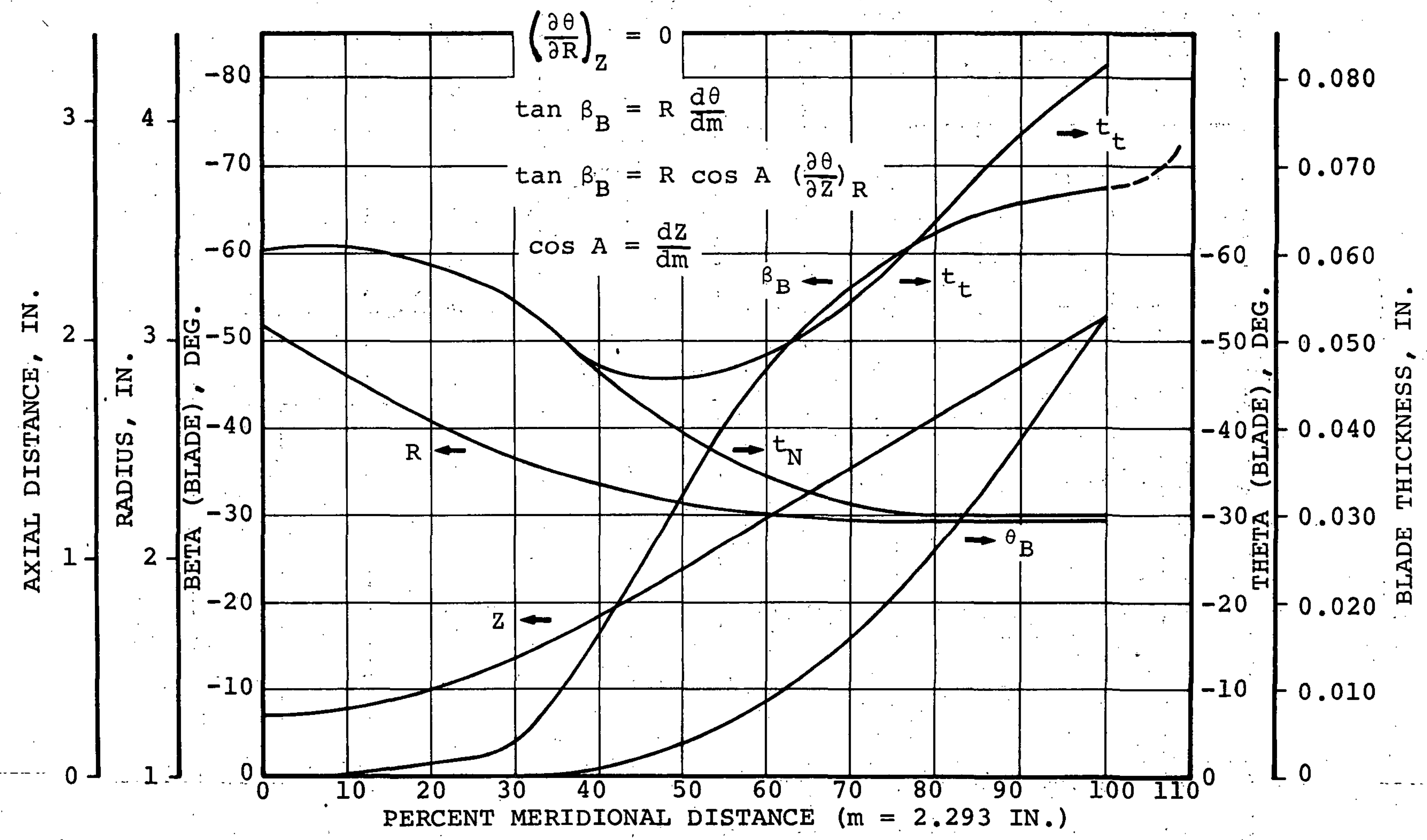

Figure 89.- Radial Turbine, Streamtube 1 - Shroud.

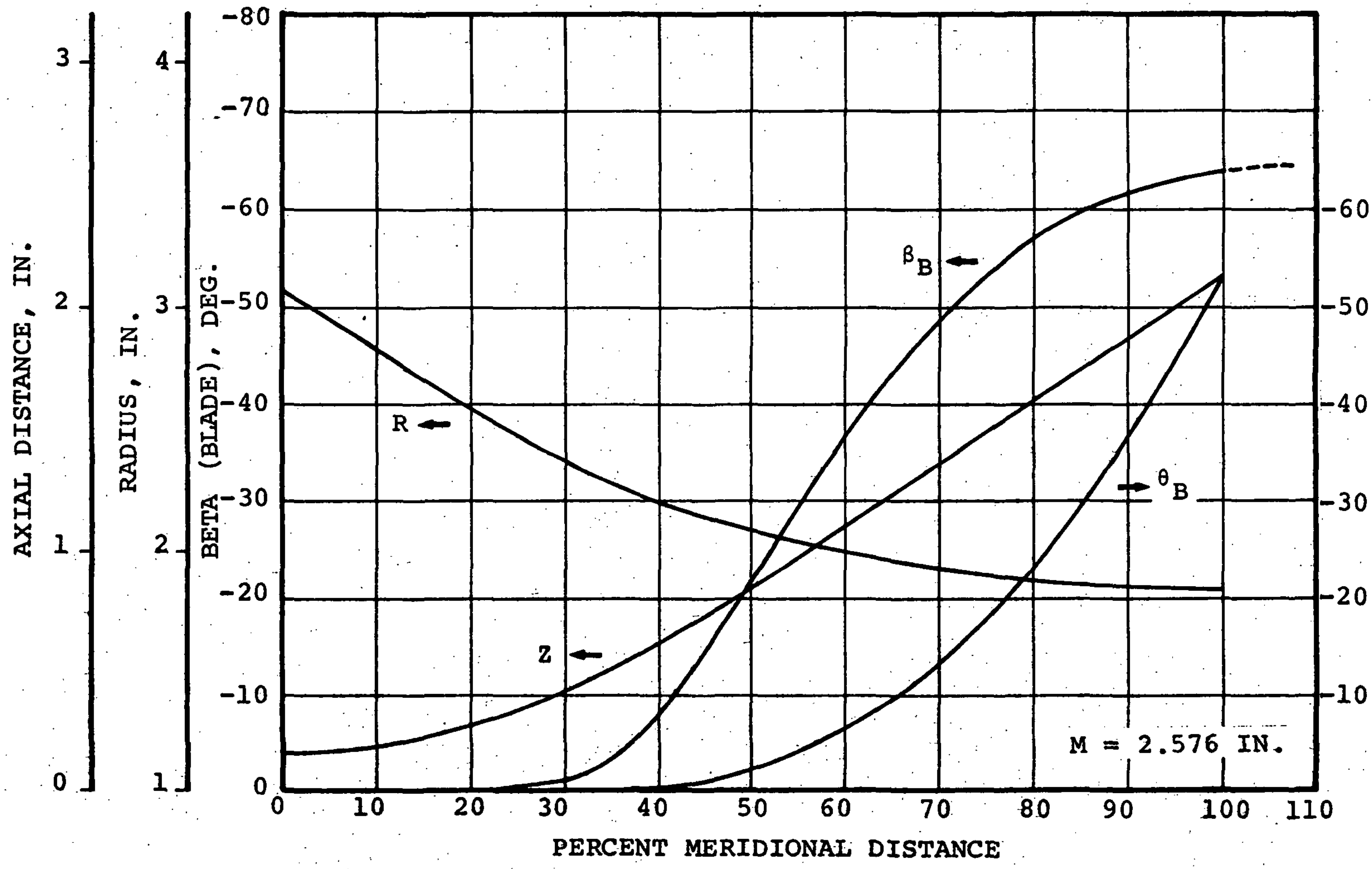

Figure 90. - Radial Turbine, Streamtube 9 - Mean.

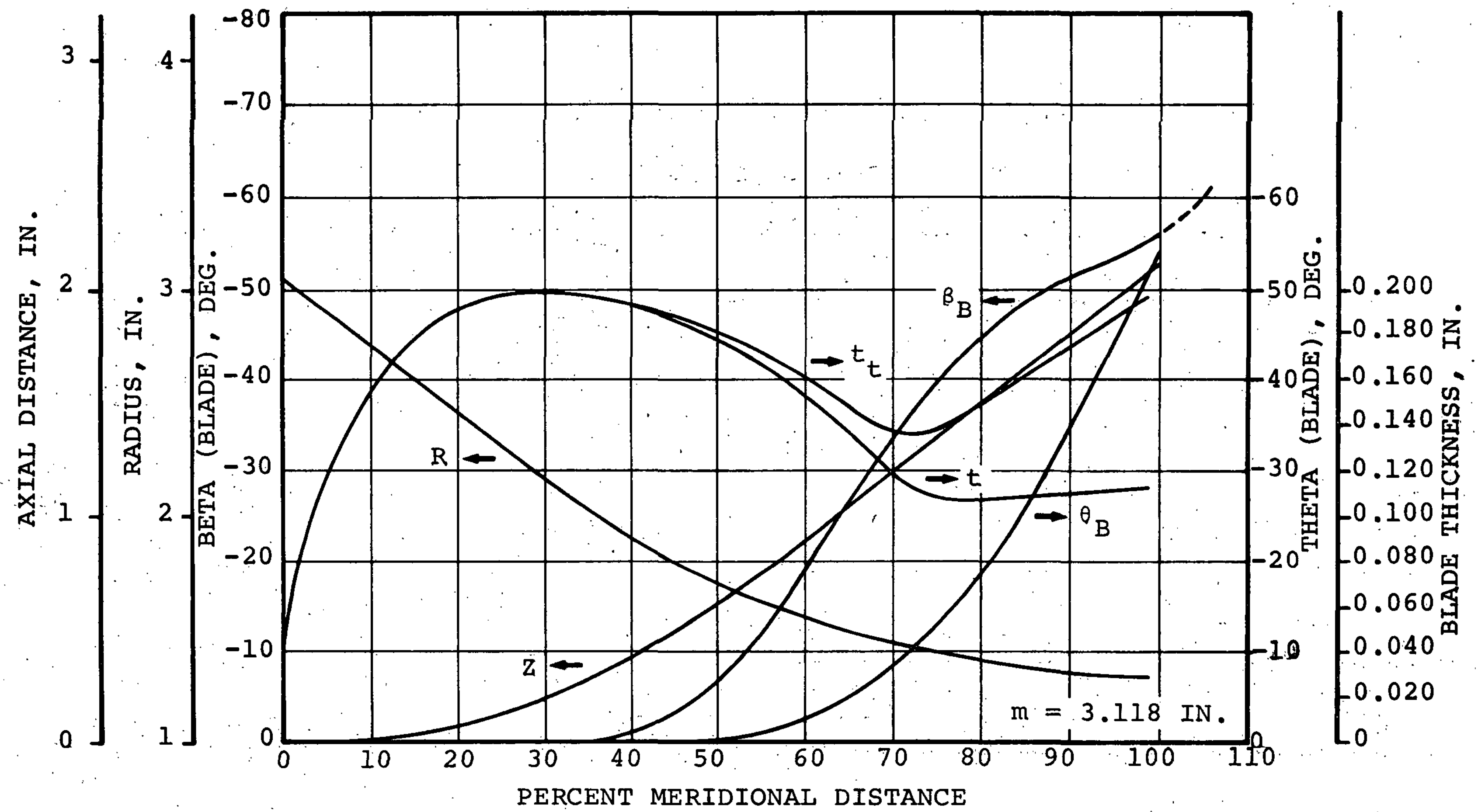

Figure 91. - Radial Turbine, Streamtube 18 - Hub.

APPENDIX A

DEVIATION ANGLE DETERMINATION FOR CASCADE/AIRFOILS

(32 pages)

DEVIATION ANGLE PREDICTION
FOR THE
CONICAL FLOW COMPRESSOR

The traditional approach to deviation or exit flow angle prediction consists of using an empirical rule derived from two-dimensional cascade data. This rule is applied to a rotor by considering flow in the relative plane and, in cases where there are significant variations from two-dimensional conditions, corrections of one form or another to account for differences in meridional velocity ratio, radius change, and other three-dimensional effects have been applied.

Measurements on transonic compressors have indicated deviation angles near the rotor hub are larger than predicted by conventional design rules which include correction factors. In cases where there are large radius and meridional velocity changes in the rotor hub regions, it has been found that these conventional design rules are even more deficient. This apparently is caused by the interacting effects of radial and circumferential equilibrium and other effects such as secondary flows, hub blade boundary layer interaction, sweep effects, and numerous other flow effects.

To account for the interacting effects of radial and circumferential equilibrium on the prediction of deviation angle at the conical flow compressor, the following analysis was used. A quasi orthogonal program was used to obtain stream sheet characteristics at several radial locations. For each stream sheet and exit flow angle, a finite difference program was used to compute blade loading. Iterations were carried out on exit flow angle until the Kutta condition was achieved (the loading diagram at the trailing edge closed). For flow in the rotor, a correction was still applied to account for other flow effects. A detailed description of this method is presented in the following section together with comparison experimental data.

BASIC CONCEPTS

Given a particular stream surface configuration (r as a function of Z), the prediction of deviation angle is equivalent to prediction of total turning and thereby the loading. Any technique to predict this total loading must first correctly predict the guided channel loading and second, correctly handle the isolated airfoil (uncovered) regions at the leading and trailing edge.

The following analysis is offered:

For the rotating blade row:

$$C_p\ (T' - T'_1) = \omega(r_2 V_{U_2} - r_1 V_{U_1})$$

Energy balance yields:

$$\dot{m}C_p\ (T' - T_1') = \int_{m_1}^{m_2} U\ (P_p - P_s)\ b\,dm$$

$$U = \omega r$$

$$\dot{m}\ (U_2 V_{U_2} - U_1 V_{U_1}) = \int_{m_1}^{m_2} U\ (P_p - P_s)\ b\,dm$$

$$V_{U_2} = \frac{U_1}{U_2} V_{U_1} + \int_{m_1}^{m_2} U/U_2\ \frac{(P_p - P_s)}{\dot{m}}\ b\,dm$$

$$V_U = W_U + U$$

$$W_{U_2} = V_{U_2} - U_2 = V_{U_1} \frac{U_1}{U_2} - U_2 + \int_{m_1}^{m_2} U/U_2 \frac{(P_p - P_s)}{\dot{m}}\ b\,dm$$

The W_m can be determined from continuity, thereby yielding the exit flow angle.

$$\tan\beta_2 = \frac{W_{U_2}}{W_m} = \frac{V_{U_1} U_1 - U_2^2}{U_2 W_m} + \int_{m_1}^{m_2} U/U_2\ \frac{(P_p - P_s)}{W_m \dot{m}}\ b\,dm$$

From this equation it can be seen that the problem of predicting β_2 rests with predicting the loading $(P_p - P_s)$ through the rotor. For stationary cascades, a similar relationship can be derived from the tangential momentum equation.

It should be noted that the upstream and downstream values of velocity represented in the above equation represent an averaged (circumferential) value of the upstream and downstream conditions. In reality the flow conditions may vary circumferentially. Secondly, the assumption is made that no flow crosses the axisymmetric stream surfaces. This assumption is violated in the cases of warped stream sheets, in separated flow regions where flow migrates towards the tip, and in the blade boundary layers.

FINITE-DIFFERENCE TECHNIQUE

The traditional approach to exit flow angle prediction consists of using an empirical rule derived from cascade data. This rule is applied to a rotor by considering flow in the relative plane and making corrections of one form or another to account for differences in meridional velocity ratio, radius change, and other three-dimensional effects. Since these corrections have not been verified experimentally, much rests on extrapolation from similar rotor designs to produce new designs. The recent advent of finite difference techniques for determining blade-to-blade solutions allows for the development of an approach more readily applicable to noncascade situations. Two such computer programs currently are in use at AiResearch for obtaining blade-to-blade solutions. Both programs are restricted to subsonic flows with reasonably successful transonic corrections. The first is an outgrowth of the program developed by Katsanis and McNally (Reference 1)* at NASA. The second is a program developed at AiResearch to handle interactions between blade rows and other objects in the flow path such as downstream struts. Because the periodic boundary conditions used in the Katsanis-derived program simplify the input requirements, this program was used for the deviation angle analysis.

*Refer to Page 30 of Appendix A for the noted reference.

The basic equation used by this program is the stream function equation:

$$\frac{1}{r^2}\frac{\partial^2 \psi}{\partial \theta_r^2} + \frac{\partial^2 \psi}{\partial m^2} - \frac{1}{r^2}\frac{1}{\rho}\frac{\partial \rho}{\partial \theta}\frac{\partial \psi}{\partial \theta_r} + \frac{\sin\alpha}{r} - \frac{1}{b\rho}\frac{\partial (b\rho)}{\partial m}\frac{\partial \psi}{\partial m} = \frac{2b\rho\omega}{m}\sin\alpha$$

The boundary conditions for its solution are shown in Figure 1. As can be seen, they are of three types. At the upstream and downstream boundaries, the flow angle is specified and assumed constant with θ_r. The straight boundaries connecting the upstream and downstream boundaries with the blade, utilize the condition of periodicity. On these boundaries

$$\psi_{upper} = \psi_{lower} + 1.$$

The blade boundaries have specified values of stream function since the flow passing between them is known.

To use this technique, the angle on the downstream boundary is specified and velocity distributions throughout the region and on the boundaries are calculated by a finite-difference relaxation technique described in Reference 1. This blade velocity distribution may take on one of the three shapes indicated in figure 2. All three loadings represent valid inviscid solutions for the cascade. However, the requirement of satisfying the Kutta condition for an airfoil is based on viscous effects and compliance with this condition must be determined on separate grounds. Reference 2 describes the Kutta condition basically as the inability of an airfoil to maintain continuous flow around the sharp trailing edge. Because of the requirement for a static pressure balance across the wake, velocities on the suction and pressure surfaces must be equal at the trailing edge. This is equivalent to stating that the stagnation point, where the dividing streamline leaves the blade, occurs in the trailing edge region.

The basic technique is then one of iteration where a variety of exit flow angles in the vicinity of the expected exit flow angle are specified until the one giving equal exit suction and pressure surface velocities is determined. In practice this is done graphically with a final computer run to verify the results at the determined exit flow angle.

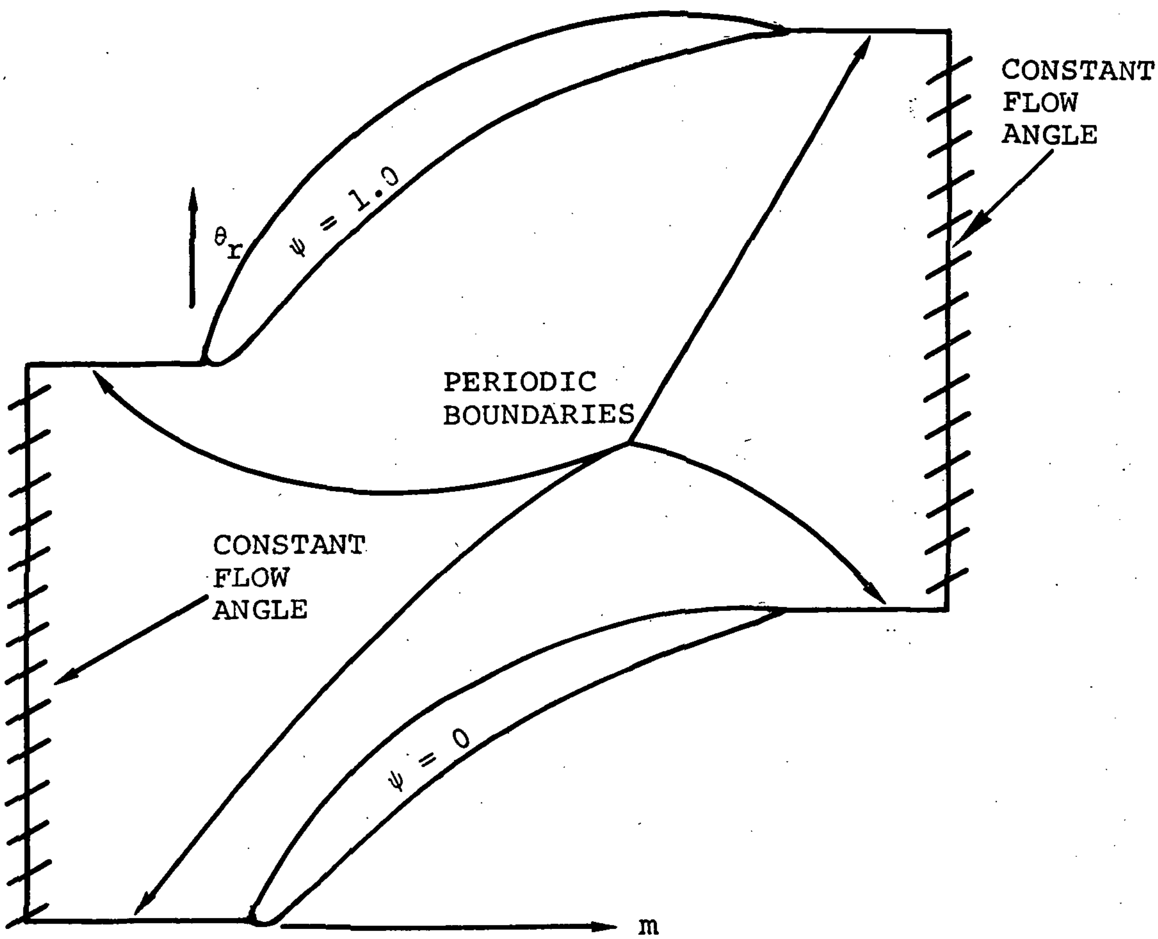

Figure 1. - Boundary conditions for solution of the stream function equation.

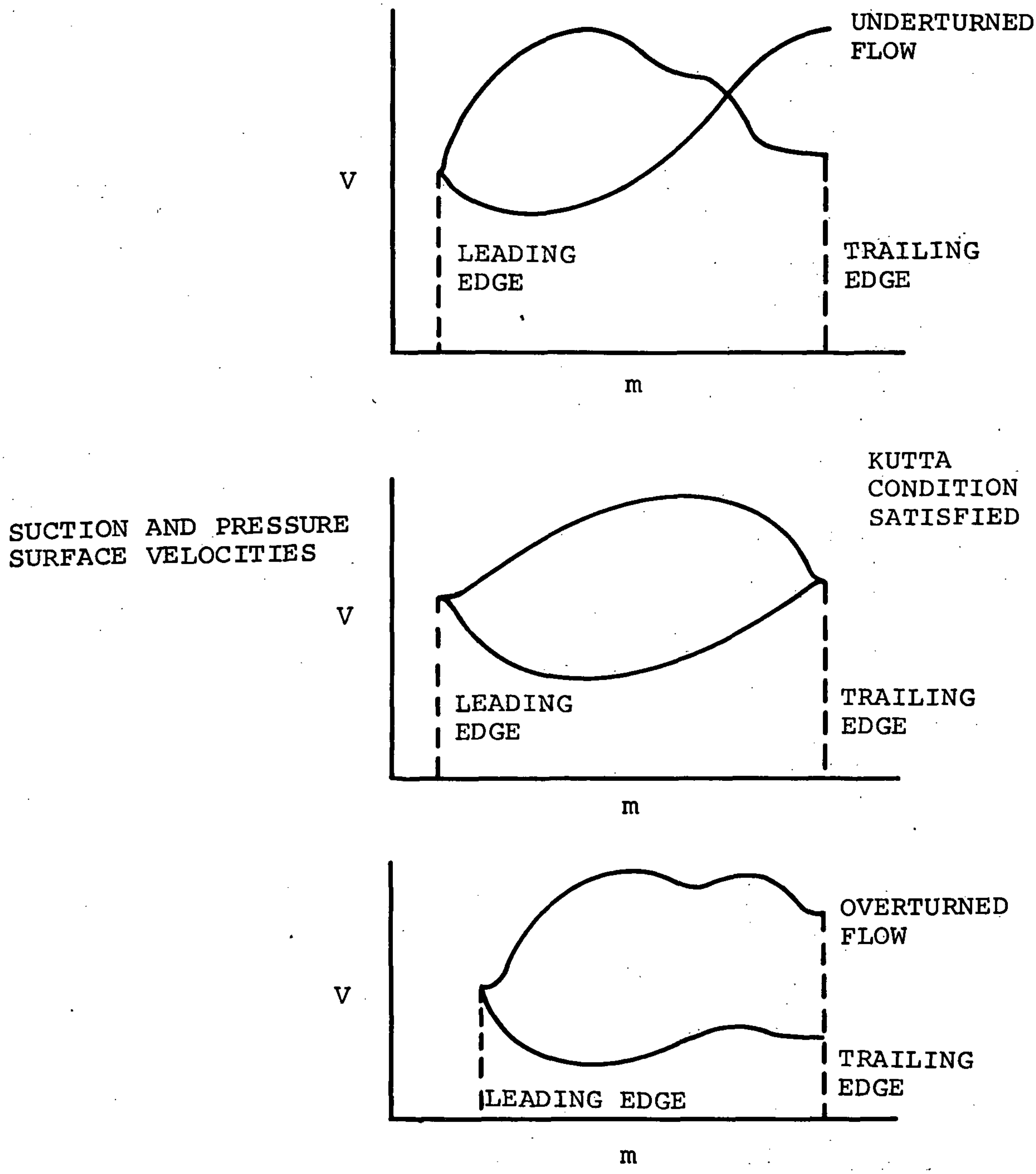

Figure 2. - Inviscid cascade solutions.

ACCURACY OF TECHNIQUE

The accuracy of the finite difference technique is expected to be influenced by the following factors:

(a) Accuracy of the inviscid solution for a given input

(b) Accuracy of the satisfaction of the trailing edge Kutta condition

(c) Accuracy of input geometries, flows, etc.

(d) The effects of viscous flows

Since integration of the solution is all that is required, the accuracy of the overall inviscid solution is expected to be excellent. To verify this point Carter's Rule can be analyzed for the effect of geometry on exit deviation angle (total turning). Since this technique represents a fit to experimental cascade data, the effect of errors in cascade parameter input and the accuracy of blade loading solutions for the finite-difference technique should be approximated. Carter's Rule is represented in Reference 3 as follows:

$$\delta = \frac{\beta_1 - i - \beta_{2e}}{\frac{\sqrt{\sigma}}{m_c} - 1} \tag{1}$$

The m-factor describes the effect of setting angle and geometry. figure 3 gives the dependence of geometry (max. camber rise point) and setting angle utilized by Reference 3. For an axial low speed cascade, equation 1 can be expressed in terms of the total turning in a cascade as follows:

$$\theta = \frac{\left(\frac{\sqrt{\sigma}}{m_c} - 1\right)(\alpha + \xi_2) + \alpha - \xi_1}{\sqrt{\sigma}/m_c} \tag{2}$$

where the angles are described in figure 4. Differentiating equation 2 the result is

$$\frac{d\theta}{dm_c} = - \delta/m_c$$

For a typical value of δ of 10 degrees and m_c of 0.25

$$\Delta\theta = -40\ \Delta m_c$$

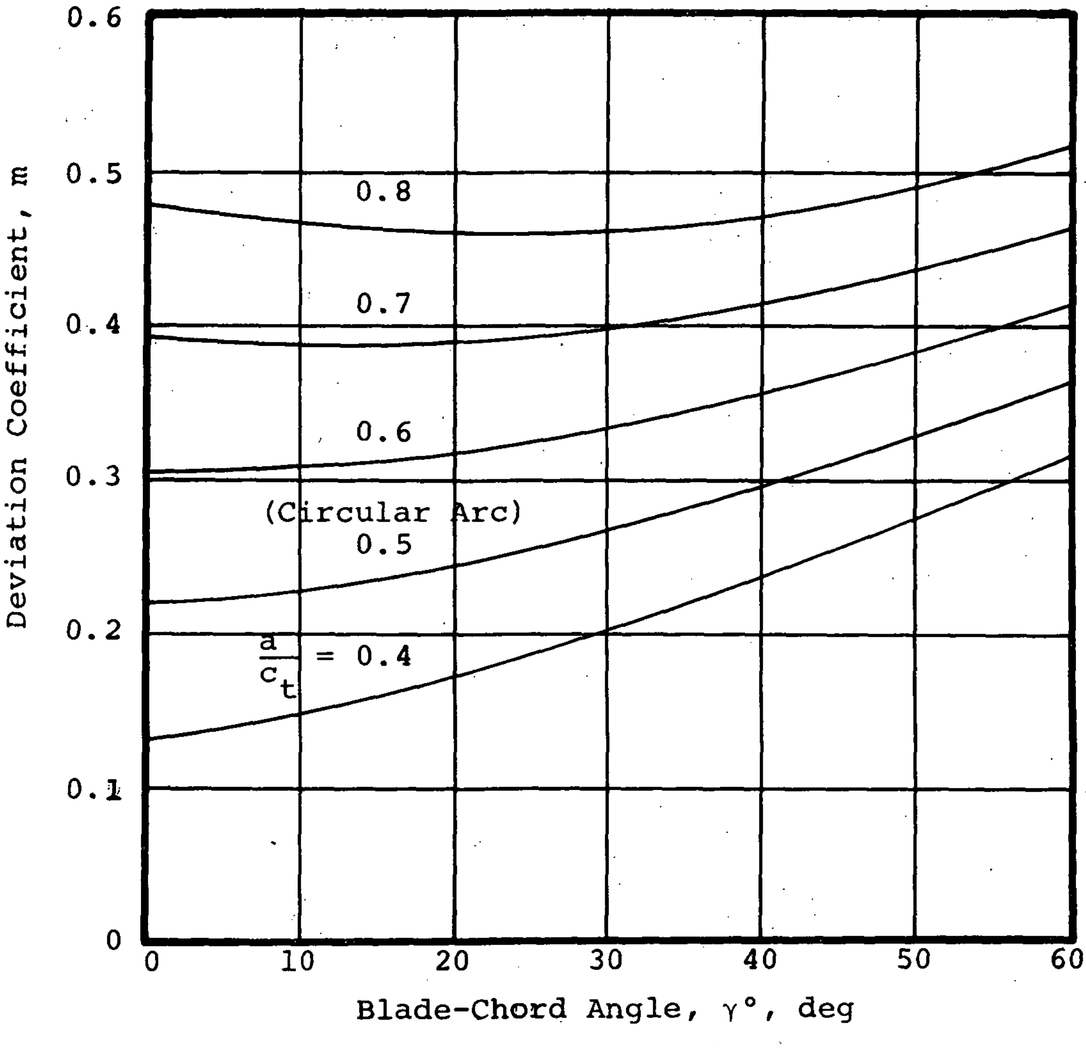

Figure 3. - Coefficients for design deviation angle rule.

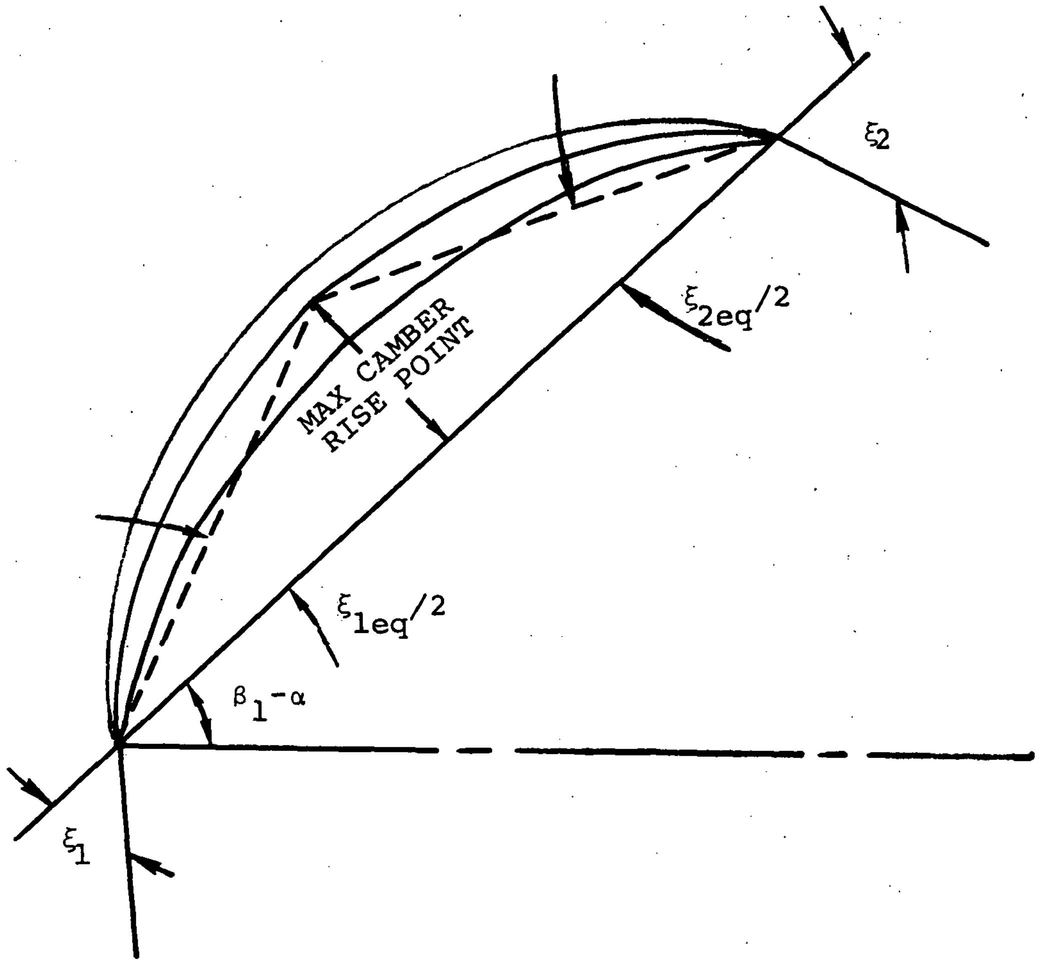

Figure 4. - Angle definitions.

To illustrate the use of this equation, if a 1-percent chord error is assumed in specifying input geometry (maximum camber rise point), the error in the turning would be 0.15 degree for the values of δ and m_c given above. This leads to the expectation that inaccuracies due to errors in input geometry specification should be slight.

Utilizing the finite-difference technique requires determination of the exit flow angle for which suction and pressure surface velocity are equal. Due to the finite-difference nature of this calculation, there is an uncertainty of the point of achievement of this equality in velocity of one-mesh spacing. The inaccuracy caused by this uncertainty in stagnation point can be evaluated as follows for the cascade situation. Assuming a triangular loading (pressure) distribution typical of compressor sections, as shown below, the uncertainty in turning can be evaluated from simple areas.

Normal values of N_m range from 20 to 40 making this error insignificant.

Real flow effects are expected to be the largest source of error. As stated earlier, this form of approximating the Kutta conditions consists of selecting θ that gives equal velocities at the trailing edge. Although the calculation differs slightly in detail, it is equivalent to the well-known technique used on isolated airfoils where the proper circulation is selected to give a dividing streamline at the trailing edge. Viscous effects including the effects of suction surface separation will modify the resultant lift. The magnitude of these effects is expected to be similar to those experienced with isolated airfoils, where useful results can be obtained for moderate cambers at nominal angles of attack.

COMPARISON WITH EXPERIMENTAL CASCADE DATA

To verify the expected accuracy of the finite-difference technique, the technique was applied to cases where experimental data was available. The obvious starting place for this comparison is with two-dimensional cascade data such as that contained in References 4, 5, and 6. This data provides the closest experimental agreement with the analysis technique since no three-dimensional flow effects were incurred. In addition, a variety of blade shapes are available for analysis. For comparison purposes data was taken from three different classes of blade shapes as follows:

(a) Front loaded, A_4K_6

(b) Mid-loaded A_{10}, circular arc

(c) Rear loaded, A_2I_{8b}

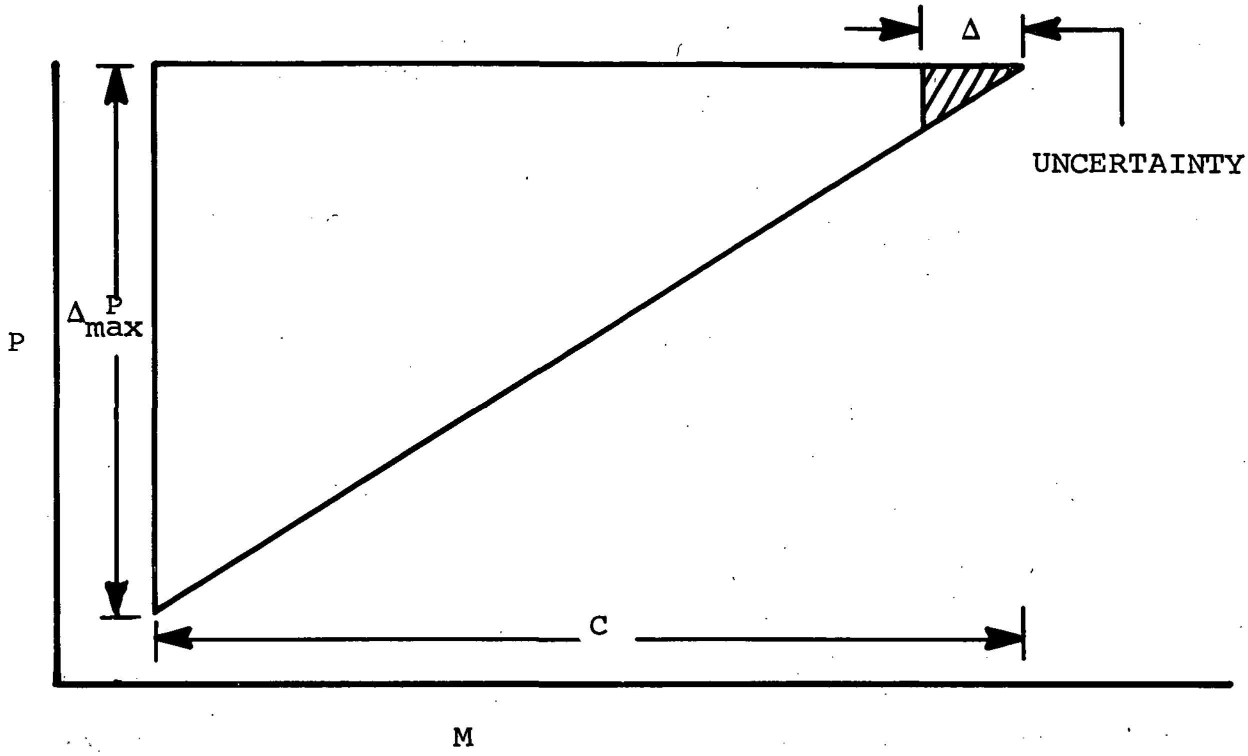

$$\Delta = C/N_m$$

where N_m is the number of mesh points between blade inlet and outlet used in the finite difference calculation

$$\frac{\Delta\theta}{\theta} = \frac{\Delta \cdot (\Delta/C)\ \Delta P_{max}}{\Delta P_{max}\ C} = \Delta^2/C^2$$

$$\frac{\Delta\theta}{\theta} = 1/N_m^2$$

Eleven cases were examined in detail. These were selected to cover a range of setting angles, inlet Mach numbers, and blade shapes.

Comparison with Carter's Rule was made utilizing the form of the rule given in Reference 3 along with the M-factor curve shown in Reference 3 and figure 3. The equations are:

$$\beta_{2e} = \tan^{-1}\left[\frac{U_1}{V_{m1}} - r_2/r_1 \left(\frac{U_2}{V_{m1}} - \frac{V_{m2}}{V_{m1}} \tan \beta_2\right)\right]$$

$$\delta^o = \frac{\beta_1 - i - \beta_{2e}}{\frac{\sqrt{\sigma}}{m_c} - 1}$$

Figures 5 through 10 show a comparison of turning angles and the ratio of change in momentum to that given by a reference turning angle, (θ Ref) for experimental data, Carter's Rule, and the finite-difference technique. Figure 11 shows the geometric angle used for the reference turning and the two approaches to Carter's Rule.

Equivalent leading and trailing edge angles were selected on the basis of the angles shown in Figure 11. For a circular-arc camber line, the true leading and trailing edge angles are equal to the equivalent leading and trailing edge angles.

An attempt was made to correlate the differences between experimental and calculated (finite-difference method) deviation angles. No correlation was found with D-factor or other conventional techniques. Stewart's calculations were also utilized and they likewise did not come close to predicting either magnitude or signs of the observed differences. What did seem consistent was that the front-loaded blades 63 (A_4K_6)06 and the 65 $(12A_{10})$10 mid-loaded blade shapes provided consistently more experimental turning than calculated. The heavily rear-loaded blades 65 $(12A_2I_{8b})$10 and the thickened circular-arc blade gave consistently less turning than calculated.

Figures 12 and 13 show the effect of Mach number on turning. As can be seen, Carter's Rule does not fit this data as well as other cases examined. Figure 14 summarizes the results on turning angle for all cases examined. The inviscid calculation has indicated a relative error of less than 5-percent error in tangential momentum change across the cascade. Although more comprisons to cascade data would be desirable, the basic characteristics and accuracy of the finite-difference method of predicting deviation angle have been demonstrated.

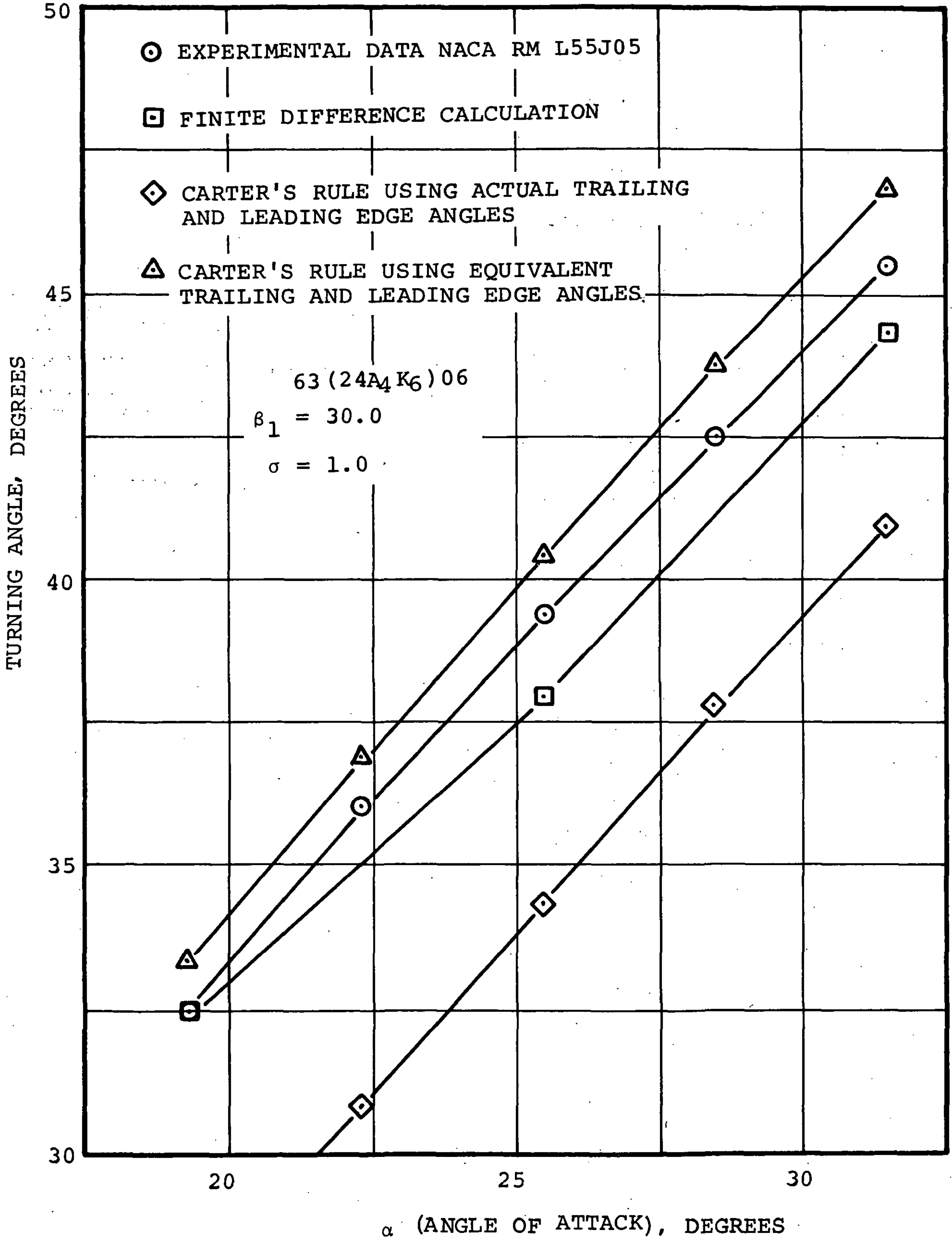

Figure 5. - Turning angle versus angle of attack.

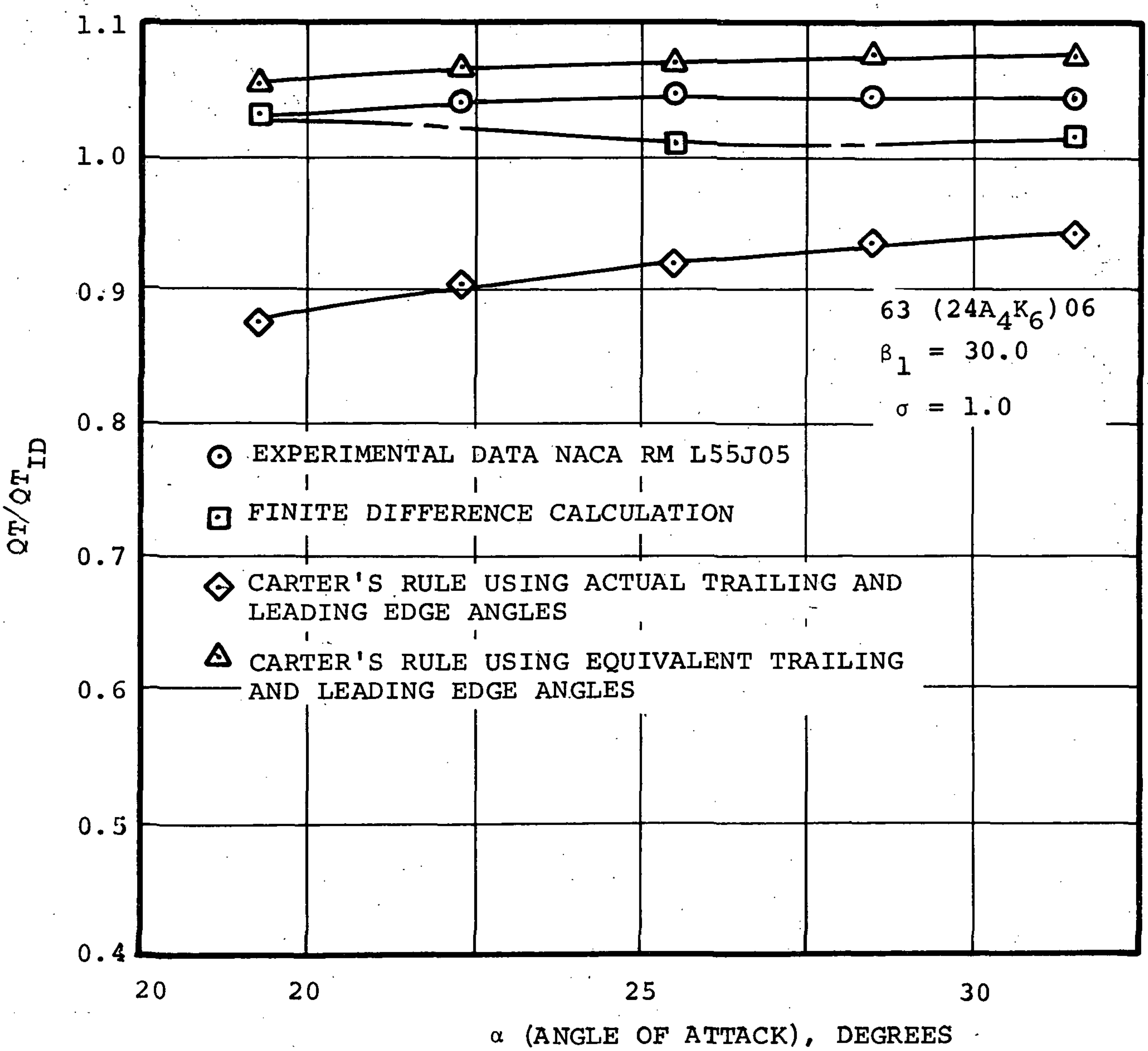

Figure 6. - Change in tangential momentum/ideal versus angle of attack.

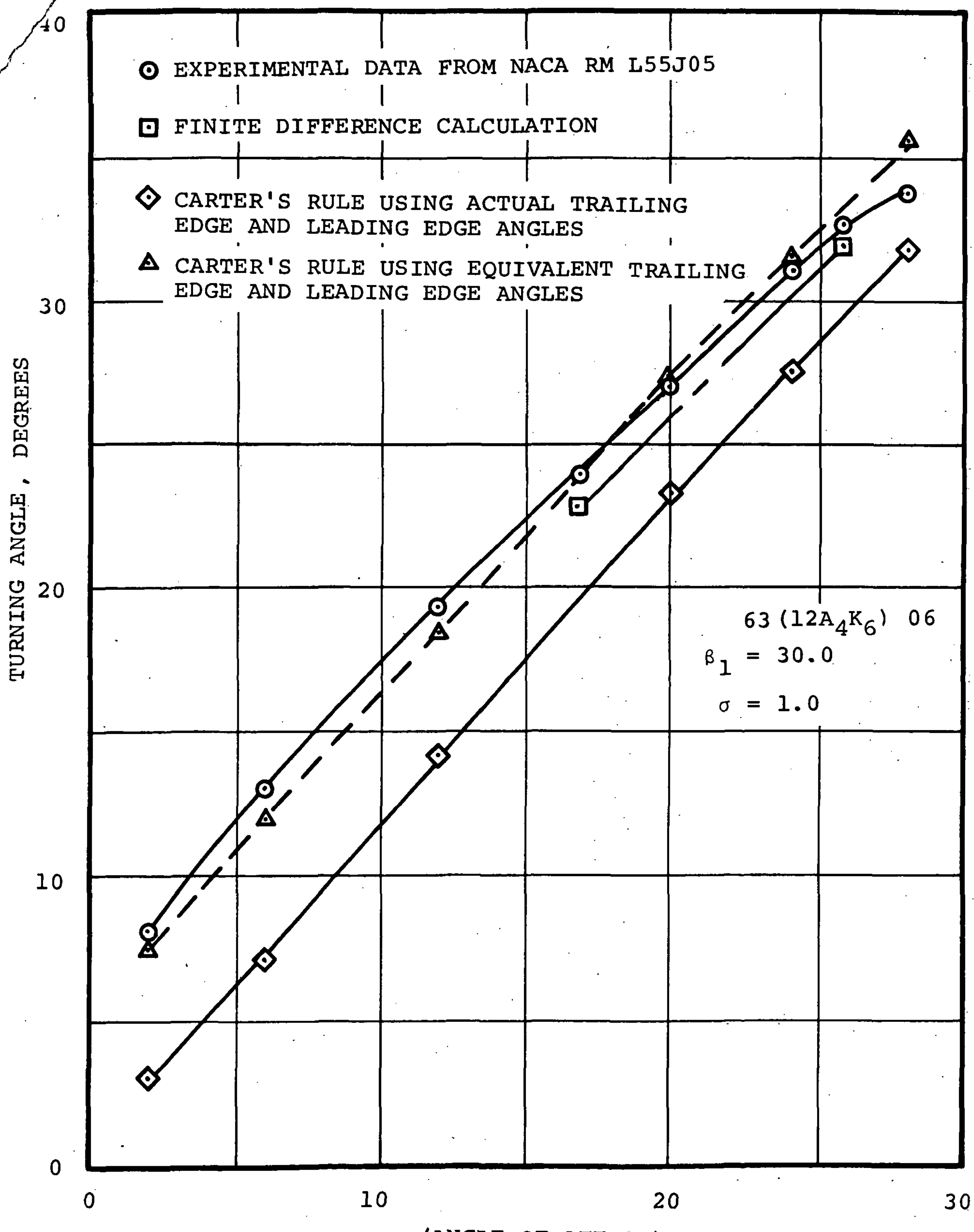

Figure 7. - Turning angle versus angle of attack.

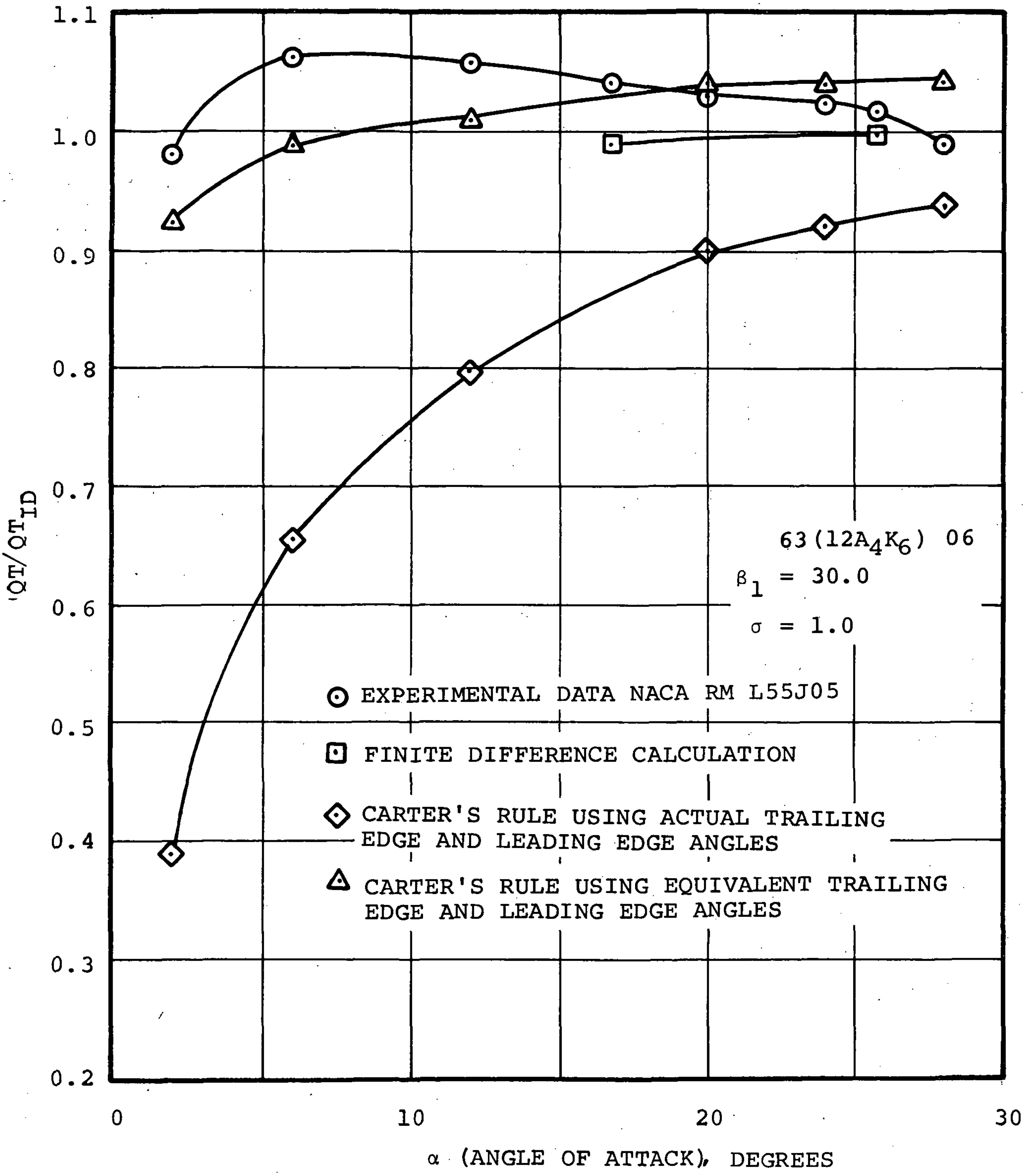

Figure 8. - Change in tangential momentum/ideal versus angle of attack.

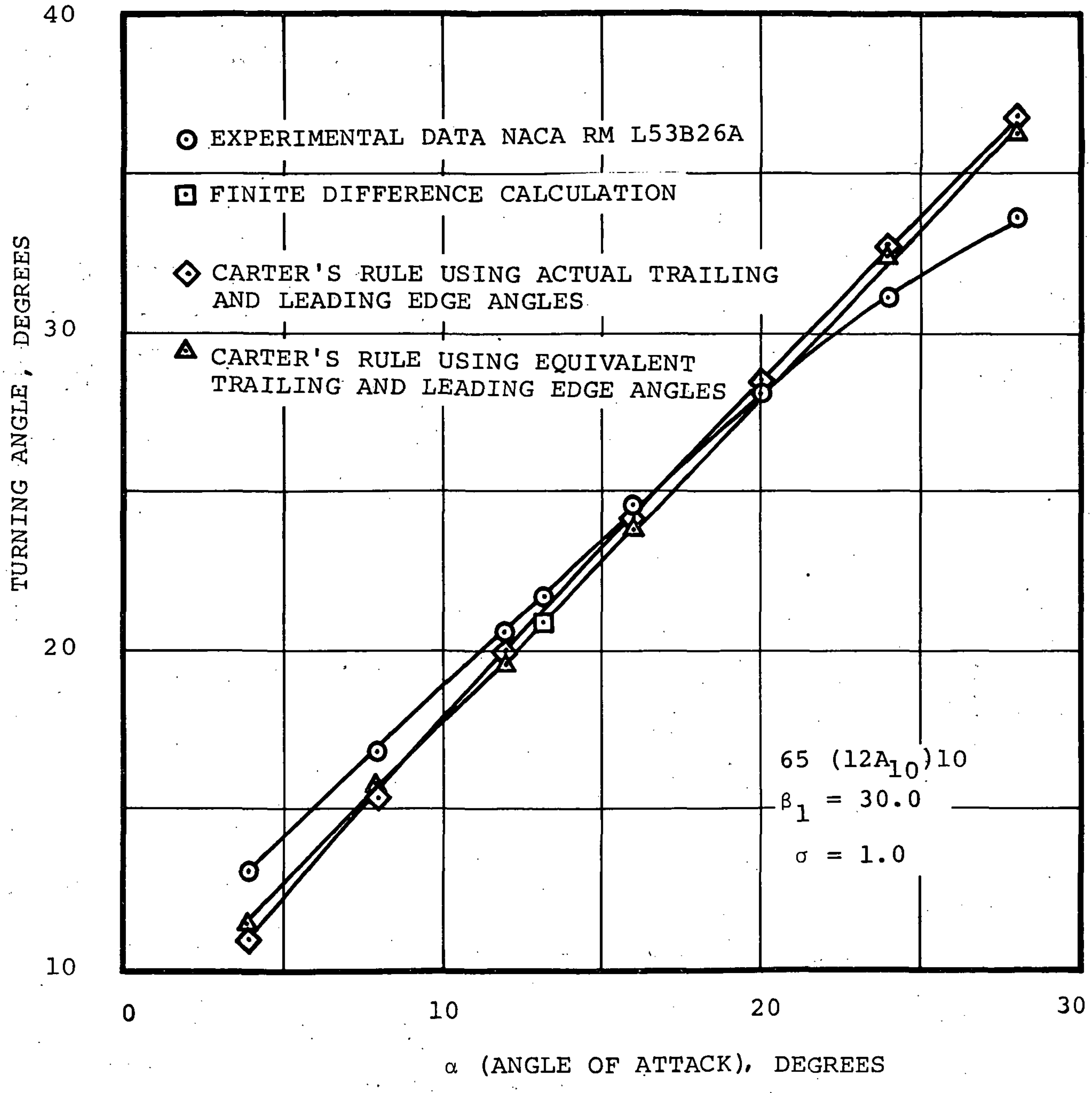

Figure 9. - Turning angle versus angle of attack.

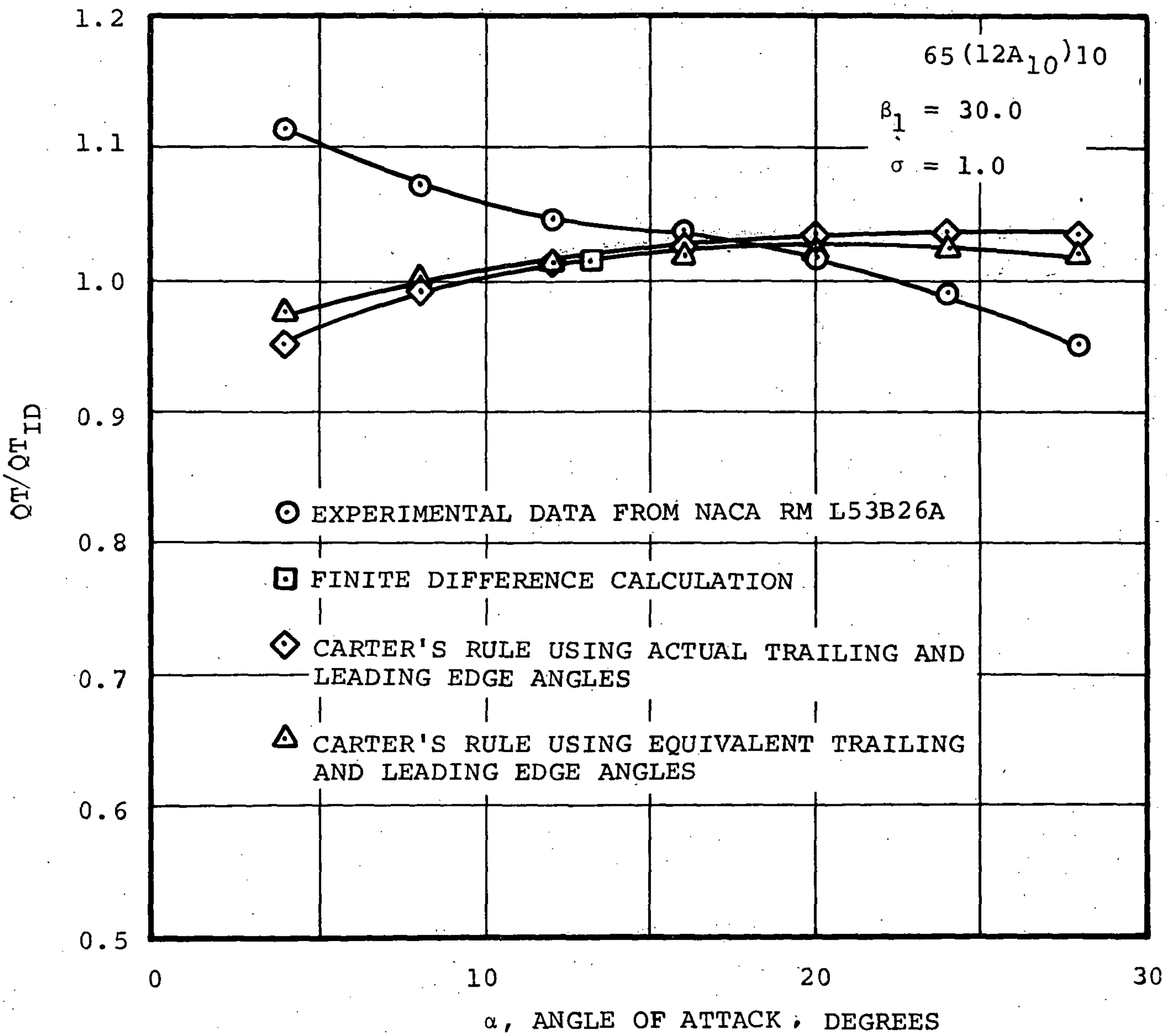

Figure 10. - Change in tangential momentum/ideal versus angle of attack.

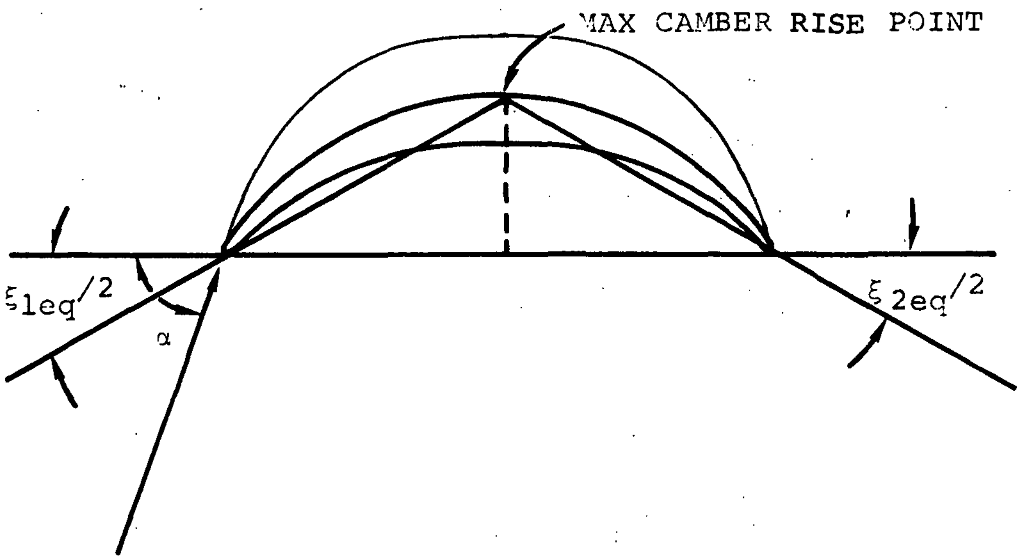

$$\theta\ \mathrm{Ref} = \alpha + \xi_{2eq}/2$$

Figure 11.

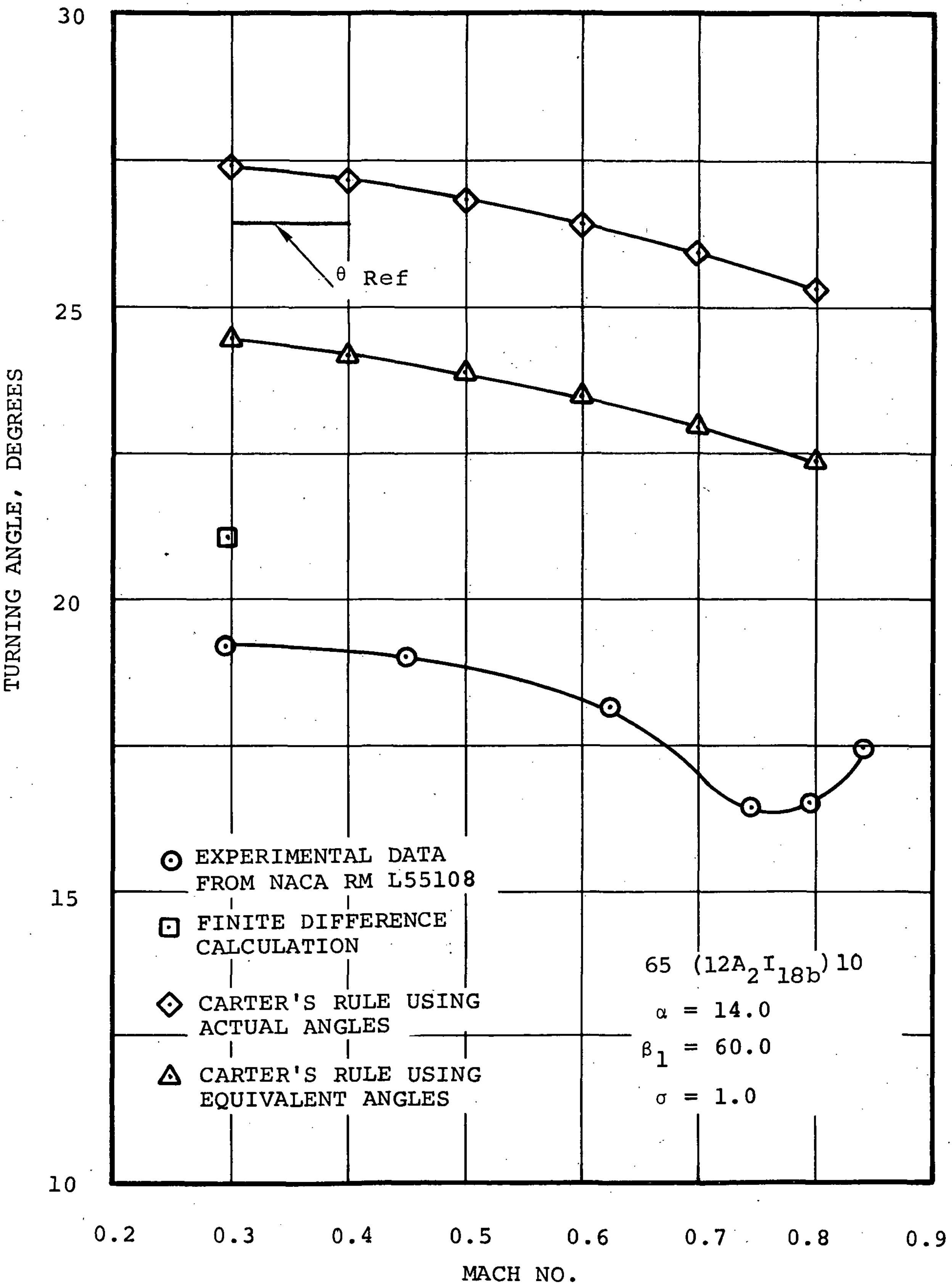

Figure 12. - Turning angle versus mach number.

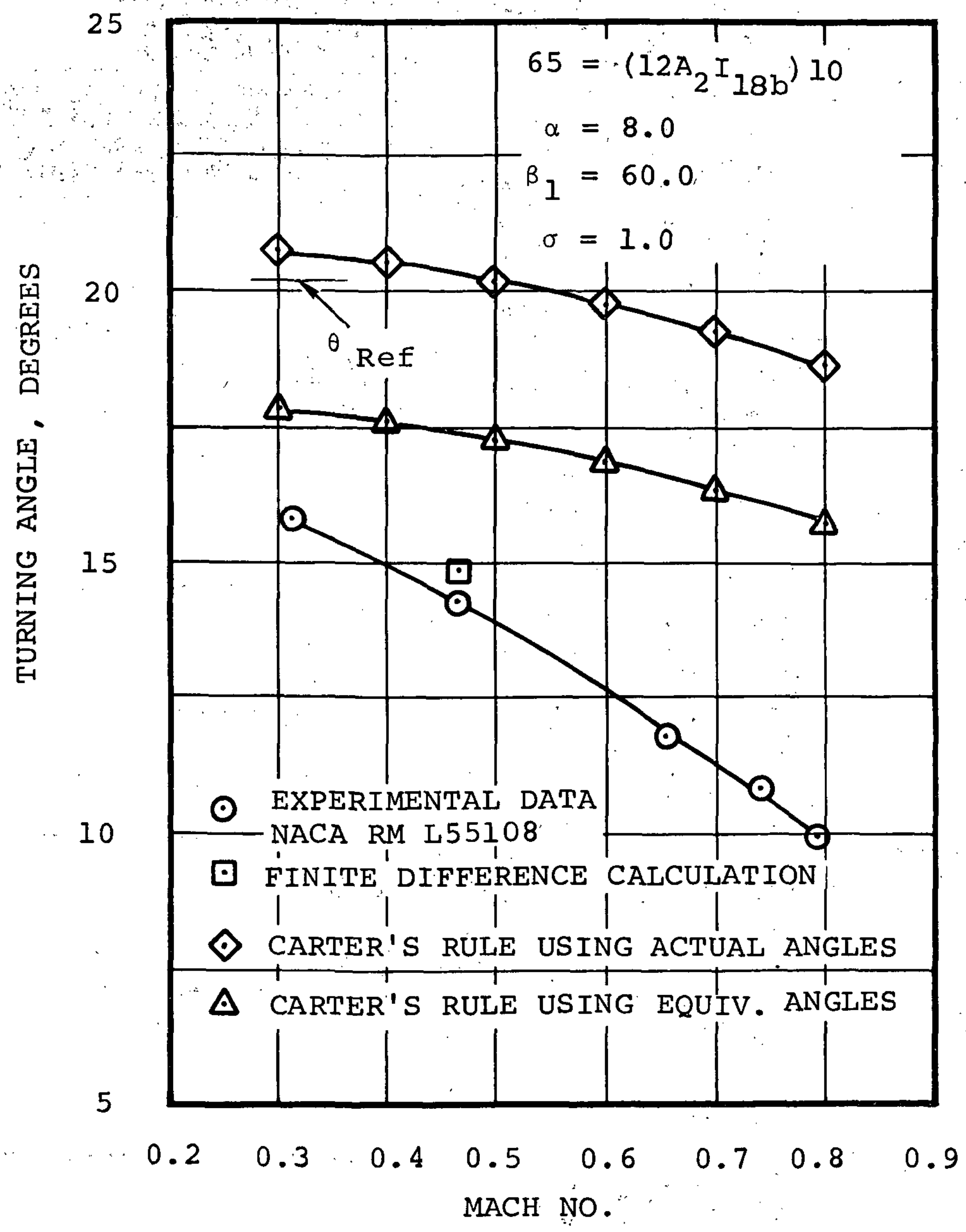

Figure 13. - Turning angle versus Mach No.

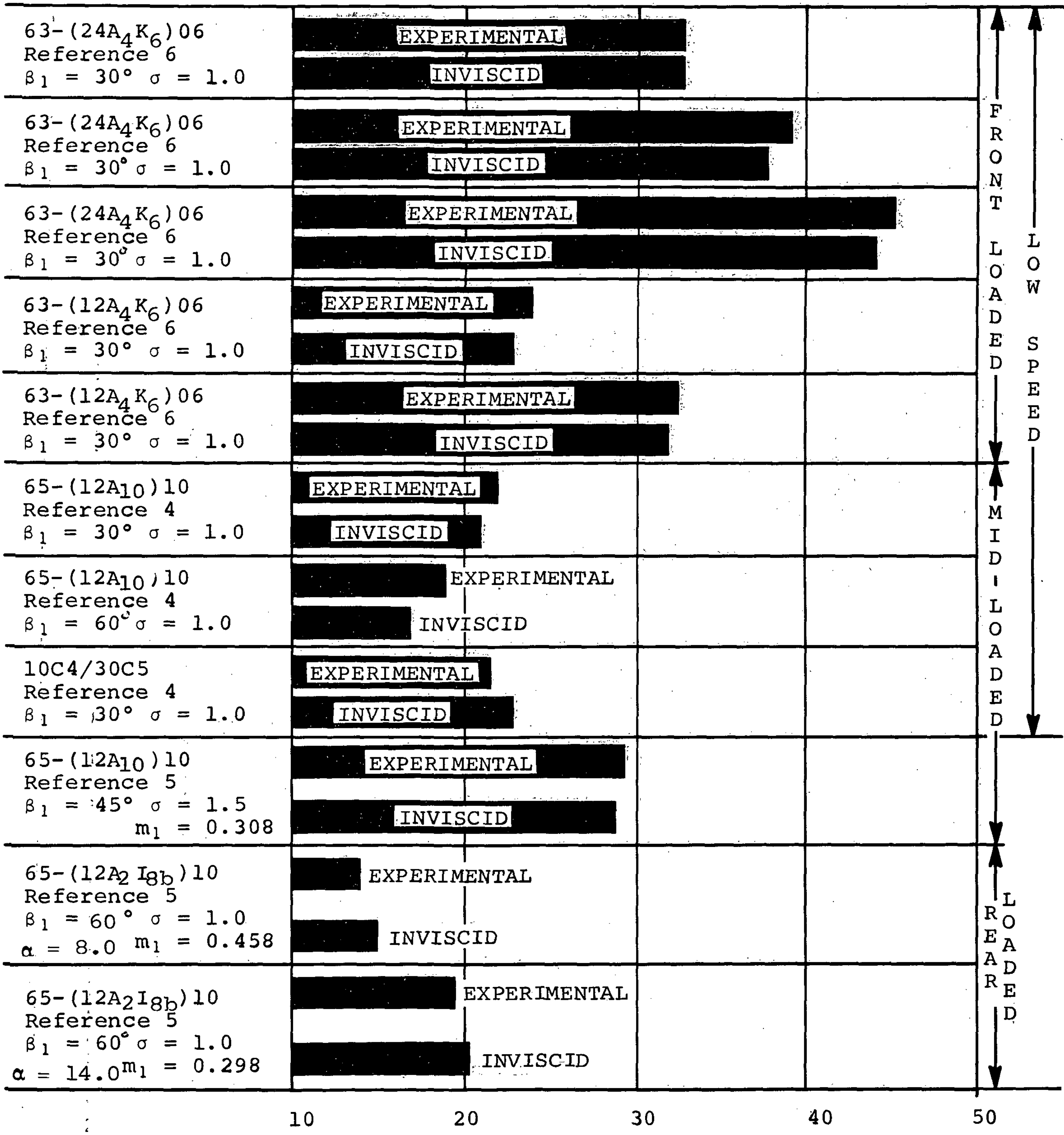

Figure 14. - Total turning θ.

APPLICATION TO THREE-DIMENSIONAL SITUATIONS

Because of the more fundamental nature of the finite-difference technique when compared to techniques used in the past, one would expect that much of the uncertainty in determining deviation angle in axial and mixed flow rotors could be eliminated. This expectation is clouded by two effects not considered by the present technique. The first is the effect of Mach number at conditions where the critical Mach number is exceeded. The finite-difference technique described herein does not provide rigorous inviscid solutions where local Mach numbers are supersonic. This restricts the direct application of this technique to the hub sections of many rotors. However, by application of this technique to lower Mach numbers for a given section and comparison with previous cascade data, the basic radius change and area change characteristics can be determined at extrapolated to high Mach numbers. There is considerable hope that the restriction in Mach number will soon be lifted resulting in a finite-difference technique of reasonable computer run times and a Mach number capability through the entire rotor design range.

The second and more serious deficiency from a long range standpoint is the effect of three-dimensional factors not taken into account by the application of successive radial equilibrum and blade-to-blade solutions. These are as follows:

(a) Secondary flow

    (1) Cross flow in boundary layer

    (2) Vorticity generation in boundary layer

(b) Blade sweep effects

(c) Stream sheet warpage and twist

(d) Effects of blade separation and the migration of low energy flow away from blade hub

Attempts to analytically evaluate these three-dimensional effects have met with limited success (Reference 7-10). Therefore, a decision was made to attempt to derive an empirical method for accounting for these effects.

Deviation angle data from a series of fan tests of an AiResearch experimental fan was employed in the empirical development. This data is presented in figure 15 which includes a comparison of design and measured deviation angles as a function of exit radius for the rotor. The design conditions shown in figure 15 are really immaterial to the following argument. A postulation is made that the difference between the measured deviation angle and that calculated by the finite difference, blade-to-blade computer program represents the viscous component of the deviation. A comparison of the measured and blade-to-blade calculated deviations for the experimental fan is presented in figure 16. The difference between the measured and calculated deviation angle for each streamline is shown in figure 17. Figures 16 and 17 indicate that most of the postulated viscous effects are in the lower half of the blade with the largest influence at the rotor hub.

Assuming that this difference represents the viscous effects on deviation, consideration is given to how these effects may be applied for other rotor configurations. Several correlating parameters were investigated with the diffusion factor (D) across the blade seeming to offer the most promise. Since the diffusion factor is representive of the losses within the blade row, the deviation correction term for a particular streamline may indeed scale directly to the ratio of diffusion factors.

The proposed approach for calculating deviation angles for the conical flow compressor is then to: (1) use the finite difference, blade-to-blade program to compute the non-viscous deviation angle, (2) obtain a deviation correction term from figure 4 for the corresponding streamline, (3) adjust the deviation correction by the corresponding diffusion factor ratios, and (4) combine the non-viscous and viscous components to get total deviation angle. A sample calculation showing this procedure is presented as table I. This tabulation shows how data from the AiResearch experimental fan was employed to predict the deviation for a rotor designed for NASA by the General Electric Company. The comparison is made at the 10-percent streamline in the hub region where considerable deviation was measured. The results of the comprison indicate very good agreement between the predicted and measured deviation for G.E. Rotor 1B. Obviously this result could just be fortuitous, but time limitations and a lack of sufficiently precise experimental information in this area did not permit further investigation.

The negative portion of the deviation correction shown in figure 17 will be neglected in the design of the conical compressor. This means the deviation angle in the region between the 90- and 50-percent streamlines will come from the finite-difference calculations without correction. The reasons for omitting the correction in this region are: (1) the correction shown is small, being less than 1 degree and (2) a reasonable explanation could not be determined for applying a negative correction for viscous effects to the deviation angle prediction.

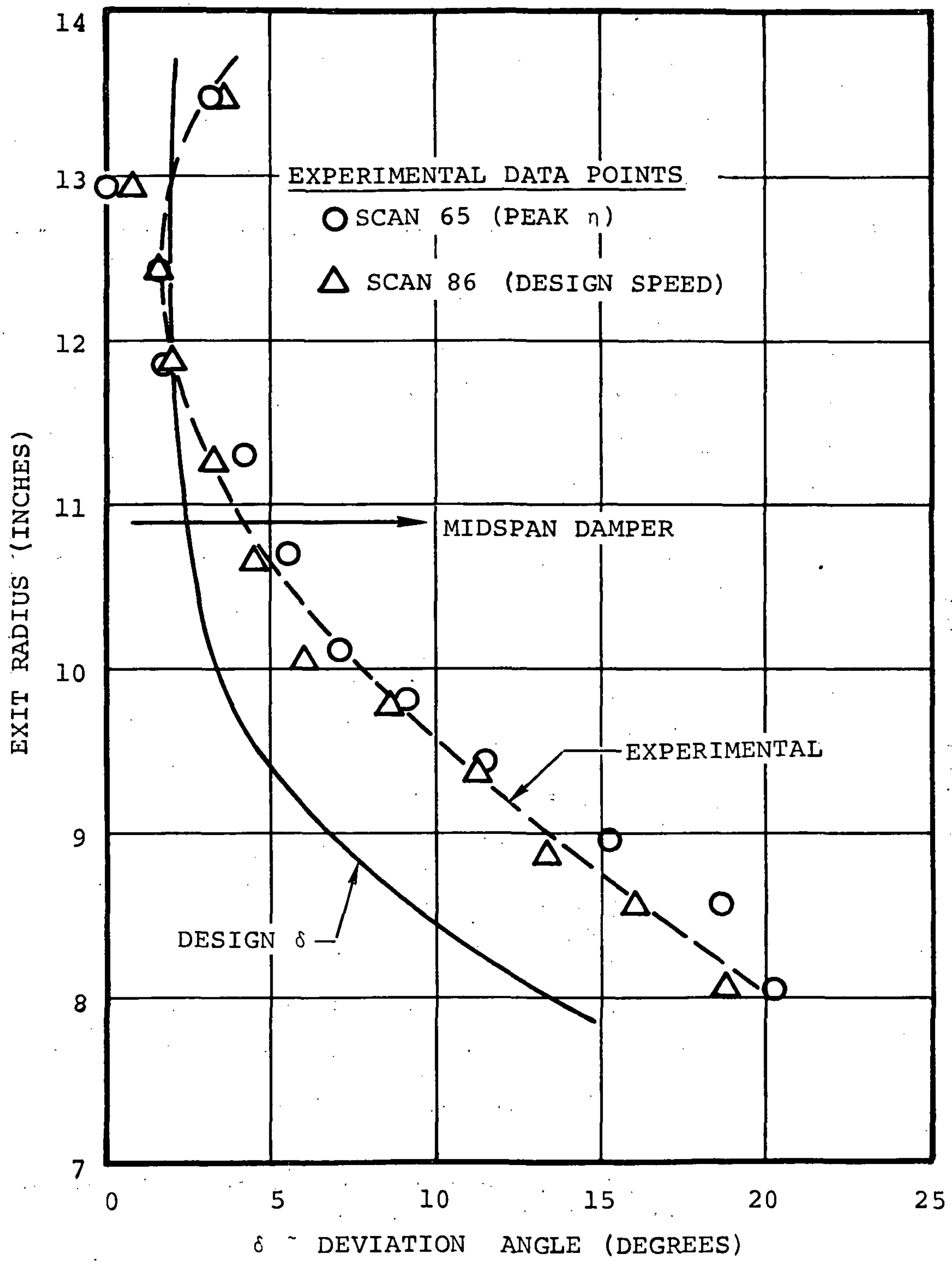

Figure 15. - AiResearch experimental fan, deviation versus blade radius.

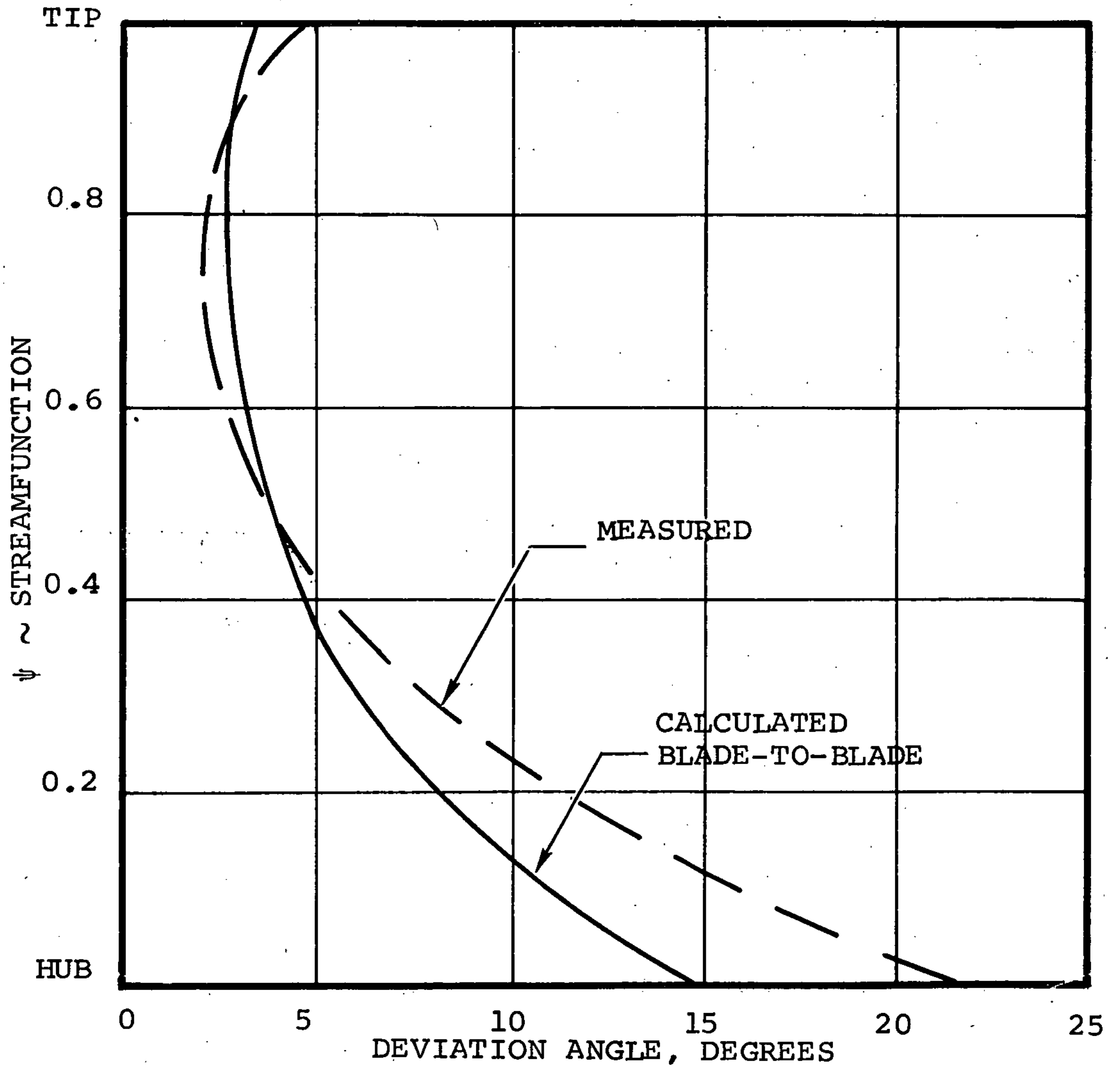

Figure 16. - AiResearch experimental fan, calculated and measured streamline deviation.

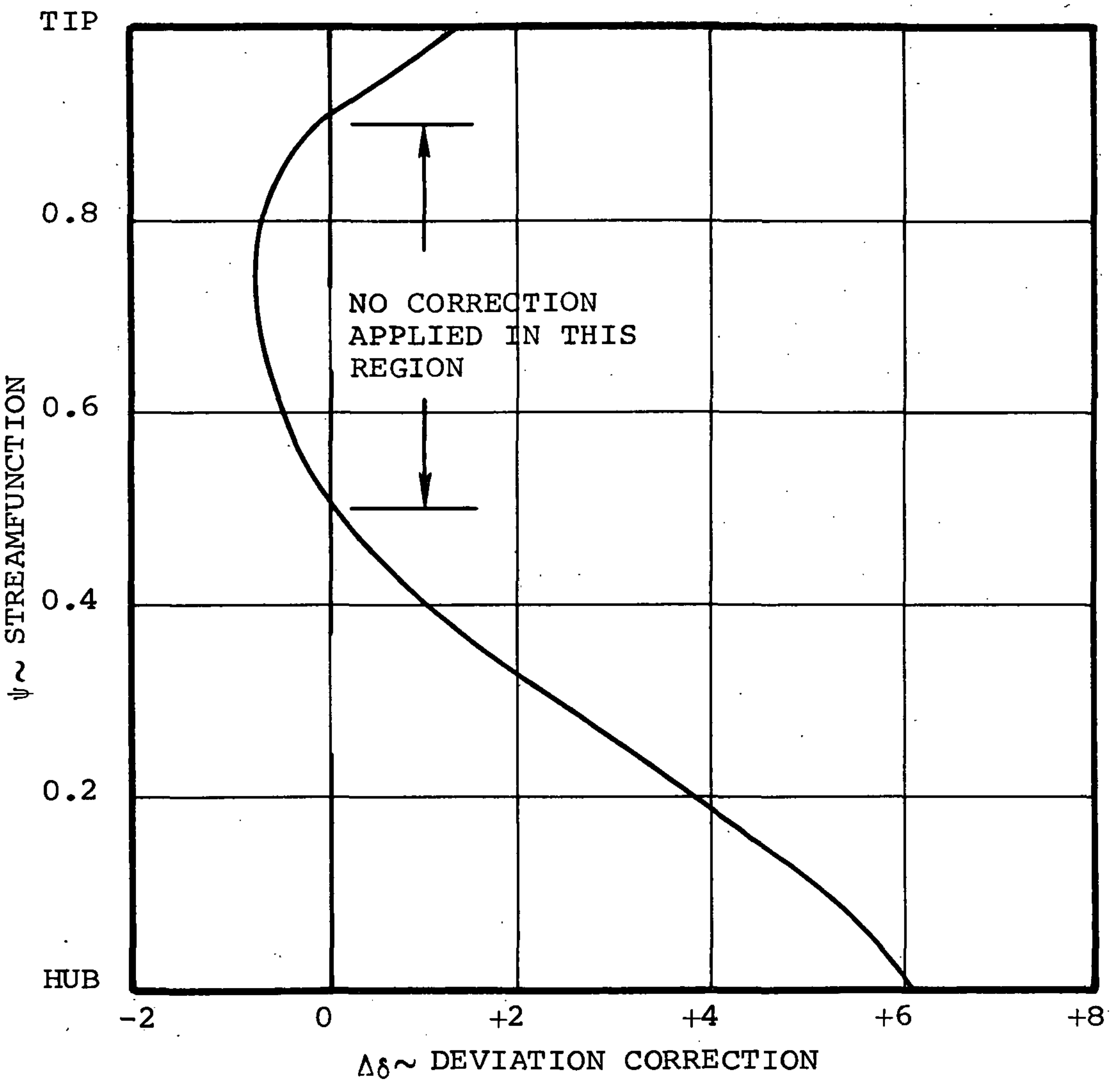

Figure 17. - AiResearch experimental fan results, deviation correction for each streamline.

TABLE I

SAMPLE CALCULATION
OF DEVIATION FOR G.E. ROTOR 1B*

10% STREAMLINE (HUB REGION)

BASIS - AIRESEARCH EXPERIMENTAL FAN RESULTS:

δ (MEASURED) = 15.8
δ (CALCULATED) = 10.6 degrees (BLADE-TO-BLADE RESULTS)

$\nabla\delta$ = 5.2 degrees

"D" FACTOR (AEF) = 0.47

ROTOR 1B RESULTS:

δ (CALCULATED) = 8.2 degrees (BLADE-TO-BLADE RESULTS)

"D" FACTOR (R-1B) = 0.49

DEVIATION CORRECTION FOR ROTOR 1B

$$\nabla\delta \text{ (R-1B)} = \nabla\delta \text{ (731)} \times \frac{\text{D (R-1B)}}{\text{D (AEF)}}$$

$$\nabla\delta = 5.2 \times \frac{0.49}{0.47} = 5.4 \text{ degrees}$$

PREDICTED DEVIATION = δ (CALC) + $\nabla\delta$ = 13.6 degrees.

MEASURED DEVIATION = 14.0 degrees.

*Seyler, D.R. and L. H. Smith Jr. Single Stage Experimental Evaluation of High Mach Number Compressor Rotor Blading, NASA CR-54581, 1967.

In summary, the foregoing discussion indicates that the finite difference, blade-to-blade program predicts most of the effects of blade loading on the air turning in compressor cascades. In the regions where the analysis indicates that the finite-difference program was lacking, an empirical correction is recommended. The combination analytical and empirical approach should provide a reasonably precise prediction of deviation angles for the conical flow compressor.

CONCLUSION

The finite-difference inviscid technique discussed herein presents a step forward in numerical determination of deviation angles. Particularly, the effects of radius change and meridional velocity ratio on the blade geometry can be evaluated to an accuracy not previously obtainable. However, three-dimensional, secondary flow effects must be evaluated when applying the technique to three-dimensional cases. These serve to make the finite-difference technique of primary use in removing many of the uncertainities associated with Carter's Rule. This does not remove the need for adder factors correlated to experimental results from existing axial compressors. However, the combined analytical-empirical approach for predicting deviation angle should instill a much higher degree of confidence in the blade angle settings than experienced through the use of sonic modification of Carter's Rule.

1. Katsanis, Theodore and William D. McNally, Fortran Program for Calculating Velocities and Streamlines on a Blade-to-Blade Stream Surface of a Tandem Blade Turbomachine, NASA, TND-5044, March 1969.

2. Milne-Thomson, L.M., Theoretical Hydrodynamics, The MacMillan Company, New York, 1960.

3. Seyler, D.R. and L.H. Smith Jr., Single Stage Experimental Evaluation of High Mach Number Compressor Rotor Blading, NASA CR-54581, 1967.

4. Felix, A. Richard and James C. Emery, A Comparison of Typical National Gas Turbine Establishment and NACA Axial-Flow Compressor Blade Sections in Cascade at Low Speed, NACA RM L53B26A, 1953.

5. Dunavant, James C., James C. Emery, Howard C. Walch, and Willard R. Westphal, High Speed Cascade Tests of the NACA 6-(RA10)10 and NACA 65-(12A2K80)10 Compressor Blade Sections, NACA RML55I08, 1955.

6. Emery, James C., Low-Speed Cascade Investigation of Loaded Leading Edge Compressor Blades, RM L55J05, 1956.

7. Lieblein, Seymour, and Richard H. Ackley, Secondary Flows in Annular Cascade and Effects on Flow in Inlet Guide Vanes, NACA RM L251627, 1951.

8. Hauser, Arthur G., and Howard Z. Herzig, Cross Flows in Laminar Incompressible Boundary Layers, NACA TN3651, 1956.

9. Lakshminarayana, B., Methods of Predicting the Tip Clearance Effects in Axial Flow Turbomachinery, ASME Paper 69-WA/FE-26, 1969.

10. Wheeler, A.J., and J.P. Johnston, Three-Dimensional Turbulent Boundary Layers - An Assessment of Prediction Methods, Stanford University, Thermoscience Division, Report MD-30, 1971.

APPENDIX A

NOTATION

b Axisymmetric streamtube thickness

c Chord

C_p Specific heat at constant pressure

i Incidence angle

m Meridional distance

$\dot{m}$ Mass flow rate

m_c Geometry constant in Carter's rule

N_m Number of mesh points leading edge to trailing edge

P_p Pressure surface static pressure

P_s Suction surface static pressure

r Radius

T' Total temperature

U Wheel speed, free stream velocity

u Boundary layer velocity

V Velocity in absolute frame

W Relative velocity

APPENDIX A

NOTATION (Contd)

α	Streamline slope
β	Relative flow angle
δ	Deviation angle
δ_{bl}	Boundary layer thickness
ω	Rotor rotational frequency
ω_v	Vorticity
ω_s	Streamwise component of vorticity
ψ	Stream function
σ	Solidity
θ	Total turning angle
θ_r	Tangential coordinate in a cylindrical coordinate system
ρ	Density
Γ	Circulation

<u>Subscripts</u>

U	Tangential direction
1	Inlet
2	Outlet
m	Meridional

APPENDIX B

DESCRIPTION OF BLADE SECTIONS FOR ROTORS AND STATORS

APPENDIX B

COMPRESSOR BLADE STACKING PROGRAM

The basic calculation performed by the Blade Stacking Program is to take the specification of airfoil shapes along a set of axisymmetric stream surfaces, interpolate the input data to cylindrical surfaces, and "stack" the blade using the cylindrical sections. The type of airfoil shape can be 65-series, multiple or double circular arc or arbitrary. Axisymmetric stream surfaces can be cylindrical, conical, or arbitrary.

Required input specification parameters for airfoil sections are mean camber line direction and tangential thickness. Each input axisymmetric stream surface must be specified by axial and radial location and slope.

The blade stacking axis must be defined on two, mutually perpendicular surfaces, the r-z plane and the r-θ plane. Normal blade stacking procedure has been to calculate the center of gravity for each cylindrical stacking section and align each section center of gravity along a straight, radial line. However, this program can stack the blade on an arbitrarily specified axis in both planes.

For purposes of this design, the axial location of the program stacking axis for rotor 1A is taken at the leading edge center location. All other sections have the stack point axial location at about the blade section center of gravity (C.G.). Tangential location of the stack point for all sections is near the section C.G. location. (Refer to center of gravity coordinates, (X, S), defined on each blade section printout).

The output from the stacking routine gives the parameters of cylindrical blade angle, tangential (or normal) thickness and the blade lean angle for input to the through-the-blade flow field calculation. It also provides the blade geometry along any axisymmetric stream surface for input to the blade-to-blade analysis program. Plane sections are also generated for blade manufacturing purposes.

COORDINATE TERMS

X - AXIAL DISTANCE FROM STACKING AXIS ON CYLINDRICAL OR PLANE SECTION

S - Rθ TANGENTIAL DISTANCE FROM STACKING AXIS ON CYLINDRICAL SECTION

Y - R SIN θ, TANGENTIAL DISTANCE FROM STACKING AXIS ON PLANE SECTION

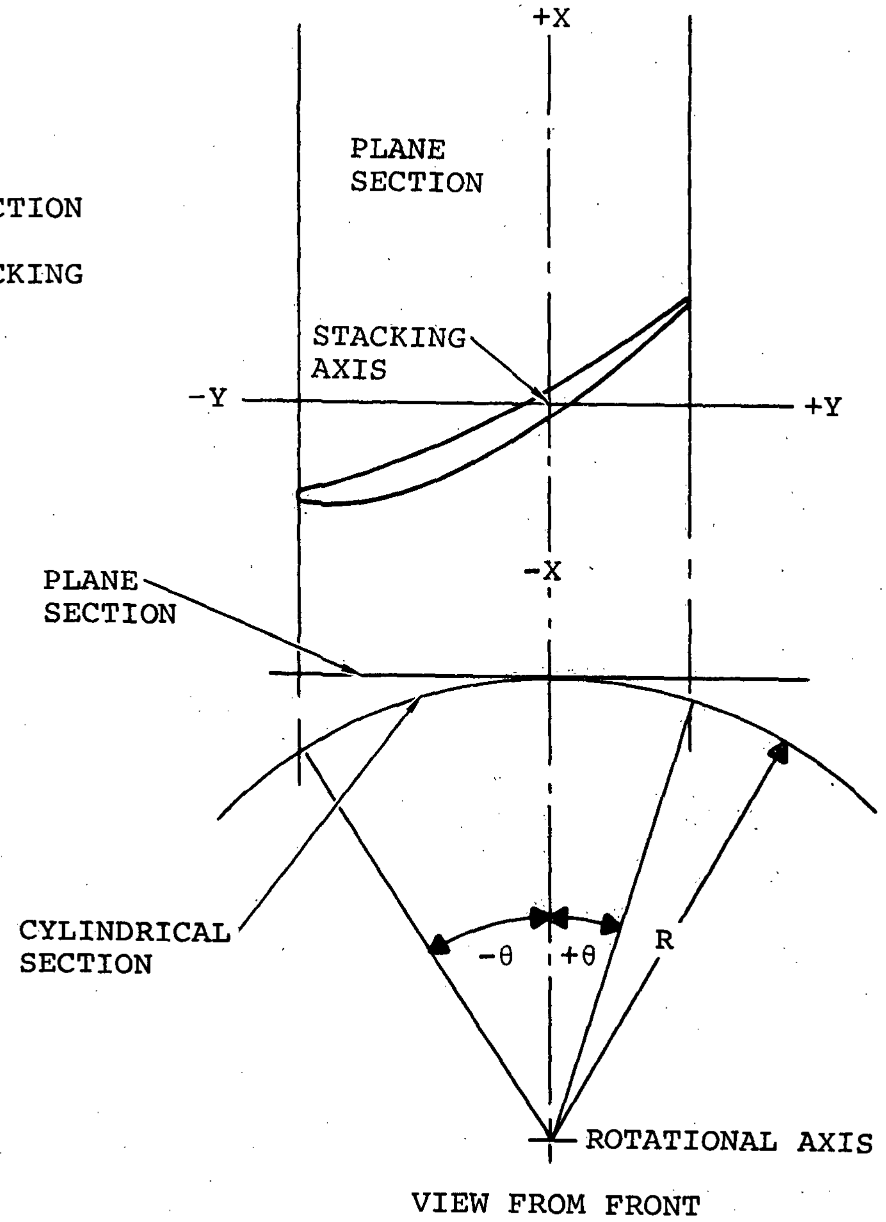

DEFINITION OF BLADE SECTION COORDINATE PARAMETERS

ADVANCED TWO-STAGE COMPRESSOR ** CONICAL FLOW ROTOR NO. 1

.... R A D I U S ....

1.000000

NUMBER OF BLADES
20

CENTER OF GRAVITY
CYLINDRICAL PROFILE
X = .280527
S = .000729

PROPERTIES OF CYLINDRICAL PROFILE

LE THICKNESS=	.009466	SPACING =	.314159
TE THICKNESS=	.022859	AXIAL CHORD=	.563783
TRUE CHORD =	.604859	SOLIDITY =	1.794577

DIRECTION OF ROTOR ROTATION = CLOCKWISE (VIEWED FROM THE TRAILING EDGE)

**** C A L C U L A T E D   C O O R D I N A T E S ****

CYLINDRICAL COORDINATES

NO.	X	S	NO.	X	S
1	.538200	-.021794	26	.019767	-.186079
2	.509376	.001537	27	.044460	-.145723
3	.481701	.015752	28	.069509	-.108351
4	.455507	.022985	29	.095011	-.074070
5	.430886	.026004	30	.121029	-.042966
6	.407296	.026023	31	.147524	-.014978
7	.383978	.023819	32	.174558	.010005
8	.361002	.019739	33	.201652	.032692
9	.337765	.013875	34	.229424	.052661
10	.314075	.006311	35	.258130	.069591
11	.288973	-.001223	36	.287721	.083333
12	.262997	-.010686	37	.318722	.091828
13	.236067	-.022301	38	.350177	.096533
14	.208469	-.036588	39	.381894	.097117
15	.180812	-.054500	40	.413268	.093329
16	.152614	-.075815	41	.444369	.084757
17	.123940	-.100701	42	.474440	.070833
18	.094750	-.129218	43	.502938	.050943
19	.065107	-.161267	44	.529956	.025536
20	.035119	-.196714	45	.555824	-.007236
21	.004816	-.235370	46	.558389	-.013422
22	.001273	-.237813	47	.554294	-.005697
23	-.002952	-.237042	48	.545919	-.025892
24	-.005374	-.233509	49	.538200	-.021794
25	-.004623	-.229285	50	.000092	-.232327
		L.E.R.C.	51	T.E.R.C. .547012	-.014515

PLANE COORDINATES

NO.	X	Y	NO.	X	Y
1	.538181	-.021725	26	.019570	-.187733
2	.509376	.001537	27	.044218	-.146696
3	.481692	.015774	28	.069318	-.108827
4	.455489	.023026	29	.094900	-.074252
5	.430865	.026052	30	.120986	-.043012
6	.407276	.026069	31	.147518	-.014982
7	.383964	.023856	32	.174558	.010005
8	.360993	.019764	33	.201621	.032691
9	.337765	.013875	34	.229336	.052675
10	.314075	.006311	35	.257961	.069642
11	.288973	-.001223	36	.287453	.083446
12	.262987	-.010686	37	.318364	.092040
13	.236061	-.022284	38	.349758	.096823
14	.208458	-.036567	39	.381447	.097465
15	.180796	-.054501	40	.412842	.093703
16	.152597	-.075906	41	.443996	.085127
17	.123932	-.101003	42	.474166	.071156
18	.094757	-.129890	43	.502790	.051160
19	.065127	-.162475	44	.529917	.025605
20	.035118	-.198554	45	.555824	-.007236
21	.004746	-.237722	46	.558389	-.013422
22	.001264	-.240167	47	.554284	-.005697
23	-.002907	-.239408	48	.545890	-.025789
24	-.005326	-.235887	49	.538181	-.021725
25	-.004576	-.231665	50	.000086	-.234695
		L.E.R.C.	51	T.E.R.C. .547001	-.014484

ADVANCED TWO-STAGE COMPRESSOR ** CONICAL FLOW ROTOR NO. 1

.... R A D I U S .....
1.200000

NUMBER OF BLADES
20

CENTER OF GRAVITY
CYLINDRICAL PROFILE
X = .251015
S = .000541

PROPERTIES OF CYLINDRICAL PROFILE

LE THICKNESS= .008613 SPACING = .376991
TE THICKNESS= .017330 AXIAL CHORD= .539732
TRUE CHORD = .631986 SOLIDITY = 1.431683

DIRECTION OF ROTOR ROTATION = CLOCKWISE (VIEWED FROM THE TRAILING EDGE)

**** C A L C U L A T E D   C O O R D I N A T E S ****

CYLINDRICAL COORDINATES

NO.	X	S	NO.	X	S
1	.521341	.051904	26	.018025	-.220372
2	.494166	.063391	27	.040830	-.178041
3	.467968	.068940	28	.064207	-.137596
4	.443300	.070770	29	.088241	-.099393
5	.419868	.069626	30	.113030	-.063778
6	.397179	.065956	31	.138334	-.030794
7	.374923	.059978	32	.164193	-.000595
8	.352621	.052028	33	.190535	.026795
9	.329952	.042102	34	.217277	.051454
10	.305392	.030666	35	.244608	.073207
11	.281745	.017400	36	.272586	.091961
12	.256451	.001149	37	.301652	.106586
13	.230569	-.018132	38	.331608	.116761
14	.204285	-.040579	39	.361930	.122813
15	.177519	-.066036	40	.392299	.124493
16	.150178	-.094337	41	.422235	.121860
17	.122362	-.125350	42	.451428	.114705
18	.093770	-.158680	43	.479385	.102890
19	.064523	-.194073	44	.505812	.086299
20	.034703	-.231205	45	.531263	.066113
21	.004343	-.269642	46	.534834	.060519
22	.001171	-.271884	47	.533403	.063974
23	-.002657	-.271226	48	.527812	.050476
24	-.004838	-.268054	49	.521341	.051904
25	-.004241	-.264226	50	.000051	-.266934
		T.E.R.C.			
		L.E.R.C.	51	.526302	.059008

PLANE COORDINATES

NO.	X	Y	NO.	X	Y
1	.521236	.052516	26	.017916	-.223640
2	.494029	.064235	27	.040659	-.180334
3	.467844	.069880	28	.064046	-.138996
4	.443208	.071705	29	.088125	-.100103
5	.419806	.070475	30	.112969	-.064047
6	.397138	.066660	31	.138317	-.030848
7	.374892	.060504	32	.164193	-.000595
8	.352596	.052371	33	.190518	.026772
9	.329933	.042287	34	.217208	.051410
10	.306380	.030741	35	.244449	.073208
11	.281741	.017416	36	.272295	.092119
12	.256451	.001149	37	.301183	.107059
13	.230565	-.018132	38	.330965	.117667
14	.204270	-.040617	39	.361135	.124216
15	.177484	-.066214	40	.391418	.126363
16	.150136	-.094825	41	.421366	.124051
17	.122270	-.126361	42	.450668	.116973
18	.093649	-.160422	43	.478805	.104943
19	.064389	-.196690	44	.505433	.087876
20	.034579	-.234699	45	.531045	.067089
21	.004264	-.273807	46	.534653	.061354
22	.001143	-.276056	47	.533215	.064848
23	-.002619	-.275394	48	.527706	.051063
24	-.004822	-.272206	49	.521236	.052516
25	-.004176	-.268358	50	.000046	-.271083
		T.E.R.C.			
		L.E.R.C.	51	.526147	.059792

ADVANCED TWO-STAGE COMPRESSOR ** CONICAL FLOW ROTOR NO. 1

.... R A D I U S .....
1.400000

NUMBER OF BLADES
20

CENTER OF GRAVITY
CYLINDRICAL PROFILE
X = .233410
S = .000300

PROPERTIES OF CYLINDRICAL PROFILE

LE THICKNESS=	.007628	SPACING =	.439823
TE THICKNESS=	.012940	AXIAL CHORD=	.516200
		SOLIDITY =	1.173654
TRUE CHORD =	.702461	=	

DIRECTION OF ROTOR ROTATION = CLOCKWISE (VIEWED FROM THE TRAILING EDGE)

**** C A L C U L A T E D   C O O R D I N A T E S ****

CYLINDRICAL COORDINATES							PLANE COORDINATES					
NO.	X	S	NO.	X	S	NO.	X	Y	NO.	X	Y	
1	.503774	.160903	26	.017398	-.261175	1	.503031	.168012	26	.017440	-.264314	
2	.479143	.161363	27	.039095	-.219724	2	.478593	.167261	27	.039096	-.222482	
3	.455945	.157796	28	.061317	-.179058	3	.455514	.162396	28	.061286	-.181198	
4	.433753	.151034	29	.084083	-.139394	4	.433378	.154376	29	.084037	-.140840	
5	.411999	.141378	30	.107502	-.101004	5	.411648	.143598	30	.107456	-.101815	
6	.390224	.128955	31	.131401	-.063960	6	.389921	.130259	31	.131373	-.064295	
7	.368129	.113784	32	.155790	-.028499	7	.367879	.114416	32	.155782	-.028565	
8	.345593	.095921	33	.180710	.005123	8	.345368	.096127	33	.180710	.005123	
9	.322412	.075436	34	.206287	.036588	9	.322284	.075433	34	.206268	.036492	
10	.298163	.052954	35	.232036	.066151	10	.298105	.052897	35	.231962	.065878	
11	.273566	.027883	36	.257997	.093558	11	.273550	.027854	36	.257824	.093119	
12	.248757	.000346	37	.284316	.118486	12	.248757	.000346	37	.283987	.117997	
13	.223777	-.029391	38	.311724	.139866	13	.223762	-.029443	38	.311179	.139566	
14	.198139	-.060645	39	.339706	.157818	14	.198077	-.060887	39	.338894	.158014	
15	.171949	-.093381	40	.368169	.171964	15	.171830	-.093977	40	.367050	.173017	
16	.145310	-.127418	41	.396962	.181912	16	.145074	-.128519	41	.395527	.184181	
17	.118171	-.162516	42	.425756	.187248	17	.117830	-.164218	42	.424047	.191030	
18	.090380	-.198312	43	.454122	.187652	18	.089963	-.200626	43	.452256	.193089	
19	.062043	-.234666	44	.481482	.182941	19	.061613	-.237494	44	.479649	.189919	
20	.033192	-.271339	45	.507410	.173322	20	.032841	-.274465	45	.505817	.181402	
21	.003813	-.308077	46	.511269	.170217	21	.003706	-.311190	46	.509787	.178342	
22	.000977	-.310052	47	.511801	.168932	22	.000922	-.313130	47	.510575	.176721	
23	-.002424	-.309444	48	.508696	.161436	23	-.002401	-.312514	48	.507816	.168848	
24	-.004399	-.306609	49	.503774	.160903	24	-.004322	-.309700	49	.503031	.168012	
25	-.003791	-.303207	50	.000011	-.305642	25	-.003713	-.306334	50	-.000002	-.308763	
				T.E.R.C.						T.E.R.C.		
		L.E.R.C.	51	.505595	.167113			L.E.R.C.	51	.504450	.174703	

ADVANCED TWO-STAGE COMPRESSOR ** CONICAL FLOW ROTOR NO. 1

.... R A D I U S .....
1.600000

NUMBER OF BLADES
20

CENTER OF GRAVITY
CYLINDRICAL PROFILE
X = .234473
S = .000337

PROPERTIES OF CYLINDRICAL PROFILE

LE THICKNESS=	.006578	AXIAL CHORD=	.494174
TE THICKNESS=	.011296	SOLIDITY =	.983128
TRUE CHORD =	.788951	SPACING =	.502655

DIRECTION OF ROTOR ROTATION = CLOCKWISE (VIEWED FROM THE TRAILING EDGE)

**** C A L C U L A T E D   C O O R D I N A T E S ****

CYLINDRICAL COORDINATES

NO.	X	S	NO.	X	S
1	.487515	.270019	26	.017717	-.295027
2	.465713	.252906	27	.039082	-.256485
3	.444055	.233183	28	.060780	-.218193
4	.422346	.211027	29	.082816	-.180222
5	.400498	.186611	30	.105188	-.142634
6	.378419	.160212	31	.127907	-.105495
7	.356028	.132106	32	.150977	-.068908
8	.333296	.102507	33	.174400	-.032984
9	.309922	.071867	34	.198580	.001879
10	.285922	.040365	35	.222972	.035944
11	.261868	.007719	36	.247410	.069165
12	.237768	-.025884	37	.271902	.101365
13	.213455	-.060139	38	.297021	.131916
14	.188346	-.094519	39	.322781	.160578
15	.162964	-.129209	40	.348883	.187283
16	.137190	-.164092	41	.375296	.211720
17	.111070	-.199055	42	.401940	.233606
18	.084614	-.234009	43	.428724	.252580
19	.057819	-.268890	44	.455558	.268185
20	.030693	-.303613	45	.482248	.280012
21	.003238	-.338116	46	.486553	.280411
22	.000741	-.339798	47	.489878	.277649
23	-.002215	-.339222	48	.490277	.273344
24	-.003897	-.336725	49	.487515	.270019
25	-.003321	-.333770	50	-.000042	-.335943
		L.E.R.C.	51	T.E.R.C. .484882	.275016

PLANE COORDINATES

NO.	X	Y	NO.	X	Y
1	.485314	.274546	26	.017755	-.296093
2	.463938	.255291	27	.039074	-.257640
3	.442632	.234099	28	.060736	-.219289
4	.421237	.211036	29	.082751	-.181145
5	.399673	.186155	30	.105119	-.143316
6	.377836	.159613	31	.127851	-.105921
7	.355649	.131566	32	.150944	-.069109
8	.333081	.102124	33	.174390	-.033034
9	.309815	.071666	34	.198580	.001879
10	.285890	.040299	35	.222955	.035880
11	.261868	.007719	36	.247336	.068926
12	.237756	-.025910	37	.271720	.100863
13	.213394	-.060272	38	.296654	.131129
14	.188245	-.094817	39	.322188	.159528
15	.162723	-.129701	40	.347999	.186097
16	.136845	-.164770	41	.374065	.210637
17	.110635	-.199876	42	.400321	.232985
18	.084135	-.234908	43	.426682	.252924
19	.057364	-.269785	44	.453091	.270134
20	.030361	-.304424	45	.479415	.284301
21	.003157	-.338783	46	.483599	.284958
22	.000730	-.340421	47	.487069	.282375
23	-.002146	-.339867	48	.487783	.278057
24	-.003789	-.337445	49	.485314	.274546
25	-.003235	-.334572	50	-.000039	-.336679
		L.E.R.C.	51	T.E.R.C. .482373	.279432

ADVANCED TWO-STAGE COMPRESSOR ** CONICAL FLOW ROTOR NO. 1

.... R A D I U S .....
. 1.800000 .
....
NUMBER OF BLADES
20

CENTER OF GRAVITY
CYLINDRICAL PROFILE
X = .236949
S = .000349

PROPERTIES OF CYLINDRICAL PROFILE

LE THICKNESS= .005650 SPACING = .565487
TE THICKNESS= .010556 AXIAL CHORD= .472722
TRUE CHORD = .825090 SOLIDITY = .835956

DIRECTION OF ROTOR ROTATION = CLOCKWISE (VIEWED FROM THE TRAILING EDGE)

**** C A L C U L A T E D   C O O R D I N A T E S ****

CYLINDRICAL COORDINATES							PLANE COORDINATES					
NO.	X	S	NO.	X	S	NO.	X	Y	NO.	X	Y
1	.468177	.309210	26	.017984	-.319783	1	.465509	.311047	26	.018019	-.322522
2	.447595	.279617	27	.039009	-.281965	2	.445439	.280400	27	.039001	-.284140
3	.426645	.249198	28	.060224	-.244419	3	.425077	.249332	28	.060181	-.246100
4	.405692	.218027	29	.081629	-.207150	4	.404449	.217819	29	.081563	-.208398
5	.384339	.186154	30	.103170	-.170133	5	.383582	.185818	30	.103095	-.170996
6	.362892	.153720	31	.124913	-.133405	6	.362348	.153392	31	.124844	-.133955
7	.341070	.120792	32	.146888	-.097009	7	.340745	.120540	32	.146838	-.097307
8	.318945	.087428	33	.169096	-.060976	8	.318791	.087230	33	.169071	-.061096
9	.295768	.054190	34	.191772	-.025495	9	.295707	.054128	34	.191766	-.025516
10	.272506	.020482	35	.214908	.009388	10	.272498	.020473	35	.214907	.009385
11	.249232	-.013678	36	.238054	.043909	11	.249229	-.013682	36	.238031	.043848
12	.225947	-.048231	37	.261213	.078014	12	.225907	-.048285	37	.261130	.077827
13	.202213	-.082822	38	.284456	.111589	13	.202091	-.082978	38	.284260	.111231
14	.177991	-.117390	39	.308752	.143872	14	.177785	-.117700	39	.308380	.143339
15	.153544	-.152056	40	.333360	.175263	15	.153234	-.152565	40	.332744	.174586
16	.128859	-.186785	41	.358273	.205685	16	.128454	-.187545	41	.357329	.204952
17	.103989	-.221573	42	.383480	.235041	17	.103496	-.222635	42	.382135	.234418
18	.078972	-.256453	43	.408857	.263313	18	.078450	-.257890	43	.407038	.263042
19	.053768	-.291396	44	.434417	.290381	19	.053284	-.293301	44	.432046	.290812
20	.028373	-.326392	45	.460166	.316084	20	.028027	-.328898	45	.457189	.317682
21	.002797	-.361434	46	.463769	.317910	21	.002706	-.364725	46	.460687	.319624
22	.000699	-.362904	47	.467608	.316653	22	.000696	-.366179	47	.464576	.318488
23	-.001817	-.362467	48	.469434	.313049	23	-.001740	-.365768	48	.466576	.314934
24	-.003288	-.360379	49	.468177	.309210	24	-.003178	-.363731	49	.465509	.311047
25	-.002850	-.357863	50	-.000032	-.359649	25	-.002772	-.361261	50	-.000033	-.362994
				T.E.R.C.						T.E.R.C.	
		L.E.R.C.	51	.464172	.312647			L.E.R.C.	51	.461352	.314367

ADVANCED TWO-STAGE COMPRESSOR ** CONICAL FLOW ROTOR NO. 1

..... R A D I U S .....
2.000000

NUMBER OF BLADES
20

CENTER OF GRAVITY
CYLINDRICAL PROFILE
X = .235465
S = .000454

PROPERTIES OF CYLINDRICAL PROFILE

LE THICKNESS= .004792 SPACING = .628319
TE THICKNESS= .010170 AXIAL CHORD= .451148
TRUE CHORD = .856056 SOLIDITY = .718024

DIRECTION OF ROTOR ROTATION = CLOCKWISE (VIEWED FROM THE TRAILING EDGE)

**** C A L C U L A T E D   C O O R D I N A T E S ****

CYLINDRICAL COORDINATES

NO.	X	S	NO.	X	S
1	.447647	.323623	26	.018217	-.355349
2	.427811	.289677	27	.038942	-.315495
3	.407689	.255461	28	.059737	-.276019
4	.387270	.220988	29	.080602	-.236915
5	.366555	.186244	30	.101462	-.198120
6	.345552	.151256	31	.122368	-.159648
7	.324242	.116020	32	.143420	-.121534
8	.302311	.080757	33	.164612	-.083793
9	.280021	.045342	34	.185947	-.046420
10	.257728	.009588	35	.207985	-.009754
11	.235431	-.026487	36	.230039	.026612
12	.213119	-.062856	37	.252097	.062667
13	.190103	-.099091	38	.274158	.098395
14	.166941	-.135543	39	.296577	.133544
15	.143644	-.172212	40	.319618	.167891
16	.120231	-.209104	41	.342961	.201587
17	.096710	-.246281	42	.366601	.234612
18	.073224	-.283793	43	.390533	.266936
19	.049669	-.321621	44	.414761	.298536
20	.026044	-.359778	45	.439276	.329399
21	.002347	-.398280	46	.442544	.331513
22	.000698	-.399579	47	.446349	.330697
23	-.001396	-.399331	48	.448463	.327429
24	-.002695	-.397682	49	.447647	.323623
25	-.002438	-.395598	50	-.000045	-.396939
		L.E.R.C.	51	.443462	.326511

(T.E.R.C. printed above row 51, X column)

PLANE COORDINATES

NO.	X	Y	NO.	X	Y
1	.444915	.322289	26	.018251	-.360162
2	.425685	.288767	27	.038934	-.318969
3	.406089	.254855	28	.059694	-.278462
4	.386109	.220593	29	.080535	-.238572
5	.365759	.185998	30	.101386	-.199185
6	.345035	.151101	31	.122295	-.160287
7	.323939	.115930	32	.143361	-.121880
8	.302166	.080715	33	.164576	-.083946
9	.279979	.045327	34	.185933	-.046464
10	.257726	.009587	35	.207984	-.009756
11	.235418	-.026494	36	.230033	.026599
12	.213053	-.062899	37	.252056	.062601
13	.189949	-.099211	38	.274047	.098239
14	.166683	-.135800	39	.296327	.133287
15	.143267	-.172696	40	.319168	.167520
16	.119714	-.209938	41	.342227	.201092
17	.096146	-.247630	42	.365501	.233984
18	.072635	-.285883	43	.388993	.266136
19	.049129	-.324743	44	.412692	.297487
20	.025660	-.364303	45	.436581	.327994
21	.002259	-.404679	46	.439799	.330031
22	.000703	-.405982	47	.443571	.329205
23	-.001294	-.405773	48	.445691	.326000
24	-.002564	-.404176	49	.444915	.322289
25	-.002363	-.402123	50	-.000050	-.403402
		L.E.R.C.	51	.440748	.325141

(T.E.R.C. printed above row 51, X column)

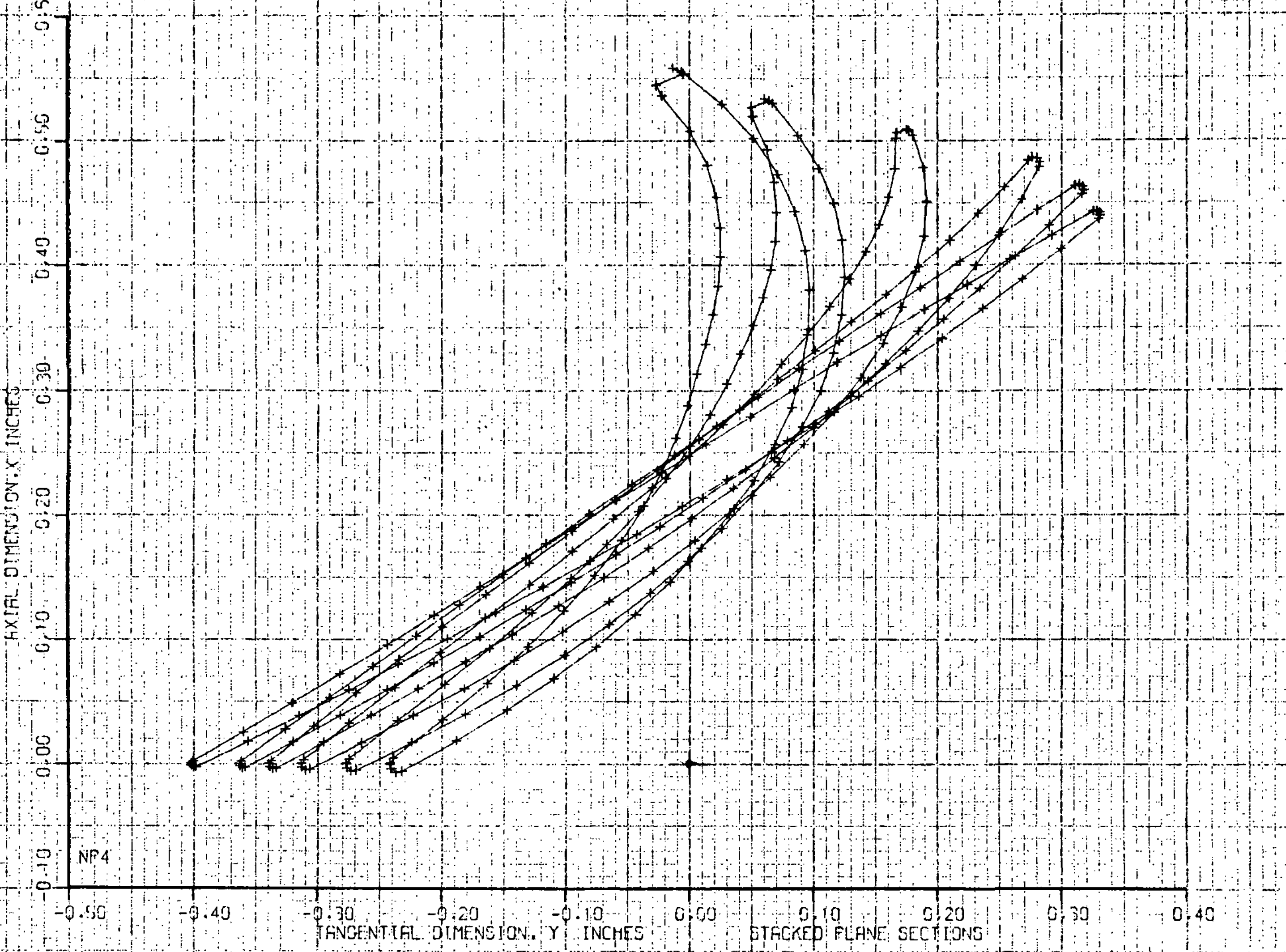

ADVANCED TWO-STAGE COMPRESSOR ** CONICAL FLOW ROTOR NO. 1

FIGURE B-1

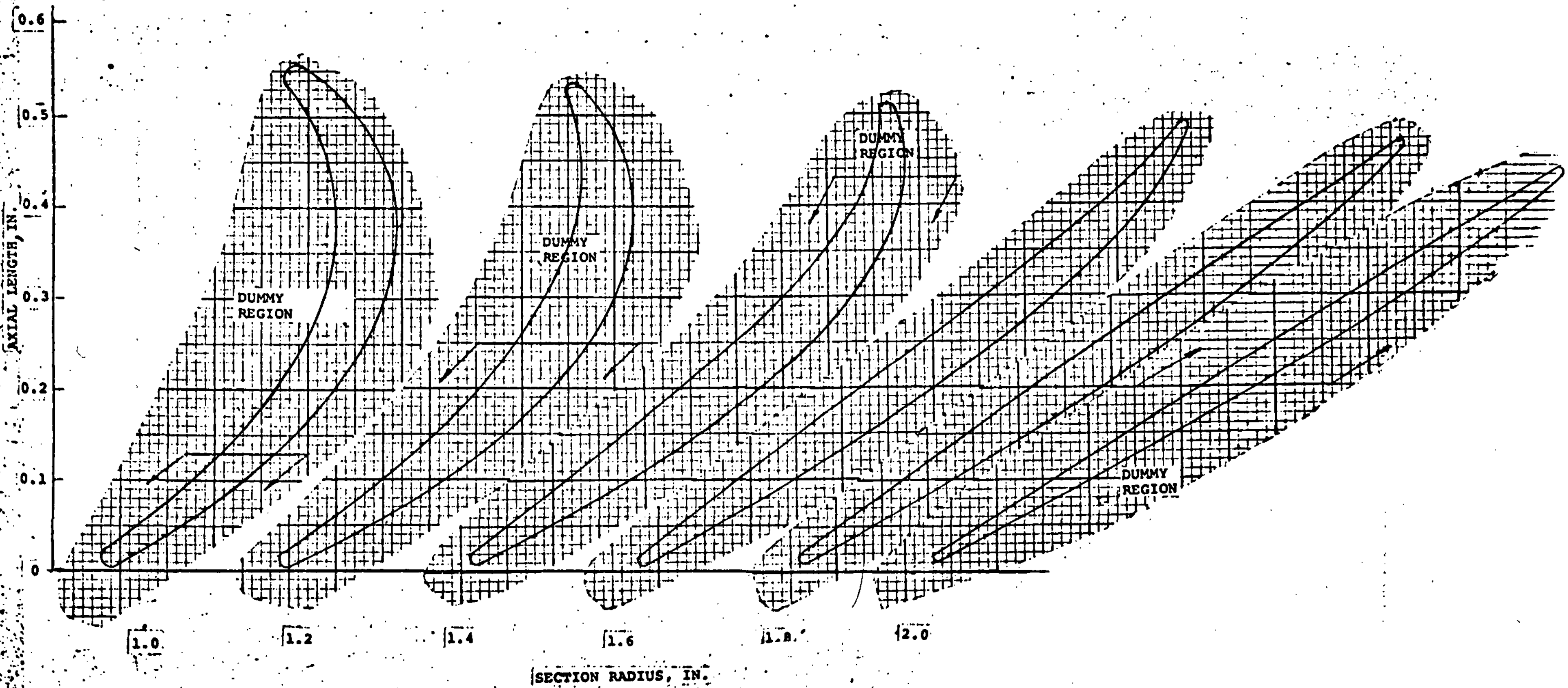

CYLINDRICAL SECTIONS FOR ROTOR 1A

FIGURE B-2

NASA10/1 ROTOR1B

..... R A D I U S .....
2.000000

NUMBER OF BLADES
20

CENTER OF GRAVITY
CYLINDRICAL PROFILE
X = .024143
S = .000511

PROPERTIES OF CYLINDRICAL PROFILE

LE THICKNESS=	.007276	SPACING =	.628319
TE THICKNESS=	.016289	AXIAL CHORD=	.348355
TRUE CHORD =	.431395	SOLIDITY =	.554424

DIRECTION OF ROTOR ROTATION = CLOCKWISE (VIEWED FROM THE TRAILING EDGE)

**** C A L C U L A T E D   C O O R D I N A T E S ****

CYLINDRICAL COORDINATES

NO.	X	S	NO.	X	S
1	.183481	.049042	26	-.138447	-.163672
2	.166577	.050150	27	-.123137	-.136547
3	.150797	.047967	28	-.107684	-.110449
4	.136127	.045069	29	-.092086	-.085482
5	.122265	.041874	30	-.076313	-.061754
6	.108354	.038132	31	-.060400	-.039295
7	.093948	.033964	32	-.044360	-.018174
8	.079084	.028437	33	-.028154	.001499
9	.063776	.021345	34	-.011747	.019659
10	.047987	.012659	35	.005031	.036080
11	.031626	.002403	36	.022336	.050516
12	.014740	-.009672	37	.040213	.062799
13	-.002520	-.023790	38	.058571	.073020
14	-.019979	-.040002	39	.077373	.081154
15	-.037605	-.058106	40	.096633	.086949
16	-.055358	-.077907	41	.116388	.089353
17	-.073251	-.099179	42	.136191	.088226
18	-.091318	-.121751	43	.155187	.083231
19	-.109531	-.145534	44	.173073	.074511
20	-.127887	-.170387	45	.189835	.064041
21	-.146372	-.196166	46	.194208	.059596
22	-.149017	-.198076	47	.194156	.059721
23	-.152237	-.197556	48	.189712	.048991
24	-.154147	-.194912	49	.183481	.049042
25	-.153628	-.191693	50	-.150000	-.193929
				T.E.R.C.	
		L.E.R.C.	51	.186658	.056542

PLANE COORDINATES

NO.	X	Y	NO.	X	Y
1	.183423	.049214	26	-.138458	-.164677
2	.166529	.050318	27	-.123165	-.137254
3	.150765	.048123	28	-.107715	-.110898
4	.136106	.045207	29	-.092112	-.085734
5	.122249	.041990	30	-.076331	-.061873
6	.108339	.038223	31	-.060409	-.039337
7	.093934	.034028	32	-.044360	-.018174
8	.079073	.028474	33	-.028154	.001499
9	.063769	.021362	34	-.011747	.019659
10	.047987	.012659	35	.005017	.036067
11	.031626	.002403	36	.022302	.050506
12	.014740	-.009672	37	.040146	.062809
13	-.002528	-.023791	38	.058459	.073073
14	-.019998	-.040017	39	.077210	.081269
15	-.037639	-.058163	40	.096414	.087147
16	-.055409	-.078047	41	.116125	.089653
17	-.073319	-.099456	42	.135921	.088605
18	-.091397	-.122228	43	.154953	.083645
19	-.109611	-.146269	44	.172901	.074897
20	-.127952	-.171417	45	.189718	.064342
21	-.146400	-.197483	46	.194112	.059862
22	-.149023	-.199411	47	.194066	.059943
23	-.152217	-.198880	48	.189654	.049167
24	-.154113	-.196228	49	.183423	.049214
25	-.153601	-.192996	50	-.150000	-.195239
				T.E.R.C.	
		L.E.R.C.	51	.186574	.056773

NASA10/1 ROTOR1B

.... R A D I U S .....
2.159000

NUMBER OF BLADES
20

CENTER OF GRAVITY
CYLINDRICAL PROFILE
X = .012659
S = .000550

PROPERTIES OF CYLINDRICAL PROFILE

LE THICKNESS=	.006301	SPACING =	.678270
TE THICKNESS=	.014566	AXIAL CHORD=	.330864
TRUE CHORD =	.470971	SOLIDITY =	.487806

DIRECTION OF ROTOR ROTATION = CLOCKWISE (VIEWED FROM THE TRAILING EDGE)

**** C A L C U L A T E D   C O O R D I N A T E S ****

CYLINDRICAL COORDINATES

NO.	X	S	NO.	X	S
1	.169586	.106235	26	-.138592	-.188962
2	.155114	.102231	27	-.123910	-.162417
3	.141384	.096890	28	-.109085	-.136255
4	.127812	.090401	29	-.094127	-.110597
5	.113986	.082617	30	-.079048	-.085564
6	.099491	.073656	31	-.063838	-.061287
7	.084530	.063035	32	-.048453	-.037932
8	.069278	.050693	33	-.032893	-.015645
9	.053647	.036937	34	-.017235	.005498
10	.037732	.021767	35	-.001567	.025472
11	.021567	.005231	36	.014268	.044064
12	.005235	-.012774	37	.030353	.061137
13	-.011107	-.032281	38	.046722	.076682
14	-.027547	-.053069	39	.063470	.090513
15	-.044162	-.074924	40	.080509	.102658
16	-.060952	-.097671	41	.098014	.112696
17	-.077873	-.121171	42	.116188	.119767
18	-.094915	-.145274	43	.134616	.123675
19	-.112090	-.169821	44	.152886	.124033
20	-.129408	-.194655	45	.170414	.120777
21	-.146857	-.219634	46	.175434	.118354
22	-.149148	-.221289	47	.177271	.113920
23	-.151938	-.220838	48	.174848	.108072
24	-.153593	-.218548	49	.169586	.106235
25	-.153143	-.215758	50	-.150000	-.217696
				T.E.R.C.	
		L.E.R.C.	51	.170000	.113506

PLANE COORDINATES

NO.	X	Y	NO.	X	Y
1	.169430	.107696	26	-.138594	-.190023
2	.154998	.103452	27	-.123933	-.163386
3	.141275	.097857	28	-.109117	-.137045
4	.127701	.091116	29	-.094160	-.111168
5	.113878	.083103	30	-.079075	-.085922
6	.099401	.073948	31	-.063856	-.061471
7	.084464	.063185	32	-.048462	-.037999
8	.069235	.050753	33	-.032893	-.015645
9	.053625	.036950	34	-.017235	.005498
10	.037725	.021766	35	-.001573	.025452
11	.021567	.005231	36	.014246	.044022
12	.005235	-.012774	37	.030305	.061092
13	-.011120	-.032315	38	.046636	.076671
14	-.027578	-.053178	39	.063328	.090593
15	-.044217	-.075163	40	.080299	.102887
16	-.061033	-.098091	41	.097719	.113143
17	-.077977	-.121804	42	.115787	.120522
18	-.095034	-.146121	43	.134116	.124805
19	-.112207	-.170836	44	.152331	.125562
20	-.129498	-.195748	45	.169886	.122648
21	-.146889	-.220678	46	.174966	.120271
22	-.149168	-.222323	47	.176938	.115700
23	-.151933	-.221863	48	.174644	.109680
24	-.153567	-.219568	49	.169430	.107696
25	-.153112	-.216781	50	-.150000	-.218730
				T.E.R.C.	
		L.E.R.C.	51	.169678	.115166

NASA10/1 ROTOR1B

•••• R A D I U S •••••
2.259000

NUMBER OF BLADES
20

CENTER OF GRAVITY
CYLINDRICAL PROFILE
X = .008795
S = .000750

PROPERTIES OF CYLINDRICAL PROFILE

		SPACING =	.709686
LE THICKNESS=	.005647	AXIAL CHORD=	.319077
TE THICKNESS=	.013401	SOLIDITY =	.449603
TRUE CHORD =	.506618		

DIRECTION OF ROTOR ROTATION = CLOCKWISE (VIEWED FROM THE TRAILING EDGE)

**** C A L C U L A T E D   C O O R D I N A T E S ****

CYLINDRICAL COORDINATES

NO.	X	S	NO.	X	S
1	.162381	.153855	26	-.138561	-.202015
2	.148595	.144055	27	-.124202	-.176961
3	.134708	.132789	28	-.109740	-.152109
4	.120619	.120132	29	-.095178	-.127462
5	.106268	.106125	30	-.080524	-.103037
6	.091638	.090835	31	-.065768	-.078878
7	.076758	.074348	32	-.050879	-.055074
8	.061575	.056813	33	-.035799	-.031763
9	.046301	.038159	34	-.020637	-.008999
10	.030817	.018591	35	-.005535	.013201
11	.015059	-.001761	36	.009659	.034610
12	-.000792	-.022931	37	.025127	.054981
13	-.016582	-.044890	38	.040805	.074255
14	-.032455	-.067396	39	.056575	.092436
15	-.048518	-.090242	40	.072647	.109223
16	-.064715	-.113339	41	.088970	.124506
17	-.081013	-.136617	42	.105571	.138072
18	-.097403	-.160029	43	.122434	.149673
19	-.113893	-.183539	44	.139499	.159065
20	-.130487	-.207136	45	.156665	.165976
21	-.147183	-.230829	46	.161788	.166222
22	-.149263	-.232301	47	.165584	.162774
23	-.151775	-.231871	48	.165830	.157651
24	-.153247	-.229790	49	.162381	.153855
25	-.152817	-.227278	50	-.150000	-.229054
				T.E.R.C.	
		L.E.R.C.	51	.159523	.159916

PLANE COORDINATES

NO.	X	Y	NO.	X	Y
1	.161912	.155934	26	-.138548	-.202313
2	.148182	.145511	27	-.124212	-.177257
3	.134353	.133734	28	-.109765	-.152415
4	.120327	.120685	29	-.095210	-.127756
5	.106043	.106400	30	-.080555	-.103287
6	.091476	.090934	31	-.065792	-.079057
7	.076653	.074353	32	-.050894	-.055175
8	.061516	.056785	33	-.035806	-.031799
9	.046276	.038134	34	-.020637	-.008999
10	.030817	.018591	35	-.005535	.013201
11	.015059	-.001761	36	.009648	.034569
12	-.000799	-.022948	37	.025095	.054891
13	-.016606	-.044953	38	.040740	.074127
14	-.032506	-.067527	39	.056460	.092307
15	-.048601	-.090445	40	.072466	.109157
16	-.064827	-.113598	41	.088704	.124590
17	-.081150	-.136897	42	.105201	.138419
18	-.097554	-.160291	43	.121941	.150418
19	-.114039	-.183762	44	.138871	.160362
20	-.130600	-.207345	45	.155904	.167987
21	-.147229	-.231119	46	.160920	.168376
22	-.149265	-.232573	47	.164769	.165010
23	-.151731	-.232160	48	.165185	.159851
24	-.153184	-.230121	49	.161912	.155934
25	-.152772	-.227649	50	-.150000	-.229385
				T.E.R.C.	
		L.E.R.C.	51	.158916	.161972

NASA10/1 ROTOR18

.... R A D I U S .....
2.320000

NUMBER OF BLADES
20

CENTER OF GRAVITY
CYLINDRICAL PROFILE
X = .006829
S = .000660

PROPERTIES OF CYLINDRICAL PROFILE

LE THICKNESS= .005157
TE THICKNESS= .011396
TRUE CHORD = .521382
SPACING = .728850
AXIAL CHORD= .311705
SOLIDITY = .427667

DIRECTION OF ROTOR ROTATION = CLOCKWISE (VIEWED FROM THE TRAILING EDGE)

**** C A L C U L A T E D   C O O R D I N A T E S ****

CYLINDRICAL COORDINATES

NO.	X	S	NO.	X	S
1	.156695	.175064	26	-.138479	-.207208
2	.142890	.161143	27	-.124302	-.182005
3	.128977	.146010	28	-.110052	-.157271
4	.114907	.129781	29	-.095722	-.132952
5	.100627	.112560	30	-.081309	-.108998
6	.086122	.094435	31	-.066803	-.085365
7	.071408	.075487	32	-.052208	-.062020
8	.056459	.055831	33	-.037513	-.038969
9	.041483	.035411	34	-.022724	-.016240
10	.026320	.014458	35	-.007854	.006128
11	.010987	-.006927	36	.007126	.028044
12	-.004457	-.028688	37	.022276	.049373
13	-.019981	-.050756	38	.037614	.069992
14	-.035599	-.073059	39	.052977	.089903
15	-.051317	-.095554	40	.068577	.108828
16	-.067125	-.118232	41	.084385	.126659
17	-.083025	-.141118	42	.100418	.143238
18	-.099008	-.164271	43	.116661	.158407
19	-.115071	-.187759	44	.133062	.172032
20	-.131208	-.211654	45	.149570	.183758
21	-.147426	-.236020	46	.153758	.185174
22	-.149270	-.237389	47	.157579	.183073
23	-.151541	-.237053	48	.158796	.178885
24	-.152909	-.235210	49	.156695	.175064
25	-.152574	-.232939	50	-.150000	-.234479
				T.E.R.C.	
		L.E.R.C.	51	.153133	.179511

PLANE COORDINATES

NO.	X	Y	NO.	X	Y
1	.156001	.176493	26	-.138468	-.207978
2	.142308	.162030	27	-.124318	-.182442
3	.128510	.146499	28	-.110082	-.157487
4	.114548	.130001	29	-.095756	-.133043
5	.100363	.112622	30	-.081341	-.109031
6	.085941	.094423	31	-.066828	-.085379
7	.071296	.075455	32	-.052225	-.062030
8	.056401	.055805	33	-.037521	-.038976
9	.041461	.035400	34	-.022724	-.016240
10	.026320	.014458	35	-.007854	.006128
11	.010987	-.006927	36	.007119	.028033
12	-.004468	-.028690	37	.022252	.049335
13	-.020014	-.050754	38	.037562	.069911
14	-.035660	-.073042	39	.052881	.089777
15	-.051409	-.095517	40	.068417	.108685
16	-.067245	-.118189	41	.084141	.126555
17	-.083166	-.141110	42	.100067	.143263
18	-.099158	-.164374	43	.116187	.158681
19	-.115214	-.188080	44	.132445	.172705
20	-.131321	-.212319	45	.148788	.185213
21	-.147478	-.237153	46	.152858	.186497
22	-.149269	-.238511	47	.156660	.184481
23	-.151487	-.238195	48	.157966	.180335
24	-.152835	-.236390	49	.156001	.176493
25	-.152523	-.234151	50	-.150000	-.235652
				T.E.R.C.	
		L.E.R.C.	51	.152396	.180859

NASA10/1 ROTOR18

.... R A D I U S .....
2.380000
NUMBER OF BLADES
20

CENTER OF GRAVITY
CYLINDRICAL PROFILE
X = .003640
S = .000577

PROPERTIES OF CYLINDRICAL PROFILE

LE THICKNESS=	.004651	SPACING =	.747699
TE THICKNESS=	.009790	AXIAL CHORD=	.304293
TRUE CHORD =	.534109	SOLIDITY =	.406973

DIRECTION OF ROTOR ROTATION = CLOCKWISE (VIEWED FROM THE TRAILING EDGE)

**** C A L C U L A T E D   C O O R D I N A T E S ****

CYLINDRICAL COORDINATES

NO.	X	S	NO.	X	S
1	.150375	.188175	26	-.138413	-.215456
2	.136622	.171407	27	-.124434	-.188842
3	.122831	.153755	28	-.110385	-.162683
4	.108913	.135367	29	-.096263	-.137052
5	.094777	.116394	30	-.082067	-.111979
6	.080452	.096908	31	-.067792	-.087487
7	.065925	.077001	32	-.053439	-.063579
8	.051277	.056684	33	-.039009	-.040235
9	.036624	.035924	34	-.024494	-.017429
10	.021744	.014900	35	-.009899	.004868
11	.006750	-.006468	36	.004794	.026670
12	-.008341	-.028208	37	.019599	.047979
13	-.023513	-.050359	38	.034630	.068714
14	-.038768	-.072954	39	.049666	.089018
15	-.054101	-.096037	40	.064823	.108763
16	-.069510	-.119641	41	.080184	.127814
17	-.084997	-.143775	42	.095730	.146082
18	-.100560	-.168427	43	.111495	.163407
19	-.116196	-.193562	44	.127380	.179718
20	-.131901	-.219127	45	.143309	.194951
21	-.147678	-.245045	46	.146745	.196447
22	-.149274	-.246308	47	.150231	.195088
23	-.151295	-.246072	48	.151735	.191661
24	-.152558	-.244476	49	.150375	.188175
25	-.152322	-.242454	50	-.150000	-.243750
				T.E.R.C.	
		L.E.R.C.	51	.146847	.191559

PLANE COORDINATES

NO.	X	Y	NO.	X	Y
1	.149565	.189431	26	-.138403	-.216852
2	.135957	.172262	27	-.124450	-.189762
3	.122313	.154303	28	-.110416	-.163248
4	.108527	.135706	29	-.096299	-.137364
5	.094490	.116610	30	-.082099	-.112124
6	.080258	.097037	31	-.067818	-.087546
7	.065804	.077075	32	-.053457	-.063597
8	.051212	.056722	33	-.039018	-.040238
9	.036595	.035940	34	-.024496	-.017429
10	.021733	.014906	35	-.009899	.004868
11	.006749	-.006467	36	.004789	.026671
12	-.008353	-.028201	37	.019580	.047985
13	-.023545	-.050346	38	.034584	.068729
14	-.038827	-.072944	39	.049579	.089049
15	-.054189	-.096053	40	.064675	.108825
16	-.069627	-.119728	41	.079953	.127934
17	-.085141	-.144010	42	.095392	.146307
18	-.100716	-.168906	43	.111023	.163810
19	-.116346	-.194403	44	.126744	.180409
20	-.132019	-.220455	45	.142497	.196058
21	-.147729	-.246969	46	.145824	.197593
22	-.149278	-.248228	47	.149273	.196293
23	-.151249	-.248006	48	.150826	.192911
24	-.152490	-.246435	49	.149565	.189431
25	-.152272	-.244432	50	-.150000	-.245702
				T.E.R.C.	
		L.E.R.C.	51	.146031	.192748

NASA10/1 ROTOR1B

.... R A D I U S .....
2.442800

NUMBER OF BLADES
20

CENTER OF GRAVITY
CYLINDRICAL PROFILE
X = -.000696
S = .000507

PROPERTIES OF CYLINDRICAL PROFILE

LE THICKNESS= .004165
TE THICKNESS= .008456
TRUE CHORD = .549258
SPACING = .767428
AXIAL CHORD= .296716
SOLIDITY = .386637

DIRECTION OF ROTOR ROTATION = CLOCKWISE (VIEWED FROM THE TRAILING EDGE)

**** C A L C U L A T E D   C O O R D I N A T E S ****

CYLINDRICAL COORDINATES

NO.	X	S	NO.	X	S
1	.143502	.199038	26	-.138353	-.227907
2	.129870	.180840	27	-.124570	-.199943
3	.116214	.162175	28	-.110727	-.172217
4	.102470	.143126	29	-.096825	-.144857
5	.088537	.123775	30	-.082867	-.117947
6	.074470	.104057	31	-.068861	-.091572
7	.060194	.083985	32	-.054772	-.065824
8	.045867	.063394	33	-.040559	-.040784
9	.031480	.042229	34	-.026252	-.016479
10	.016870	.020543	35	-.011905	.007096
11	.002178	-.001806	36	.002431	.029966
12	-.012504	-.024900	37	.016848	.052086
13	-.027226	-.048710	38	.031488	.073381
14	-.042041	-.073186	39	.046186	.094000
15	-.056980	-.098274	40	.060937	.113997
16	-.071999	-.123945	41	.075897	.133300
17	-.087066	-.150147	42	.090989	.151996
18	-.102192	-.176777	43	.106269	.170055
19	-.117375	-.203734	44	.121632	.187547
20	-.132620	-.230917	45	.137025	.204473
21	-.147920	-.258179	46	.139900	.205961
22	-.149300	-.259331	47	.142983	.204988
23	-.151090	-.259169	48	.144474	.202121
24	-.152242	-.257789	49	.143502	.199038
25	-.152080	-.255998	50	-.150000	-.257089
				T.E.R.C.	
		L.E.R.C.	51	.140267	.201754

PLANE COORDINATES

NO.	X	Y	NO.	X	Y
1	.142588	.200016	26	-.138344	-.230110
2	.129127	.181618	27	-.124588	-.201486
3	.115637	.162793	28	-.110760	-.173226
4	.102026	.143639	29	-.096865	-.145447
5	.088215	.124190	30	-.082902	-.118232
6	.074250	.104373	31	-.068890	-.091686
7	.060055	.084205	32	-.054791	-.065852
8	.045788	.063526	33	-.040567	-.040783
9	.031442	.042294	34	-.026254	-.016477
10	.016856	.020566	35	-.011905	.007096
11	.002178	-.001805	36	.002425	.029980
12	-.012513	-.024889	37	.016826	.052138
13	-.027255	-.048688	38	.031436	.073498
14	-.042098	-.073182	39	.046091	.094198
15	-.057068	-.098346	40	.060774	.114297
16	-.072121	-.124178	41	.075651	.133687
17	-.087220	-.150670	42	.090644	.152455
18	-.102361	-.177717	43	.105787	.170614
19	-.117539	-.205225	44	.120981	.188252
20	-.132746	-.233070	45	.136191	.205379
21	-.147971	-.261110	46	.138987	.206855
22	-.149309	-.262261	47	.142018	.205898
23	-.151052	-.262108	48	.143510	.203067
24	-.152179	-.260741	49	.142588	.200016
25	-.152030	-.258959	50	-.150000	-.260035
				T.E.R.C.	
		L.E.R.C.	51	.139387	.202700

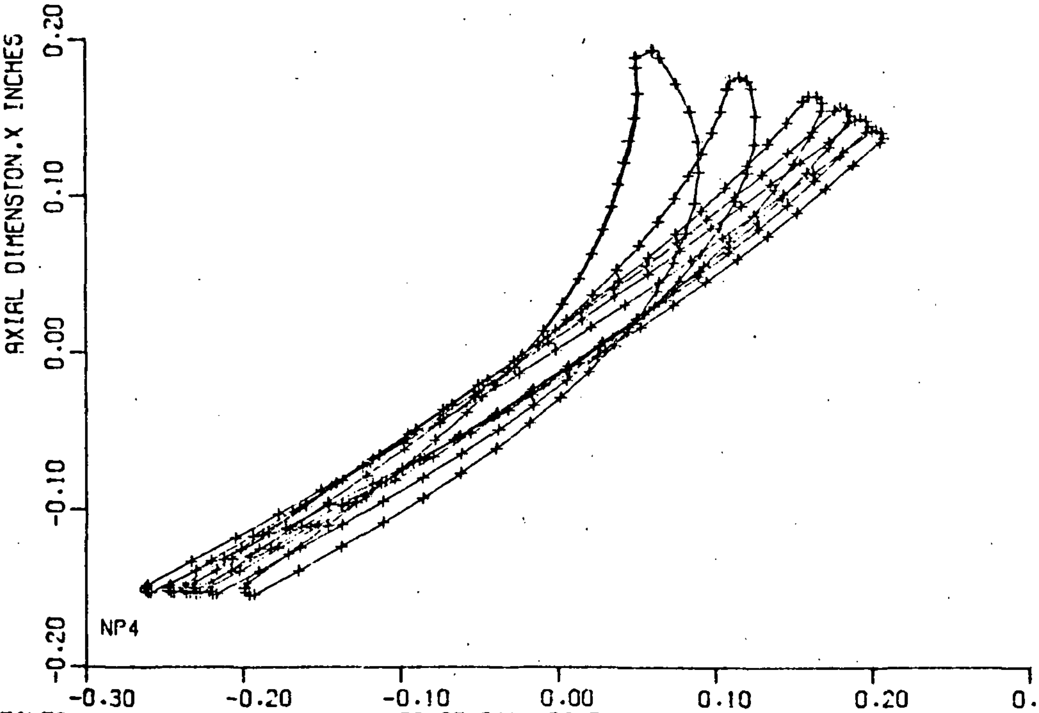

PROFILES

STACKED PLANE SECTIONS

NASA10/1 ROTOR1B

FIGURE B-3

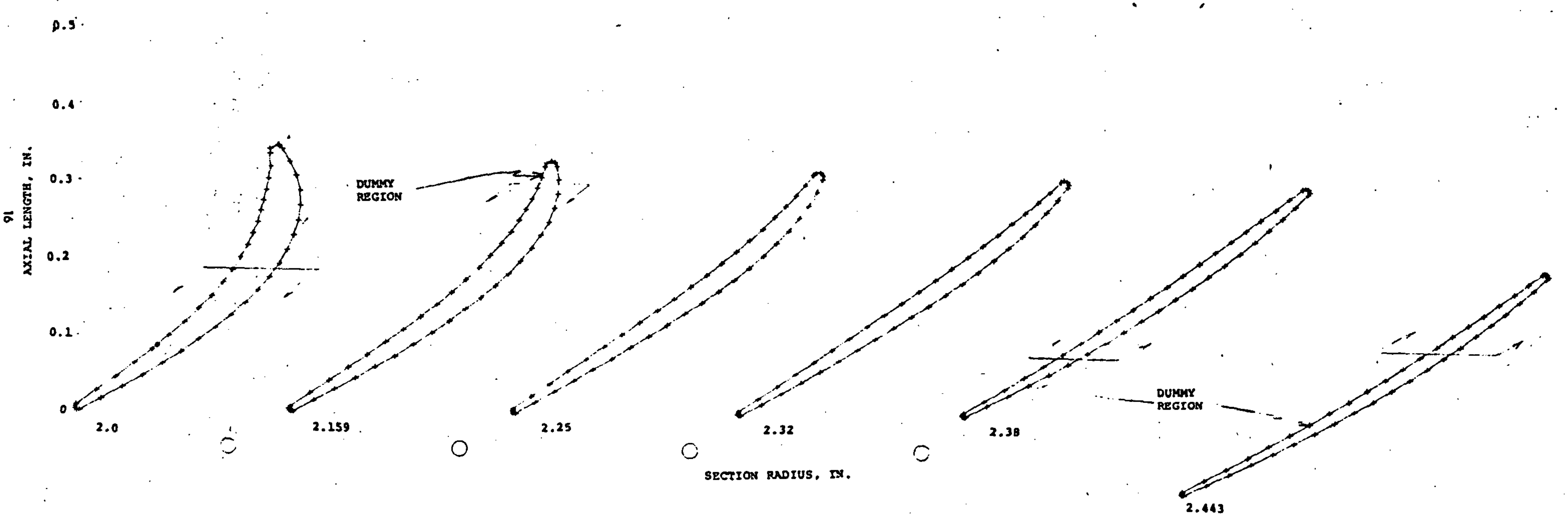

CYLINDRICAL SECTIONS FOR ROTOR 1B

FIGURE B-4

NASA 10-1 S1A STACKED CYL./PLANE SECTIONS. 20MARCH1972.

.... R A D I U S .....

2.500000

NUMBER OF VANES

53

CENTER OF GRAVITY
CYLINDRICAL PROFILE
X = -.013939
S = -.000107

PROPERTIES OF CYLINDRICAL PROFILE

LE THICKNESS= .007660
TE THICKNESS= .009501
TRUE CHORD = .562741
SPACING = .296377
AXIAL CHORD= .357040
SOLIDITY = 1.204683

DIRECTION OF ROTOR ROTATION = COUNTER CLOCKWISE (VIEWED FROM THE TRAILING EDGE)

**** C A L C U L A T E D C O O R D I N A T E S ****

CYLINDRICAL COORDINATES

NO.	X	S	NO.	X	S
1	.176087	-.199456	26	-.163505	.194955
2	.159829	-.183770	27	-.147953	.165197
3	.143636	-.167416	28	-.132102	.136545
4	.127420	-.150468	29	-.115903	.108980
5	.111122	-.132965	30	-.099317	.082498
6	.094751	-.114885	31	-.082453	.057009
7	.078287	-.096244	32	-.065246	.032558
8	.061704	-.077054	33	-.047820	.009037
9	.044984	-.057306	34	-.030389	-.013713
10	.028111	-.036990	35	-.012948	-.035706
11	.011069	-.016094	36	.004815	-.056694
12	-.006295	.005289	37	.022748	-.076801
13	-.023670	.027440	38	.040833	-.096036
14	-.041055	.050375	39	.059055	-.114407
15	-.058648	.073969	40	.077397	-.131921
16	-.076589	.098158	41	.095831	-.148594
17	-.094809	.123038	42	.114338	-.164428
18	-.113415	.148586	43	.132928	-.179373
19	-.132369	.174895	44	.151541	-.193470
20	-.151622	.202085	45	.170088	-.206823
21	-.171146	.230290	46	.173570	-.207865
22	-.173824	.232345	47	.176770	-.206140
23	-.177172	.231905	48	.177813	-.202657
24	-.179227	.229226	49	.176087	-.199456
25	-.178787	.225879	50	-.174966	.228084
				T.E.R.C.	
		L.E.R.C.	51	.173087	-.203139

PLANE COORDINATES

NO.	X	Y	NO.	X	Y
1	.175287	-.198131	26	-.163532	.193445
2	.159182	-.182712	27	-.147992	.164309
3	.143125	-.166595	28	-.132143	.136072
4	.127026	-.149854	29	-.115939	.108761
5	.110829	-.132525	30	-.099344	.082416
6	.094543	-.114586	31	-.082469	.056989
7	.078149	-.096056	32	-.065246	.032557
8	.061620	-.076948	33	-.047821	.009037
9	.044941	-.057256	34	-.030390	-.013712
10	.028094	-.036973	35	-.012959	-.035692
11	.011066	-.016092	36	.004783	-.056648
12	-.006295	.005289	37	.022684	-.076701
13	-.023677	.027442	38	.040722	-.095857
14	-.041076	.050372	39	.058883	-.114124
15	-.058688	.073936	40	.077148	-.131508
16	-.076648	.098047	41	.095491	-.148025
17	-.094885	.122770	42	.113891	-.163678
18	-.113500	.148045	43	.132361	-.178420
19	-.132449	.173926	44	.150845	-.192286
20	-.151676	.200493	45	.169251	-.205384
21	-.171148	.227845	46	.172719	-.206404
22	-.173839	.229848	47	.175924	-.204704
23	-.177192	.229405	48	.176988	-.201278
24	-.179241	.226773	49	.175287	-.198131
25	-.178787	.223496	50	-.174967	.225670
				T.E.R.C.	
		L.E.R.C.	51	.172268	-.201758

NASA 10-1 S1A STACKED CYL./PLANE SECTIONS. 20MARCH1972.

.... R A D I U S .....
2.600000

NUMBER OF VANES
53

CENTER OF GRAVITY
CYLINDRICAL PROFILE
X = -.017407
S = -.000074

PROPERTIES OF CYLINDRICAL PROFILE
LE THICKNESS= .007609
TE THICKNESS= .009232
TRUE CHORD = .529704
SPACING = .308232
AXIAL CHORD= .346910
SOLIDITY = 1.125484

DIRECTION OF ROTOR ROTATION = COUNTER CLOCKWISE (VIEWED FROM THE TRAILING EDGE)

**** C A L C U L A T E D   C O O R D I N A T E S ****

CYLINDRICAL COORDINATES

NO.	X	S	NO.	X	S
1	.165899	-.185541	26	-.163829	.177139
2	.150140	-.170522	27	-.148633	.150297
3	.134434	-.154845	28	-.133167	.124683
4	.118649	-.138637	29	-.117401	.100161
5	.102785	-.121887	30	-.101275	.076640
6	.086839	-.104596	31	-.084898	.053920
7	.070798	-.086790	32	-.068258	.031965
8	.054645	-.068493	33	-.051256	.010739
9	.038369	-.049731	34	-.034279	-.009999
10	.021959	-.030528	35	-.017294	-.030250
11	.005336	-.010968	36	-.000118	-.049844
12	-.011479	.008951	37	.017273	-.068728
13	-.028302	.029369	38	.034796	-.086931
14	-.045130	.050279	39	.052444	-.104423
15	-.062260	.071454	40	.070202	-.121174
16	-.079683	.092935	41	.088056	-.137153
17	-.097356	.114849	42	.105992	-.152331
18	-.115390	.137256	43	.124007	-.166660
19	-.133724	.160412	44	.142100	-.180093
20	-.152328	.184576	45	.160141	-.192757
21	-.171185	.210028	46	.163537	-.193736
22	-.173939	.212031	47	.166629	-.192027
23	-.177301	.211499	48	.167607	-.188632
24	-.179303	.208746	49	.165899	-.185541
25	-.178772	.205384	50	-.174978	.207706
				T.E.R.C.	
		L.E.R.C.	51	.163028	-.189149

PLANE COORDINATES

NO.	X	Y	NO.	X	Y
1	.165235	-.184556	26	-.163844	.175959
2	.149607	-.169709	27	-.148660	.149515
3	.134014	-.154193	28	-.133197	.124204
4	.118328	-.138128	29	-.117429	.099898
5	.102549	-.121505	30	-.101297	.076518
6	.086674	-.104324	31	-.084911	.053878
7	.070691	-.086610	32	-.068234	.031957
8	.054582	-.068388	33	-.051256	.010739
9	.038336	-.049683	34	-.034279	-.009999
10	.021947	-.030513	35	-.017300	-.030238
11	.005336	-.010968	36	-.000138	-.049798
12	-.011479	.008951	37	.017226	-.068626
13	-.028310	.029370	38	.034708	-.086751
14	-.045150	.050265	39	.052305	-.104143
15	-.062296	.071389	40	.070000	-.120778
16	-.079735	.092766	41	.087777	-.136631
17	-.097421	.114508	42	.105622	-.151676
18	-.115462	.136672	43	.123535	-.165867
19	-.133793	.159508	44	.141514	-.179157
20	-.152378	.183276	45	.159437	-.191664
21	-.171194	.208260	46	.162815	-.192630
22	-.173941	.210224	47	.165912	-.190949
23	-.177295	.209704	48	.166914	-.187604
24	-.179294	.207005	49	.165235	-.184556
25	-.178765	.203707	50	-.174979	.205984
				T.E.R.C.	
		L.E.R.C.	51	.162336	-.188111

NASA 10-1 S1A STACKED CYL./PLANE SECTIONS. 20MARCH1972.

.... R A D I U S .....
2.700000
....
NUMBER OF VANES
53

CENTER OF GRAVITY
CYLINDRICAL PROFILE
X = -.021817
S = -.000079

PROPERTIES OF CYLINDRICAL PROFILE

=	.260747	SPACING =	.320087
LE THICKNESS=	.007369	AXIAL CHORD=	.336449
TE THICKNESS=	.008870	SOLIDITY =	1.051118
TRUE CHORD =	.502615		

DIRECTION OF ROTOR ROTATION = COUNTER CLOCKWISE (VIEWED FROM THE TRAILING EDGE)

**** C A L C U L A T E D   C O O R D I N A T E S ****

CYLINDRICAL COORDINATES

NO.	X	S	NO.	X	S
1	.155767	-.170729	26	-.164084	.165080
2	.140523	-.155774	27	-.149284	.138242
3	.125240	-.140401	28	-.134240	.113090
4	.109875	-.124692	29	-.118928	.089441
5	.094430	-.108696	30	-.103260	.067190
6	.078899	-.092436	31	-.087349	.046102
7	.063283	-.075980	32	-.071212	.026054
8	.047569	-.059367	33	-.054676	.007104
9	.031750	-.042607	34	-.038151	-.011167
10	.015815	-.025681	35	-.021645	-.028865
11	-.000392	-.008687	36	-.005058	-.045986
12	-.016680	.008643	37	.011802	-.062417
13	-.032951	.026497	38	.028776	-.078375
14	-.049208	.044972	39	.045857	-.093910
15	-.065866	.063838	40	.063036	-.109050
16	-.082749	.083371	41	.080299	-.123796
17	-.099875	.103734	42	.097648	-.138094
18	-.117358	.125051	43	.115077	-.151877
19	-.135109	.147657	44	.132589	-.165054
20	-.153102	.171890	45	.150139	-.177585
21	-.171315	.198052	46	.153387	-.178571
22	-.173884	.200042	47	.156391	-.176971
23	-.177102	.199626	48	.157367	-.173723
24	-.179082	.197057	49	.155767	-.170729
25	-.178666	.193839	50	-.174991	.195951
				T.E.R.C.	
		L.E.R.C.	51	.152953	-.174157

PLANE COORDINATES

NO.	X	Y	NO.	X	Y
1	.155228	-.169524	26	-.164103	.164717
2	.140094	-.154813	27	-.149314	.137943
3	.124904	-.139678	28	-.134271	.112868
4	.109621	-.124184	29	-.118954	.089293
5	.094245	-.108359	30	-.103278	.067105
6	.078771	-.092248	31	-.087359	.046063
7	.063201	-.075890	32	-.071216	.026042
8	.047522	-.059335	33	-.054676	.007104
9	.031727	-.042602	34	-.038151	-.011167
10	.015807	-.025683	35	-.021652	-.028873
11	-.000392	-.008687	36	-.005077	-.045997
12	-.016680	.008643	37	.011763	-.062417
13	-.032957	.026485	38	.028709	-.078339
14	-.049223	.044934	39	.045752	-.093803
15	-.065892	.063754	40	.062882	-.108828
16	-.082786	.083223	41	.080085	-.123413
17	-.099920	.103508	42	.097361	-.137507
18	-.117408	.124741	43	.114705	-.151057
19	-.135157	.147279	44	.132119	-.163988
20	-.153138	.171447	45	.149565	-.176275
21	-.171323	.197611	46	.152804	-.177244
22	-.173876	.199582	47	.155804	-.175668
23	-.177082	.199180	48	.156809	-.172471
24	-.179063	.196640	49	.155228	-.169524
25	-.178659	.193448	50	-.174992	.195530
				T.E.R.C.	
		L.E.R.C.	51	.152396	-.172900

NASA 10-1 S1A STACKED CYL./PLANE SECTIONS. 20MARCH1972.

.... R A D I U S .....
2.800000

NUMBER OF VANES
53

CENTER OF GRAVITY
CYLINDRICAL PROFILE
X = -.028058
S = -.000130

PROPERTIES OF CYLINDRICAL PROFILE

LE THICKNESS= .007233
TE THICKNESS= .009188
TRUE CHORD = .487637
SPACING = .331942
AXIAL CHORD= .326293
SOLIDITY = .982982

DIRECTION OF ROTOR ROTATION = COUNTER CLOCKWISE (VIEWED FROM THE TRAILING EDGE)

**** C A L C U L A T E D   C O O R D I N A T E S ****

CYLINDRICAL COORDINATES

NO.	X	S	NO.	X	S
1	.145615	-.156826	26	-.164470	.165611
2	.130771	-.143645	27	-.150126	.136980
3	.115885	-.130302	28	-.135561	.110339
4	.100947	-.116791	29	-.120739	.085487
5	.085947	-.103089	30	-.105580	.062307
6	.070888	-.089142	31	-.090164	.040601
7	.055762	-.074902	32	-.074516	.020238
8	.040556	-.060316	33	-.058484	.001253
9	.025257	-.045327	34	-.042379	-.016709
10	.009854	-.029871	35	-.026278	-.033810
11	-.005841	-.014049	36	-.010184	-.050133
12	-.021529	.002514	37	.006203	-.065442
13	-.037212	.019904	38	.022603	-.079956
14	-.052969	.038149	39	.039276	-.093732
15	-.069111	.057130	40	.055939	-.106831
16	-.085484	.077156	41	.072669	-.119314
17	-.102113	.098394	42	.089458	-.131244
18	-.119081	.121004	43	.106309	-.142669
19	-.136304	.145297	44	.123211	-.153645
20	-.153750	.171580	45	.140157	-.164217
21	-.171395	.200209	46	.143569	-.165065
22	-.173760	.202220	47	.146582	-.163251
23	-.176853	.201969	48	.147429	-.159838
24	-.178864	.199605	49	.145615	-.156826
25	-.178614	.196512	50	-.175004	.198360
				T.E.R.C.	
		L.E.R.C.	51	.142886	-.160522

PLANE COORDINATES

NO.	X	Y	NO.	X	Y
1	.145173	-.156489	26	-.164491	.165698
2	.130412	-.143436	27	-.150156	.136959
3	.115603	-.130182	28	-.135590	.110294
4	.100732	-.116730	29	-.120762	.085450
5	.085788	-.103066	30	-.105596	.062285
6	.070777	-.089140	31	-.090172	.040591
7	.055689	-.074909	32	-.074516	.020238
8	.040512	-.060326	33	-.058484	.001253
9	.025234	-.045335	34	-.042379	-.016709
10	.009845	-.029976	35	-.026288	-.033816
11	-.005841	-.014049	36	-.010208	-.050144
12	-.021529	.002514	37	.006158	-.065456
13	-.037212	.019904	38	.022620	-.079968
14	-.052979	.038136	39	.039169	-.093736
15	-.069130	.057102	40	.055791	-.106819
16	-.085514	.077107	41	.072472	-.119276
17	-.102153	.098321	42	.089204	-.131166
18	-.119126	.120915	43	.105990	-.142531
19	-.136348	.145227	44	.122818	-.153422
20	-.153783	.171618	45	.139677	-.163883
21	-.171403	.200545	46	.143097	-.164719
22	-.173746	.202565	47	.146125	-.162899
23	-.176826	.202332	48	.146983	-.159490
24	-.178842	.199982	49	.145173	-.156489
25	-.178610	.196891	50	-.175006	.198718
				T.E.R.C.	
		L.E.R.C.	51	.142425	-.160186

NASA 10-1 S1A STACKED CYL./PLANE SECTIONS. 20MARCH1972.

.... R A D I U S .....
. 2.900000 .
....

NUMBER OF VANES
53

CENTER OF GRAVITY
CYLINDRICAL PROFILE
X = -.034888
S = -.000224

PROPERTIES OF CYLINDRICAL PROFILE

LE THICKNESS=	.006996	SPACING =	.343797
TE THICKNESS=	.009555	AXIAL CHORD=	.316029
TRUE CHORD =	.490315	SOLIDITY =	.919231

DIRECTION OF ROTOR ROTATION = COUNTER CLOCKWISE (VIEWED FROM THE TRAILING EDGE)

**** C A L C U L A T E D   C O O R D I N A T E S ****

CYLINDRICAL COORDINATES

NO.	X	S	NO.	X	S
1	.135486	-.155510	26	-.164914	.174732
2	.121080	-.143695	27	-.151125	.142543
3	.106685	-.131566	28	-.137106	.112998
4	.092243	-.119191	29	-.122819	.085786
5	.077758	-.106486	30	-.108193	.060691
6	.063235	-.093418	31	-.093289	.037466
7	.048657	-.079937	32	-.078148	.015920
8	.034007	-.065997	33	-.062664	-.003997
9	.019267	-.051495	34	-.047018	-.022531
10	.004328	-.036467	35	-.031370	-.039925
11	-.010807	-.020766	36	-.015723	-.056292
12	-.025940	-.004079	37	.000110	-.071526
13	-.041076	.013710	38	.016161	-.085680
14	-.056373	.032612	39	.032292	-.098927
15	-.072013	.052663	40	.048495	-.111350
16	-.087891	.074156	41	.064754	-.123025
17	-.104045	.097306	42	.081050	-.134027
18	-.120541	.122359	43	.097390	-.144392
19	-.137303	.149702	44	.113776	-.154157
20	-.154296	.179745	45	.130152	-.163437
21	-.171502	.212983	46	.133735	-.164162
22	-.173581	.215015	47	.136782	-.162141
23	-.176489	.214982	48	.137507	-.158557
24	-.178522	.212903	49	.135486	-.155510
25	-.178489	.209995	50	-.174995	.211489
		T.E.R.C.			
		L.E.R.C.	51	.132819	-.159473

PLANE COORDINATES

NO.	X	Y	NO.	X	Y
1	.135061	-.155574	26	-.164943	.175447
2	.120735	-.143802	27	-.151164	.142898
3	.106411	-.131699	28	-.137143	.113152
4	.092030	-.119327	29	-.122848	.085838
5	.077599	-.106429	30	-.108212	.060700
6	.063120	-.093547	31	-.093298	.037463
7	.048579	-.080043	32	-.078149	.015920
8	.033958	-.066064	33	-.062664	-.003997
9	.019240	-.051544	34	-.047018	-.022531
10	.004316	-.036491	35	-.031385	-.039947
11	-.010807	-.020766	36	-.015754	-.056341
12	-.025940	-.004079	37	.000064	-.071610
13	-.041076	.013710	38	.016077	-.085803
14	-.056379	.032603	39	.032172	-.099087
15	-.072026	.052649	40	.048333	-.111541
16	-.087913	.074152	41	.064546	-.123234
17	-.104078	.097345	42	.080786	-.134236
18	-.120581	.122502	43	.097067	-.144584
19	-.137347	.150047	44	.113388	-.154310
20	-.154334	.180451	45	.129693	-.163533
21	-.171521	.214307	46	.133280	-.164251
22	-.173581	.216362	47	.136339	-.162217
23	-.176475	.216343	48	.137076	-.158624
24	-.178509	.214259	49	.135061	-.155574
25	-.178489	.211330	50	-.175005	.212818
				T.E.R.C.	
		L.E.R.C.	51	.132377	-.159553

NASA 10-1 S1A STACKED CYL./PLANE SECTIONS. 20MARCH1972.

.... R A D I U S .....
3.000000

NUMBER OF VANES
53

CENTER OF GRAVITY CYLINDRICAL PROFILE		PROPERTIES OF CYLINDRICAL PROFILE			
X =	-.041326	LE THICKNESS=	.006729	SPACING =	.355652
S =	-.000332	TE THICKNESS=	.009942	AXIAL CHORD=	.306096
		TRUE CHORD =	.508857	SOLIDITY =	.860661

DIRECTION OF ROTOR ROTATION = COUNTER CLOCKWISE (VIEWED FROM THE TRAILING EDGE)

**** C A L C U L A T E D   C O O R D I N A T E S ****

CYLINDRICAL COORDINATES							PLANE COORDINATES				
NO.	X	S	NO.	X	S	NO.	X	Y	NO.	X	Y
1	.125428	-.166162	26	-.165471	.191168	1	.124971	-.166892	26	-.165470	.192025
2	.111539	-.155120	27	-.152242	.155430	2	.111168	-.155739	27	-.152265	.155883
3	.097666	-.143591	28	-.138794	.122797	3	.097370	-.144099	28	-.138824	.123023
4	.083777	-.131567	29	-.125087	.092823	4	.083547	-.131966	29	-.125113	.092925
5	.069871	-.118968	30	-.111074	.065184	5	.069698	-.119267	30	-.111091	.065223
6	.055927	-.105737	31	-.096773	.039606	6	.055801	-.105948	31	-.096781	.039616
7	.041919	-.091914	32	-.082223	.015862	7	.041831	-.091952	32	-.082223	.015862
8	.027822	-.077137	33	-.067347	-.006148	8	.027765	-.077219	33	-.067347	-.006148
9	.013622	-.061626	34	-.052149	-.026543	9	.013589	-.061667	34	-.052155	-.026543
10	-.000867	-.045353	35	-.036941	-.045655	10	-.000884	-.045370	35	-.036959	-.045661
11	-.015436	-.028047	36	-.021722	-.063573	11	-.015442	-.028051	36	-.021761	-.063594
12	-.030015	-.009566	37	-.006422	-.080313	12	-.030015	-.009566	37	-.006492	-.080364
13	-.044606	.010181	38	.009165	-.095721	13	-.044606	.010181	38	.009058	-.095818
14	-.059517	.031093	39	.024856	-.109977	14	-.059521	.031095	39	.024703	-.110139
15	-.074755	.053362	40	.040637	-.123129	15	-.074766	.053375	40	.040432	-.123376
16	-.090243	.077265	41	.056480	-.135239	16	-.090262	.077308	41	.056217	-.135586
17	-.106018	.103044	42	.072362	-.146371	17	-.106044	.103151	42	.072037	-.146830
18	-.122099	.131022	43	.098261	-.156594	18	-.122128	.131252	43	.087871	-.157171
19	-.138639	.161640	44	.104176	-.165953	19	-.138664	.162093	44	.103719	-.166646
20	-.154997	.195437	45	.120076	-.174541	20	-.155006	.196289	45	.119550	-.175339
21	-.171767	.233107	46	.123823	-.175206	21	-.171738	.234666	46	.123295	-.176017
22	-.173621	.235124	47	.126942	-.173027	22	-.173572	.236705	47	.126434	-.173823
23	-.176358	.235240	48	.127606	-.169280	23	-.176293	.236834	48	.127128	-.170042
24	-.178374	.233396	49	.125428	-.166162	24	-.178308	.234976	49	.124971	-.166892
25	-.178490	.230649	50	-.175128	.231978	25	-.178436	.232220	50	-.175086	.233443
				T.E.R.C.						T.E.R.C.	
		L.E.R.C.	51	.122755	-.170352			L.E.R.C.	51	.122261	-.171115

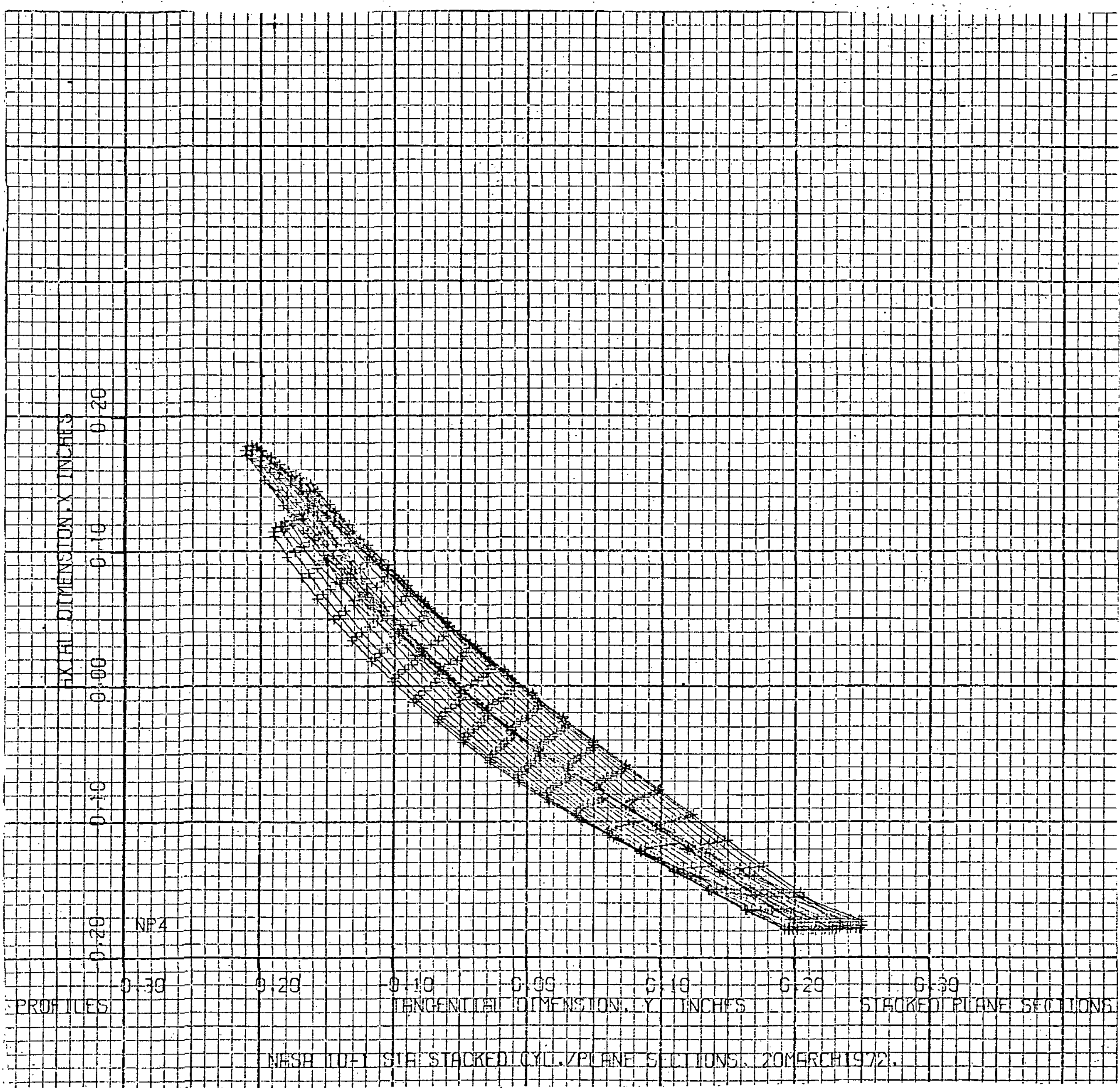
AXIAL DIMENSION, X INCHES
0.20
0.10
0.00
0.10
0.20
NP4
0.30
0.20
0.10
0.00
0.10
0.20
0.30
PROFILES
TANGENTIAL DIMENSION, Y INCHES
STACKED PLANE SECTIONS
NASA 10+1 STA STACKED CYL./PLANE SECTIONS, 20MARCH1972.

Figure B5.

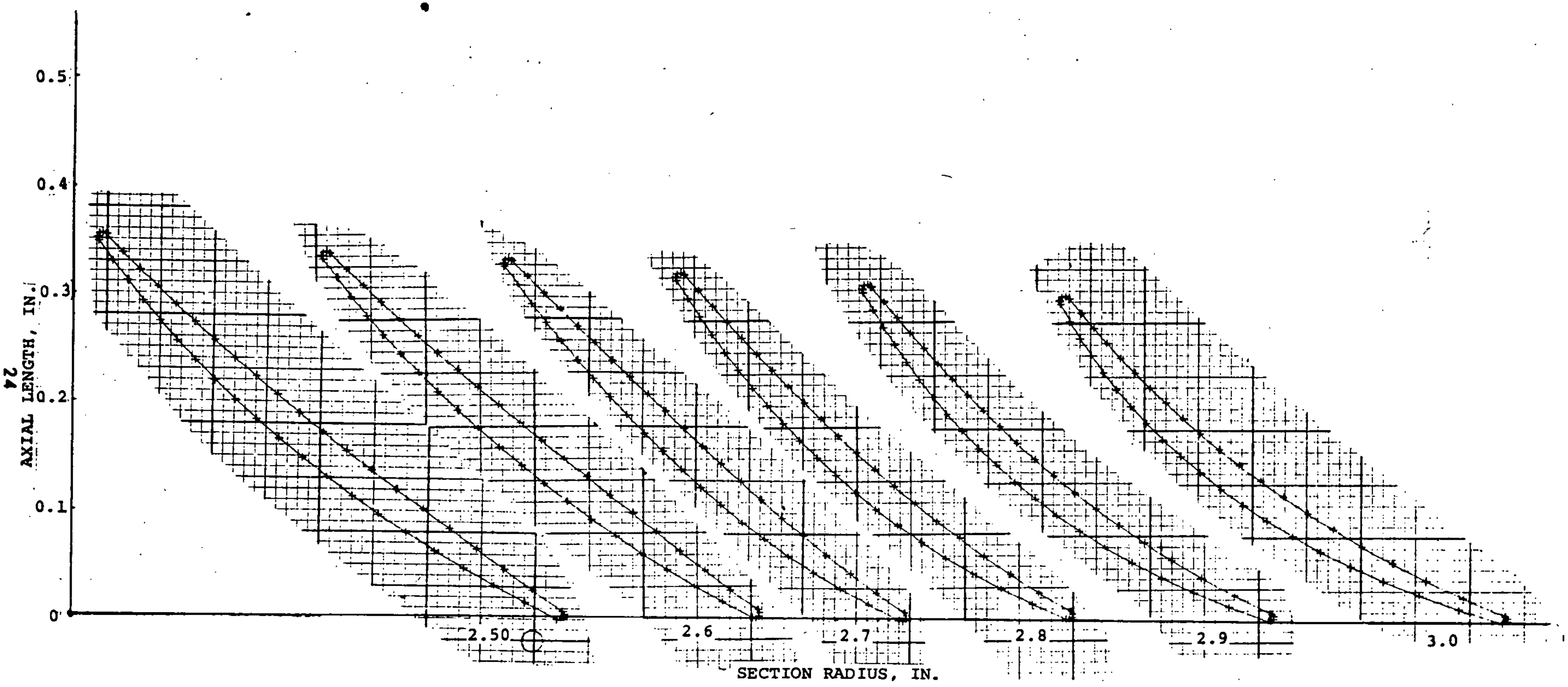

Figure B-6. Cylindrical Section for Stator 1A

NASA 10-1 S1B STACKED CYLINDRICAL/PLANE SECTIONS. 21MARCH1972.

.... R A D I U S .....
2.954000

NUMBER OF VANES
53

CENTER OF GRAVITY
CYLINDRICAL PROFILE
X = .001017
S = -.000027

PROPERTIES OF CYLINDRICAL PROFILE

LE THICKNESS=	.006343	SPACING =	.350199
TE THICKNESS=	.009988	AXIAL CHORD=	.499655
TRUE CHORD =	.530952	SOLIDITY =	1.426776

DIRECTION OF ROTOR ROTATION = COUNTER CLOCKWISE (VIEWED FROM THE TRAILING EDGE)

**** C A L C U L A T E D   C O O R D I N A T E S ****

CYLINDRICAL COORDINATES

NO.	X	S	NO.	X	S
1	.254955	-.049725	26	-.215180	.100445
2	.230671	-.047216	27	-.191836	.078957
3	.206527	-.044106	28	-.168149	.059367
4	.182501	-.040470	29	-.144151	.041559
5	.158569	-.036306	30	-.119885	.025399
6	.134701	-.031610	31	-.095392	.010781
7	.110884	-.026380	32	-.070702	-.002369
8	.087100	-.020595	33	-.045760	-.013926
9	.063325	-.014220	34	-.020666	-.024060
10	.039468	-.007482	35	.004432	-.033102
11	.015568	-.000001	36	.029532	-.041098
12	-.008334	.008478	37	.054675	-.047887
13	-.032240	.017997	38	.079900	-.053208
14	-.056298	.028312	39	.105116	-.057385
15	-.080608	.039337	40	.130299	-.060449
16	-.105115	.051338	41	.155431	-.062433
17	-.129849	.064430	42	.180499	-.063354
18	-.154851	.078737	43	.205473	-.063213
19	-.180164	.094424	44	.230329	-.062020
20	-.205820	.111723	45	.255045	-.059783
21	-.231852	.130878	46	.258563	-.058288
22	-.235208	.132095	47	.259994	-.054835
23	-.238443	.130583	48	.258499	-.051226
24	-.239661	.127226	49	.254955	-.049795
25	-.238148	.123991	50	-.235000	.127434
				T.E.R.C.	
		L.E.R.C.	51	.255000	-.054789

PLANE COORDINATES

NO.	X	Y	NO.	X	Y
1	.254955	-.049780	26	-.215180	.100407
2	.230670	-.047204	27	-.191836	.078935
3	.206526	-.044097	28	-.168149	.059356
4	.182500	-.040464	29	-.144151	.041554
5	.158569	-.036302	30	-.119885	.025397
6	.134701	-.031608	31	-.095392	.010781
7	.110884	-.026379	32	-.070702	-.002369
8	.087100	-.020595	33	-.045760	-.013926
9	.063325	-.014220	34	-.020666	-.024060
10	.039468	-.007482	35	.004432	-.033102
11	.015568	-.000001	36	.029533	-.041097
12	-.008334	.008478	37	.054676	-.047884
13	-.032240	.017996	38	.079901	-.053203
14	-.056298	.028310	39	.105117	-.057377
15	-.080608	.039333	40	.130300	-.060438
16	-.105115	.051330	41	.155432	-.062419
17	-.129849	.064415	42	.180500	-.063337
18	-.154851	.078714	43	.205474	-.063193
19	-.180164	.094389	44	.230330	-.061998
20	-.205820	.111672	45	.255046	-.059760
21	-.231851	.130807	46	.258563	-.058266
22	-.235207	.132023	47	.259994	-.054817
23	-.238443	.130514	48	.258499	-.051210
24	-.239661	.127161	49	.254955	-.049780
25	-.238149	.123930	50	-.235000	.127368
				T.E.R.C.	
		L.E.R.C.	51	.255000	-.054770

NASA 10-1 S1B STACKED CYLINDRICAL/PLANE SECTIONS. 21MARCH1972.

.... R A D I U S .....
3.050000

NUMBER OF VANES
53

CENTER OF GRAVITY
CYLINDRICAL PROFILE
X = .000763
S = -.000023

PROPERTIES OF CYLINDRICAL PROFILE

LE THICKNESS=	.006391	AXIAL CHORD=	.499675
TE THICKNESS=	.009999	SOLIDITY =	1.381923
TRUE CHORD =	.529646	SPACING =	.361580

DIRECTION OF ROTOR ROTATION = COUNTER CLOCKWISE (VIEWED FROM THE TRAILING EDGE)

**** C A L C U L A T E D   C O O R D I N A T E S ****

CYLINDRICAL COORDINATES

NO.	X	S	NO.	X	S
1	.254863	-.046847	26	-.215193	.099392
2	.230540	-.044740	27	-.191835	.077812
3	.206364	-.042079	28	-.168132	.058174
4	.182314	-.038865	29	-.144109	.040363
5	.158366	-.035093	30	-.119814	.024254
6	.134494	-.030756	31	-.095288	.009741
7	.110679	-.025847	32	-.070565	-.003255
8	.086900	-.020346	33	-.045599	-.014614
9	.063134	-.014223	34	-.020494	-.024528
10	.039283	-.007704	35	.004612	-.033340
11	.015388	-.000430	36	.029717	-.041098
12	-.008506	.007845	37	.054866	-.047649
13	-.032401	.017168	38	.080100	-.052725
14	-.056435	.027301	39	.105321	-.056629
15	-.080712	.038179	40	.130506	-.059392
16	-.105186	.050082	41	.155634	-.061043
17	-.129891	.063130	42	.180686	-.061604
18	-.154868	.077452	43	.205636	-.061081
19	-.180165	.093210	44	.230460	-.059490
20	-.205807	.110630	45	.255137	-.056842
21	-.231828	.129955	46	.258631	-.055281
22	-.235191	.131189	47	.259998	-.051982
23	-.238442	.129685	48	.258437	-.048213
24	-.239677	.126322	49	.254863	-.046847
25	-.238172	.123071	50	-.235000	.126513
		T.E.R.C.			
		L.E.R.C.	51	.255000	-.051844

PLANE COORDINATES

NO.	X	Y	NO.	X	Y
1	.254863	-.046833	26	-.215193	.099350
2	.230540	-.044729	27	-.191835	.077789
3	.206364	-.042071	28	-.168132	.058163
4	.182314	-.038859	29	-.144109	.040358
5	.158366	-.035089	30	-.119814	.024253
6	.134494	-.030754	31	-.095288	.009741
7	.110679	-.025846	32	-.070565	-.003255
8	.086900	-.020346	33	-.045599	-.014614
9	.063134	-.014223	34	-.020494	-.024528
10	.039283	-.007704	35	.004612	-.033340
11	.015388	-.000430	36	.029718	-.041097
12	-.008506	.007845	37	.054867	-.047646
13	-.032401	.017168	38	.080101	-.052720
14	-.056435	.027299	39	.105322	-.056621
15	-.080712	.038175	40	.130507	-.059381
16	-.105186	.050074	41	.155635	-.061029
17	-.129891	.063116	42	.180687	-.061587
18	-.154868	.077430	43	.205637	-.061062
19	-.180165	.093175	44	.230461	-.059470
20	-.205807	.110576	45	.255138	-.056821
21	-.231829	.129874	46	.258631	-.055261
22	-.235191	.131106	47	.259998	-.051965
23	-.238442	.129604	48	.258437	-.048198
24	-.239677	.126246	49	.254863	-.046833
25	-.238172	.122999	50	-.235000	.126437
				T.E.R.C.	
		L.E.R.C.	51	.255000	-.051827

NASA 10-1 S18 STACKED CYLINDRICAL/PLANE SECTIONS. 21MARCH1972.

.... R A D I U S .....
. 3.150000 .
....

NUMBER OF VANES
53

CENTER OF GRAVITY
CYLINDRICAL PROFILE
X = .000552
S = -.000016

PROPERTIES OF CYLINDRICAL PROFILE

LE THICKNESS= .006406 SPACING = .373435
TE THICKNESS= .010007 AXIAL CHORD= .499691
TRUE CHORD = .528030 SOLIDITY = 1.338095

DIRECTION OF ROTOR ROTATION = COUNTER CLOCKWISE (VIEWED FROM THE TRAILING EDGE)

**** C A L C U L A T E D C O O R D I N A T E S ****

CYLINDRICAL COORDINATES

NO.	X	S	NO.	X	S
1	.254766	-.043567	26	-.215186	.097899
2	.230402	-.041960	27	-.191814	.076370
3	.206192	-.039775	28	-.168095	.056786
4	.182115	-.037012	29	-.144052	.039046
5	.158148	-.033664	30	-.119729	.023038
6	.134269	-.029718	31	-.095174	.008661
7	.110454	-.025164	32	-.070419	-.004158
8	.086680	-.019980	33	-.045428	-.015304
9	.062921	-.014140	34	-.020310	-.024981
10	.039079	-.007871	35	.004807	-.033541
11	.015193	-.000830	36	.029921	-.041036
12	-.008690	.007221	37	.055079	-.047317
13	-.032572	.016331	38	.080320	-.052112
14	-.056581	.026271	39	.105546	-.055709
15	-.080826	.036989	40	.130731	-.058136
16	-.105271	.048771	41	.155852	-.059421
17	-.129948	.061737	42	.180885	-.059590
18	-.154905	.076011	43	.205808	-.058658
19	-.180186	.091743	44	.230598	-.056643
20	-.205814	.109140	45	.255234	-.053563
21	-.231821	.128434	46	.258699	-.051934
22	-.235197	.129669	47	.259998	-.048798
23	-.238458	.128154	48	.258369	-.044866
24	-.239693	.124778	49	.254766	-.043567
25	-.238179	.121517	50	-.235000	.124975
				T.E.R.C.	
		L.E.R.C.	51	.255000	-.048565

PLANE COORDINATES

NO.	X	Y	NO.	X	Y
1	.254766	-.043554	26	-.215186	.097862
2	.230402	-.041950	27	-.191814	.076350
3	.206191	-.039767	28	-.168095	.056776
4	.182114	-.037006	29	-.144052	.039042
5	.158148	-.033660	30	-.119729	.023038
6	.134269	-.029716	31	-.095174	.008661
7	.110454	-.025163	32	-.070419	-.004158
8	.086680	-.019980	33	-.045428	-.015304
9	.062921	-.014140	34	-.020310	-.024981
10	.039079	-.007871	35	.004807	-.033541
11	.015193	-.000830	36	.029922	-.041035
12	-.008690	.007221	37	.055080	-.047315
13	-.032572	.016331	39	.080321	-.052107
14	-.056581	.026269	39	.105547	-.055701
15	-.080826	.036985	40	.130733	-.058125
16	-.105271	.048764	41	.155854	-.059407
17	-.129948	.061724	42	.180886	-.059573
18	-.154905	.075990	43	.205809	-.058639
19	-.180186	.091711	44	.230599	-.056623
20	-.205814	.109092	45	.255234	-.053543
21	-.231821	.128362	46	.258699	-.051915
22	-.235197	.129595	47	.259998	-.048782
23	-.238458	.128082	48	.258369	-.044852
24	-.239693	.124710	49	.254766	-.043554
25	-.238179	.121453	50	-.235000	.124907
				T.E.R.C.	
		L.E.R.C.	51	.255000	-.048549

NASA 10-1 S18 STACKED CYLINDRICAL/PLANE SECTIONS. 21MARCH1972.

.... R A D I U S .....
3.250000

NUMBER OF VANES
53

CENTER OF GRAVITY
CYLINDRICAL PROFILE
X = .000321
S = -.000010

PROPERTIES OF CYLINDRICAL PROFILE

LE THICKNESS= .006416
TE THICKNESS= .010010
TRUE CHORD = .526554
SPACING = .385290
AXIAL CHORD= .499697
SOLIDITY = 1.296938

DIRECTION OF ROTOR ROTATION = COUNTER CLOCKWISE (VIEWED FROM THE TRAILING EDGE)

**** C A L C U L A T E D   C O O R D I N A T E S ****

CYLINDRICAL COORDINATES

NO.	X	S	NO.	X	S
1	.254657	-.040111	26	-.215175	.096895
2	.230245	-.039075	27	-.191793	.075378
3	.205995	-.037439	28	-.168065	.055794
4	.181888	-.035195	29	-.144013	.038054
5	.157902	-.032331	30	-.119678	.022059
6	.134017	-.028827	31	-.095106	.007720
7	.110208	-.024665	32	-.070330	-.005029
8	.086447	-.019827	33	-.045315	-.016067
9	.062709	-.014284	34	-.020173	-.025592
10	.038892	-.008264	35	.004969	-.033963
11	.015031	-.001433	36	.030108	-.041231
12	-.008827	.006443	37	.055291	-.047246
13	-.032685	.015413	38	.080553	-.051738
14	-.056670	.025247	39	.105792	-.054988
15	-.080894	.035897	40	.130983	-.057026
16	-.105322	.047647	41	.156098	-.057883
17	-.129987	.060613	42	.181112	-.057592
18	-.154935	.074911	43	.206005	-.056181
19	-.180207	.090690	44	.230755	-.053674
20	-.205825	.108109	45	.255343	-.050097
21	-.231816	.127413	46	.258773	-.048392
22	-.235201	.128649	47	.259993	-.045447
23	-.238469	.127129	48	.258288	-.041331
24	-.239704	.123744	49	.254657	-.040111
25	-.238184	.120477	50	-.235000	.123945
				T.E.R.C.	
		L.E.R.C.	51	.255000	-.045104

PLANE COORDINATES

NO.	X	Y	NO.	X	Y
1	.254657	-.040101	26	-.215175	.096875
2	.230245	-.039068	27	-.191793	.075368
3	.205995	-.037434	28	-.168065	.055789
4	.181888	-.035191	29	-.144013	.038052
5	.157902	-.032329	30	-.119678	.022059
6	.134017	-.028826	31	-.095106	.007720
7	.110208	-.024665	32	-.070330	-.005029
8	.086447	-.019827	33	-.045315	-.016067
9	.062709	-.014284	34	-.020173	-.025592
10	.038892	-.008264	35	.004969	-.033963
11	.015031	-.001433	36	.030108	-.041231
12	-.008827	.006443	37	.055292	-.047245
13	-.032685	.015413	38	.080554	-.051736
14	-.056670	.025247	39	.105793	-.054984
15	-.080894	.035895	40	.130984	-.057019
16	-.105322	.047643	41	.156099	-.057874
17	-.129987	.060606	42	.181113	-.057581
18	-.154935	.074899	43	.206006	-.056168
19	-.180207	.090562	44	.230756	-.053659
20	-.205825	.108082	45	.255344	-.050081
21	-.231816	.127373	46	.258773	-.048377
22	-.235201	.128608	47	.259993	-.045435
23	-.238468	.127089	48	.258288	-.041320
24	-.239704	.123707	49	.254657	-.040101
25	-.238184	.120443	50	-.235000	.123908
				T.E.R.C.	
		L.E.R.C.	51	.255000	-.045092

NASA 10-1 S1B STACKED CYLINDRICAL/PLANE SECTIONS. 21MARCH1972.

..... R A D I U S .....
. 3.350000 .
....
NUMBER OF VANES
53

CENTER OF GRAVITY
CYLINDRICAL PROFILE
X = .000265
S = -.000004

PROPERTIES OF CYLINDRICAL PROFILE
LE THICKNESS= .006428
TE THICKNESS= .010004
TRUE CHORD = .525633
SPACING = .397145
AXIAL CHORD= .499688
SOLIDITY = 1.258201

DIRECTION OF ROTOR ROTATION = COUNTER CLOCKWISE (VIEWED FROM THE TRAILING EDGE)

**** C A L C U L A T E D C O O R D I N A T E S ****

CYLINDRICAL COORDINATES

NO.	X	S	NO.	X	S
1	.254534	-.037492	26	-.215166	.096649
2	.230087	-.037052	27	-.191772	.075112
3	.205817	-.035935	28	-.168035	.055510
4	.181701	-.034141	29	-.143977	.037751
5	.157718	-.031661	30	-.119640	.021735
6	.133842	-.028478	31	-.095064	.007373
7	.110047	-.024585	32	-.070285	-.005396
8	.086305	-.019968	33	-.045264	-.016449
9	.062587	-.014603	34	-.020111	-.025974
10	.038793	-.008723	35	.005047	-.034309
11	.014953	-.001992	36	.030207	-.041500
12	-.008889	.005822	37	.055413	-.047393
13	-.032736	.014767	38	.080695	-.051714
14	-.056715	.024613	39	.105953	-.054749
15	-.080936	.035303	40	.131158	-.056524
16	-.105360	.047108	41	.156282	-.057066
17	-.130023	.060136	42	.181299	-.056410
18	-.154965	.074496	43	.206183	-.054573
19	-.180228	.090326	44	.230913	-.051579
20	-.205834	.107819	45	.255466	-.047452
21	-.231810	.127190	46	.258851	-.045664
22	-.235196	.128430	47	.259980	-.042938
23	-.238468	.126913	48	.258192	-.038622
24	-.239709	.123526	49	.254534	-.037492
25	-.238190	.120255	50	-.235000	.123722
				T.E.R.C.	
		L.E.R.C.	51	.255000	-.042472

PLANE COORDINATES

NO.	X	Y	NO.	X	Y
1	.254534	-.037489	26	-.215166	.096635
2	.230097	-.037050	27	-.191772	.075106
3	.205817	-.035934	28	-.168035	.055508
4	.181701	-.034140	29	-.143977	.037750
5	.157718	-.031661	30	-.119640	.021735
6	.133842	-.028478	31	-.095064	.007373
7	.110047	-.024585	32	-.070285	-.005396
8	.086305	-.019968	33	-.045264	-.016449
9	.062587	-.014603	34	-.020111	-.025974
10	.038793	-.008723	35	.005047	-.034309
11	.014953	-.001992	36	.030207	-.041499
12	-.008889	.005822	37	.055413	-.047392
13	-.032736	.014767	38	.080695	-.051712
14	-.056715	.024613	39	.105953	-.054747
15	-.080936	.035302	40	.131158	-.056521
16	-.105360	.047106	41	.156282	-.057063
17	-.130023	.060132	42	.181299	-.056406
18	-.154965	.074489	43	.206183	-.054569
19	-.180228	.090315	44	.230913	-.051574
20	-.205834	.107800	45	.255466	-.047447
21	-.231810	.127159	46	.258851	-.045660
22	-.235196	.128398	47	.259980	-.042935
23	-.238468	.126882	48	.258192	-.038619
24	-.239708	.123497	49	.254534	-.037489
25	-.238190	.120228	50	-.235000	.123693
				T.E.R.C.	
		L.E.R.C.	51	.255000	-.042468

NASA 10-1 S1B STACKED CYLINDRICAL/PLANE SECTIONS. 21MARCH1972.

..... R A D I U S .....
3.450000

NUMBER OF VANES
53

CENTER OF GRAVITY
CYLINDRICAL PROFILE
X = .000134
S = .000002

PROPERTIES OF CYLINDRICAL PROFILE

LE THICKNESS= .006440
TE THICKNESS= .009996
TRUE CHORD = .525331
SPACING = .409000
AXIAL CHORD= .499690
SOLIDITY = 1.221736

DIRECTION OF ROTOR ROTATION = COUNTER CLOCKWISE (VIEWED FROM THE TRAILING EDGE)

**** C A L C U L A T E D   C O O R D I N A T E S ****

CYLINDRICAL COORDINATES

NO.	X	S	NO.	X	S
1	.254468	-.036598	26	-.215156	.096637
2	.230011	-.036479	27	-.191750	.075130
3	.205739	-.035620	28	-.168007	.055545
4	.181628	-.034028	29	-.143946	.037791
5	.157651	-.031703	30	-.119610	.021765
6	.133782	-.028637	31	-.095038	.007381
7	.109992	-.024833	32	-.070261	-.005421
8	.086254	-.020281	33	-.045241	-.016513
9	.062538	-.014960	34	-.020084	-.026072
10	.038751	-.009100	35	.005080	-.034423
11	.014920	-.002367	36	.030249	-.041612
12	-.008916	.005470	37	.055462	-.047484
13	-.032759	.014454	38	.080746	-.051774
14	-.056739	.024355	39	.106008	-.054764
15	-.080962	.035106	40	.131218	-.056474
16	-.105390	.045968	41	.156349	-.056928
17	-.130054	.060044	42	.181372	-.056149
18	-.154993	.074440	43	.206261	-.054146
19	-.180250	.090291	44	.230989	-.050937
20	-.205844	.107793	45	.255532	-.046537
21	-.231804	.127156	46	.258890	-.044706
22	-.235200	.128397	47	.259970	-.042099
23	-.238479	.126873	48	.258138	-.037677
24	-.239720	.123477	49	.254468	-.036598
25	-.238196	.120198	50	-.235000	.123677
		T.E.R.C.			
		L.E.R.C.	51	.255000	-.041569

PLANE COORDINATES

NO.	X	Y	NO.	X	Y
1	.254468	-.036596	26	-.215156	.096624
2	.230011	-.036477	27	-.191750	.075124
3	.205739	-.035619	28	-.168007	.055543
4	.181628	-.034027	29	-.143946	.037790
5	.157651	-.031703	30	-.119610	.021766
6	.133782	-.028637	31	-.095038	.007381
7	.109992	-.024833	32	-.070261	-.005421
8	.086254	-.020281	33	-.045241	-.016513
9	.062538	-.014960	34	-.020084	-.026072
10	.038751	-.009100	35	.005080	-.034423
11	.014920	-.002367	36	.030249	-.041611
12	-.008916	.005470	37	.055462	-.047483
13	-.032759	.014454	38	.080746	-.051772
14	-.056739	.024355	39	.106008	-.054762
15	-.080962	.035105	40	.131218	-.056471
16	-.105390	.046966	41	.156349	-.056925
17	-.130054	.060040	42	.181372	-.056145
18	-.154993	.074434	43	.206261	-.054142
19	-.180250	.090280	44	.230989	-.050933
20	-.205844	.107775	45	.255532	-.046533
21	-.231804	.127126	46	.258890	-.044702
22	-.235200	.128367	47	.259970	-.042096
23	-.238479	.126844	48	.258138	-.037674
24	-.239720	.123450	49	.254468	-.036596
25	-.238196	.120173	50	-.235000	.123650
				T.E.R.C.	
		L.E.R.C.	51	.255000	-.041565

NASA 10-1 S18 STACKED CYLINDRICAL/PLANE SECTIONS. 21MARCH1972.

.... R A D I U S .....
3.530000

NUMBER OF VANES
53

CENTER OF GRAVITY
CYLINDRICAL PROFILE
X = .000031
S = .000008

PROPERTIES OF CYLINDRICAL PROFILE

LE THICKNESS= .006450
TE THICKNESS= .009991
TRUE CHORD = .525092
SPACING = .418484
AXIAL CHORD= .499692
SOLIDITY = 1.194052

DIRECTION OF ROTOR ROTATION = COUNTER CLOCKWISE (VIEWED FROM THE TRAILING EDGE)

**** C A L C U L A T E D   C O O R D I N A T E S ****

CYLINDRICAL COORDINATES

NO.	X	S	NO.	X	S
1	.254415	-.035883	26	-.215148	.096627
2	.229950	-.036021	27	-.191732	.075144
3	.205677	-.035368	28	-.167985	.055573
4	.181570	-.033938	29	-.143921	.037823
5	.157597	-.031737	30	-.119586	.021791
6	.133734	-.028764	31	-.095017	.007387
7	.109948	-.025031	32	-.070242	-.005441
8	.086213	-.020531	33	-.045223	-.016564
9	.062499	-.015246	34	-.020062	-.026150
10	.038717	-.009402	35	.005106	-.034514
11	.014894	-.002667	36	.030283	-.041702
12	-.008938	.005188	37	.055501	-.047557
13	-.032777	.014204	38	.080787	-.051822
14	-.056758	.024149	39	.106052	-.054776
15	-.080983	.034948	40	.131266	-.056434
16	-.105414	.046856	41	.156403	-.056818
17	-.130079	.059970	42	.181430	-.055940
18	-.155015	.074395	43	.206323	-.053804
19	-.180268	.090263	44	.231050	-.050423
20	-.205852	.107772	45	.255585	-.045805
21	-.231799	.127129	46	.258921	-.043940
22	-.235203	.128371	47	.259962	-.041428
23	-.238488	.126841	48	.258095	-.036921
24	-.239730	.123438	49	.254415	-.035883
25	-.238201	.120152	50	-.235000	.123641
				T.E.R.C.	
		L.E.R.C.	51	.255000	-.040845

PLANE COORDINATES

NO.	X	Y	NO.	X	Y
1	.254415	-.035881	26	-.215148	.096615
2	.229950	-.036019	27	-.191732	.075139
3	.205676	-.035367	28	-.167984	.055571
4	.181569	-.033937	29	-.143921	.037822
5	.157597	-.031736	30	-.119586	.021791
6	.133734	-.028764	31	-.095017	.007387
7	.109948	-.025031	32	-.070242	-.005441
8	.086213	-.020531	33	-.045223	-.016564
9	.062499	-.015246	34	-.020062	-.026150
10	.038717	-.009402	35	.005106	-.034514
11	.014894	-.002667	36	.030283	-.041701
12	-.008938	.005188	37	.055501	-.047556
13	-.032777	.014203	38	.080787	-.051820
14	-.056758	.024148	39	.106052	-.054774
15	-.080983	.034947	40	.131266	-.056431
16	-.105414	.046854	41	.156403	-.056815
17	-.130079	.059967	42	.181431	-.055937
18	-.155016	.074389	43	.206324	-.053801
19	-.180268	.090253	44	.231050	-.050419
20	-.205852	.107755	45	.255585	-.045801
21	-.231799	.127101	46	.258921	-.043936
22	-.235203	.128342	47	.259962	-.041425
23	-.238488	.126813	48	.258095	-.036919
24	-.239730	.123412	49	.254415	-.035881
25	-.238201	.120128	50	-.235000	.123615
				T.E.R.C.	
		L.E.R.C.	51	.255000	-.040842

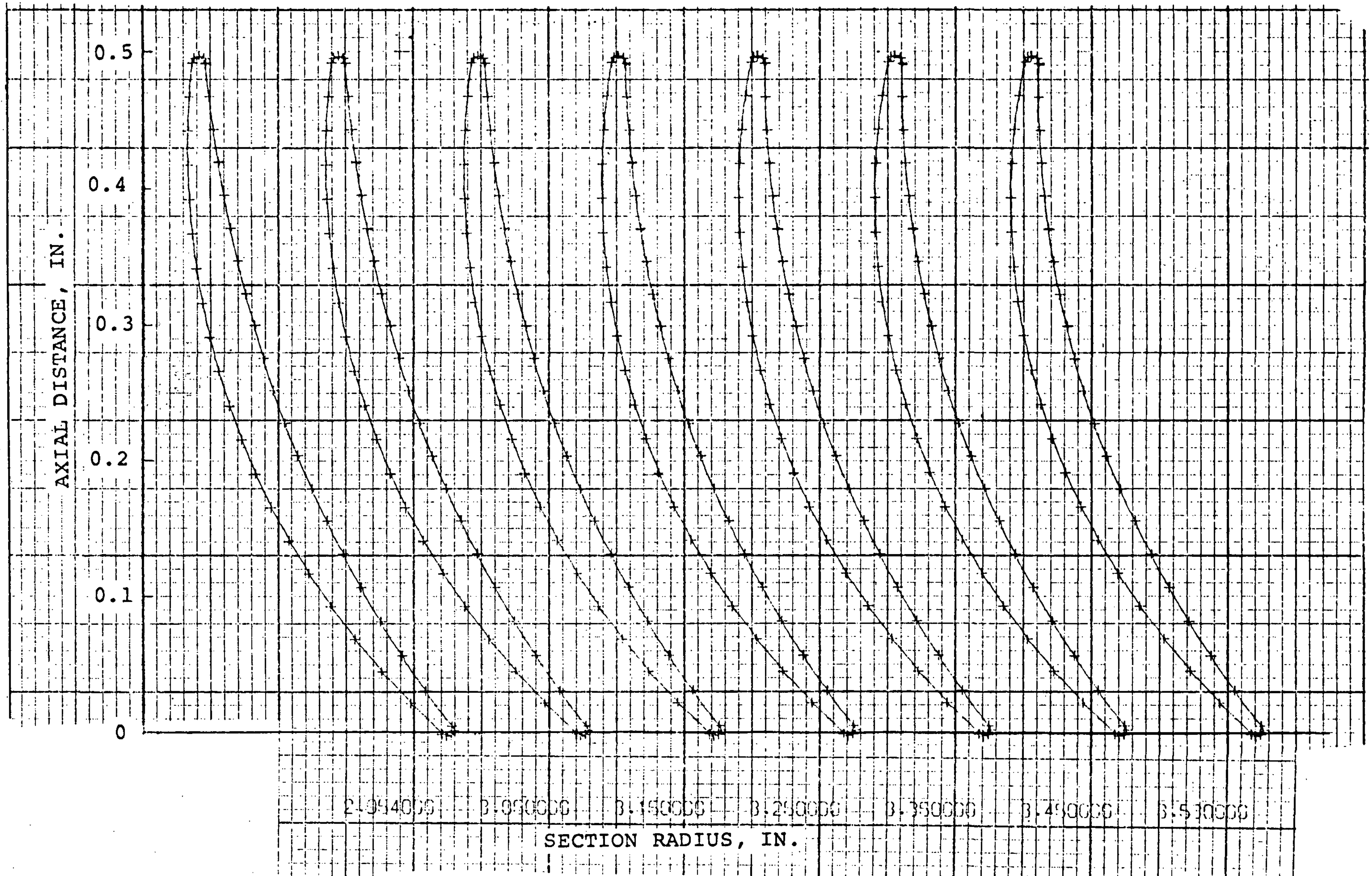

Figure B-7. Cylindrical Sections for Stator 1B

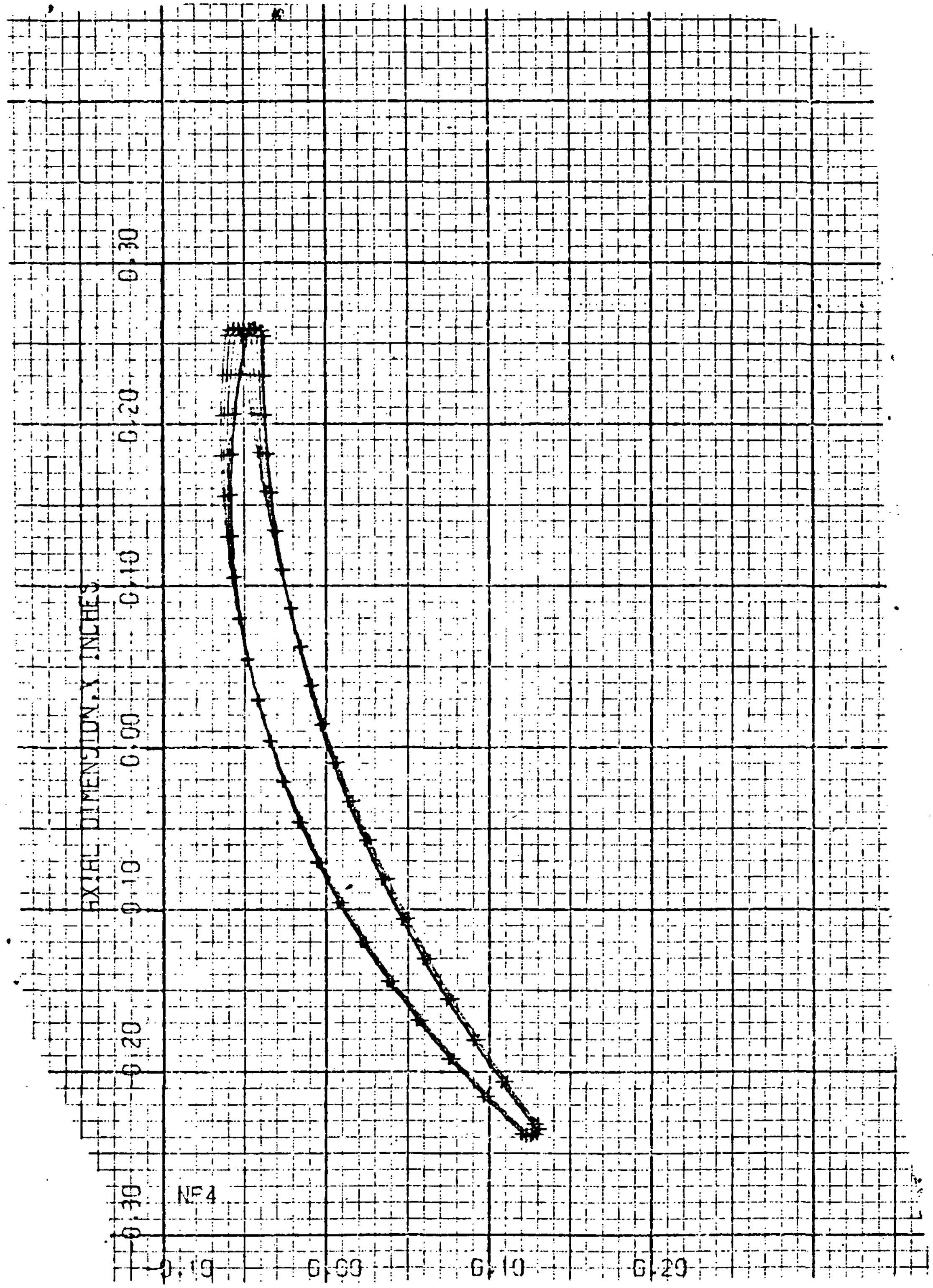

TANGENTIAL DIMENSION, Y IN.

Figure B-8. Advanced Two-Stage Compressor, Stator 1B

APPENDIX C

TURBINE BLADE SECTIONS

(9 pages)

D_T	G	Z_G				Z_H	M	W	C	V
6.138 6.134	2.851	0.297-0.300				2.095-2.105	.060 .050	3.7406	20	0.11 0.08

TRAILING EDGE CONTOUR TO BE A 4/1 ELLIPSE, TRUE WITHIN 3.5/1 TO 4.5/1, CENTERED ON THE BLADE CONTOUR WITH THE MINOR AXIS EQUAL TO THE BLADE THICKNESS

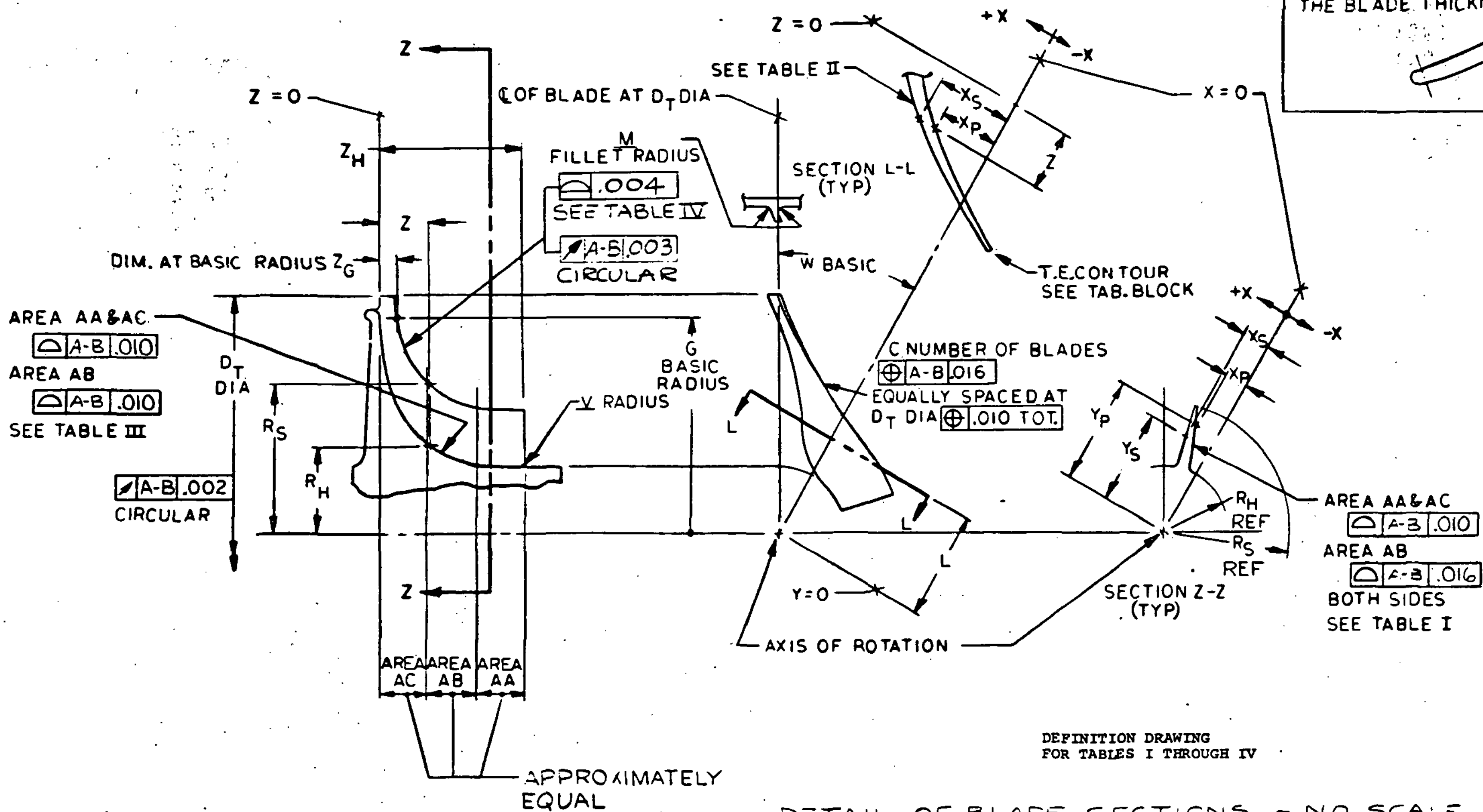

DEFINITION DRAWING FOR TABLES I THROUGH IV

DETAIL OF BLADE SECTIONS - NO SCALE

BLADE CONTOUR MUST FAIR SMOOTHLY BETWEEN SECTIONS. THE ALLOWABLE WAVINESS RATE OF CHANGE OF BLADE CONTOUR OR BLEND BETWEEN SECTIONS SHALL NOT BE MORE THAN .005 IN./IN.

TABLE I

Z = 0.0375				Z = 0.1175				Z = 0.2175			
SUCTION SIDE		PRESSURE SIDE		SUCTION SIDE		PRESSURE SIDE		SUCTION SIDE		PRESSURE SIDE	
X_S	Y_S	X_P	Y_P	X_S	Y_S	X_P	Y_P	X_S	Y_S	X_P	Y_P
0.0932	2.5100	-0.0932	2.5100	0.1000	2.2325	-0.1000	2.2325	0.1040	2.0250	-0.1040	2.0250
0.0890	2.5604	-0.0890	2.5604	0.0941	2.3116	-0.0941	2.3116	0.0966	2.1237	-0.0966	2.1237
0.0864	2.5886	-0.0864	2.5886	0.0909	2.3536	-0.0909	2.3536	0.0925	2.1762	-0.0925	2.1762
0.0836	2.6167	-0.0836	2.6167	0.0878	2.3956	-0.0878	2.3956	0.0885	2.2286	-0.0885	2.2286
0.0807	2.6449	-0.0807	2.6449	0.0845	2.4376	-0.0845	2.4376	0.0845	2.2811	-0.0845	2.2811
0.0779	2.6731	-0.0779	2.6731	0.0813	2.4796	-0.0813	2.4796	0.0805	2.3335	-0.0805	2.3335
0.0749	2.7013	-0.0749	2.7013	0.0780	2.5217	-0.0780	2.5217	0.0766	2.3860	-0.0766	2.3860
0.0712	2.7295	-0.0712	2.7295	0.0746	2.5637	-0.0746	2.5637	0.0726	2.4384	-0.0726	2.4384
0.0681	2.7577	-0.0681	2.7577	0.0712	2.6057	-0.0712	2.6057	0.0687	2.4909	-0.0687	2.4909
0.0650	2.7859	-0.0650	2.7859	0.0675	2.6477	-0.0675	2.6477	0.0647	2.5433	-0.0647	2.5433
0.0619	2.8141	-0.0619	2.8141	0.0637	2.6897	-0.0637	2.6897	0.0606	2.5958	-0.0606	2.5958
0.0584	2.8423	-0.0584	2.8423	0.0598	2.7317	-0.0598	2.7317	0.0567	2.6483	-0.0567	2.6483
0.0548	2.8705	-0.0548	2.8705	0.0557	2.7738	-0.0557	2.7738	0.0527	2.7007	-0.0527	2.7007
0.0513	2.8987	-0.0513	2.8987	0.0516	2.8158	-0.0516	2.8158	0.0487	2.7532	-0.0487	2.7532
0.0468	2.9269	-0.0468	2.9269	0.0473	2.8578	-0.0473	2.8578	0.0447	2.8056	-0.0447	2.8056
0.0429	2.9551	-0.0429	2.9551	0.0431	2.8998	-0.0431	2.8998	0.0406	2.8581	-0.0406	2.8581
0.0388	2.9833	-0.0388	2.9833	0.0385	2.9418	-0.0385	2.9418	0.0366	2.9105	-0.0366	2.9105
0.0343	3.0115	-0.0343	3.0115	0.0340	2.9839	-0.0340	2.9839	0.0327	2.9630	-0.0327	2.9630
0.0296	3.0397	-0.0296	3.0397	0.0294	3.0259	-0.0294	3.0259	0.0288	3.0154	-0.0288	3.0154
0.0230	3.0800	-0.0230	3.0800	0.0220	3.0950	-0.0220	3.0950	0.0229	3.1000	-0.0229	3.1000

TABLE I (Contd)

Z = 0.3000				Z = 0.5000				Z = 0.7725			
SUCTION SIDE		PRESSURE SIDE		SUCTION SIDE		PRESSURE SIDE		SUCTION SIDE		PRESSURE SIDE	
X_s	Y_s	X_p	Y_p	X_s	Y_s	X_p	Y_p	X_s	Y_s	X_p	Y_p
0.1012	1.9250	-0.1012	1.9250	0.0980	1.7250	-0.0970	1.7250	0.1200	1.5209	-0.0600	1.5245
0.0952	2.0193	-0.0952	2.0193	0.0915	1.8059	-0.0906	1.8059	0.1100	1.6170	-0.0462	1.6201
0.0913	2.0711	-0.0913	2.0711	0.0882	1.8457	-0.0872	1.8457	0.1065	1.6568	-0.0411	1.6597
0.0872	2.1228	-0.0872	2.1228	0.0849	1.8854	-0.0839	1.8855	0.1029	1.6965	-0.0359	1.6992
0.0831	2.1746	-0.0831	2.1746	0.0815	1.9252	-0.0804	1.9252	0.0999	1.7362	-0.0314	1.7388
0.0788	2.2263	-0.0788	2.2263	0.0783	1.9649	-0.0772	1.9650	0.0970	1.7759	-0.0269	1.7784
0.0748	2.2781	-0.0748	2.2781	0.0748	2.0047	-0.0737	2.0047	0.0942	1.8156	-0.0226	1.8179
0.0703	2.3299	-0.0703	2.3299	0.0712	2.0444	-0.0701	2.0445	0.0918	1.8553	-0.0186	1.8575
0.0663	2.3816	-0.0663	2.3816	0.0679	2.0842	-0.0667	2.0842	0.0893	1.8950	-0.0145	1.8971
0.0621	2.4334	-0.0621	2.4334	0.0641	2.1240	-0.0630	2.1240	0.0871	1.9347	-0.0108	1.9367
0.0577	2.4852	-0.0577	2.4852	0.0606	2.1637	-0.0594	2.1638	0.0849	1.9744	-0.0070	1.9762
0.0530	2.5369	-0.0530	2.5369	0.0568	2.2035	-0.0556	2.2035	0.0828	2.0141	-0.0034	2.0158
0.0489	2.5887	-0.0489	2.5887	0.0529	2.2432	-0.0517	2.2433	0.0808	2.0538	0.0002	2.0554
0.0441	2.6405	-0.0441	2.6405	0.0492	2.2830	-0.0480	2.2830	0.0788	2.0935	0.0038	2.0950
0.0400	2.6922	-0.0400	2.6922	0.0453	2.3228	-0.0440	2.3228	0.0769	2.1332	0.0073	2.1346
0.0355	2.7440	-0.0355	2.7440	0.0416	2.3625	-0.0403	2.3625	0.0749	2.1729	0.0108	2.1742
0.0320	2.7958	-0.0320	2.7958	0.0377	2.4023	-0.0364	2.4023	0.0730	2.2126	0.0142	2.2138
0.0281	2.8475	-0.0281	2.8475	0.0338	2.4420	-0.0324	2.4420	0.0712	2.2523	0.0176	2.2534
0.0250	2.8993	-0.0250	2.8993	0.0308	2.4818	-0.0294	2.4818	0.0693	2.2920	0.0211	2.2929
0.0207	2.9950	-0.0207	2.9950	0.0257	2.5500	-0.0243	2.5500	0.0665	2.3561	0.0265	2.3569

TABLE I (Contd)

$Z=1.0350$				$Z=1.2000$				$Z=1.2100$			
SUCTION SIDE		PRESSURE SIDE		SUCTION SIDE		PRESSURE SIDE		SUCTION SIDE		PRESSURE SIDE	
X_s	Y_s	X_p	Y_p	X_s	Y_s	X_p	Y_p	X_s	Y_s	X_p	Y_p
0.1970	1.3964	0.0375	1.4098	0.2709	1.2989	0.1318	1.3203	0.2917	1.2953	0.1240	1.3219
0.1931	1.4793	0.0551	1.4909	0.2826	1.4009	0.1512	1.4211	0.3017	1.3941	0.1450	1.4190
0.1919	1.5216	0.0633	1.5323	0.2864	1.4446	0.1608	1.4639	0.3055	1.4379	0.1550	1.4618
0.1908	1.5638	0.0714	1.5738	0.2894	1.4884	0.1711	1.5065	0.3091	1.4817	0.1651	1.5046
0.1901	1.6060	0.0791	1.6153	0.2924	1.5322	0.1813	1.5492	0.3116	1.5258	0.1764	1.5472
0.1899	1.6482	0.0863	1.6568	0.2952	1.5760	0.1919	1.5919	0.3148	1.5697	0.1870	1.5900
0.1897	1.6903	0.0935	1.6984	0.2984	1.6198	0.2019	1.6346	0.3177	1.6136	0.1979	1.6327
0.1902	1.7324	0.1000	1.7399	0.3012	1.6636	0.2124	1.6773	0.3203	1.6576	0.2090	1.6753
0.1906	1.7745	0.1066	1.7815	0.3049	1.7073	0.2221	1.7201	0.3227	1.7017	0.2204	1.7179
0.1914	1.8166	0.1128	1.8232	0.3083	1.7511	0.2319	1.7628	0.3251	1.7457	0.2317	1.7605
0.1924	1.8586	0.1188	1.8648	0.3124	1.7947	0.2411	1.8057	0.3278	1.7897	0.2427	1.8032
0.1935	1.9007	0.1246	1.9064	0.3166	1.8384	0.2503	1.8486	0.3308	1.8336	0.2535	1.8459
0.1951	1.9427	0.1301	1.9481	0.3212	1.8819	0.2589	1.8915	0.3344	1.8775	0.2637	1.8887
0.1966	1.9847	0.1355	1.9898	0.3261	1.9254	0.2674	1.9345	0.3384	1.9213	0.2735	1.9316
0.1985	2.0267	0.1406	2.0315	0.3313	1.9689	0.2754	1.9775	0.3427	1.9650	0.2829	1.9745
0.2004	2.0687	0.1457	2.0732	0.3373	2.0123	0.2828	2.0206	0.3474	2.0087	0.2920	2.0175
0.2024	2.1106	0.1507	2.1150	0.3427	2.0557	0.2907	2.0637	0.3526	2.0523	0.3005	2.0605
0.2045	2.1526	0.1556	2.1567	0.3490	2.0990	0.2976	2.1069	0.3588	2.0957	0.3081	2.1037
0.2067	2.1946	0.1604	2.1984	0.3556	2.1423	0.3044	2.1501	0.3656	2.1390	0.3150	2.1471
0.2090	2.2365	0.1651	2.2402	0.3618	2.1856	0.3115	2.1933	0.3722	2.1824	0.3222	2.1903

TABLE I (Contd)

Z = 1.4600				Z = 1.7100				Z = 1.9000			
SUCTION SIDE		PRESSURE SIDE		SUCTION SIDE		PRESSURE SIDE		SUCTION SIDE		PRESSURE SIDE	
X_s	Y_s	X_p	Y_p	X_s	Y_s	X_p	Y_p	X_s	Y_s	X_p	Y_p
0,4657	1,1635	0.2943	1,2182	0,6679	1,0011	0,5094	1,0903	0,8488	0,8540	0,5972	0,9817
0,4891	1,2627	0.3326	1,3126	0,7140	1,1102	0,5787	1,1863	0,9073	0,9435	0,7754	1,0546
0,5000	1,3081	0.3501	1,3559	0,7333	1,1545	0,6066	1,2258	0,9348	0,9841	0,8107	1,0885
0,5106	1,3536	0.3678	1,3992	0,7527	1,1988	0,6344	1,2654	0,9620	1,0248	0,8462	1,1223
0,5210	1,3992	0.3857	1,4424	0,7727	1,2428	0,6616	1,3053	0,9900	1,0649	0,8810	1,1567
0,5315	1,4447	0.4035	1,4856	0,7927	1,2867	0,6889	1,3451	1,0178	1,1052	0,9160	1,1910
0,5420	1,4903	0.4213	1,5288	0,8131	1,3304	0,7156	1,3853	1,0462	1,1450	0,9503	1,2257
0,5527	1,5358	0,4390	1,5720	0,8335	1,3742	0,7425	1,4254	1,0744	1,1849	0,9849	1,2603
0,5633	1,5813	0,4567	1,6153	0,8543	1,4176	0,7688	1,4657	1,1031	1,2244	1,0189	1,2953
0,5737	1,6269	0,4746	1,6585	0,8750	1,4612	0,7953	1,5061	1,1317	1,2640	1,0531	1,3302
0,5841	1,6725	0,4926	1,7016	0,8964	1,5043	0,8211	1,5467	1,1609	1,3031	1,0866	1,3657
0,5944	1,7181	0,5106	1,7448	0,9177	1,5475	0,8470	1,5874	1,1901	1,3422	1,1202	1,4011
0,6049	1,7636	0,5284	1,7880	0,9396	1,5904	0,8722	1,6283	1,2198	1,3809	1,1533	1,4369
0,6158	1,8090	0,5458	1,8314	0,9615	1,6333	0,8976	1,6693	1,2495	1,4196	1,1864	1,4727
0,6275	1,8542	0,5625	1,8749	0,9837	1,6760	0,9225	1,7104	1,2795	1,4580	1,2191	1,5089
0,6396	1,8992	0,5787	1,9187	1,0060	1,7186	0,9474	1,7516	1,3096	1,4963	1,2517	1,5451
0,6520	1,9442	0,5946	1,9625	1,0291	1,7608	0,9716	1,7932	1,3405	1,5340	1,2837	1,5819
0,6649	1,9890	0,6100	2,0065	1,0523	1,8030	0,9955	1,8350	1,3715	1,5716	1,3154	1,6189
0,6783	2,0336	0,6249	2,0506	1,0762	1,8447	1,0188	1,8770	1,4032	1,6086	1,3465	1,6564
0,6923	2,0780	0.6393	2,0949	1,1003	1,8864	1.0419	1,9192	1,4351	1,6454	1,3773	1,6941

TABLE I (Contd)

$Z = 2.1000$			
SUCTION SIDE		PRESSURE SIDE	
X_S	Y_S	X_P	Y_P
1.0215	0.6386	0.8937	0.8078
1.0932	0.7093	0.9813	0.8575
1.1292	0.7432	1.0237	0.8828
1.1648	0.7773	1.0663	0.9078
1.2011	0.8107	1.1083	0.9336
1.2373	0.8442	1.1504	0.9592
1.2739	0.8771	1.1921	0.9854
1.3104	0.9102	1.2339	1.0115
1.3473	0.9428	1.2753	1.0380
1.3841	0.9754	1.3168	1.0645
1.4214	1.0075	1.3579	1.0916
1.4589	1.0392	1.3986	1.1190
1.4964	1.0710	1.4395	1.1463
1.5341	1.1025	1.4801	1.1740
1.5721	1.1336	1.5204	1.2021
1.6102	1.1646	1.5606	1.2302
1.6488	1.1948	1.6002	1.2591
1.6877	1.2247	1.6396	1.2884
1.7271	1.2539	1.6785	1.3183
1.7668	1.2829	1.7172	1.3485

TABLE II BLADE COORDINATES

'L' SECTION R = 1.3000			'L' SECTION R = 1.5200			'L' SECTION R = 1.7400			'L' SECTION R = 1.8500			'L' SECTION R = 1.9600			'L' SECTION R = 2.0700			'L' SECTION R = 2.1800		
	SUCTION SIDE	PRESSURE SIDE		SUCTION SIDE	PRESSURE SIDE		SUCTION SIDE	PRESSURE SIDE		SUCTION SIDE	PRESSURE SIDE		SUCTION SIDE	PRESSURE SIDE		SUCTION SIDE	PRESSURE SIDE		SUCTION SIDE	PRESSURE SIDE
Z	YS	YP	Z	YS	YP	Z	YS	YP	Z	YS	YP	Z	YS	YP	Z	YS	YP	Z	YS	YP
0.0000	0.0000	0.0000	0.0000	0.0000	0.0000	0.0000	0.0000	0.0000	0.0000	0.0000	0.0000	0.0000	0.0000	0.0000	0.0000	0.0000	0.0000	0.0000	0.0000	0.0000
0.0375	0.0000	0.0000	0.0375	0.0000	0.0000	0.0375	0.0000	0.0000	0.0375	0.0000	0.0000	0.0375	0.0000	0.0000	0.0375	0.0000	0.0000	0.0375	0.0000	0.0000
0.0700	0.0000	0.0000	0.0700	0.0000	0.0000	0.0700	0.0000	0.0000	0.0700	0.0000	0.0000	0.0700	0.0000	0.0000	0.0700	0.0000	0.0000	0.0700	0.0000	0.0000
0.1500	0.0000	0.0000	0.1500	0.0000	0.0000	0.1500	0.0000	0.0000	0.1500	0.0000	0.0000	0.1500	0.0000	0.0000	0.1500	0.0000	0.0000	0.1500	0.4332	0.2349
0.2175	0.0000	0.0000	0.2175	0.0000	0.0000	0.2175	0.0000	0.0000	0.2175	0.0000	0.0000	0.2175	0.0000	0.0000	0.2175	0.4170	0.2170	0.2175	0.4255	0.2427
0.3000	0.0000	0.0000	0.3000	0.0000	0.0000	0.3000	0.0000	0.0000	0.3000	0.0000	0.0000	0.3000	0.3991	0.2015	0.3000	0.4076	0.2266	0.3000	0.4156	0.2548
0.3525	0.0000	0.0000	0.3525	0.0000	0.0000	0.3525	0.0000	0.0000	0.3525	0.3840	0.1826	0.3525	0.3950	0.2074	0.3525	0.4017	0.2338	0.3525	0.4095	0.2610
0.5000	0.0000	0.0000	0.5000	0.0000	0.0000	0.5000	0.3616	0.1700	0.5000	0.3694	0.1962	0.5000	0.3768	0.2226	0.5000	0.3839	0.2496	0.5000	0.3902	0.2769
0.6500	0.0000	0.0000	0.6500	0.0000	0.0000	0.6500	0.3342	0.1772	0.6500	0.3410	0.2033	0.6500	0.3464	0.2290	0.6500	0.3556	0.2543	0.6500	0.3630	0.2794
0.7725	0.0000	0.0000	0.7725	0.2909	0.1153	0.7725	0.2963	0.1673	0.7725	0.3015	0.1900	0.7725	0.3076	0.2151	0.7725	0.3162	0.2379	0.7725	0.3216	0.2603
0.9000	0.0000	0.0000	0.9000	0.2408	0.0874	0.9000	0.2433	0.1339	0.9000	0.2463	0.1539	0.9000	0.2512	0.1759	0.9000	0.2584	0.1913	0.9000	0.2634	0.2103
1.0350	0.0000	0.0000	1.0350	0.1704	0.0391	1.0350	0.1655	0.0751	1.0350	0.1658	0.0902	1.0350	0.1677	0.1036	1.0350	0.1709	0.1157	1.0350	0.1749	0.1271
1.1500	0.0000	0.0000	1.1500	0.0975	-0.0267	1.1500	0.0829	-0.0217	1.1500	0.0758	0.0075	1.1500	0.0763	0.0151	1.1500	0.0752	0.0215	1.1500	0.0759	0.0259
1.2000	0.0000	0.0000	1.2000	0.0628	-0.0625	1.2000	0.0432	-0.0414	1.2000	0.0365	-0.0365	1.2000	0.0293	-0.0293	1.2000	0.0266	-0.0266	1.2000	0.0258	-0.0258
1.2500	0.0000	0.0000	1.2500	0.0250	-0.1027	1.2500	0.0000	-0.0859	1.2500	-0.0102	-0.0857	1.2500	-0.0178	-0.0922	1.2500	-0.0265	-0.0792	1.2500	-0.0298	-0.0816
1.3500	-0.0212	-0.1944	1.3500	-0.0563	-0.1927	1.3500	-0.0935	-0.1921	1.3500	-0.1132	-0.1943	1.3500	-0.1303	-0.1957	1.3500	-0.1445	-0.2000	1.3500	-0.1544	-0.2085
1.4600	-0.1179	-0.2897	1.4600	-0.1707	-0.3266	1.4600	-0.2241	-0.3229	1.4600	-0.2511	-0.3310	1.4600	-0.2754	-0.3419	1.4600	-0.2969	-0.3553	1.4600	0.0000	0.0000
1.6000	-0.2681	-0.4311	1.6000	-0.3493	-0.4713	1.6000	-0.4256	-0.5140	1.6000	-0.4623	-0.5373	1.6000	-0.4567	-0.5629	1.6000	-0.5292	-0.5914	1.6000	0.0000	0.0000
1.7100	-0.4114	-0.5620	1.7100	-0.5164	-0.6255	1.7100	-0.6137	-0.6953	1.7100	-0.6599	-0.7325	1.7100	-0.7033	-0.7730	1.7100	0.0000	0.0000	1.7100	0.0000	0.0000
1.8000	-0.5410	-0.6935	1.8000	-0.6688	-0.7787	1.8000	-0.7853	-0.8717	1.8000	-0.8444	-0.9216	1.8000	-0.8969	-0.9744	1.8000	0.0000	0.0000	1.8000	0.0000	0.0000
1.9000	-0.7120	-0.8646	1.9000	-0.8700	-0.9791	1.9000	-1.0168	-1.1036	1.9000	-1.0838	-1.1714	1.9000	0.0000	0.0000	1.9000	0.0000	0.0000	1.9000	0.0000	0.0000
1.9750	-0.8663	-1.0155	1.9750	-1.0498	-1.1573	1.9750	-1.2176	-1.3137	1.9750	0.0000	0.0000	1.9750	0.0000	0.0000	1.9750	0.0000	0.0000	1.9750	0.0000	0.0000
2.0500	-1.0503	-1.1922	2.0500	-1.2616	-1.3661	2.0500	0.0000	0.0000	2.0500	0.0000	0.0000	2.0500	0.0000	0.0000	2.0500	0.0000	0.0000	2.0500	0.0000	0.0000
2.1000	-1.1922	-1.3285	2.1000	-1.4222	-1.5344	2.1000	0.0000	0.0000	2.1000	0.0000	0.0000	2.1000	0.0000	0.0000	2.1000	0.0000	0.0000	2.1000	0.0000	0.0000

TABLE III

HUB CONTOUR COORDINATES

Z	R_H		Z	R_H	
2.1000	1.2500		0,1696	2,1600	
2.0109	1.2512		0,1540	2,1893	
1.9218	1.2546		0,1394	2,2186	
1.8327	1.2599		0,1258	2,2479	
1.7436	1.2671		0,1131	2,2772	
1.6545	1.2762		0,1013	2,3065	
1.5654	1.2873		0,0904	2,3358	
1.4850	1.2994		0,0803	2,3650	
1.3950	1.3225		0,0710	2,3943	*
1.3050	1.3489		0,0624	2,4236	*
1.2150	1.3785		0,0545	2,4529	*
1.1250	1.4116		0,0473	2,4822	*
1.0350	1.4483		0,0408	2,5115	*
0.9450	1.4889		0,0349	2,5407	*
0.8550	1.5338		0,0296	2,5700	*
0.7650	1.5836		0,0249	2,5993	*
0.6750	1.6390		0,0206	2,6286	*
0.5850	1.7013		0,0169	2,6579	*
0.5216	1.7500		0,0137	2,6872	*
0.4862	1.7793		0,0108	2,7165	*
0.4527	1.8086		0,0085	2,7458	*
0.4211	1.8379		0,0064	2,7750	*
0.3911	1.8672		0,0047	2,8043	*
0.3628	1.8965		0,0034	2,8336	*
0.3360	1.9257		0,0023	2,8629	*
0.3106	1.9550		0,0015	2,8922	*
0.2867	1.9843		0,0009	2,9215	*
0.2641	2.0136		0,0005	2,9508	*
0.2428	2.0429		0,0002	2,9800	*
0.2228	2.0722		0,0001	3,0093	*
0.2039	2.1015		0,0000	3,0386	*
0.1862	2.1308		0,0000	3,9000	*

TABLE IV

OUTSIDE EDGE CONTOUR COORDINATES

Z	R_S			Z	R_S
0.2695	3.2000	*			
0.2695	3.0680				
0.2717	3.0060				
0.2786	2.9440				
0.2903	2.8819				
0.3071	2.8199				
0.3294	2.7578				
0.3579	2.6957				
0.3935	2.6336				
0.4373	2.5715				
0.4913	2.5093				
0.5223	2.4788				
0.5972	2.4167				
0.6932	2.3547				
0.8236	2.2929				
0.9308	2.2560				
1.0377	2.2285				
1.1445	2.2082				
1.2511	2.1936				
1.3575	2.1834				
1.4638	2.1766				
1.5700	2.1723				
1.6761	2.1699				
1.7822	2.1686				
1.8882	2.1681				
1.9941	2.1680				
2.1000	2.1680				

* FOR CONSTRUCTION PURPOSES

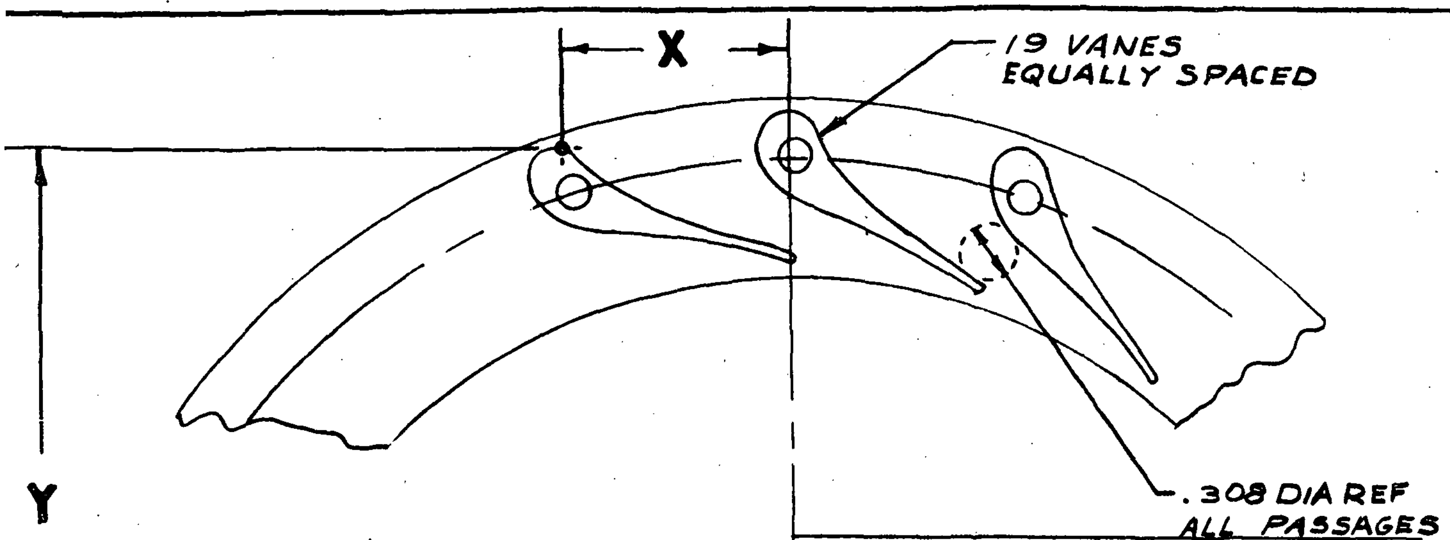

SUCTION		PRESSURE	
X	Y	X	Y
.0142	3.1692	.0140	3.1692
.0068	3.1606	.0135	3.1806
-.0045	3.1597	.0050	3.1882
-.0996	3.1880	-.0365	3.2023
-.1501	3.2017	-.0797	3.2152
-.2478	3.2260	-.1237	3.2290
-.3733	3.2527	-.1708	3.2430
-.5012	3.2751	-.2191	3.2580
-.6284	3.2932	-.2714	3.2740
-.7579	3.3074	-.3266	3.2919
-.8890	3.3184	-.3864	3.3117
-1.0225	3.3258	-.4522	3.3339
-1.0505	3.3278	-.5289	3.3616
-1.0785	3.3312	-.6060	3.3918
-1.1064	3.3363	-.6989	3.4307
-1.1340	3.3429	-.8041	3.4819
-1.1613	3.3514	-.9267	3.5510
-1.1882	3.3614	-1.0672	3.6500
-1.2145	3.3734	-1.0925	3.6699
-1.2400	3.3873	-1.1178	3.6901
-1.2646	3.4031	-1.1431	3.7105
-1.2880	3.4209	-1.1684	3.7267
-1.3101	3.4406	-1.2864	3.7356
-1.3304	3.4625		
-1.3486	3.4863		
-1.3645	3.5122		
-1.3773	3.5398		
-1.3740	3.6560		
-1.2864	3.7356		

PROJECT AUTHORIZATION — For Development Only

Alternate / Rework — for Dwg No. NASA 10/1 RIG — Next Assy

W. O. No. — Outline

AIRESEARCH MANUFACTURING COMPANY OF ARIZONA
PHOENIX, ARIZONA

Title: NOZZLE, RADIAL TURBINE

APPD M. D. Toomey	11-15-71
APPD	
CHK	
DFT	
PAP	216124

FORM P8725B

APPENDIX D

COMPLETE RADIAL EQUILIBRIUM FLOW SOLUTION ALL BLADE ROWS

(61 pages)

10/1 NASA COMP.#3/30/72**THRU THE BLADE**ALL STAGES** FINAL

DATE04/05/72 TIME17:54:48

CODE	RADIUS	SPEED	FLOW	STRMLNS	MAX IT
70000.00000	.08333	610.00000	2.00000	6	19

GAMMA	SPEC HEAT	TEMP	PRESSURE	DENSITY	RPM
1.39470	6065.37000	518.68800	2116.22000	.076474	69900.88

MAJOR ITERS	FLOW TOL	CUR TOL	SENSE SW	SHOK LOC	OD LOSS
20	.00100	.00100	89	-0.00000	-0.00000
FLOW					
.10000	.15000	.25000	.25000	.25000	

STATIONS	DM(M-1)	DM(N+1)	ANGL DAMP	ROT DELW	DEL LOSS
30	1.00000	.30000	.95000	.30000	-0.00000
SLOPE M-1					
-5.23000	-5.61700	-6.09160	-6.58860	-6.86600	-6.33000
SLOPE N+1					
22.00000	22.00000	22.00000	22.00000	22.00000	22.50000
CURVATURE M-1					
-.08240	-.10324	-.11402	-.12200	-.12515	-.09970
CURVATURE N+1					
-.25000	-.25000	-.26000	-.31200	-.31200	-.31200

	STATION	AVERAGE P/P	AVERAGE T/T	AVERAGE EFF
	.03000	1.00000	1.00000	1.00000
	.04000	1.00000	1.00000	1.00000
	.05000	1.00000	1.00000	1.00000
	.50000	1.00000	1.00000	1.00000
	.06000	1.00000	1.00000	1.00000
	.07000	1.00000	1.00000	1.00000
Rotor 1A Inlet	1.00000	1.00000	1.00000	1.00000
	1.20000	1.14542	1.04028	.96102
	1.40000	1.32628	1.08659	.95856
	1.60000	1.52199	1.13212	.95688
	1.80000	1.70059	1.17001	.95597
Rotor 1A Exit	2.00000	1.78018	1.18605	.95509
Rotor 1B Inlet	3.00000	1.77876	1.18605	.95364
	3.20000	2.12780	1.24888	.95890
	3.40000	2.43015	1.29793	.96042
	3.60000	2.78528	1.35027	.96144
	3.80000	3.10595	1.39515	.95811
Rotor 1B Exit	4.00000	3.24146	1.41210	.95963
Stator 1A Inlet	5.00000	3.24146	1.41210	.95963
	5.10000	3.21130	1.41210	.95073
	5.20000	3.18373	1.41210	.94254
	5.30000	3.15247	1.41210	.93319
	5.40000	3.12463	1.41210	.92480
Stator 1A Exit	5.50000	3.09619	1.41210	.91617
Stator 1B Inlet	6.00000	3.09619	1.41210	.91617
	6.10000	3.09036	1.41210	.91439
	6.20000	3.08335	1.41210	.91225
	6.30000	3.07634	1.41210	.91010
	6.40000	3.06934	1.41210	.90795
Stator 1B Exit	6.50000	3.06243	1.41210	.90583

```
STATION        .03000  STATOR   XI =      0.00000

P =   -0.   ZTIP =   -4.12500   AR =    1.30000    XN =    0.     BNXT =  -0.
  =    0.   ZHUB =   -4.12500   LOSS =    1.   EXP =    .8000  BLADES =  -0.

RADIUS
   3.54000     3.47000     3.32000     3.15000     2.75000     2.28000
SLOPE
 -14.32000   -16.00000   -17.00000   -19.00000   -20.00000   -18.14000
CURVATURE
   -.22220     -.19000     -.21000     -.23000     -.25000     -.28540
LOSS COEFF
  -0.00000    -0.00000    -0.00000    -0.00000    -0.00000    -0.00000
SOLIDITY
   1.00000     1.00000     1.00000     1.00000     1.00000     1.00000
AERO BLOCKAGE
    .99600      .99600      .99600      .99600      .99600      .99600
TOTAL BLOCKAGE
    .99600      .99600      .99600      .99600      .99600      .99600
BLADE ANGLE
  -0.00000    -0.00000    -0.00000    -0.00000    -0.00000    -0.00000
LEAN
  -0.00000    -0.00000    -0.00000    -0.00000    -0.00000    -0.00000
Y
  -0.00000    -0.00000    -0.00000    -0.00000    -0.00000    -0.00000

MINOR ITERS =  1  AREA RATIO =  .99938  EXP =  .80000  CHOKE =  .26613

 DIUS
   3.54000     3.42314     3.24461     2.93771     2.61665     2.28000
Z
  -4.12500    -4.12500    -4.12500    -4.12500    -4.12500    -4.12500
CROSS PASSAGE DIST P
   1.26000     1.14314      .96461      .65771      .33665     0.00000
SLOPE
 -14.32000   -15.23712   -15.97222   -17.39095   -18.47023   -18.14000
CURVATURE
   -.22220     -.20663     -.20057     -.20908     -.22670     -.28540
DELTA CURVATURE
   0.00000     -.00001     -.00015     -.00006      .00010     0.00000
VM
 152.62197   156.30901   162.17091   173.40452   187.53331   207.89497
VU2
   0.00000     0.00000     0.00000     0.00000     0.00000     0.00000
U
2159.40000  2088.11380  1979.21147  1792.00433  1596.15566  1390.80000
VR
 -37.74911   -41.08026   -44.62479   -51.82892   -59.41279   -64.72603
BETA2
   0.00000     0.00000     0.00000     0.00000     0.00000     0.00000
BETA2*
   0.00000     0.00000     0.00000     0.00000     0.00000     0.00000
```

```
INCIDENCE
    0.00000     0.00000     0.00000     0.00000     0.00000     0.00000

     .13722      .14054      .14584      .15599      .16876      .18721
V2
  152.62197   156.30901   162.17091   173.40452   187.53331   207.89497
TOTAL TEMP
    1.00000     1.00000     1.00000     1.00000     1.00000     1.00000
TOTAL PRESS
    1.00000     1.00000     1.00000     1.00000     1.00000     1.00000
EFFICIENCY
    0.00000     0.00000     0.00000     0.00000     0.00000     0.00000
STATIC TEMP
     .99630      .99612      .99582      .99522      .99441      .99313
STATIC PRESS
     .98698      .98635      .98531      .98322      .98039      .97594
DENSITY
     .99065      .99019      .98944      .98794      .98590      .98269
DELTA T
    0.00000     0.00000     0.00000     0.00000     0.00000     0.00000
WORK COEF = 2*CP*DELT/U**2
    0.00000     0.00000     0.00000     0.00000     0.00000     0.00000
FLOW COEF = VM/U
     .07068      .07486      .08194      .09677      .11749      .14948
R BAR
    3.54000     3.42314     3.24461     2.93771     2.61665     2.28000
D-FACTOR
    0.00000     0.00000     0.00000     0.00000     0.00000     0.00000
VM2/VM1
    1.00000     1.00000     1.00000     1.00000     1.00000     1.00000
DELP/Q
    0.00000     0.00000     0.00000     0.00000     0.00000     0.00000
TANG BLADE FORCE LB/IN
    0.00000     0.00000     0.00000     0.00000     0.00000     0.00000
AXIAL BLADE FORCE LB/IN
    0.00000     0.00000     0.00000     0.00000     0.00000     0.00000
VEL HEAD 2
     .01302      .01365      .01469      .01678      .01961      .02406
Q=E**(-S/CP)
    1.00000     1.00000     1.00000     1.00000     1.00000     1.00000
RVU/
    0.00000     0.00000     0.00000     0.00000     0.00000     0.00000
DRVU/DM
   -0.00000    -0.00000    -0.00000    -0.00000    -0.00000    -0.00000
STRMLN DIST M
   -4.12500    -4.12500    -4.12500    -4.12500    -4.12500    -4.12500
```

STATION .04000 STATOR XI = 0.00000

P = -0. ZTIP = -3.12500 AR = 1.40000 XN = -0. BNXT = -0.
= -0. ZHUB = -3.12500 LOSS = 1. EXP = .8000 BLADES = -0.

RADIUS					
3.16000	3.09000	2.89000	2.68000	2.25000	1.77000
SLOPE					
-26.90000	-26.00000	-28.00000	-30.00000	-32.00000	-35.30000
CURVATURE					
-.18410	-.20000	-.18000	-.16000	-.13000	-.23290
LOSS COEFF					
-0.00000	-0.00000	-0.00000	-0.00000	-0.00000	-0.00000
SOLIDITY					
1.00000	1.00000	1.00000	1.00000	1.00000	1.00000
AERO BLOCKAGE					
.99500	.99500	.99500	.99500	.99500	.99500
TOTAL BLOCKAGE					
.99500	.99500	.99500	.99500	.99500	.99500
BLADE ANGLE					
-0.00000	-0.00000	-0.00000	-0.00000	-0.00000	-0.00000
LEAN					
-0.00000	-0.00000	-0.00000	-0.00000	-0.00000	-0.00000
Y					
-0.00000	-0.00000	-0.00000	-0.00000	-0.00000	-0.00000

MINOR ITERS = 1 AREA RATIO = .99955 EXP = .80000 CHOKE = .31431

DIUS					
3.16000	3.03550	2.84602	2.51674	2.16501	1.77000
Z					
-3.12500	-3.12500	-3.12500	-3.12500	-3.12500	-3.12500
CROSS PASSAGE DIST P					
1.39000	1.26550	1.07602	.74674	.39501	0.00000
SLOPE					
-26.90000	-26.92155	-27.94293	-29.20354	-30.97242	-35.30000
CURVATURE					
-.18410	-.19573	-.19355	-.17729	-.17489	-.23290
DELTA CURVATURE					
0.00000	.00004	.00036	.00024	-.00003	0.00000
VM					
174.29387	180.49529	189.66782	206.04046	225.55094	250.64984
VU2					
0.00000	0.00000	0.00000	0.00000	0.00000	0.00000
U					
1927.60000	1851.65420	1736.07441	1535.20893	1320.65751	1079.70000
VR					
-78.85663	-81.72291	-88.87682	-100.52999	-116.07429	-144.83998
BETA2					
0.00000	0.00000	0.00000	0.00000	0.00000	0.00000
BETA2*					
0.00000	0.00000	0.00000	0.00000	0.00000	0.00000

```
INCIDENCE
    0.00000     0.00000     0.00000     0.00000     0.00000     0.00000

     .15679      .16240      .17070      .18553      .20323      .22606
V2
  174.29387   180.49529   189.66782   206.04046   225.55094   250.64984
TOTAL TEMP
    1.00000     1.00000     1.00000     1.00000     1.00000     1.00000
TOTAL PRESS
    1.00000     1.00000     1.00000     1.00000     1.00000     1.00000
EFFICIENCY
    0.00000     0.00000     0.00000     0.00000     0.00000     0.00000
STATIC TEMP
     .99517      .99482      .99428      .99325      .99191      .99002
STATIC PRESS
     .98304      .98182      .97994      .97636      .97172      .96516
DENSITY
     .98781      .98693      .98558      .98299      .97964      .97490
DELTA T
    0.00000     0.00000     0.00000     0.00000     0.00000     0.00000
WORK COEF = 2*CP*DELT/U**2
    0.00000     0.00000     0.00000     0.00000     0.00000     0.00000
FLOW COEF = VM/U
     .09042      .09748      .10925      .13421      .17079      .23215
R BAR
    3.35000     3.22932     3.04532     2.72722     2.39083     2.02500
D-FACTOR
    -.14200     -.15473     -.16956     -.18821     -.20272     -.20566
VM2/VM1
    1.14200     1.15473     1.16956     1.18821     1.20272     1.20566
DELP/Q
    -.30230     -.33122     -.36519     -.40832     -.44197     -.44787
TANG BLADE FORCE LB/IN
    0.00000     0.00000     0.00000     0.00000     0.00000     0.00000
AXIAL BLADE FORCE LB/IN
    -.84090     -.84793     -.94707    -1.06570    -1.24716    -1.74702
VEL HEAD 2
     .01696      .01818      .02006      .02364      .02828      .03484
Q=E**(-S/CP)
    1.00000     1.00000     1.00000     1.00000     1.00000     1.00000
RVU/
    0.00000     0.00000     0.00000     0.00000     0.00000     0.00000
DRVU/DM
   -0.00000    -0.00000    -0.00000    -0.00000    -0.00000    -0.00000
STRMLN DIST M
   -3.05308    -3.05064    -3.04653    -3.03808    -3.02556    -2.99825
```

```
STATION        .05000  STATOR   XI =      0.00000

P =  -0.  ZTIP =  -2.12500   AR =    1.50000    XN =  -0.     BNXT =  -0.
  =  -0.  ZHUB =  -2.12500   LOSS =    1.  EXP =     .8000  BLADES =  -0.

RADIUS
     2.54000      2.46000      2.26000      2.03000      1.58000      1.00600
SLOPE
   -35.08000    -34.50000    -32.90000    -30.85000    -29.78000    -34.40000
CURVATURE
     -.06112      0.00000       .05000       .08000       .15000       .24700
LOSS COEFF
    -0.00000     -0.00000     -0.00000     -0.00000     -0.00000     -0.00000
SOLIDITY
     1.00000      1.00000      1.00000      1.00000      1.00000      1.00000
AERO BLOCKAGE
      .99400       .99400       .99400       .99400       .99400       .99400
TOTAL BLOCKAGE
      .99400       .99400       .99400       .99400       .99400       .99400
BLADE ANGLE
    -0.00000     -0.00000     -0.00000     -0.00000     -0.00000     -0.00000
LEAN
    -0.00000     -0.00000     -0.00000     -0.00000     -0.00000     -0.00000
Y
    -0.00000     -0.00000     -0.00000     -0.00000     -0.00000     -0.00000

MINOR ITERS =  1  AREA RATIO =  .99909  EXP =  .80000  CHOKE =  .40515

 )IUS
     2.54000      2.41891      2.23506      1.91191      1.53748      1.00600
Z
    -2.12500     -2.12500     -2.12500     -2.12500     -2.12500     -2.12500
CROSS PASSAGE DIST P
     1.53400      1.41291      1.22906       .90591       .53148      0.00000
SLOPE
   -35.08000    -34.11692    -32.60263    -30.56561    -29.79860    -34.40000
CURVATURE
     -.06112      -.01536       .03878       .11473       .19184       .24700
DELTA CURVATURE
     0.00000      -.00007      -.00051      -.00067      -.00055      0.00000
VM
   245.72929    254.46730    265.03657    275.91751    275.72465    255.08052
VU2
     0.00000      0.00000      0.00000      0.00000      0.00000      0.00000
U
  1549.40000   1475.53422   1363.38743   1166.26276    937.86308    613.66000
VR
  -141.22550   -142.72655   -142.80425   -140.31093   -137.02219   -144.11213
BETA2
     0.00000      0.00000      0.00000      0.00000      0.00000      0.00000
BETA2*
     0.00000      0.00000      0.00000      0.00000      0.00000      0.00000
```

INCIDENCE					
0.00000	0.00000	0.00000	0.00000	0.00000	0.00000
. .					
.22158	.22954	.23918	.24912	.24894	.23010
V2					
245.72929	254.46730	265.03657	275.91751	275.72465	255.08052
TOTAL TEMP					
1.00000	1.00000	1.00000	1.00000	1.00000	1.00000
TOTAL PRESS					
1.00000	1.00000	1.00000	1.00000	1.00000	1.00000
EFFICIENCY					
0.00000	0.00000	0.00000	0.00000	0.00000	0.00000
STATIC TEMP					
.99040	.98971	.98884	.98790	.98792	.98966
STATIC PRESS					
.96650	.96411	.96111	.95790	.95796	.96394
DENSITY					
.97586	.97413	.97196	.96963	.96967	.97401
DELTA T					
0.00000	0.00000	0.00000	0.00000	0.00000	0.00000
WORK COEF = 2*CP*DELT/U**2					
0.00000	0.00000	0.00000	0.00000	0.00000	0.00000
FLOW COEF = VM/U					
.15860	.17246	.19440	.23658	.29399	.41567
R BAR					
2.85000	2.72720	2.54054	2.21432	1.85125	1.38800
D-FACTOR					
-.40986	-.40983	-.39737	-.33914	-.22245	-.01768
VM2/VM1					
1.40986	1.40983	1.39737	1.33914	1.22245	1.01768
DELP/Q					
-.97570	-.97476	-.93920	-.78116	-.48682	-.03520
TANG BLADE FORCE LB/IN					
0.00000	0.00000	0.00000	0.00000	0.00000	0.00000
AXIAL BLADE FORCE LB/IN					
-2.09020	-1.99288	-1.68336	-1.10594	-.49723	.01465
VEL HEAD 2					
.03350	.03589	.03889	.04210	.04204	.03606
Q=E**(-S/CP)					
1.00000	1.00000	1.00000	1.00000	1.00000	1.00000
RVU/					
0.00000	0.00000	0.00000	0.00000	0.00000	0.00000
DRVU/DM					
-0.00000	-0.00000	-0.00000	-0.00000	-0.00000	-0.00000
STRMLN DIST M					
-1.87648	-1.87582	-1.87466	-1.86940	-1.84497	-1.73980

```
STATION          .50000  STATOR   XI =       0.00000

P =   -0.  ZTIP =  -1.42500   AR =   4.00000    XN =  -0.     BNXT =  -0.
.  =  -0.  ZHUB =  -1.42500   LOSS =   1.  EXP =    .8000  BLADES =  -0.

RADIUS
    2.07530     1.97900     1.83000     1.55000     1.20000      .63660
SLOPE
  -29.56000   -26.30000   -23.90000   -20.00000   -17.00000   -19.55000
CURVATURE
     .28750      .31000      .36000      .41600      .45600      .49144
LOSS COEFF
   -0.00000    -0.00000    -0.00000    -0.00000    -0.00000    -0.00000
SOLIDITY
    1.00000     1.00000     1.00000     1.00000     1.00000     1.00000
AERO BLOCKAGE
     .99000      .99000      .99000      .99000      .99000      .99000
TOTAL BLOCKAGE
     .99000      .99000      .99000      .99000      .99000      .99000
BLADE ANGLE
   -0.00000    -0.00000    -0.00000    -0.00000    -0.00000    -0.00000
LEAN
   -0.00000    -0.00000    -0.00000    -0.00000    -0.00000    -0.00000
Y
   -0.00000    -0.00000    -0.00000    -0.00000    -0.00000    -0.00000

MINOR ITERS =  1  AREA RATIO =  .99960  EXP =  .80000  CHOKE =  .51896

  DIUS
    2.07530     1.98155     1.83549     1.56235     1.21659      .63660
Z
   -1.42500    -1.42500    -1.42500    -1.42500    -1.42500    -1.42500
CROSS PASSAGE DIST P
    1.43870     1.34495     1.19889      .92575      .57999     0.00000
SLOPE
  -29.56000   -27.07022   -24.44119   -20.49675   -17.50555   -19.55000
CURVATURE
     .28750      .31778      .33380      .35811      .39100      .49144
DELTA CURVATURE
    0.00000      .00033     -.00006     -.00035     -.00061     0.00000
VM
  382.37042   384.52282   380.44635   362.41394   331.20066   260.09312
VU2
    0.00000     0.00000     0.00000     0.00000     0.00000     0.00000
U
 1265.93300  1208.74730  1119.65136   953.03341   742.11704   388.32600
VR
 -188.63668  -174.98953  -157.41317  -126.90085   -99.62459   -87.03483
BETA2
    0.00000     0.00000     0.00000     0.00000     0.00000     0.00000
BETA2*
    0.00000     0.00000     0.00000     0.00000     0.00000     0.00000
```

INCIDENCE	0.00000	0.00000	0.00000	0.00000	0.00000	0.00000
	.34720	.34920	.34541	.32868	.29984	.23467
V2	382.37042	384.52282	380.44635	362.41394	331.20066	260.09312
TOTAL TEMP	1.00000	1.00000	1.00000	1.00000	1.00000	1.00000
TOTAL PRESS	1.00000	1.00000	1.00000	1.00000	1.00000	1.00000
EFFICIENCY	0.00000	0.00000	0.00000	0.00000	0.00000	0.00000
STATIC TEMP	.97676	.97650	.97700	.97913	.98257	.98925
STATIC PRESS	.92028	.91941	.92106	.92817	.93975	.96252
DENSITY	.94217	.94153	.94274	.94796	.95642	.97298
DELTA T	0.00000	0.00000	0.00000	0.00000	0.00000	0.00000
WORK COEF = 2*CP*DELT/U**2	0.00000	0.00000	0.00000	0.00000	0.00000	0.00000
FLOW COEF = VM/U	.30205	.31812	.33979	.38027	.44629	.66978
R BAR	2.30765	2.20023	2.03528	1.73713	1.37703	.82130
D-FACTOR	-.55606	-.51109	-.43545	-.31349	-.20120	-.01965
VM2/VM1	1.55606	1.51109	1.43545	1.31349	1.20120	1.01965
DELP/Q	-1.37969	-1.24535	-1.02971	-.70610	-.43310	-.03915
TANG BLADE FORCE LB/IN	0.00000	0.00000	0.00000	0.00000	0.00000	0.00000
AXIAL BLADE FORCE LB/IN	-1.68566	-.97244	-.29188	.44067	.70291	.58296
VEL HEAD 2	.07972	.08059	.07894	.07183	.06025	.03748
Q=E**(-S/CP)	1.00000	1.00000	1.00000	1.00000	1.00000	1.00000
RVU/	0.00000	0.00000	0.00000	0.00000	0.00000	0.00000
DRVU/DM	-0.00000	-0.00000	-0.00000	-0.00000	-0.00000	-0.00000
STRMLN DIST M	-1.03627	-1.05043	-1.06865	-1.08596	-1.07344	-.94609

STATION .06000 STATOR XI = 0.00000

P = -0. ZTIP = -.92500 AR = 4.00000 γN = -0. BNXT = -0.
= -0. ZHUB = -.92500 LOSS = 1. EXP = .8000 BLADES = -0.

RADIUS					
1.86100	1.79800	1.66500	1.41200	1.11200	.52900
SLOPE					
-15.26000	-13.30000	-10.80000	-7.10000	-3.50000	-4.23000
CURVATURE					
.64400	.55000	.55000	.50000	.55000	.67400
LOSS COEFF					
-0.00000	-0.00000	-0.00000	-0.00000	-0.00000	-0.00000
SOLIDITY					
1.00000	1.00000	1.00000	1.00000	1.00000	1.00000
AERO BLOCKAGE					
.99200	.99200	.99200	.99200	.99200	.99200
TOTAL BLOCKAGE					
.99200	.99200	.99200	.99200	.99200	.99200
BLADE ANGLE					
-0.00000	-0.00000	-0.00000	-0.00000	-0.00000	-0.00000
LEAN					
-0.00000	-0.00000	-0.00000	-0.00000	-0.00000	-0.00000
Y					
-0.00000	-0.00000	-0.00000	-0.00000	-0.00000	-0.00000

MINOR ITERS = 1 AREA RATIO = 1.00050 EXP = .80000 CHOKE = .59568

DIUS					
1.86100	1.78713	1.66710	1.43122	1.11439	.52900
Z					
-.92500	-.92500	-.92500	-.92500	-.92500	-.92500
CROSS PASSAGE DIST P					
1.33200	1.25813	1.13810	.90222	.58539	0.00000
SLOPE					
-15.26000	-13.52046	-11.27682	-7.75818	-4.38250	-4.23000
CURVATURE					
.64400	.58437	.55928	.51867	.52899	.67400
DELTA CURVATURE					
0.00000	.00092	.00015	.00019	-.00080	0.00000
VM					
525.71339	507.87795	480.81325	429.94544	368.21261	253.36926
VU2					
0.00000	0.00000	0.00000	0.00000	0.00000	0.00000
U					
1135.21000	1090.14947	1016.93365	873.04370	679.77695	322.69000
VR					
-138.36761	-118.73817	-94.02279	-58.03937	-28.13678	-18.68862
BETA2					
0.00000	0.00000	0.00000	0.00000	0.00000	0.00000
BETA2*					
0.00000	0.00000	0.00000	0.00000	0.00000	0.00000

INCIDENCE	0.00000	0.00000	0.00000	0.00000	0.00000	0.00000
	.48249	.46541	.43963	.39163	.33405	.22854
V2	525.71339	507.87795	480.81325	429.94544	368.21261	253.36926
TOTAL TEMP	1.00000	1.00000	1.00000	1.00000	1.00000	1.00000
TOTAL PRESS	1.00000	1.00000	1.00000	1.00000	1.00000	1.00000
EFFICIENCY	0.00000	0.00000	0.00000	0.00000	0.00000	0.00000
STATIC TEMP	.95608	.95901	.96326	.97062	.97845	.98980
STATIC PRESS	.85323	.86251	.87610	.89999	.92591	.96441
DENSITY	.89243	.89938	.90952	.92723	.94631	.97435
DELTA T	0.00000	0.00000	0.00000	0.00000	0.00000	0.00000
WORK COEF = 2*CP*DELT/U**2	0.00000	0.00000	0.00000	0.00000	0.00000	0.00000
FLOW COEF = VM/U	.46310	.46588	.47281	.49247	.54167	.78518
R BAR	1.96815	1.88434	1.75130	1.49678	1.16549	.58280
D-FACTOR	-.37488	-.32080	-.26381	-.18634	-.11175	.02585
VM2/VM1	1.37488	1.32080	1.26381	1.18634	1.11175	.97415
DELP/Q	-.84101	-.70598	-.56947	-.39223	-.22953	.05037
TANG BLADE FORCE LB/IN	0.00000	0.00000	0.00000	0.00000	0.00000	0.00000
AXIAL BLADE FORCE LB/IN	2.01929	1.82111	1.55149	1.01093	.55108	.21490
VEL HEAD 2	.14677	.13749	.12390	.10001	.07409	.03559
Q=E**(-S/CP)	1.00000	1.00000	1.00000	1.00000	1.00000	1.00000
RVU/	0.00000	0.00000	0.00000	0.00000	0.00000	0.00000
DRVU/DM	-0.00000	-0.00000	-0.00000	-0.00000	-0.00000	-0.00000
STRMLN DIST M	-.49087	-.51270	-.53990	-.56799	-.56199	-.43312

```
STATION          .07000  STATOR   XI =      0.00000

P =  -0.  ZTIP =    -.42500   AR =   4.00000    XN =  -0.     BNXT =  -0.
  =  -0.  ZHUB =    -.42500   LOSS =   1.  EXP =   1.5000  BLADES =  -0.

RADIUS
    1.81450      1.74500      1.64060      1.43400      1.14900       .60000
SLOPE
    4.49000      2.87000      4.37000      7.31000     10.15000     20.18000
CURVATURE
     .70287       .60400       .56000       .60000       .75000       .80000
LOSS COEFF
   -0.00000     -0.00000     -0.00000     -0.00000     -0.00000     -0.00000
SOLIDITY
    1.00000      1.00000      1.00000      1.00000      1.00000      1.00000
AERO BLOCKAGE
     .99100       .99100       .99100       .99100       .99100       .99100
TOTAL BLOCKAGE
     .99100       .99100       .99100       .99100       .99100       .99100
BLADE ANGLE
   -0.00000     -0.00000     -0.00000     -0.00000     -0.00000     -0.00000
LEAN
   -0.00000     -0.00000     -0.00000     -0.00000     -0.00000     -0.00000
Y
   -0.00000     -0.00000     -0.00000     -0.00000     -0.00000     -0.00000

MINOR ITERS =  1  AREA RATIO = 1.00028  EXP = 1.50000  CHOKE =  .65051

  DIUS
    1.81450      1.75004      1.64433      1.43403      1.14673       .60000
Z
    -.42500      -.42500      -.42500      -.42500      -.42500      -.42500
CROSS PASSAGE DIST P
    1.21450      1.15004      1.04433       .83403       .54673      0.00000
SLOPE
    4.49000      4.64561      5.93979      8.54635     11.81866     20.18000
CURVATURE
     .70287       .67334       .64514       .63737       .69777       .80000
DELTA CURVATURE
    0.00000       .00144       .00096      -.00062      -.00154      0.00000
VM
  633.45865    605.67597    563.88868    490.16335    401.62704    264.40266
VU2
    0.00000      0.00000      0.00000      0.00000      0.00000      0.00000
U
 1106.84500   1067.52709   1003.04067    874.75960    699.50432    366.00000
VR
   49.59039     49.05518     58.35309     72.84291     82.25918     91.21118
BETA2
    0.00000      0.00000      0.00000      0.00000      0.00000      0.00000
BETA2*
    0.00000      0.00000      0.00000      0.00000      0.00000      0.00000
```

INCIDENCE	0.00000	0.00000	0.00000	0.00000	0.00000	0.00000
	.58751	.56010	.51932	.44852	.36513	.23860
V2	633.45865	605.67597	563.88868	490.16335	401.62704	264.40266
TOTAL TEMP	1.00000	1.00000	1.00000	1.00000	1.00000	1.00000
TOTAL PRESS	1.00000	1.00000	1.00000	1.00000	1.00000	1.00000
EFFICIENCY	0.00000	0.00000	0.00000	0.00000	0.00000	0.00000
STATIC TEMP	.93623	.94170	.94946	.96182	.97436	.98889
STATIC PRESS	.79227	.80875	.83257	.87147	.91232	.96129
DENSITY	.84624	.85882	.87688	.90607	.93632	.97209
DELTA T	0.00000	0.00000	0.00000	0.00000	0.00000	0.00000
WORK COEF = 2*CP*DELT/U**2	0.00000	0.00000	0.00000	0.00000	0.00000	0.00000
FLOW COEF = VM/U	.57231	.56736	.56218	.56034	.57416	.72241
R BAR	1.83775	1.76859	1.65572	1.43263	1.13056	.56450
D-FACTOR	-.20495	-.19256	-.17278	-.14006	-.09075	-.04355
VM2/VM1	1.20495	1.19256	1.17278	1.14006	1.09075	1.04355
DELP/Q	-.41540	-.39100	-.35135	-.28520	-.18355	-.08773
TANG BLADE FORCE LB/IN	0.00000	0.00000	0.00000	0.00000	0.00000	0.00000
AXIAL BLADE FORCE LB/IN	1.45106	.96504	.39911	-.16793	-.34909	-.22459
VEL HEAD 2	.20773	.19125	.16743	.12853	.08768	.03871
Q=E**(-S/CP)	1.00000	1.00000	1.00000	1.00000	1.00000	1.00000
RVU/	0.00000	0.00000	0.00000	0.00000	0.00000	0.00000
DRVU/DM	-0.00000	-0.00000	-0.00000	-0.00000	-0.00000	-0.00000
STRMLN DIST M	.01379	-.00922	-.03749	-.06629	-.05927	.07574

```
STATION        1.00000  ROTOR     XI =       0.00000

P =    1.   ZTIP =    0.00000   AR =    3.40000     XN =    0.      BNXT =    1.
  =    0.   ZHUB =    0.00000   LOSS =    3.   EXP =  -0.0000   BLADES =    1.

RADIUS
     1.91300      1.84000      1.74000      1.56000      1.33000       .86450
SLOPE
    20.33000     21.10000     22.23000     28.53000     35.00000     42.53000
CURVATURE
      .49296       .28700       .28600       .52900       .59900       .56700
LOSS COEFF
     1.00000      1.00000      1.00000      1.00000      1.00000      1.00000
SOLIDITY
     1.00000      1.00000      1.00000      1.00000      1.00000      1.00000
BLADE THICKNESS
      .01174       .01201       .01255       .01432       .01835       .02630
AERO BLOCKAGE
      .98000       .98000       .98000       .98000       .98000       .98000
TOTAL BLOCKAGE
      .97904       .97898       .97887       .97857       .97785       .97525
BLADE ANGLE
    59.26314     58.35051     57.17567     56.57143     57.55473     56.48617
LEAN
      .94632      2.23809      3.55011      4.35245      2.60429      5.91810
Y
     0.00000      0.00000      0.00000      0.00000      0.00000      0.00000

   NOR ITERS =  1   AREA RATIO = 1.00082  EXP = 1.50000  CHOKE =   .74162

RADIUS
     1.91300      1.85028      1.75006      1.56071      1.31442       .86450
Z
     0.00000      0.00000      0.00000      0.00000      0.00000      0.00000
CROSS PASSAGE DIST P
     1.04850       .98578       .88556       .69621       .44992      0.00000
SLOPE
    20.33000     20.24422     20.64932     24.97660     31.49755     42.53000
CURVATURE
      .49296       .40247       .34868       .44057       .55846       .56700
DELTA CURVATURE
     0.00000       .00351       .00671       .00603       .00303      0.00000
VM
   675.36652    656.86940    636.21722    592.00793    498.98170    371.73075
VU2
  1166.93000   1128.66885   1067.53566    952.03020    801.79782    527.34500
U
  1166.93000   1128.66885   1067.53566    952.03020    801.79782    527.34500
VR
   234.64044    227.29167    224.36034    249.97430    260.69912    251.28121
BETA2
    59.93965     59.80117     59.20638     58.12508     58.10479     54.81959
BETA2*
    61.51117     61.36391     60.85240     60.59075     62.04793     62.54969
```

INCIDENCE	2.22555	2.76422	3.29834	3.55899	4.27953	5.03112
	1.25633	1.21428	1.15293	1.03531	.86477	.58546
V2	1348.27503	1305.89846	1242.74081	1121.08648	944.38471	645.19493
TOTAL TEMP	1.00000	1.00000	1.00000	1.00000	1.00000	1.00000
TOTAL PRESS	1.00000	1.00000	1.00000	1.00000	1.00000	1.00000
EFFICIENCY	0.00000	0.00000	0.00000	0.00000	0.00000	0.00000
STATIC TEMP	.92751	.93143	.93567	.94430	.96043	.97804
STATIC PRESS	.76651	.77800	.79060	.81667	.86704	.92453
DENSITY	.82641	.83528	.84496	.86485	.90276	.94529
SUCT SURF VEL	0.00000	0.00000	0.00000	0.00000	0.00000	0.00000
PRESS SURF VEL	0.00000	0.00000	0.00000	0.00000	0.00000	0.00000
DELTA T	0.00000	0.00000	0.00000	0.00000	0.00000	0.00000
WORK COEF = 2*CP*DELT/U**2	0.00000	0.00000	0.00000	0.00000	0.00000	0.00000
FLOW COEF = VM/U	.57875	.58199	.59597	.62184	.62233	.70491
R BAR	1.86375	1.80016	1.69719	1.49737	1.23058	.73225
D-FACTOR	-1.12843	-1.15610	-1.20388	-1.28717	-1.35140	-1.44020
VM2/VM1	1.06616	1.08452	1.12827	1.20778	1.24240	1.40593
DELP/Q	-.12401	-.16076	-.25064	-.42636	-.51634	-.94954
TANG BLADE FORCE LB/IN	0.00000	0.00000	0.00000	0.00000	0.00000	0.00000
AXIAL BLADE FORCE LB/IN	-4.26027	-3.95459	-3.70427	-4.14983	-3.71917	-2.05651
VEL HEAD 2	.61641	.59445	.56096	.49239	.38518	.20649
Q=E**(-S/CP)	1.00000	1.00000	1.00000	1.00000	1.00000	1.00000
RVU/	0.00000	0.00000	0.00000	0.00000	0.00000	0.00000
DRVU/DM	1.53101	1.98077	2.38156	2.92120	3.00299	2.46391
STRMLN DIST M	.45144	.42879	.40167	.37871	.39987	.57951

STATION 1.20000 ROTOR XI = .81762

P = 1. ZTIP = .08600 AR = 10.00000 XN = 0. BNXT = 1.
= 0. ZHUB = .10000 LOSS = 3. EXP = -0.0000 BLADES = 20.

RADIUS	1.94700	1.87700	1.77800	1.59700	1.35500	.96600
SLOPE	23.00000	26.00000	27.00000	32.00000	36.00000	46.40000
CURVATURE	.48400	.41000	.39000	.37000	.35000	.39900
LOSS COEFF	.99760	.99715	.99848	.99915	.99949	.99937
SOLIDITY	1.00000	1.00000	1.00000	1.00000	1.00000	1.00000
BLADE THICKNESS	.03884	.04130	.04638	.05614	.07071	.05472
AERO BLOCKAGE	.97800	.97800	.97800	.97800	.97800	.97800
TOTAL BLOCKAGE	.91590	.90950	.89679	.86857	.81556	.80167
BLADE ANGLE	59.17886	58.35729	57.22589	56.37186	55.95303	48.13260
LEAN	.46646	1.15476	1.77076	.16200	-2.88071	.34465
Y	-.17150	-.22400	-.27580	-.36000	-.41000	-.45000

VOR ITERS = 2 AREA RATIO = 1.00053 EXP = 1.50000 CHOKE = .79880

RADIUS	1.94700	1.88408	1.78557	1.60363	1.37143	.96600
Z	.08600	.08690	.08830	.09090	.09421	.10000
CROSS PASSAGE DIST P	.98110	.91817	.81966	.63770	.40547	0.00000
SLOPE	23.00000	24.30210	25.51653	28.96800	33.38571	46.40000
CURVATURE	.48400	.50565	.58653	.49929	.31142	.39900
DELTA CURVATURE	0.00000	.00190	.00361	.00206	-.00194	0.00000
VM	679.10299	682.26624	682.41207	657.34676	574.68693	329.97218
VU2	1133.93862	1076.76211	994.97995	841.27789	654.20934	304.86549
U	1187.67000	1149.28576	1089.20059	978.21685	836.57348	589.26000
VR	265.34678	280.78528	293.96380	318.36697	316.23456	238.95664
BETA2	59.08306	57.64050	55.55550	51.99708	48.70245	42.73522
BETA2*	61.13291	59.99437	58.24423	55.64306	53.74036	53.26189

INCIDENCE	1.97828	1.48051	.73095	-.81329	-1.72876	5.00144
	1.21917	1.17261	1.10666	.97234	.78509	.39858
V2	1321.74039	1274.71717	1206.51205	1067.63910	870.77834	449.24894
TOTAL TEMP	1.02028	1.02649	1.03262	1.04258	1.04849	1.05327
TOTAL PRESS	1.06446	1.08580	1.11411	1.15527	1.18001	1.19860
EFFICIENCY	.87928	.88958	.95188	.97919	.98897	.98754
STATIC TEMP	.94653	.95168	.95720	.97092	.99072	1.02307
STATIC PRESS	.81655	.83102	.85219	.89828	.96584	1.08150
DENSITY	.86267	.87322	.89029	.92518	.97489	1.05712
SUCT SURF VEL	1474.02201	1447.33108	1390.36306	1258.98112	1050.77412	597.63334
PRESS SURF VEL	1169.45877	1102.10325	1022.66104	876.29708	690.78256	300.86454
DELTA T	10.52123	13.74201	16.91985	22.08538	25.15279	27.62936
WORK COEF = 2*CP*DELT/U**2	.09048	.12621	.17301	.27998	.43598	.96526
FLOW COEF = VM/U	.57179	.59364	.62653	.67198	.68695	.55998
R BAR	1.93000	1.86718	1.76782	1.58217	1.34293	.91525
D-FACTOR	.03978	.05190	.06744	.10958	.17654	.53632
VM2/VM1	1.00553	1.03866	1.07261	1.11037	1.15172	.88766
DELP/Q	.04063	.04649	.06096	.10302	.18189	.65245
TANG BLADE FORCE LB/IN	5.27018	6.77611	8.15294	9.77808	9.03406	5.62317
AXIAL BLADE FORCE LB/IN	8.12354	9.65081	11.80633	14.62866	14.88641	12.39769
VEL HEAD 2	.59704	.57188	.53464	.45366	.33344	.10335
Q=E**(-S/CP)	.99760	.99715	.99848	.99915	.99949	.99937
RVU/	.17150	.22400	.27580	.36000	.41000	.45037
DRVU/DM	3.30292	3.61985	3.70066	3.65233	3.41331	2.57688
STRMLN DIST M	.54392	.52203	.49685	.47924	.50999	.72200

```
STATION        1.40000  ROTOR    XI =       1.76046

P =     1.   ZTIP =     .17200   AR =    9.00000    XN =    0.     BNXT =   1.
  =     0.   ZHUB =     .20000   LOSS =    3.   EXP =   -0.0000  BLADES =  20.

RADIUS
   1.98500      1.91700      1.82500      1.65300      1.42500      1.07400
SLOPE
  25.56000     29.00000     33.00000     36.00000     42.00000     49.25000
CURVATURE
    .47100       .41000       .45000       .39000       .32000       .27400
LOSS COEFF
    .99155       .99147       .99612       .99793       .99900       .99877
SOLIDITY
   1.00000      1.00000      1.00000      1.00000      1.00000      1.00000
BLADE THICKNESS
    .05372       .06013       .06590       .07658       .08744       .07592
AERO BLOCKAGE
    .97600       .97600       .97600       .97600       .97600       .97600
TOTAL BLOCKAGE
    .89193       .87855       .86381       .83207       .78537       .75640
BLADE ANGLE
  59.07060     58.30032     57.19764     55.91262     53.52590     38.79420
LEAN
    .34847       .25606       .10707     -1.86332     -3.57562      -.34511
Y
   -.62050      -.69020      -.72360      -.75000      -.76000      -.74000

  NOR ITERS =  2  AREA RATIO = 1.00097  EXP = 1.50000  CHOKE =  .80065

RADIUS
   1.98500      1.92408      1.82947      1.65489      1.43316      1.07400
Z
    .17200       .17387       .17678       .18215       .18896       .20000
CROSS PASSAGE DIST P
    .91143       .85048       .75583       .58116       .35933      0.00000
SLOPE
  25.56000     27.50226     30.56697     33.64937     37.53989     49.25000
CURVATURE
    .47100       .38531       .40496       .47264       .45323       .27400
DELTA CURVATURE
   0.00000       .00219       .00224       .00283       .00243      0.00000
VM
 622.95147    643.54557    665.15009    652.40416    599.14774    450.69835
VU2
1020.16738    954.86873    874.70747    733.02958    550.75036    234.34766
U
1210.85000   1173.68647   1115.97723   1009.48298    874.23033    655.14000
VR
 268.77629    297.17890    338.25900    361.50323    365.06904    341.43339
BETA2
  58.59021     56.02149     52.74968     48.33055     42.58992     27.47287
BETA2*
  61.15066     59.12901     56.78507     53.46582     49.21866     38.53960
```

INCIDENCE						
	2.13580	.74484	-.50880	-2.16403	-3.50747	-.00879
	1.06951	1.02913	.98318	.87672	.72447	.44981
V2						
	1195.32841	1151.48825	1098.88025	981.30706	813.82060	507.98408
TOTAL TEMP						
	1.07339	1.08163	1.08558	1.08871	1.08989	1.08763
TOTAL PRESS						
	1.24641	1.28020	1.31842	1.34044	1.35070	1.33973
EFFICIENCY						
	.87641	.88698	.95078	.97459	.98788	.98473
STATIC TEMP						
	1.00594	1.00820	1.00602	1.00891	1.01621	1.02710
STATIC PRESS						
	.99097	.99860	1.00749	1.02433	1.05472	1.09432
DENSITY						
	.98512	.99047	1.00147	1.01528	1.03790	1.06545
SUCT SURF VEL						
	1435.74494	1395.25521	1326.97959	1173.23247	974.75540	633.81377
PRESS SURF VEL						
	954.91189	907.72129	870.78090	789.38166	652.88581	382.15439
DELTA T						
	27.54538	28.60057	27.47176	23.92583	21.47190	17.82176
WORK COEF = 2*CP*DELT/U**2						
	.22791	.25186	.26759	.28481	.34081	.50370
FLOW COEF = VM/U						
	.51447	.54831	.59602	.64628	.68534	.68794
R BAR						
	1.96600	1.90408	1.80752	1.62926	1.40230	1.02000
D-FACTOR						
	.14834	.15525	.15184	.14925	.15283	.06262
VM2/VM1						
	.91732	.94325	.97470	.99248	1.04256	1.36587
DELP/Q						
	.14417	.15096	.15863	.16899	.18395	.10285
TANG BLADE FORCE LB/IN						
	13.96201	14.45875	13.69554	11.09546	8.36079	3.89658
AXIAL BLADE FORCE LB/IN						
	25.33687	24.52577	22.01105	16.52824	11.24311	2.69990
VEL HEAD 2						
	.51288	.48865	.46041	.39289	.29409	.12921
Q=E**(-S/CP)						
	.99155	.99147	.99612	.99793	.99900	.99877
RVU/						
	.62050	.69020	.72360	.75000	.76000	.74087
DRVU/DM						
	5.26826	5.05612	4.44283	3.53191	2.83097	1.90756
STRMLN DIST M						
	.63794	.61776	.59562	.58390	.62307	.86918

```
STATION        1.60000  ROTOR    XI =        2.88642

F =      1.   ZTIP =     .25800   AR =    8.50000     XN =    0.     BNXT =    1.
  =      0.   ZHUB =     .30000   LOSS =    3.   EXP =  -0.0000   BLADES =  20.

RADIUS
    2.02800     1.96200     1.87500     1.71300     1.50000     1.19500
SLOPE
   28.05000    30.00000    33.00000    37.00000    44.00000    51.17000
CURVATURE
 -   .43850      .38000      .40000      .37000      .30000      .16800
LOSS COEFF
     .98453      .98554      .99389      .99681      .99852      .99818
SOLIDITY
    1.00000     1.00000     1.00000     1.00000     1.00000     1.00000
BLADE THICKNESS
     .05866      .06151      .06646      .07406      .07946      .07774
AERO BLOCKAGE
     .97400      .97400      .97400      .97400      .97400      .97400
TOTAL BLOCKAGE
     .88431      .87680      .86411      .83997      .80977      .77230
BLADE ANGLE
   58.76147    58.10414    56.97868    54.73916    50.63974    28.24758
LEAN
     .17521      .22499     -.35545    -1.59983    -2.23997     3.66601
Y
   -1.17550    -1.20720    -1.16840    -1.11500    -1.06500    -1.03000

  VOR ITERS =  1   AREA RATIO =   .99921  EXP = 1.50000  CHOKE =   .76550

RADIUS
    2.02800     1.97022     1.88049     1.71516     1.50516     1.19500
Z
     .25800      .26091      .26544      .27377      .28436      .30000
CROSS PASSAGE DIST P
     .83406      .77621      .68636      .52083      .31056     0.00000
SLOPE
   28.05000    29.32366    31.36749    35.38910    40.82717    51.17000
CURVATURE
     .43850      .39979      .32942      .25764      .30264      .16800
DELTA CURVATURE
    0.00000      .00107     -.00013      .00136      .00419     0.00000
VM
  582.55347   592.07595   610.76159   594.97936   576.57891   553.41793
VU2
  883.50258   828.07518   768.08661   649.69959   486.53656   203.56435
U
 1237.08000  1201.83595  1147.09697  1046.25044   918.15046   728.95000
VR
  273.94116   289.96491   317.91694   344.56821   376.95563   431.11810
BETA2
   56.60039    54.43511    51.50921    47.51727    40.15877    20.19509
BETA2*
   59.80412    58.06109    55.82523    53.25587    48.11667    30.39765
```

INCIDENCE	1.07353	-.17743	-1.23243	-1.18776	-1.85675	-.95057
	.92016	.88526	.85693	.77130	.66275	.52159
V2	1058.27471	1017.96976	981.31889	880.97105	754.42763	589.66927
TOTAL TEMP	1.13903	1.14278	1.13819	1.13188	1.12596	1.12173
TOTAL PRESS	1.49916	1.52218	1.54610	1.53180	1.51284	1.49106
EFFICIENCY	.87326	.88427	.94968	.97262	.98677	.98323
STATIC TEMP	1.06523	1.06487	1.05608	1.05062	1.04352	1.02928
STATIC PRESS	1.18316	1.18604	1.18666	1.17729	1.15639	1.10025
DENSITY	1.11071	1.11379	1.12365	1.12056	1.10816	1.06895
SUCT SURF VEL	1305.99580	1247.92872	1177.64426	1047.41850	903.33513	719.57768
PRESS SURF VEL	810.55363	788.01081	784.99352	714.52361	605.52013	459.76085
DELTA T	34.04829	31.71706	27.28771	22.39212	18.71122	17.69092
WORK COEF = 2*CP*DELT/U**2	.26989	.26637	.25157	.24815	.26925	.40387
FLOW COEF = VM/U	.47091	.49264	.53244	.56868	.62798	.75920
R BAR	2.00650	1.94715	1.85498	1.68503	1.46916	1.13450
D-FACTOR	.18524	.18628	.17354	.16957	.15078	-.00819
VM2/VM1	.93515	.92002	.91823	.91198	.96233	1.22791
DELP/Q	.18421	.19642	.20841	.23074	.23137	.03650
TANG BLADE FORCE LB/IN	17.77488	16.73405	14.52202	10.91417	7.79031	5.03029
AXIAL BLADE FORCE LB/IN	30.54475	28.03795	25.58445	18.99156	11.39760	2.33108
VEL HEAD 2	.42074	.39839	.38011	.32447	.25454	.16873
Q=E**(-S/CP)	.98453	.98554	.99389	.99681	.99852	.99818
RVU/	1.17550	1.20720	1.16840	1.11500	1.06500	1.02924
DRVU/DM	5.17283	4.58244	3.70900	2.98142	2.44438	1.81881
STRMLN DIST M	.73409	.71627	.69790	.69357	.74259	1.02616

STATION 1.80000 ROTOR XI = 4.24198

P = I. ZTIP = .34400 AR = 8.00000 XN = 0. BNXT = 1.
= 0. ZHUB = .40000 LOSS = 3. EXP = -0.0000 BLADES = 20.

RADIUS					
2.07600	2.01400	1.93500	1.78400	1.58700	1.32100
SLOPE					
30.36000	33.00000	35.00000	39.00000	46.00000	52.22000
CURVATURE					
.39500	.36000	.39000	.37000	.28000	.10420
LOSS COEFF					
.97917	.98124	.99235	.99604	.99806	.99761
SOLIDITY					
1.00000	1.00000	1.00000	1.00000	1.00000	1.00000
BLADE THICKNESS					
.04829	.04956	.05155	.05429	.05278	.04982
AERO BLOCKAGE					
.97200	.97200	.97200	.97200	.97200	.97200
TOTAL BLOCKAGE					
.90004	.89586	.88958	.87784	.86911	.85531
BLADE ANGLE					
57.80893	57.40181	56.47022	53.50556	46.75384	15.13302
LEAN					
-1.03805	-.52280	-.31771	-.54264	1.58310	9.81008
Y					
-1.62450	-1.60210	-1.48920	-1.41300	-1.36000	-1.31900

VOR ITERS = 1 AREA RATIO = .99980 EXP = 1.50000 CHOKE = .72113

RADIUS					
2.07600	2.02196	1.93658	1.78181	1.58784	1.32100
Z					
.34400	.34801	.35434	.36582	.38021	.40000
CROSS PASSAGE DIST P					
.75707	.70288	.61727	.46208	.26758	0.00000
SLOPE					
30.36000	32.20885	33.65790	37.22678	43.60244	52.22000
CURVATURE					
.39500	.39718	.46160	.41899	.34295	.10420
DELTA CURVATURE					
0.00000	.00151	.00160	.00074	.00242	0.00000
VM					
569.05498	560.62979	573.51394	552.09384	534.22265	556.09083
VU2					
789.02618	750.06049	712.23189	603.16532	446.11491	196.82175
U					
1266.36000	1233.39444	1181.31282	1086.90387	968.58454	805.81000
VR					
287.61842	298.81973	317.86045	334.00108	368.42700	439.51704
BETA2					
54.20039	53.22384	51.15775	47.53125	39.86433	19.49080
BETA2*					
58.10558	57.68981	56.16815	53.91441	49.06945	30.01650

```
INCIDENCE
     .49658       .34722      -.27445       .63285      1.56243      2.66848

     .83070       .80036       .78640       .70561       .60321       .51713
V2
  972.82367    936.42752    914.43562    817.68944    695.99738    589.89475
TOTAL TEMP
    1.19214      1.18949      1.17614      1.16712      1.16086      1.15598
TOTAL PRESS
    1.72744      1.72675      1.72656      1.70245      1.68236      1.65490
EFFICIENCY
     .87076       .88224       .94892       .97234       .98600       .98229
STATIC TEMP
    1.10446      1.10241      1.08889      1.08149      1.07211      1.04792
STATIC PRESS
    1.31878      1.31995      1.31493      1.30057      1.27022      1.16991
DENSITY
    1.19405      1.19734      1.20758      1.20257      1.18478      1.11642
SUCT SURF VEL
 1136.09084   1077.71637   1028.70432    926.84144    807.70420    696.69691
PRESS SURF VEL
  809.55650    795.13868    800.16692    708.53743    584.29056    483.09260
DELTA T
   27.54538     24.22643     19.68053     18.28179     18.09774     17.76461
WORK COEF = 2*CP*DELT/U**2
     .20836       .19318       .17108       .18773       .23401       .33188
FLOW COEF = VM/U
     .44936       .45454       .48549       .50795       .55155       .69010
R BAR
    2.05200      1.99609      1.90853      1.74849      1.54650      1.25800
D-FACTOR
     .14381       .13938       .12040       .13084       .15457       .11868
VM2/VM1
     .97683       .94689       .93901       .92792       .92654      1.00483
DELP/Q
     .15781       .17051       .17628       .21801       .28829       .31195
TANG BLADE FORCE LB/IN
   15.25267     13.19168     10.87085      9.25958      7.99653      6.36669
AXIAL BLADE FORCE LB/IN
   23.00964     20.06602     17.88906     15.82280     12.83092      7.79054
VEL HEAD 2
     .36310       .34338       .33429       .28192       .21733       .16617
Q=E**(-S/CP)
     .97917       .98124       .99235       .99604       .99806       .99761
RVU/
    1.62450      1.60210      1.48920      1.41300      1.36000      1.31881
DRVU/DM
    3.14583      2.67227      2.07773      1.86961      1.70276      1.34754
STRMLN DIST M
     .83258       .81758       .80302       .80721       .86917      1.18702
```

Rotor 1A Exit

```
STATION         2.00000  ROTOR    XI =       5.91192

P =     1.  ZTIP =     .43000   AR =    7.50000    XN =    0.     BNXT =    1.
  =     0.  ZHUB =     .50000   LOSS =     3.  EXP =  -0.0000  BLADES =    1.

RADIUS
    2.13000      2.08300      2.00700      1.86700      1.69200      1.45400
SLOPE
   32.54000     34.10000     36.20000     40.10000     45.50000     53.40000
CURVATURE
     .35550       .27500       .28400       .23900       .19200       .10670
LOSS COEFF
     .97719       .97969       .99180       .99577       .99761       .99706
SOLIDITY
    1.00000      1.00000      1.00000      1.00000      1.00000      1.00000
BLADE THICKNESS
     .01230       .01242       .01269       .01315       .01254       .01237
AERO BLOCKAGE
     .96900       .96900       .96900       .96900       .96900       .96900
TOTAL BLOCKAGE
     .96811       .96808       .96803       .96791       .96786       .96769
BLADE ANGLE
   56.26243     56.19262     55.43665     51.94140     40.38929     -4.48826
LEAN
   -5.07140     -3.45422     -1.09982      2.06675      9.18285     21.12723
Y
   -1.79600     -1.74920     -1.60560     -1.54170     -1.49950     -1.46470

  NOR ITERS =  1   AREA RATIO = 1.00052  EXP = 1.50000  CHOKE =   .67449

RADIUS
    2.13000      2.07962      1.99985      1.85675      1.68272      1.45400
Z
     .43000       .43522       .44348       .45829       .47632       .50000
CROSS PASSAGE DIST P
     .67961       .62896       .54877       .40491       .22994      0.00000
SLOPE
   32.54000     34.37235     36.54114     40.38325     46.03186     53.40000
CURVATURE
     .35550       .32311       .37959       .39267       .30595       .10670
DELTA CURVATURE
    0.00000       .00081       .00157       .00232       .00173      0.00000
VM
  533.75767    520.44278    531.17269    513.16549    494.64680    492.21442
VU2
  784.95258    755.48596    730.16081    626.12523    482.87482    272.26824
U
 1299.30000   1268.56680   1219.90639   1132.62029   1026.45714    886.94000
VR
  287.10210    293.82584    316.26026    332.47861    356.01024    395.15846
BETA2
   55.78478     55.43761     53.96508     50.66230     44.31002     28.94915
BETA2*
   60.17691     60.37760     59.69481     58.02329     54.58017     42.85372
```

INCIDENCE	5.25179	5.27168	4.90401	5.94908	9.70528	14.19160
' -	.80309	.77722	.77015	.69277	.59376	.48693
V2	949.23538	917.39834	902.92814	809.55026	691.26229	562.49892
TOTAL TEMP	1.21242	1.20689	1.18990	1.18235	1.17735	1.17329
TOTAL PRESS	1.82049	1.80754	1.79552	1.78050	1.76557	1.74073
EFFICIENCY	.86981	.88152	.94862	.97257	.98413	.98009
STATIC TEMP	1.12510	1.12200	1.10694	1.09972	1.09151	1.07469
STATIC PRESS	1.39790	1.39690	1.39086	1.37839	1.35113	1.27649
DENSITY	1.24247	1.24501	1.25649	1.25339	1.23786	1.18778
SUCT SURF VEL	0.00000	0.00000	1804.31950	0.00000	0.00000	0.00000
PRESS SURF VEL	0.00000	0.00000	1.53678	0.00000	0.00000	0.00000
DELTA T	10.52123	9.02433	7.14094	7.89552	8.55808	8.97689
WORK COEF = 2*CP*DELT/U**2	.07560	.06803	.05821	.07466	.09853	.13843
FLOW COEF = VM/U	.41080	.41026	.43542	.45308	.48190	.55496
R BAR	2.10300	2.05079	1.96821	1.81928	1.63528	1.38750
D-FACTOR	.04981	.04368	.03231	.03634	.04419	.10097
VM2/VM1	.93797	.92832	.92617	.92949	.92592	.88513
DELP/Q	.10523	.11148	.11500	.15240	.22941	.45712
TANG BLADE FORCE LB/IN	6.31613	5.23518	4.17981	4.25519	4.07574	3.66045
AXIAL BLADE FORCE LB/IN	10.09841	9.16290	7.89000	8.22464	8.77219	10.91845
VEL HEAD 2	.34515	.32832	.32372	.27368	.21154	.14921
Q=E**(-S/CP)	.97719	.97969	.99180	.99577	.99761	.99706
RVU/	1.79600	1.74920	1.60560	1.54170	1.49950	1.46514
DRVU/DM	1.29161	1.06866	.80059	.79600	.73766	.59052
STRMLN DIST M	.93413	.92212	.91233	.92624	1.00422	1.35342

Rotor 1B Inlet

STATION 3.00000 ROTOR XI = 0.00000

P = 1. ZTIP = .70000 AR = 6.00000 XN = 0. BNXT = 1.
= -0. ZHUB = .70000 LOSS = 3. EXP = -0.0000 BLADES = 1.

RADIUS					
2.32000	2.27700	2.21070	2.08780	1.93780	1.73000
SLOPE					
36.59429	37.15283	38.57043	42.26202	47.34751	54.44440
CURVATURE					
.10760	.08914	.08409	.09035	.00719	-0.00000
LOSS COEFF					
.97791	.98049	.99034	.99548	.99711	.99811
SOLIDITY					
1.00000	1.00000	1.00000	1.00000	1.00000	1.00000
BLADE THICKNESS					
.01168	.01225	.01327	.01510	.01698	.01955
AERO BLOCKAGE					
.96100	.96100	.96100	.96100	.96100	.96100
TOTAL BLOCKAGE					
.96023	.96018	.96008	.95989	.95966	.95927
BLADE ANGLE					
59.33508	58.61771	58.23417	58.29549	58.27538	58.69649
LEAN					
-2.46299	-1.98986	-1.78518	-1.98243	-1.58136	-.02982
Y					
-1.79603	-1.74922	-1.60563	-1.54172	-1.49950	-1.46465

VOR ITERS = 1 AREA RATIO = 1.00017 EXP = 1.50000 CHOKE = .76461

RADIUS					
2.32000	2.27686	2.20915	2.08457	1.93523	1.73000
Z					
.70000	.70000	.70000	.70000	.70000	.70000
CROSS PASSAGE DIST P					
.59000	.54686	.47915	.35457	.20523	0.00000
SLOPE					
36.59429	37.31240	39.18222	43.04870	48.18286	54.44440
CURVATURE					
.10760	.00969	-.06598	-.11688	-.12324	-0.00000
DELTA CURVATURE					
0.00000	-.00224	-.00272	-.00178	.00006	0.00000
VM					
659.79561	655.37553	648.12690	625.72504	575.42108	487.70786
VU2					
942.96797	920.24467	904.22478	820.44093	707.83470	538.82859
U					
1415.20000	1388.88351	1347.57905	1271.58847	1180.48946	1055.30000
VR					
393.33391	397.26293	409.47944	427.13243	428.84802	396.77563
BETA2					
55.01946	54.54245	54.36792	52.66833	50.89123	47.85091
BETA2*					
60.67385	60.47176	60.94332	60.86737	61.54112	62.24107

INCIDENCE	1.99044	2.48105	3.42964	3.44488	4.26901	4.14459
	.98126	.96503	.95543	.88781	.78437	.62383
V2	1150.87742	1129.76428	1112.51559	1031.82127	912.21675	726.77039
TOTAL TEMP	1.21243	1.20689	1.18991	1.18235	1.17735	1.17324
TOTAL PRESS	1.82525	1.81277	1.78622	1.77868	1.76244	1.74697
EFFICIENCY	.87392	.88619	.93947	.97069	.98081	.98720
STATIC TEMP	1.10780	1.10372	1.09191	1.08777	1.08923	1.09304
STATIC PRESS	1.32686	1.32194	1.31836	1.32483	1.33881	1.36024
DENSITY	1.19775	1.19771	1.20739	1.21793	1.22913	1.24446
SUCT SURF VEL	0.00000	0.00000	0.00000	0.00000	0.00000	0.00000
PRESS SURF VEL	0.00000	0.00000	0.00000	0.00000	0.00000	0.00000
DELTA T	.00184	.00123	.00184	.00123	0.00000	-.02386
WORK COEF = 2*CP*DELT/U**2	.00001	.00001	.00001	.00001	0.00000	-.00026
FLOW COEF = VM/U	.46622	.47187	.48096	.49208	.48744	.46215
R BAR	2.22500	2.17824	2.10450	1.97066	1.80897	1.59200
D-FACTOR	-.21242	-.23148	-.23211	-.27456	-.31964	-.29191
VM2/VM1	1.23613	1.25927	1.22018	1.21934	1.16330	.99084
DELP/Q	-.09642	-.10978	-.10890	-.10311	-.03400	.37408
TANG BLADE FORCE LB/IN	.00107	.00069	.00103	.00063	0.00000	-.00819
AXIAL BLADE FORCE LB/IN	-4.24324	-3.69989	-5.14662	-3.03693	1.13279	11.75259
VEL HEAD 2	.45922	.44909	.44306	.40003	.33297	.23008
Q=E**(-S/CP)	.97791	.98049	.99034	.99548	.99711	.99811
RVU/	1.79603	1.74922	1.60563	1.54172	1.49950	1.46475
DRVU/DM	6.67514	6.57895	5.44380	5.44477	3.96447	3.91197
STRMLN DIST M	1.26428	1.25230	1.24340	1.25839	1.34156	1.69426

```
STATION       3.20000  ROTOR    XI =        .84563

P =    1.  ZTIP =     .75700   AR =    6.00000    XN =    0.     BNXT =   1.
  =   -0.  ZHUB =     .76500   LOSS =    3.   EXP =   -0.0000   BLADES =  40.

RADIUS
    2.36200     2.31930     2.25660     2.14210     2.00680     1.82000
SLOPE
   38.00376    38.12298    38.29803    41.82005    46.92217    53.25115
CURVATURE
     .15000      .34853      .09474     -.20976     -.15283     -.04800
LOSS COEFF
     .97496      .97768      .98929      .99506      .99688      .99782
SOLIDITY
    1.00000     1.00000     1.00000     1.00000     1.00000     1.00000
BLADE THICKNESS
     .02596      .02771      .03034      .03492      .03812      .04425
AERO BLOCKAGE
     .96100      .96100      .96100      .96100      .96100      .96100
TOTAL BLOCKAGE
     .89376      .88791      .87874      .86127      .84479      .81225
BLADE ANGLE
   59.21263    58.36701    57.40559    56.60486    54.75606    51.76280
LEAN
    -.96817    -1.37002    -2.15564    -3.59881    -3.25803    -2.45331
Y
   -2.37000    -2.32900    -2.10850    -2.10000    -1.97130    -2.04000

  NOR ITERS =  2   AREA RATIO = 1.00078   EXP = 1.50000   CHOKE =   .79636

RADIUS
    2.36200     2.32053     2.25643     2.14046     2.00462     1.82000
Z
     .75700      .75761      .75856      .76027      .76228      .76500
CROSS PASSAGE DIST P
     .54206      .50059      .43648      .32049      .18464     0.00000
SLOPE
   38.00376    37.61596    38.44405    41.92147    47.09760    53.25115
CURVATURE
     .15000      .22837     -.04398     -.27358     -.22420     -.04800
DELTA CURVATURE
    0.00000     -.00586     -.00910     -.00528     -.00463     0.00000
VM
  658.11611   669.15864   659.76570   677.55026   620.42896   568.25061
VU2
  828.75395   803.30054   806.41302   707.21106   622.95619   426.28117
U
 1440.82000  1415.52593  1376.42197  1305.68056  1222.81740  1110.20000
VR
  405.21092   408.43172   410.20956   452.67926   454.47331   455.31993
BETA2
   51.54678    50.20529    50.71171    46.22704    45.11644    36.87590
BETA2*
   57.96454    56.58136    57.34877    54.51663    55.86312    51.42517
```

INCIDENCE					
-1.14065	-1.63380	.48323	-1.13020	2.47947	.93493
.88485	.87691	.88015	.83105	.74727	.60355
V2					
1058.27687	1045.49751	1041.91781	979.39871	879.20789	710.36920
TOTAL TEMP					
1.28031	1.27546	1.24938	1.24838	1.23316	1.24135
TOTAL PRESS					
2.18924	2.18145	2.11426	2.15203	2.07408	2.13024
EFFICIENCY					
.88563	.89665	.94634	.97517	.98350	.98879
STATIC TEMP					
1.15194	1.14473	1.12857	1.11850	1.11479	1.11562
STATIC PRESS					
1.50713	1.48864	1.47599	1.45966	1.45200	1.46069
DENSITY					
1.30834	1.30043	1.30784	1.30502	1.30249	1.30930
SUCT SURF VEL					
1256.56349	1257.72594	1210.69616	1150.19510	1024.98909	862.48547
PRESS SURF VEL					
859.99025	833.26909	873.13947	808.60232	733.42668	558.25293
DELTA T					
35.21207	35.56850	30.85021	34.24952	28.94412	35.32421
WORK COEF = 2*CP*DELT/U**2					
.20576	.21534	.19753	.24371	.23481	.34766
FLOW COEF = VM/U					
.45676	.47273	.47933	.51892	.50738	.51185
R BAR					
2.34100	2.29870	2.23279	2.11252	1.96992	1.77500
D-FACTOR					
.14544	.14268	.12520	.12892	.11626	.15870
VM2/VM1					
.99745	1.02103	1.01796	1.08282	1.07822	1.16515
DELP/Q					
.15999	.15469	.15029	.15264	.16937	.24713
TANG BLADE FORCE LB/IN					
21.38554	21.61404	18.24042	18.87127	13.20959	12.18578
AXIAL BLADE FORCE LB/IN					
37.37248	36.61744	34.40019	31.78009	24.08295	19.93177
VEL HEAD 2					
.39813	.39302	.39510	.36333	.30886	.21754
Q=E**(-S/CP)					
.97496	.97768	.98929	.99506	.99688	.99782
RVU/					
2.37000	2.32900	2.10850	2.10000	1.97130	2.04054
DRVU/DM					
7.15604	7.49107	6.08454	5.75185	4.90195	4.69454
STRMLN DIST M					
1.33508	1.32459	1.31867	1.34058	1.43480	1.80528

STATION 3.40000 ROTOR XI = 1.96300

R = 1. ZTIP = .81100 AR = 6.00000 XN = 0. BNXT = 1.
= -0. ZHUB = .82800 LOSS = 3. EXP = -0.0000 BLADES = 40.

RADIUS					
2.40500	2.36030	2.29970	2.19290	2.07060	1.90900
SLOPE					
38.72212	38.83091	39.07845	41.09818	46.27763	53.84123
CURVATURE					
.17500	.01196	-.02285	.07902	-.09458	-.08000
LOSS COEFF					
.97200	.97487	.98825	.99464	.99666	.99753
SOLIDITY					
1.00000	1.00000	1.00000	1.00000	1.00000	1.00000
BLADE THICKNESS					
.03180	.03461	.03828	.04339	.04729	.05488
AERO BLOCKAGE					
.96100	.96100	.96100	.96100	.96100	.96100
TOTAL BLOCKAGE					
.88011	.87129	.85916	.83995	.82127	.78512
BLADE ANGLE					
58.46244	57.50910	56.31321	54.03466	50.00377	43.70551
LEAN					
2.53867	1.24787	-.42408	-2.51336	-2.20933	-1.72651
Y					
-2.80000	-2.81140	-2.50030	-2.47000	-2.39000	-2.50000

NOR ITERS = 1 AREA RATIO = .99966 EXP = 1.50000 CHOKE = .78809

RADIUS					
2.40500	2.36248	2.29995	2.19192	2.06891	1.90900
Z					
.81100	.81246	.81460	.81830	.82252	.82800
CROSS PASSAGE DIST P					
.49629	.45375	.39118	.28309	.16000	0.00000
SLOPE					
38.72212	38.05880	37.82425	40.96159	46.14184	53.84123
CURVATURE					
.17500	.04437	-.19296	.02532	-.08146	-.08000
DELTA CURVATURE					
0.00000	.00484	-.00094	-.00308	-.00366	0.00000
VM					
566.27296	607.81630	622.80998	678.95802	641.73171	627.34216
VU2					
756.86289	715.20340	739.82818	649.68724	557.35986	365.72191
U					
1467.05000	1441.11493	1402.96688	1337.07402	1262.03211	1164.49000
VR					
354.22873	374.70059	381.93302	445.09305	462.72544	506.50686
BETA2					
53.19672	49.64040	49.90828	43.73793	40.97511	30.24091
BETA2*					
59.72680	56.21135	56.37774	51.72049	51.41847	44.65542

INCIDENCE						
	.78628	-1.75854	.17045	-1.57220	2.44375	1.88908
	.77434	.77211	.80433	.78852	.71493	.61255
V2						
	945.25473	938.59286	967.07704	939.72204	849.98211	726.16162
TOTAL TEMP						
	1.33117	1.33252	1.29573	1.29214	1.28268	1.29566
TOTAL PRESS						
	2.48547	2.52050	2.39571	2.42702	2.38182	2.47571
EFFICIENCY						
	.88745	.89930	.94852	.97629	.98484	.98918
STATIC TEMP						
	1.20005	1.19006	1.16419	1.14378	1.13831	1.13174
STATIC PRESS						
	1.72296	1.69031	1.64119	1.57730	1.56195	1.53505
DENSITY						
	1.43574	1.42036	1.40973	1.37902	1.37216	1.35636
SUCT SURF VEL						
	1121.98774	1112.18154	1138.26550	1091.68953	1002.55302	869.87035
PRESS SURF VEL						
	768.52172	765.00417	795.88858	787.75455	697.41121	582.45289
DELTA T						
	26.37976	29.59441	24.03626	22.69886	25.68652	28.17153
WORK COEF = 2*CP*DELT/U**2						
	.14869	.17286	.14814	.15402	.19564	.25201
FLOW COEF = VM/U						
	.38599	.42177	.44392	.50779	.50849	.53873
R BAR						
	2.38350	2.34151	2.27819	2.16619	2.03676	1.86450
D-FACTOR						
	.15879	.16235	.12217	.09370	.10455	.08351
VM2/VM1						
	.86045	.90833	.94399	1.00208	1.03434	1.10399
DELP/Q						
	.21649	.20923	.17136	.14122	.16944	.18310
TANG BLADE FORCE LB/IN						
	16.13329	18.69729	15.06031	13.92480	13.17996	11.23414
AXIAL BLADE FORCE LB/IN						
	36.24671	35.94245	31.18779	24.66660	23.01029	15.04917
VEL HEAD 2						
	.32645	.32499	.34596	.33567	.28793	.22309
Q=E**(-S/CP)						
	.97200	.97487	.98825	.99464	.99666	.99753
RVU/						
	2.80000	2.81140	2.50030	2.47000	2.39000	2.49975
DRVU/DM						
	6.72371	6.16753	6.19900	5.01324	4.92320	4.24534
STRMLN DIST M						
	1.40411	1.39364	1.38962	1.41815	1.52290	1.91432

STATION 3.60000 ROTOR XI = 2.88747

P = 1. ZTIP = .86700 AR = 6.00000 XN = 0. BNXT = 1.
= -0. ZHUB = .89000 LOSS = 3. EXP = -0.0000 BLADES = 40.

RADIUS					
2.45000	2.40520	2.34510	2.24370	2.13240	1.99400
SLOPE					
39.50742	38.59819	38.84416	40.86195	45.25754	53.14836
CURVATURE					
.20000	.07639	.09166	.01780	.28169	-.11920
LOSS COEFF					
.96906	.97207	.98720	.99423	.99643	.99725
SOLIDITY					
1.00000	1.00000	1.00000	1.00000	1.00000	1.00000
BLADE THICKNESS					
.03097	.03396	.03838	.04447	.04788	.05525
AERO BLOCKAGE					
.96100	.96100	.96100	.96100	.96100	.96100
TOTAL BLOCKAGE					
.88366	.87462	.86087	.83974	.82363	.79148
BLADE ANGLE					
57.25140	55.83620	54.34767	50.91125	43.81139	32.82765
LEAN					
7.36479	5.71752	3.55145	1.27933	1.59436	1.71574
Y					
-3.32000	-3.19400	-3.00000	-2.88000	-2.83000	-2.95000

NOR ITERS = 2 AREA RATIO = .99981 EXP = 1.50000 CHOKE = .75771

RADIUS					
2.45000	2.40684	2.34379	2.24274	2.13054	1.99400
Z					
.86700	.86918	.87236	.87745	.88311	.89000
CROSS PASSAGE DIST P					
.45658	.41336	.35024	.24906	.13671	0.00000
SLOPE					
39.50742	38.20198	37.67940	40.11559	44.83716	53.14836
CURVATURE					
.20000	.07274	.20614	-.19219	-.06571	-.11920
DELTA CURVATURE					
0.00000	-.00050	.00643	-.00040	-.00267	0.00000
VM					
517.27854	524.57425	595.94359	627.72697	650.80176	647.60327
VU2					
667.88776	658.66926	648.92864	584.74504	489.36428	313.92687
U					
1494.50000	1468.17118	1429.71411	1368.07215	1299.62875	1216.34000
VR					
329.08142	324.41549	364.26616	404.46456	458.87674	518.20656
BETA2					
52.24222	51.46563	47.43717	42.96971	36.94098	25.86186
BETA2*					
59.13918	57.95953	53.98950	50.61539	46.67899	38.94733

INCIDENCE	.20215	.74811	-1.29818	-.68550	2.07200	3.52469
	.68037	.68137	.72132	.70857	.67756	.60151
V2	844.77876	842.03524	881.05456	857.88572	814.26060	719.68054
TOTAL TEMP	1.39268	1.37777	1.35483	1.34063	1.33472	1.34890
TOTAL PRESS	2.88452	2.80752	2.79416	2.76045	2.73897	2.85143
EFFICIENCY	.89027	.89814	.95113	.97729	.98576	.98937
STATIC TEMP	1.24155	1.22989	1.20150	1.18049	1.16306	1.15284
STATIC PRESS	1.92222	1.87967	1.82782	1.76099	1.68394	1.63694
DENSITY	1.54824	1.52832	1.52129	1.49174	1.44785	1.41993
SUCT SURF VEL	1012.06728	979.44960	1052.17825	1002.46777	978.18002	855.21794
PRESS SURF VEL	677.49023	704.62087	709.93088	713.30368	650.34118	584.14314
DELTA T	31.90110	23.47185	30.65573	25.15279	26.99324	27.61311
WORK COEF = 2*CP*DELT/U**2	.17326	.13209	.18193	.16303	.19387	.22641
FLOW COEF = VM/U	.34612	.35730	.41683	.45884	.50076	.53242
R BAR	2.42750	2.38466	2.32187	2.21733	2.09972	1.95150
D-FACTOR	.17541	.15501	.15683	.14710	.11722	.10580
VM2/VM1	.91348	.86305	.95686	.92454	1.01413	1.03230
DELP/Q	.23863	.23267	.21499	.23049	.19316	.23117
TANG BLADE FORCE LB/IN	18.88538	14.44547	19.97937	16.28372	15.55246	12.76721
AXIAL BLADE FORCE LB/IN	38.46296	31.87692	36.89320	32.86703	25.67952	19.99862
VEL HEAD 2	.26575	.26638	.29205	.28383	.26395	.21628
Q=E**(-S/CP)	.96906	.97207	.98720	.99423	.99643	.99725
RVU/	3.32000	3.19400	3.00000	2.88000	2.83000	2.94986
DRVU/DM	6.20156	5.05842	5.89303	4.71978	4.99793	3.82061
STRMLN DIST M	1.47595	1.46564	1.46214	1.49613	1.60933	2.01953

STATION 3.80000 ROTOR XI = 4.25158

P = 1. ZTIP = .92500 AR = 6.00000 XN = 0. BNXT = 1.
= -0. ZHUB = .95600 LOSS = 3. EXP = -0.0000 BLADES = 40.

RADIUS					
2.49600	2.45260	2.39450	2.29810	2.19620	2.07900
SLOPE					
40.39805	39.58730	39.39818	41.37679	45.24561	51.93587
CURVATURE					
.22000	-.01659	-.00959	.23315	-.19928	-.18000
LOSS COEFF					
.96611	.96925	.98150	.99381	.99621	.99696
SOLIDITY					
1.00000	1.00000	1.00000	1.00000	1.00000	1.00000
BLADE THICKNESS					
.02357	.02623	.02945	.03385	.03769	.04408
AERO BLOCKAGE					
.95300	.95300	.95300	.95300	.95300	.95300
TOTAL BLOCKAGE					
.89571	.88811	.87838	.86364	.84888	.82436
BLADE ANGLE					
55.65959	54.43986	52.19366	46.98038	36.48599	18.45993
LEAN					
11.93187	10.32751	8.86219	8.23414	9.05259	9.51482
Y					
-3.70000	-3.55400	-3.37240	-3.22000	-3.27350	-3.31000

NOR ITERS = 1 AREA RATIO = 1.00088 EXP = 1.50000 CHOKE = .73301

RADIUS					
2.49600	2.45335	2.39165	2.29561	2.19420	2.07900
Z					
.92500	.92817	.93276	.93990	.94744	.95600
CROSS PASSAGE DIST P					
.41815	.37538	.31351	.21721	.11551	0.00000
SLOPE					
40.39805	38.67128	39.12227	41.03700	44.88034	51.93587
CURVATURE					
.22000	.00146	.22293	.54400	.13125	-.18000
DELTA CURVATURE					
0.00000	-.00069	.00206	.00090	.00109	0.00000
VM					
475.93052	485.77793	558.24571	616.12253	645.74998	685.08553
VU2					
618.31321	612.87712	598.76248	544.69213	428.40587	296.81333
U					
1522.56000	1496.54275	1458.90664	1400.32407	1338.45924	1268.19000
VR					
308.44782	303.53914	352.24058	404.51311	455.65977	539.38250
BETA2					
52.41363	51.59897	47.00558	41.47874	33.56123	23.42466
BETA2*					
59.62152	58.24943	54.12159	49.52911	43.11484	35.09604

INCIDENCE	1.03619	1.23387	-.57047	-.44542	1.27974	4.76099
	.62093	.62553	.66193	.67253	.63769	.62024
V2	780.26988	782.04767	818.62982	822.37248	774.93524	746.61927
TOTAL TEMP	1.43762	1.42035	1.39887	1.38085	1.38718	1.39157
TOTAL PRESS	3.19255	3.09437	3.06522	3.05976	3.13621	3.17989
EFFICIENCY	.88867	.89610	.93512	.97756	.98642	.98920
STATIC TEMP	1.27167	1.25875	1.23176	1.20416	1.18928	1.16694
STATIC PRESS	2.06969	2.01933	1.95535	1.88616	1.82050	1.70705
DENSITY	1.62754	1.60424	1.58744	1.56637	1.53076	1.46284
SUCT SURF VEL	872.34953	892.25923	914.09841	919.58301	883.86019	838.56459
PRESS SURF VEL	688.19023	671.83612	723.16123	725.16195	666.01029	654.67396
DELTA T	23.31235	22.08538	22.84610	20.85841	27.20796	22.13368
WORK COEF = 2*CP*DELT/U**2	.12199	.11962	.13021	.12904	.18424	.16694
FLOW COEF = VM/U	.31259	.32460	.38265	.43999	.48246	.54021
R BAR	2.47300	2.43009	2.36772	2.26918	2.16237	2.03650
D-FACTOR	.13184	.12490	.12530	.09467	.12512	.03765
VM2/VM1	.92007	.92604	.93674	.98151	.99224	1.05788
DELP/Q	.21196	.20462	.16913	.17935	.22614	.15519
TANG BLADE FORCE LB/IN	13.73014	13.22218	15.24277	14.16186	17.46869	12.18285
AXIAL BLADE FORCE LB/IN	28.24647	26.46145	21.70808	23.80633	26.66630	16.98435
VEL HEAD 2	.22828	.23114	.25401	.26075	.23873	.22785
Q=E**(-S/CP)	.96611	.96925	.98150	.99381	.99621	.99696
RVU/	3.70000	3.55400	3.37240	3.22000	3.27350	3.31064
DRVU/DM	3.35252	3.97501	3.17291	2.99272	3.07067	2.42315
STRMLN DIST M	1.54998	1.54077	1.53920	1.57795	1.69983	2.12715

Rotor 1B Exit

```
STATION        4.00000   ROTOR    XI =      5.98088

P =    1.   ZTIP =     .98000   AR =    6.00000    XN =    0.     BNXT =   -0.
  =   -0.   ZHUB =    1.02000   LOSS =    3.   EXP =  -0.0000  BLADES =    1.

RADIUS
    2.54080      2.50020      2.44280      2.35350      2.25910      2.15900
SLOPE
   40.34944     40.20571     40.53980     42.37657     45.85692     50.86984
CURVATURE
     .24280       .31647       .30135       .06521       .00277      -.25180
LOSS COEFF
     .96317       .96646       .98517       .99339       .99598       .99668
SOLIDITY
    1.00000      1.00000      1.00000      1.00000      1.00000      1.00000
BLADE THICKNESS
     .01078       .01188       .01298       .01408       .01408       .01365
AERO BLOCKAGE
     .95300       .95300       .95300       .95300       .95300       .95300
TOTAL BLOCKAGE
     .95236       .95228       .95219       .95209       .95205       .95204
BLADE ANGLE
   53.46013     52.87353     50.15388     42.06407     26.71148     -1.28609
LEAN
   14.67896     13.99358     13.72569     15.32252     18.48976     20.99815
Y
   -3.81677     -3.78400     -3.48920     -3.36928     -3.38680     -3.46765

  NOR ITERS =   1   AREA RATIO = 1.00089   EXP = 1.50000   CHOKE =   .67667

RADIUS
    2.54080      2.49839      2.44013      2.35017      2.25727      2.15900
Z
     .98000       .98444       .99055       .99997      1.00970      1.02000
CROSS PASSAGE DIST P
     .38389       .34124       .28267       .19222       .09880      0.00000
SLOPE
   40.34944     39.71951     40.92017     43.15562     46.06735     50.86984
CURVATURE
     .24280       .43332       .38684       .17027       .03806      -.25180
DELTA CURVATURE
    0.00000       .00437       .00344       .00497       .00302      0.00000
VM
  407.76993    439.03627    514.82116    551.20328    596.47451    644.54236
VU2
  633.55074    600.12438    616.22463    559.09199    461.68960    337.07818
VU1
  916.33726    923.89194    872.25395    874.51425    915.24316    979.91182
U
 1549.88800   1524.01632   1488.47858   1433.60624   1376.93275   1316.99000
VR
  264.00977    280.55734    337.21150    377.01336    429.55475    499.98089
BETA2
   57.23358     53.81169     50.12311     45.40706     37.74096     27.60834
  .TA1
   66.01092     64.58276     59.45005     57.77689     56.90722     56.66484
BETA2*
   63.87138     60.63288     57.73656     54.27609     48.12812     39.64818
```

BETA1*	71.26618	69.92173	65.96390	65.30698	65.66914	67.45669
CIDENCE	-63.84075	-65.85982	-73.85987	-82.25337	87.21228	72.49670
M2	.59494	.58951	.64461	.63563	.61512	.59798
M1	.79198	.81096	.81309	.83690	.89091	.96426
V2	753.43404	743.57388	802.97797	785.11713	754.28054	727.36273
V1	1002.97073	1022.90233	1012.85131	1033.73122	1092.45223	1172.88620
TOTAL TEMP	1.45143	1.44756	1.41269	1.39850	1.40058	1.41021
TOTAL PRESS	3.26688	3.27539	3.21566	3.19548	3.24193	3.32967
EFFICIENCY	.88159	.89152	.94923	.97680	.98594	.98859
STATIC TEMP	1.29156	1.28126	1.24965	1.22867	1.21090	1.19151
STATIC PRESS	2.16292	2.12811	2.08486	2.02232	1.93860	1.83564
DENSITY	1.67466	1.66094	1.66836	1.64594	1.60096	1.54060
SUCT SURF VEL	690.93919	0.00000	711.70516	0.00000	0.00000	0.00000
PRESS SURF VEL	915.92890	0.00000	894.25078	0.00000	0.00000	0.00000
DELTA T	7.16364	14.11010	7.16548	9.15807	6.95076	9.66864
WORK COEF = 2*CP*DELT/U**2	.03618	.07370	.03923	.05405	.04447	.06762
FLOW COEF = VM/U	.26310	.28808	.34587	.38449	.43319	.48941
R, BAR	2.51840	2.47587	2.41589	2.32289	2.22573	2.11900
D-FACTOR	.05252	.08543	.03713	.06914	.04669	.05617
VM2/VM1	.85678	.90378	.92221	.89463	.92369	.94082
DELP/Q	.15228	.17919	.19451	.20467	.20686	.25528
TANG BLADE FORCE LB/IN	4.24229	8.71048	5.04456	6.72546	5.08468	6.72325
AXIAL BLADE FORCE LB/IN	13.85118	18.38775	21.24493	18.35825	17.02458	22.74738
VEL HEAD 2	.21226	.20895	.24308	.23744	.22468	.21412
VEL HEAD 1	.33793	.35027	.35166	.36713	.40202	.44861
Q=E**(-S/CP)	.96317	.96646	.98517	.99339	.99598	.99668
RVU/	3.81677	3.78400	3.48920	3.36928	3.38680	3.46825
DRVU/DM	-.06030	2.40705	-.07603	.68625	-.51399	.65352
STRMLN DIST M	1.62092	1.61284	1.61463	1.65910	1.78846	2.22960

```
STATION        5.00000   STATOR    XI =        0.00000

P =    0.   ZTIP =    1.30000    AR =    3.00000     XN =   -0.      BNXT =   -0.
  =   -0.   ZHUB =    1.30000    LOSS =    2.    EXP =   -0.0000   BLADES =    1.

RADIUS
     2.82900      2.80000      2.73000      2.64000      2.56000      2.47300
SLOPE
    42.17000     41.00000     42.00000     44.00000     45.00000     46.00000
CURVATURE
     -.08767      -.13000      -.15000      -.16000      -.18000      -.13050
LOSS COEFF
     1.00000      1.00000      1.00000      1.00000      1.00000      1.00000
SOLIDITY
     1.00000      1.00000      1.00000      1.00000      1.00000      1.00000
BLADE THICKNESS
      .01821       .01772       .01722       .01665       .01649       .01708
AERO BLOCKAGE
      .94500       .94500       .94500       .94500       .94500       .94500
TOTAL BLOCKAGE
      .94403       .94405       .94405       .94405       .94403       .94396
BLADE ANGLE
   -64.05654    -62.67773    -61.24885    -59.10606    -58.72378    -60.71567
LEAN
     2.17206       .02951     -3.30363    -10.28877    -15.69511    -17.14941
Y
    -0.00000     -0.00000     -0.00000     -0.00000     -0.00000     -0.00000

  NOR ITERS =   1   AREA RATIO = 1.00029   EXP = 1.50000   CHOKE =   .67317

RADIUS
     2.82900      2.79243      2.73898      2.65199      2.56267      2.47300
Z
     1.30000      1.30000      1.30000      1.30000      1.30000      1.30000
CROSS PASSAGE DIST P
      .35600       .31943       .26598       .17899       .08967      0.00000
SLOPE
    42.17000     42.60118     43.52334     44.63871     45.63315     46.00000
CURVATURE
     -.08767      -.18711      -.18604      -.18796      -.12816      -.13050
DELTA CURVATURE
     0.00000      -.00175       .00042       .00037      -.00047      0.00000
VM
   479.06562    490.77282    528.43361    543.45949    575.73768    609.02632
VU2
   822.98682    826.60621    777.08113    774.98706    806.17146    855.52931
U
  1725.69000   1703.38231   1670.77963   1617.71615   1563.22611   1508.53000
VR
   321.61249    332.19989    363.90594    381.85318    411.58200    438.09702
BETA2
    59.79603     59.30151     55.78334     54.95993     54.46696     54.55402
BETA2*
    66.66309     66.39333     63.75295     63.48191     63.46344     63.68726
```

INCIDENCE					
3.52232	4.53728	2.06065	2.17932	.99235	-1.04916
.74740	.75643	.74763	.75790	.79687	.84805
V2					
952.26633	961.31982	939.73249	946.54802	990.64944	1050.16354
TOTAL TEMP					
1.45143	1.44756	1.41269	1.39850	1.40058	1.41021
TOTAL PRESS					
3.26688	3.27539	3.21566	3.19548	3.24193	3.32967
EFFICIENCY					
.88159	.89152	.94923	.97680	.98594	.98859
STATIC TEMP					
1.30731	1.30068	1.27234	1.25611	1.24460	1.23493
STATIC PRESS					
2.25760	2.24429	2.22173	2.18647	2.13609	2.08318
DENSITY					
1.72690	1.72547	1.74618	1.74067	1.71628	1.68688
SUCT SURF VEL					
0.00000	0.00000	0.00000	0.00000	0.00000	0.00000
PRESS SURF VEL					
0.00000	0.00000	0.00000	0.00000	0.00000	0.00000
DELTA T					
0.00000	0.00000	0.00000	0.00000	0.00000	0.00000
WORK COEF = 2*CP*DELT/U**2					
0.00000	0.00000	0.00000	0.00000	0.00000	0.00000
FLOW COEF = VM/U					
.27761	.28812	.31628	.33594	.36830	.40372
R BAR					
2.68490	2.64541	2.58956	2.50108	2.40997	2.31600
D-FACTOR					
.05055	.06020	.07219	.08434	.09319	.10465
VM2/VM1					
1.17484	1.11784	1.02644	.98595	.96523	.94490
DELP/Q					
.08577	.10127	.12104	.13992	.15152	.16575
TANG BLADE FORCE LB/IN					
-.00000	-.00000	-.00000	-.00000	-.00000	.00650
AXIAL BLADE FORCE LB/IN					
29.95129	31.87609	31.72610	35.37090	42.08068	55.46356
VEL HEAD 2					
.30894	.31480	.30909	.31576	.34111	.37436
Q=E**(-S/CP)					
.96317	.96646	.98517	.99339	.99598	.99668
RVU/					
3.81677	3.78400	3.48920	3.36928	3.38680	3.46840
DRVU/DM					
-7.54163	-7.12164	-5.92516	-4.83079	-3.75732	-2.92013
STRMLN DIST M					
2.05157	2.04416	2.04483	2.08468	2.20981	2.65031

STATION 5.10000 STATOR XI = .83443

P = 0. ZTIP = 1.36000 AR = 4.00000 XN = 1. BNXT = 0.
= -0. ZHUB = 1.36500 LOSS = 2. EXP = -0.0000 BLADES = 53.

RADIUS					
2.88260	2.84000	2.79000	2.70000	2.62000	2.53930
SLOPE					
41.68900	42.00000	43.00000	44.00000	45.00000	45.33150
CURVATURE					
-.12135	-.14000	-.14000	-.14000	-.14000	-.15075
LOSS COEFF					
.99691	.99695	.99744	.99830	.99733	.99603
SOLIDITY					
1.00000	1.00000	1.00000	1.00000	1.00000	1.00000
BLADE THICKNESS					
.04100	.03978	.03918	.03867	.03979	.04285
AERO BLOCKAGE					
.94331	.94335	.94335	.94337	.94338	.94336
TOTAL BLOCKAGE					
.83013	.83189	.83160	.82940	.82252	.80908
BLADE ANGLE					
-58.01493	-56.74558	-55.49516	-53.62422	-53.45886	-55.59224
LEAN					
-2.55017	-3.72303	-4.55138	-7.80551	-10.13416	-9.26323
Y					
-50.70000	-50.20000	-48.08000	-47.62000	-47.80000	-48.64000

VOR ITERS = 1 AREA RATIO = .99944 EXP = 1.50000 CHOKE = .91667

RADIUS					
2.88260	2.84845	2.79748	2.71297	2.62730	2.53930
Z					
1.36000	1.36050	1.36124	1.36247	1.36372	1.36500
CROSS PASSAGE DIST P					
.34334	.30919	.25821	.17369	.08801	0.00000
SLOPE					
41.68900	42.10591	42.74873	43.30337	44.51415	45.33150
CURVATURE					
-.12135	-.30510	-.42811	-.50772	-.44498	-.15075
DELTA CURVATURE					
0.00000	-.00115	-.00385	-.00412	-.00383	0.00000
VM					
536.35408	546.67429	558.86425	586.51717	626.11142	663.59530
VU2					
655.29714	660.56095	629.86729	643.29447	690.10885	753.68468
U					
1758.38600	1737.55593	1706.46566	1654.91356	1602.65195	1548.97300
VR					
356.72225	366.54695	379.34848	402.26946	438.95773	471.93990
BETA2					
50.70000	50.38913	48.41820	47.64330	47.78363	48.63709
BETA2*					
58.56586	58.45025	56.91341	56.43560	57.09914	58.24362

INCIDENCE					
-.08326	.60754	-.01940	.34850	.43898	-.16576
.65710	.66703	.66276	.69103	.74419	.80604
V2					
846.81169	857.43429	842.05823	870.53441	931.80778	1004.19088
TOTAL TEMP					
1.45143	1.44756	1.41269	1.39850	1.40058	1.41021
TOTAL PRESS					
3.23135	3.24018	3.18669	3.17635	3.21151	3.28325
EFFICIENCY					
.87202	.88197	.94061	.97088	.97666	.97500
STATIC TEMP					
1.33746	1.33071	1.30000	1.27806	1.26258	1.24994
STATIC PRESS					
2.42042	2.40664	2.37555	2.31059	2.22604	2.14373
DENSITY					
1.80971	1.80854	1.82735	1.80789	1.76308	1.71506
SUCT SURF VEL					
1022.28594	1026.61076	995.85888	1013.53923	1063.74831	1123.01222
PRESS SURF VEL					
671.33745	688.25781	688.25757	727.52960	799.86724	885.36953
DELTA T					
0.00000	0.00000	0.00000	0.00000	0.00000	0.00000
WORK COEF = 2*CP*DELT/U**2					
0.00000	0.00000	0.00000	0.00000	0.00000	0.00000
FLOW COEF = VM/U					
.30503	.31462	.32750	.35441	.39067	.42841
K BAR					
2.85580	2.82044	2.76823	2.68248	2.59498	2.50615
D-FACTOR					
.19150	.18675	.17436	.14136	.10857	.08213
VM2/VM1					
1.11958	1.11391	1.05759	1.07923	1.08749	1.08960
DELP/Q					
.16132	.15746	.15476	.12301	.08134	.04858
TANG BLADE FORCE LB/IN					
-25.71603	-25.38746	-22.87246	-19.75665	-16.34520	-13.09659
AXIAL BLADE FORCE LB/IN					
50.52536	49.71053	44.01699	37.59349	28.90475	21.06481
VEL HEAD 2					
.25096	.25725	.25454	.27256	.30686	.34707
Q=E**(-S/CP)					
.96019	.96351	.98265	.99170	.99333	.99273
RVU/					
3.09665	3.08455	2.88860	2.86105	2.97233	3.13743
DRVU/DM					
-8.70669	-8.31977	-7.26621	-6.67322	-6.22702	-5.80077
STRMLN DIST M					
2.13202	2.12662	2.12953	2.17198	2.30057	2.74315

STATION 5.20000 STATOR XI = 1.72583

P = -0. ZTIP = 1.41500 AR = 4.00000 XN = 1. BNXT = -0.
= -0. ZHUB = 1.42500 LOSS = 2. EXP = -0.0000 BLADES = 53.

RADIUS	2.93108	2.89000	2.84000	2.76000	2.67000	2.59919
SLOPE	41.11230	42.00000	43.00000	43.00000	44.00000	44.52400
CURVATURE	-.15349	-.16000	-.17000	-.17000	-.18000	-.18223
LOSS COEFF	.99717	.99723	.99763	.99843	.99752	.99636
SOLIDITY	1.00000	1.00000	1.00000	1.00000	1.00000	1.00000
BLADE THICKNESS	.04564	.04430	.04332	.04309	.04417	.04715
AERO BLOCKAGE	.94178	.94186	.94183	.94186	.94187	.94187
TOTAL BLOCKAGE	.81808	.82009	.82065	.81783	.81044	.79774
BLADE ANGLE	-52.62893	-51.41668	-50.23110	-49.03793	-49.04520	-51.36890
LEAN	-4.98158	-5.82798	-5.92520	-6.22135	-6.72153	-4.14150
Y	-45.50000	-44.83000	-43.38000	-42.30000	-42.40000	-42.60000

VOR ITERS = 1 AREA RATIO = .99966 EXP = 1.50000 CHOKE = .83773

RADIUS	2.93108	2.89769	2.84802	2.76517	2.68295	2.59919
Z	1.41500	1.41601	1.41750	1.42000	1.42248	1.42500
CROSS PASSAGE DIST P	.33204	.29864	.24895	.16605	.08379	0.00000
SLOPE	41.11230	41.40934	41.86401	41.96615	43.13245	44.52400
CURVATURE	-.15349	-.13664	-.10039	-.05288	-.12327	-.18223
DELTA CURVATURE	0.00000	.00072	-.00048	-.00283	-.00232	0.00000
VM	506.08948	521.86408	523.08847	553.13392	585.29689	631.06646
VU2	515.00075	521.67700	498.46310	503.82078	533.98048	580.28705
U	1787.95880	1767.59113	1737.29456	1686.75112	1636.59655	1585.50590
VR	332.77268	345.17884	349.09103	369.87601	400.16010	442.50898
BETA2	45.50000	44.98971	43.61909	42.32873	42.37493	42.59957
BETA2*	53.48427	53.12011	51.99156	50.77466	51.34340	52.21193

INCIDENCE	-.72718	-.37631	-.48717	-.61181	-.25534	-.71660
	.55388	.56761	.56231	.58673	.62338	.67648
V2	722.04733	737.89498	722.55588	748.19283	792.28000	857.30854
TOTAL TEMP	1.45143	1.44756	1.41269	1.39850	1.40058	1.41021
TOTAL PRESS	3.19921	3.20853	3.16008	3.15872	3.18343	3.24123
EFFICIENCY	.86329	.87333	.93264	.96541	.96804	.96258
STATIC TEMP	1.36857	1.36102	1.32971	1.30954	1.30082	1.29340
STATIC PRESS	2.59917	2.58053	2.55156	2.50404	2.45187	2.38792
DENSITY	1.89918	1.89603	1.91888	1.91215	1.88488	1.84624
SUCT SURF VEL	875.69116	891.14155	864.82969	890.21071	937.37929	1005.39156
PRESS SURF VEL	568.40349	584.64842	580.28207	606.17495	647.18072	709.22552
DELTA T	0.00000	0.00000	0.00000	0.00000	0.00000	0.00000
WORK COEF = 2*CP*DELT/U**2	0.00000	0.00000	0.00000	0.00000	0.00000	0.00000
FLOW COEF = VM/U	.28305	.29524	.30109	.32793	.35763	.39802
K BAR	2.90684	2.87307	2.82275	2.73907	2.65512	2.56924
D-FACTOR	.22441	.21450	.21394	.21437	.22663	.22486
VM2/VM1	.94357	.95462	.93598	.94308	.93481	.95098
DELP/Q	.22043	.20862	.21700	.22344	.22917	.21429
TANG BLADE FORCE LB/IN	-24.08355	-23.98616	-22.60406	-24.20329	-26.58490	-28.41719
AXIAL BLADE FORCE LB/IN	44.42298	43.48173	41.98918	45.98877	51.77275	54.93544
VEL HEAD 2	.18756	.19573	.19256	.20726	.22980	.26327
Q=E**(-S/CP)	.95748	.96084	.98032	.99014	.99086	.98912
RVU/	2.47460	2.47813	2.32727	2.28385	2.34859	2.47258
DRVU/DM	-6.97910	-6.88229	-6.23984	-6.12844	-6.33107	-6.58885
STRMLN DIST M	2.20534	2.20082	2.20515	2.24965	2.38150	2.82793

STATION 5.30000 STATOR XI = 3.62137

P = -0. ZTIP = 1.47500 AR = 4.00000 XN = 1. BNXT = -0.
= -0. ZHUB = 1.49500 LOSS = 2. EXP = -0.0000 BLADES = 53.

RADIUS					
2.98275	2.95000	2.89000	2.82000	2.74000	2.66674
SLOPE					
40.33100	41.00000	41.00000	42.00000	42.00000	43.39600
CURVATURE					
-.19161	-.20000	-.20000	-.20000	-.20000	-.22377
LOSS COEFF					
.99694	.99683	.99737	.99819	.99712	.99572
SOLIDITY					
1.00000	1.00000	1.00000	1.00000	1.00000	1.00000
BLADE THICKNESS					
.04002	.03915	.03862	.03854	.03935	.04104
AERO BLOCKAGE					
.94012	.94016	.94014	.94013	.94013	.94012
TOTAL BLOCKAGE					
.83371	.83492	.83417	.83175	.82624	.81808
BLADE ANGLE					
-46.84601	-45.48986	-44.19821	-43.80426	-43.99808	-46.56846
LEAN					
-6.71432	-7.46853	-7.18996	-5.15956	-3.88857	.19175
Y					
-41.70000	-40.70000	-39.50000	-37.80000	-37.55000	-37.15000

NOR ITERS = 1 AREA RATIO = 1.00055 EXP = 1.50000 CHOKE = .76556

RADIUS					
2.98275	2.95044	2.90256	2.82243	2.74462	2.66674
Z					
1.47500	1.47704	1.48007	1.48515	1.49007	1.49500
CROSS PASSAGE DIST P					
.31664	.28427	.23630	.15601	.07804	0.00000
SLOPE					
40.33100	40.63542	40.77724	41.37999	42.04346	43.39600
CURVATURE					
-.19161	-.16847	-.18299	-.16119	-.14714	-.22377
DELTA CURVATURE					
0.00000	-.00023	-.00008	.00188	.00307	0.00000
VM					
470.71372	489.20562	484.84543	522.42112	552.31914	595.25271
VU2					
419.39089	420.96115	402.88279	405.97415	424.87807	450.98375
U					
1819.47750	1799.76974	1770.56380	1721.68531	1674.21813	1626.71140
VR					
304.64712	318.59205	316.66228	345.34654	369.88498	408.96065
BETA2					
41.70000	40.71196	39.72490	37.85081	37.56970	37.14879
BETA2*					
49.44947	48.59112	47.65674	46.00365	46.00887	46.19693

INCIDENCE					
.05374	.09476	.24297	-.11385	.21843	-.27571
.48017	.49278	.48697	.51504	.54359	.58297
V2					
630.44438	645.39169	630.38848	661.61835	696.83414	746.80127
TOTAL TEMP					
1.45143	1.44756	1.41269	1.39850	1.40058	1.41021
TOTAL PRESS					
3.16476	3.17269	3.13079	3.13852	3.15118	3.19252
EFFICIENCY					
.85388	.86346	.92380	.95910	.95808	.94804
STATIC TEMP					
1.38826	1.38136	1.34953	1.32893	1.32340	1.32157
STATIC PRESS					
2.70430	2.68900	2.66358	2.62071	2.57927	2.53812
DENSITY					
1.94798	1.94664	1.97371	1.97204	1.94897	1.92053
SUCT SURF VEL					
735.14932	753.29718	730.49010	759.63035	796.16420	851.91157
PRESS SURF VEL					
525.73944	537.48619	530.28687	563.60634	597.50407	641.69097
DELTA T					
0.00000	0.00000	0.00000	0.00000	0.00000	0.00000
WORK COEF = 2*CP*DELT/U**2					
0.00000	0.00000	0.00000	0.00000	0.00000	0.00000
FLOW COEF = VM/U					
.25871	.27182	.27384	.30344	.32990	.36592
R BAR					
2.95691	2.92407	2.87529	2.79380	2.71378	2.63296
D-FACTOR					
.18742	.18784	.18778	.17487	.18245	.19660
VM2/VM1					
.93010	.93742	.92689	.94447	.94366	.94325
DELP/Q					
.17521	.17273	.18407	.17822	.17414	.17602
TANG BLADE FORCE LB/IN					
-16.86146	-18.13250	-16.95246	-17.64193	-19.54492	-23.04548
AXIAL BLADE FORCE LB/IN					
24.34687	25.29719	25.34783	26.22906	28.51699	33.02691
VEL HEAD 2					
.14550	.15245	.14923	.16498	.18149	.20498
Q=E**(-S/CP)					
.95455	.95779	.97774	.98835	.98801	.98489
RVU/					
2.05072	2.03610	1.91704	1.87842	1.91169	1.97157
DRVU/DM					
-4.37341	-4.43345	-4.05731	-3.88111	-3.94372	-4.18526
STRMLN DIST M					
2.28452	2.28149	2.28816	2.33639	2.47300	2.92521

STATION 5.40000 STATOR XI = 3.68557

P = -0. ZTIP = 1.53500 AR = 4.00000 XN = 1. BNXT = -0.
= -0. ZHUB = 1.55500 LOSS = 2. EXP = -0.0000 BLADES = 53.

RADIUS					
3.03287	3.00000	2.95000	2.87000	2.79000	2.72238
SLOPE					
39.38000	40.00000	40.00000	41.00000	41.00000	42.25380
CURVATURE					
-.23374	-.23000	-.23000	-.23000	-.23000	-.26448
LOSS COEFF					
.99697	.99704	.99748	.99839	.99752	.99633
SOLIDITY					
1.00000	1.00000	1.00000	1.00000	1.00000	1.00000
BLADE THICKNESS					
.02769	.02721	.02707	.02733	.02799	.02923
AERO BLOCKAGE					
.93848	.93858	.93854	.93860	.93863	.93862
TOTAL BLOCKAGE					
.86620	.86677	.86590	.86321	.85918	.85361
BLADE ANGLE					
-40.96506	-39.57368	-38.31786	-38.66671	-39.55225	-42.38635
LEAN					
-8.37788	-8.91084	-8.39222	-4.77394	-1.92047	2.81818
Y					
-39.34000	-38.15000	-37.35000	-35.03000	-34.84000	-34.20000

NOR ITERS = 1 AREA RATIO = 1.00047 EXP = 1.50000 CHOKE = .70798

RADIUS					
3.03287	3.00088	2.95349	2.87406	2.79825	2.72238
Z					
1.53500	1.53706	1.54011	1.54523	1.55011	1.55500
CROSS PASSAGE DIST P					
.31113	.27907	.23159	.15199	.07603	0.00000
SLOPE					
39.38000	39.72089	39.95845	40.50369	41.22299	42.25380
CURVATURE					
-.23374	-.23201	-.16813	-.21618	-.20055	-.26448
DELTA CURVATURE					
0.00000	-.00031	.00030	-.00123	-.00280	0.00000
VM					
437.87178	457.16175	449.53830	491.02652	517.33267	559.06760
VU2					
358.90489	359.42973	343.61025	345.60601	360.35491	379.91410
U					
1850.05070	1830.53398	1801.63031	1753.17380	1706.93287	1660.65180
VR					
277.81255	292.14854	288.70797	318.92038	340.91783	375.92607
BETA2					
39.34000	38.17512	37.39293	35.13955	34.85964	34.19803
BETA2*					
46.67967	45.62816	44.91960	42.78940	42.80262	42.55487

INCIDENCE	1.94096	1.80515	2.32239	1.55092	2.07392	1.47942
	.42933	.44204	.43512	.46529	.48923	.52448
V2	566.16641	581.53813	565.82037	600.45863	630.46709	675.93735
TOTAL TEMP	1.45143	1.44756	1.41269	1.39850	1.40058	1.41021
TOTAL PRESS	3.13102	3.13967	3.10303	3.12075	3.12362	3.15133
EFFICIENCY	.84458	.85431	.91538	.95354	.94950	.93562
STATIC TEMP	1.40049	1.39381	1.36181	1.34120	1.33740	1.33760
STATIC PRESS	2.75965	2.74675	2.72580	2.69188	2.65357	2.61437
DENSITY	1.97049	1.97068	2.00160	2.00706	1.98412	1.95453
SUCT SURF VEL	604.41277	629.95351	606.00545	641.94606	681.46075	735.45028
PRESS SURF VEL	527.92006	533.12275	525.63529	558.97119	579.47343	616.42443
DELTA T	0.00000	0.00000	0.00000	0.00000	0.00000	0.00000
WORK COEF = 2*CP*DELT/U**2	0.00000	0.00000	0.00000	0.00000	0.00000	0.00000
FLOW COEF = VM/U	.23668	.24974	.24952	.28008	.30308	.33666
H BAR	3.00781	2.97566	2.92803	2.84825	2.77144	2.69456
D-FACTOR	.14478	.14148	.14429	.13291	.13609	.13673
VM2/VM1	.93023	.93450	.92718	.93991	.93666	.93921
DELP/Q	.12020	.11939	.13317	.13744	.12992	.11652
TANG BLADE FORCE LB/IN	-10.56195	-11.02472	-10.40531	-11.03889	-11.74725	-13.05149
AXIAL BLADE FORCE LB/IN	11.35957	11.90294	12.34327	14.84290	14.63525	15.02985
VEL HEAD 2	.11861	.12515	.12157	.13743	.15048	.17039
Q=E**(-S/CP)	.95166	.95495	.97528	.98676	.98556	.98127
RVU/	1.78445	1.76820	1.66369	1.62835	1.65305	1.69553
DRVU/DM	-1.48180	-1.84514	-1.51614	-1.52427	-1.87340	-2.18208
STRMLN DIST M	2.36270	2.35988	2.36689	2.41561	2.55351	3.00703

```
STATION        5.50000  STATOR   XI =      5.74866

r =    0.  ZTIP =    1.59000   AR =   3.00000    XN =   1.     BNXT =  -0.
  =   -0.  ZHUB =    1.62000   LOSS =    2.  EXP =  -0.0000  BLADES =  53.

RADIUS
     3.07700      3.04000      3.00000      2.90000      2.82000      2.77900
SLOPE
    38.35000     38.50000     39.00000     39.00000     40.00000     40.35000
CURVATURE
     -.27690      -.15000      -.20000      -.25000      -.25000      -.29450
LOSS COEFF
      .99725       .99704       .99759       .99832       .99730       .99600
SOLIDITY
     1.00000      1.00000      1.00000      1.00000      1.00000      1.00000
BLADE THICKNESS
      .01200       .01183       .01160       .01150       .01150       .01136
AERO BLOCKAGE
      .93700       .93700       .93700       .93700       .93700       .93700
TOTAL BLOCKAGE
      .90618       .90624       .90644       .90567       .90476       .90470
BLADE ANGLE
   -35.37778    -33.94082    -32.57263    -33.30880    -34.90349    -37.35585
LEAN
   -10.05552    -10.35747     -9.82442     -5.06253      -.38821      4.51900
Y
   -41.00000    -38.50000    -39.02000    -35.50000    -36.00000    -34.50000

  NOR ITERS =   1   AREA RATIO = 1.00078  EXP = 1.50000  CHOKE =   .67707

RADIUS
     3.07700      3.04636      3.00098      2.92407      2.85208      2.77900
Z
     1.59000      1.59309      1.59765      1.60540      1.61264      1.62000
CROSS PASSAGE DIST P
      .29951       .26871       .22310       .14580       .07345      0.00000
SLOPE
    38.35000     38.56134     39.11304     39.26516     40.21386     40.35000
CURVATURE
     -.27690      -.22466      -.21224      -.16328      -.24100      -.29450
DELTA CURVATURE
     0.00000      -.00085       .00017       .00179       .00198      0.00000
VM
   411.03116    434.23695    419.30620    461.20854    477.95310    516.24041
VU2
   357.30416    348.31419    339.63694    341.13623    344.71382    354.63262
U
  1876.97000   1858.27681   1830.59704   1783.68058   1739.77074   1695.19000
VR
   255.02998    270.68262    264.52040    291.90370    308.58690    334.24260
BETA2
    41.00000     38.73410     39.00737     36.48873     35.80023     34.48720
BETA2*
    47.94451     45.73015     46.23157     43.69192     43.36396     42.03117
```

INCIDENCE	7.30093	5.94156	7.80873	6.73144	7.27017	6.53811
	.41243	.42246	.41426	.44370	.45592	.48412
V2	544.62177	556.67271	539.60258	573.66126	589.29346	626.31338
TOTAL TEMP	1.45143	1.44756	1.41269	1.39850	1.40058	1.41021
TOTAL PRESS	3.10075	3.10693	3.07670	3.10229	3.09396	3.10706
EFFICIENCY	.83618	.84516	.90734	.94772	.94021	.92214
STATIC TEMP	1.40429	1.39831	1.36641	1.34620	1.34539	1.34787
STATIC PRESS	2.75929	2.74923	2.73510	2.71137	2.68422	2.64827
DENSITY	1.96490	1.96611	2.00167	2.01409	1.99513	1.96478
SUCT SURF VEL	539.17143	565.41498	537.46396	571.66057	600.22227	646.55703
PRESS SURF VEL	550.07211	547.93044	541.74119	575.66196	578.36466	606.06974
DELTA T	0.00000	0.00000	0.00000	0.00000	0.00000	0.00000
WORK COEF = 2*CP*DELT/U**2	0.00000	0.00000	0.00000	0.00000	0.00000	0.00000
FLOW COEF = VM/U	.21899	.23368	.22905	.25857	.27472	.30453
H BAR	3.05494	3.02362	2.97724	2.89906	2.82517	2.75069
D-FACTOR	.04121	.04774	.04764	.04584	.07238	.08652
VM2/VM1	.93870	.94985	.93275	.93927	.92388	.92340
DELP/Q	-.00096	.00632	.02467	.04545	.06520	.06312
TANG BLADE FORCE LB/IN	.72260	-1.21542	.30033	.31642	-1.93443	-3.97202
AXIAL BLADE FORCE LB/IN	-3.35485	-1.84184	-1.35962	1.66176	2.74449	4.01748
VEL HEAD 2	.11012	.11513	.11103	.12601	.13243	.14766
Q=E**(-S/CP)	.94905	.95213	.97293	.98510	.98290	.97735
RVU/	1.80234	1.73949	1.67089	1.63525	1.61173	1.61561
DRVU/DM	.20652	-.32210	.07747	.06986	-.38966	-.70945
STRMLN DIST M	2.43321	2.43205	2.44149	2.49384	2.63602	3.09324

```
STATION        6.00000  STATOR   XI =     0.00000

P =    0.  ZTIP =   1.84000   AR =   3.00000    XN =  -0.     BNXT =  -0.
  =   -0.  ZHUB =   1.84000   LOSS =   2.  EXP =  -0.0000  BLADES =   1.

RADIUS
    3.25800     3.23000     3.18000     3.10000     3.00000     2.95400
SLOPE
   33.38000    33.00000    34.00000    34.50000    35.00000    36.08000
CURVATURE
    -.28210     -.28000     -.28000     -.28000     -.28000     -.29350
LOSS COEFF
    1.00000     1.00000     1.00000     1.00000     1.00000     1.00000
SOLIDITY
    1.00000     1.00000     1.00000     1.00000     1.00000     1.00000
BLADE THICKNESS
     .01277      .01276      .01275      .01273      .01270      .01263
AERO BLOCKAGE
     .93100      .93100      .93100      .93100      .93100      .93100
TOTAL BLOCKAGE
     .93042      .93041      .93041      .93039      .93037      .93037
BLADE ANGLE
  -42.56001   -42.56017   -42.57532   -42.61664   -42.63979   -42.43921
LEAN
   -2.51652    -2.66727    -2.87708    -3.04335    -3.06200    -2.86163
Y
   -0.00000    -0.00000    -0.00000    -0.00000    -0.00000    -0.00000

  NOR ITERS =  1  AREA RATIO = 1.00015  EXP = 1.50000  CHOKE =  .51304

RADIUS
    3.25800     3.22812     3.18326     3.10517     3.03053     2.95400
Z
    1.84000     1.84000     1.84000     1.84000     1.84000     1.84000
CROSS PASSAGE DIST P
     .30400      .27412      .22926      .15117      .07653     0.00000
SLOPE
   33.38000    33.60852    34.24905    35.12798    35.48099    36.08000
CURVATURE
    -.28210     -.29582     -.33810     -.31722     -.30995     -.29350
DELTA CURVATURE
    0.00000     -.00067     -.00044      .00045      .00018     0.00000
VM
  393.26146   410.33761   384.81860   417.30214   419.55221   438.70681
VU2
  337.45393   328.70200   320.18873   321.24025   324.41611   333.62886
U
 1987.38000  1969.15193  1941.78717  1894.15267  1848.62277  1801.94000
VR
  216.36833   227.12826   216.57259   240.11774   243.52194   258.36080
BETA2
   40.63256    38.69655    39.76217    37.58915    37.71275    37.25234
BETA2*
   45.77997    43.88547    45.18832    43.26590    43.51827    43.25781
```

INCIDENCE					
2.28982	.36530	1.53990	-.46897	-.26758	-.28765
.39180	.39824	.38341	.40608	.40873	.42382
V2					
518.19854	525.75846	500.60582	526.62736	530.34882	551.15504
TOTAL TEMP					
1.45143	1.44756	1.41269	1.39850	1.40058	1.41021
TOTAL PRESS					
3.10075	3.10693	3.07670	3.10229	3.09396	3.10706
EFFICIENCY					
.83618	.84516	.90734	.94772	.94021	.92214
STATIC TEMP					
1.40875	1.40362	1.37286	1.35443	1.35587	1.36193
STATIC PRESS					
2.79040	2.78636	2.78098	2.77036	2.75890	2.74721
DENSITY					
1.98076	1.98512	2.02568	2.04541	2.03477	2.01714
SUCT SURF VEL					
0.00000	0.00000	0.00000	0.00000	0.00000	0.00000
PRESS SURF VEL					
0.00000	0.00000	0.00000	0.00000	0.00000	0.00000
DELTA T					
0.00000	0.00000	0.00000	0.00000	0.00000	0.00000
WORK COEF = 2*CP*DELT/U**2					
0.00000	0.00000	0.00000	0.00000	0.00000	0.00000
FLOW COEF = VM/U					
.19788	.20838	.19818	.22031	.22695	.24346
R BAR					
3.16750	3.13724	3.09212	3.01462	2.94131	2.86650
D-FACTOR					
.04852	.05553	.07227	.08199	.10003	.12001
VM2/VM1					
.95677	.94496	.91775	.90480	.87781	.84981
DELP/Q					
.09112	.10379	.13429	.15090	.18226	.21566
TANG BLADE FORCE LB/IN					
0.00000	-.00000	-.00000	-.00000	-.00000	.00116
AXIAL BLADE FORCE LB/IN					
10.31254	11.20353	11.63334	13.05247	15.37957	17.89691
VEL HEAD 2					
.10009	.10318	.09612	.10699	.10830	.11582
Q=E**(-S/CP)					
.94905	.95213	.97293	.98510	.98290	.97735
RVU/					
1.80234	1.73949	1.67089	1.63525	1.61173	1.61564
DRVU/DM					
-3.46478	-2.93009	-3.13213	-2.52160	-2.49886	-2.57883
STRMLN DIST M					
2.74186	2.73865	2.74474	2.79022	2.92504	3.37435

STATION 6.10000 STATOR XI = 0.00000

P = 0. ZTIP = 1.92500 AR = 4.00000 XN = 1. BNXT = 0.
= -0. ZHUB = 1.92500 LOSS = 2. EXP = -0.0000 BLADES = 53.

RADIUS					
3.31230	3.27000	3.23000	3.15000	3.08000	3.01380
SLOPE					
31.75800	32.00000	33.00000	33.00000	33.00000	34.28300
CURVATURE					
-.27834	-.27000	-.27000	-.27000	-.27000	-.28133
LOSS COEFF					
.99943	.99945	.99952	.99957	.99949	.99916
SOLIDITY					
1.00000	1.00000	1.00000	1.00000	1.00000	1.00000
BLADE THICKNESS					
.02960	.02965	.02973	.02984	.02995	.03007
AERO BLOCKAGE					
.92902	.92915	.92910	.92909	.92912	.92910
TOTAL BLOCKAGE					
.85899	.85808	.85698	.85485	.85291	.85092
BLADE ANGLE					
-33.29322	-33.27384	-33.24764	-33.23007	-33.28473	-33.32775
LEAN					
-1.21188	-1.31286	-1.47931	-1.73056	-1.86968	-1.91519
Y					
-29.90000	-29.78000	-29.40000	-29.50000	-29.30000	-28.90000

VOR ITERS = 1 AREA RATIO = .99954 EXP = 1.50000 CHOKE = .60600

RADIUS					
3.31230	3.28334	3.23933	3.16352	3.08982	3.01380
Z					
1.92500	1.92500	1.92500	1.92500	1.92500	1.92500
CROSS PASSAGE DIST P					
.29850	.26954	.22553	.14972	.07602	0.00000
SLOPE					
31.75800	32.01613	32.57193	33.07773	33.50506	34.28300
CURVATURE					
-.27834	-.33836	-.33176	-.41787	-.32499	-.28133
DELTA CURVATURE					
0.00000	-.00063	-.00082	-.00432	-.00363	0.00000
VM					
428.72926	435.23229	414.53995	438.18863	442.45862	457.75676
VU2					
246.53038	249.75379	234.41757	247.74486	248.73348	252.70689
U					
2020.50300	2002.83572	1975.99211	1929.74777	1884.78778	1838.41800
VR					
225.65429	230.74193	223.17100	239.15309	244.24193	257.84574
BETA2					
29.90000	29.84892	29.48765	29.48311	29.34303	28.90110
BETA2*					
34.06966	34.08931	33.86282	34.00904	33.98733	33.74817

INCIDENCE	.23767	.23434	-.02750	.01225	-.12547	-.44200
	.37342	.37957	.36424	.38761	.39064	.40137
V2	494.55637	501.80085	476.22996	503.37540	507.58051	522.87859
TOTAL TEMP	1.45143	1.44756	1.41269	1.39850	1.40058	1.41021
TOTAL PRESS	3.09447	3.10087	3.07153	3.09762	3.08835	3.09784
EFFICIENCY	.83443	.84346	.90575	.94625	.93844	.91932
STATIC TEMP	1.41256	1.40754	1.37664	1.35823	1.35963	1.36676
STATIC PRESS	2.81142	2.80840	2.80344	2.79376	2.78095	2.77351
DENSITY	1.99030	1.99526	2.03643	2.05691	2.04537	2.02926
SUCT SURF VEL	619.12829	620.97376	591.56011	604.89570	607.15459	622.36372
PRESS SURF VEL	369.98445	382.62794	360.89980	401.85509	408.00642	423.39346
DELTA T	0.00000	0.00000	0.00000	0.00000	0.00000	0.00000
WORK COEF = 2*CP*DELT/U**2	0.00000	0.00000	0.00000	0.00000	0.00000	0.00000
FLOW COEF = VM/U	.21219	.21731	.20979	.22707	.23475	.24899
R BAR	3.28515	3.25573	3.21129	3.13434	3.06017	2.98390
D-FACTOR	.12870	.11598	.12952	.10890	.10905	.11939
VM2/VM1	1.09019	1.06067	1.07723	1.05005	1.05460	1.04342
DELP/Q	.06772	.06877	.07596	.07050	.06582	.07309
TANG BLADE FORCE LB/IN	-17.50736	-15.33166	-15.82773	-13.95749	-13.94192	-14.82801
AXIAL BLADE FORCE LB/IN	13.71605	12.27059	12.76375	12.06016	11.64992	11.91641
VEL HEAD 2	.09147	.09432	.08728	.09809	.09954	.10469
Q=E**(-S/CP)	.94850	.95160	.97247	.98468	.98239	.97653
RVU/	1.33866	1.34430	1.24485	1.28483	1.25990	1.24854
DRVU/DM	-4.29822	-4.11463	-3.97232	-3.50433	-3.43930	-3.42878
STRMLN DIST M	2.84272	2.84001	2.84657	2.89332	3.02867	3.47828

STATION 6.20000 STATOR XI = 0.00000

P = 0. ZTIP = 2.02500 AR = 4.00000 XN = 1. BNXT = 0.
= -0. ZHUB = 2.02500 LOSS = 2. EXP = -0.0000 BLADES = 53.

RADIUS					
3.37200	3.33000	3.29000	3.21000	3.14000	3.07950
SLOPE					
29.92500	30.00000	30.00000	30.00000	30.00000	32.36080
CURVATURE					
-.27042	-.27000	-.27000	-.27000	-.27000	-.27868
LOSS COEFF					
.99937	.99924	.99943	.99950	.99939	.99900
SOLIDITY					
1.00000	1.00000	1.00000	1.00000	1.00000	1.00000
BLADE THICKNESS					
.03624	.03632	.03645	.03666	.03688	.03716
AERO BLOCKAGE					
.92686	.92660	.92684	.92686	.92690	.92685
TOTAL BLOCKAGE					
.84284	.84136	.84023	.83757	.83507	.83250
BLADE ANGLE					
-22.98716	-22.96542	-22.95318	-22.97066	-23.14303	-23.43325
LEAN					
-.22307	-.27711	-.37393	-.51419	-.58997	-.60406
Y					
-20.80000	-19.37000	-20.45000	-20.50000	-20.60000	-20.60000

VOR ITERS = 1 AREA RATIO = 1.00082 EXP = 1.50000 CHOKE = .56170

RADIUS					
3.37200	3.34336	3.30013	3.22554	3.15376	3.07950
Z					
2.02500	2.02500	2.02500	2.02500	2.02500	2.02500
CROSS PASSAGE DIST P					
.29250	.26386	.22063	.14604	.07426	0.00000
SLOPE					
29.92500	30.00666	30.17291	30.49287	31.01146	32.36080
CURVATURE					
-.27042	-.24247	-.25919	-.22648	-.29044	-.27868
DELTA CURVATURE					
0.00000	-.00083	-.00180	-.00014	.00154	0.00000
VM					
418.24868	429.44417	405.17255	434.48819	435.55481	449.28407
VU2					
158.87785	152.42625	149.42925	162.31818	163.56271	168.87337
U					
2056.92000	2039.45124	2013.07830	1967.57963	1923.79184	1878.49500
VR					
208.65011	214.76541	203.64436	220.47293	224.40209	240.47895
BETA2					
20.80000	19.54172	20.24417	20.48491	20.58252	20.59983
BETA2*					
23.66778	22.28750	23.10325	23.43903	23.66088	23.98810

INCIDENCE	.51587	-.72943	-.02159	.20572	.24392	.20685
	.33698	.34383	.32953	.35635	.35721	.36751
V2	447.40824	455.69294	431.84939	463.81805	465.25342	479.97333
TOTAL TEMP	1.45143	1.44756	1.41269	1.39850	1.40058	1.41021
TOTAL PRESS	3.08762	3.09256	3.06539	3.09218	3.08169	3.08686
EFFICIENCY	.83252	.84112	.90387	.94453	.93634	.91595
STATIC TEMP	1.41962	1.41455	1.38305	1.36431	1.36617	1.37360
STATIC PRESS	2.85504	2.85053	2.84411	2.83323	2.82243	2.81285
DENSITY	2.01113	2.01514	2.05640	2.07667	2.06594	2.04780
SUCT SURF VEL	552.29279	566.78215	534.70406	566.23879	563.59389	575.00833
PRESS SURF VEL	342.52368	344.60374	328.99472	361.39731	366.91296	384.93832
DELTA T	0.00000	0.00000	0.00000	0.00000	0.00000	0.00000
WORK COEF = 2*CP*DELT/U**2	0.00000	0.00000	0.00000	0.00000	0.00000	0.00000
FLOW COEF = VM/U	.20334	.21057	.20127	.22082	.22640	.23917
R BAR	3.34215	3.31335	3.26973	3.19453	3.12179	3.04665
D-FACTOR	.18029	.18523	.17868	.15948	.16313	.15787
VM2/VM1	.97555	.98670	.97740	.99156	.98440	.98149
DELP/Q	.15411	.14403	.15169	.12988	.13496	.12131
TANG BLADE FORCE LB/IN	-18.05150	-20.37243	-16.84984	-17.59822	-16.96104	-16.30954
AXIAL BLADE FORCE LB/IN	13.02157	13.50688	12.47174	13.19989	12.87090	11.33118
VEL HEAD 2	.07533	.07826	.07219	.08375	.08413	.08877
Q=E**(-S/CP)	.94791	.95088	.97192	.98420	.98179	.97555
RVU/	.87826	.83544	.80842	.85830	.84563	.85253
DRVU/DM	-3.41230	-3.59005	-3.34453	-3.34736	-3.22739	-3.13175
STRMLN DIST M	2.95919	2.95664	2.96360	3.01099	3.14737	3.59793

STATION 6.30000 STATOR XI = 0.00000

R = 0. ZTIP = 2.12500 AR = 4.00000 XN = 1. BNXT = 0.
= -0. ZHUB = 2.12500 LOSS = 2. EXP = -0.0000 BLADES = 53.

RADIUS					
3.42750	3.39000	3.34000	3.27000	3.20000	3.14064
SLOPE					
28.18870	29.00000	29.00000	30.00000	30.00000	30.50800
CURVATURE					
-.25880	-.25000	-.25000	-.25000	-.25000	-.27248
LOSS COEFF					
.99935	.99941	.99944	.99950	.99930	.99901
SOLIDITY					
1.00000	1.00000	1.00000	1.00000	1.00000	1.00000
BLADE THICKNESS					
.03441	.03450	.03463	.03482	.03505	.03535
AERO BLOCKAGE					
.92461	.92462	.92460	.92462	.92433	.92461
TOTAL BLOCKAGE					
.84630	.84525	.84375	.84158	.83892	.83682
BLADE ANGLE					
-13.15601	-13.16994	-13.19334	-13.36500	-13.69501	-14.13522
LEAN					
.37921	.36250	.34761	.37343	.43254	-.52372
Y					
-13.50000	-12.20000	-12.20000	-12.35000	-12.50000	-12.50000

NOR ITERS = 1 AREA RATIO = 1.00020 EXP = 1.50000 CHOKE = .53144

RADIUS					
3.42750	3.39918	3.35637	3.28308	3.21319	3.14064
Z					
2.12500	2.12500	2.12500	2.12500	2.12500	2.12500
CROSS PASSAGE DIST P					
.28686	.25854	.21573	.14244	.07255	0.00000
SLOPE					
28.18870	28.57299	28.66508	29.36327	29.88712	30.50800
CURVATURE					
-.25880	-.27205	-.27921	-.30472	-.23322	-.27248
DELTA CURVATURE					
0.00000	.00076	.00125	.00038	-.00097	0.00000
VM					
406.78347	416.70086	393.36177	428.49523	429.08505	443.21211
VU2					
97.66011	91.74046	85.04786	93.54715	94.95269	98.25733
U					
2090.77500	2073.49855	2047.38828	2002.68134	1960.04382	1915.79040
VR					
192.15521	199.29889	188.69133	210.11061	213.81008	225.00055
BETA2					
13.50000	12.41610	12.20000	12.31532	12.47795	12.49994
BETA2*					
15.23684	14.07350	13.84237	14.06305	14.31819	14.43013

INCIDENCE					
2.03097	.97533	.74640	.82926	.81640	.00445
.31464	.32148	.30667	.33652	.33695	.34712
V2					
418.34231	426.68011	402.45076	438.58777	439.46557	453.97299
TOTAL TEMP					
1.45143	1.44756	1.41269	1.39850	1.40058	1.41021
TOTAL PRESS					
3.08050	3.08608	3.05931	3.08672	3.07402	3.07605
EFFICIENCY					
.83053	.83930	.90200	.94281	.93392	.91262
STATIC TEMP					
1.42362	1.41862	1.38695	1.36793	1.36988	1.37746
STATIC PRESS					
2.87692	2.87357	2.86683	2.85482	2.84250	2.83093
DENSITY					
2.02085	2.02561	2.06701	2.08696	2.07500	2.05519
SUCT SURF VEL					
509.11301	515.56572	488.43764	529.16008	528.12211	539.43613
PRESS SURF VEL					
327.57161	337.79451	316.46389	348.01546	350.80904	368.50985
DELTA T					
0.00000	0.00000	0.00000	0.00000	0.00000	0.00000
WORK COEF = 2*CP*DELT/U**2					
0.00000	0.00000	0.00000	0.00000	0.00000	0.00000
FLOW COEF = VM/U					
.19456	.20097	.19213	.21396	.21892	.23135
R BAR					
3.39975	3.37127	3.32825	3.25431	3.18347	3.11007
D-FACTOR					
.13104	.12804	.14032	.12609	.12657	.12500
VM2/VM1					
.97259	.97033	.97085	.98621	.98515	.98649
DELP/Q					
.09405	.09523	.10270	.08338	.07741	.06598
TANG BLADE FORCE LB/IN					
-12.94938	-13.03610	-13.15202	-14.81712	-14.25732	-14.49429
AXIAL BLADE FORCE LB/IN					
6.00297	5.85769	5.90540	6.27725	5.62460	5.69144
VEL HEAD 2					
.06609	.06886	.06291	.07513	.07531	.07969
Q=E**(-S/CP)					
.94729	.95031	.97137	.98370	.98110	.97458
RVU/					
.54874	.51122	.46795	.50348	.50017	.50589
DRVU/DM					
-2.82062	-2.75349	-2.66624	-2.81695	-2.76638	-2.67704
STRMLN DIST M					
3.07356	3.07116	3.07833	3.12636	3.26370	3.71514

```
STATION        6.40000   STATOR    XI =       0.00000

P =    0.   ZTIP =    2.22500    AR =    4.00000     XN =   1.     BNXT =    0.
   =  -0.   ZHUB =    2.22500    LOSS =    2.   EXP =  -0.0000  BLADES =  53.

RADIUS
    3.47930      3.45000      3.40000      3.33000      3.26000      3.19750
SLOPE
   26.56550     27.00000     27.00000     27.00000     27.00000     28.74200
CURVATURE
    -.24372      -.25000      -.25000      -.25000      -.25000      -.26270
LOSS COEFF
     .99931       .99924       .99944       .99949       .99939       .99901
SOLIDITY
    1.00000      1.00000      1.00000      1.00000      1.00000      1.00000
BLADE THICKNESS
     .02607       .02612       .02621       .02635       .02649       .02668
AERO BLOCKAGE
     .92222       .92209       .92237       .92234       .92211       .92238
TOTAL BLOCKAGE
     .86393       .86319       .86239       .86078       .85892       .85747
BLADE ANGLE
   -3.58613     -3.61283     -3.69188     -3.94111     -4.46423     -5.16844
LEAN
     .69020       .72157       .79733       .99723      1.27698     -1.51457
Y
   -6.13000     -5.30000     -5.50000     -5.40000     -5.35000     -5.90000

   NOR ITERS =   1   AREA RATIO =   .99917   EXP = 1.50000   CHOKE =   .50186

RADIUS
    3.47930      3.45121      3.40876      3.33633      3.26830      3.19750
Z
    2.22500      2.22500      2.22500      2.22500      2.22500      2.22500
CROSS PASSAGE DIST P
     .28180       .25371       .21126       .13883       .07080      0.00000
SLOPE
   26.56550     26.76860     26.88784     27.02864     27.44866     28.74200
CURVATURE
    -.24372      -.24397      -.22638      -.26674      -.37492      -.26270
DELTA CURVATURE
    0.00000      -.00027      -.00041      -.00109      -.00196      0.00000
VM
  388.19074    397.48668    373.75262    411.63113    412.49350    424.08728
VU2
   41.69123     37.01687     35.86525     38.96125     38.65305     43.80101
U
 2122.37300   2105.23827   2079.34369   2035.16049   1993.66219   1950.47500
VR
  173.60696    179.02344    169.02796    187.06000    190.14047    203.92938
BETA2
    6.13000      5.32046      5.48131      5.40699      5.35331      5.89677
BETA2*
    6.84706      5.95473      6.14089      6.06527      6.02770      6.71826
```

INCIDENCE	3.22945	2.41868	2.55757	2.36682	2.02908	.63911
	.29328	.30040	.28576	.31685	.31726	.32553
V2	390.42311	399.20660	375.46949	413.47088	414.30055	426.34323
TOTAL TEMP	1.45143	1.44756	1.41269	1.39850	1.40058	1.41021
TOTAL PRESS	3.07296	3.07785	3.05324	3.08118	3.06743	3.06527
EFFICIENCY	.82842	.83697	.90013	.94105	.93184	.90929
STATIC TEMP	1.42721	1.42223	1.39028	1.37133	1.37330	1.38132
STATIC PRESS	2.89552	2.89173	2.88553	2.87480	2.86147	2.84909
DENSITY	2.02880	2.03324	2.07550	2.09636	2.08365	2.06258
SUCT SURF VEL	454.10807	473.14639	439.46148	480.24168	472.77691	491.08079
PRESS SURF VEL	326.73816	325.26680	311.47750	346.70008	355.82418	361.60566
DELTA T	0.00000	0.00000	0.00000	0.00000	0.00000	0.00000
WORK COEF = 2*CP*DELT/U**2	0.00000	0.00000	0.00000	0.00000	0.00000	0.00000
FLOW COEF = VM/U	.18290	.18881	.17975	.20226	.20690	.21743
R BAR	3.45340	3.42519	3.38257	3.30971	3.24074	3.16907
D-FACTOR	.13238	.12737	.12698	.11828	.12002	.11944
VM2/VM1	.95429	.95389	.95015	.96064	.96133	.95685
DELP/Q	.09139	.08544	.09716	.08618	.08194	.07406
TANG BLADE FORCE LB/IN	-12.25050	-12.17310	-10.35787	-12.39567	-12.38497	-11.74902
AXIAL BLADE FORCE LB/IN	3.40931	3.24050	3.31056	4.54100	4.33940	3.10238
VEL HEAD 2	.05774	.06047	.05493	.06698	.06714	.07053
Q=E**(-S/CP)	.94663	.94960	.97082	.98320	.98051	.97361
RVU/	.23780	.20943	.20042	.21309	.20710	.22960
DRVU/DM	-1.89095	-2.19422	-1.90196	-1.98762	-1.74397	-1.93782
STRMLN DIST M	3.18618	3.18389	3.19122	3.23966	3.37788	3.83017

STATION 6.50000 STATOR XI = 0.00000

P = 0. ZTIP = 2.33000 AR = 3.00000 XN = 1. BNXT = 1.
* -0. ZHUB = 2.33000 LOSS = 2. EXP = -0.0000 BLADES = 53.

RADIUS	3.53000	3.51000	3.48000	3.40000	3.33000	3.25000
SLOPE	25.00000	25.00000	25.50000	26.00000	26.50000	27.00000
CURVATURE	-.28200	-.26900	-.27000	-.27200	-.27400	-.29350
LOSS COEFF	.99936	.99938	.99941	.99948	.99942	.99894
SOLIDITY	1.00000	1.00000	1.00000	1.00000	1.00000	1.00000
BLADE THICKNESS	.01005	.01005	.01005	.01005	.01004	.01002
AERO BLOCKAGE	.92000	.92000	.92000	.92000	.92000	.92000
TOTAL BLOCKAGE	.89790	.89777	.89758	.89707	.89661	.89607
BLADE ANGLE	6.33938	6.29478	6.14885	5.71909	4.96198	3.92472
LEAN	.59872	.71747	.93884	1.42878	2.00686	-2.54859
Y	-3.30000	0.00000	-1.00000	-1.00000	-2.75000	-1.60000

IOR ITERS = 1 AREA RATIO = 1.00006 EXP = 1.50000 CHOKE = .47065

RADIUS	3.53000	3.50233	3.46035	3.38825	3.32094	3.25000
Z	2.33000	2.33000	2.33000	2.33000	2.33000	2.33000
CROSS PASSAGE DIST P	.28000	.25233	.21035	.13825	.07094	0.00000
SLOPE	25.00000	25.23034	25.55112	25.81480	26.04749	27.00000
CURVATURE	-.28200	-.15563	-.16866	-.14005	-.14975	-.29350
DELTA CURVATURE	0.00000	.00168	.00168	.00192	.00126	0.00000
VM	366.65550	376.60561	349.80675	388.48895	383.39979	387.81359
VU2	21.14123	2.02184	6.10590	8.99769	18.67358	10.82864
VU1	2132.15877	2134.39949	2104.71006	2057.83532	2007.10201	1971.67136
U	2153.30000	2136.42133	2110.81596	2066.83300	2025.77559	1982.50000
VR	154.95537	160.53134	150.87740	169.17288	168.35704	176.06376
BETA2	3.30000	.30759	1.00000	1.32677	2.78840	1.59941
BETA1	80.24256	79.99337	80.56356	79.30919	79.18552	78.87235
BETA2*	3.64027	.34003	1.10838	1.47379	3.10305	1.79494

BETA1*	81.14153	80.93131	81.47214	80.35495	80.26176	80.05957
INCIDENCE	74.24256	73.99776	74.63323	73.59784	74.17218	76.52902
M2	.27561	.28312	.26599	.29744	.29353	.29570
M1	1.62355	1.62933	1.62212	1.60297	1.56259	1.53156
V2	367.26449	376.61103	349.86004	388.59313	383.85428	387.96474
V1	2163.45494	2167.37006	2133.58131	2094.18477	2043.39274	2009.44951
TOTAL TEMP	1.45143	1.44756	1.41269	1.39850	1.40058	1.41021
TOTAL PRESS	3.06596	3.07105	3.04683	3.07549	3.06115	3.05379
EFFICIENCY	.82646	.83505	.89816	.93925	.92985	.90574
STATIC TEMP	1.42999	1.42501	1.39323	1.37451	1.37716	1.38629
STATIC PRESS	2.90892	2.90537	2.90114	2.89301	2.88409	2.87464
DENSITY	2.03422	2.03884	2.08231	2.10477	2.09423	2.07362
SUCT SURF VEL	370.41478	418.73161	382.73456	416.69578	385.62224	422.73746
PRESS SURF VEL	364.11421	334.49046	316.98552	360.49048	382.08631	353.19203
DELTA T	0.00000	0.00000	0.00000	0.00000	0.00000	0.00000
WORK COEF = 2*CP*DELT/U**2	0.00000	0.00000	0.00000	0.00000	0.00000	0.00000
FLOW COEF = VM/U	.17028	.17628	.16572	.18796	.18926	.19562
R BAR	3.50465	3.47677	3.43456	3.36229	3.29462	3.22375
D-FACTOR	.08505	.10007	.10742	.09595	.09705	.12816
VM2/VM1	.94452	.94747	.93593	.94378	.92947	.91447
DELP/Q	.07553	.07329	.09309	.08823	.10982	.11819
TANG BLADE FORCE LB/IN	-4.56362	-8.01992	-6.39560	-7.01188	-4.47242	-7.29953
AXIAL BLADE FORCE LB/IN	.95699	1.09990	1.10046	1.64145	1.93936	1.71364
VEL HEAD 2	.05122	.05395	.04782	.05933	.05784	.05866
VEL HEAD 1	.77236	.77431	.77188	.76529	.75086	.73928
Q=E**(-S/CP)	.94602	.94900	.97025	.98269	.97994	.97258
RVU/	.12234	.01161	.03464	.04998	.10166	.05769
DRVU/DM	-.08942	-1.19365	-.93215	-.79745	-.05131	-.99084
STRMLN DIST M	3.30278	3.30067	3.30821	3.35679	3.49533	3.94757

APPENDIX E

MECHANICAL DESIGN ANALYSIS OF NASA 10/1 ADVANCED COMPRESSOR RIG

(11 pages)

MECHANICAL DESIGN ANALYSIS
OF NASA 10/1 ADVANCED
COMPRESSOR RIG

This report summarizes the mechanical design analyses completed on the NASA 10/1 Advanced Compressor Test Rig. The analyses include (1) the first stage compressor blade stress and vibration and (2) the first-stage compressor disk stress.

First-Stage Compressor Blade Stress and Vibration Analysis

The first-stage compressor consists of two blade rows, rotor 1A and rotor 1B. The compressor is made of titanium (90Ti-6Al-4V). The material properties at room temperatures are as follows:

Tensile Strength = 130,000 psi

Yield Strength = 120,000 psi

Rotor 1A has 20 blades and rotor 1B has 40 blades. A finite element program has been employed to analyze the aerodynamically designed blade for the centrifugal, thermal, and gas pressure stresses. The same program also computes the natural frequencies and mode shapes of the compressor blade.

The distributions of centrifugal stresses in the blades of rotors 1A and 1B are shown in Figures 1 and 2. The stresses are based on the 100-percent operating speed (70,000 rpm). The distributions of the combined stresses due to centrifugal force, thermal gradient and gas pressure in the blades of rotors 1A and 1B are shown in Figure 3 and Figure 4. The tangential and axial forces acting on the blades resulting from gas pressure difference are listed in Table I. The temperature distribution of the blade is assumed to equal the total relative gas temperature. The calculated blade stresses are not excessive and they are within the acceptable level.

The interference diagrams drawn for the natural frequencies of the blades are shown in Figures 5 and 6. In Figure 5, a 10-percent to 20-percent increase of the first bending resonant frequency due to blade variations, as observed in the salt pattern test of NASA 6/1 Advanced Compressor rotor blade,would interfere with four-per-revolution excitation very close to the 100-percent operating speed. Four struts are currently used upstream of this rotor in the inlet duct. The interference possibility of seven and eleven struts is also indicated.

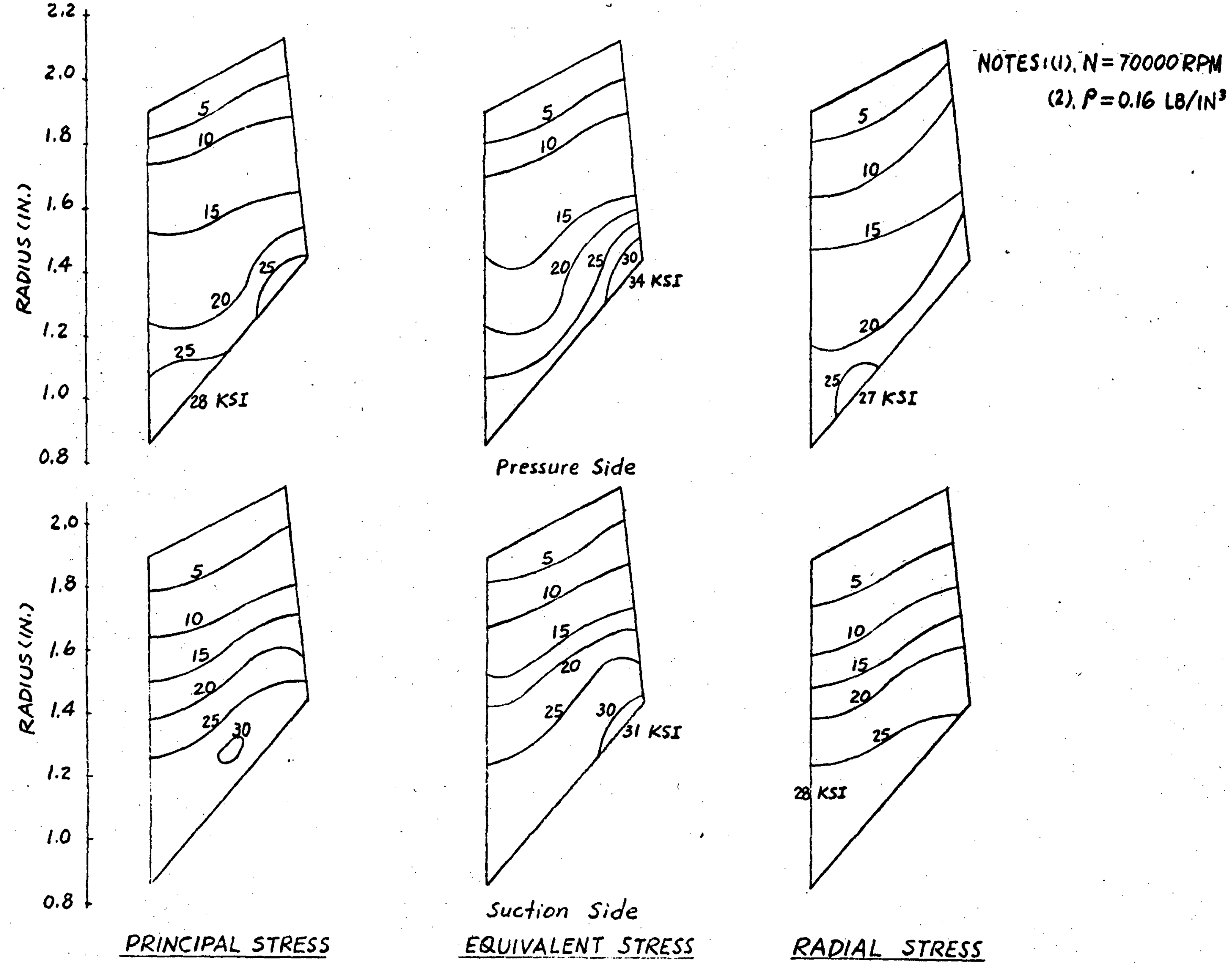

BLADE STRESSES DUE TO CENTRIFUGAL FORCE - ROTOR 1A

FIGURE 1

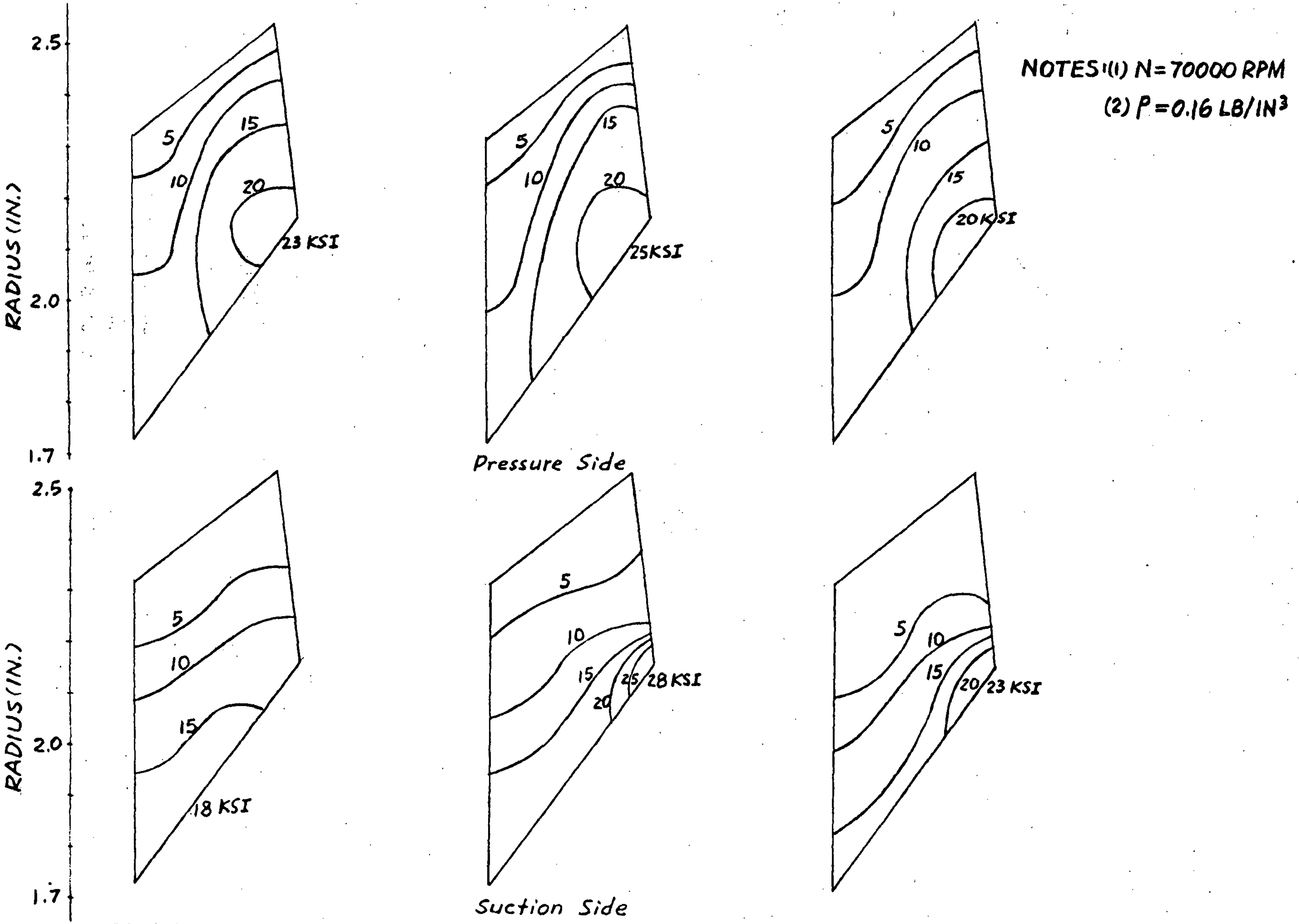

PRINCIPAL STRESS EQUIVALENT STRESS RADIAL STRESS

BLADE STRESSES DUE TO CENTRIFUGAL FORCE - ROTOR 1B

FIGURE 2

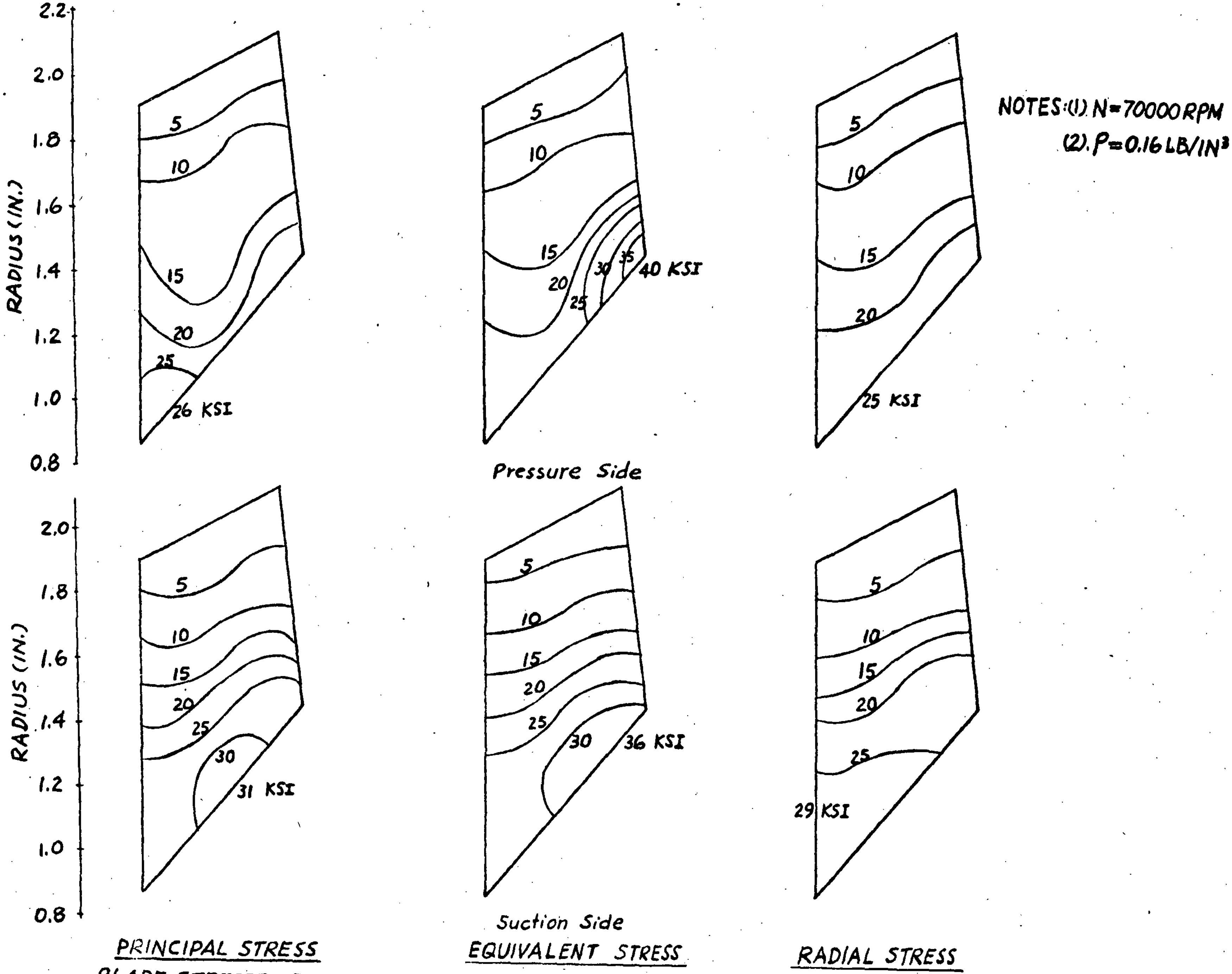

BLADE STRESSES DUE TO CENTRIFUGAL AND THERMAL FORCES AND GAS PRESSURE - ROTOR 1A FIGURE 3

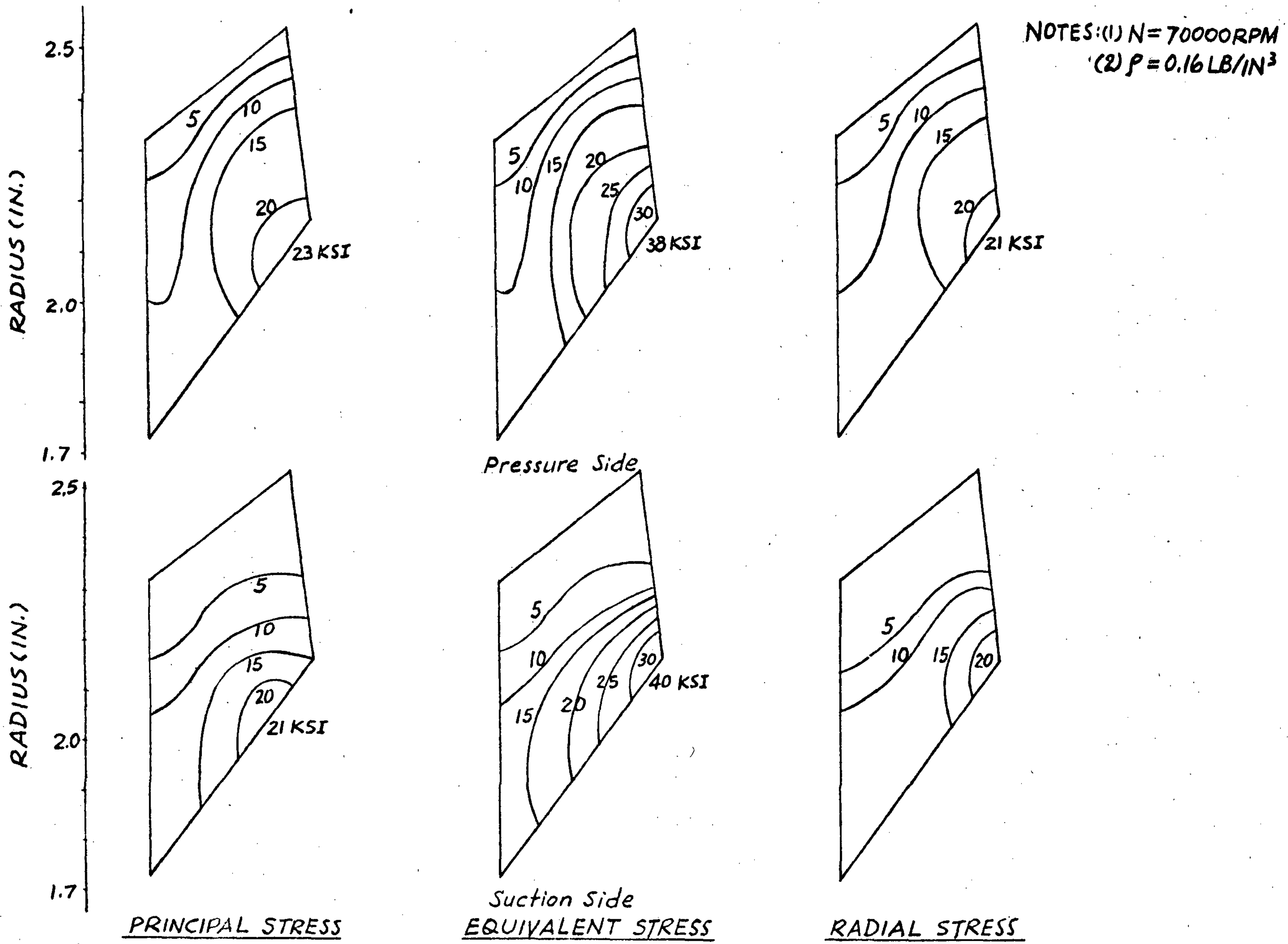

BLADE STRESSES DUE TO CENTRIFUGAL AND THERMAL FORCES AND GAS PRESSURE – ROTOR 1B FIGURE 4

A seven-strut inlet indicates the rotor 1A blade to be free of resonance (Figure 5), whereas the rotor 1B has a possible resonance condition near 100-percent speed (Figure 6). Eleven inlet struts apprear to be a better configuration in that the interference (resonance) occurs at a low speed during a start transient.

TABLE I

PRESSURE LOADS vs. RADIUS

Rotor 1A 20 Blades

Radius, in.	2.13	2.083	2.008	1.871	1.7	1.454
Tang., lb/in.	66.0*	61.8	54.7	46.36	36.87	25.14
Axial, lb/in.	93.84	90.57	86.86	77.91	64.25	41.72

Rotor 1B 40 Blades

Radius, in.	2.541	2.503	2.447	2.360	2.264	2.159
Tang., lb/in.	81.34	80.28	76.7	72.75	70.3	64.84
Axial, lb/in.	147.9	144.3	143.3	134.1	123.3	108.4

* Loads indicated are pounds per radial inch and are totals for indicated blade numbers.

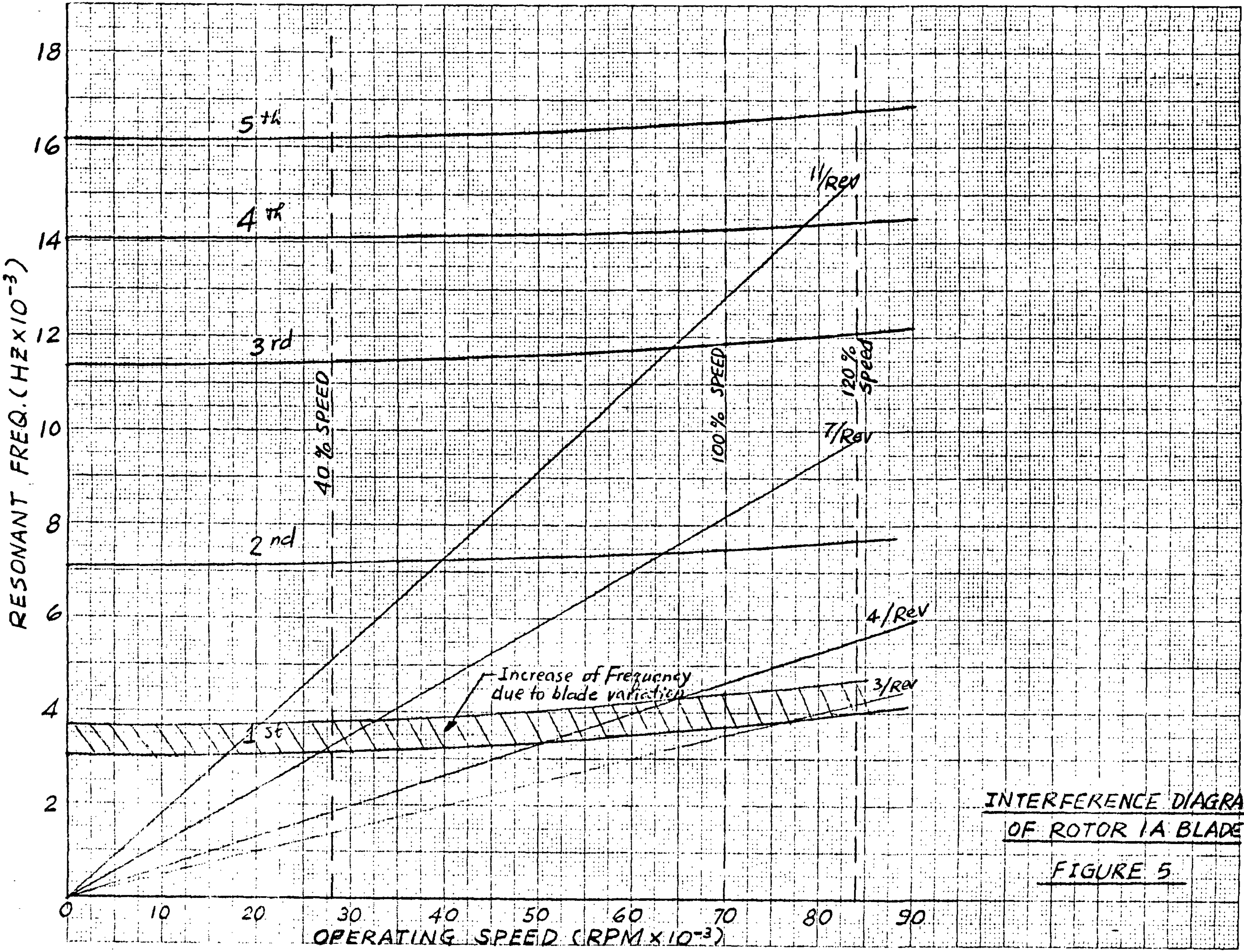

INTERFERENCE DIAGRAM OF ROTOR 1A BLADE

FIGURE 5

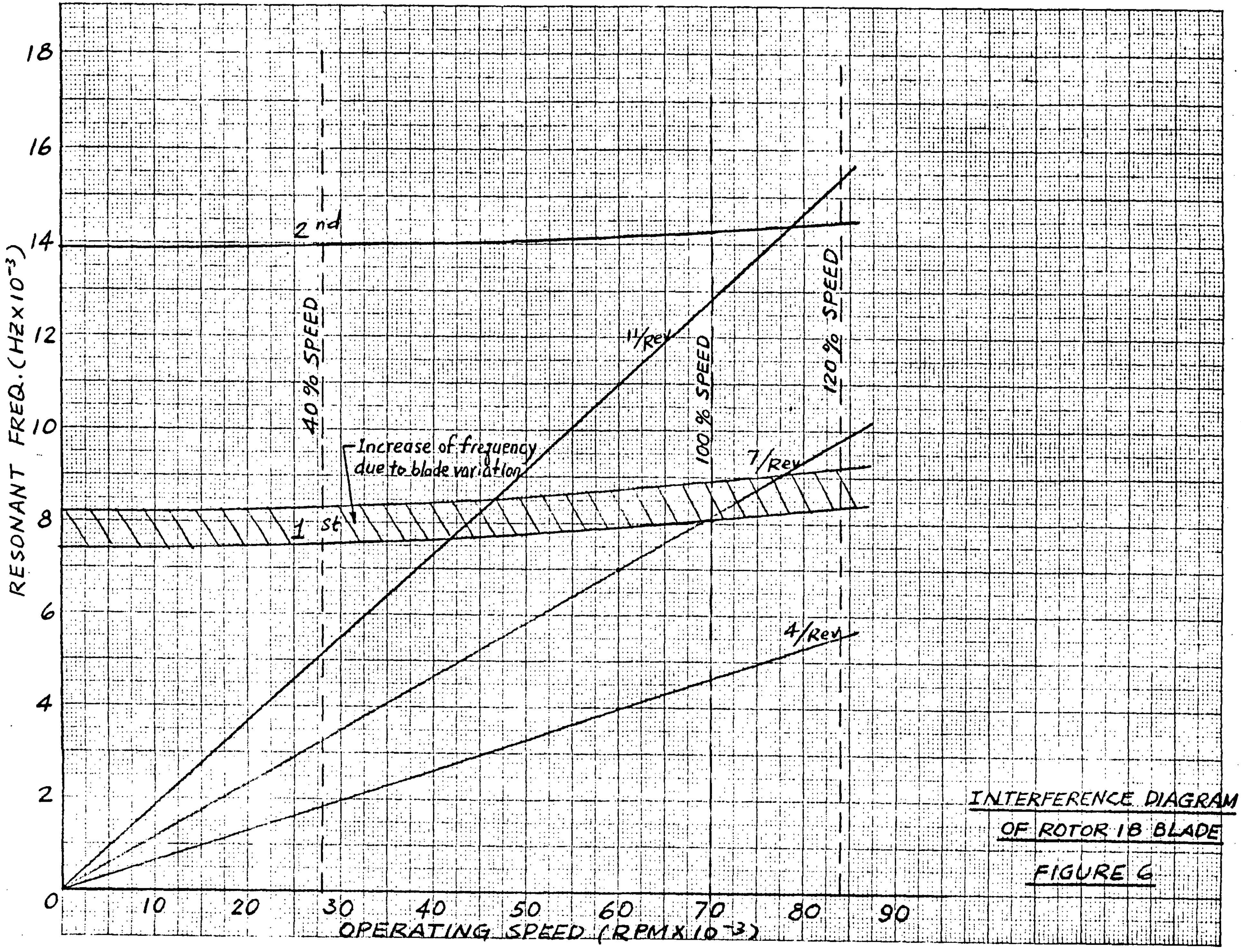

INTERFERENCE DIAGRAM OF ROTOR 1B BLADE

FIGURE 6

First-Stage Compressor Disk Stress Analysis

A finite element program has been employed to analyze the centrifugal and thermal stresses of the disks. The calculated tangential, radial, and equivalent stresses of rotor 1A and rotor 1B are shown in Figures 7 and 8. A summary of pertinent information is listed in Table II. The stresses based on 100-percent operating speed (70,000 RPM) are satisfactory.

TABLE II

	ROTOR 1A	ROTOR 1B
Weight, pounds	0.56	0.55
Polar Moment of Inertia, in-lb-sec^2	0.00123	0.00293
Diametric Moment of Inertia, in-lb-sec^2	0.00129	0.0015
Maximum Tangential Stress at Bore, psi	38,000	66,000
Average Tangential Stress, psi	14,077	36,697
Average Burst Speed, rpm	190,100	117,800
Average Burst Margin, percent	271	168
Blade Tip Radial Growth, in.	0.003	0.005
Blade Tip Axial Growth, in.	0.005	0.008

NOTES: (1) N = 70,000 rpm
(2) δ = 0.16 lb/in^2
(3) Burst Factor Assumed = 0.8

NOTE: (1). MATERIAL: TITANIUM (90Ti-6Al-4V)

(2). 100% OPERATING SPEED 70000 RPM

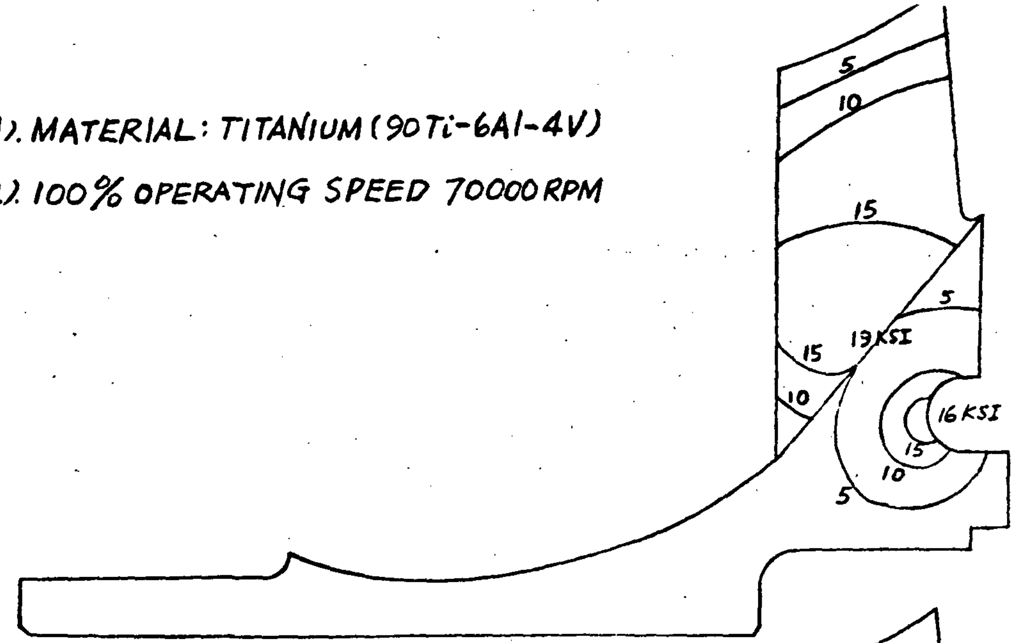

RADIAL STRESS

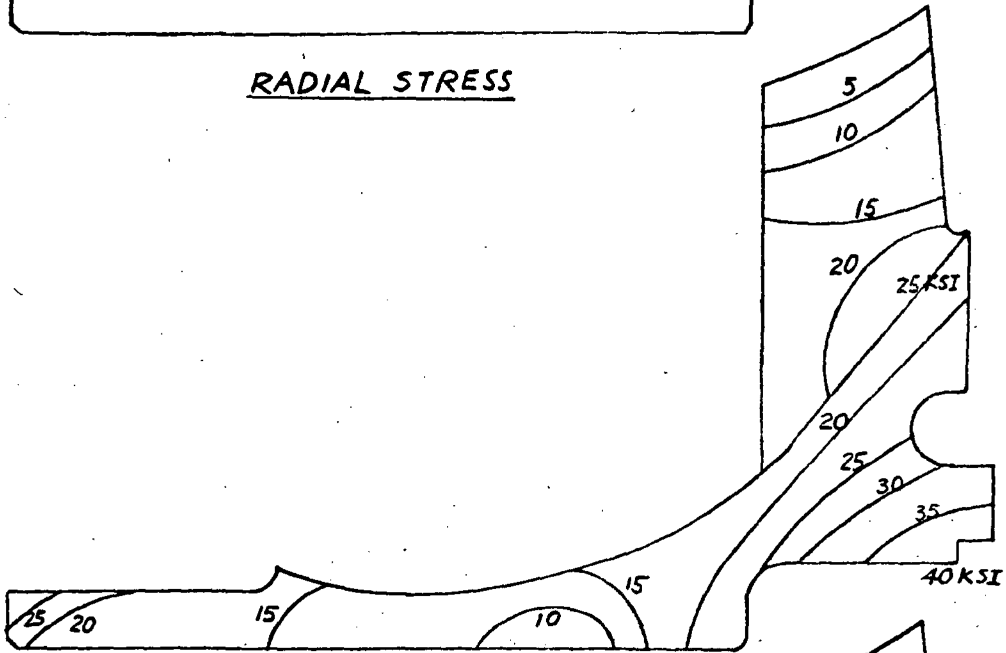

EQUIVALENT STRESS

STRESS DISTRIBUTIONS IN IMPELLER DISK - ROTOR IA

FIGURE 7

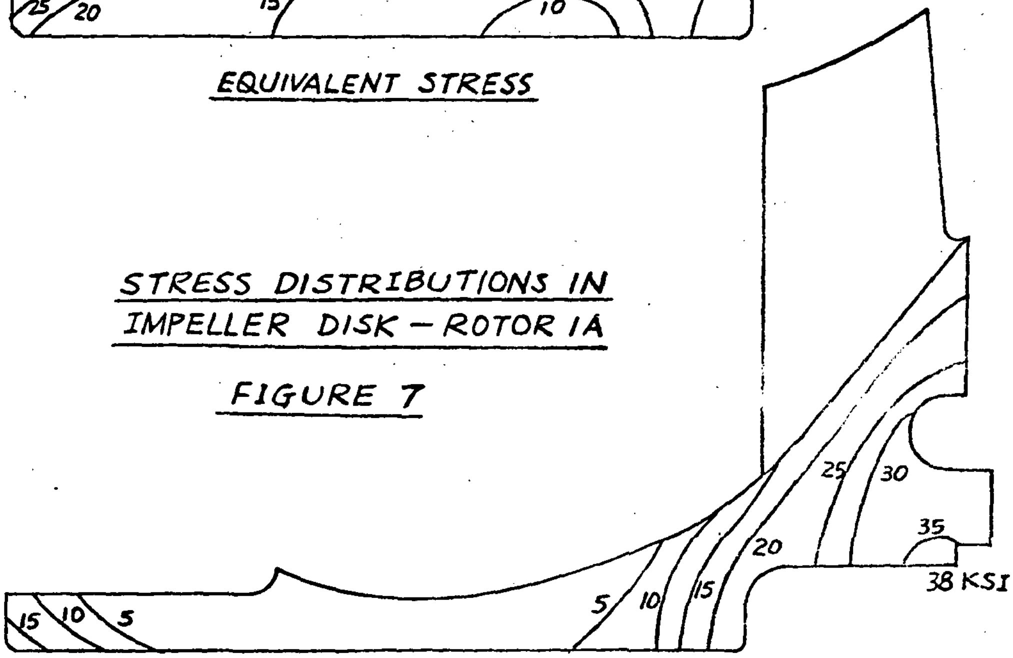

TANGENTIAL STRESS

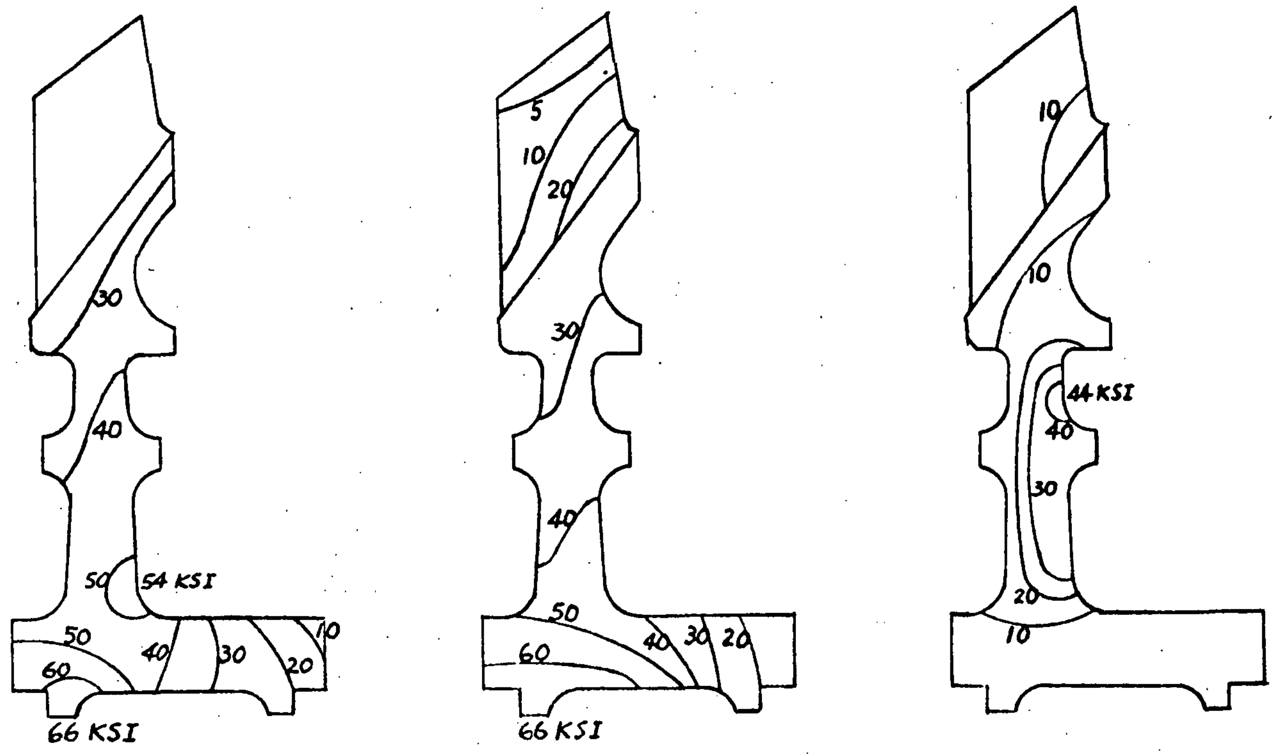

TANGENTIAL STRESS   EQUIVALENT STRESS   RADIAL STRESS

NOTE: (1) MATERIAL: TITANIUM (90Ti-6Al-4V)
(2) 100 % OPERATING SPEED 70000 RPM

STRESS DISTRIBUTION OF IMPELLER DISK - ROTOR 1B
FIGURE 8

APPENDIX F

REFERENCES

(1 page)

REFERENCES

1. Love, G., "Pressure Rise Associated with Shock-Induced Boundary-Layer Separation," NACA TN 3601, 1955.

2. Johnsen, I. A. and Bullock, R. O., "Aerodynamic Design of Axial-Flow Compressors," NASA SP-36, 1965.

3. Stark, U., "Flow Investigations Around Swept Cascades at Compressible Subsonic Flow," Institure for Aerodynamics of the German Research Laboratory for Aeronautics and Space, DFL Report No. 0331, June 1966.

4. Smith, L. H. Jr. and Yeh, H., "Sweep and Dihedral Effects in Axial Flow Turbomachinery," Trans-of ASME, Journal of Basic Engineering, Series D, Volume 85, No. 3, September 1963.

5. Beatty, L. A., Savage M., and Emery, J. C., "Low-Speed Cascade Tests of Two 45° Swept Compressor Blades with Constant Spanwise Loading," NACA RM L53L07, March 1954.

6. Godwin, W. R., "Effect of Sweep on Performance of Compressor Blade Sections as Indicated by Swept-Blade Rotor, Unswept - Blade Rotor, and Cascade Tests," NACA TN 4062, July 1957.

7. Gothert, B., "High-Speed Measurements on a Swept-Back Wing (Sweepback Angle $\Phi = 35°$)," NACA TM 1102, 1947.

8. Katsanis, T. and McNally, W. D., "Fortran Program for Calculating Velocities and Streamlines on a Blade-to-Blade Stream Surface of a Tandem Blade Turbomachine," NASA TN D-5044, March 1969.

9. Pampreen, R. C., "Design and Test of a Cascade Radial Diffuser," AiResearch Internal Report AD-5100-R, June 1966.

10. Keenan, M. J. and Bartok, J. A., "Experimental Evaluation of Transonic Stators," NASA CR-72298, 1969.

11. Von Doenhoff, A. E. and Tetervin, N., "Determination of General Relations for the Behavior of Turbulent Boundary Layers," NACA Rep. 772, 1943.

12. Garner, H. C., "The Development of Turbulent Boundary Layers," ARC Rep. 2133, 1944.

13. K. G. Harley, J. Harris, and E. A. Burdsall, P&W Report, "High Loading Low-Speed Fan Study," NASA CR-72895, 1972.

14. Seyler, D. R. and Smith, L. H., Jr. "Single Stage Experimental Evaluation of High Mach Number Compressor Rotor Blading," NASA CR-54581, 1967.

APPENDIX G

PERFORMANCE PARAMETER DEFINITIONS
SYMBOL DEFINITIONS

(4 pages)

PERFORMANCE PARAMETERS

Diffusion Factor

For the rotor,

$$D = 1.0 - \frac{V_2'}{V_1'} + \frac{r_2 V_{u_2} - r_1 V_{u_1}}{2\bar{r}\sigma V_1'}$$

and for the stator

$$D = 1.0 - \frac{V_2}{V_1} + \frac{r_2 V_{u_2} - r_1 V_{u_1}}{2\bar{r}\sigma V_1}$$

Loss Coefficient

For the rotor,

$$\bar{\omega} = \frac{P'_{T_1}\left[T_2'/T_1'\right]^{\alpha/\alpha-1} - P'_{T_2}}{P'_{T_1} - P_{S_1}}$$

and for the stator

$$\bar{\omega} = \frac{P_{T_1} - P_{T_2}}{P_{T_1} - P_{S_1}}$$

SYMBOL DEFINITIONS

a	Distance along chord line to point of maximum camber line rise (inches)
A	Flow area (square inches)
A*	Critical flow area (square inches)
AR	Blade aspect ratio (mean blade height/mean chord)
C	Blade chord (inches)
H_{act}	Actual stage enthalpy rise (feet)
i	Incidence angle (degrees), $\beta'_{air} - \beta_{blade}$
L	Distance along chord line from leading edge (inches)
m	Meridional length (inches)
M	Mach number
N	Shaft speed (rpm)
N_b	Number of blades
N_s	Specific speed defined on Figure 1
P	Pressure (psia)
PR	Pressure ratio
Q_{av}	Volumetric flow rate (cubic feet/second)
R,r	Radius (inches)
Re	Reynold's number, $\frac{2 \rho U_T R_T}{\mu_1}$
s	Blade circumferential spacing (inches)
t	Blade thickness (inches)
U_t REF	Reference tip speed = 610 feet/second
U_t	Rotor tip speed (feet/second)
V	Velocity (feet/second)

μ	Viscosity, lb/ft-sec
ρ	Density, slugs/ft^3
$\overset{\circ}{W}$	Weight flow rate (pounds mass/second)
Z	Axial length
β	Relative air angle or blade angle (degrees)
α	Specific heat ratio
δ	Reduced pressure or deviation angle (degrees)
ψ	Stream function
η_{ad}	Adiabatic efficiency, $\frac{(P_2/P_1)^{\alpha-1/\alpha} - 1}{T_2/T_1 - 1}$
η_p	Polytropic efficiency, $\frac{\alpha-1/\alpha \ \ln\left(P_2/P_1\right)}{\ln\left(T_2/T_1\right)}$
Θ	Reduced temperature, T/518.68
θ^*	Boundary layer momentum thickness
σ	Solidity, $\frac{CN_b}{2\pi\bar{r}}$
Φ	Blade camber, $\beta_2 - \beta_1$
$\bar{\omega}$	Total pressure loss parameter

<u>Subscript</u>

1	Upstream
2	Downstream
eff	Effective
geo	Geometric
LE	Leading edge
SS	Supersonic

SYMBOL DEFINITIONS (Contd)

Subscript (Contd)

s	Static condition
t	Tip
T	Stagnation condition
TE	Trailing edge
u, θ	Tangential component

Superscript

$'$	Relative condition
$\bar{\ }$	Averaged value